Exploration of Morita-Baylis-Hillman Adducts of Pyrazoledione and 3-Methyleneoxindole to Access Multifunctional Spiroheterocycles with Contiguous Chiral Centres

विद्या वाचस्पति की
उपाधि की अपेक्षाओं की आंशिक पूर्ति में प्रस्तुत शोध प्रबंध

A thesis submitted in partial fulfillment of the requirements of the degree of Doctor of Philosophy

द्वारा / By

अभिजीत शामराव साबळे/ Abhijeet Shamrao Sabale

पंजीकरण सं. /Registration No.:20193632

प्रो. रामकृष्ण जी. भट्ट / Prof. Ramakrishna G. Bhat



भारतीय विज्ञान शिक्षा एवं अनुसंधान संस्थान पुणे
INDIAN INSTITUTE OF SCIENCE EDUCATION AND RESEARCH PUNE
2025

This thesis is dedicated to ….

My parents, whose unwavering support and love have been my greatest strength, and to my entire family, for their constant encouragement and inspiration throughout this journey

CERTIFICATE

Certified that the work incorporated in the thesis entitled **"Exploration of Morita-Baylis-Hillman Adducts of Pyrazoledione and 3-Methyleneoxindole to Access Multifunctional Spiroheterocycles with Contiguous Chiral Centres"** submitted by Abhijeet Shamrao Sabale, was carried out by the candidate, under my supervision. The work presented here or any part of it has not been included in any other thesis submitted previously for the award of any degree or diploma from any other University or institution.



Prof. Ramakrishna G. Bhat

Date: 24-6-2025

Declaration by Student

Declaration by Student

Name of Student: Abhijeet Shamrao Sabale
Thesis Supervisor(s): Prof. Ramakrishna G. Bhat

Department Chemistry
Date of joining program: 1-5-2019
Date of Pre-Synopsis Seminar: 21-11-2024

Title of Thesis: **Exploration of Morita-Baylis-Hillman Adducts of Pyrazoledione and 3-Methyleneoxindole to Access Multifunctional Spiroheterocycles with Contiguous Chiral Centers**

I declare that this written submission represents my idea in my own words, and where others' ideas have been included, I have adequately cited and referenced the original sources. I declare that I have acknowledged collaborative work and discussions wherever such work has been included. I also declare that I have adhered to all principles of academic honesty and integrity and have not misrepresented or fabricated, or falsified any idea/data/fact/source in my submission. I understand that violation of the above will be cause for disciplinary action by the Institute and can also evoke penal action from the sources which have thus not been properly cited or from whom proper permission has not been taken when needed.

The work reported in this thesis is the original work done by me under the guidance of Prof. Ramakrishna G. Bhat



Signature of the student

ACKNOWLEDGEMENTS

First and foremost, I would like to express my heartfelt gratitude to my thesis advisor, Prof. Ramakrishna G. Bhat, for his exceptional mentorship, unwavering support, and insightful guidance throughout the course of my doctoral research. I am deeply thankful for the trust he placed in me and the academic freedom he allowed, which greatly enriched my learning experience. His advice and thoughtful feedback were invaluable during the writing of this thesis, the preparation of research articles, and the development of scientific presentations. I have learned much more than just science under his mentorship—his emphasis on independent thinking, attention to detail, and the importance of soft skills have significantly contributed to my growth as a researcher. Beyond academics, I thoroughly enjoyed our conversations on history and was constantly inspired by his vast knowledge of literature and scripture. It has truly been a privilege to work under his supervision, and I consider myself very fortunate to have had such a dedicated and knowledgeable advisor. Words fall short in conveying the depth of my appreciation for his consistent encouragement and interest, which played a pivotal role in the successful completion of this work.

I sincerely thank Prof. Jayant B. Udgaonkar (Former Director, IISER Pune) and Prof. Sunil S. Bhagwat (Director, IISER Pune) for ensuring a highly conducive research environment and access to world-class infrastructure and facilities at IISER Pune, which greatly supported the progress of my doctoral studies.

I am deeply thankful to the members of my Research Advisory Committee, Dr. Gnanaprakasam Boopathy (IISER Pune) and Dr. Ravindar Kontham (NCL Pune), for their insightful feedback and constructive suggestions provided during the RAC evaluations, which greatly contributed to the improvement of my research work.

It gives me great pleasure to extend my heartfelt thanks to all the members of our research group. I am especially grateful to my seniors, Dr. Prakash Warghude, Dr. Pankaj Dharpure, Dr. Vikas Khade, Dr. Debasish Laha, Dr. Javed Shaikh, and Dr. Anindita Bhowmick, for their guidance and support during the early phase of my Ph.D.

I would like to express my deepest appreciation to Dr. Prakash Warghude, under whose mentorship I completed my initial lab training and began my research journey. His encouragement and support played a key role in shaping my approach toward scientific work,

and I firmly believe the values, skills, and mindset I developed under his guidance will benefit me throughout my career. It was truly an honor to learn from him.

I also feel incredibly fortunate to have shared this journey with my labmates Kajal, Mousumi, Onkar, Archana, Sidharth, Saswata, Ganesh, Chhabi, Mohit, Shubham, Hrishik, Omkar, Snehal, Bhavya, and Abhinav. Their camaraderie, insightful discussions, and constant support made my time in the lab both productive and enjoyable. These moments will always remain special and memorable.

I would like to extend my sincere thanks to the technical staff for their assistance in operating and accessing various instruments essential to my research. I am grateful to Mr. Ravinder and Mr. Parven Nasa for their support with SCXRD, Mr. Sandeep Kanade for help with HRMS, Mr. Nitin Dalvi and Dr. Sandeep for their guidance with NMR, and Mr. Mahesh Jadhav for his assistance with HPLC. I also appreciate the continuous support provided by the IT department. My heartfelt thanks go to Dr. V. S. Rao, Mr. Mayuresh Kulkarni, Mr. Tushar Kulkarni, Ms. Dipali Dalvi, Ms. Nayana Shirole, and the Dean of the Doctoral Studies Office for addressing academic and fellowship-related matters throughout my Ph.D. journey. Additionally, I am thankful to the administrative team, chemistry department office staff, technical team, security personnel, and housekeeping staff for their consistent support and contributions that helped make my research experience smooth and productive.

I gratefully acknowledge the University Grants Commission (UGC) and IISER Pune for supporting my research through the provision of a fellowship throughout the duration of my doctoral studies.

I truly cherished the time spent with my friends from both IISER and NCL. I am also sincerely grateful to Sandeep Kaulage for his assistance in solving and refining the X-ray crystallographic data.

I would also like to express my gratitude to the Alchemist team for contributing to my well-being and keeping my spirits high throughout this journey.

I feel truly fortunate to have Jyoti as my wife. Despite her demanding MPSC preparation schedule, she has been a constant source of care and encouragement. Her presence has inspired me to grow into a better person, and she has stood by me through every high and low. I am confident that our mutual support and understanding will continue to guide us through all the phases of our life ahead.

No words can truly capture the depth of my gratitude for the blessings, love, and unwavering support of my parents, Ms. Shalan Sabale and Shri. Shamrao Sabale, as well as the encouragement from my extended family members, Ms. Latika, Ms. Archana, Ms. Reshama, Ms. Madhavi, and Ms. Shital (my sisters), also thanks my nephew (Shubham, Ritesh, Samarth, Tanishq, Aryan, Vedant) and niece (Akshada, Vedita). Their constant emotional support, patience, trust, and sacrifices have been the foundation of this journey. They have been my greatest source of motivation and continue to inspire every accomplishment. I have reached those I hope to achieve in the future.

I also extend my heartfelt thanks to all those whose names may have been inadvertently omitted, yet whose unwavering support and contributions have been an integral part of my Ph.D. journey. Lastly, I am deeply thankful to the Almighty for blessing me with this life and the many opportunities it has offered along the way.

Abhijeet S. Sabale

CONTENTS

Contents……..i

Abbreviations……...vi

Synopsis……...xi

List of Publications……..…...xxvii

Chapter 1: *Organocatalysis, Photocatalysis, and Base-Catalyzed Synthesis of Spirocycles via Morita-Baylis-Hillman Adducts and 3-Methyleneoxindole*

1.1 Introduction…….....2

1.2 Synthesis of spiroheterocyclic scaffolds via organocatalysis……...……4

1.2.1 Covalent organocatalysis……..……....4

1.2.2 Non-covalent organocatalysis ……..…….....5

1.3 The Morita-Baylis-Hillman (MBH) reaction……6

1.4 MBH reaction mechanism ……...…….……...……....7

1.5 Morita-Baylis-Hillman (MBH) adducts……..…….....10

1.6 Functional group transformations in Morita-Baylis-Hillman adduct...……...11

1.7 Utilization of Morita-Baylis-Hillman adducts in the synthesis of spirocyclic framework via organocatalysis ……..…….....12

1.8 Utilization of morita-baylis-hillman adducts in spirocyclic framework synthesis via base……...16

1.9 Utilization of visible light for the synthesis of spirocyclic framework……17

1.10 Conclusions……..…...20

1.11 References…….....21

Chapter 2: *A streamlined Synthesis of SpirooxindolePpyrazoloneFfused Cyclopentenes via Diastereoselective [3+2] Annulation*

2.1 Introduction……24

2.2 Recent developments in the synthesis of spirooxindole fused pyrazolone …….25

2.3 Proposed hypothesis and synthetic approach …….....28

2.4 Results and Discussion …….....29

2.5 Conclusions……....37

2.6 Experimental section…….....38

2.6.1 General……..……...38

2.6.2 General procedure for the synthesis of spiropyrazolone fused oxindole …….....38

2.6.3 General procedure for the synthesis of spiroxindole fused pyrazolone……39

2.6.4 Procedure for the synthesis of 3a on mmol scale……..…..….39

2.6.5 Synthetic transformations……....40

2.7 Experimental Data…….....42

2.8 Appendix II: ^{1}H, ^{13}C spectral data of representative compound…….55

2.9 References……..……..…..……..….. 61

Chapter 3: *Visible-Light-Induced Diastereoselective [4+2] Cyclization for Efficient Synthesis of 3,4-Fused Spirooxindoles from 3-Methyleneoxindoles*

3.1 Introduction……64

3.2 Recent developments in the synthesis of 3,4-fused indole and oxindole skeleton ……..65

3.3 Results and Discussion…….....68

3.4 Conclusions……..…….....83

3.5 Experimental section……..……....83

3.5.1 General……..…….....83

3.5.2 General procedure for the synthesis of 2a (GP1)……..…..84

3.5.3 General procedure for the synthesis of 2a under sunlight.....84

3.5.4 Procedure for the synthesis of 2a on mmol scale……..……..85

3.5.5 Procedure for the reaction using TEMPO…….……...…86

3.5.6 Procedure for the reaction using BHT…….……...88

3.5.7 Procedure for UV-visible absorption spectra without light…….....89

3.6 Experimental Data……..……....90

3.7 Appendix III ^{1}H, ^{13}C spectral data of representative compounds……106

3.8 References…….……..……..…..……...…...111

Chapter 4: *One-Pot Oxa-Michael-Initiated [4+2] Cycloaddition Cascade Between Pyrazoledione-Based Morita–Baylis–Hillman Alcohols and Arylidene Pyrazolones: A Concise Route to Dispiropyrazolone-Fused Tetrahydropyrans*

4.1 Introduction……..114

4.2 Recent developments in the synthesis of dispiropyrazolone……116

4.3 Results and Discussion…….....119

4.4 Conclusions……..…….....127

4.5 Experimental section……..……...128

4.5.1 General……..…….....128

4.5.2 General procedure for the synthesis of Pyro-MBH alcohols 1a−1f.……128

4.5.3 General procedure for the synthesis of arylidene ayrazolone derivatives 2a–2af…....129

4.5.4 General procedure for the synthesis of Tetrahydro-dispiro[indolinone-3,2′-pyran-5′,4″-pyrazolone] scaffolds (3a–3ak)……..130

4.5.5 Procedure for the synthesis of 3a on mmol Scale…….……..…130

4.5.6 Procedure for the synthesis of 7a…….…….....131

4.5.7 Procedure for the synthesis of 9a……..……131

4.6 Experimental Data……..……..132

4.7 Appendix IV ^{1}H, ^{13}C spectral data of representative compounds……..162

4.8 References…….……..……..…..……...…....169

Chapter 5: *Efficient Synthesis of Spiropyrazolone Pyrrolidinediones Fused Tetrahydropyran via Base-Induced [4+2] Cycloaddition*

5.1 Introduction……..172

5.2 Recent advances in the synthesis of spiropyrazolone and spiropyrrolidinediones scaffolds ……173

5.3 Results and Discussion…….....176

5.4 Conclusions……..…….....181

5.5 Experimental Section……..……..182

5.5.1 General……..…….....182

5.5.2 General Procedure for the Synthesis of Pyro-MBH alcohols 1a−1e……182

5.5.3 General Procedure for the synthesis of pyrrolidinedione derivatives 2a-2t ….….....183

5.5.4 General Procedure for the Synthesis of spiropyrazolone pyrrolidinediones fused tetrahydropyran scaffolds (3a–3x)……..……...184

5.6 Experimental Data……..……..185

5.7 Appendix V ^{1}H, ^{13}C, ^{19}F spectral data of representative compounds……204

5.8 References…….……..…….…..……...…....212

Summary…….....214

Rights and Permission……...216

List of Abbreviations

Å	angstrom (s)
Ag	argentums (Silver)
Ar	aryl
BHT	butylated hydroxytoluene
Bn	benzyl
^{t}Boc	*tert*-butoxycarbonyl
bs	broad singlet
C	carbon
°C	degree Celsius
Calcd.	calculated
Cat.	Catalytic
CCDC	Cambridge Crystallographic Data Centre
$CeCl_3$	Cerium(III) chloride
CFL	Compact Fluorescent Lamp
$CHCl_3$	chloroform
cm^{-1}	wavenumber(s)
Cs_2CO_3	cesium carbonate
d	day (s); doublet (spectral)
DCM	dichloromethane
dd	doublet of doublet

DABCO	1,4-Diazabicyclo[2.2.2]octane
DBU	1,8-Diazabicyclo[5.4.0]undec-7-ene
DMAP	*N, N'*-dimethylaminopyridine
DIPEA	*N, N*-diisopropylethylamine
DMF	dimethylformamide
DMSO	dimethylsulfoxide
dr	diastereomeric ratio
ee	enantiomeric excess
E	electrophile
equiv	equivalent
ESI	electrospray ionisation
EtOAc	ethyl acetate
EDG	electron-donating group
EWG	electron-withdrawing group
g	gram(s)
FTIR	fourier transform infrared
H	hydrogen
h	hour(s)
HPLC	high High-performance liquid chromatography
HRMS	high-resolution mass spectrometry
Hz	hertz
^{i}Pr	isopropyl
Isa-MBHCs	Isatin derived Morita-Baylis-Hillman Carbonates

J	Spin coupling constant
K_2CO_3	Potassium Carbonate
kcal	kilocalories
K_3PO_4	tripotassium phosphate
KO*t*-Bu	Potassium tert-butoxide
LB	Lewis Base
M	multiplet (spectral)
m	meta
M	molar (mol L^{-1})
MBH	Morita-Baylis-Hillman
MBHCs	Morita-Baylis-Hillman Carbonates
m/z	mass-to-charge ratio
Me	methyl
MeCN	acetonitrile
mg	milligram
min.	minute(s)
mL	millilitres
mmL	microlitre
MS	molecular seives
mmol	millimole
mol	mole
m.p.	melting point
MTBE	methyl tert-butyl ether
N	nitrogen
Et_3N	triethylamine

Nu	nucleophile
O	oxygen
o	ortho
ORTEP	Oak Ridge Thermal-Ellipsoid Plot Program
p	para
P	phosphorus
PPh_3	Triphenylphosphine
Ph	phenyl
Pyro-MBHCs	Pyrazolonedione-based Morita−Baylis−Hillman Carbonates
Pyro-MBHAs	Pyrazolonedione-based Morita−Baylis−Hillman Alcohol
q	quartet
R_f	retention factor
rt	room temperature
s	singlet (NMR)
t	triplet (NMR)
t-, tert-	tertiary (branched alkyl chain)
td	triplet of doublet
TEMPO	2,2,6,6-Tetramethylpiperidin-1-yl)oxyl
THF	tetrahydrofuran
TLC	thin-layer chromatography
TMS	trimethylsilyl
TS	transition state
UV	ultraviolet

W	watts
XRD	X-ray diffraction
δ	chemical shift in ppm downfield from trimethylsilane
2*40	two 40-watt Kessil blue LEDs

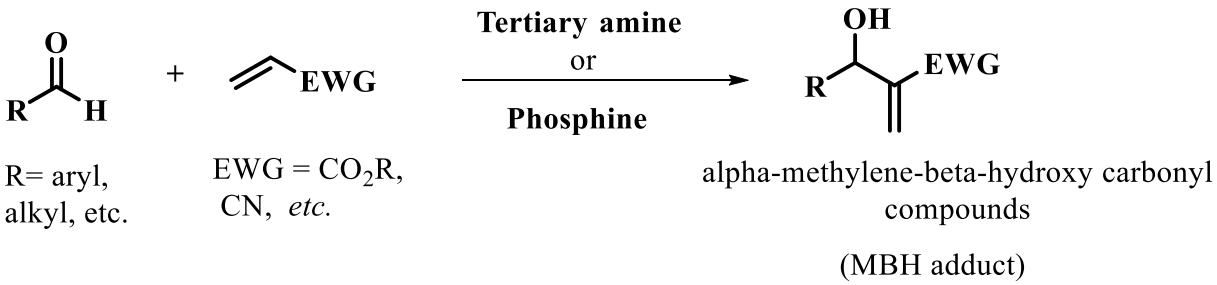
SYNOPSIS

The thesis entitled *Exploration of Morita-Baylis-Hillman Adducts of* Pyrazoledione *and 3-Methyleneoxindole to Access Multifunctional Spiroheterocycles with Contiguous Chiral Centres* is organized into five chapters.

Chapter 1: *Organocatalysis, Photocatalysis, and Base-Catalyzed Synthesis of Spirocycles via Morita-Baylis-Hillman Adducts and 3-Methyleneoxindole*

This introductory chapter presents a brief overview of spiropyrazolone and spirooxindole scaffolds, emphasizing their structural significance and synthetic methodologies. The reactivity and applications of Morita–Baylis–Hillman (MBH) adducts as key intermediates and their utility in constructing spiropyrazolone and spirooxindole frameworks have been highlighted. Additionally, the chapter explores the application of 3-methyleneoxindole as a crucial precursor in synthesizing spirooxindole derivatives has been presented. The strategic importance of these approaches in developing structurally complex and pharmacologically relevant spirocyclic architectures has been discussed as well.

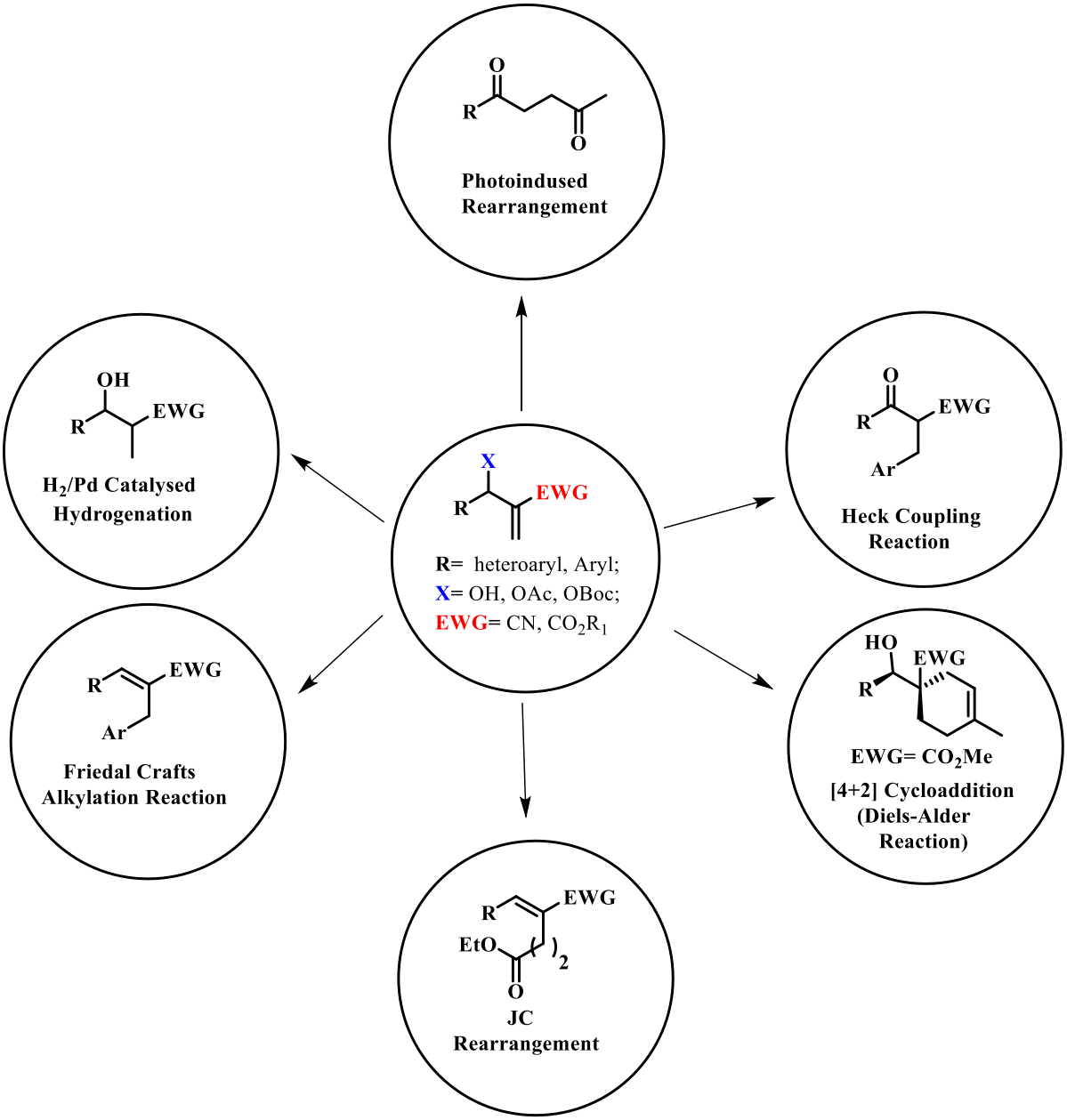
Among the various strategies for the carbon–carbon bond formation, the Morita–Baylis–Hillman (MBH) reaction has emerged as a highly significant and versatile method for the



Scheme 1.1 Representative example of Morita-Baylis-Hillman reaction

efficient construction of C–C and C–X bonds under mild reaction conditions. This classical transformation facilitates the formation of a carbon–carbon (C–C) bond by coupling the α-position of an activated alkene with an aldehyde in the presence of a nucleophilic catalyst, such as a tertiary amine or phosphine (Scheme 1.1). The MBH reaction has gained considerable prominence due to its atom economy, broad substrate scope, and operational simplicity, making it an invaluable tool in modern synthetic organic chemistry.

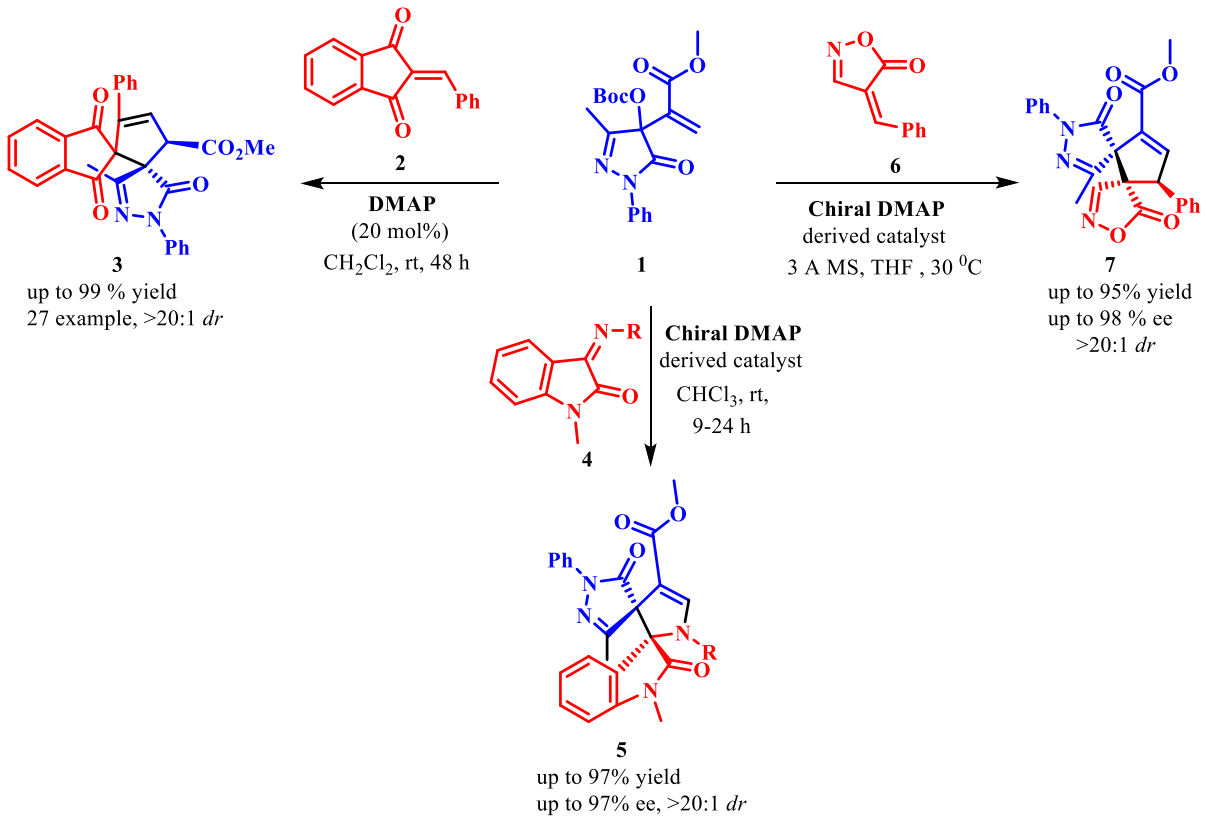
The products of the Morita–Baylis–Hillman (MBH) reaction, commonly referred to as MBH adducts, are usually highly functionalized molecules that feature diverse functional groups,



Scheme 1.2 Some examples of the transformation of Morita-Baylis-Hillman (MBH) adducts

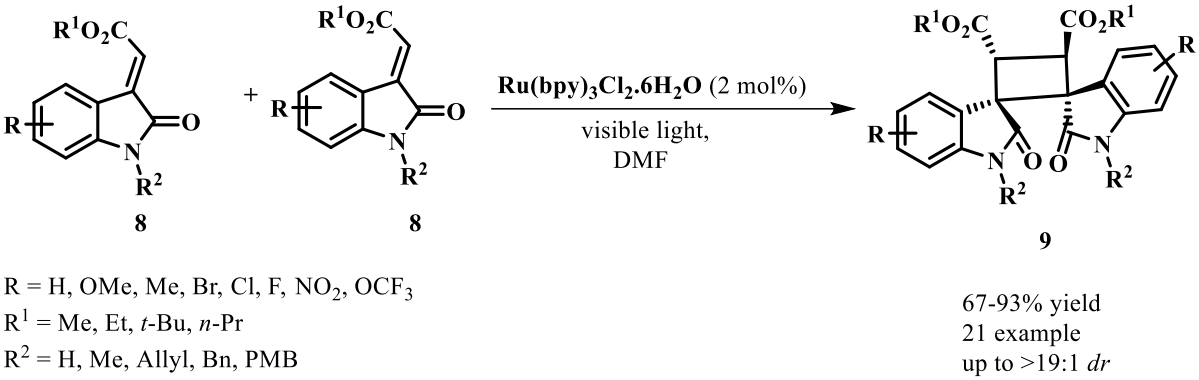
including allylic alcohols, activated alkenes, and electron-withdrawing substituents in the near vicinity. Due to this dense functionalization, MBH adducts serve as versatile synthetic precursors, enabling various useful chemical transformations. They have been extensively utilized in various synthetic methodologies, such as photochemical reactions, Friedel–Crafts reactions, Diels–Alder cycloadditions, Heck coupling, hydrogenation reaction, and Johnson-Claisen rearrangement processes (Scheme 1.2). Their broad applicability highlights their significance in the development of complex molecular Architectures.

In addition to their known transformations, Morita-Baylis-Hillman (MBH) carbonates have been recognized for their diverse annulation reactions, which are instrumental in synthesizing various spirocyclic compounds. Notably, MBH carbonates derived from pyrazolonedione, designated as **1**, have proven to be valuable precursors for generating biologically pertinent spirocyclic scaffolds, including cyclopentadiene pyrazolones **3**, **5**, **7**. This has been achieved through [3+2] annulation reaction with substrates such as 2-arylideneindane-1,3-diones **2**, isatin-derived N-Boc-ketimine **4**, and 4-benzylidene-3-pheny isoxazol-5-one **6**, among others (Scheme 1.3).



Scheme 1.3 Cycloaddition of Morita-Baylis-Hillman (MBH) carbonates of pyrrazolone

In addition to these transformations, visible light driven photocatalysis facilitates various annulation reactions, which play a crucial role in synthesizing structurally diverse spirocyclic compounds. Some of the photocatalyzed reactions enabled the construction of complex molecular frameworks with enhanced functionality and unique architectures. In 2012, Xiao and coworkers disclosed a highly diastereoselective and regioselective [2+2] cycloaddition of 3-methyleneoxindoles **8** via visible-light photocatalysis (Scheme 1.4).



Scheme 1.4 Visible light mediated dimerization of 3-methyleneoxindole in the presence of $Ru(bpy)_3Cl_2.6H_2O$ photocatalyst

Although MBH adduct **1** and 3-methyleneoxindole **8** have been extensively employed in diverse annulation strategies for constructing spirocyclic frameworks, substantial scope remains for further advancements. The strategic utilization of MBH adducts holds promise for accessing structurally intricate and pharmaceutically significant spirocyclic architectures. Moreover, current methodologies involving pyrazoledione-based MBH adducts often fall short in achieving the desired levels of stereoselectivity, necessitating further refinement. In addition, exploring novel and practical synthetic applications of MBH carbonates derived from pyrazolone **1** and 3-methyleneoxindole **8** represents a formidable yet highly rewarding challenge in contemporary organic synthesis.

Chapter 2: *A streamlined Synthesis of Spirooxindole-Pyrazolone Fused Cyclopentenes via Diastereoselective [3+2] Annulation*

This chapter elucidates the development of an innovative, regio- and diastereoselective strategy for the synthesis of spiropyrazolone **10** and spirooxindole **13** through a [3+2]

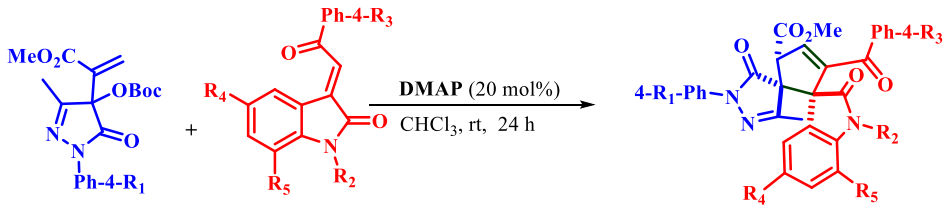
annulation reaction. This transformation employs Morita–Baylis–Hillman (MBH) carbonates derived from pyrazolonedione **1** in conjunction with 3-methyleneoxindoles **8**, as well as MBH carbonates of isatin **11** coupled with arylidenepyrazolones **12** facilitated by tertiary amine catalysis (Scheme 2.1 and Scheme 2.2).

The chapter commences with an overview of the significance of dispiropyrazolone and dispiro oxindole scaffolds, along with a discussion of selected synthetic methodologies reported for their construction. These spirocyclic frameworks represent highly versatile and structurally distinct motifs, garnering considerable interest due to their prominent pharmacological relevance. Consequently, significant research efforts have been dedicated to the regio- and stereoselective synthesis of diverse spiropyrazolone and spirooxindole derivatives. However, existing synthetic protocols often suffer from inherent limitations, such as restricted substrate scope, reliance on transition metal catalysis, the necessity for stoichiometric bases, and elevated reaction temperatures.

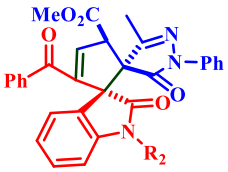
In response to these challenges, a streamlined and efficient synthetic approach has been developed for the construction of dispiropyrazolones **10** and dispirooxindoles **13**. This methodology leverages the [3+2] cycloaddition strategy through Lewis base organocatalysis, offering a metal-free and operationally simple alternative pathway for the generation of these structurally intricate architectures. Upon establishing the optimized reaction conditions, the scope of the [3+2] annulation was systematically explored using various combinations of substituted 3-methyleneoxindoles (**8a**–**8v**) and MBH carbonates (**1a**–**1c**). This investigation led to synthesizing dispiropyrazolone derivatives (**10a**–**10x**), as summarized in Scheme 2.1. All examined substrates smoothly participated in the annulation process, furnishing the desired dispiropyrazolone products (**10a**–**10x**) with adjacent quaternary spirocenters consistently in high to excellent yields (up to 96%, Scheme 2.1). The transformation exhibited remarkable diastereoselectivity (*dr* >20:1), underscoring the efficiency of the developed protocol. Notably, the presence of electron-donating or weakly electron-withdrawing substituents on the 3-methyleneoxindole framework **8** or the MBH carbonates **1** had no significant impact on the reaction outcome. Both the yields and stereoselectivity remained unaffected, highlighting the robustness and broad applicability of the developed synthetic strategy.

In a similar manner, the substrate scope of the [3+2] annulation involving MBH carbonates of isatin **11** and arylidenepyrazolones **12** was systematically evaluated under the optimized reaction conditions (Scheme 2.2). The reaction proceeded efficiently with a range of MBH

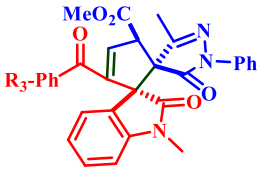
Scheme 2.1 Substrate scope of [3 + 2] annulation to access dispiropyrazolone derivatives[a-c]



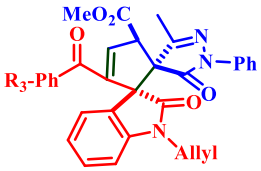
1a-1c **8a-8v** **10a-10x**



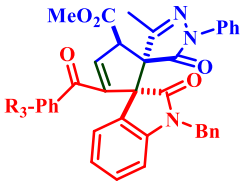
10a, R_2= Me, 92%, *dr* >20:1
10b, R_2= allyl, 98%, *dr* >20:1
10c, R_2= Bn, 76%, *dr* >20:1



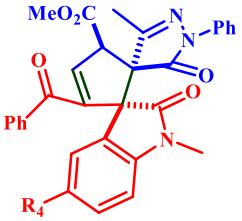
10d, R_3= 4-Me, 86%, *dr* >20:1
10e, R_3= 4-Br, 86%, *dr* >20:1



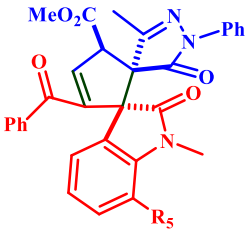
10f, R_3= 4-Me, 96%, *dr* >20:1
10g, R_3= 4-Br, 77%, *dr* >20:1



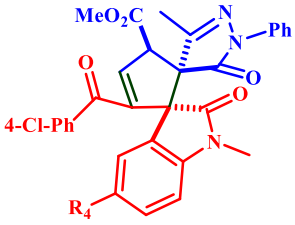
10h, R_3= 4-Cl, 88%, *dr* >20:1
10i, R_3= 4-Br, 73%, *dr* >20:1



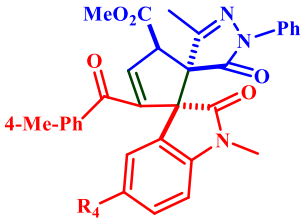
10j, R_4= F, 95%, *dr* >20:1
10k, R_4= Br, 86%, *dr* >20:1
10l, R_4= Cl, 77%, *dr* >20:1



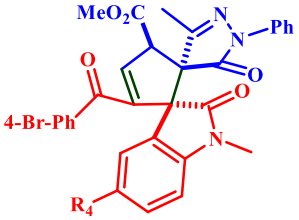
10m, R_5= F, 88%, *dr* >20:1



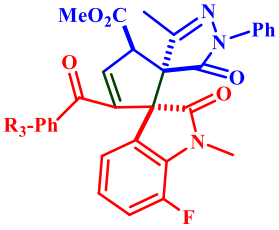
10n, R_4= F, 79%, *dr* >20:1
10o, R_4= Br, 79%, *dr* >20:1
10p, R_4= Cl, 96%, *dr* >20:1



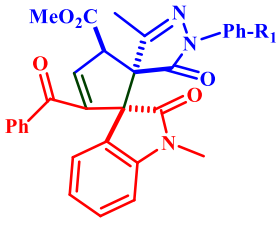
10q, R_4= F, 81%, *dr* >20:1
10r, R_4= Br, 72%, *dr* >20:1
10s, R_4= Cl, 96%, *dr* >20:1



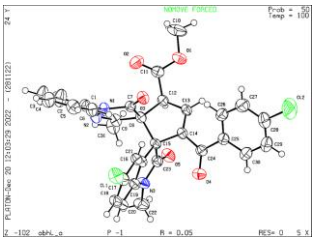
10t, R_4= F, 83%, *dr* >20:1



10u, R_3= 4-Me, 77%, *dr* >20:1
10v, R_3= 4-Cl, 82%, *dr* >20:1



10w, R_1= 4-Cl, 89%, *dr* >20:1
130x, R_1= 4-Me, 90%, *dr* >20:1

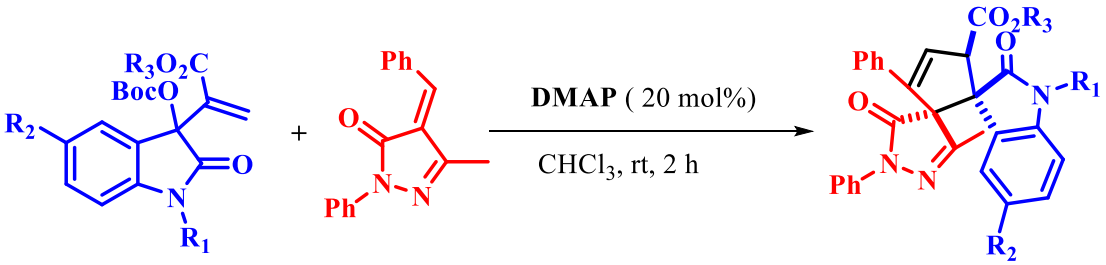


(Molecular Structure of Compound **10p**)
CCDC-2189452

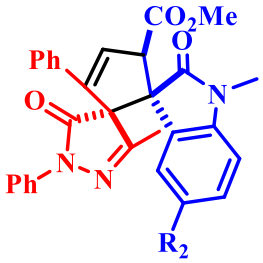
[a]**Reaction Conditions:** Unless stated otherwise, reactions were performed using **1a-1c** [0.094 mmol], **8a-8v** [0.112 mmol], and the DMAP [20 mol%] in 2.0 mL of the specified solvent at the indicated temperature and reaction time. [b]Yields represent isolated products following purification by column chromatography. [c]Diastereomeric ratios were determined via ^{1}H NMR analysis.

carbonates (**11a**–**11e**) derived from isatin and arylidenepyrazolones **12** in the presence of 4-dimethylaminopyridine (DMAP) as a Lewis base catalyst (20 mol%), in chloroform at ambient temperature. This transformation resulted in the formation of the desired spirooxindole derivatives (**13a**–**13e**) in excellent yields (up to 98%) with outstanding diastereoselectivity (up to *dr* >20:1, Scheme 2.2). The reaction conditions proved to be highly efficient and tolerant of various substituents, underscoring the robustness and general applicability of this organocatalytic approach in constructing complex spirocyclic architectures with precise stereocontrol.

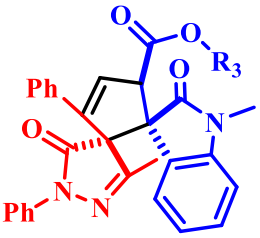
Scheme 2.2 Substrate scope of [3 + 2] annulation to access dispirooxindole derivatives[a-c]



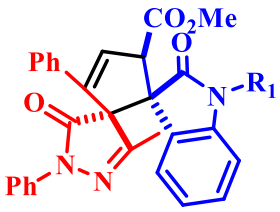
11a-11e **12** **13a-13e**



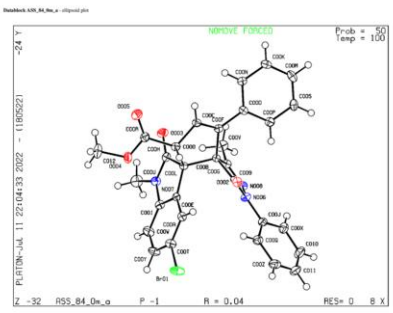
13a, R_2= H, 94%, *dr* >96:4
13b, R_2=Br, 94%, *dr* >97:3
13c, R_2= F, 94%, *dr* >95:5



13d, R_3=^{t}Bu, 91%, *dr* >20:1



13e, R_1=Bn, 98%, *dr* >91:9



(Molecular Structure of Compound **13b**)
CCDC-2183100

[a]**Reaction Conditions:** Unless otherwise specified, reactions were conducted with **11a-11e** (0.115 mmol), **12** (0.138 mmol), and the DMAP (20 mol%) in chloroform at room temperature for 2 h. [b]Yields represent isolated products obtained after purification via column chromatography. [c]Diastereomeric ratios were determined through ^{1}H NMR spectroscopy.

We have successfully established a highly efficient and versatile strategy for synthesizing structurally diverse dispiropyrazolone **10** and dispirooxindole **13** derivatives. This approach is based on [3+2] annulation reaction involving Morita–Baylis–Hillman (MBH) carbonates derived from pyrazolonedione **1** and 3-methyleneoxindoles **8**, as well as MBH carbonates of isatin **11** in combination with arylidenepyrazolones **12**.

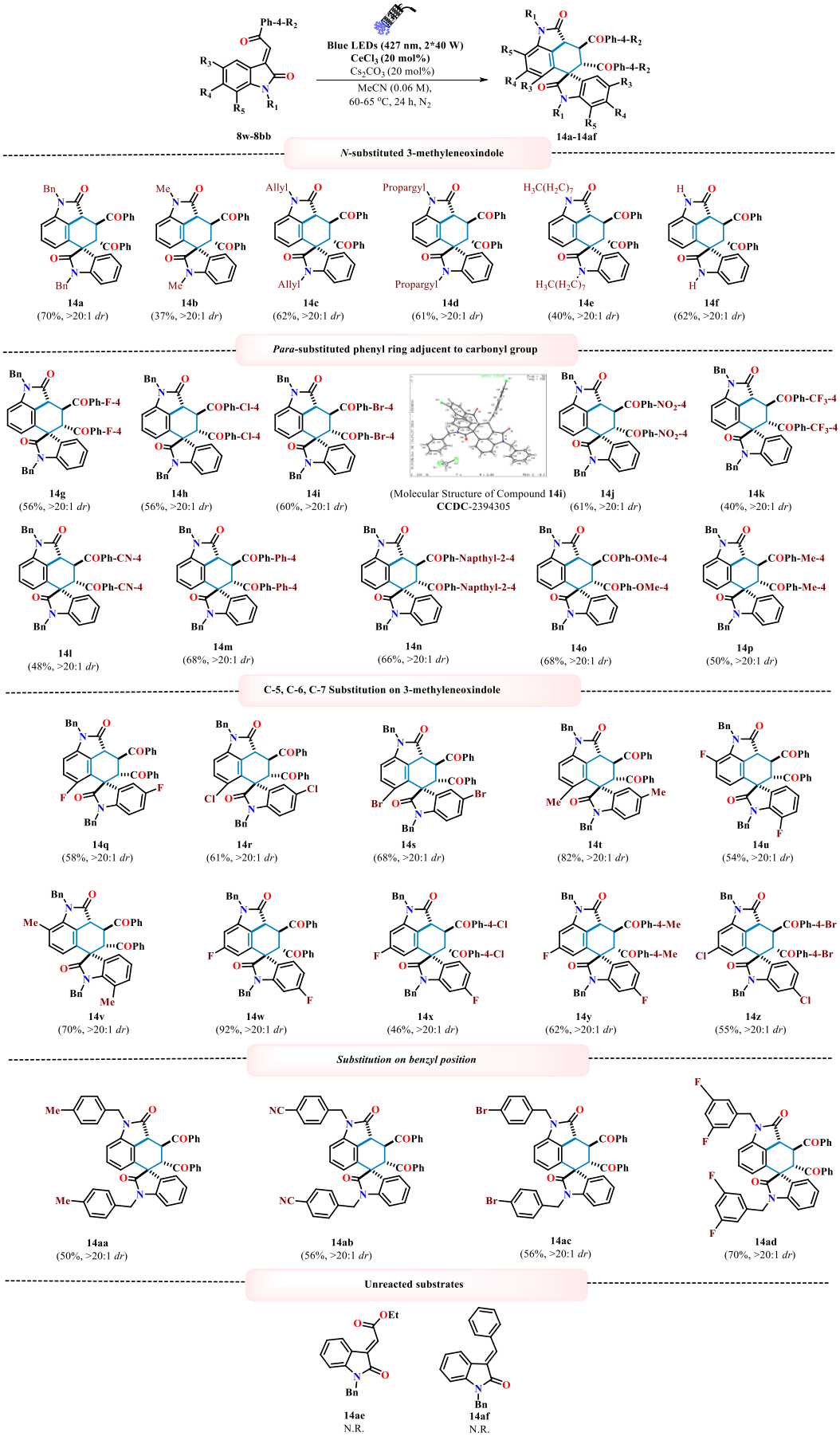
The developed protocol enabled the construction of spiropyrazolone **10** and spirooxindole **13** frameworks in consistently high yields and excellent diastereoselectivity. The efficiency, practicality, and broad applicability of this methodology have been substantiated through the successful synthesis of spiroheterocycles (a total of 29 distinct examples). This highlights the synthetic utility of the protocol for the generation of complex spirocyclic architectures under mild and practical reaction conditions.

Chapter 3: *Visible-Light-Induced Diastereoselective [4+2] Cyclization for Efficient Synthesis of 3,4-Fused Spirooxindoles from 3-Methyleneoxindoles*

This chapter presents an innovative visible-light-driven strategy for the direct functionalization of the unactivated C4 position of 3-methyleneoxindoles **8** for the direct synthesis of 3,4-fused spirooxindoles **14** via a formal [4+2] cycloaddition. This approach circumvents the necessity for the pre-functionalization steps, thus making it an economical and direct synthetic pathway. 3-Methyleneoxindoles **8** undergo an efficient cyclization process in the presence of a catalytic amount of $CeCl_3$ and alkaline conditions under visible-light irradiation, affording the complex 3,4-fused spirooxindole **14** frameworks featuring four contiguous stereocenters. The protocol has demonstrated remarkable chemo- and regioselectivity, affording the target 3,4-fused spirooxindole **14** in moderate to good yields (Scheme 3.1).

The chapter begins by highlighting the significance of 3,4-fused spirooxindole scaffolds, emphasizing their synthetic and pharmacological relevance. A critical discussion on some of the selected synthetic methodologies for the construction of 3,4-fused spirooxindole has been provided along with their structural diversity and synthetic versatility. 3,4-Fused spirooxindole framework has attracted considerable attention due to its potential biological activities, prompting extensive research into regio- and stereo-selective approaches for its synthesis.

Scheme 3.1 Substrate scope of [4+2] annulation: access 3,4-fused spirooxindole derivatives[a-b]



Standard reaction conditions: [a]3-Methyleneoxindole **8w-8bb** (2 mmol, 1 equiv), $CeCl_3$ (20 mol%), Cs_2CO_3 (20 mol%) in MeCN (0.06 M), irradiated with two Kessil Blue LED (427 nm, 100% intensity, 60–65 °C, fan switched off, 2*40 W) under a nitrogen atmosphere. [b]Diastereomeric ratio (>20:1 *dr*) was determined using ^{1}H NMR spectroscopy.

However, many existing synthetic strategies exhibit intrinsic limitations, including the requirement for pre-functionalized substrates, elevated reaction temperatures, and sub-optimal diastereoselectivity, necessitating more efficient and selective methodologies.

To address these challenges, an expedient and efficient synthetic strategy has been developed for the construction of 3,4-fused spirooxindole framework. This approach exploits a [4+2] cycloaddition mechanism under visible-light activation, providing an operationally straightforward and robust alternative for the synthesis of these architecturally complex structures. By harnessing the strength of photocatalysis, this method successfully circumvented the limitations of conventional protocols, facilitating the selective and efficient assembly of 3,4-fused spirooxindole derivatives.

Having obtained the optimum reaction conditions, the substrate scope of the [4+2] annulation was systematically investigated by employing a diverse range of substituted 3-methyleneoxindoles. This comprehensive study enabled the efficient synthesis of a series of 3,4-fused spirooxindole derivatives (**14a**–**14ad**), the details of which are summarized in Scheme 3.1.

All tested substrates underwent annulation smoothly, affording the desired 3,4-fused spirooxindole derivatives (**14a**–**14ad**) in moderate to excellent yields (up to 92%). This transformation demonstrated exceptional diastereoselectivity (>20:1 *dr*), highlighting the efficiency of the developed methodology. Notably, the electronic nature of substituents on the 3-methyleneoxindole framework **8**, particularly electron-donating or electron-deactivating groups, exhibited a discernible influence on the reaction outcome. These findings underscore the robustness and broad applicability of this synthetic strategy.

In conclusion, we have developed an efficient visible-light-driven strategy for the direct C4–H functionalization of 3-methyleneoxindoles, facilitating the synthesis of 3,4-fused spirooxindoles **14** via a formal [4+2] cycloaddition. This methodology utilizes a catalytic amount of $CeCl_3$ under basic conditions, affording the desired spirooxindole derivatives in moderate to good yields with outstanding chemo- and regio-selectivity. Furthermore, the protocol is scalable and effective even under the direct exposure of sunlight. Given its

operational simplicity and broad applicability, this approach represents a valuable tool for constructing architecturally complex molecular frameworks.

Chapter 4: *One-Pot Oxa-Michael-Initiated [4+2] Cycloaddition Cascade Between Pyrazoledione-Based Morita–Baylis–Hillman Alcohols and Arylidene Pyrazolones: A Concise Route to Dispiropyrazolone-Fused Tetrahydropyrans*

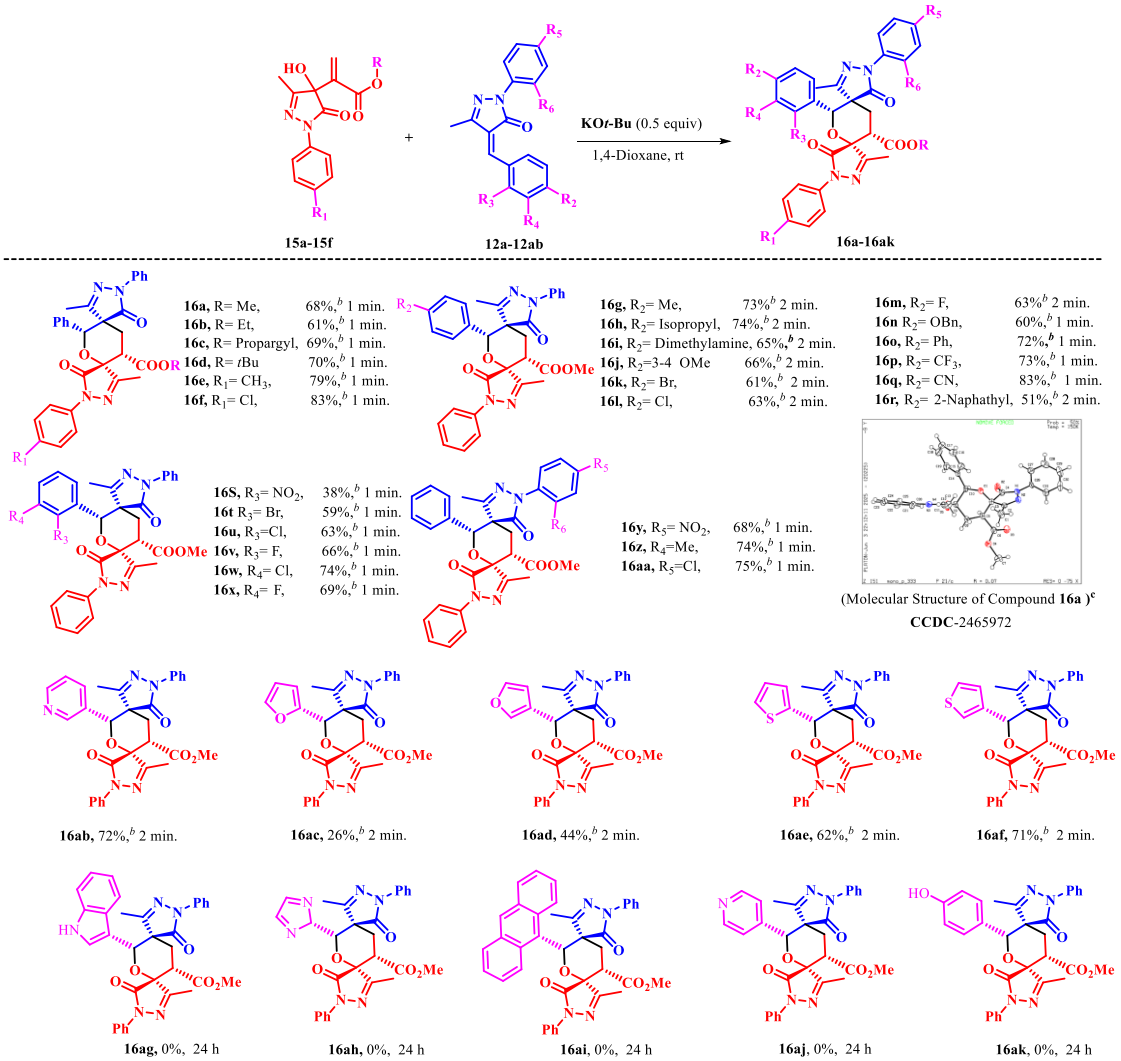
This chapter discloses the development of a novel and regioselective metal-free oxa-Michael strategy for the synthesis of dispiropyrazolone fused tetrahydropyrans compounds via a [4+2] annulation reaction. This transformation leverages oxa-Michael donor: Morita–Baylis–Hillman (MBH) alcohols **15** derived from pyrazolonedione, in combination with arylidenepyrazolone **12** under the catalytic influence of tertiary butoxide anion. The methodology offers an efficient and selective approach for constructing complex molecular architectures without requiring any transition metal catalysts.

The chapter begins with a comprehensive overview of the significance of dispiropyrazolone scaffolds, emphasizing their structural diversity and synthetic versatility. Some of the selected representative synthetic methodologies for the construction of dispiropyrazolone scaffolds have been discussed and highlighting the relevance of the compounds in medicinal chemistry due to their notable pharmacological properties. As a result, extensive research has been devoted to the regio- and stereo-selective synthesis of diverse dispiropyrazolone derivatives. However, existing synthetic approaches often suffer from inherent limitations, including prolonged reaction times, dependence on transition-metal catalysis, low diastereoselective and a restricted substrate scope, necessitating the development of more efficient and broadly applicable methodologies.

To address some of these challenges, a streamlined and highly efficient synthetic strategy has been developed to construct dispiropyrazolones **16**. This approach exploits a [4+2] cycloaddition mechanism under tertiary butoxide catalysis, providing a transition metal-free and operationally straightforward alternative for assembling these architecturally complex frameworks. This methodology enhances sustainability while ensuring high selectivity and efficiency in the synthesis of dispiropyrazolone fused tetrahydropyrans derivatives in very rapid reaction time (within 1-2 min.).

Having established the optimum reaction conditions, the scope of the [4+2] annulation was systematically explored using a diverse array of substituted Morita–Baylis–Hillman (MBH) alcohols **15a-15f** derived from pyrazolonedione, along with various arylidenepyrazolones **12a-12ab**. This protocol facilitated the efficient synthesis of a series of dispiropyrazolone derivatives (**16a**–**16af)** Scheme 4.1.

Scheme 4.1 Substrate scope of [4+2] annulation to access dispiropyrazolone fused tetrahydropyrans [a-c]



[a]**Reaction conditions:** Unless stated otherwise, reactions were performed using Pyro-MBH alcohol **15a-15f** (1 equiv, 0.2 mmol), **12a-12ak** (1 equiv, 0.2 mmol) and KOt-Bu (50 mol%, 0.1 mmol) in 1,4-Dioxane (1.0 mL) at room temperature for 1–2 min.[b] Single diastereomer. [c]Thermal ellipsoids at the 50% probability level.

All evaluated substrates participated smoothly in the annulation process, affording the desired dispiropyrazolone derivatives (**16a**–**16af**) in modest to very good yields (up to 83%). This efficient transformation has demonstrated the high selectivity in constructing the complex

scaffold in very rapid reaction time. Notably, the electronic properties of substituents on the arylidenepyrazolones **12**, particularly electron-donating, electron-activating and electron-withdrawing groups, significantly influenced the reaction outcome. Additionally, variations in the substituents on the Morita–Baylis–Hillman (MBH) alcohol **15** derived from pyrazolonedione also had a noticeable impact on the efficiency and selectivity of the transformation (Scheme 4.1). These findings highlight the broad applicability and versatility of this synthetic approach.

In conclusion, a rapid and transition metal-free oxa-Michael cascade [4+2] annulation strategy has been developed for the efficient construction of structurally complex dispiropyrazolone-fused tetrahydropyran frameworks. This method leverages pyrazolonedione-derived Morita–Baylis–Hillman (Pyro-MBH) alcohols as novel oxa-Michael donors, demonstrating exceptional atom economy. Notably, this is the first report where unprotected Pyro-MBH alcohols have been directly utilized for the synthesis of pyrazolone-based spirocyclic compounds. The reaction proceeds within a remarkably short time frame, forming two tertiary and two quaternary stereocenters with excellent diastereoselectivity. Additionally, the protocol is operationally simple, scalable to gram quantities, and compatible with post-synthetic functionalization via Suzuki coupling. Importantly, the methodology avoids the use of costly reagents or catalysts, offering a highly efficient and sustainable route to complex spiroheterocyclic architectures.

Chapter 5: *Efficient Synthesis of Spiropyrazolone Pyrrolidinediones Fused Tetrahydropyran via Base-Induced [4+2] Cycloaddition*

In this chapter, presents the design and development of a novel, transition metal-free oxa-Michael cascade [4+2] annulation strategy aimed at the efficient construction of spiropyrazolone pyrrolidinediones fused tetrahydropyran framework. This expedient and facile synthetic approach is notable for its atom-economical nature, providing a sustainable and environmentally friendly alternative to the traditional transition metal-catalyzed reactions. The methodology capitalizes on the unique reactivity of pyrazolonedione-derived Morita–Baylis–Hillman (Pyro-MBH) alcohols **15**, which have been specifically adapted to function as potent oxa-Michael donors.

The reaction system is carefully planned to achieve high levels of chemo- and regio-selectivity,

ensuring that the cascade process proceeds smoothly without the need for external additives. Pyro-MBH alcohols **15**, owing to their activated hydroxyl groups adjacent to electron-deficient pyrazolone moiety, demonstrate exceptional nucleophilicity, making them ideally suited for participation in the oxa-Michael addition. Their engagement with suitably designed arylidene-substituted pyrrolidinediones **17** resulted in an elegant sequence of bond-forming events, culminating in the rapid and efficient assembly of highly functionalized, structurally complex spiropyrazolone pyrrolidinediones fused tetrahydropyran hybrids **18**.

The chapter gives a brief overview on the importance as well as exploration of spiropyrazolone and spiropyrrolidinediones frameworks, underlining their remarkable structural diversity and synthetic adaptability. It presents a critical analysis of key synthetic strategies previously reported for the construction of these scaffolds, with particular emphasis on their prominent role in medicinal chemistry owing to their diverse pharmacological activities. As a result of their significant bioactivity, substantial efforts have been dedicated for the development of regio- and stereoselective methods towards the synthesis of various spiropyrazolones and spiropyrrolidinediones.

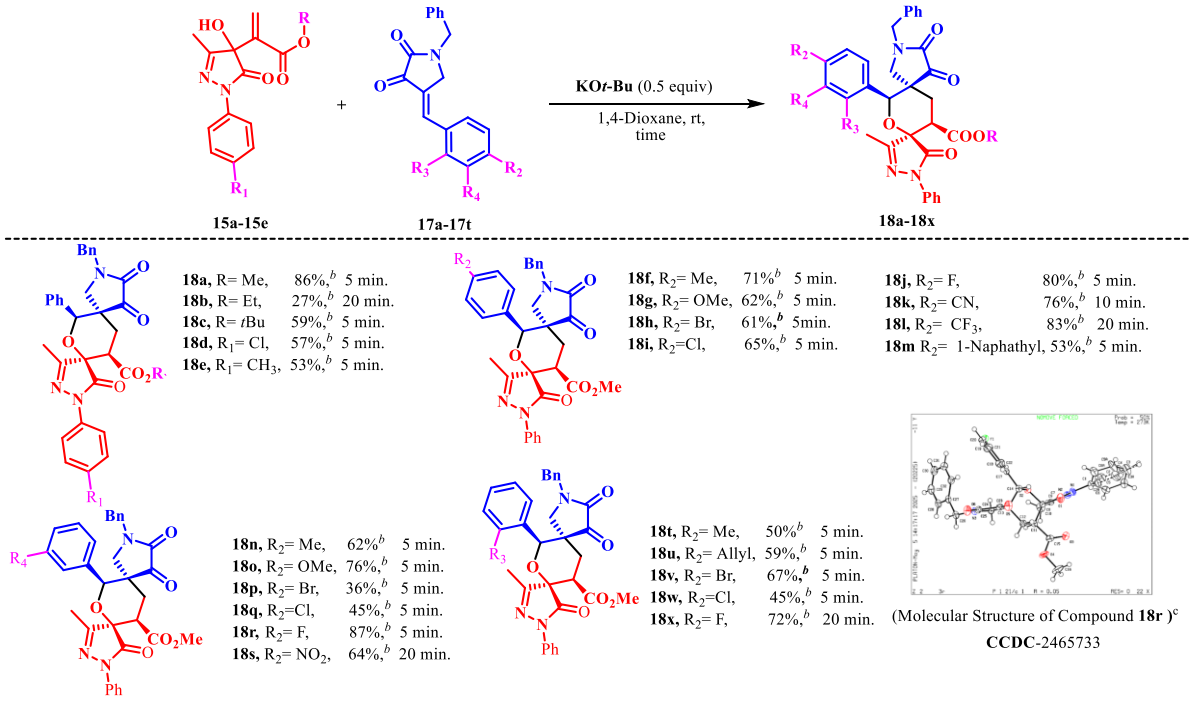
Nevertheless, many of the existing synthetic routes are hindered by certain inherent drawbacks, such as extended reaction durations, reliance on transition metal catalysis, and a limited range of applicable substrates. These limitations have underscored the need for more practical, efficient, and broadly applicable synthetic methodologies.

In this regard, we designed and developed an expedient synthetic strategy for the construction of spiropyrazolone pyrrolidinediones fused tetrahydropyran **18**. This newly developed approach harnesses a [4+2] cycloaddition pathway, promoted by sub-catalytic amount of tertiary butoxide there by offering a transition metal-free and operationally simple alternative strategy for building the structurally intricate molecules. The method proved to be high stereoselective and efficient for the synthesis of spiropyrazolone pyrrolidinediones fused tetrahydropyran **18**.

Having obtained the optimum reaction conditions, the substrate scope of the [4+2] annulation reaction was thoroughly investigated by employing a wide range of substituted Morita–Baylis–Hillman (MBH) alcohols **15a-15e** derived from pyrazolonedione, in combination with various arylidene pyrrolidinediones derivatives **17a-17t**. The protocol enabled the efficient synthesis of a series of spiropyrazolone pyrrolidinediones fused tetrahydropyran products (**18a**–**18x**) in moderate to very good yields (up to 87%, Scheme 5.1). The transformation exhibited excellent

selectivity and efficiency, underscoring the reliability and robustness of the developed synthetic protocol to access the desired spirocyclic compounds in very short reaction time (5-20 min.). Importantly, we observed that the electronic nature of the substituents on the arylidene-pyrrolidinediones scaffolds **17** has a pronounced effect on the reaction outcomes. Substrates bearing electron-donating or mildly electron-withdrawing groups on the aryl moiety significantly influenced the reaction efficiency and product yields. Furthermore, modifications to the substituents on the pyrazolonedione-derived MBH alcohols **15** also impacted the overall reaction performance, affecting both yield and selectivity.

Scheme 5.1 Substrate scope of [4+2] annulation to access dispiropyrazolone derivatives[a-c]



[a]**Reaction Conditions:** Unless stated otherwise, reactions were performed using **18a-18e** (0.2 mmol), **20a-20t** (0.2 mmol) and the KOt-Bu [50 mol%] in 1.0 mL of the 1,4-Dioxane at the room temperature for 5-20 min. [b] Single diastereomer. [c]Thermal ellipsoids at the 50% probability level.

We observed that the protocol demonstrated a broad functional group tolerance and wide applicability of the methodology, establishing it as a powerful and versatile strategy for the synthesis of complex spiropyrazolone pyrrolidinediones fused tetrahydropyran architecture.

In summary, we have developed a facile transition metal-free oxa-Michael cascade [4+2] annulation to access structurally complex spiropyrazolone pyrrolidinediones fused tetrahydropyran framework in a regioselective and efficient manner. The strategy employed pyrazolonedione-derived Morita–Baylis–Hillman alcohols as oxa-Michael donors to access

spiropyrazolone pyrrolidinediones fused tetrahydropyran with two tertiary and two quaternary stereocenters in remarkably short reaction time (5–20 min.) in atom economic manner. It is also important to highlight that we explored the pyrazolonedione-derived Morita–Baylis–Hillman alcohols without any protection of alcohol moiety.

*****

Please note that the numbering of substrates and products in the synopsis may differ from those used in the main thesis. Compound numbers have been assigned independently within each chapter for clarity and convenience, and as a result, some compound numbers may vary between chapters.

List of Research Publications

(Based on the research work included the thesis)

1. **Sabale, A. S**.; Warghude, P. K.; Bhat, R. G. *Synlett* **2023**, *34*, 1732-1738.
2. **Sabale, A. S**.; Bhowmick, A.; Pattanaik, S.; Bankar, O. S.; Bhat, R. G. *Asian J. Org. Chem.* **2025**, *11*, https://doi.org/10.1002/ajoc.202500424.
3. **Sabale, A. S**.; Khandeparkar, M.; Bhat. R. G. One-Pot Oxa-Michael-Initiated [4+2] Cycloaddition Cascade Between Pyrazoledione-Based Morita–Baylis–Hillman Alcohols and Arylidene Pyrazolones: A Concise Route to Dispiropyrazolone-Fused Tetrahydropyrans, *Manuscript is ready to be communicated.*
4. **Sabale, A. S**.; Khandeparkar, M.; Pattanaik, S.; Bhat. R. G. Efficient Synthesis of Spiropyrazolone pyrrolidinediones Fused Tetrahydropyran via Base-Induced [4+2] Cycloaddition, *Manuscript under preparation.*

(Publications as a co-author)

1. Warghude, P. K.; **Sabale, A. S**.; Bhat, R. G. *Org. Biomol. Chem.* **2020**, *18*, 1794-1799.
2. Warghude, P. K.; **Sabale, A. S**.; Dixit, R.; Vanka, K.; Bhat, R. G. *Org. Biomol. Chem.* **2021**, *19*, 4338.
3. Bankar, O. S.; Pal, C.; Laha, D.; **Sabale, A. S**.; Bhat, R. G. *Organic Lett.* **2024**, DOI: 10.1021/acs.orglett.4c03117.
4. Bankar, O. S.; Pal, C.; Bhavya; **Sabale, A. S**.; Bhat, R. G. *DOI:10.26434/chemrxiv-2025-f6k87*.

Book Chapter

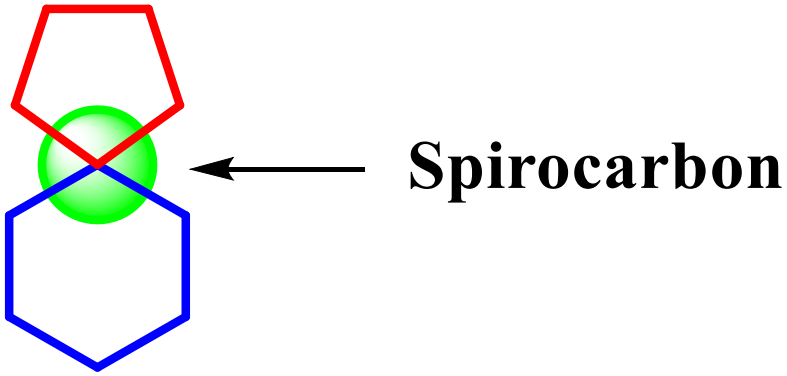
1. Warghude, P. K.; **Sabale, A. S.**; Bhat, R. G. Synthesis of hybrid spirooxindoles

Elsevier, **2024**, 309-331. DOI: 10.1016/B978-0-443-22324-2.00012-6

1 Organocatalysis, Photocatalysis, and Base-Catalyzed Synthesis of Spirocycles via Morita-Baylis-Hillman Adducts and 3-Methyleneoxindole

Abstract

This chapter highlights the importance of spirocyclic compounds and gives a brief overview of the selected synthesis of spirocyclic compounds using Morita-Baylis-Hillman (MBH) adducts and 3-methyleneoxindoles through organocatalysis, photocatalysis, and base-catalyzed strategies. Spirohetreocycles are characterized by their unique three-dimensional architectures, and they are known to exhibit significant pharmaceutical and biological activities. The MBH reaction is a powerful carbon-carbon bond-forming strategy that serves as a key platform for accessing diverse spiroheterocyclic frameworks. Recent advancements have enabled the development of highly regio- and stereo-selective catalytic approaches, overcoming limitations of traditional methods. Some of the mechanistic insights, synthetic versatility, and practical applications of these catalytic transformations have also been highlighted. Some of these transformations inspired and made the foundation for the subsequent novel research methods that are described in the later part of this thesis.



1 Organocatalysis, Photocatalysis, and Base-Catalyzed Synthesis of Spirocycles via Morita-Baylis-Hillman Adducts and 3-Methyleneoxindole

1.1 Introduction

Among many natural compounds, spiroheterocyclic scaffold compounds are quite unique due to their unique structural framework. Spiroheterocyclic compounds are formed by two cyclic structures intersecting at a single shared carbon atom, known as the spiroatom. Many spirohetreocycles are known for their bioactivity, and the spiro scaffold has been increasingly included as a structural component in many drug candidates and several classes of chiral ligands that are employed in asymmetric synthesis. Recent advancements in organic synthetic strategies have led to a marked increase in the exploration of spirocyclic structures in drug discovery. These compounds, with their unique three-dimensional frameworks, are now recognized for their potential to enhance molecular diversity and improve pharmacological properties, making them increasingly attractive targets in medicinal chemistry.[1] Due to our continued interest in the synthesis of interesting and useful spirocyclic compounds, we became more interested in reviewing the literature on spirocyclic compounds. There are different types of biologically important spirocyclic compounds present in bioactive compounds and drug molecules in the literature. We became particularly interested in spiropyrazolone and spirooxindole motifs, as many of the drugs, natural products, and pharmaceuticals contain either spiropyrazolone or spirooxindole spirocyclic scaffolds.

In spirooxindoles, 2-oxindole derivatives fused with another cyclic system at the C-3 position have gained significant interest among synthetic and medicinal chemists worldwide. Some of the spirooxindole-containing natural products and bioactive compounds include horsfiline, spindomycin B, gelsemine, alstonisine, NNRTIs HIV-1 inhibitor, cipagamin, SPX-F (Figure 1.1).

Additionally, several synthetic molecules, such as CFI-400945 and SAR-405838, have been developed based on this scaffold, with some showing promising anticancer properties (Figure 1.1). Compounds having a spirooxindole scaffold have demonstrated a range of biological activities, including anticancer and antiparasitic effects, and some of the compounds are progressing to phase I clinical trials due to their potent anticancer potential as well.[2]

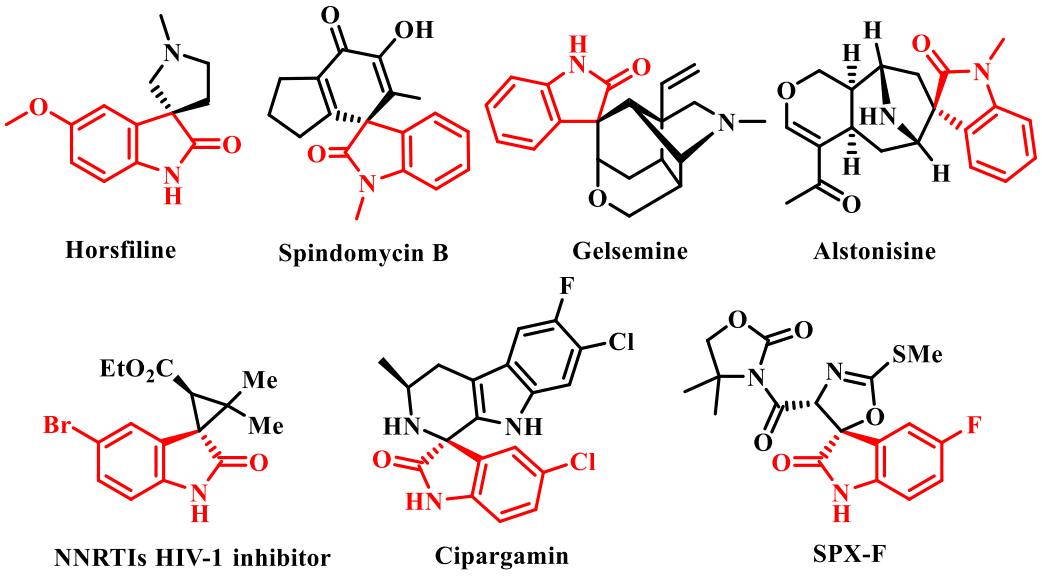


Figure 1.1 Representative natural products and bioactive compounds having spirooxindole motif

Spiropyrazolones, a distinctive subclass of pyrazolone derivatives characterized by the fusion of an additional cyclic moiety at the C-4 position. Over the years, spiropyrazolones have gained substantial interest from the community of synthetic and medicinal chemists from across the globe. The structural complexity and unique pharmacological profiles of these compounds render them valuable in various therapeutic contexts. Notably, spiropyrazolones exhibit a

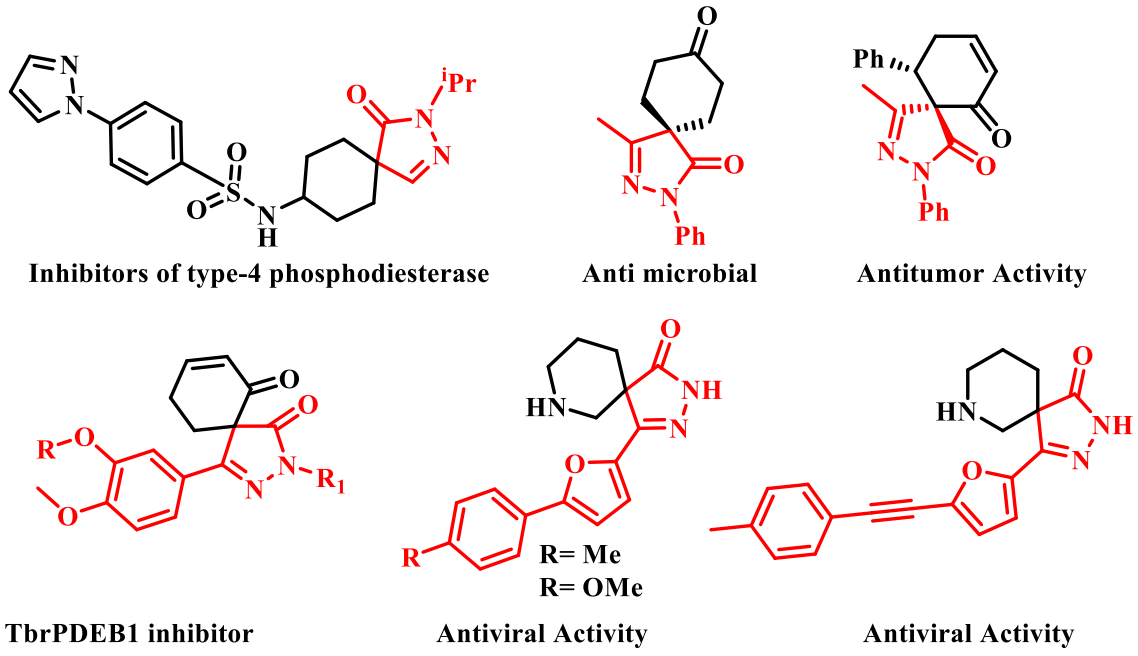


Figure 1.2 Representative bioactive compounds with spiropyrazolone motif

spectrum of biological activities, functioning as inhibitors of type-4 phosphodiesterase and also demonstrating significant antimicrobial and antitumor properties. Furthermore, they have been identified as inhibitors of TbrPDEB1 and possess noteworthy antiviral activity, underscoring their potential as multifaceted agents in drug development and biomedical research (Figure 1.2).[3]

The importance of spiropyrazolone and spirooxindole scaffolds from a biological perspective is really significant, as various strategies have been disclosed in the literature. Undoubtedly, these unique molecular structures have attracted considerable attention due to their diverse pharmacological activities and potential therapeutic applications.[4] Various synthetic strategies, such as alkylation, metal-catalysis, ring-closure, cycloadditions, radical, and rearrangement pathways, have been explored to synthesize different compounds with spiropyrazolone and spirooxindole scaffolds. Some of the relevant topics, such as organocatalysis, building blocks such as Morita-Baylis-Hillman (MBH) adduct and their utility, and some selected synthesis of spiropyrazolone and spirooxindole scaffolds using cycloaddition strategies have been discussed.

1.2 Synthesis of spiroheterocyclic scaffolds via organocatalysis

Organocatalysis, within the realm of organic chemistry, leverages organic molecules to accelerate chemical reactions to construct complex molecular architecture. Unlike the metal catalysts, organocatalysts are derived from chiral pools of natural or nature-inspired compounds and are primarily composed of elements like carbon, hydrogen, and sulfur, along with other nonmetallic elements commonly found in organic compounds. They function by interacting with reactants to lower the energy barrier of the reaction, thereby increasing its rate. Organocatalysis offers advantages such as environmental friendliness due to the absence of heavy metals, readily available and often inexpensive starting materials, and the potential for high selectivity and control over reaction outcomes.[5] Over the years, organocatalysis has grown rapidly by expanding the field of chemical synthesis. Organocatalysis is broadly classified into two primary categories based on the nature of the interaction established between the substrate and the organocatalyst. This classification hinges on the fundamental bonding principles and the resulting impact on the overall catalytic mechanism.[6]

1.2.1 Covalent organocatalysis: This branch is characterized by forming a transient, covalent bond between the organocatalyst and the substrate. This interaction leads to the generation of a reactive intermediate, often resulting in a change in the electronic structure and reactivity of

the substrate. Upon completion of the catalytic cycle, the organocatalyst is regenerated, facilitating the transformation of the substrate.

1.2.2 Non-covalent organocatalysis: In contrast, non-covalent organocatalysis relies on weaker, non-covalent interactions to mediate the catalytic process. A prominent example is the utilization of hydrogen bonding. Through specific functional groups, the organocatalyst establishes hydrogen bonds with the substrate, leading to substrate preorganization, activation, or stabilization of transition states. Though weaker than covalent bonds, these interactions can still significantly influence the reaction pathway and enhance the rate of the reaction and stereoselectivity. Some of the examples of covalent and noncovalent organocatalysts have been highlighted in Figure 1. 3.

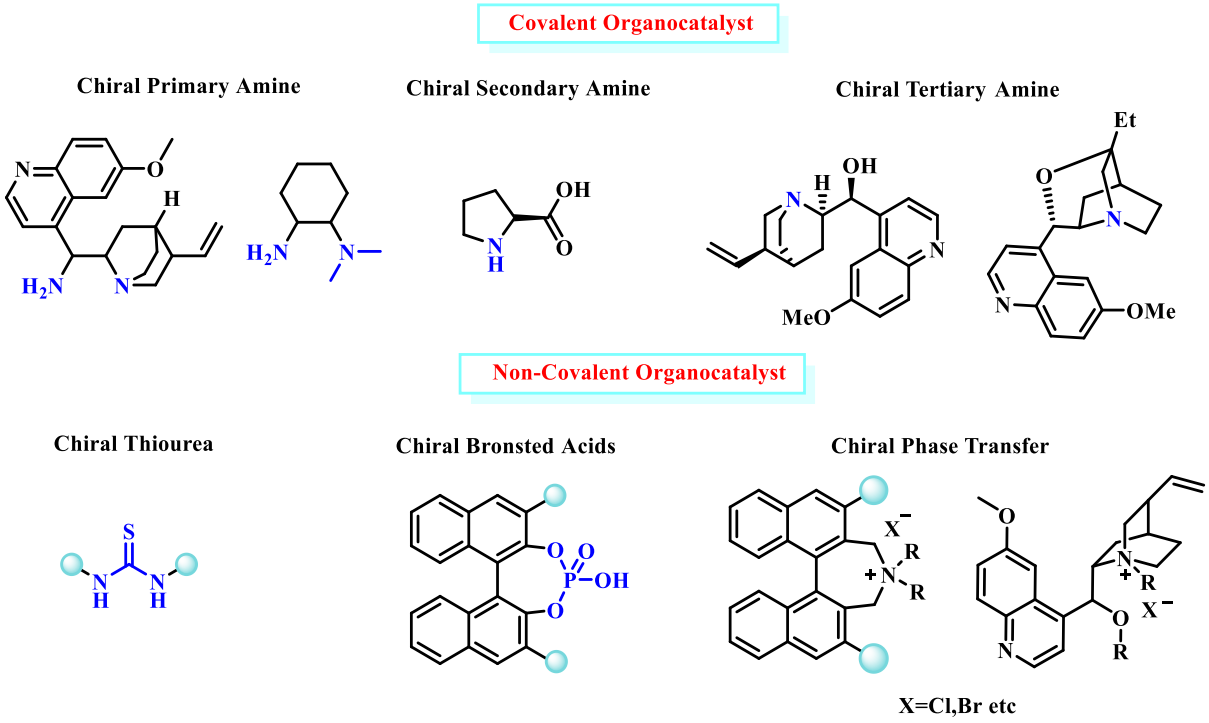
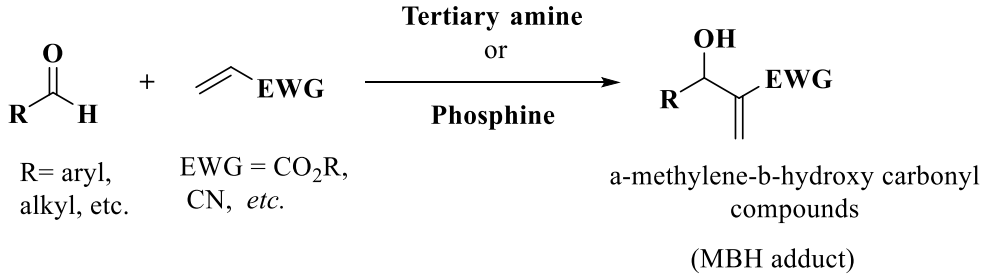


Figure 1.3 Representative examples of covalent and non-covalent organocatalysts

These covalent and noncovalent organocatalysis used for different organic transformations such as Aldol Reaction, Mannich Reaction, Michael Addition, Diels–Alder reaction, Friedel–Crafts reaction, Morita-Baylis-Hillman Reaction, Reduction, Henry reaction etc. As the thesis work is mainly focused on the Morita-Baylis-Hillman (MBH) adduct, some of the selected MBH reactions have been presented.

1.3 The Morita-Baylis-Hillman (MBH) reaction

The Morita-Baylis-Hillman (MBH) reaction is a powerful carbon-carbon bond-forming reaction. It facilitated the formation of α-methylene-β-hydroxy carbonyl compounds. This reaction involves the coupling of an activated alkene (at the α-position) with an aldehyde, catalyzed either by a phosphine (Morita, 1968)[7] or by using a tertiary amine (Baylis and Hillman, 1972)[8] (Scheme 1.1). Furthermore, the MBH reaction can be extended using activated imines instead of aldehydes as well. This variation results in the formation of α-methylene-β-amino carbonyl compounds and is termed the aza-Morita-Baylis-Hillman (aza-MBH) reaction.



Scheme 1.1 Representative example of Morita-Baylis-Hillman reaction

While the MBH reaction holds considerable promise now, initially this was not explored to the fullest, and the lack of widespread adoption within the synthetic organic chemistry community limited its full synthetic potential. Since, 1980s MBH reaction and its diverse applications have gained a lot of importance with substantial attention to utilizing the MBH adducts in organic synthesis.

The MBH (Morita-Baylis-Hillman) reaction is a versatile chemical transformation, widely utilized for the synthesis of various valuable compounds and synthetic intermediates. Its popularity stems from several key advantages and its broad applicability across diverse chemical applications. Here are some of the notable merits of the MBH reaction:

- **Atom Economy:** The MBH reaction is generally considered atom-economical, as most (if not all) of the atoms of the starting materials are usually incorporated into the final product. This greatly minimizes waste and increases atom efficiency.
- **Formation of Multiple Bonds:** The reaction elegantly constructs carbon-carbon double bonds (alkenes) and often introduces functionalized groups. This is crucial for building complex molecular architectures.
- **Functional Group Tolerance:** The MBH reaction displays good functional group tolerance under various reaction conditions. It can often be utilized in the presence of a variety of other reactive groups without being significantly affected. Thus, it greatly offers flexibility in synthetic planning.

- **Mild Reaction Conditions:** Usually, the reactions can often be performed under relatively mild conditions (e.g., moderate temperatures, use of catalysts). This is really advantageous for sensitive compounds, and it greatly reduces the likelihood of side reactions.
- **Stereoselectivity:** The MBH reactions can lead to selective formation of specific stereoisomers depending on the substrates, and this is vital as well as useful while designing and the synthesis of chiral molecules or molecules with desired three-dimensional shapes.
- **Ease of Execution:** The reaction setup and execution are typically straightforward, making it a relatively easy and accessible process for both experienced chemists as well as for those relatively new to synthetic methodologies.

- **Wide Substrate Scope:** The MBH reaction exhibits a broader substrate scope and allows for the scope for the use of various aldehydes, activated alkenes (e.g., acrylates, vinyl ketones), and catalysts, expanding its utility in different contexts.

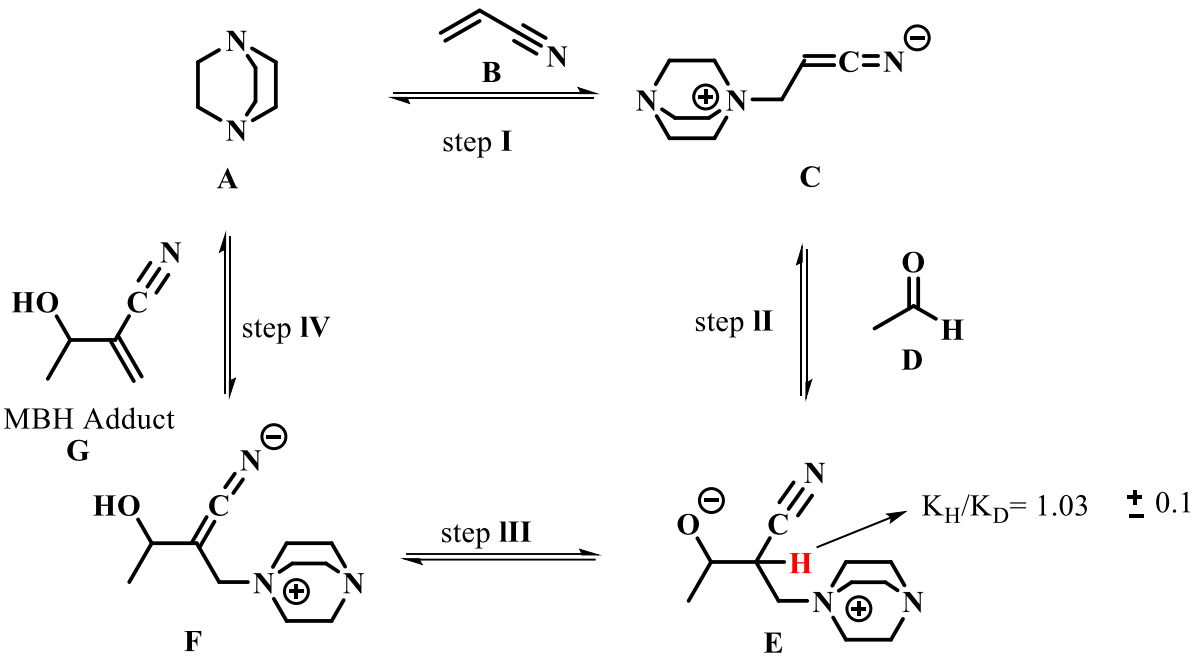
1.4 MBH reaction mechanism

In 1983, Hoffmann[9] proposed the initial reaction mechanism for the Morita-Baylis-Hillman (MBH) reaction. Later, Hill and Isaacs[10] and other research groups refined the understanding of this mechanism. The general mechanism usually involves several key steps and has been depicted in Scheme 1.2.

A tertiary amine catalyst (**A**), such as DABCO, reacts with an activated alkene (**B**), an α,β-unsaturated carbonyl compound like acrolein, methyl acrylate, or methyl vinyl ketone via a 1,4-conjugate addition (Michael addition) to form a zwitterionic aza-enolate intermediate (**C**). This intermediate (**C**) then undergoes an aldol-type reaction with an aldehyde (**D**), such as acetaldehyde or benzaldehyde, to generate another intermediate (**E**). This subsequently undergoes an intramolecular proton shift, leading to the formation of intermediate (**F**). This finally affords MBH adduct (**G**) via either an E2 or E1cb elimination reaction, along with the subsequent release of the catalyst (**A**) to complete the catalytic cycle.

Hill and Isaacs[10] investigated the reaction mechanism using kinetic isotope effect (KIE) measurements involving acrolein, acetaldehyde, and DABCO. The KIE was found to be 1.03 ± 0.1. However, when α-deuterated acrylonitrile was used, no significant KIE was observed. Based on these results, it was concluded that the aldol addition step, which involves the formation of a carbon-carbon bond, is the rate-determining step (RDS). This conclusion is

supported by the fact that the RDS involves all three reactants (**A**, **B**, and **D**, as described in Scheme 1.2).

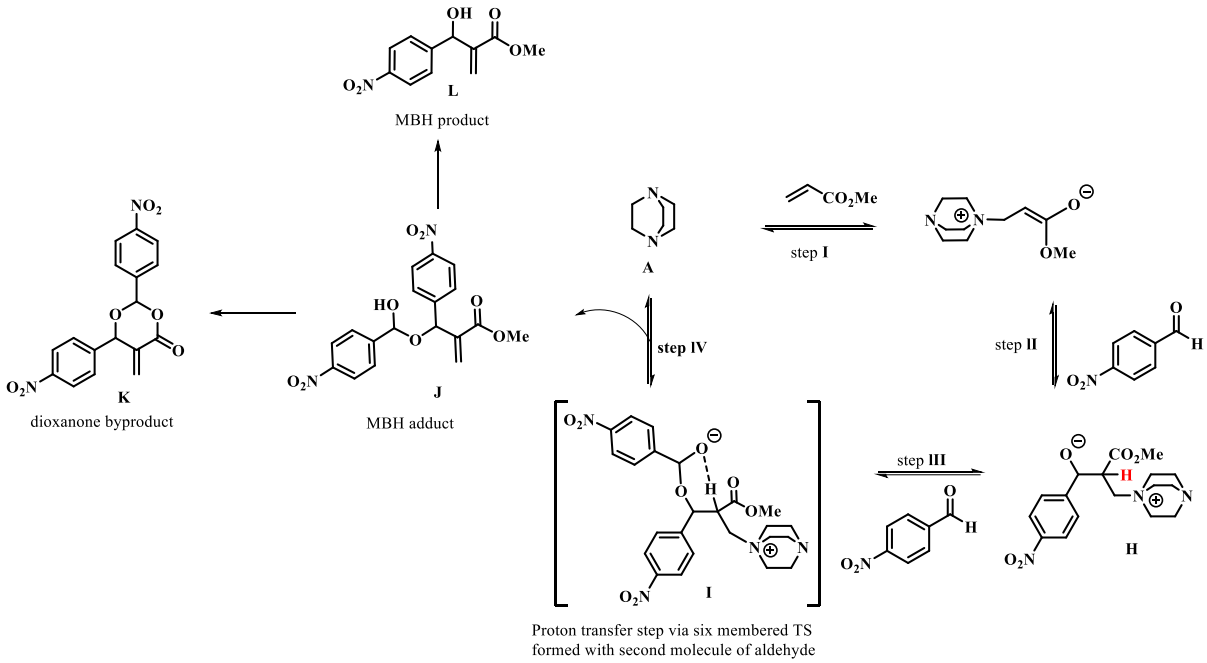


Scheme 1.2 Hoffman/Hill and Isaacs proposed a plausible mechanism for the MBH reaction

However, the mechanism that was originally suggested by Hoffmann, Hill, and Isaacs raised several queries and doubts. Some of these queries were not adequately clarified on certain aspects as follows:

1. It did not satisfactorily account for the autocatalytic effect, where the accumulation of the product leads to an increase in the reaction rate.
2. The mechanism also could not explain the significant formation of an unusual dioxanone by-product when the reaction was conducted with aryl aldehydes and acrylates.

In order to deepen the understanding of the MBH reaction mechanism, the research groups of McQuade and co-workers[11] and Aggarwal and co-workers[12] have systematically re-examined the MBH reaction mechanism. Their studies concentrated on both the kinetic and theoretical aspects, particularly emphasizing the role of the proton transfer step. McQuade and co-workers discovered that the MBH reaction follows first-order kinetics with respect to both DABCO and methyl acrylate, while it is second-order with respect to aldehyde (*p*-nitrobenzaldehyde). They also measured a pronounced kinetic isotope effect (k-H/k-D) of 5.2 ± 0.6 in DMSO, which,

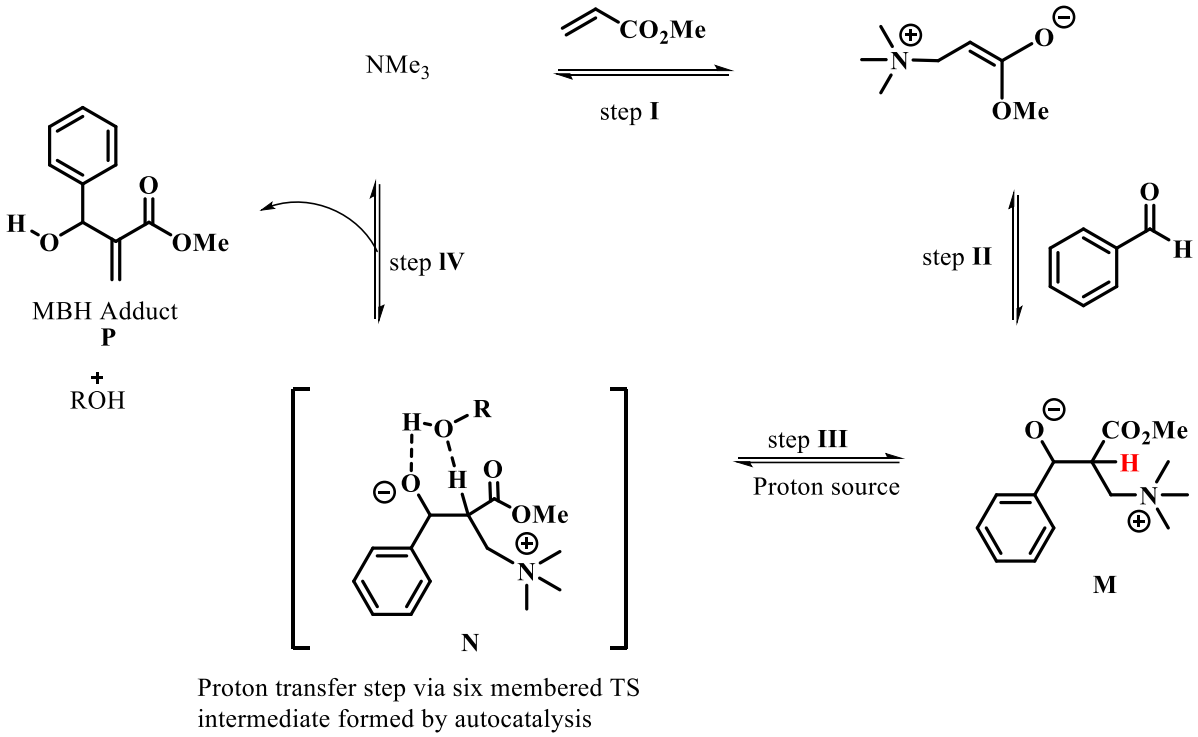


Scheme 1.3 McQuade and co-workers proposed a plausible mechanism for the MBH reaction

together with values consistently above 2 in solvents such as Chloroform, acetonitrile, and tetrahydrofuran strongly suggest that proton abstraction is involved in the rate-determining step. Based on these kinetic findings, McQuade proposed a revised mechanism in which the initial steps (I and II, Scheme 1.3) are essentially the same as those outlined earlier by Hill and Isaacs (see Scheme 1.2). After the initial aldol reaction (step II), a second aldehyde molecule is incorporated, forming a hemiacetal alkoxide intermediate (**I**) as depicted in Scheme 1.3. This intermediate then undergoes a proton transfer through a six-membered transition state-which is identified as the rate-determining step to furnish MBH adduct **J**. Ultimately, this adduct **J** converts either into the final MBH product **L** or rearranges to form the dioxanone by-product **K** (Scheme 1.3).

Aggarwal and co-workers proposed that proton transfer is the rate-determining step (RDS) initially, occurring when less than 20% of the reaction has progressed (Scheme 1.4). As the reaction proceeds and the concentration of product increases, however, step II becomes the RDS. This elevation in product concentration improves the efficiency of the proton transfer process. They further suggested that the MBH adduct **P** could serve as a proton donor, thereby facilitating the proton-transfer step through a six-membered intermediate **N** as illustrated in Scheme 1.4.

Based on recent mechanistic studies, it has been concluded that the rate-determining (RDS) step involves the 1,3-proton shift.



Scheme 1.4 Plausible mechanism for the MBH reaction by Aggarwal and coworkers

1.5 Morita-Baylis-Hillman (MBH) adducts

The utilization of Morita-Baylis-Hillman (MBH) adducts in organic synthesis has seen a substantial increase over recent decades, owing to their versatile structural features and diverse functionalities. These adducts are characterized by multifaceted functional groups, including allylic alcohols and amines, which contribute significantly to their reactivity and utility in

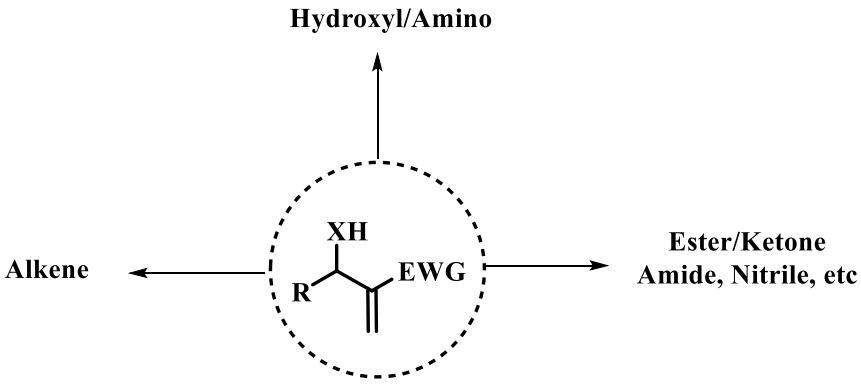


Figure 1.4 Densely functionalized MBH adducts: versatile intermediates in organic synthesis

various synthetic pathways. Additionally, MBH adducts incorporate activated alkenes that serve as Michael acceptors, facilitating conjugate addition reactions. Incorporating electron-withdrawing groups (EWGs) further enhances their reactivity and compatibility with numerous synthetic methodologies (as depicted in Figure 1.4). The rich functionalization endows MBH

adducts with the capability to participate in a wide array of chemical transformations, thus establishing them as important intermediates in the field of organic chemistry.[13]

1.6 Functional group transformations in Morita-Baylis-Hillman adducts

Morita-Baylis-Hillman (MBH) adducts possess multiple functional groups in close spatial proximity, rendering them highly versatile intermediates for diverse synthetic transformations.

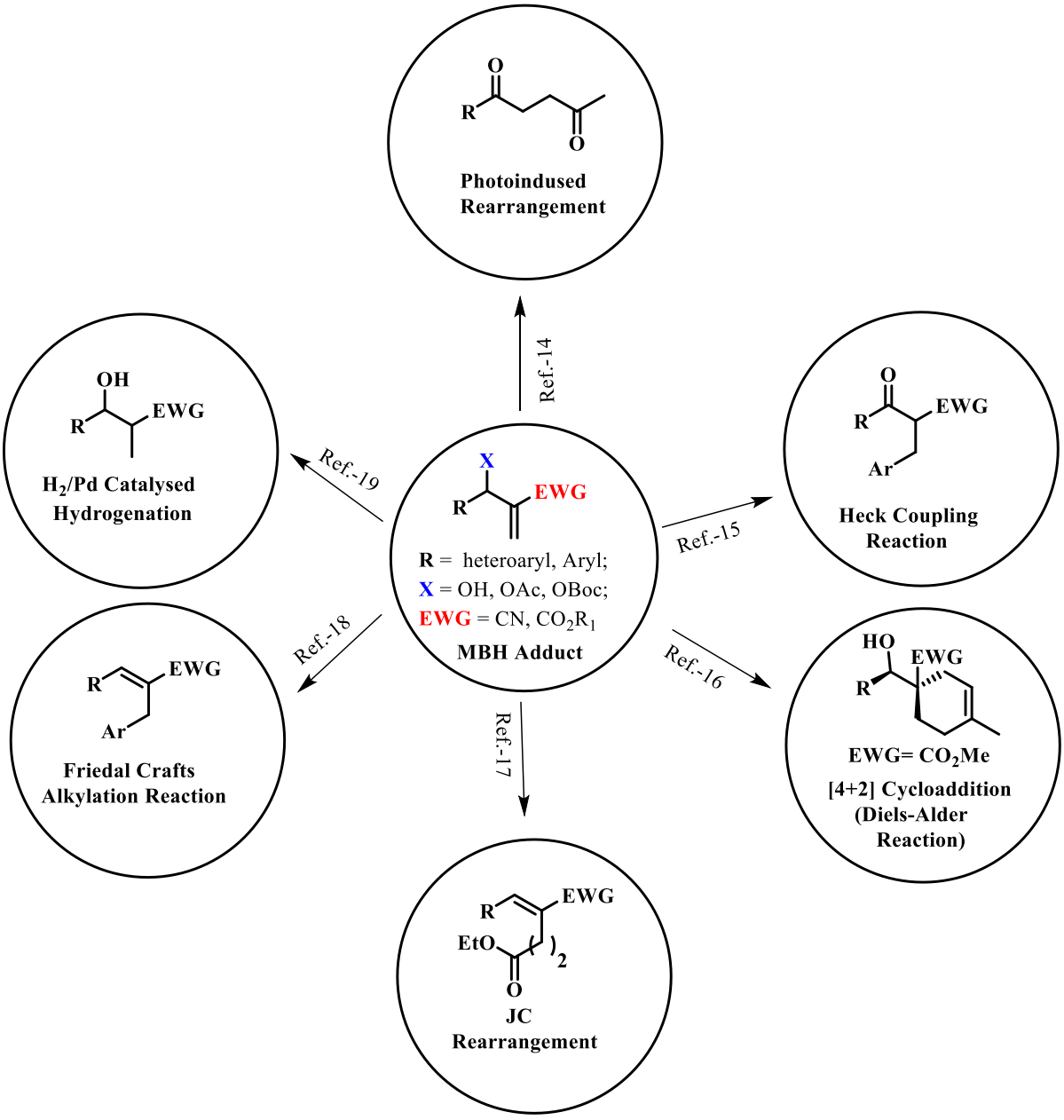


Figure 1.5 Selected transformations of Morita-Baylis-Hillman (MBH) adducts

Their unique structural framework enables the participation in a wide array of synthetic reactions, including the Claisen rearrangement, Friedel-Crafts alkylation and acylation, Heck

coupling, Diels-Alder cycloaddition, catalytic hydrogenation, and Michael-type conjugate additions, among others. These transformations significantly enhance the synthetic utility of MBH adducts, facilitating the construction of complex molecular architectures with high efficiency and selectivity.[13]

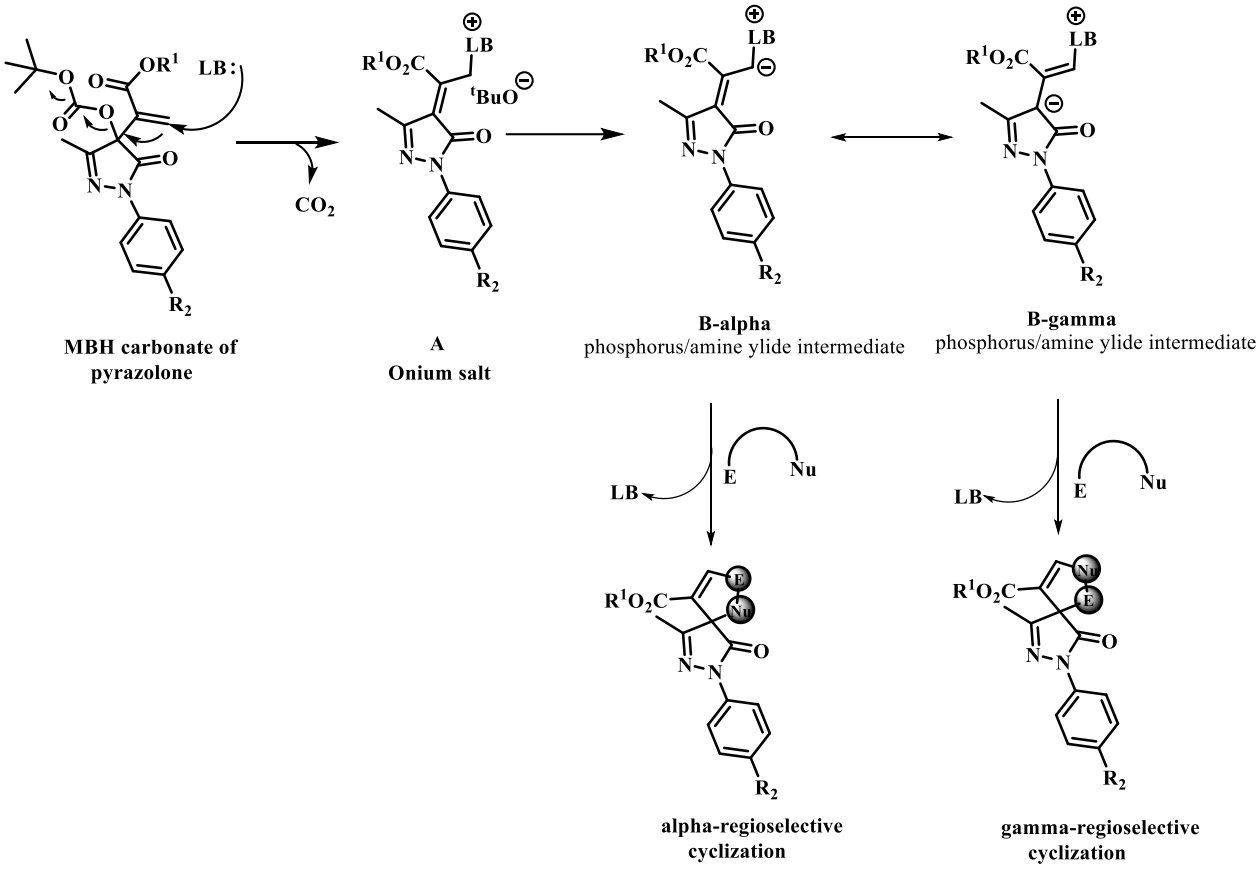
1.7 Utilization of Morita-Baylis-Hillman adducts in the synthesis of spirocyclic framework via organocatalysis

Carbocyclic and heterocyclic scaffolds have garnered immense attention in synthetic organic chemistry owing to their structural complexity, diverse reactivity, and profound significance in medicinal chemistry, agrochemicals, and materials science. These cyclic frameworks serve as core building blocks in the synthesis of many bioactive compounds, including pharmaceuticals, natural products, and advanced functional materials. Their unique electronic and steric properties contribute to their widespread utility in designing and constructing new chemical entities (NCEs), to modulate the interactions with biological targets, and to harness the potential therapeutic activity. Additionally, their applications extend to the fine chemical industry, where they play a crucial role in the synthesis of dyes, polymers, and specialty chemicals. As a result, the exploration of efficient synthetic methodologies for the construction of carbocyclic and heterocyclic systems remains a fundamental pursuit in contemporary organic synthesis.[20]

In recent years, isatin and pyrazolone-derived Morita-Baylis-Hillman adducts have emerged as versatile and excellent precursors for the construction of structurally diverse spirocyclic scaffolds.[21] Isatin-derived MBH (Morita-Baylis-Hillman) adducts and pyrazoledione-derived MBH (Morita–Baylis–Hillman) adducts easily undergo cycloaddition reactions through a similar mechanism. Both involve an electron-deficient alkene system that facilitates nucleophilic attack, followed by cyclization to form the desired heterocyclic structure. It is well known that the electronic nature of the substituents on isatin and pyrazolone influences the reactivity and regioselectivity of the reaction. While the core mechanism remains comparable, variations in steric and electronic effects can lead to differences in reaction rates as well as product distribution. The general reactivity of pyrazoledione-derived MBH (Morita–Baylis–Hillman) adducts follows a well-defined mechanistic pathway, as outlined in Scheme 1.5. The process is initiated by the nucleophilic attack of a Lewis base catalyst (LB), such as phosphines (PR_3), amines (NR_3), or sulfides (SR_2), on the MBH carbonate of pyrazolone via an S_N2 mechanism. This nucleophilic displacement leads to the formation of a transient phosphonium or ammonium salt intermediate (**A**), accompanied by the elimination of carbon dioxide (CO_2)

and tert-butoxide as a leaving group (Scheme 1.5). Subsequently, the in situ generated Brønsted base (tert-butoxide) facilitates the deprotonation of intermediate **A**, resulting in the formation of an allylic phosphorus/amine ylide intermediate (**B**). This ylide species exhibits high nucleophilicity and can undergo further transformations depending on the nature of the dipolarophile present in the reaction medium.

The reactivity of intermediate **B** is dictated by its ability to engage in annulation pathways through either the **B-α** or **B-γ** position, leading to the formation of distinct annulated products. The reaction proceeds via a cyclization step, wherein the ylide undergoes regioselective addition to the dipolarophile to furnish the α-annulation or γ-annulation products (Scheme 1.5). Importantly, the Lewis base catalyst (LB) is regenerated at the end of the reaction cycle, making the process catalytic and highly efficient.

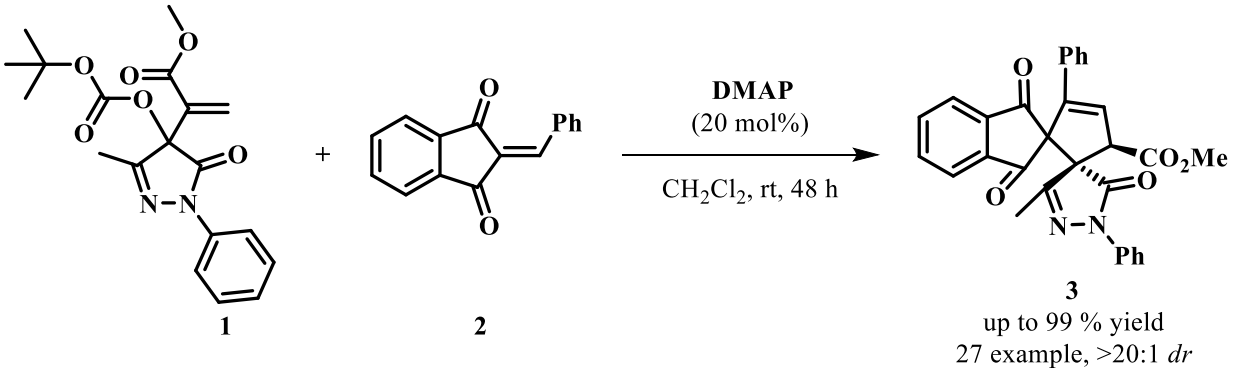


Scheme 1.5 General mechanistic pathway for cycloaddition of pyrazoledione-derived MBH (Morita–Baylis–Hillman) adduct with dienophile

This mechanistic pathway underscores the versatility of pyrazoledione-derived MBH (Morita–Baylis–Hillman) adducts as key intermediates in annulation reactions, providing access to structurally diverse cyclic frameworks with potential applications in organic synthesis and drug discovery as well.

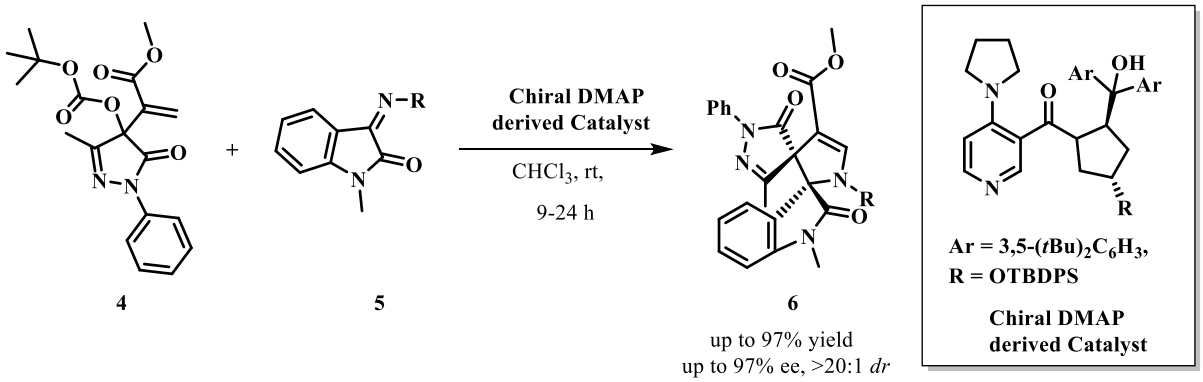
Some of the pyrazoledione-derived MBH (Morita–Baylis–Hillman) adducts and isatin-derived MBH (Morita-Baylis-Hillman) adducts have been utilized for the synthesis of the spirocyclic scaffold via the organocatalytic cycloaddition pathway.

In 2022, Guo and coworkers[22] reported a [3+2] annulation reaction catalyzed by 4-(dimethylamino)pyridine (DMAP) by employing pyrazoledione-derived Morita–Baylis–Hillman (MBH) carbonates **1** and 2-arylideneindane-1,3-diones **2** as key reactants (Scheme 1.6). This transformation efficiently furnished a range of multifunctional spiropyrazolone derivatives **3** in modest to excellent yields with very good diastereoselectivities (up to 99%, varying from 3:2 to greater than > 20:1 *dr*). As a class of Lewis-base receptors, pyrazoledione derived MBH carbonates serve as crucial substrates in organocatalyzed annulation processes, facilitating the synthesis of structurally diverse pyrazolinone-containing dispirocyclic frameworks.



Scheme 1.6 Organocatalysed synthesis of spiropyrazolone via Pyro-MBH carbonate

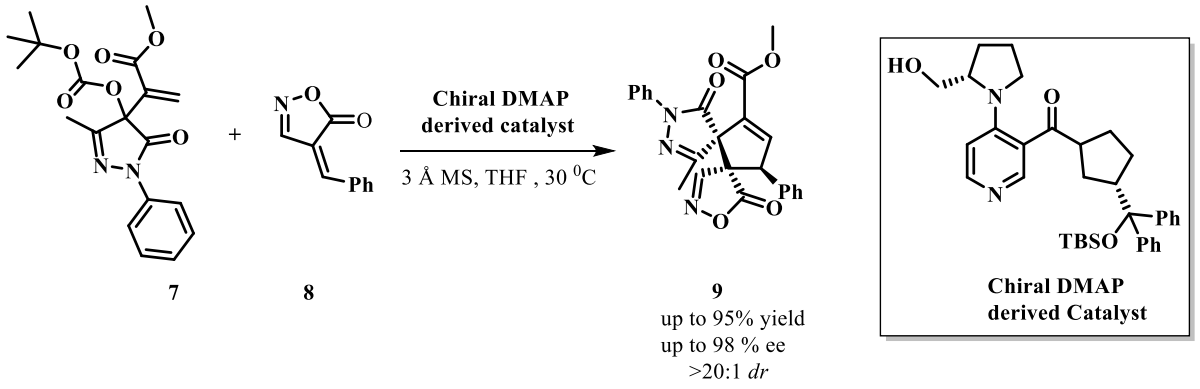
In 2022, Han and coworkers[23] reported the catalytic asymmetric synthesis of the bis-spiro[pyrazolone–dihydropyrrole–oxindole] **6** frameworks using a chiral DMAP-derived



Scheme 1.7 Organocatalysed synthesis of bispiro[pyrazolone–dihydropyrrole–oxindole framework via Pyro-MBH carbonate with isatin derived imine

catalyst. In this transformation, pyrazoledione-derived MBH (Morita–Baylis–Hillman) carbonate **4** and isatin-derived imine **5** have been utilized, and the reaction proceeded with exceptional stereoselectivity to afford the desired product in high yields (Scheme 1.7). The proposed transition state analysis suggested that intermolecular hydrogen bonding and π–π interactions played a pivotal role in governing the stereoselective nature and outcome of the chemical transformation.

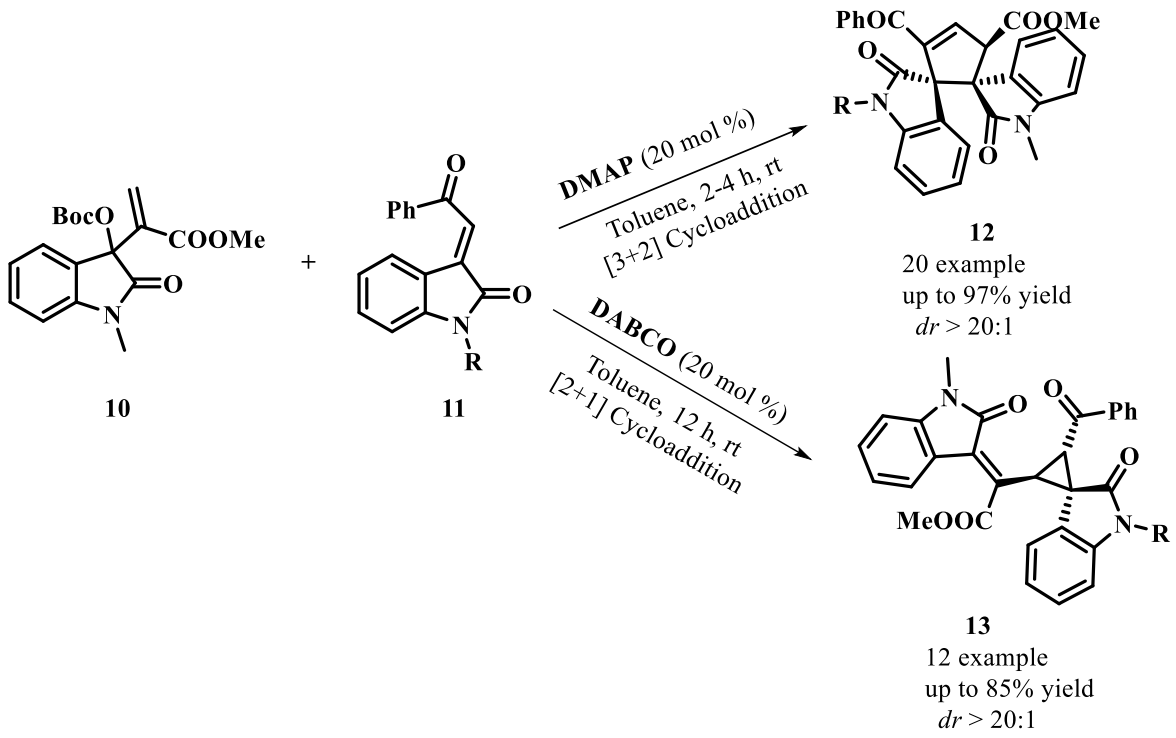
In 2024, Wang and coworkers[24] introduced a highly enantioselective [3+2] cyclization approach for synthesizing bis-spirocyclic pyrazolones **9** using pyrazolone-based Morita–Baylis–Hillman (MBH) adducts **7** and arylidenyl isoxazolones **8**. This transformation was catalyzed by a chiral DMAP-derived organocatalyst for the formation of complex spirocyclic architectures. This spirocyclic compound was constructed with vicinal all-carbon quaternary stereocenters embedded in a cyclopentene framework. The reaction proceeded under mild reaction conditions to afford the desired spiroheterocycles in high yields with exceptional stereoselectivity (up to 95%, 98% *ee*, and >20:1 *dr*, see Scheme 1.8). This protocol provided a powerful strategy for the asymmetric synthesis of structurally intricate spirocyclic compounds, offering potential applications in synthetic and medicinal chemistry.



Scheme 1.8 Organocatalysed synthesis of bis-spirocyclic pyrazolones framework via Pyro-MBH Carbonate with arylidenyl isoxazolones

In 2018, our research group[25] reported a highly diastereoselective organocatalytic synthesis of cyclopentenyl bis-spirooxindoles **12** and cyclopropyl spirooxindoles **13** via [3+2] and [2+1] annulations. The tertiary amine catalysts (DMAP and DABCO) have been effectively employed to tune the cycloaddition of isatin-derived MBH carbonates **10** and 3-methyleneoxindoles **11** to access two different spirooxindole frameworks with vicinal quaternary spiro centers and three contiguous stereocenters. The reactions worked under mild

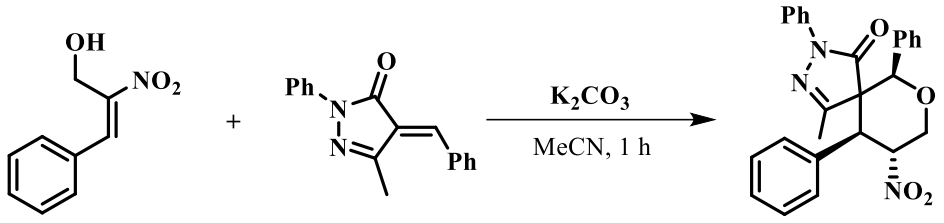
and practical conditions to afford the spirooxindoles in good to excellent yields with very high diastereoselectivity (Scheme 1.9)



Scheme 1.9 Organocatalysed synthesis of isatin-derived bis-spirocyclic framework via Is-MBH carbonate with 3-methyleneoxindole

1.8 Utilization of Morita-Baylis-Hillman adducts in spirocyclic framework synthesis via base

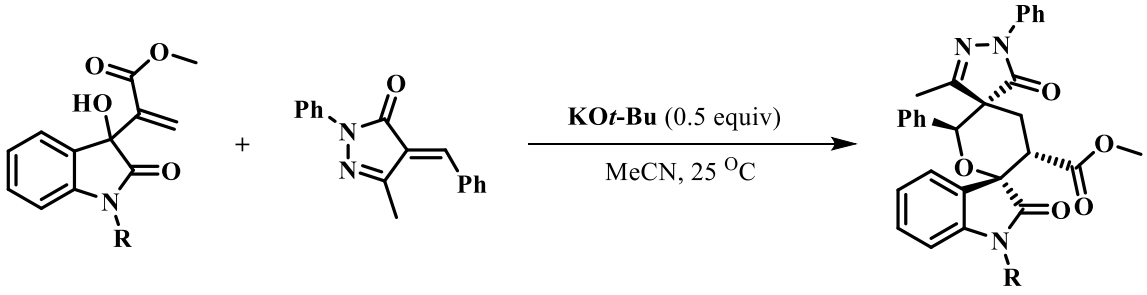
Numerous studies in the literature describe the synthesis of spirocyclic frameworks utilizing a base in conjunction with Michael addition of MBH adducts. In 2022, Anwar and coworkers[26] developed an efficient transition metal-free strategy for synthesizing spiro-pyrazolone tetrahydropyran frameworks under ambient conditions. This transformation involved a formal [4+2] cyclization between *trans*-β-nitrostyrene-derived Morita–Baylis–Hillman (MBH) alcohol **14** and α-arylidene pyrazolone **15** (Scheme 1.10). The reaction proceeded via an oxa-Michael/Michael cascade mechanism, facilitating the formation of new C–C and C–O bonds. This elegant protocol utilized quinine-derived organocatalyst to afford the spirocyclic compounds **16** in excellent yields with impressive enantioselectivity and diastereoselectivity (up to 93%, 94% *ee*, and >20:1 *dr*, Scheme 1.10). This protocol proved to be very effective and robust for the stereoselective spirocyclization under very mild and simple reaction conditions.



14 **15** **16**
13 example
up to 93 % yield
>20:1 *dr*

Scheme 1.10 Base mediated [4+2] cyclization between *trans*-β-nitrostyrene-derived Morita–Baylis–Hillman (MBH) alcohol and α-arylidene pyrazolone

Very recently in 2023, Kesavan and coworkers[27] reported a transition metal-free oxa-Michael cascade [4+2] annulation strategy that facilitated the reaction of isatin-derived Morita–Baylis–Hillman (Is-MBH) alcohols **17** with α-arylidene pyrazolones **18** (Scheme 1.11). This innovative approach enabled the efficient construction of a structurally diverse tetrahydro-dispiro[indolinone-3,2′-pyran-5′,4″-pyrazolone] **19** framework, effectively incorporating two tertiary and two quaternary stereogenic centers. The utilization of Is-MBH alcohols as oxa-Michael donors marks a pioneering foray into highly atom-economical reaction pathways. This method showcased an exceptional performance by affording a broad spectrum of bioinspired tetrahydro-dispirooxindole-pyran-pyrazolone derivatives with remarkable efficiency, with impressive diastereoselectivity in an exceptionally short reaction time of 15 min at room temperature.



17 **18** **19**
35 example
up to 96% yield
>20:1 *dr*

Scheme 1.11 Base-mediated [4+2] cyclization via Is-MBH-derived alcohol and α-arylidene pyrazolone

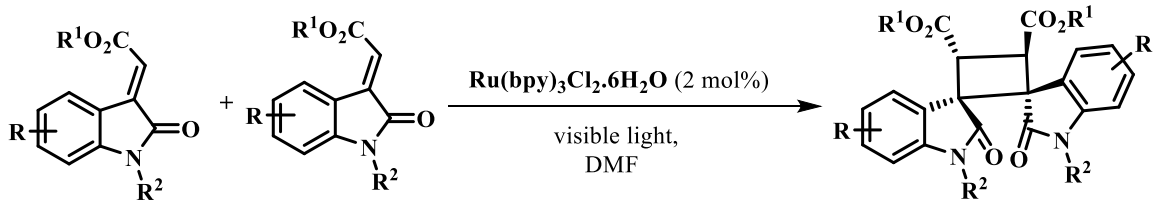
1.9 Utilization of visible light for the synthesis of Spirocyclic framework

Several studies in the literature describe the visible light-mediated synthesis of a spirocyclic framework. These approaches are generally categorized into two types: those that utilize

external photocatalysts and those that do not. Most reported methods focus on synthesizing a spirocyclic framework without the use of external photocatalysts. The visible light photochemical reactions that proceed without the requirement of any external photocatalysts can be further classified into five categories.[28]

1. Visible light photoexcitation of a single substrate
2. Visible light photoexcitation of reaction intermediates
3. Visible light photoexcitation of EDA complexes between substrates
4. Visible light photoexcitation of EDA complexes between substrates and reaction intermediates
5. Visible light photoexcitation of products

Attempts have been made to synthesize different spirocyclic compounds with and without the use of a photocatalyst. In 2012, Xiao and coworkers[29] disclosed a highly diastereoselective and regioselective visible light-mediated [2+2] cycloaddition of 3-methyleneoxindoles **20** in the presence of a metal photocatalyst (Scheme 1.12). This photochemical strategy provided a rapid and efficient route to access structurally complex and functionally diverse oxindole derivatives **21**, featuring two spirocyclic frameworks and four stereogenic centers, including two fully substituted all-carbon quaternary centers. The developed methodology exemplified the power of visible-light-mediated transformations in the construction of architecturally intricate molecular scaffolds.



20 **20**

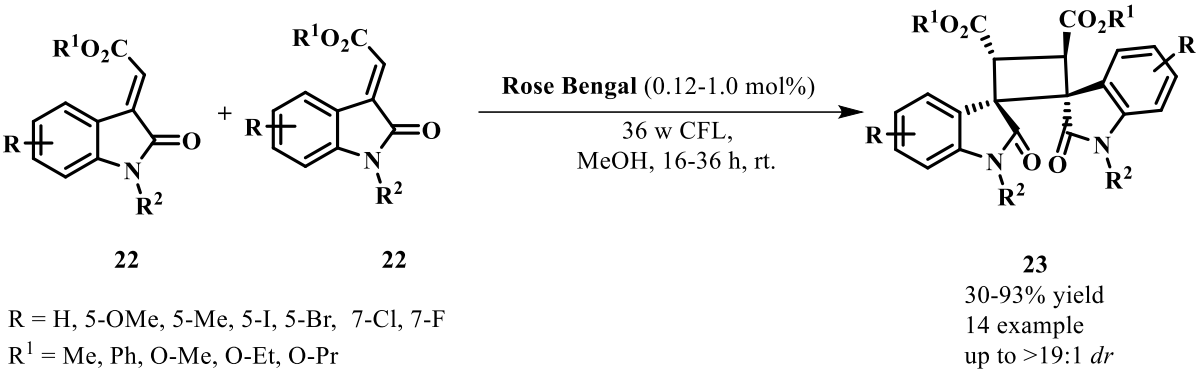
R = H, OMe, Me, Br, Cl, F, NO_2, OCF_3
R^1 = Me, Et, *t*-Bu, *n*-Pr
R^2 = H, Me, Allyl, Bn, PMB

21
67-93% yield
21 example
up to >19:1 *dr*

Scheme 1.12 Visible light-mediated dimerization of 3-methyleneoxindole in the presence of $Ru(bpy)_3Cl_2.6H_2O$ photocatalyst

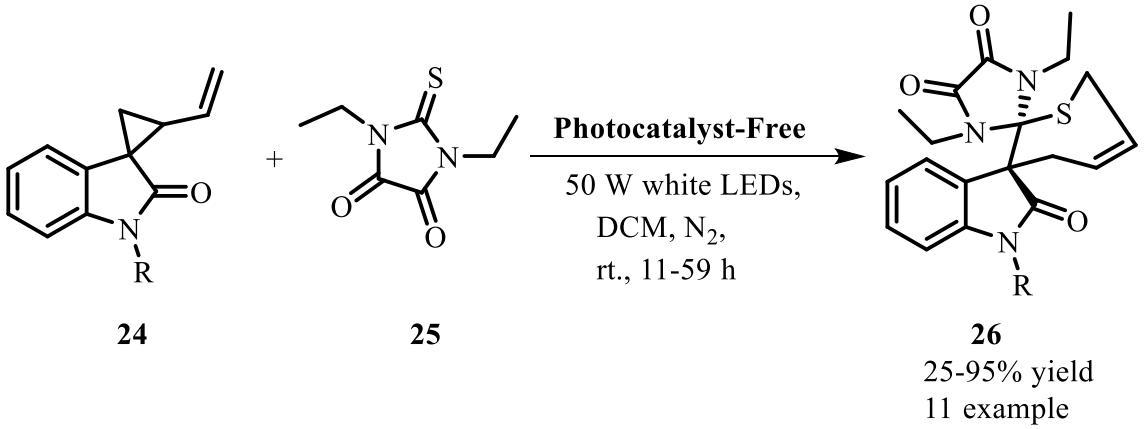
In 2017, He and coworkers[30] reported a Rose Bengal-sensitized intermolecular [2+2] cycloaddition of 3-methyleneoxindoles **22**, enabling the efficient synthesis of spirocyclic oxindoles **23** under visible-light irradiation (Scheme 1.13). This transformation proceeded with

high diastereoselectivity and regioselectivity to afford the cycloadducts (up to 93%, >19:1 *dr*). Notably, the reaction required only a minimal loading of Rose Bengal (0.125 mol%) as a triplet sensitizer, highlighting its remarkable catalytic efficiency. This protocol underscores the significant potential of Rose Bengal as a photocatalyst in visible-light-mediated organic transformations.



Scheme 1.13 Visible light-mediated dimerization of 3-methyleneoxindole in the presence of Rose Bengal photocatalyst

In 2021, Zhang and coworkers[31] introduced an innovative method that employed the strength of visible light to facilitate [5+2] cycloaddition between vinylcyclopropanes (VCPs) **24** and thioparabanates **25** (Scheme 1.14). This elegant protocol worked smoothly without the need for any catalysts or additional additives. The approach proved to be environmentally friendly and atom-efficient to synthesize a diverse functionalized sulfur-containing seven-membered heterocycles **26** using visible light (White LEDs). Notably, the resultant compounds incorporated two adjacent fully substituted stereogenic centers under mild reaction conditions, marking a significant advancement in synthetic chemistry.



Scheme 1.13 Visible light mediated synthesis of sulfur-containing seven-membered spiroheterocycles in the absence of a photocatalyst

Over the years, we have been exploring the organocatalytic cycloaddition strategies for the synthesis of spiropyrazolone and spirooxindole scaffolds.[25, 32] Novel cycloaddition approaches to construct complex spiroheterocycles are challenging, and they offer a great opportunity to build newer scaffolds which may have potential applications in various fields, including medicinal chemistry and materials science. As we have been working in the area of organocatalysis as well as visible light photocatalysis, we aimed to synthesize complex spirocyclic scaffolds via organocatalytic, photochemical cycloaddition strategies under milder and transition metal-free reaction conditions.

1.10 Conclusions

In summary, Morita-Baylis-Hillman (MBH) adducts, notable for their accessibility and functional diversity, have been recognized as effective building blocks in organic synthesis. The MBH adducts facilitate the construction of a wide range of structurally unique compounds through various reaction pathways. Specifically, MBH adducts derived from pyrazolonediones have proven to be particularly valuable, serving as key intermediates in synthesizing diverse spiropyrazolones structures found in numerous natural products and have significant pharmacological relevance.

This introductory chapter offers a succinct overview of the history and applications of the Morita-Baylis-Hillman (MBH) reaction in organic synthesis. It highlights some of the selected innovative methods that effectively utilize MBH adducts and 3-methyleneoxindole. These methods do open more avenues, and there remains significant potential to explore the potential of MBH adducts and 3-methyleneoxindole in synthesizing intriguing and complex spirocyclic compounds. Additionally, existing methodologies related to MBH adducts derived from pyrazolonedione and 3-methyleneoxindole have yet to achieve high levels of stereoselectivity as well. Consequently, there are great opportunities to explore novel and practical applications of pyrazolonedione-based MBH adducts and 3-methyleneoxindole to access newer spiroheterocyclic compounds via novel synthetic pathways.

In the subsequent chapters, we have delved into the synthetic advantages and diverse applications of MBH adducts and 3-methyleneoxindole, focusing on their role in creating innovative spiroheterocyclic compounds by designing and developing novel methodologies.

1.10 References

1. Zheng, Y.; Tice, C. M.; Singh, S. B. *Bioorg. Med. Chem. Lett.* **2014**, *24*, 3673.
2. (a) Yu, B.; Yu, D. Q.; Liu, H. M. *Eur. J. Med. Chem.* **2015**, *97*, 673. (b)Yu, B.; Yu, Z.; Qi, P. P.; Yu, D. Q.; Liu, H. M. *Eur. J. Med. Chem.* **2015**, *95*, 35. (c) Gollner, A.; Rudolph, D.; Arnhof, H.; Bauer, M.; Blake, S. M.; Boehmelt, G.; Cockroft, X.-L.; Dahmann, G.; Ettmayer, P.; Gerstberger, T.; Karolyi-Oezguer, J.; Kessler, D.; Kofink, C.; Ramharter, J.; Rinnenthal, J.; Savchenko, A.; Schnitzer, R.; Weinstabl, H.; Weyer-Czernilofsky, U.; Wunberg, T.; McConnell, D. B. *J. Med. Chem.*, **2016**, *59*, 10147. (d) Zhou, L. M.; Qu, R. Y.; Yang, G. F. *Expert Opin. Drug Dis.* **2020**, *15*, 603.
3. (a) Zhao, Z.; Dai, X.; Li, C.; Wang, X.; Tian, J.; Feng, Y.; Xie, J.; Ma, C.; Nie, Z.; Fan, P.; Qian, M.; He, X.; Wu, S.; Zhang, Y.; Zheng, X. *Eur. J. Med. Chem.* **2019**, *186*, 111893. (b) Reddy, Y. P.; Anwar, S. *RSC Adv.* **2022**, *12*, 34634.
4. Rios, R. *Chem. Soc. Rev.* **2012**, *41*, 1060.
5. (a) Dalko, P. I.; Moisan, L. *Angew. Chem. Int. Ed.* **2004**, *43*, 5138. (b) Gaunt, M. J.; Johansson, C. C. C.; McNally, A.; Vo, N. T. *Drug Discov. Today* **2007**, *12*, 8.
6. Berkessel, A.; Gröger, H. *Asymmetric Organocatalysis* **2005**, doi:10.1002/3527604677.
7. (a) Morita, K.; Suzuki, Z.; Hirose, H. Bull. *Chem. Soc. Jpn*. **1968**, *41*, 2815. (b) Morita, K. *Japan Patent* **1968**, *69*, 58828s.
8. Baylis, A. B.; M. E. D. Hillman, *German Patent* **1972**, *77*, 34174q.
9. Hoffmann, H. M. R.; Rabe, J. *Angew. Chem., Int. Ed.* **1983**, *22*, 796.
10. Hill, J. S.; Isaacs, N. S. *J. Phys. Org. Chem.* **1990**, *3*, 285.
11. (a) Price, K. E.; Broadwater, S. J.; Jung, H. M.; McQuade, D. T. *Org. Lett.* **2005**, *7*, 147. (b) Price, K. E.; Broadwater, S. J.; Walker, B. J.; McQuade, D. T. *J. Org. Chem.* **2005**, *70*, 3980.
12. Aggarwal, V. K.; Fulford, S. Y.; Lloyd-Jones, G. C. *Angew. Chem., Int. Ed.* **2005**, *44*, 1706.
13. Basavaiah, D.; Veeraraghavaiah, G. *Chem. Soc. Rev.* **2012**, *41*, 68.
14. Matsumoto, S.; Okubo, Y.; Mikami, K. *J. Am. Chem. Soc.* **1998**, *120*, 4015.
15. Basavaiah, D.; Muthukumaran, K. *Tetrahedron* **1998**, *54*, 4943.
16. Aggarwal, V. K.; Patin, A.; Tisserand, S. *Org. Lett.* **2005**, *7*, 2555.
17. Basavaiah, D.; Pandiaraju, S. *Tetrahedron Lett.* **1995**, *36*, 757.
18. Basavaiah, D.; Krishnamacharyulu, M.; Hyma, R. S.; Pandiaraju, S. *Tetrahedron Lett.* **1997**, *38*, 2141.

19. Mateus, C. R.; Almeida, W. P.; Coelho, F. *Tetrahedron Lett.* **2000**, *41*, 2533.

20. (a) Fuji, K. *Chem. Rev.* **1993**, *93*, 2037. (b) Corey, E. J.; Guzman-Perez, A. *Angew. Chem. Int. Ed.* **1998**, *37*, 388. (c) O'Hagan, D. *Nat. Prod. Rep.* **2000**, *17*, 435. (d) Christoffers, J.; Mann, A. *Angew. Chem., Int. Ed.* **2001**, *40*, 4591. (e) Buffat, M. G. P. *Tetrahedron* **2004**, *60*, 1701. (f) Michael, J. P. *Nat. Prod. Rep.* **2004**, *21*, 625.

21. (a) Chen, Z. C.; Chen, Z.; Du, W.; Chen, Y. C. *Chem. Rec*. **2020**, *20*, 541. (b) Warghude, P. K.; Sabale, A. S.; Bhat, R. G. *Elsevier* **2024**, 309.

22. Liao, J.; Xu, J.; Wu, Y.; Hou, Y.; Guoa, H. *Adv. Synth. Catal*. **2022**, *364*, 1074.

23. Tian, Z.; Jiang, J.; Yan, Z.-H.; Luo, Q.-Q.; Zhan, G.; Huang, W.; Li, X.; and Han, B. *Chem. Commun.* **2022**, *58*, 5363.

24. Yang, M.; Xue, A.; Wei, X.; Huang, Y.; Qu, J.; and Wang, B. *Eur. J. Org. Chem.* **2024**, *27*, e202400305.

25. Warghude, P. K.; Dharpure, P. D.; Bhat, R. G. *Tetrahedron Lett.* **2018,** *59*, 4076.

26. Reddy, Y. P.; Anwar, S. *RSC Adv.* **2022**, *12*, 34634.

27. Lokesh, K.; Kumarswamyreddy N.; Kesavan, V. *J. Org. Chem.* **2023**, *88*, 15540.

28. Wei, Y.; Zhou, Q.-Q.; Tan, F.; Lu, L.-Q.; Xiao, W.-J. Synth. **2019**, *51*, 3021.

29. Zou, Y. Q.; Duan, S. W.; Meng, X. G.; Hu, X. Q.; Gao, S.; Chen, J. R.; Xiao, W.J. *Tetrahedron* **2012**, *68*, 6914.

30. Wu, L. L.; Yang, G. H.; Guan, Z.; He, Y. H. *Tetrahedron* **2017**, *73*, 1854.

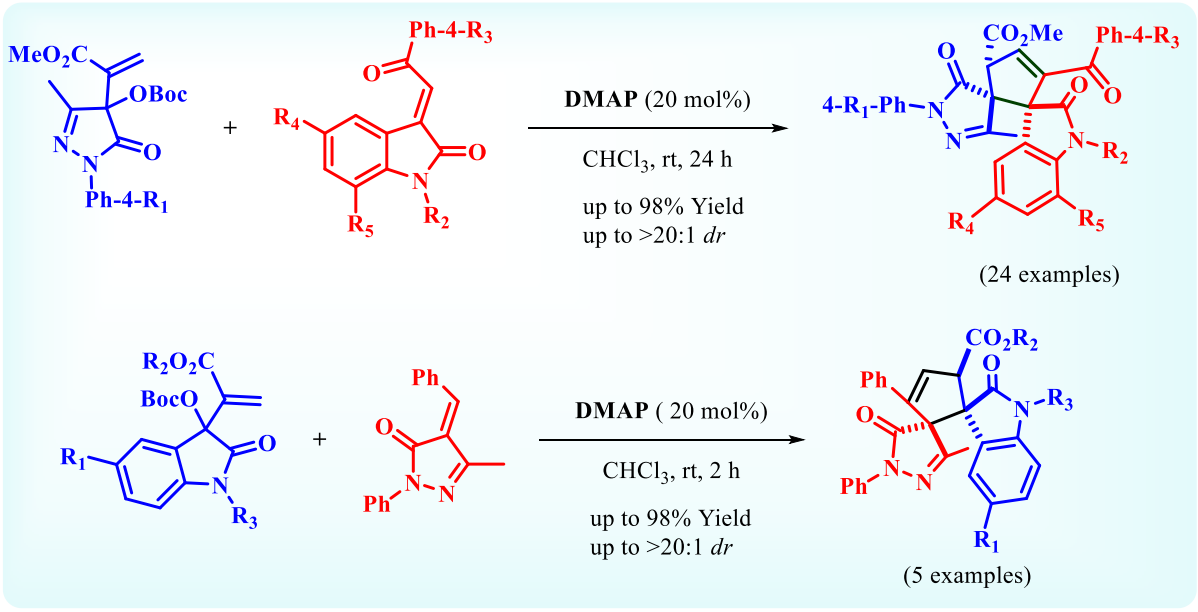
31. Huang, X.; Wang, R.; Zhou, C.; Gao, R.; Zhang, H.; Zheng, Y.; Zhang, X. *Org. Chem. Front.* **2021**, *8*, 5454.

32. (a) Warghude, P. K.; Sabale, A. S.; and Bhat, R. G. *Org. Biomol. Chem.* **2020**, *18,* 1794. (b) Warghude, P. K.; Sabale, A. S.; Dixit, R.; Vanka, R.; Bhat, R. G. *Org. Biomol. Chem.*, **2021**, *19*, 4338.

2 A Streamlined Synthesis of Spirooxindole-Pyrazolone Fused Cyclopentenes via Diastereoselective [3+2] Annulation

Abstract

A highly diastereoselective [3+2] cycloaddition catalyzed by DMAP has been established, utilizing pyrazolonedione-derived Morita-Baylis-Hillman (MBH) carbonates and 3-methyleneoxindoles as substrates. This method enabled the efficient synthesis of structurally intricate spiropyrazolone-fused oxindoles featuring three consecutive chiral centers in remarkable yields (up to 98%) with an exceptional diastereoselectivity (up to 99:1). Furthermore, the synthetic versatility of this approach has been demonstrated through subsequent Suzuki coupling and hydrolysis reaction.



Sabale, A. S.; Warghude, P. K.; Bhat, R. G. *Synlett* **2023,** *34,* 1732.

2 A Streamlined Synthesis of Spirooxindole-Pyrazolone Fused Cyclopentenes via Diastereoselective [3+2] Annulation

2.1 Introduction

Synthesis of spiro carbocyclic and heterocyclic frameworks has gained significant interest among synthetic and medicinal chemistry researchers over recent decades.[1] The three-dimensional architecture of spirocyclic frameworks enhances physicochemical properties, including metabolic stability, aqueous solubility, and lipophilicity, compared to their monocyclic counterparts.[2] Spiro-cyclopentane-pyrazolone and spiro-cyclopentane-oxindole derivatives, as multifunctional spirocyclic compounds, have attracted substantial attention in organic synthesis and pharmaceutical research due to their diverse biological activities (Figure 2.1). Notably, the spiropyrazolone cyclopentane derivative **I** function as a PPAR-α antagonist.[3] Furthermore, spirocyclic compounds **II** and **III** are recognized for their potent inhibitory effects on type-4 phosphodiesterases.[4] Additionally, spiro-cyclopentane-oxindole derivatives, such as

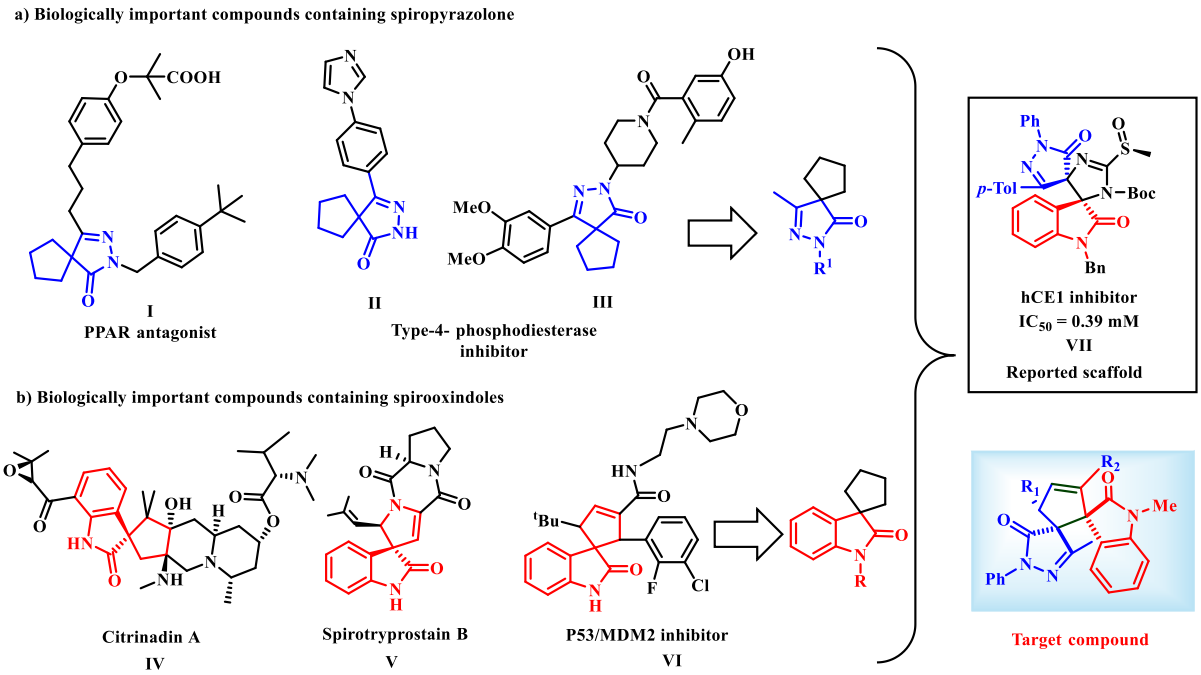


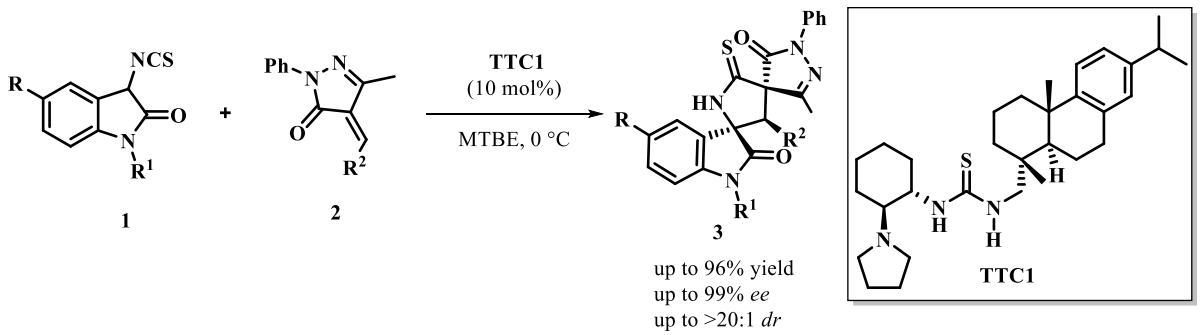
Figure 2.1 Notable examples of bioactive compounds featuring spirooxindole and spiropyrazolone frameworks

citrinadin A (**IV**) and spirotryprostatin B (**V**), have been identified as naturally occurring compounds.[5] The spirooxindole compound **VI** demonstrates inhibitory activity against the P53/MDM2 interaction.[6] In recent years, the integration of diverse pharmacologically significant scaffolds has emerged as a prominent and effective strategy for the design and development of novel biologically active compounds.[7] In this context, the fusion of spiropyrazolone and spirooxindole frameworks offers a promising strategy for constructing structurally diverse and intriguing spiro-heterocyclic compounds, potentially facilitating the discovery of bioactive candidates. Notably, the combining approach has recently enabled the successful synthesis of compound **VII**, which exhibits hCE1 inhibitory activity.[8]

2.2 Recent developments in the synthesis of spirooxindole fused pyrazolone

Design and synthesis of spirocyclic compounds incorporating heterocyclic frameworks, such as oxindole and pyrazolone scaffolds, holds significant relevance, particularly in contemporary drug discovery initiatives. Given the importance of these structural motifs, numerous methodologies have been established for synthesizing spirooxindole-pyrazolone derivatives under organocatalytic conditions.[9]

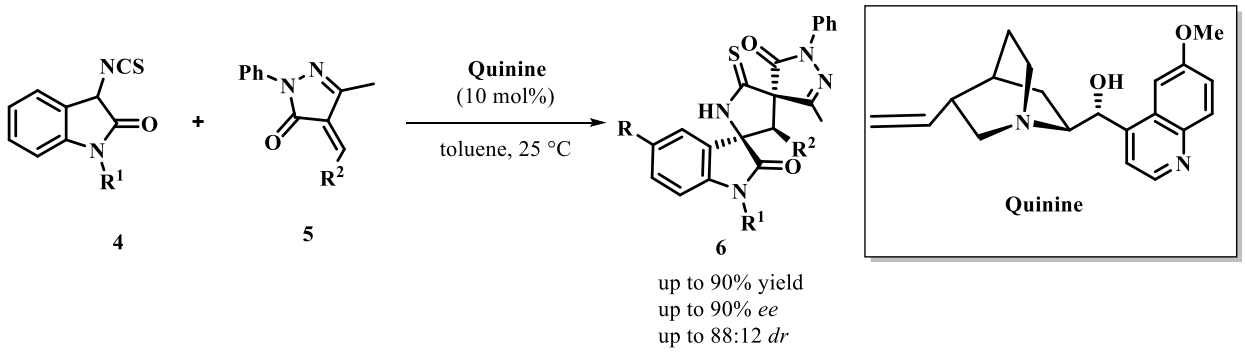
In 2013 Wang and coworkers[10] disclosed a pioneering organocatalytic Michael-cyclization cascade reaction, involving isothiocyanato oxindoles **1** and unsaturated pyrazolones **2** in the presence of the bifunctional thiourea catalyst **TTC1**. This approach enabled the efficient synthesis of multicyclic spiro[oxindole/thiobutyrolactam/pyrazolone] frameworks **3**, featuring three consecutive stereogenic centers, including two spiro-quaternary centers. The method achieved remarkable diastereoselectivity (up to >20:1 *dr*) and enantioselectivity (up to 99% *ee*) (Scheme 2.1).



Scheme 2.1 Synthesis of spiro[oxindole/thiobutyrolactam/pyrazolone] via chiral thiourea catalyzed [3 + 2] cycloaddition

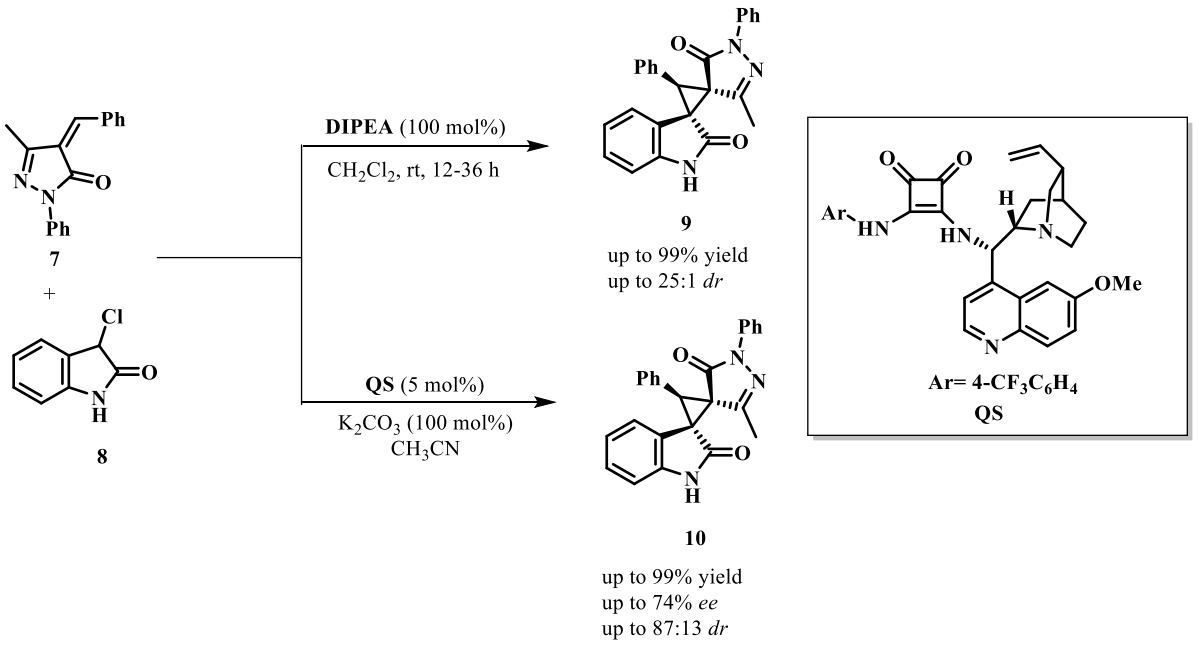
The following year, Yuan and coworkers [11] introduced an efficient organocatalytic approach

for the diastereo- and enantioselective synthesis of spirocyclic oxindole derivatives. This method employed commercially available quinine as a catalyst to construction the spirocyclic frameworks featuring two spiro-quaternary centers and three consecutive stereocenters via a domino Michael/cyclization sequence. The reactions between 3-isothiocyanato oxindoles **4** and unsaturated pyrazolones **5** proceeded under mild conditions, delivering spirocyclic oxindoles **6** in high to excellent yields (up to 90%) with moderate to good levels of diastereoselectivity (up to 88:12 *dr*) and enantioselectivity (up to 90% *ee*). A plausible dual activation mechanism was proposed to rationalize the stereochemical outcomes of the domino Michael/cyclization process (Scheme 2.2).



Scheme 2.2 Synthesis of spiro[oxindole/thiobutyrolactam/pyrazolone] via quinine-catalyzed asymmetric domino Michael-cyclization reaction

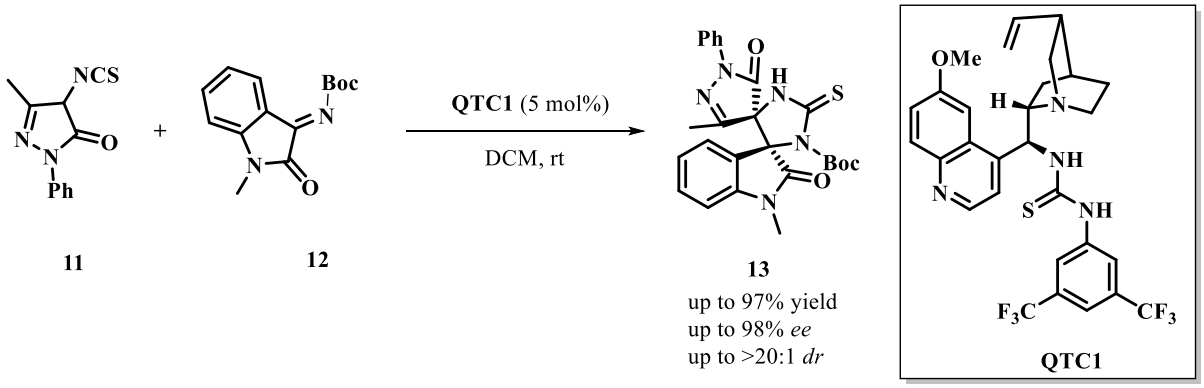
In 2015, the Du research group[12] introduced an effective diastereoselective Michael/alkylation cascade reaction between arylidenepyrazolones **7** and 3-chlorooxindoles **8**, catalyzed by



Scheme 2.3 Synthesis of spiro-pyrazolone-cyclopropane-oxindoles via DIPEA-catalyzed and squaramide-catalyzed [2+1] cycloaddition reaction

DIPEA. This strategy facilitated the synthesis of a diverse array of highly functionalized spiro-pyrazolone-cyclopropane-oxindoles **9** with excellent yields (up to 99%) and impressive diastereoselectivities (up to >25:1 *dr*). Additionally, squaramide-catalyzed **QS** asymmetric variants of this reaction provided chiral spirocyclic heterocycles **10** in outstanding yields (up to 99%) with moderate diastereoselectivities (up to 87:13 *dr*), and moderate to high enantioselectivities (up to 74% *ee*) (Scheme 2.3).

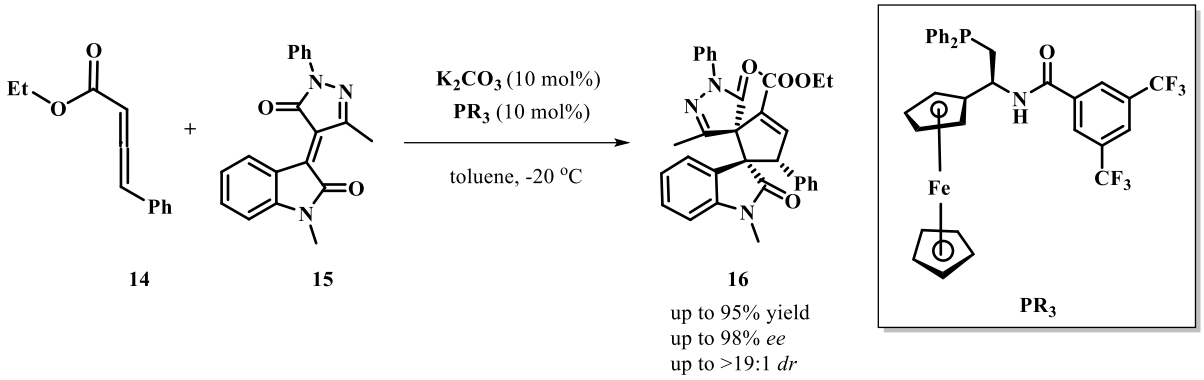
In 2018, Wang, Zou, and Ge collaboratively[13] developed an asymmetric [3+2] cycloaddition strategy to synthesize spiropyrazolone-fused oxindole derivatives. This methodology employed novel 4-isothiocyanato pyrazolones **11** and ketimines derived from isatin **12** as key substrates, affording a diverse array of dispirotriheterocyclic compounds **13**. The process achieved remarkable efficiency, in yields (up to 97%), with an exceptional diastereoselectivity (up to >20:1 *dr*), and high enantioselectivity (up to 98% *ee*). A chiral sulfoxide derivative of the resulting dispirocyclic product was identified as a promising human carboxylesterase 1 (hCE1) inhibitor. It's very important to highlight here that there was a significant difference in biological activity observed between the two enantiomers, which underscores the critical importance of the asymmetric synthesis (Scheme 2.4).



Scheme 2.4 Synthesis of dispirotriheterocyclic compounds via asymmetric [3+2] cycloaddition

Zhong and coworkers[14] developed a highly regioselective, diastereoselective, and enantioselective method for synthesizing spirocyclopentene-fused oxindole-pyrazolone derivatives **16**. This strategy enables the formation of complex molecular architectures featuring three contiguous stereocenters, including two adjacent spiro quaternary stereogenic centers, with excellent diastereoselectivity (up to 19:1) and enantioselectivity (up to 98% *ee*).

The transformation is achieved through an enantioselective [3+2] annulation between γ-substituted allenoates **14** and pyrazoloneyldiene oxindoles **15**, catalyzed by a ferrocenyl-based bifunctional phosphine (**PR_3**) (Scheme 2.5). In this context, developing a highly efficient one-pot strategy for synthesizing multifunctionalized spirocyclic pyrazolones and oxindoles represents a significant and challenging objective in synthetic organic chemistry.



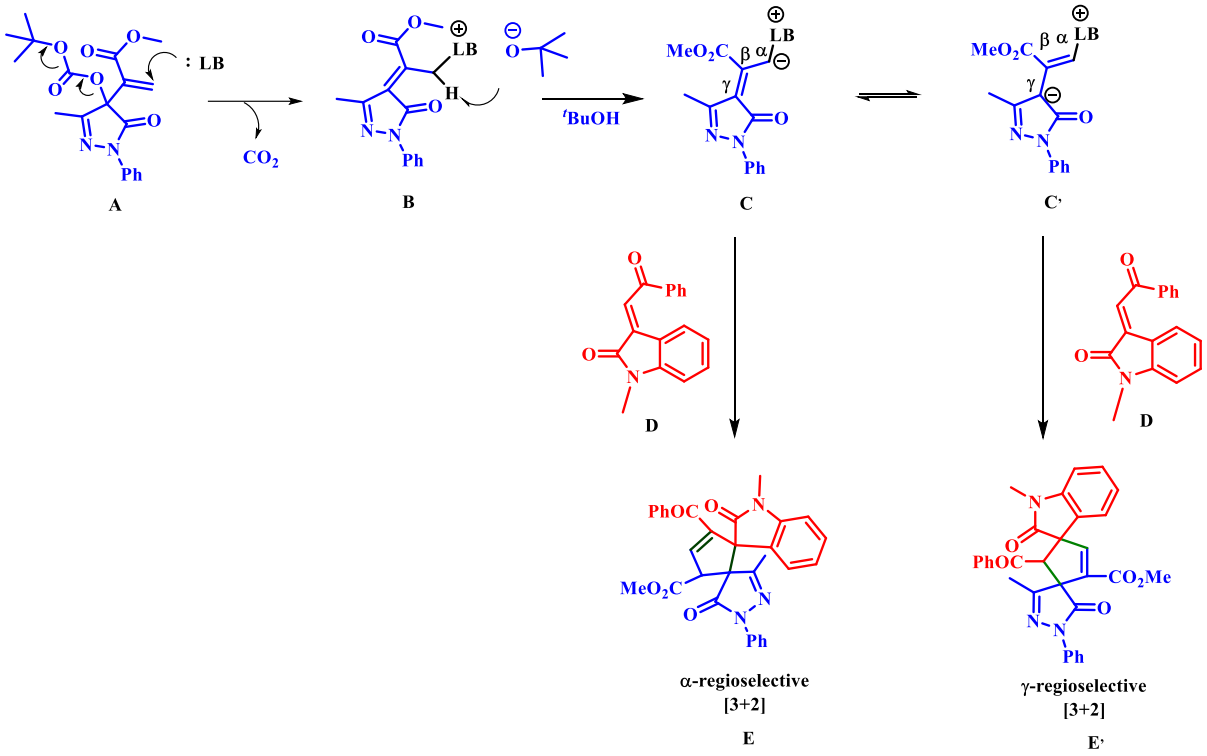
Scheme 2.5 Synthesis of spiropyrazolone-fused oxindole derivatives

2.3 Proposed hypothesis and synthetic approach

We have been working on the synthesis of spirocyclic compounds, and with our continued interest in the synthesis of spirocyclic compounds and cycloaddition reactions involving isatin-derived Morita-Baylis-Hillman carbonates,[15] we directed our focus towards the design and development of spirooxindole-fused pyrazolone framework.

In recent years, isatin-derived Morita-Baylis-Hillman (MBH) carbonates have been extensively utilized as three-carbon synthons for the synthesis of multifunctional hetero-spirocyclic compounds.[16] Similarly, pyrazolonedione-based MBH carbonates have gained recognition as versatile intermediates for the construction of spiropyrazolone frameworks.[17] Additionally, 3-methyleneoxindole derivatives have demonstrated significant utility as valuable synthons in cycloaddition reactions, enabling the formation of structurally diverse spirocyclic oxindole architectures. Their broad reactivity has provided a robust platform for developing various synthetic compounds and molecular building blocks, including bioactive entities.[18]

Based on the earlier experience, we postulated that a Lewis base catalyst, such as an amine or phosphine, would initiate an S_N2 reaction on the MBH carbonate **A**, forming intermediate **B** with the concurrent extrusion of CO_2 and tert-butoxide (Scheme 2.6). The tert-butoxide, generated in situ as a Brønsted base, is expected to abstract a proton from intermediate **B**, forming a zwitterionic ylide intermediate **C** or **C'**. This reactive intermediate could subsequently interact with 3-methyleneoxindole **D**, facilitating the formation of compounds **E** or **E'**, which incorporates the desired spiropyrazolone-oxindole framework.



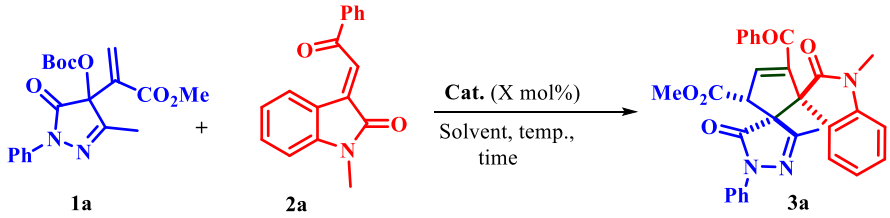
Scheme 2.6 Proposed synthesis of spirooxindole-fused pyrazolone

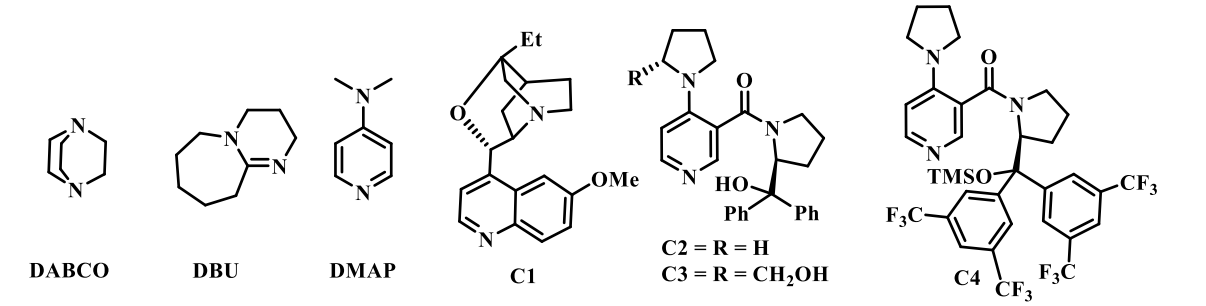
2.4 Results and Discussion

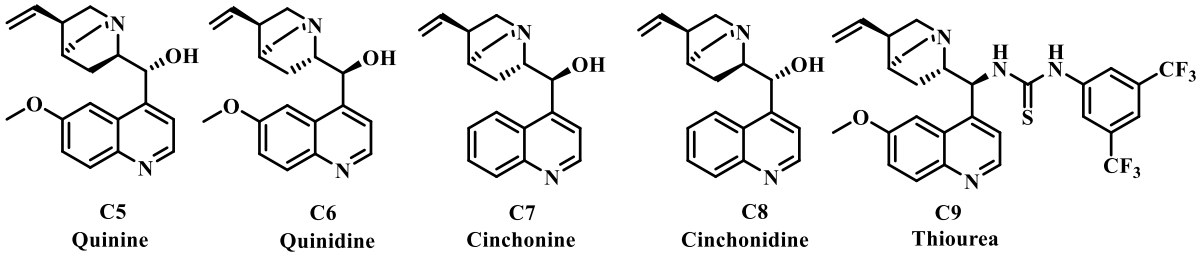
In order to validate our hypothesis, a model reaction was performed using pyrazolonedione-derived MBH carbonate **1a** and (*E*)-1-methyl-3-(2-oxo-2-phenylethylidene)indolin-2-one **2a**. The reaction proceeded under catalytic conditions employing DABCO (20 mol%) in dichloromethane (DCM) at room temperature. Gratifyingly, the reaction furnished the α-regioselective [3+2] annulation product **3a** in moderate yield (30%) with excellent diastereoselectivity (>20:1 *dr*, Table 2.1, entry 1).

To improve the yield of **3a**, independent reactions of **1a** and **2a** were conducted using PPh_3 (20 mol%) and DBU (20 mol%) as catalysts (Table 2.1, entries 2–3). Unexpectedly, no product formation was observed, even after extended reaction times (Table 2.1, entries 2–3). However, when 4-dimethylaminopyridine (DMAP, 20 mol%) was employed as the catalyst, the desired [3+2] annulation product **3a** was obtained with a remarkable yield (90%) and excellent diastereoselectivity (>20:1 *dr*, Table 2.1, entry 4). Motivated by this significant improvement, efforts were directed towards developing an asymmetric variant of this α-regioselective [3+2] annulation reaction.

Table 2.1 Screening of catalysts and solvents for cycloaddition reaction[a-d]







Entry	Catalyst [mol%]	Solvent	Temp [° C]	Time [h]	Yield [%][b]	*dr*[c]	*ee* [%][d]
1	DABCO [20]	CH_2Cl_2	rt	36	30	>20:1	-
2	PPh_3 [20]	CH_2Cl_2	rt	72	NR	-	-
3	DBU [20]	CH_2Cl_2	rt	72	NR	-	-
4	DMAP [20]	CH_2Cl_2	rt	24	90	>20:1	-
5	C1 [20]	CH_2Cl_2	rt	72	NR	-	-
6	C2 [20]	CH_2Cl_2	rt	24	65	>20:1	15
7	C3 [20]	CH_2Cl_2	rt	24	68	>20:1	21
8	C4 [20]	CH_2Cl_2	rt	24	73	>20:1	23
9	C1 [20]	$CHCl_3$	rt	72	NR	-	-

10	C2 [20]	$CHCl_3$	rt	24	68	>20:1	10
11	C3 [20]	$CHCl_3$	rt	24	70	>20:1	12
12	C4 [20]	$CHCl_3$	rt	24	74	>20:1	15
13	C5 [20]	$CHCl_3$	rt	24	NR	-	-
14	C6 [20]	$CHCl_3$	rt	24	NR	-	-
15	C7 [20]	$CHCl_3$	rt	24	NR	-	-
16	C8 [20]	$CHCl_3$	rt	24	NR	-	-
17	C9 [20]	$CHCl_3$	rt	24	NR	-	-
18	C2 [20]	$CHCl_3$	0	36	63	>20:1	10
19	C3 [20]	$CHCl_3$	0	36	60	>20:1	10
20	C4 [20]	$CHCl_3$	0	36	65	>20:1	12
21	DMAP [20]	$CHCl_3$	rt	24	92	>20:1	-
22	DMAP [20]	MeCN	rt	24	81	>20:1	-
23	DMAP [20]	THF	rt	24	80	>20:1	-
24	DMAP [20]	DMF	rt	24	82	>20:1	-
25	DMAP [20]	EtOAc	rt	24	85	>20:1	-
26	DMAP [20]	$PhCH_3$	rt	24	87	>20:1	-
27	DMAP [20]	PhCl	rt	24	89	>20:1	-
28	DMAP [20]	MeOH	rt	24	85	>20:1	-
29	DMAP [20]	EtOH	rt	24	78	>20:1	-
30	DMAP [20]	PrOH	rt	24	84	>20:1	-
31	DMAP [15]	$CHCl_3$	rt	24	78	>20:1	-

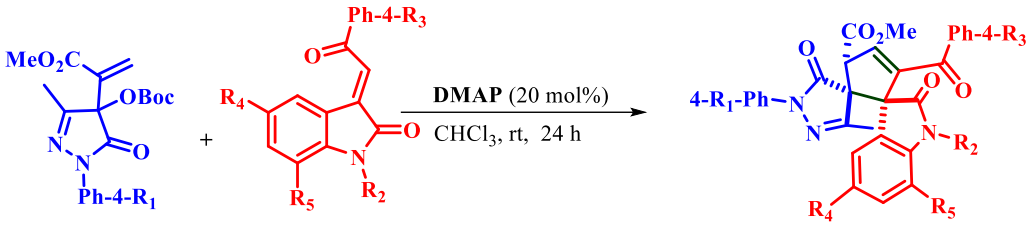
[a]**Reaction Conditions:** Unless stated otherwise, reactions were performed using **1a** [0.094 mmol], **2a** [0.112 mmol], and the catalyst [20 mol%] in 2.0 mL of the specified solvent at the indicated temperature and reaction time. [b]Yields represent isolated products following purification by column chromatography. [c]Diastereomeric ratios were determined via ^{1}H NMR analysis. [d]Enantiomeric excess [*ee*] was measured by HPLC utilizing a chiral stationary phase.

In pursuit of an asymmetric variant, we evaluated several chiral tertiary amine catalysts (Table 2.1, entries 5–8). Unfortunately, we did not observe any desired product in the presence of cinchona-derived catalyst **C1**, even after an extended reaction period (Table 2.1, entry 5). Subsequently, chiral DMAP-based catalysts **C2**–**C4** were employed to synthesize the optically enriched product **3a**. Gratifyingly, all three catalysts successfully furnished the [3+2] annulation product **3a**. However, the enantioselectivity achieved was consistently low across these catalysts, with enantiomeric excesses ranging from 15% to 23% (Table 2.1, entries 6–8).

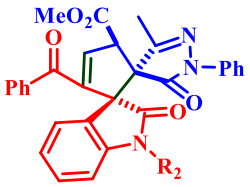
Despite our extensive efforts to achieve enantioselectivity, including the evaluation of various chiral catalysts under diverse reaction conditions, all the attempts proved to be unsuccessful (Table 2.1, entries 9–20). Given the significant relevance of spiropyrazolone and spirooxindole scaffolds in synthetic and medicinal chemistry, we further investigated the diastereoselective variant of this α-regioselective [3+2] annulation reaction. To refine the reaction conditions, a variety of solvents were evaluated, including chloroform, acetonitrile, tetrahydrofuran, dimethylformamide, ethyl acetate, toluene, chlorobenzene, methanol, ethanol, and propanol (Table 2.1, entries 21–30). Among all, chloroform emerged as the most effective solvent, room temperature facilitating the formation of spirooxindole-pyrazolone **3a** in an excellent yield of 92% with outstanding diastereoselectivity (>20:1 *dr*, Table 2.1, entry 21). Reducing the catalyst loading resulted in a slightly lower yield of 78%, while the diastereoselectivity remained unaffected (Table 2.1, entry 31). Based on exhaustive screening for the [3+2] cycloaddition reaction, MBH carbonate of pyrazolone **1a** (1.0 equiv), (*E*)-1-methyl-3-(2-oxo-2-phenylethylidene)indolin-2-one **2a** (1.2 equiv.), and **DMAP** (20 mol%) in chloroform under room temperature proved to be the optimum reaction conditions to obtain spiropyrazolone-fused oxindole derivatives efficiently with high selectivity and yield.

To investigate the substrate scope of the [3+2] annulation reaction, we initially synthesized a range of pyrazolonedione-derived MBH carbonates (**1a**–**1c**) and various 3-methyleneoxindole derivatives (**2a**–**2v**). Under the optimized reaction conditions, pyrazolonedione-derived MBH carbonates **1a**–**1c** reacted smoothly with a variety of 3-methyleneoxindoles **2a**–**2v** to afford the corresponding spiropyrazolone-oxindole derivatives **3a**–**3x** in good to excellent yields. The reactions exhibited exceptional diastereoselectivity with diastereomeric ratios exceeding >20:1 and afforded the desired products in excellent yields (98%, Scheme 2.7). Notably, all the substrates underwent the [3+2] annulation reaction by affording the corresponding spiropyrazolone-oxindole derivatives **3a**-**3x** featuring vicinal quaternary spirocenters under the optimized reaction conditions. It was observed that the presence of electron-donating groups

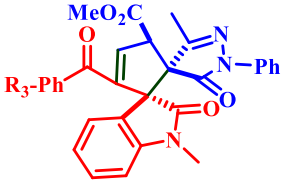
Scheme 2.7 Exploration of substrate scope for the [3+2] annulation reaction[a]



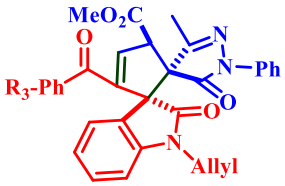
1a-1c 2a-2v 3a-3x



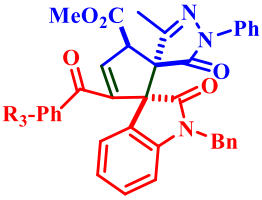
3a, R_2= Me, 92%, *dr* >20:1
3b, R_2= allyl, 98%, *dr* >20:1
3c, R_2= Bn, 76%, *dr* >20:1



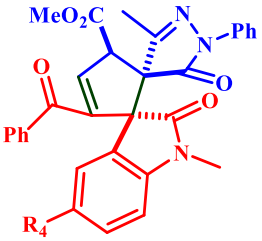
3d, R_3= 4-Me, 86%, *dr* >20:1
3e, R_3= 4-Br, 86%, *dr* >20:1



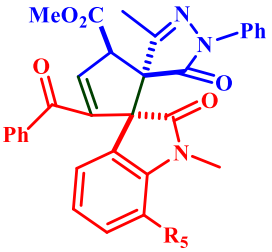
3f, R_3= 4-Me, 96%, *dr* >20:1
3g, R_3= 4- Br, 77%, *dr* >20:1



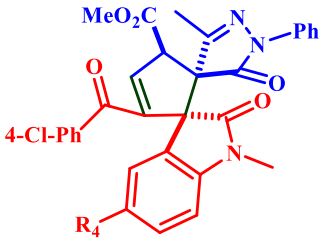
3h, R_3= 4-Cl, 88%, *dr* >20:1
3i, R_3= 4-Br, 73%, *dr* >20:1



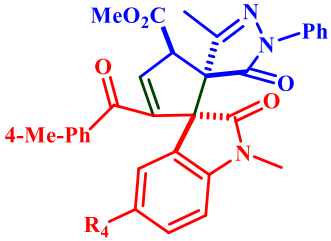
3j, R_4=F, 95%, *dr* >20:1
3k, R_4= Br, 86%, *dr* >20:1
3l, R_4= Cl, 77%, *dr* >20:1



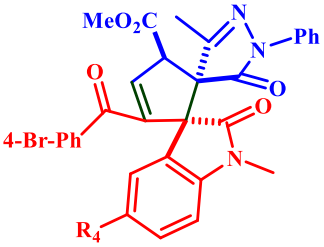
3m, R_5= F, 88%, *dr* >20:1



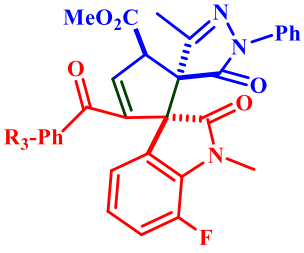
3n, R_4=F, 79%, *dr* >20:1
3o, R_4= Br, 79%, *dr* >20:1
3p, R_4= Cl, 96%, *dr* >20:1



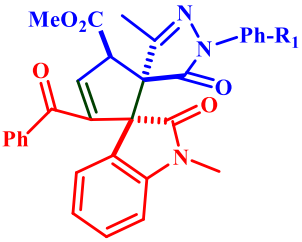
3q, R_4=F, 81%, *dr* >20:1
3r, R_4= Br, 72%, *dr* >20:1
3s, R_4= Cl, 96%, *dr* >20:1



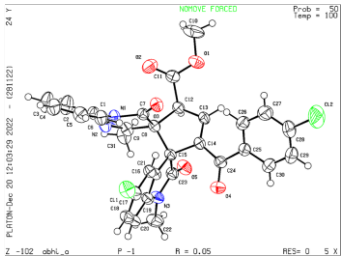
3t, R_4=F, 83%, *dr* >20:1



3u, R_3= 4-Me, 77%, *dr* >20:1
3v, R_3= 4-Cl, 82%, *dr* >20:1



3w, R_1=Cl, 89%, *dr* >20:1
3x, R_1= Me, 90%, *dr* >20:1



(Molecular Structure of compound **3p**)

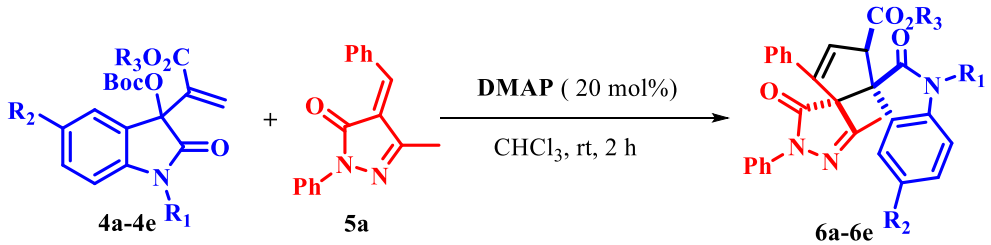
CCDC-2189452

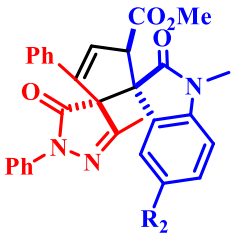
[a]**Reaction Conditions:** Unless otherwise specified, reactions were conducted with **1a-1c** (0.094 mmol), **2a-2v** (0.112 mmol), and the **DMAP** (20 mol%) in chloroform at room temperature for 24 hours. [b]Yields represent isolated products obtained after purification via

column chromatography. [c]Diastereomeric ratios were determined through ^{1}H NMR spectroscopy.

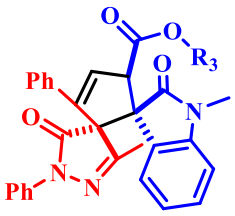
(EDG) as well as electron-deactivating groups (e.g., Br, Cl, F) on the 3-methyleneoxindoles **2** had no significant impact either on the yield or on the diastereoselectivity of the spirooxindole products. Additionally, 3-methyleneoxindoles with *N*-allyl or *N*-benzyl protecting groups participated efficiently in the reaction, affording the spirooxindole-fused pyrazolones in excellent yields with high Diastereoselectivity (Scheme 2.7). Furthermore, the molecular structure of compound **3p** was unequivocally confirmed through single-crystal X-ray diffraction analysis (Scheme 2.7).[19]

Scheme 2.8 Exploration of substrate scope for the [3+2] annulation reaction of MBH carbonate of isatin and arylidene pyrazolone [a]

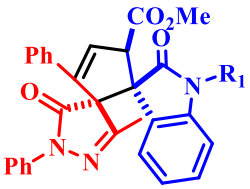




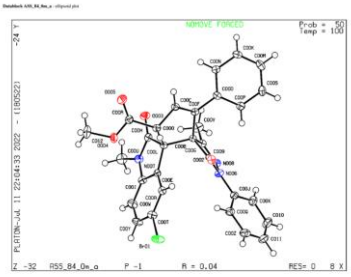
6a, R_2= H, 94%, *dr* >96:4
6b, R_2=Br, 94%, *dr* >97:3
6c, R_2= F, 94%, *dr* >95:5



6d, R_3=^{t}Bu, 91%, *dr* >20:1



6e, R_1=Bn, 98%, *dr* >91:9



(Molecular Structure of compound **6b**)

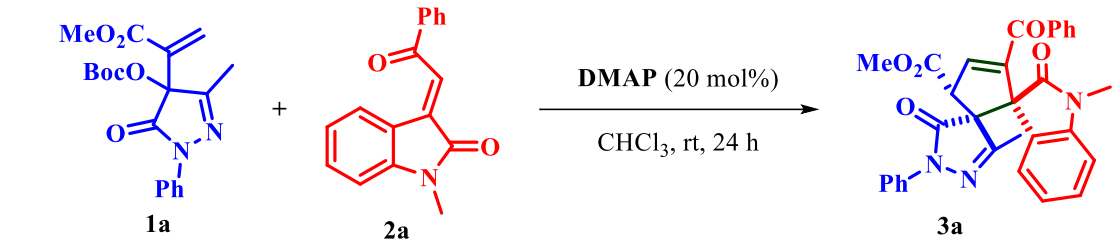
CCDC-2183100

[a]**Reaction Conditions:** Unless otherwise specified, reactions were conducted with **4a-4e** (0.115 mmol), **5a** (0.138 mmol), and the **DMAP** (20 mol%) in chloroform at room temperature

for 24 hours. [b]Yields represent isolated products obtained after purification via column chromatography. [c]Diastereomeric ratios were determined through ^{1}H NMR spectroscopy.

Inspired by the promising result, we further extended the approach to employ MBH carbonates derived from isatin for the construction of spirooxindole-pyrazolone derivatives **6a**-**6e** via [3+2] cycloaddition reaction. To the best of our knowledge, the utilization of arylidene pyrazolones **5a** for the synthesis of spiropyrazolone-fused oxindole compounds bearing adjacent quaternary spirocenters has not been reported to date. In this context, MBH carbonates of isatin (**4a**–**4e**) were synthesized and subsequently treated with arylidene pyrazolone **5a** under the optimized reaction conditions (Scheme 2.8). Gratifyingly, all reactions proceeded efficiently, affording the corresponding highly functionalized spiropyrazolone-fused oxindole derivatives (**6a**–**6e**) in excellent yields with excellent diastereoselectivity (up to 98% yield, *dr* ranging from 91:9 to 99:1, Scheme 2.8). The molecular structure of compound **6b** was unambiguously confirmed by single-crystal X-ray diffraction analysis (Scheme 2.8).[20] Additionally, the structures of all other products were inferred based on analogy and corroborated by detailed spectroscopic data.

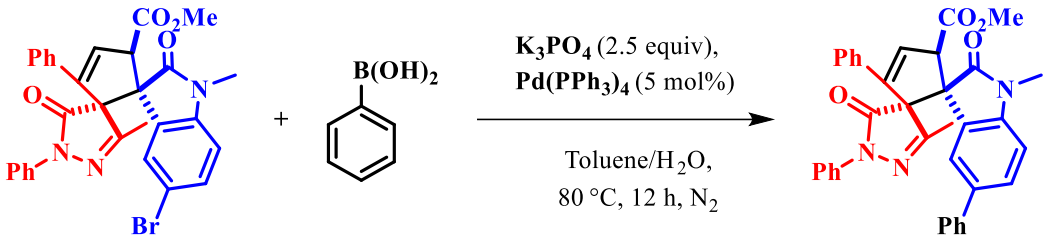
To validate the practicality of this [3+2] annulation protocol, we explored the scaled-up reaction of pyrazolonedione-derived MBH carbonate **1a** and 3-methyleneoxindole **2a** under the optimized conditions to afford the spirooxindole **3a** in an isolated yield of 83% (Scheme 2.9).



Scheme 2.9 Scale up synthesis

To illustrate the synthetic potential of the developed protocol, a Suzuki coupling was carried out using compound **6b**. The reaction of phenylboronic acid **7** with spirooxindole-fused pyrazolone **6b** in the presence of $Pd(PPh_3)_4$ and K_3PO_4 at 80 °C successfully furnished the corresponding product **8a** in very good yield with high diastereoselectivity (80%, Scheme 2.10a).

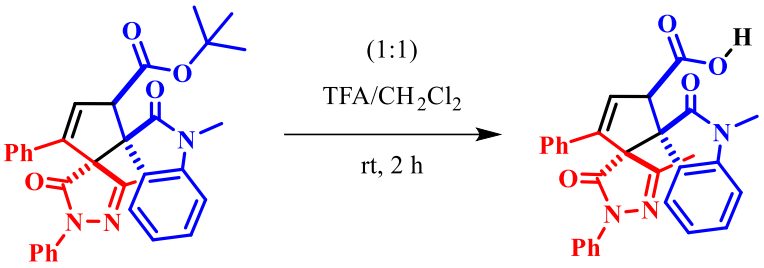
[a] Suzuki coupling



6b **7** **8a**

80%, *dr* > 97:3

[b] Hydrolysis



6d **9a**

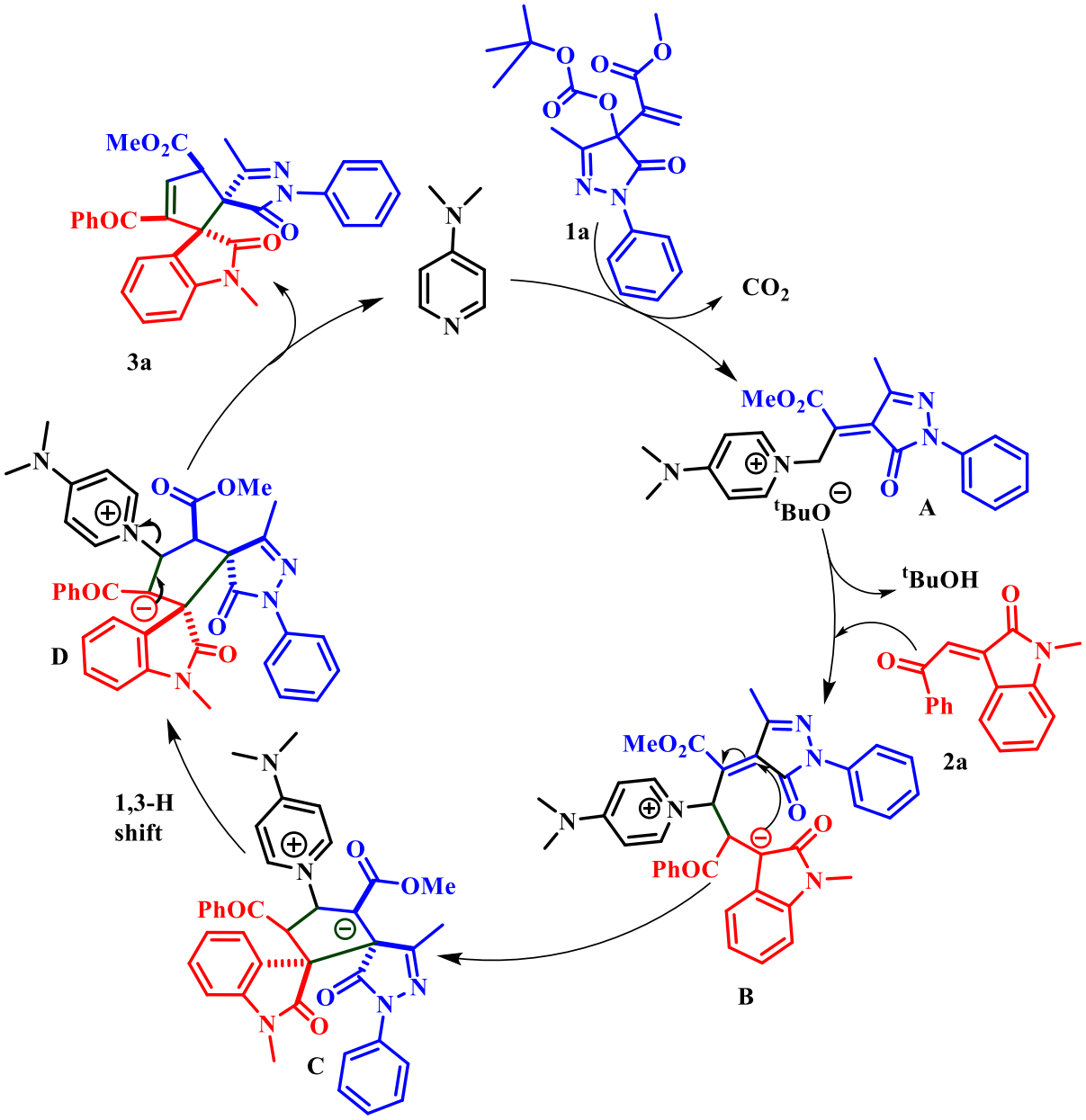
94%, *dr* >20:1

Scheme 2.10 Synthetic modifications

Additionally, the treatment of compound **6d** with a mixture of trifluoroacetic acid (TFA) and dichloromethane (DCM) in a 1:1 (v/v) ratio successfully afforded the corresponding carboxylic acid derivative **9a** in excellent yield (94%, Scheme 2.10b)

Based on our experimental findings and prior literature reports[15, 17, 21] a plausible catalytic cycle for the [3+2] cycloaddition reaction has been outlined (Scheme 2.11).

The catalytic cycle begins with the nucleophilic attack of DMAP on the pyrazolonedione-derived MBH carbonate **1a**, resulting in the formation of quaternary ammonium salt **A** and the release of tert-butoxide anion and carbon dioxide. The tert-butoxide anion, acting as a Brønsted base, subsequently abstracts a proton from the substrate **A**, generating an allylic nitrogen ylide. This reactive intermediate undergoes nucleophilic addition at the α-position of 3-methyleneoxindole **2a**, leading to the formation of intermediate **B**. An intramolecular Michael addition then occurs, yielding the cyclic intermediate **C**. The process concludes with a 1,3-proton shift to form intermediate **D**, which undergoes final reorganization to furnish the spirooxindole product **3a** while regenerating the catalyst (Scheme 2.11).



Scheme 2.11 Proposed reaction mechanism for the [3+2] annulation

2.5 Conclusions

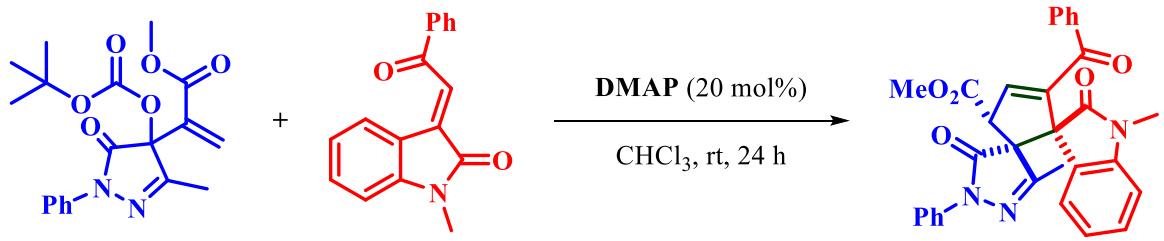
In conclusion, we have developed an efficient [3+2] annulation protocol involving Morita-Baylis-Hillman (MBH) carbonates of pyrazolonedione and 3-methyleneoxindoles under mild reaction conditions. 4-dimethylaminopyridine (DMAP) proved to be an efficient catalyst for the synthesis of highly functionalized and medicinally significant spiro-heterocyclic compounds. The method also successfully gave access to spirooxindole-pyrazolone-fused cyclopentene derivatives featuring two adjacent spiro-quaternary centers in excellent yields with outstanding diastereoselectivity.

2.6 Experimental Section

2.6.1 General

Unless otherwise specified, all reagents were purchased from commercial suppliers and used as received without further purification. HPLC-grade solvents were obtained from RANKEM. Reactions were performed in glassware that had been dried in an oven. Thin-layer chromatography (TLC) was conducted on silica gel 60 GF254 pre-coated aluminum-backed plates (2.5 mm), with visualization achieved by UV light irradiation at 254 nm. Phosphomolybdic acid (PMA) solution was utilized for staining the products. Column chromatography was performed using silica gel (100-200 mesh), and elution was carried out with a mixture of petroleum ether and ethyl acetate. Nuclear magnetic resonance (NMR) spectra were recorded with tetramethylsilane (TMS) as the internal standard. ^{1}H NMR spectra were acquired at 400 MHz, while ^{13}C{^{1}H} NMR spectra were recorded at 100 MHz using Bruker and Jeol instruments. Chemical shifts (δ) are reported in parts per million (ppm) relative to $CDCl_3$ (δ = 7.26 ppm) for ^{1}H NMR and the central resonance of $CDCl_3$ (δ = 77.16 ppm) for ^{13}C{^{1}H} NMR. Coupling constants (J) are expressed in hertz (Hz), and integrations were performed. Melting points were determined using a BUCHI M-560 melting point apparatus, measured in open glass capillaries, and uncorrected values were reported. Substrates **1a**–**1c** were synthesized following the procedure outlined in the literature,[22] while substrates **2a**–**2v** were prepared based on the methods described in the literature.[10,11,12]

2.6.2 General procedure for the synthesis of spiro-pyrazolone fused oxindole:

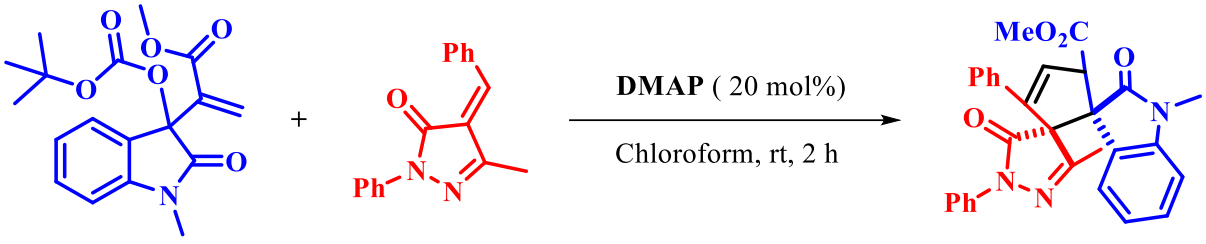


1a **2a** **3a**

In an oven-dried round-bottom flask, a mixture of Methyl-2-(4-((tert-butoxycarbonyl)oxy)-3-methyl-5-oxo-1-phenyl-4,5-dihydro-1H-pyrazol-4-yl)acrylate **1a** (35 mg, 0.094 mmol), (*E*)-1-methyl-3-(2-oxo-2-phenylethylidene)indolin-2-one **2a** (24 mg, 0.112 mmol), and DMAP (20 mol%) (2.28 mg, 0.019 mmol) in chloroform (2 mL) was stirred at room temperature for 24

hours. The progress of the reaction was monitored by thin-layer chromatography (TLC). Upon completion, the solvent was removed under reduced pressure, and the crude product was purified directly by column chromatography on silica gel (100-200 mesh), using a petroleum ether/ethyl acetate mixture (70:30) as the eluent. The desired product **3a** was obtained as a brown solid (45 mg, 92% yield, >20:1 diastereomeric ratio).

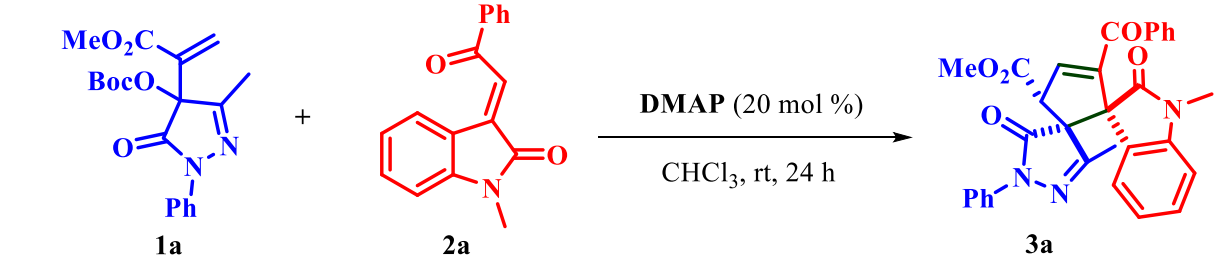
2.6.3 General procedure for the synthesis of spiroxindole fused pyrazolone:



4a **5a** **6a**

In an oven-dried round-bottom flask, a mixture of methyl 2-(3-((tert-butoxycarbonyl)oxy)-1-methyl-2-oxoindolin-3-yl)acrylate **4a** (40 mg, 0.115 mmol), (*Z*)-4-benzylidene-5-methyl-2-phenyl-2,4-dihydro-3H-pyrazol-3-one **5a** (36.3 mg, 0.138 mmol), and DMAP (20 mol%) (2.81 mg, 0.023 mmol) in chloroform (2 mL) was stirred at ambient temperature for 2 hours. The reaction's progress was monitored by thin-layer chromatography (TLC). After the reaction was complete, as confirmed by TLC, the solvent was removed under reduced pressure. The crude mixture was then subjected to column chromatography over silica gel (100-200 mesh), using a petroleum ether/ethyl acetate mixture (70:30) as the eluent. The purified product **6a** was obtained as a white solid (53 mg, 94% yield, 90:10 diastereomeric ratio).

2.6.4 Procedure for the synthesis of 3a on mmol scale:



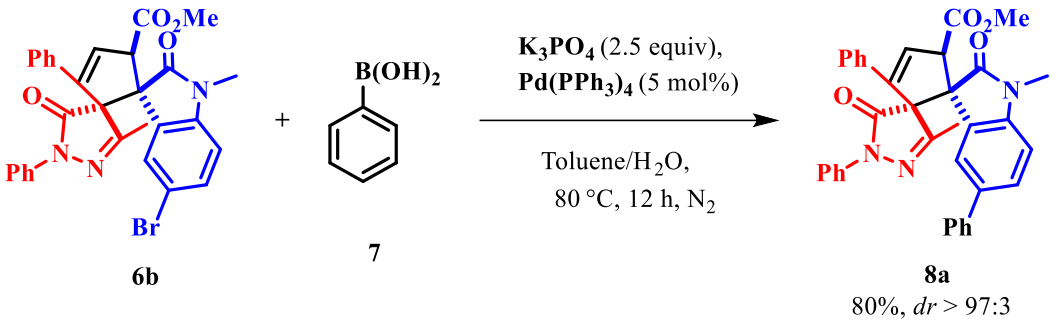
1a (400 mg, 1.07 mmol) **2a** (333 mg, 1.28 mmol) **3a** 83%, *dr* >20:1

In a reaction vessel, morita-Baylis-Hillman carbonate **1a** (400 mg, 1.07 mmol) was dissolved in chloroform (15 mL). To this solution, 3-methyleneoxindole **2a** (333 mg, 1.28 mmol) and DMAP (26.11 mg, 214 µmol) were added sequentially at room temperature. The reaction

mixture was stirred continuously for 24 hours. Upon completion of the reaction, as confirmed by thin-layer chromatography (TLC), the solvent was removed under reduced pressure. The crude residue was purified by column chromatography on silica gel (100–200 mesh) using a petroleum ether/ethyl acetate mixture (70:30) as the eluent. The desired product, **3a**, was obtained as a brown solid with a yield of 83% (460 mg).

2.6.5 Synthetic Transformations:

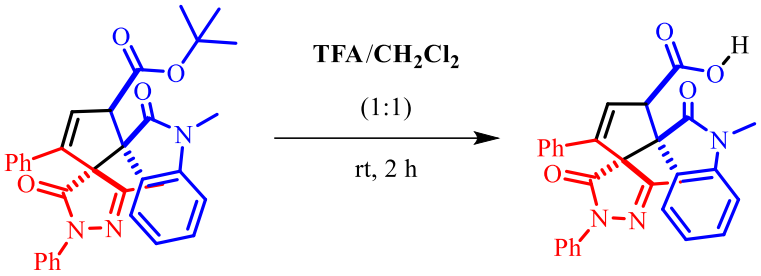
[a] Procedure for the Synthesis of Compound 8a



A solution of compound **6b** (50 mg, 1.0 equivalent) in a mixture of toluene (1 mL) and water (0.3 mL) was prepared at room temperature. Phenylboronic acid **7** (16.0 mg, 1.5 equivalents), $Pd(PPh_3)_4$ (6.1 mg, 0.06 equivalents), and K_3PO_4 (46.5 mg, 2.5 equivalents) were added sequentially under a nitrogen atmosphere. The reaction mixture was heated to 80 °C and stirred continuously at this temperature for 12 h, with the reaction progress monitored by thin-layer chromatography (TLC). After completion of the reaction, it was cooled to room temperature, and the reaction mixture was filtered through a Celite bed. The solvent was removed under reduced pressure, and the resulting crude residue was purified by column chromatography on silica gel (100-200 mesh) to furnish the desired compound **8a** as a white solid (40 mg, 80% isolated yield, 97:3 diastereomeric ratio).

[b] Procedure for the Synthesis of Compound 9a

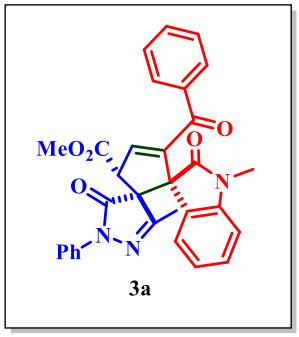
Ester **6d** (50 mg, 93.70 µmol) was dissolved in dichloromethane (2 mL), and trifluoroacetic acid (2 mL) was added to the solution. The reaction mixture was stirred at ambient temperature for 2 hours. The solvent was removed under reduced pressure upon completion, and the residue was partitioned between dichloromethane and water. The aqueous layer was extracted twice



with dichloromethane (10 mL each). The combined organic extracts were dried over anhydrous sodium sulfate, filtered, and concentrated under a vacuum to obtain the target compound **9a** as a white solid (42 mg, 94% yield).

2.7 Experimental Data

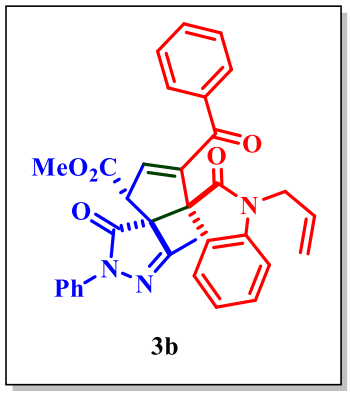
Methyl -3'-benzoyl-1, 3''-dimethyl-2, 5''-dioxo-1''-phenyl-1'', 5''-dihydrodispiro [indoline-3, 2'-cyclopentane-1', 4''-pyrazol]-3'-ene-5'-carboxylate (3a)



3a

Brown solid (45 mg, 92% yield). R_f = 0.5 (petroleum ether/EtOAc 70:30). MP: 78-80 °C. ^{1}H NMR (400 MHz, $CDCl_3$): δ 8.0 (d, *J* = 7.0 Hz, 2H), 7.6 (m, 3H), 7.5 – 7.4 (m, 2H), 7.4 – 7.3 (m, 3H), 7.2 – 7.1 (m,2H), 7.1 (d, *J* = 2.2 Hz, 1H), 6.8 (d, *J* = 25.2 Hz, 2H), 4.9 (d, *J* = 2.3 Hz, 1H), 3.7 (s, 3H), 3.3 (s, 3H), 2.2 (s, 3H); ^{13}C {^{1}H} NMR (100 MHz, $CDCl_3$): δ 190.9, 174.1, 172.5, 169.1, 156.5, 144.7, 143.3, 142.8, 137.3, 136.8, 133.6, 130.1, 129.9, 128.9, 128.8, 125.9, 125.0, 124.0, 123.4, 119.7, 108.6, 67.2, 65.0, 53.8, 53.0, 26.9, 15.9; HRMS: (ESI TOF) *m/z* calcd for $C_{31}H_{26}N_3O_5$ $[M + H]^+$ 520.1872, found 520.1876.

Methyl -1-allyl-3'-benzoyl-3''-methyl-2, 5''-dioxo-1''-phenyl-1'', 5''-dihydrodispiro[indoline-3, 2'-cyclopentane-1', 4''-pyrazol]-3'-ene-5'-carboxylate (3b)

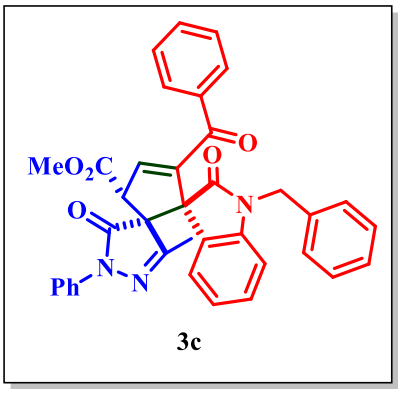


3b

Brown solid (50 mg, 98% yield). R_f = 0.5 (petroleum ether/EtOAc 70:30). MP: 154-156 °C. ^{1}H NMR (400 MHz, $CDCl_3$): δ 8.0 – 7.9 (m, 2H), 7.6 – 7.5 (m, 3H), 7.5 (d, *J* = 7.8 Hz, 2H), 7.4 – 7.3 (m, 3H), 7.2 (s, 2H), 7.1 (d, *J* = 2.2 Hz, 1H), 6.8 (m, 2H), 6.0 – 5.9 (m, 1H), 5.5 – 5.3 (m, 2H), 4.9 (d, *J* = 2.2 Hz, 1H), 4.5 – 4.4 (m, 2H), 3.7 (s, 3H), 2.2 (s, 3H); ^{13}C{ ^{1}H} NMR (100 MHz, $CDCl_3$): δ 190.9, 174.0, 172.5, 169.1, 156.9, 144.0, 143.3, 142.8, 137.3, 137.0, 133.5, 130.7, 129.9, 129.9, 128.9, 128.8, 125.7, 125.1, 124.0, 123.2, 119.9, 118.2, 109.6, 67.2, 65.0, 53.8, 42.9, 16.1; HRMS: (ESI TOF) *m/z* calcd for $C_{33}H_{28}N_3O_5$ $[M + H]^+$ 546.2029, found 546.2025.

Methyl-3'-benzoyl-1-benzyl-3''-methyl-2, 5''-dioxo-1''-phenyl-1'', 5''-dihydrodispiro[indoline-3, 2'-cyclopentane-1', 4''-pyrazol]-3'-ene-5'-carboxylate (3c)

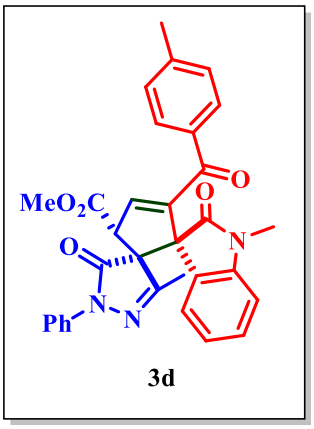
Red solid (45 mg, 76% yield). R_f = 0.5 (petroleum ether/EtOAc 70:30). MP: 173-175 °C. ^{1}H NMR (400 MHz, $CDCl_3$): δ 8.0 (m, 2H), 7.6 (m, 3H), 7.5 (s, 2H), 7.5 – 7.4 (m, 2H), 7.4 – 7.3 (m, 6H), 7.2 (s, 1H), 7.0 (d, *J* = 2.2 Hz, 1H), 7.1 (d, *J* = 1.3 Hz, 1H), 6.8 (d, *J* = 1.0 Hz, 1H), 6.7 (s, 1H), 5.2 (d, *J* = 16.0 Hz, 1H), 5.0 – 4.9 (m, 2H), 3.7 (s, 3H), 2.1 (s, 3H); ^{13}C {^{1}H} NMR



3c

(100 MHz, $CDCl_3$): δ 190.8, 174.3, 172.5, 169.2, 156.7, 144.1, 143.2, 142.8, 137.3, 136.9, 135.1, 133.5, 129.9, 129.9, 129.0, 128.9, 128.8, 127.8, 127.2, 125.7, 125.2, 124.0, 123.3, 119.9, 109.7, 67.2, 65.0, 53.7, 52.9, 43.8, 15.8; HRMS: (ESI TOF) *m/z* calcd for $C_{37}H_{30}N_3O_5$ $[M + H]^+$ 596.2185, found 596.2188.

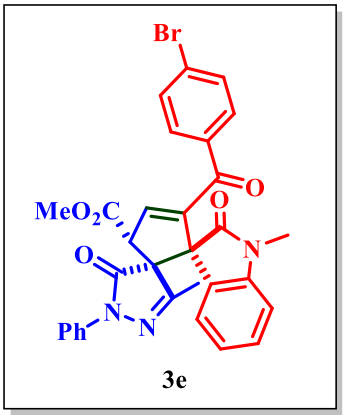
Methyl -1, 3''-dimethyl-3'-(4-methylbenzoyl)-2, 5''-dioxo-1''-phenyl-1'', 5''-dihydrodispiro[indoline-3, 2'-cyclopentane-1', 4''-pyrazol]-3'-ene-5'-carboxylate (3d)



3d

Brown solid (43 mg, 86% yield). R_f = 0.5 (petroleum ether/EtOAc 70:30). MP: 230-232 °C. ^{1}H NMR (400 MHz, $CDCl_3$): δ 7.9 (d, *J* = 8.2 Hz, 2H), 7.6 (m, 2H), 7.3 (s, 3H), 7.3 (m, 2H), 7.2 (m, 2H), 7.1 (d, *J* = 2.2 Hz, 1H), 6.8 (m, 2H), 4.9 (s, 1H), 3.7 (s, 3H), 3.3 (s, 3H), 2.4 (s, 3H), 2.2 (s, 3H); ^{13}C{^{1}H} NMR (100 MHz, $CDCl_3$): δ 190.5, 174.1, 172.4, 169.1, 156.6, 144.7, 144.4, 142.8, 142.6, 137.3, 134.4, 130.0, 129.4, 128.9, 128.8, 125.7, 125.0, 124.0, 123.2, 119.8, 108.5, 67.1, 65.0, 53.7, 52.9, 26.8, 21.8, 15.8; HRMS: (ESI TOF) *m/z* calcd for $C_{32}H_{28}N_3O_5$ $[M + H]^+$ 534.2029, found 534.2029.

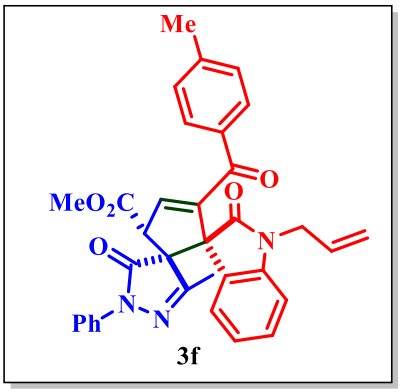
Methyl 3'-(4-bromobenzoyl)-1, 3''-dimethyl-2,5''-dioxo-1''-phenyl-1'', 5''-dihydrodispiro[indoline-3, 2'-cyclopentane-1', 4''-pyrazol]-3'-ene-5'-carboxylate (3e)



3e

Yellow solid (45 mg, 80% yield). R_f = 0.5 (petroleum ether/EtOAc 70:30). MP: 103-105 °C. ^{1}H NMR (400 MHz, $CDCl_3$): δ 7.8 (d, *J* = 8.5 Hz, 2H), 7.6 (dd, *J* = 9.2, 7.9 Hz, 4H), 7.4 – 7.3 (m, 3H), 7.2 (d, *J* = 1.3 Hz, 2H), 7.1 (d, *J* = 2.2 Hz, 1H), 6.8 (d, *J* = 7.8 Hz, 2H), 4.9 (d, *J* = 2.2 Hz, 1H), 3.7 (s, 3H), 3.3 (s, 3H), 2.2 (s, 3H); ^{13}C{^{1}H} NMR (100 MHz, $CDCl_3$): δ189.8, 173.9, 172.4, 169.0, 156.5, 144.7, 143.5, 142.5, 137.2, 135.6, 132.1, 131.3, 130.1, 128.9, 128.8, 125.7, 124.9, 123.8, 123.3, 119.8, 108.6, 67.1, 64.9, 53.7, 53.0, 26.9, 15.8; HRMS: (ESI TOF) *m/z* calcd for $C_{31}H_{25}BrN_3O_5$ $[M + H]^+$ 598.0977, found 598.0980.

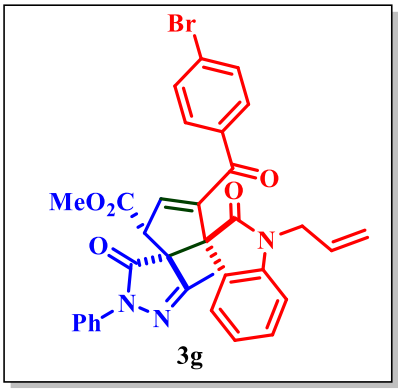
Methyl -1-allyl-3''-methyl-3'-(4-methylbenzoyl)-2, 5''-dioxo-1''-phenyl-1'', 5''-dihydrodispiro[indoline-3, 2'-cyclopentane-1', 4''-pyrazol]-3'-ene-5'-carboxylate (3f)



3f

Brown solid (50 mg, 96% yield). R_f = 0.5 (petroleum ether/EtOAc 70:30). MP: 202-204 °C. ^{1}H NMR (400 MHz, $CDCl_3$): δ 7.9 (d, *J* = 8.2 Hz, 2H), 7.7 – 7.6 (m, 2H), 7.4 (dd, *J* = 8.6, 7.5 Hz, 3H), 7.3 (m, 2H), 7.2 (m, 2H), 7.1 (d, *J* = 2.2 Hz, 1H), 6.8 – 6.7 (m, 2H), 5.9 (ddd, *J* = 12.2, 10.4, 5.2 Hz, 1H), 5.5 – 5.3 (m, 2H), 4.9 (d, *J* = 2.3 Hz, 1H), 4.5 (dd, *J* = 30.0, 5.0 Hz, 2H), 3.7 (s, 3H), 2.4 (s, 3H), 2.2 (s, 3H); ^{13}C{^{1}H} NMR (100 MHz, $CDCl_3$): δ 190.5, 174.0, 172.5, 169.3, 156.8, 144.5, 144.1, 142.9, 142.6, 137.3, 134.5, 130.7, 130.1, 129.9, 129.5, 128.9, 125.7, 125.2, 124.1, 123.2, 119.9, 118.2, 109.5, 67.2, 65.1, 53.7, 52.9, 42.9, 21.9, 16.1; HRMS (ESI TOF) *m/z* calcd for $C_{34}H_{30}N_3O_5$ $[M + H]^+$ 560.2185, found 560.2186.

Methyl -1-allyl-3'-(4-bromobenzoyl)-3''-methyl-2, 5''-dioxo-1''-phenyl-1'', 5''-dihydrodispiro[indoline-3,2'-cyclopentane-1', 4''-pyrazol]-3'-ene-5'-carboxylate (3g)

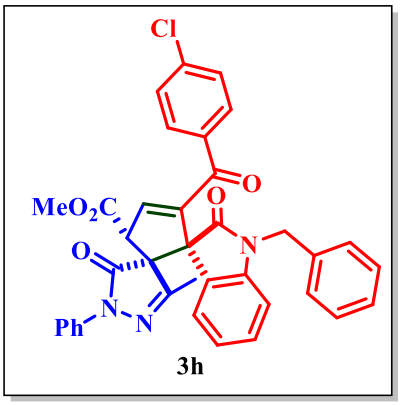


3g

Brown solid (45 mg, 77% yield). R_f = 0.5 (petroleum ether/EtOAc 70:30). MP: 157-159 °C. ^{1}H NMR (400 MHz, $CDCl_3$): δ 7.9 – 7.8 (m, 2H), 7.6 (m, 4H), 7.4 – 7.3 (m, 3H), 7.2 – 7.1 (m, 2H), 7.1 (d, *J* = 2.2 Hz, 1H), 6.9 – 6.7 (m, 2H), 5.9 (ddd, *J* = 22.1, 10.2, 5.0 Hz, 1H), 5.5 – 5.3 (m, 2H), 4.9 (d, *J* = 2.2 Hz, 1H), 4.5 – 4.4 (m, 2H), 3.7 (s, 3H), 2.2 (s, 3H); ^{13}C{^{1}H} NMR (100 MHz, $CDCl_3$): δ 189.8, 173.7, 172.4, 169.0, 156.6, 144.0, 143.5, 142.5, 137.2, 135.6, 132.1, 131.3, 130.5, 130.0, 128.9, 128.8, 125.8, 125.0, 123.8, 123.2, 119.8, 118.2, 109.6, 67.2, 64.9, 53.7, 53.0, 42.9, 16.0; HRMS (ESI TOF) *m/z* calcd for $C_{33}H_{27}BrN_3O_5$ $[M + H]^+$ 624.1134, found 624,1138.

Methyl 1-benzyl-3'-(4-chlorobenzoyl)-3''-methyl-2, 5''-dioxo-1''-phenyl-1'', 5''-dihydrodispiro[indoline-3, 2'-cyclopentane-1', 4''-pyrazol]-3'-ene-5'-carboxylate (3h)

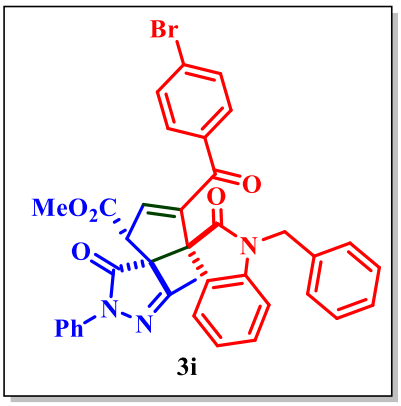
Grey solid (52 mg, 88% yield). R_f = 0.5 (petroleum ether/EtOAc 70:30). MP: 200-202 °C. ^{1}H NMR (400 MHz, $CDCl_3$): δ 8.0 – 7.9 (m, 2H), 7.6 (dd, *J* = 8.4, 1.3 Hz, 2H), 7.5 – 7.4 (m, 4H),



3h

7.4 (ddt, *J* = 12.7, 10.9, 7.2 Hz, 6H), 7.2 – 7.1 (m, 1H), 7.1 – 7.1 (m, 2H), 6.8 (td, *J* = 7.7, 1.0 Hz, 1H), 6.7 (d, *J* = 7.9 Hz, 1H), 5.2 (d, *J* = 15.9 Hz, 1H), 5.0 – 4.9 (m, 2H), 3.7 (s, 3H), 2.1 (s, 3H); $^{13}C\{^{1}H\}$ NMR (100 MHz, $CDCl_3$): δ 189.7, 174.1, 172.5, 169.1, 156.6, 144.1, 143.4, 142.6, 140.1, 137.2, 135.3, 135.1, 131.3, 130.1, 129.2, 129.0, 128.9, 127.9, 127.2, 125.8, 125.1, 123.9, 123.3, 119.9, 109.8, 67.3, 65.0, 53.7, 53.0, 44.5, 15.9; HRMS **(**ESI TOF) *m/z* calcd for $C_{37}H_{29}ClN_3O_5$ $[M + H]^+$ 630.1796, found 630.1794.

Methyl -1-benzyl-3'-(4-bromobenzoyl)-3''-methyl-2, 5''-dioxo-1''-phenyl-1'' ,5''-dihydrodispiro[indoline-3, 2'-cyclopentane-1', 4''-pyrazol]-3'-ene-5'-carboxylate (3i)

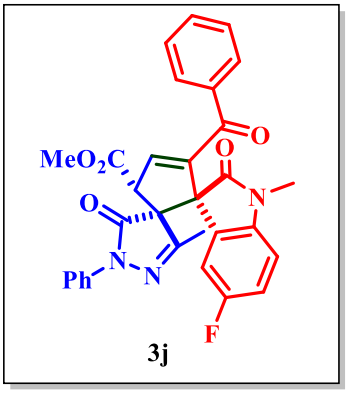


3i

Brown solid (45 mg, 76% yield). R_f = 0.5 (petroleum ether/EtOAc 70:30). MP: 206-208 °C. ^{1}H NMR (400 MHz, $CDCl_3$): δ 7.9 (d, *J* = 8.5 Hz, 2H), 7.7 – 7.6 (m, 4H), 7.5 – 7.3 (m, 8H), 7.2 (s, 1H), 7.1 (dd, *J* = 8.1, 1.7 Hz, 2H), 6.8 (d, *J* = 1.0 Hz, 1H), 6.7 (d, *J* = 7.9 Hz, 1H), 5.1 (d, 1H), 4.9 (m, *J* = 2.2 Hz, 2H), 3.7 (s, 3H), 2.1 (s, 3H); $^{13}C\{^{1}H\}$ NMR (100 MHz, $CDCl_3$): δ 189.9, 174.2, 172.5, 169.1, 156.7, 144.1, 143.5, 142.6, 137.3, 135.7, 135.1, 132.2, 131.4, 130.1, 129.1, 129.0, 128.9, 127.9, 127.2, 125.8, 125.1, 123.9, 123.4, 119.9, 109.8, 67.3, 65.0, 53.7, 53.0, 44.5, 15.9; HRMS: (ESI TOF) *m/z* calcd for $C_{37}H_{29}BrN_3O_5$ $[M + H]^+$ 674.1290, found 674.1298.

Methyl (1-3'-benzoyl-5-fluoro-1, 3''-dimethyl-2, 5''-dioxo-1''-phenyl-1'',5''-dihydrodispiro[indoline-3, 2'-cyclopentane-1', 4''-pyrazol]-3'-ene-5'-carboxylate (3j)

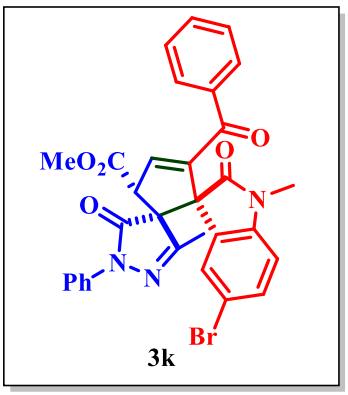
Brown solid (48 mg, 95% yield). R_f : (petroleum ether/EtOAc 70:30). MP: 98-100 °C. ^{1}H NMR (400 MHz, $CDCl_3$): δ 8.0 – 7.9 (m, 2H), 7.7 – 7.6 (m, 3H), 7.5 (dd, *J* = 8.3, 7.1 Hz, 2H), 7.4 – 7.3 (m, 2H), 7.2 (d, *J* = 7.4 Hz, 1H), 7.2 (dd, *J* = 8.1, 2.4 Hz, 2H), 6.9 (d, *J* = 2.6 Hz, 1H), 6.8 (dd, *J* = 8.6, 4.2 Hz, 1H), 4.9 (d, *J* = 2.3 Hz, 1H), 3.7 (s, 3H), 3.3 (s, 3H), 2.2 (s, 3H); $^{13}C\{^{1}H\}$ NMR (100 MHz, $CDCl_3$): δ 190.7, 173.9, 172.2, 169.0, 158.1, 156.5, 143.8, 141.6 (d, $J_{(C-F)}$ =



3j

158.0 Hz), 137.2, 136.8, 133.7, 129.8, 129.0, 128.9, 125.9, 125.7 (d, $J_{(C-F)}$ = 8.5 Hz), 119.7, 119.5, 116.4 (d, $J_{(C-F)}$ = 23.6 Hz), 113.4 (d, $J_{(C-F)}$ = 26.1 Hz), 109.1 (d, $J_{(C-F)}$ = 8.2 Hz), 67.0, 65.0, 53.9, 53.0, 27.0, 15.8; ^{19}F NMR (377 MHz, $CDCl_3$): δ -119.4; HRMS: (ESI TOF) *m/z* calcd for $C_{31}H_{25}FN_3O_5$ $[M + H]^+$ 538.1778, found 538.1774.

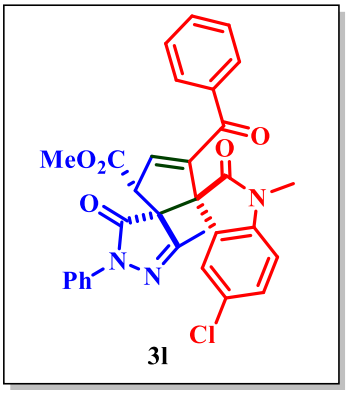
Methyl 3'-benzoyl-5-bromo-1,3''-dimethyl-2, 5''-dioxo-1''-phenyl-1'', 5''-dihydrodispiro[indoline-3, 2'-cyclopentane-1', 4''-pyrazol]-3'-ene-5'-carboxylate (3k)



3k

Gray solid (48 mg, 86% yield). R_f = 0.5 (petroleum ether/EtOAc 70:30); MP: 168-170 °C; ^{1}H NMR (400 MHz, $CDCl_3$): δ 8.0 (d, *J* = 6.9 Hz, 2H), 7.7 – 7.6 (m, 3H), 7.5 – 7.5 (m, 3H), 7.4 – 7.3 (m, 3H), 7.2 (d, *J* = 2.2 Hz, 2H), 6.7 (d, *J* = 8.3 Hz, 1H), 4.9 (d, *J* = 2.2 Hz, 1H), 3.7 (s, 3H), 3.3 (s, 3H), 2.2 (s, 3H); ^{13}C{^{1}H} NMR (100 MHz, CDCl3): δ 190.6, 173.6, 172.2, 169.0, 156.3, 144.1, 143.8, 142.2, 137.0, 136.7, 133.7, 132.9, 129.9, 129.1, 128.9, 128.2, 126.1, 126.0, 120.0, 116.0, 110.0, 66.9, 64.8, 53.7, 53.1, 27.0, 15.8; HRMS: (ESI TOF) *m/z* calcd for $C_{31}H_{25}BrN_3O_5$ $[M + H]^+$ 598.0978, found 598.0976.

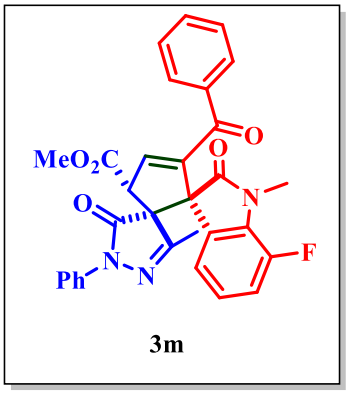
Methyl 3'-benzoyl-5-chloro-1, 3''-dimethyl-2, 5''-dioxo-1''-phenyl-1'', 5''-dihydrodispiro[indoline-3, 2'-cyclopentane-1' ,4''-pyrazol]-3'-ene-5'-carboxylate (3l)



3l

brown solid (40 mg, 77% yield). R_f = 0.5 (petroleum ether/EtOAc 70:30). MP: 108-110 °C. ^{1}H NMR (400 MHz, $CDCl_3$): δ 8.0 – 7.9 (m, 2H), 7.7 – 7.6 (m, 3H), 7.5 (s, 2H), 7.4 – 7.3 (m, 3H), 7.2 – 7.1 (m, 3H), 6.8 (d, *J* = 8.4 Hz, 1H), 4.9 (d, *J* = 2.2 Hz, 1H), 3.7 (s, 3H), 3.3 (s, 3H), 2.2 (s, 3H); ^{13}C{^{1}H} NMR (100 MHz, $CDCl_3$): δ 190.6, 173.6, 172.0, 168.8, 156.2, 144.0, 143.3, 142.2, 137.0, 136.7, 133.7, 130.0, 129.8, 129.0, 128.9, 128.7, 125.9, 125.7, 125.5, 119.9, 109.5, 66.8, 64.9, 53.7, 53.0, 27.0, 15.8; HRMS: (ESI TOF) *m/z* calcd for $C_{31}H_{25}ClN_3O_5$ $[M + H]^+$ 554.1483, found 554.1481.

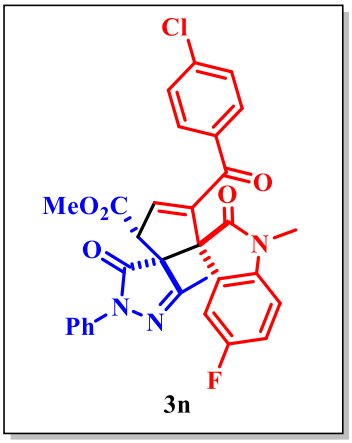
Methyl -3'-benzoyl-7-fluoro-1, 3''-dimethyl-2, 5''-dioxo-1''-phenyl-1'', 5''-dihydrodispiro[indoline-3, 2'-cyclopentane-1', 4''-pyrazol]-3'-ene-5'-carboxylate (3m)



3m

Brown solid (44 mg, 88% yield). R_f = 0.5 (petroleum ether/EtOAc 70:30). MP: 152-154 °C. ^{1}H NMR (400 MHz, $CDCl_3$): δ 8.0 – 7.9 (m, 2H), 7.7 – 7.6 (m, 3H), 7.5 – 7.5 (m, 2H), 7.4 – 7.3 (m, 2H), 7.2 – 7.1 (m, 3H), 6.9 (ddd, J = 11.5, 8.4, 1.1 Hz, 1H), 6.7 (ddd, J = 8.5, 7.6, 4.6 Hz, 1H), 4.9 (d, J = 2.2 Hz, 1H), 3.7 (s, 3H), 3.5 (s, 3H), 2.2 (s, 3H); ^{13}C{^{1}H} NMR (100 MHz, $CDCl_3$): δ 190.7, 172.9 (d, $J_{(C-F)}$ = 157.3 Hz), 169.0, 156.4, 147.7 (d, $J_{(C-F)}$= 243.8 Hz), 143.6, 142.4, 136.9 (d, $J_{(C-F)}$ = 64.6 Hz), 133.6, 131.5, 131.4, 129.8, 128.9, 128.8, 126.8, 126.8, 125.8, 123.7 (d, $J_{(C-F)}$ = 6.4 Hz), 120.9 (d, $J_{(C-F)}$ = 3.6 Hz), 119.7, 118.1 (d, $J_{(C-F)}$ = 18.9 Hz), 67.2, 65.0, 53.7, 53.0, 29.4 (d, $J_{(C-F)}$ = 6.2 Hz), 15.8; ^{19}F NMR: (377 MHz, $CDCl_3$) δ -135.9; HRMS: (ESI TOF) *m/z* calcd for $C_{31}H_{25}FN_3O_5$ $[M + H]^+$ 538.1778, found 538.1778.

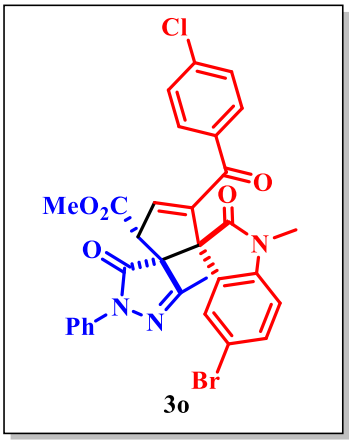
Methyl (3'-(4-chlorobenzoyl)-5-fluoro-1, 3''-dimethyl-2, 5''-dioxo-1''-phenyl-1'', 5''-dihydrodispiro[indoline-3, 2'-cyclopentane-1', 4''-pyrazol]-3'-ene-5'-carboxylate (3n)



3n

Red solid (42 mg, 79% yield). R_f = 0.5 (petroleum ether/EtOAc 70:30). MP: 78-80 °C. ^{1}H NMR (400 MHz, $CDCl_3$): δ 7.97 – 7.86 (m, 2H), 7.67 – 7.58 (m, 2H), 7.51 – 7.42 (m, 2H), 7.41 – 7.32 (m, 2H), 7.22 – 7.16 (m, 1H), 7.15 – 7.09 (m, 2H), 6.93 (td, J = 8.7, 2.6 Hz, 1H), 6.77 (dd, J = 8.6, 4.2 Hz, 1H), 4.91 (d, J = 2.3 Hz, 1H), 3.70 (s, 3H), 3.31 (s, 3H), 2.18 (s, 3H); ^{13}C{^{1}H} NMR (100 MHz, $CDCl_3$): δ 189.5, 173.7, 172.2, 168.9, 159.3 (d, $J_{(C-F)}$ = 241.9 Hz), 156.4, 144.0, 142.2, 140.8 (d, $J_{(C-F)}$ = 2.2 Hz), 140.3, 137.1, 135.1, 131.2, 129.3, 129.1, 126.0, 125.5 (d, $J_{(C-F)}$ = 8.6 Hz), 119.7, 116.5 (d, $J_{(C-F)}$ = 23.5 Hz), 113.3 (d, $J_{(C-F)}$ = 26.3 Hz), 109.2 (d, $J_{(C-F)}$ = 8.1 Hz), 67.0, 65.0, 53.9, 53.1, 27.1, 15.8; ^{19}F NMR (377 MHz, $CDCl_3$): δ -119.3; HRMS (ESI TOF) *m/z* calcd for $C_{31}H_{24}ClFN_3O_5$ $[M + H]^+$ 572.1388, found 572.1389.

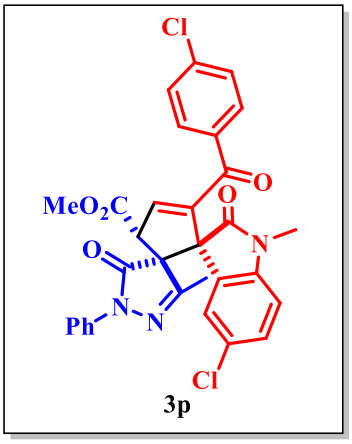
Methyl 5-bromo-3'-(4-chlorobenzoyl)-1, 3''-dimethyl-2, 5''-dioxo-1''-phenyl-1'', 5''-dihydrodispiro[indoline-3, 2'-cyclopentane-1', 4''-pyrazol]-3'-ene-5'-carboxylate (3o)



3o

Gray solid (47 mg, 79% yield). R_f = 0.5 (petroleum ether/EtOAc 70:30). MP: 172-174 °C. ^{1}H NMR (400 MHz, $CDCl_3$): δ 7.9 (d, *J* = 8.5 Hz, 2H), 7.6 (m, 2H), 7.5 – 7.4 (m, 3H), 7.4-7.3 (dd, *J* = 8.5, 7.5 Hz, 3H), 7.2 (s, 1H), 7.1 (d, *J* = 2.3 Hz, 1H), 6.7 (s, 1H), 4.9 (s, 1H), 3.7 (s, 3H), 3.3 (s, 3H), 2.2 (s, 3H). ^{13}C NMR{^{1}H} (100 MHz, $CDCl_3$): δ 189.4, 173.5, 172.2, 168.9, 156.3, 144.3, 143.8, 142.0, 140.3, 136.9, 134.9, 133.0, 131.2, 129.3, 129.0, 128.2, 126.1, 125.9, 120.0, 116.1, 110.1, 66.9, 64.8, 53.7, 53.1, 27.0, 15.8; HRMS: (ESI TOF) *m/z* calcd for $C_{31}H_{24}BrClN_3O_5$ [M + H]$^+$ 632.0588, found 632.0586.

Methyl 5-chloro-3'-(4-chlorobenzoyl)-1, 3''-dimethyl-2, 5''-dioxo-1''-phenyl-1'', 5''-dihydrodispiro[indoline-3, 2'-cyclopentane-1', 4''-pyrazol]-3'-ene-5'-carboxylate (3p)

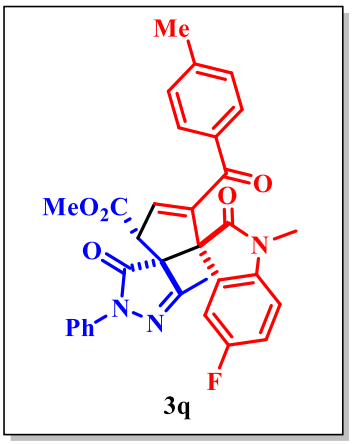


3p

Gray solid (53 mg, 96% yield). R_f = 0.5 (petroleum ether/EtOAc 70:30). MP: 169-171 °C. ^{1}H NMR (400 MHz, $CDCl_3$): δ 7.9 – 7.9 (m, 2H), 7.6 – 7.6 (m, 2H), 7.5 (d, *J* = 8.6 Hz, 2H), 7.4 – 7.3 (m, 3H), 7.2 (dd, *J* = 8.4, 2.0 Hz, 2H), 7.1 (s, 1H), 6.8 (d, *J* = 8.3 Hz, 1H), 4.9 (d, *J* = 2.3 Hz, 1H), 3.7 (s, 3H), 3.3 (s, 3H), 2.2 (s, 3H); ^{13}C{^{1}H} NMR (100 MHz, $CDCl_3$): δ 189.3, 173.4, 172.1, 168.7, 156.2, 144.1, 143.2, 141.9, 140.2, 136.8, 134.9, 131.1, 130.0, 129.2, 128.9, 128.7, 125.9, 125.4, 125.3, 119.9, 109.5, 66.7, 64.7, 53.6, 53.0, 26.9, 15.6; HRMS: (ESI TOF) *m/z* calcd for $C_{31}H_{24}Cl_2N_3O_5$ [M + H]$^+$ 588.1093, found 588.1094.

Methyl-5-fluoro-1,3''-dimethyl-3'-(4-methylbenzoyl)-2,5''-dioxo-1''-phenyl-1'',5'' dihydrodispiro[indoline-3,2'-cyclopentane-1',4''-pyrazol]-3'-ene-5'-carboxylate (3q)

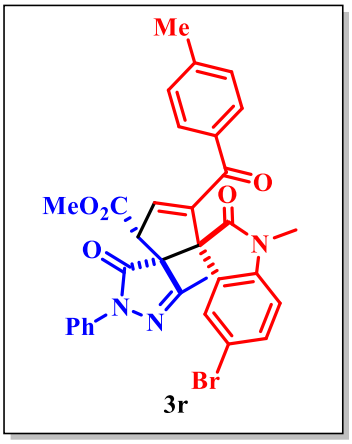
Red solid (42 mg, 81% yield). R_f = 0.5 (petroleum ether/EtOAc 70:30). MP: 207-209 °C. ^{1}H NMR (400 MHz, $CDCl_3$): δ 7.9 (d, *J* = 8.2 Hz, 2H), 7.7 – 7.6 (m, 2H), 7.4 – 7.3 (m, 2H), 7.3 (d, *J* = 8.0 Hz, 2H), 7.2 – 7.1 (m, 3H), 6.9 (td, *J* = 8.7, 2.6 Hz, 1H), 6.8 (dd, *J* = 8.6, 4.2 Hz, 1H), 4.9 (d, *J* = 2.2 Hz, 1H), 3.7 (s, 3H), 3.3 (s, 3H), 2.4 (s, 3H), 2.2 (s, 3H); ^{13}C{^{1}H} NMR (100 MHz, $CDCl_3$): δ 190.4, 173.9, 172.2, 169.0, 159.3(d, $J_{(C-F)}$ =241.6 Hz), 156.5, 144.7, 143.1, 142.5,



3q

140.8 (d, $J_{(C-F)}$ = 2 Hz), 137.2, 134.2, 129.9, 129.6, 129.0, 125.9, 125.8, 119.7, 119.5, 116.3 (d, $J_{(C-F)}$ = 23.7 Hz), 113.3 (d, $J_{(C-F)}$ = 26.1 Hz), 109.1 (d, $J_{(C-F)}$ = 8.3 Hz), 66.9, 65.0 (d, $J_{(C-F)}$ = 1.9 Hz), 53.9, 52.9, 27.0, 21.9, 15.8; ^{19}F NMR (377 MHz, $CDCl_3$): δ -119.51; HRMS: (ESI TOF) *m/z* calcd for $C_{32}H_{27}FN_3O_5$ $[M + H]^+$ 552.1934, found 552.1937.

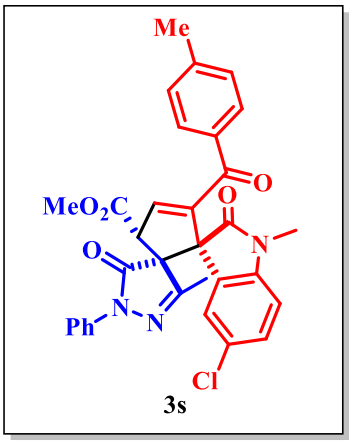
Methyl 5-bromo-1, 3''-dimethyl-3'-(4-methylbenzoyl)-2, 5''-dioxo-1''-phenyl-1'',5''-dihydrodispiro[indoline-3, 2'-cyclopentane-1', 4''-pyrazol]-3'-ene-5'-carboxylate (3r)



3r

Gray solid (41 mg, 72% yield). R_f = 0.5 (petroleum ether/EtOAc 70:30); MP: 196-198 °C; ^{1}H NMR (400 MHz, $CDCl_3$): δ 7.9 (d, *J* = 8.2 Hz, 2H), 7.6 (dd, *J* = 8.7, 1.2 Hz, 2H), 7.5 (d, *J* = 2.0 Hz, 1H), 7.4 – 7.3 (m, 5H), 7.2 (s, 1H), 7.1 (d, *J* = 2.2 Hz, 1H), 6.7 (d, *J* = 8.3 Hz, 1H), 4.9 (d, *J* = 2.2 Hz, 1H), 3.7 (s, 3H), 3.3 (s, 3H), 2.4 (s, 3H), 2.2 (s, 3H); ^{13}C{^{1}H} NMR (100 MHz, $CDCl_3$): δ 190.3, 173.7, 172.2, 169.0, 156.3, 144.7, 143.8, 143.3, 142.2, 137.1, 134.2, 132.9, 130.0, 129.6, 129.0, 128.2, 126.1, 126.0, 120.0, 116.0, 110.0, 66.8, 64.9, 53.7, 53.0, 27.0, 21.9, 15.8; HRMS: (ESI TOF) *m/z* calcd for $C_{32}H_{27}BrN_3O_5$ $[M + H]^+$ 612.1134, found 612.1136.

Methyl 5-chloro-1, 3''-dimethyl-3'-(4-methylbenzoyl)-2, 5''-dioxo-1''-phenyl-1'', 5''-dihydrodispiro [indoline-3, 2'-cyclopentane-1', 4''-pyrazol]-3'-ene-5'-carboxylate (3s)

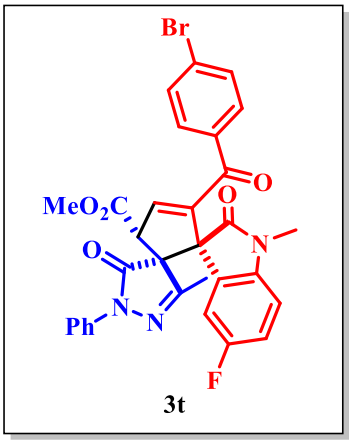


3s

Brown solid (51 mg, 96% yield). R_f = 0.5 (petroleum ether/EtOAc 70:30). MP: 182-184 °C. ^{1}H NMR (400 MHz, $CDCl_3$): δ 7.9 – 7.8 (m, 2H), 7.6 (dd, *J* = 8.7, 1.2 Hz, 2H), 7.4 (t, *J* = 1.6 Hz, 3H), 7.3 – 7.3 (m, 2H), 7.2 – 7.2 (m, 2H), 7.1 (d, *J* = 2.2 Hz, 1H), 6.8 (d, *J* = 8.4 Hz, 1H), 4.9 (d, *J* = 2.2 Hz, 1H), 3.7 (s, 3H), 3.3 (s, 3H), 2.4 (s, 3H), 2.2 (s, 3H); ^{13}C NMR{^{1}H} (100 MHz, $CDCl_3$): δ 190.3, 173.8, 172.2, 169.0, 156.4, 144.7, 143.4, 143.3, 142.3, 137.0, 134.2, 130.0, 130.0, 129.6, 129.0, 128.7, 126.0, 125.8, 125.5, 119.9, 109.5, 66.8, 64.9, 53.7, 53.0, 27.0,

21.9, 15.8; HRMS: (ESI TOF) *m/z* calcd for $C_{32}H_{27}ClN_3O_5$ $[M + H]^+$ 568.1639, found 568.1635.

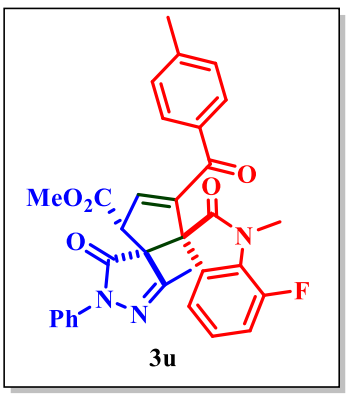
Methyl-3'-(4-bromobenzoyl)-5-fluoro-1,3''-dimethyl-2,5''-dioxo-1''-phenyl-1'',5'' dihydrodispiro[indoline-3,2'-cyclopentane-1',4''-pyrazol]-3'-ene-5'-carboxylate (3t)



3t

Red solid (48 mg, 83% yield). R_f = 0.5 (petroleum ether/EtOAc 70:30). MP: 105-107 °C. ^{1}H NMR (400 MHz, $CDCl_3$): δ 7.8 (d, *J* = 8.5 Hz, 2H), 7.7 – 7.6 (m, 4H), 7.4 (t, *J* = 7.9 Hz, 2H), 7.2 (t, *J* = 7.4 Hz, 1H), 7.1 (dt, *J* = 5.0, 2.7 Hz, 2H), 6.9 (td, *J* = 8.7, 2.6 Hz, 1H), 6.8 (dd, *J* = 8.6, 4.2 Hz, 1H), 4.9 (d, *J* = 2.2 Hz, 1H), 3.7 (s, 3H), 3.3 (s, 3H), 2.2 (s, 3H); ^{13}C{^{1}H} NMR (100 MHz, $CDCl_3$): δ 189.6, 173.6, 172.0, 168.7, 159.2 (d, $J_{(C-F)}$ = 241.9 Hz), 156.3, 143.9, 142.0, 140.7 (d, $J_{(C-F)}$ = 2.0 Hz), 136.9, 135.4, 132.1, 131.1, 128.9, 125.9, 125.4 (d, $J_{(C-F)}$ = 8.4 Hz), 119.6, 116.4 (d, $J_{(C-F)}$ = 23.7 Hz), 113.2 (d, $J_{(C-F)}$ = 26.1 Hz), 109.1 (d, $J_{(C-F)}$ = 8.2 Hz), 66.9, 64.8, 53.8, 52.9, 26.9, 15.7; ^{19}F NMR (377 MHz, $CDCl_3$): δ -119.25; HRMS: (ESI TOF) *m/z* calcd for $C_{31}H_{24}BN_3O_5$ $[M + H]^+$ 616.0883, found 616.0880.

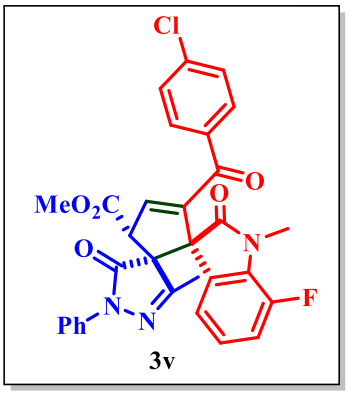
Methyl -7-fluoro-1, 3''-dimethyl-3'-(4-methylbenzoyl)-2, 5''-dioxo-1''-phenyl-1'', 5''-dihydrodispiro [indoline-3, 2'-cyclopentane-1', 4''-pyrazol]-3'-ene-5'-carboxylate (3u)



3u

Yellow solid (40 mg, 77% yield). R_f = 0.5 (petroleum ether/EtOAc 70:30). MP: 162-164 °C. ^{1}H NMR (400 MHz, $CDCl_3$): δ 7.9 – 7.8 (m, 2H), 7.6 (m, 2H), 7.4 – 7.3 (m, 2H), 7.3 (d, *J* = 8.0 Hz, 2H), 7.2 (s, 1H), 7.1 (m, 2H), 7.0 – 6.9 (m, 1H), 6.7 – 6.6 (m, 1H), 4.9 (d, *J* = 2.2 Hz,1H), 3.7 (s, 3H), 3.5 (s, 3H), 2.4 (s, 3H), 2.2 (s, 3H); ^{13}C{^{1}H} NMR (100 MHz, $CDCl_3$): δ 190.2, 172.9 (d, $J_{(C-F)}$ = 163.1 Hz), 169.0, 156.4, 147.6 (d, $J_{(C-F)}$ = 243.5 Hz), 144.5, 142.8, 142.5, 135.6 (d, $J_{(C-F)}$ = 301.0 Hz), 131.4, 131.3, 129.9, 129.4, 128.8, 126.8, 126.8, 125.6, 123.5 (d, $J_{(C-F)}$ = 6.5 Hz), 120.8 (d, $J_{(C-F)}$ = 3.4 Hz), 119.6, 118.0 (d, $J_{(C-F)}$ = 19.1 Hz), 67.0, 65.0, 53.6, 52.8, 29.3 (d, $J_{(C-F)}$ = 6.1 Hz), 21.8, 15.7; ^{19}F NMR (377 MHz, $CDCl_3$): δ -135.9; HRMS**:** (ESI TOF) *m/z* calcd for $C_{32}H_{27}FN_3O_5$ $[M + H]^+$ 552.1934, found 552.1938.

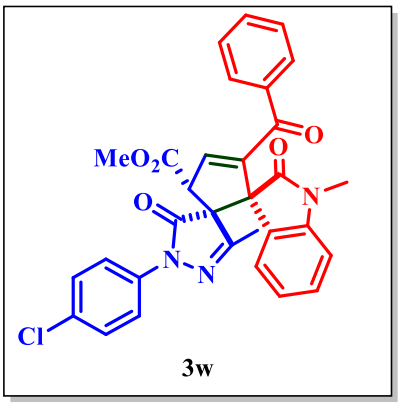
Methyl -3'-(4-chlorobenzoyl)-7-fluoro-1, 3''-dimethyl-2, 5''-dioxo-1''-phenyl-1'', 5''-dihydrodispiro[indoline-3, 2'-cyclopentane-1', 4''-pyrazol]-3'-ene-5'-carboxylate (3v)



3v

Red solid (44 mg, 82% yield). R_f = 0.5 (petroleum ether/EtOAc 70:30). MP: 164-166 °C. ^{1}H NMR (400 MHz, $CDCl_3$): δ 7.9 (m, 2H), 7.6 (m, 2H), 7.5 (d, *J* = 8.6 Hz, 2H), 7.3 (dd, *J* = 8.5, 7.5 Hz, 2H), 7.2 (s, 1H), 7.1 (m, 2H), 6.9 (ddd, *J* = 11.5, 8.6, 1.1 Hz, 1H), 6.7 (ddd, *J* = 8.5, 7.6, 4.6 Hz, 1H), 4.9 (d, *J* = 2.2 Hz, 1H), 3.7 (s, 3H), 3.5 (s, 3H), 2.2 (s, 3H); ^{13}C{^{1}H} NMR (100 MHz, $CDCl_3$): δ 189.5, 172.9 (d, $J_{(C-F)}$ = 147.2 Hz), 168.9, 156.4, 147.8 (d, $J_{(C-F)}$ = 248.0 Hz), 143.8, 142.3, 140.3, 136.1 (d, $J_{(C-F)}$ = 208.0 Hz), 131.5, 131.4, 131.2, 129.3, 129.0, 126.7 (d, $J_{(C-F)}$ = 3.2 Hz), 125.9, 123.8, 123.8, 120.9 (d, *J* = 3.2 Hz), 119.7, 118.2 (d, $J_{(C-F)}$ = 19.1 Hz), 67.2, 65.0, 53.7, 53.1, 29.5 (d, $J_{(C-F)}$ = 6.2 Hz), 15.6; ^{19}F NMR (377 MHz, $CDCl_3$): δ -135.7; HRMS: (ESI TOF) *m/z* calcd for $C_{31}H_{24}ClFN_3O_5$ [M + H]$^+$ 572.1388, found 572.1392.

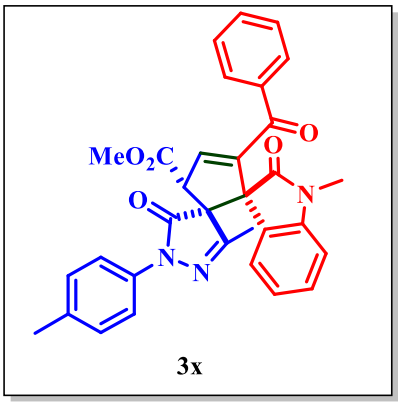
Methyl -3'-benzoyl-1''-(4-chlorophenyl)-1, 3''-dimethyl-2, 5''-dioxo-1'',5''-dihydrodispiro [indoline-3, 2'-cyclopentane-1', 4''-pyrazol]-3'-ene-5'-carboxylate (3w)



3w

Red solid (46 mg, 89% yield). R_f = 0.5 (petroleum ether/EtOAc 70:30). MP: 156-158 °C. ^{1}H NMR (400 MHz, $CDCl_3$): δ 8.0 – 7.9 (m,2H), 7.7 (m, 3H), 7.5 (s, 2H), 7.4 (dd, *J* = 3.0, 1.7 Hz, 3H), 7.2 (m, 3H), 6.8 (d, *J* = 8.4 Hz, 1H), 4.9 (d, *J* = 2.2 Hz, 1H), 3.7 (s, 3H), 3.3 (s, 3H), 2.2 (s, 3H). ^{13}C{^{1}H} NMR (100 MHz, $CDCl_3$): δ 190.6, 173.7, 172.2, 169.0, 156.4, 144.0, 143.3, 142.2, 137.0, 136.7, 133.7, 130.0, 129.9, 129.6, 128.9, 128.7, 126.0, 125.8, 125.5, 119.9, 109.5, 64.9, 66.9, 53.7, 53.0, 27.0, 15.8; HRMS: (ESI TOF) *m/z* calcd for $C_{31}H_{25}ClN_3O_5$ [M + H]$^+$ 554.1483, found 554.1483.

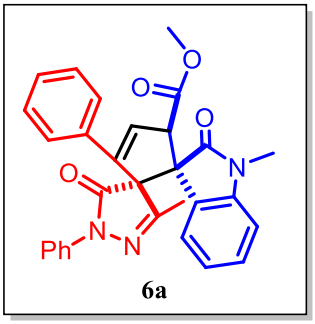
Methyl -3'-benzoyl-1, 3''-dimethyl-2, 5''-dioxo-1''-(p-tolyl)-1'', 5''-dihydrodispiro[indoline-3, 2'-cyclopentane-1', 4''-pyrazol]-3'-ene-5'-carboxylate (3x)



3x

Yellow solid (45 mg, 90% yield). R_f = 0.5 (petroleum ether/EtOAc 70:30). MP: 162-164 °C. ^{1}H NMR (400 MHz, $CDCl_3$): δ 8.0 – 8.0 (m, 2H), 7.6 – 7.5 (m, 1H), 7.5 – 7.4 (m, 4H), 7.3 (dd, *J* = 7.7, 1.2 Hz, 1H), 7.2 (d, *J* = 1.2 Hz, 1H), 7.2 – 7.1 (m, 3H), 6.9 – 6.8 (m, 2H), 4.9 (d, *J* = 2.2 Hz, 1H), 3.7 (s, 3H), 3.3 (s, 3H), 2.3 (s, 3H), 2.2 (s, 3H); ^{13}C{^{1}H} NMR (100 MHz, $CDCl_3$): δ 190.7, 174.0, 172.2, 169.1, 156.3, 144.6, 143.2, 142.7, 136.8, 135.4, 134.7, 133.4, 129.9, 129.8, 129.3, 128.7, 125.0, 124.0, 123.1, 119.8, 108.5, 67.0, 64.9, 53.6, 52.8, 26.8, 21.0, 15.7; HRMS: (ESI TOF) *m/z* calcd for $C_{32}H_{27}N_3O_5$ [M + H]$^+$ 534.2029, found 534.2031.

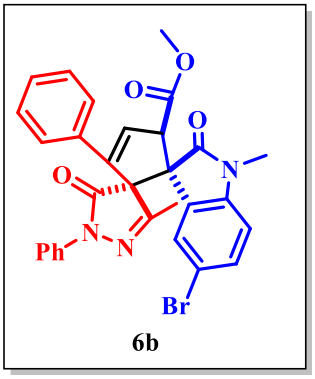
Methyl -1, 3''-dimethyl-2, 5''-dioxo-1'', 3'-diphenyl-1'', 5''-dihydrodispiro[indoline-3, 1'-cyclopentane-2', 4''-pyrazol]-3'-ene-5'-carboxylate (6a)



6a

White solid (53 mg, 94% yield). R_f = 0.4 (petroleum ether/EtOAc 70:30). MP: 254-256 °C. ^{1}H NMR (400 MHz, $CDCl_3$): δ 7.7 – 7.7 (m, 2H), 7.5 (dd, *J* = 7.7, 1.2 Hz, 1H), 7.4 (d, *J* = 1.2 Hz, 2H), 7.3 (d, *J* = 4.5 Hz, 1H), 7.3 – 7.2 (m, 3H), 7.2 (s, 1H), 7.1 – 7.1 (m, 2H), 6.9 – 6.9 (m, 2H), 6.8 (d, *J* = 7.9 Hz, 1H), 4.9 (d, *J* = 2.3 Hz, 1H),3.7 (s, 3H), 3.2 (s, 3H), 1.8 (s, 3H); ^{13}C{^{1}H} NMR (100 MHz, $CDCl_3$): δ 175.4, 171.7, 170.5, 158.7, 144.3, 139.6, 137.4, 133.8, 132.0, 129.8, 128.6, 128.5, 125.7, 125.5, 124.6, 124.5, 122.8, 119.8, 119.4, 108.3, 73.1, 62.3, 55.3, 52.4, 26.4, 16.3; HRMS: (ESI TOF) *m/z* calcd for $C_{30}H_{26}N_3O_4$ [M + H]$^+$ 492.1923, found 492.1928.

Methyl -5-bromo-1, 3''-dimethyl-2, 5''-dioxo-1'', 3'-diphenyl-1'', 5''-dihydrodispiro[indoline-3, 1'-cyclopentane-2', 4''-pyrazol]-3'-ene-5'-carboxylate (6b)

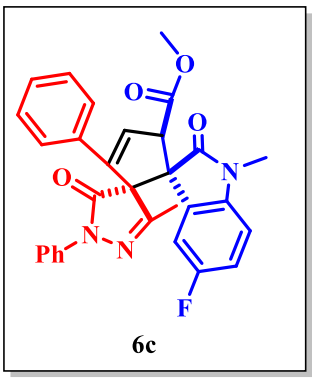


6b

Brown solid (62 mg, 94% yield). R_f = 0.4 (petroleum ether/EtOAc 70:30). MP: 260-262 °C. ^{1}H NMR (400 MHz, $CDCl_3$): δ 7.7 (m, 3H), 7.4 (dd, *J* = 8.5, 7.5 Hz, 2H), 7.4 (dd, *J* = 8.3, 2.0 Hz, 1H), 7.3 (d, *J* = 2.3 Hz, 3H), 7.2 (s, 1H), 7.2 – 7.1 (m,2H), 6.9 (d, *J* = 2.3 Hz, 1H), 6.7 (d, *J* = 8.3 Hz, 1H), 4.9 (d, *J* = 2.3 Hz, 1H), 3.7 (s, 3H), 3.2 (s, 3H), 1.8 (s, 3H); ^{13}C{^{1}H} NMR (100 MHz, $CDCl_3$): δ 174.9, 171.4, 170.3, 158.4, 143.4, 139.4, 137.1, 133.6, 132.7, 131.7, 129.1,

129.0, 128.6, 127.8, 126.6, 125.9, 125.4, 119.5, 115.6, 109.7, 72.9, 62.1, 55.3, 52.5, 26.5, 16.6; HRMS: (ESI TOF) *m/z* calcd for $C_{30}H_{25}BrN_3O_4$ $[M + H]^+$ 570.1028, found 570.1031.

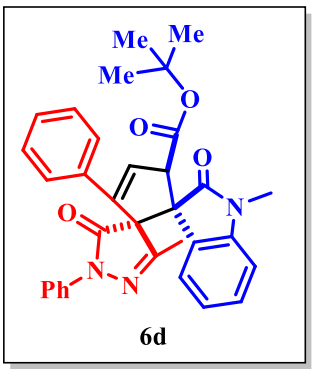
Methyl -5-fluoro-1, 3''-dimethyl-2, 5''-dioxo-1'', 3'-diphenyl-1'', 5''-dihydrodispiro[indoline-3, 1'-cyclopentane-2', 4''-pyrazol]-3'-ene-5'-carboxylate (6c)



6c

Brown solid (55 mg, 94% yield). R_f = 0.4 (petroleum ether/EtOAc 70:30). MP: 242-244 °C. ^{1}H NMR (400 MHz, $CDCl_3$): δ 7.8 – 7.7 (m, 2H), 7.4 (dd, *J* = 7.6, 1.0 Hz, 3H), 7.3 (d, *J* = 4.2 Hz, 2H), 7.3 – 7.2 (m, 2H), 7.1 (d, *J* = 3.6 Hz, 2H), 6.9 (td, *J* = 8.7, 2.7 Hz, 1H), 6.9 (d, *J* = 2.2 Hz, 1H), 6.7 (dd, *J* = 8.6, 4.2 Hz, 1H), 4.9 (d, *J* = 2.3 Hz, 1H), 3.7 (s, 3H), 3.2 (s, 3H), 1.8 (s, 3H); ^{13}C{^{1}H} NMR (100 MHz, $CDCl_3$): δ 175.1, 171.4, 170.2, 160.2, 158.2 (d, $J_{(C-F)}$ = 64.2 Hz), 140.3, 138.4 (d, $J_{(C-F)}$ = 235.3 Hz), 133.5, 131.7, 129.2, 129.0, 128.9, 128.6 (d, $J_{(C-F)}$ = 4.4 Hz), 125.7, 125.7, 125.4, 119.2, 116.0 (d, $J_{(C-F)}$ = 23.6 Hz), 112.9 (d, $J_{(C-F)}$ = 26.2 Hz), 108.7 (d, $J_{(C-F)}$ = 8.2 Hz), 72.9, 62.2, 55.4, 52.4, 26.5, 16.6; ^{19}F NMR (377 MHz, $CDCl_3$): δ -119.9; HRMS: (ESI TOF) *m/z* calcd for $C_{30}H_{25}FN_3O_4$ $[M + H]^+$ 510.1829, found 510.1830.

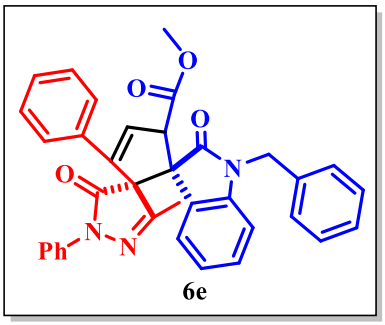
Tert-butyl -1, 3''-dimethyl-2, 5''-dioxo-1'', 3'-diphenyl-1'', 5''-dihydrodispiro[indoline-3,1 '-cyclopentane-2', 4''-pyrazol]-3'-ene-5'-carboxylate (6d)



6d

Yellow solid (54 mg, 91% yield). R_f = 0.4 (petroleum ether/EtOAc 70:30). MP: 177-179 °C. ^{1}H NMR (400 MHz, $CDCl_3$): δ 7.5 (dd, *J* = 7.7, 1.2 Hz, 1H), 7.4 (d, *J* = 2.0 Hz, 1H), 7.2 (d, *J* = 8.6 Hz, 5H), 7.2 – 7.1 (m, 5H), 7.1 – 7.0 (m, 1H), 6.9 (td, *J* = 7.7, 1.1 Hz, 1H), 6.8 (d, *J* = 7.7 Hz, 1H), 5.2 (d, *J* = 2.0 Hz, 1H), 3.3 (s, 3H), 2.3 (s, 3H), 1.1 (s, 9H); ^{13}C{^{1}H} NMR (100 MHz, $CDCl_3$): δ 174.8, 169.5, 161.8, 156.1, 146.6, 144.3, 138.9, 136.9, 135.0, 133.8, 129.3, 128.6, 128.5, 128.1, 126.7, 125.5, 123.3, 119.8, 108.2, 81.3, 73.2, 63.5, 53.4, 29.9, 27.8, 26.7, 16.1; HRMS: (ESI TOF) *m/z* calcd for $C_{33}H_{32}N_3O_4$ $[M + H]^+$ 534.2393, found 534.2389.

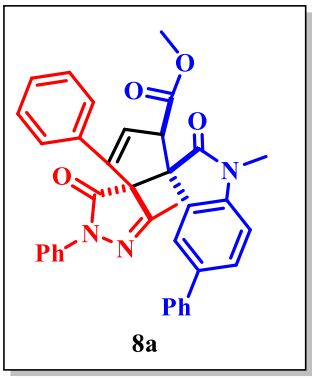
Methyl -1-benzyl-3''-methyl-2, 5''-dioxo-1'', 3'-diphenyl-1'', 5''-dihydrodispiro[indoline-3, 1'-cyclopentane-2', 4''-pyrazol]-3'-ene-5'-carboxylate (6e)



6e

Brown solid (64 mg, 98% yield). R_f = 0.5 (petroleum ether/EtOAc 70:30). MP: 263-264 °C. ^{1}H NMR (400 MHz, $CDCl_3$): δ 7.7 (dd, *J* = 8.8, 1.1 Hz, 2H), 7.6 – 7.5 (m, 1H), 7.4 (dd, *J* = 8.5, 7.5 Hz, 2H), 7.3 – 7.2 (m, 3H), 7.2 (s, 1H), 7.2 – 7.1 (m, 3H), 7.1 (dd, *J* = 4.4, 3.2 Hz, 2H), 6.9 – 6.8 (m, 2H), 6.8 (s, 1H), 5.9 – 5.7 (m, 1H), 5.4 – 5.2 (m, 2H), 4.9 (d, *J* = 2.3 Hz, 1H), 4.4 – 4.2 (m, 2H), 3.6 (s, 3H), 1.8 (s, 3H); ^{13}C{^{1}H} NMR (100 MHz, $CDCl_3$): δ 175.2, 171.7, 170.3, 158.8, 143.6, 139.6, 137.4, 133.8, 132.0, 131.0, 129.7, 129.2, 128.9, 128.8, 128.6, 128.5, 125.7, 125.5, 124.6, 122.8, 119.5, 119.1, 118.4, 109.3, 73.2, 62.3, 55.5, 52.4, 42.7, 16.9; HRMS: (ESI TOF) *m/z* calcd for $C_{36}H_{30}N_3O_4$ [M + H]$^+$ 568.2236, found 568.2235.

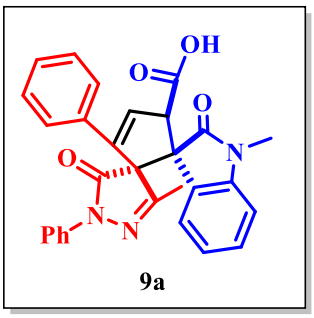
Methyl -1, 3''-dimethyl-2, 5''-dioxo-1'',3',5-triphenyl-1'',5''-dihydrodispiro[indoline-3,1'-cyclopentane-2',4''-pyrazol]-3'-ene-5'-carboxylate (8a)



8a

White solid (40 mg, 80% yield). R_f = 0.4 (petroleum ether/EtOAc 70:30). MP: 278-280 °C. ^{1}H NMR (400 MHz, $CDCl_3$): δ 7.7 (dt, *J* = 6.9, 1.1 Hz, 4H), 7.4 – 7.3 (m, 4H), 7.3 – 7.3 (m, 2H), 7.3 – 7.2 (m, 5H), 7.1 – 7.1 (m, 2H), 6.9 (d, *J* = 2.3 Hz, 1H), 6.7 (d, *J* = 8.3 Hz, 1H), 4.9 (d, *J* = 2.3 Hz, 1H), 3.7 (s, 3H), 3.2 (s, 3H), 1.8 (s, 3H); ^{13}C{^{1}H} NMR (100 MHz, $CDCl_3$): δ 175.0, 171.4, 170.3, 158.5, 143.4, 139.4, 137.1, 133.6, 132.7, 131.8, 129.3, 129.3, 129.1, 129.0, 128.7, 127.8, 126.7, 125.9, 125.8, 125.5, 119.6, 115.6, 109.8, 72.9, 62.2, 55.4, 52.6, 26.5, 16.6; *Rf*: (petroleum ether/EtOAc 65:35); HRMS: (ESI TOF) *m/z* calcd for $C_{36}H_{29}N_3O_4$ [M + H]$^+$ 568.2236, found 568.2235.

1,3''-Dimethyl-2 ,5''-dioxo-1'', 3'-diphenyl-1'' ,5''-dihydrodispiro[indoline-3,1'-cyclopentane-2',4''-pyrazol]-3'-ene-5'-carboxylic acid (9a)



9a

White solid (42 mg, 94% yield). MP: 210-212 °C. ^{1}H NMR (400 MHz, DMSO-d_6): δ 7.5 (d, *J* =2.0 Hz, 1H), 7.3 – 7.2 (m, 4H), 7.2 – 7.2 (m, 4H), 7.2 – 7.1 (m, 3H), 7.0 (dd, *J* = 8.6, 7.4 Hz, 2H), 6.9 (d, *J* = 1.0 Hz, 1H), 5.2 (d, *J* = 2.0 Hz, 1H), 3.2 (s, 3H), 2.2 (s, 3H); ^{13}C{^{1}H} NMR (100 MHz, DMSO-d_6): δ 173.7, 169.2, 163.7, 156.7, 146.8, 144.1, 137.5, 136.4, 135.1, 129.4, 128.8, 128.5, 128.2, 127.8, 125.9, 125.4, 125.4, 122.5, 118.9, 108.9, 72.5, 63.2, 52.5, 26.5, 15.5; HRMS: (ESI TOF) *m/z* calcd for $C_{36}H_{29}N_3O_4$ [M + H]$^+$ 478.1761, found 478.1767.

2.8 Appendix II ^{1}H, ^{13}C spectral data of representative compounds

Compound No.	Figure AII.X	Data	Page No
3p	Figure AII.1 and AII.2	^{1}H and ^{13}C	56
3s	Figure AII.3 and AII.4	^{1}H and ^{13}C	57
6a	Figure AII.5 and AII.6	^{1}H and ^{13}C	58
6d	Figure AII.7 and AII.8	^{1}H and ^{13}C	59
3p	Figure AII.9	ORTEP plot	60
6b	Figure AII.10	ORTEP plot	61

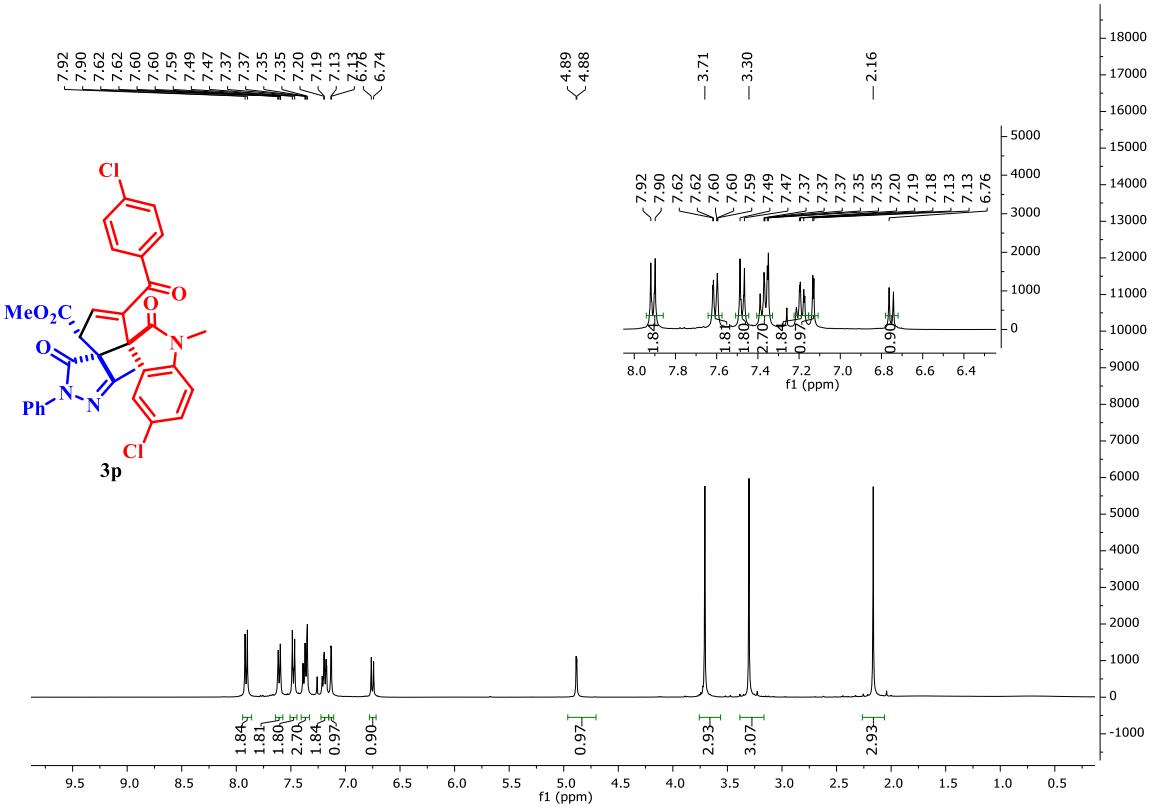


Figure AII.1 ^{1}H NMR (400 MHz, $CDCl_3$) spectrum of compound **3p**

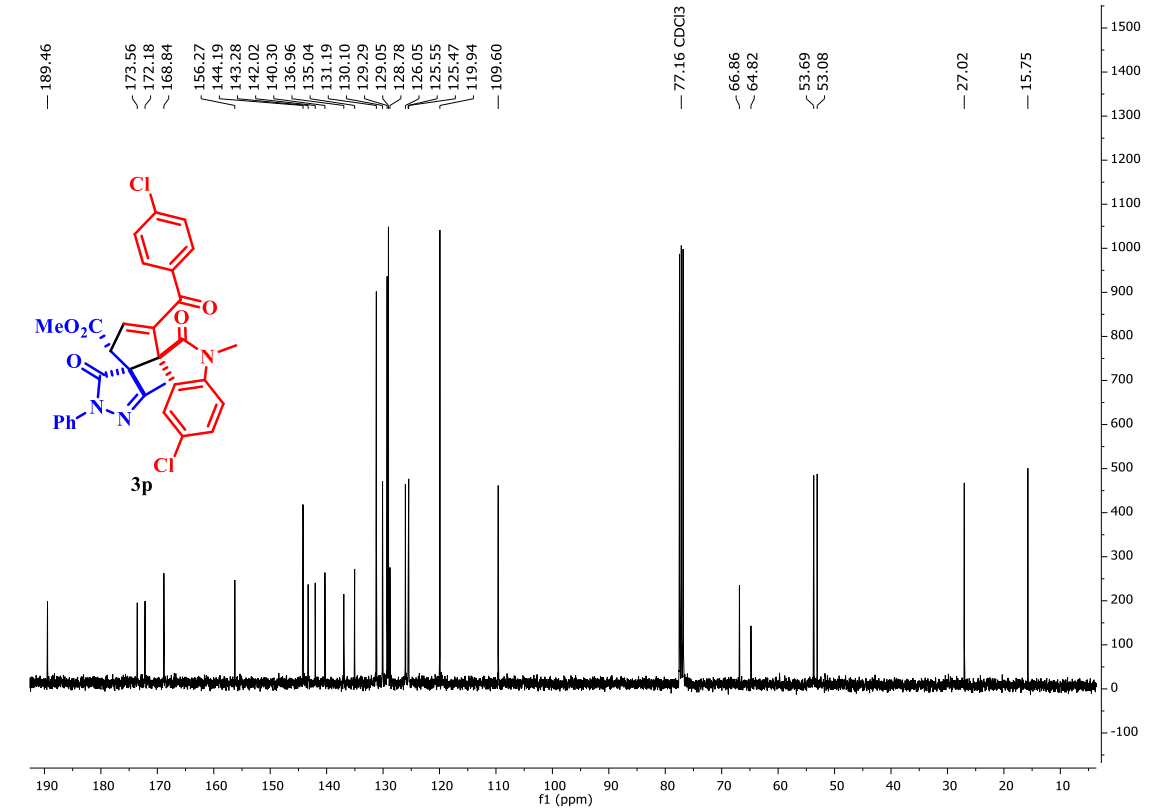


Figure AII.2 $^{13}C\{^{1}H\}$ NMR (100 MHz, $CDCl_3$) spectrum of compound **3p**

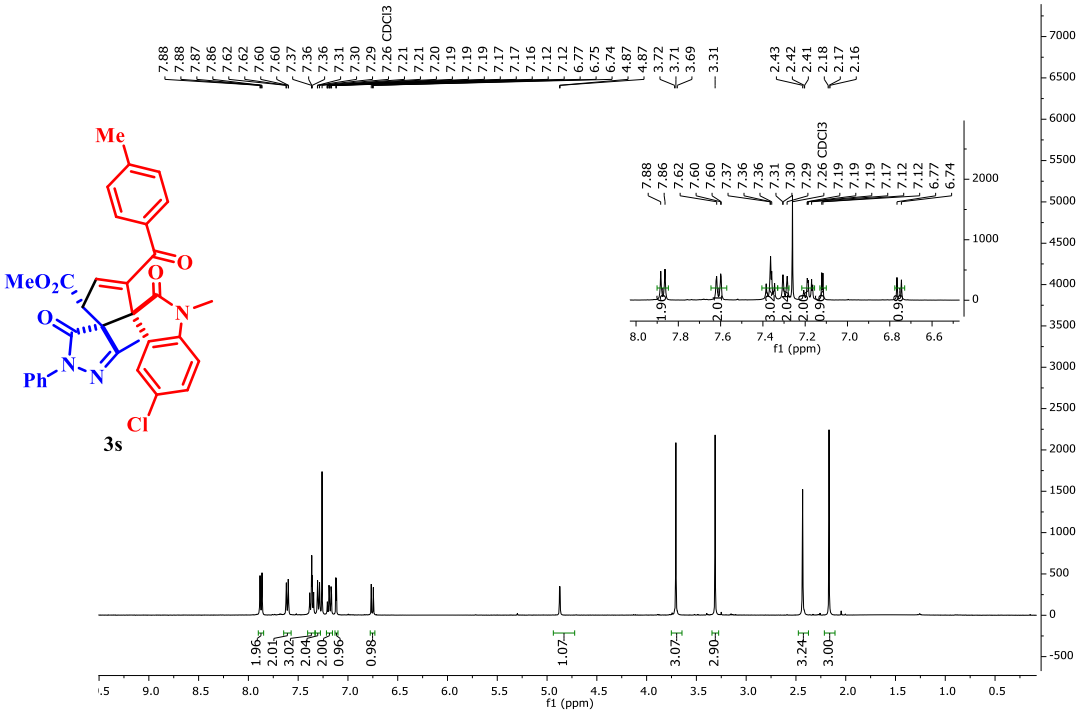


Figure AII.3 ^{1}H NMR (400 MHz, $CDCl_3$) spectrum of compound **3s**

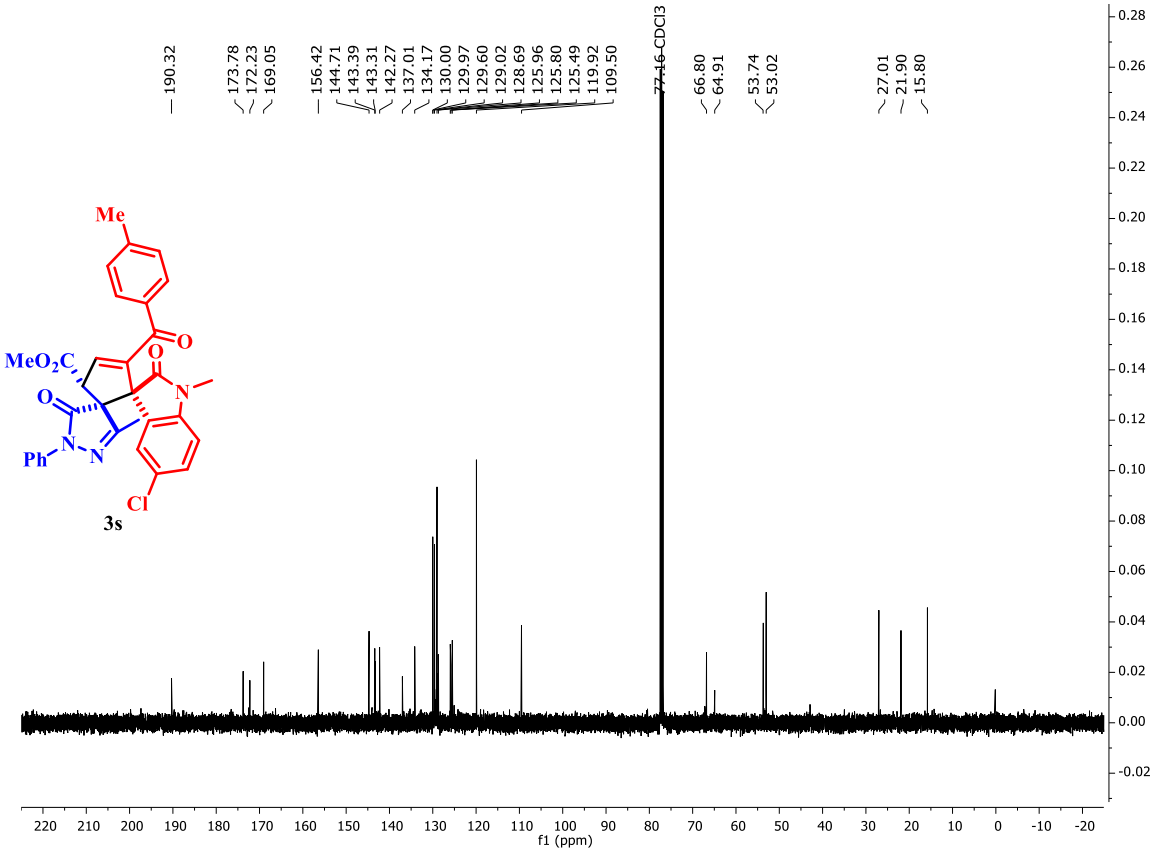


Figure AII.4 ^{13}C{^{1}H} NMR (100 MHz, $CDCl_3$) spectrum of compound **3s**

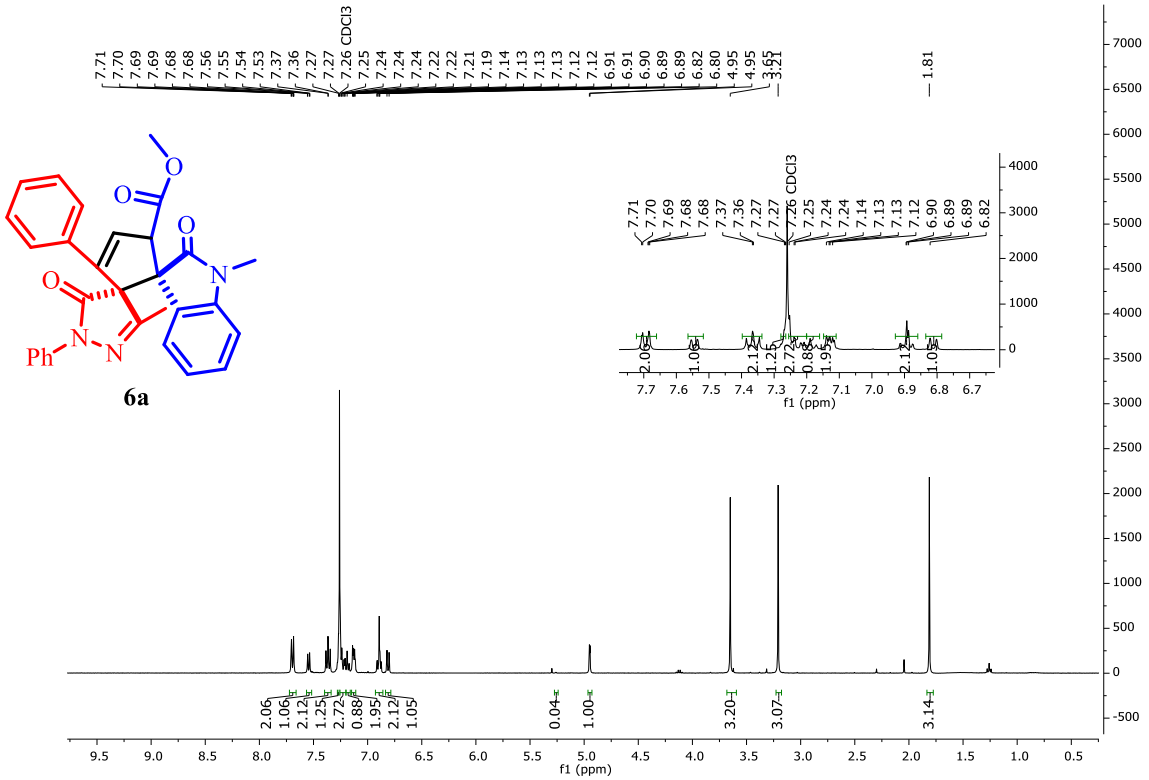


Figure AII.5 ^{1}H NMR (400 MHz, $CDCl_3$) spectrum of compound **6a**

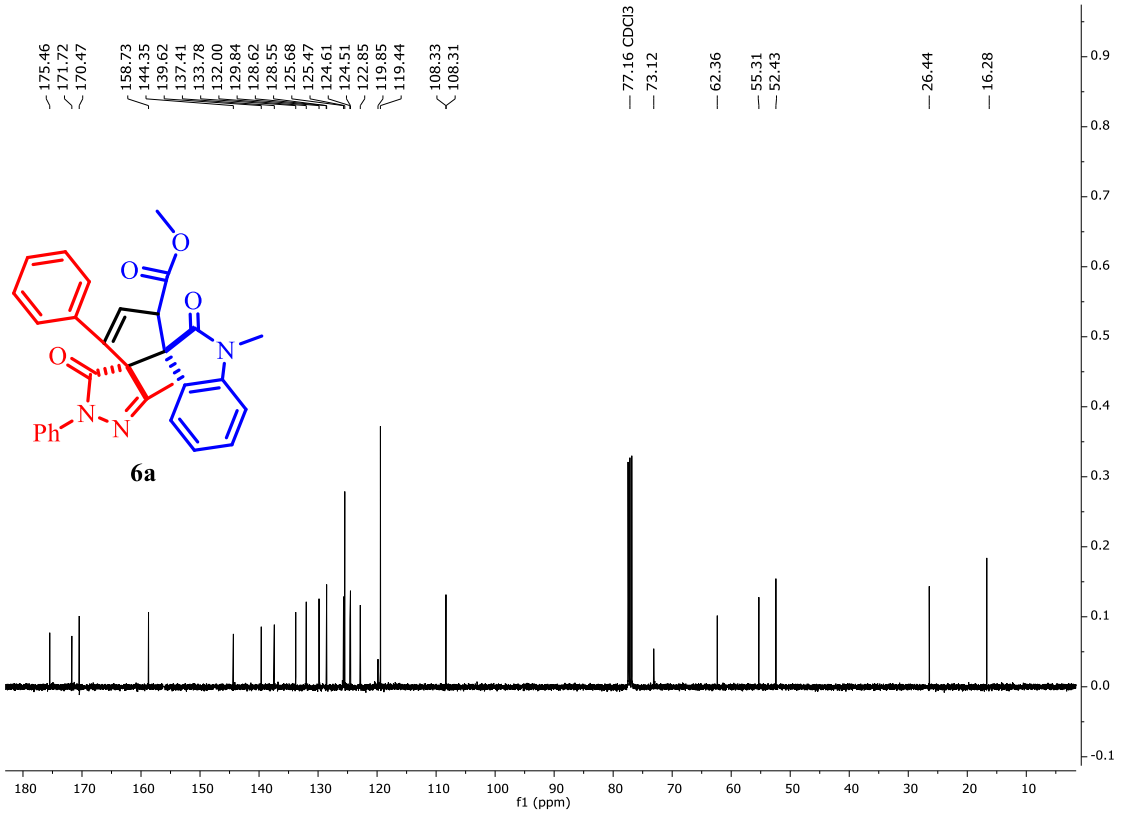


Figure AII.6 $^{13}C\{^{1}H\}$ NMR (100 MHz, $CDCl_3$) spectrum of compound **6a**

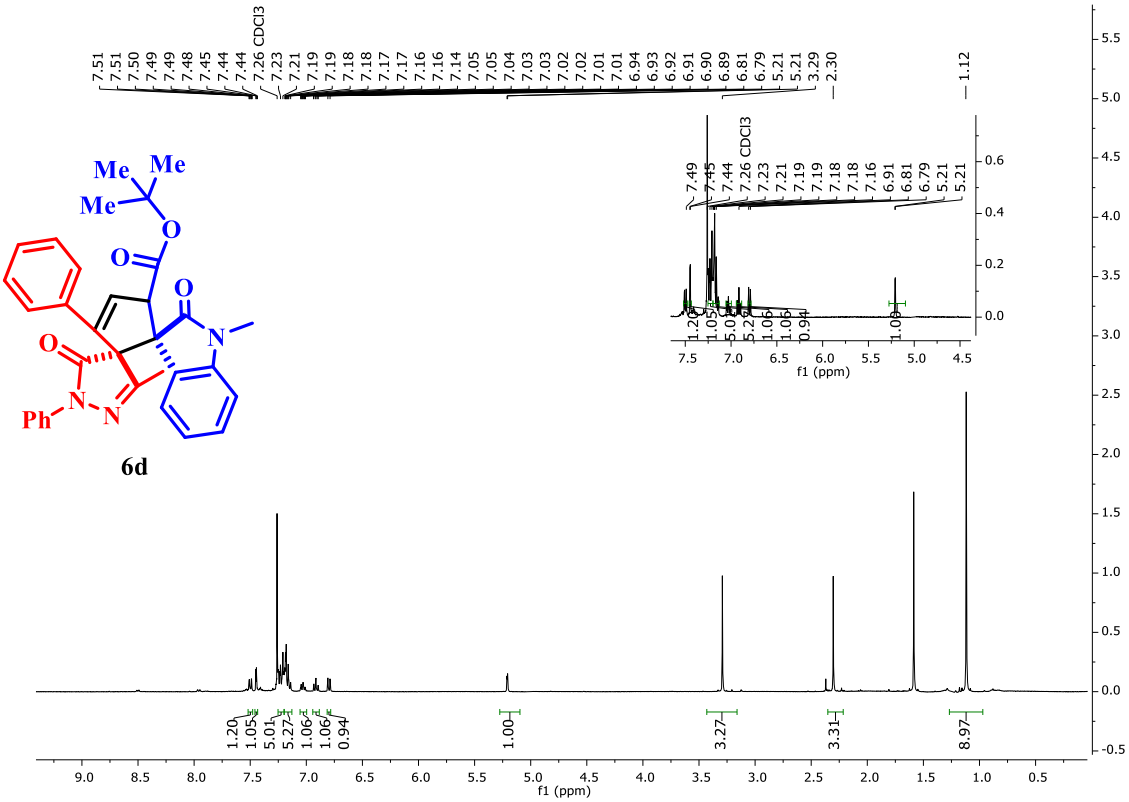


Figure AII.7 ^{1}H NMR (400 MHz, $CDCl_3$) spectrum of compound **6d**

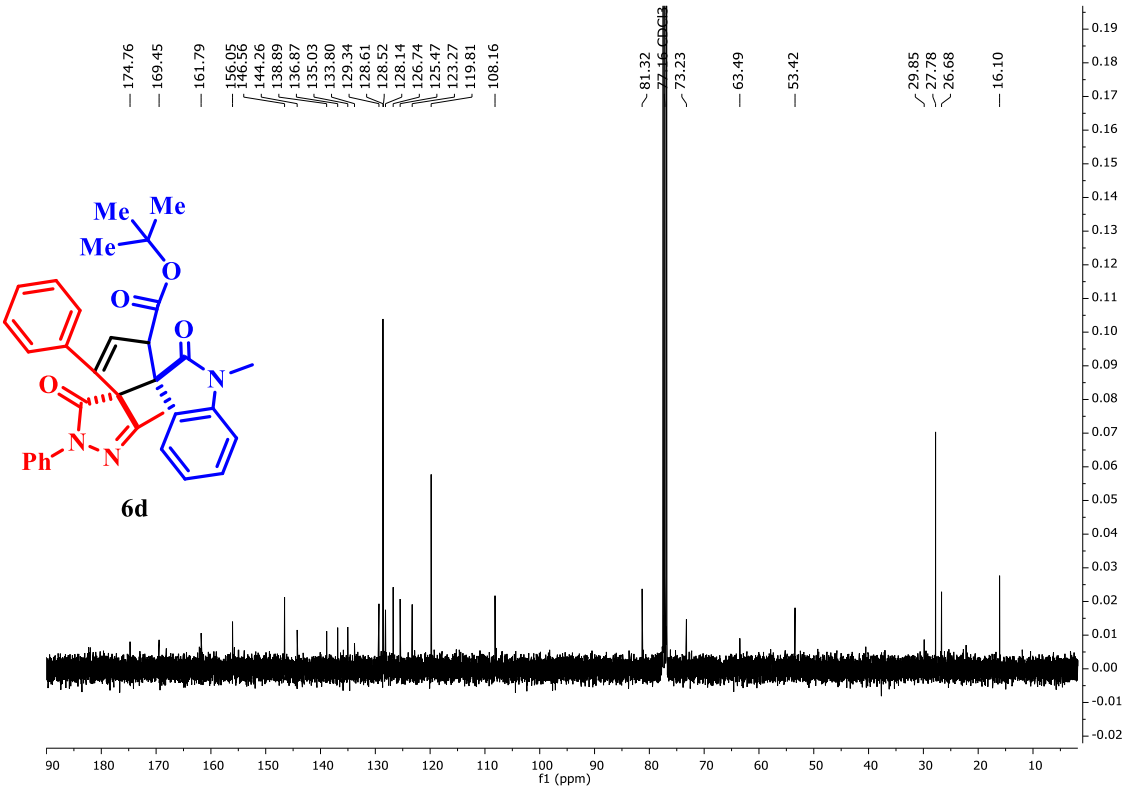


Figure AII.8 $^{13}C\{^{1}H\}$ NMR (100 MHz, $CDCl_3$) spectrum of compound **6d**

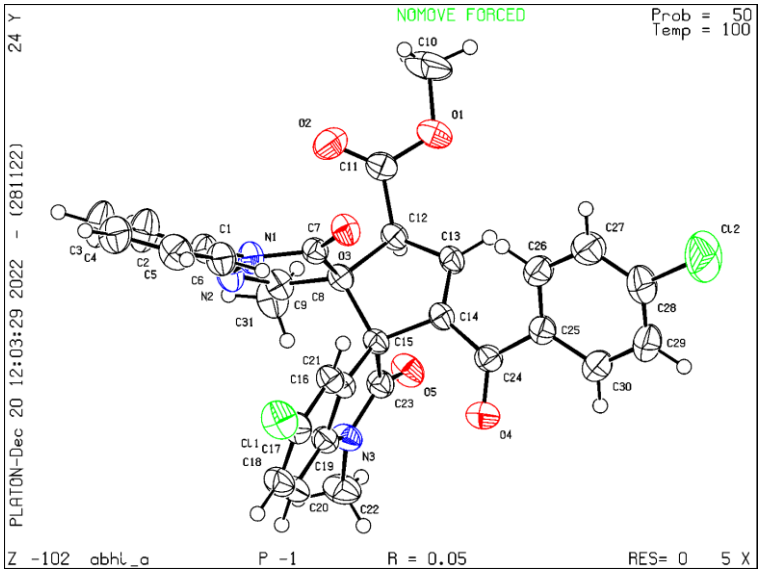


Figure AII.9 An ORTEP diagram showing thermal ellipsoids at a 50% probability level was created to represent the structures determined by single-crystal X-ray diffraction analysis of compound **3p**.

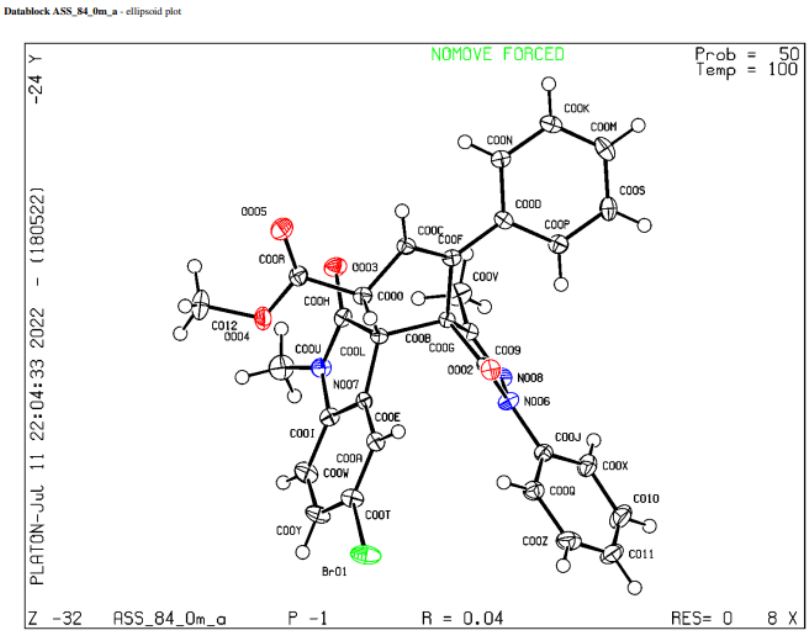


Figure AII.10 An ORTEP diagram showing thermal ellipsoids at a 50% probability level was created to represent the structures determined by single-crystal X-ray diffraction analysis of compound **6b**

2.8 References

1. (a) Rios, R. *Chem. Soc. Rev.* **2012**, *41*, 1060. (b) Carreira, E. M.; Fessard, T. C. *Chem. Rev.* **2014**, *114*, 8257. (c) Cao, Z.-Y.; Zhou. *J. Org. Chem. Front.* **2015**, *2*, 849. (d) James, M. J.; O′Brien, P.; Taylor, R. J. K.; Unsworth, W. P. *Chem. Eur. J.* **2016**, *22*, 2856. (e) Reddy, C. R.; Prajapti, S. K.; Warudikar, K.; Ranjan, R.; Rao, B. B. *Org. Biomol. Chem.* **2017**, *15*, 3130. (f) Kotha, S.; Panguluri, N. R.; Ali, R. *Eur. J. Org. Chem.* **2017**, *2017*, 5316.
2. (a) Ritchie, T. J.; MacDonald, S. J. F.; Young, R. J.; Pickett, S. D. *Drug Discov. Today* **2011**, *16*, 164. (b) Ritchie, T. J.; and MacDonald, S. J. F. *Drug Discov. Today* **2009**, *14*, 1011. (c) Müller, G.; Berkenbosch, T.; Benningshof, J. C. J.; Stumpfe, D.; Bajorath, J. *Chem. Eur. J.* **2017**, *23*, 703. (d) Degorce, S. L.; Bodnarchuk, M. S.; Scott, J. S. *ACS Med. Chem. Lett.* **2019**, *10*, 1198.
3. Tada, I.; Motoki, M.; Takahashi, N.; and Miyata, T.; Takechi, T.; Uchida, T.; Takagi, Y. *Pestic. Sci.* **1996**, *48*, 165.
4. (a) Schmidt, B.; Scheufler, C.; Volz, J.; Feth, M.-P.; Hatzeimann, R.-P.; Zitt, C.; Wohlsen, A.; Marx, D.; Kley, H.-P.; Marx, D.; Ockert, D.; Heuser, A.; Christiaans, J.-A. M.; Sterk, G.-J.; and Menge, W.-M. P. B. *Germany Patent WO2008138939,* **2008**. (b) Schlemminger, I.; Schmidt, B.; Flockerzi, D.; Tenor, H.; Zitt, C.; Hatzelmann, A.; Marx, D.; Braun, C.; Kuelzer, R.; Heuser, A.; kley, H.-P.; Sterk, G. J. *Germany Patent WO2010055083*, **2010**.
5. (a) Cui, C. B.; Kakeya, H.; Osada, H. Spirotryprostatin B, *J. Antibiot.* **1996**, *49*, 832. (b) Masashi, T.; Yuu, K.; Haruaki, I.; Eri, F.; Jun, K.; Masayuki, W.; Kenichi, A.; and Jun'ichi, K. *J. Org. Chem.* **2005**, *70*, 9430. (c) Mercado-Marin, E.; Garcia-Reynaga, P.; and Romminger, S. *Nature* **2014**, *509*, 318.
6. Gicquel, M.; Gomez, C.; Alvarez, M. C. C.; Pamlard, O.; Jacquet, V. G. E.; Bignon, J.; Voituriez, A.; and Marinetti, A. *J. Med. Chem.* **2018**, *61*, 9386.
7. Wang, B.; Peng, F.; Huang, W.; Zhou, J.; Zhang, N.; Sheng, J.; Haruehanroengra, P.; He, G.; and Han, B. *Acta Pharm. Sin. B* **2020**, *10*, 1492.
8. Bao, X.; Wei, S.; Qian, X.; Qu, J.; Wang, B.; Zou, L.; and Ge, G. *Org. Lett.* **2018**, *20*, 3394.
9. (a) Liu, S.; Baoa, X.; Wang, B. *Chem. Commun.* **2018**, *54*, 11515. (b) Zhou, L. M.; Qu, R. Y.; Yang, G. F. *Expert Opin Drug Discov.* **2020**, *15*, 603. (c) Boddy, A. J.; Bull, J. A. *Org. Chem. Front.* **2021**, *8*, 1026. (d) Carceller-Ferrer, L.; Blay, G.; Pedro, J. R.; Vila, C. *Synthesis* **2021**, *53*, 215.

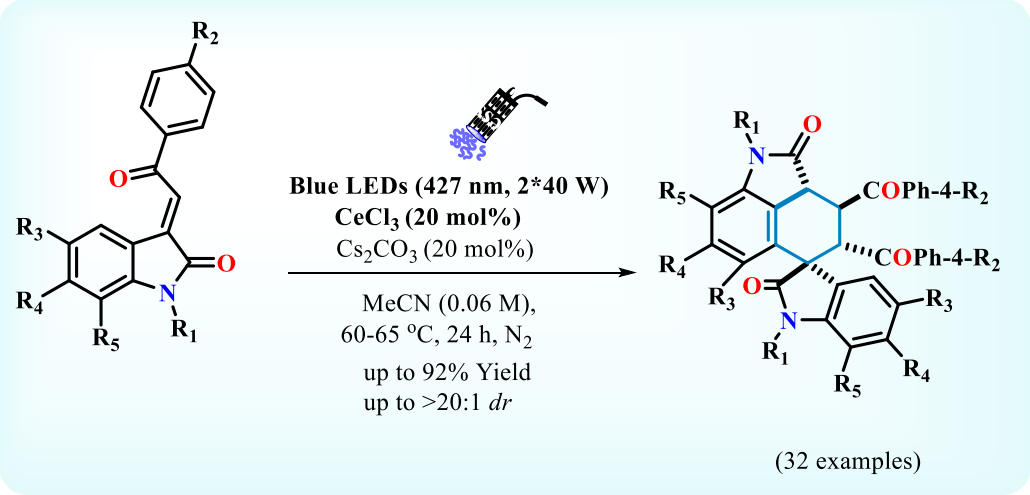
10. Chen, Q.; Liang, J.; Wang, S.; Wang D.; and Wang, R. *Chem. Commun.* **2013**, *49*, 1657.
11. Cui, B.D.; Li, S.W.; Zuo, J.; Wu, Z.J.; Zhang, X.M.; Yuan, W.C. *Tetrahedron* **2014**, *70*, 1895.
12. Li, J. H.; Feng, T.F.; Du, D. M. *J. Org. Chem.* **2015**, *80*, 11369.
13. Bao, X.; Wei, S.; Qian, X.; Qu, J.; Wang, B.; Zou, L.; and Ge, G. *Org. Lett.* **2018**, *20*, 3394.
14. Luo, W.; Shao, B.; Li, J.; Xiao, X.; Song, D.; Ling, F.; Zhong, W. *Org. Chem. Front.* **2020**, *7*, 1016.
15. (a) Warghude, P. K.; Dharpure, P. D.; Bhat, R. G. *Tetrahedron Lett.* **2018**, *59*, 4076. (b) Warghude, P. K.; Sabale, A. S.; Bhat. R. G. *Org. Biomol. Chem.* **2020**, *18*, 1794. (c) Warghude, P. K.; Sabale, A. S.; Dixit, R.; Vanka, K.; Bhat, R. G. *Org. Biomol. Chem.* **2021**, *19*, 4338. (d) Warghude, P.K.; Bhowmick, A.; Bhat, R.G. *Tetrahedron Lett.* **2022**, *97*, 153.
16. Chen, Z.; Chen, Z.; Du W.; and Chen, Y. *Chem. Rec.* **2020**, *20*, 541.
17. (a) Tian, Z.; Jiang, J.; Yan, Z.-H.; Luo, Q.-Q.; Zhan, G.; Huang, W.; Li, X.; and Han, B. *Chem. Commun.* **2022**, *58*, 5363. (b) Huang, S.; Wen, H.; Tian, Y.; Wang, P.; Qin W.; and Yan, H. *Angew. Chem., Int. Ed.* **2021**, *60*, 21486. (c) Liao, J.; Xu, J.; Wu, Y.; Hou, Y.; and Guo, H. *Adv. Synth. Catal.* **2022**, *364*, 1074. (d) Wei, X.; Huang, Y.; Wang, W.; Wei, S.; Qu, J.; and Wang, B. Chem. Commun. **2022**, *58*, 9504. (e) Luo, Q.; Tian, Z.; Tang, J.; Wang, Y.; Tian, Y.; Peng, C.; Zhan, G.; and Han B. *ACS Catal.* **2022**, *12*, 7221.
18. Saeed, R.; Sakla, A. P.; and Shankaraiah, N. *Org. Biomol. Chem.* **2021**, *19*, 7768.
19. CCDC 2189452 contains crystallographic data for compound **3p.**
20. CCDC 2183100 contains crystallographic data for compound **6b.**
21. (a) Peng, J.; Huang, X.; Jiang, L.; Cui, H. L.; Chen. Y. C. *Org. Lett.* **2011**, *13*, 4584. (b) Wei, F.; Huang, H. Y.; Zhong, N. J.; Gu, C. L.; Wang, D.; Liu. L. *Org. Lett.* **2015**, *17*, 1688.
22. Tian, Z.; Jiang, J.; Yan, Z-H.; Luo, Q-Q.; Zhan, G.; Huang, W.; Li, X.; Han, B. *Chem. Commun.* **2022**, *35*, 5363.

3 Visible-Light-Induced Diastereoselective [4+2] Cyclization for Efficient Synthesis of 3,4-Fused Spirooxindoles from 3-Methyleneoxindoles

Abstracts

A novel visible light-mediated approach has been established for the direct functionalization at the unactivated C4 position of 3-methyleneoxindole, enabling the synthesis of 3,4-fused spirooxindoles via a formal [4+2] cycloaddition. This strategy eliminates the need for any pre-functionalization steps. Upon exposure to the visible light in the presence of a catalytic amount of $CeCl_3$ under alkaline conditions, 3-methyleneoxindoles undergo efficient cyclization to furnish the intricate 3,4-fused spirooxindole frameworks, incorporating four contiguous stereocenters. The method exhibits excellent chemo- and regio-selectivity, furnishing the desired spirooxindoles in moderate to good yields. Furthermore, the protocol operates effectively under the direct exposure of sunlight and method proved to be scalable on gram quantity. This method offers a powerful and precise approach for constructing complex molecular architectures with high efficiency and precision.

.



Sabale, A. S.; Bhowmick, A.; Pattanaik, S.; Bankar, O. S.; Bhat, R. G. *Asian J. Org. Chem.* **2025**, *11*, e202500424.

3 Visible-Light-Induced Diastereoselective [4+2] Cyclization for Efficient Synthesis of 3,4-Fused Spirooxindoles from 3-Methyleneoxindoles

3.1 Introduction

The 3,4-fused indole and oxindole frameworks are prominent structural motifs frequently encountered in numerous natural products, pharmaceuticals, and biologically active molecules.[1] These fused systems often exhibit remarkable pharmacological properties, contributing to their widespread presence in medicinal chemistry. Representative examples of compounds having this scaffold include lysergic acid,[2] rugulovasine A,[3] chanoclavine-I,[4] dehydrobufotenine,[5] chuangxinmycin,[6] hapalindole U,[7] and ammosamide B,[1d] alongside their structural analogs[1g] (Figure 3.1).

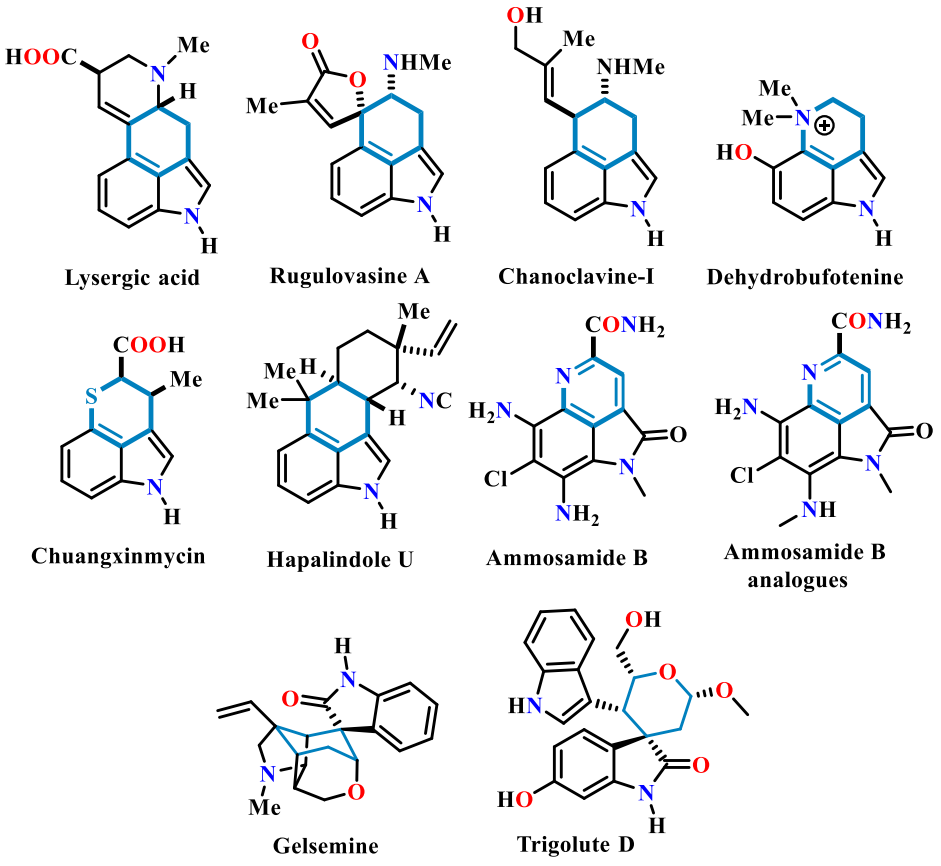


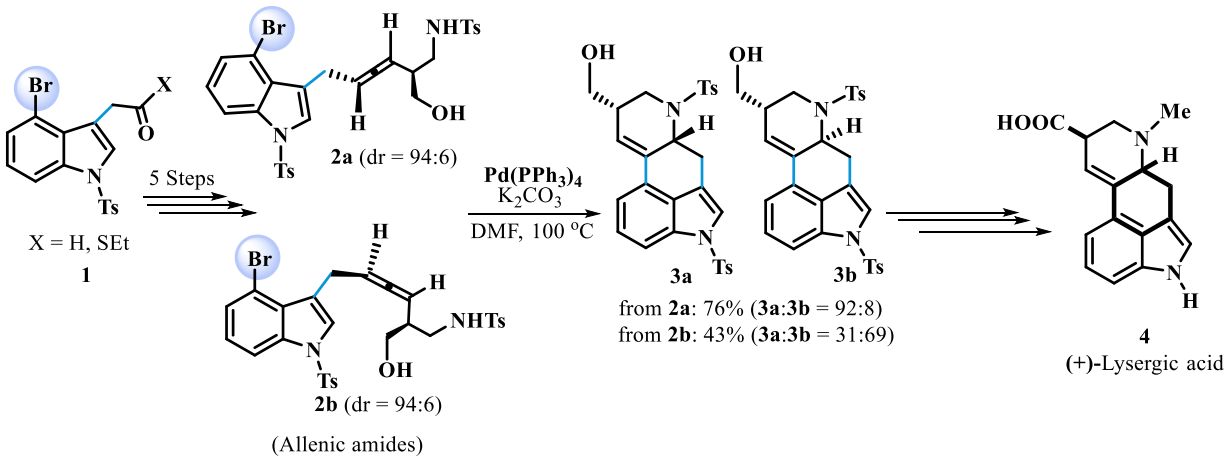
Figure 3.1 Natural products featuring 3,4-fused indole, oxindole, and spirooxindole frameworks

Due to their pronounced biological significance, extensive research has been devoted to the synthesis and functionalization of these fused frameworks. As a result, the continuous development of innovative and efficient synthetic approaches to construct complex 3,4-fused indole and oxindole derivatives remains a critical objective in the field of drug discovery as well.[8]

3.2 Recent developments in the synthesis of 3,4-fused indole and oxindole skeleton

Given the biological importance of the 3,4-fused indole and oxindole scaffold and the synthetic complexity associated with its construction, the development of stereoselective strategies for assembling molecules with 3,4-fused indole and oxindole core is highly desirable and greatly sought after due to their relevance. Several synthetic approaches have been devised to construct significant 3,4-fused indole and oxindole frameworks featuring six-membered rings.

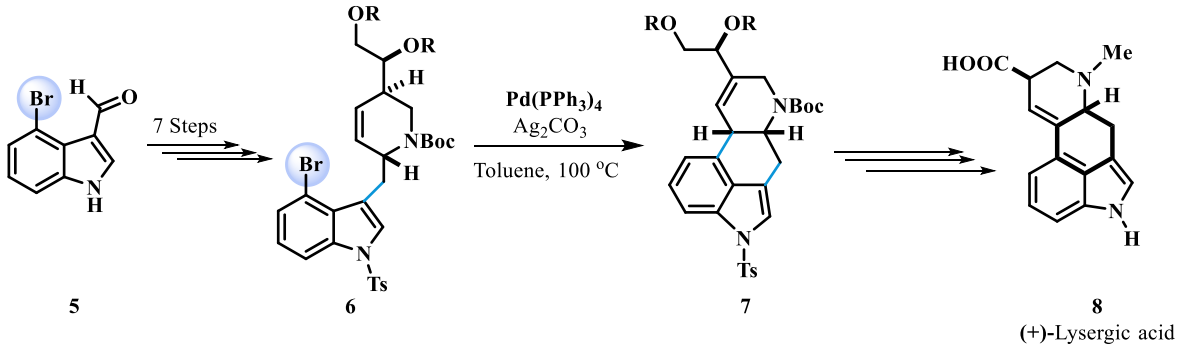
Fujii, Hiroaki Ohno, and colleagues[9] reported a concise one-step total synthesis of (+)-lysergic acid **4** via a palladium-catalyzed domino cyclization of 4-haloindole-based allenic amides (**2a** and **2b**). These intermediates were obtained as a diastereomeric mixture in a 94:6 ratio, due to difficulties in separating the individual diastereomers. Treatment of amide **2a** with 5 mol% $Pd(PPh_3)_4$ and K_2CO_3 in DMF at 100 °C afforded the cyclized products **3a** and **3b** with high diastereoselectivity (**3a**:**3b** = 92:8). Similarly, cyclization of isomer **2b** under the same reaction conditions provided **3a** and **3b** in a reversed diastereomeric ratio of 31:69. The overall yield for this transformation was reported to be 4%, as depicted in Scheme 3.1.



Scheme 3.1 Pd-catalyzed synthesis of 3,4-fused indole skeletons from 4-haloindole derivatives

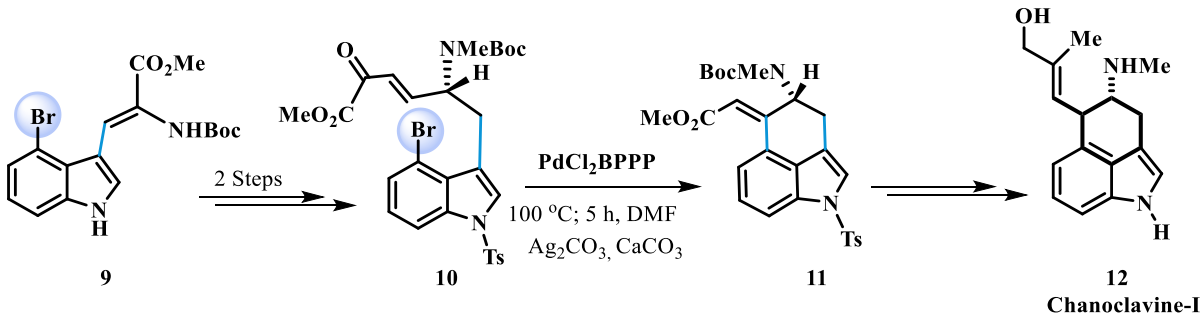
Fukuyama and coworkers[2a] successfully synthesized lysergic acid **8**, utilizing a palladium-catalyzed cyclization reaction at an elevated temperature of 100 °C. This approach enabled the

efficient formation of 3,4-substituted indoline **7** as a key intermediate in the synthetic pathway. The overall yield for this transformation was reported to be 10.6 %, as depicted in Scheme 3.2



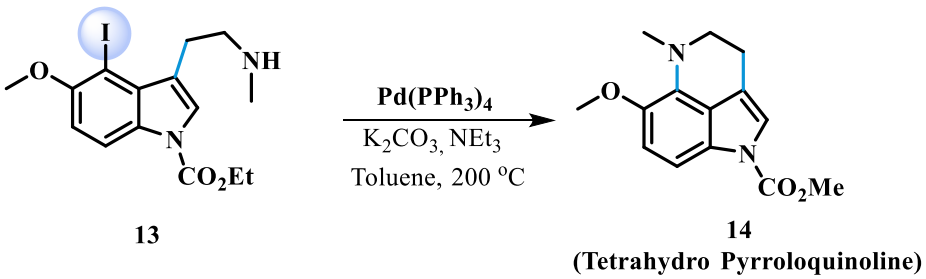
Scheme 3.2 Pd-catalyzed synthesis of 3,4-fused indole skeletons from 4-haloindole derivatives

Murakami and coworkers[4] achieved the enantioselective total synthesis of optically active clianochvine-I **12**, an ergot alkaloid, through a palladium-catalyzed intramolecular cyclization via the Heck reaction. This key transformation was performed at an elevated temperature of 100 °C, facilitating the construction of the desired molecular framework (Scheme 3.3).



Scheme 3.3 Pd-catalyzed synthesis of 3,4-fused indole skeletons (chanoclavine) from 4-haloindole derivatives

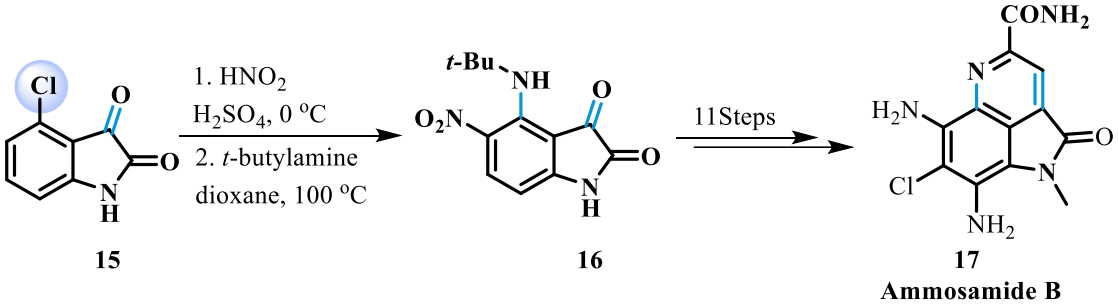
Buchwald and his team[5a] developed a method for synthesizing tetrahydropyrroloquinolines **14** through a palladium-catalyzed intramolecular cyclization of iodoindole derivative **13.** This transformation was performed at an elevated temperature of 200 °C to facilitate the efficient assembly of the 3,4-indoline core framework **14.** The overall yield for this transformation was reported to be 17 %, as depicted in Scheme 3.4.



13 14
(Tetrahydro Pyrroloquinoline)

Scheme 3.4 Pd-catalyzed synthesis of 3,4-fused indole skeletons (tetrahydropyrroloquinolines) from 4-haloindole derivatives

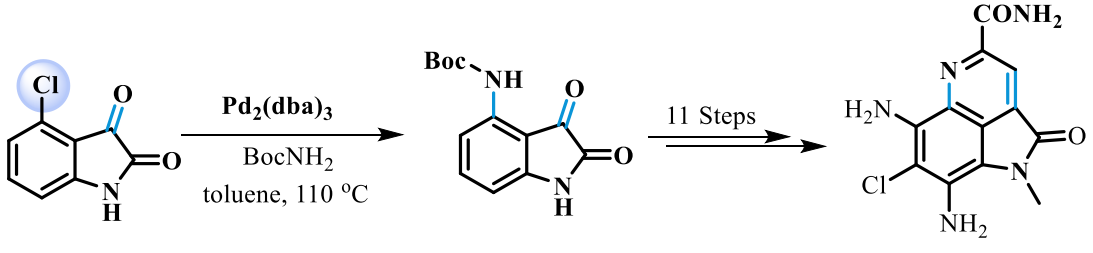
Fenica and coworkers[1d] successfully accomplished the total synthesis of ammosamide B **17**, via a C4 pre-functionalization step at an elevated temperature of 100 °C. This approach facilitated the formation of the desired structural framework, demonstrating its applicability in the construction of complex molecules such as ammosamide B **17**. The overall yield for this transformation was reported to be 8%, as depicted in Scheme 3.5.



15 16 17
Ammosamide B

Scheme 3.5 Synthesis of 3,4-fused oxindole skeletons (ammosamide B) from 4-haloxindole derivatives

Sun, Wang, and their team[1g] reported the total synthesis of ammosamide B **20** through a palladium-catalyzed cyclization reaction conducted at 110 °C. This method enabled the efficient construction of 3,4-substituted oxindoles, showcasing the versatility of transition-metal catalysis in accessing complex molecular architecture. The use of palladium catalysis facilitated selective bond formation, contributing to the streamlined synthesis of the target



18 19 20
Ammosamide B

Scheme 3.6 Pd-catalyzed synthesis of 3,4-fused oxindole skeletons (ammosamide B) from 4-haloxindole derivatives

compound such ammosamide B **20**. The overall yield for this transformation was reported to be 23 %, as depicted in Scheme 3.6.

Notably, all existing methodologies rely on pre-functionalized substrates to enable C–H functionalization at the unactivated C4 position. This limitation arises due to the relatively low reactivity of the C4–H bond toward electrophiles, thus making cyclization challenging without prior functionalization.[10]

Additionally, some literature-reported approaches for synthesizing 3,4-fused oxindoles using 3-methyleneoxindole as a model substrate face significant limitations. Common challenges include the requirement of elevated temperature, limited to restricted substrate scope, use of environmentally harmful solvents such as acetic anhydride, DMF, and poor product yields. These drawbacks highlight the necessity for the development of more efficient, sustainable, and broadly applicable synthetic strategies.[11]

The construction of complex molecules like 3,4-fused spirooxindoles from a single substrate remains unexplored, particularly under visible light conditions. Developing an efficient and straightforward methodology for assembling 3,4-fused indole frameworks at room temperature presents a significant challenge as well as a valuable opportunity. In contrast, 3,3-disubstituted spirooxindole frameworks have been synthesized extensively due to their notable biological importance (Figure 3.1).[12] In this chapter, we report a cerium-catalyzed, visible light-driven approach for directly synthesizing 3,4-fused spirooxindole framework featuring a six-membered ring. This strategy employs 3-methyleneoxindole as the key substrate.[13]

3.3 Results and Discussion

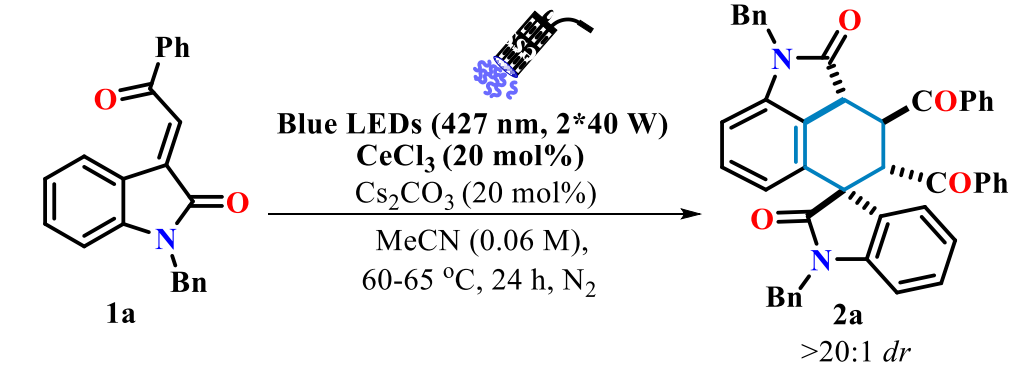
Drawing inspiration from existing literature, we aimed to investigate a visible-light-driven strategy employing a Ligand-to-Metal Charge Transfer (LMCT) complex for the construction of a 3,4-fused spirooxindole framework. Our hypothesis suggested that 3-methyleneoxindole could engage with cerium chloride ($CeCl_3$), promoting LMCT-mediated cyclization under visible-light irradiation through an electron transfer from Ce(III) to Ce(IV). In order to validate this concept, we commenced with *N*-benzyl 3-methyleneoxindole **1a** as a model substrate, and this was synthesized following the previously reported method.[14] Upon subjecting **1a** to a reaction with $CeCl_3$ (20 mol%) and cesium carbonate (20 mol%) in acetonitrile under the exposure of 456 nm blue LED light (Kessil lamp) in an inert atmosphere, the desired product **2a** was obtained, albeit in very low yield (11%, see Table 3.2, entry 1).

Encouraged by this initial result, we carried out a comprehensive screening of LEDs with varying wavelengths and intensities to optimize the reaction conditions (see Table 3.2, entries

2–4). Among the tested light sources, blue LED (427 nm, 50% intensity, 20 W) proved to be efficient, resulting in the desired product **2a** in a modest yield (20%). Notably, when the reaction of **1a** was performed using two blue LEDs (427 nm, 40 W) under otherwise identical conditions, the yield of the desired product **2a** significantly improved to 70% (see Table 3.2, entries 5–8). However, we observed that due to the two LEDs reaction temperature was increased to 60–65 °C. To assess the influence of temperature on the reaction outcome and overall impact on the higher yield, a control experiment was carried out in the absence of light, maintaining elevated temperature at 70 °C (Table 3.1, entry 3). Interestingly, we observed that product **2a** did not form even after the prolonged reaction time. This result unequivocally confirmed the indispensable role of light in driving the reaction. It is plausible that the increase in the reaction temperature due to intense LED illumination might have accelerated the reaction rate, thus contributing to the observed enhancement in the yield of **2a**. This observation underscores the synergistic effect of light and thermal energy in facilitating the smooth transformation.

Interestingly, when the reaction was performed in the absence of Cs_2CO_3 while maintaining other conditions, the desired product **2a** was still formed, though in modest yield. This highlighted the role of the base in facilitating the reaction and yield of the product (refer to Table 3.1, entry 4). Surprisingly, even in the absence of both $CeCl_3$ and Cs_2CO_3, the reaction proceeded to form **2a**, albeit in modest yield (35%, Table 3.1, entry 5). This result raised some concern about the necessity of $CeCl_3$ and the proposed Ligand-to-Metal Charge Transfer (LMCT) mechanism.

Table 3.1 Optimization studies were conducted for the visible light-mediated C4 unactivated C– H functionalization to construct the 3,4-fused spirooxindole framework.[a]



Entry	Variation from the optimized condition [a]	[Yield[b] %]
1[d]	**None**	**70**
2[d]	No light	NR
3[d]	Reaction in the absence of light at 70 °C.	NR
4[d]	Absence of Cs_2CO_3	48
5[d]	Absence of $CeCl_3$ and Cs_2CO_3	35
6[d]	Open air instead of inert atmosphere	36
7[d]	Presence of molecular oxygen	ND

Reaction conditions: [a]3-Methyleneoxindole **1a** (0.2 mmol, 1 equiv), $CeCl_3$ (20 mol%), Cs_2CO_3 (20 mol%), in MeCN (0.06 M), under Kessil Blue LED (427 nm, 100% intensity, 60–65 °C with fan off, 2*40 W) in a nitrogen atmosphere. [b]Yields were determined after purification by column chromatography. [c]Diastereomeric ratio (>20:1 *dr*) was analyzed using ^{1}H NMR spectroscopy. [d]A.R. grade MeCN was used. NR = No reaction. ND = Not Detected

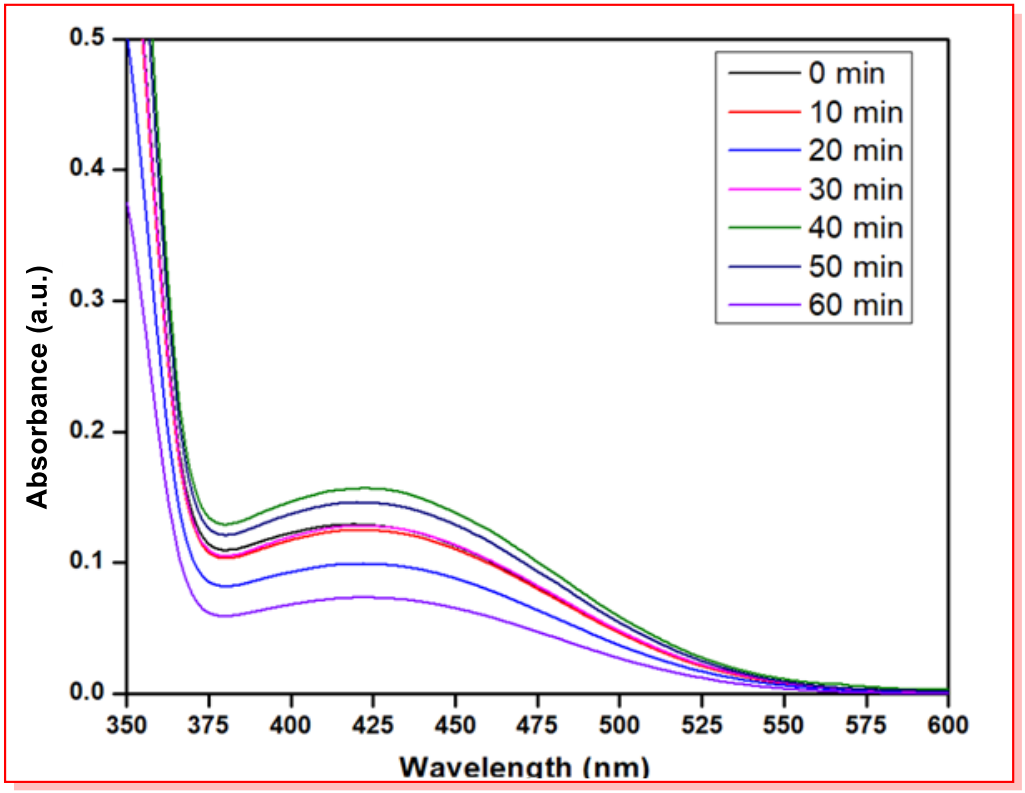


Figure 3.2 UV-visible absorption spectra of the reaction mixture in the absence of light

In order to understand the reaction mechanism and role of $CeCl_3$, systematic UV-visible absorption studies were carried out by recording the spectra of the reaction mixture at 10-minute intervals over a one-hour period. Notably, no significant changes were observed in the absorption maxima of 3-methyleneoxindole **1a**, and no new peaks emerged (see Figure 3.2). These findings clearly suggested that a single-electron transfer (SET) from $CeCl_3$ to **1a** does not occur. Hence, oxidation of Ce(III) to Ce(IV) is an unlikely event during the course of the reaction.

Furthermore, FT-IR spectroscopic analysis of 3-methyleneoxindole **1a**, $CeCl_3$, and the mixture of 3-methyleneoxindole **1a** + $CeCl_3$ showed notable shifts in vibrational frequencies, suggesting potential interactions or structural alterations. These observations offer important insights into the reaction mechanism and the intermediates involved (See Figures 3.3, 3.4, 3.5). Considering these findings and the earlier results highlighting the requirement of $CeCl_3$, it is plausible that $CeCl_3$ acts as a Lewis acid additive, facilitating the reaction much faster and resulting higher yield of the desired product **2a**.[15]

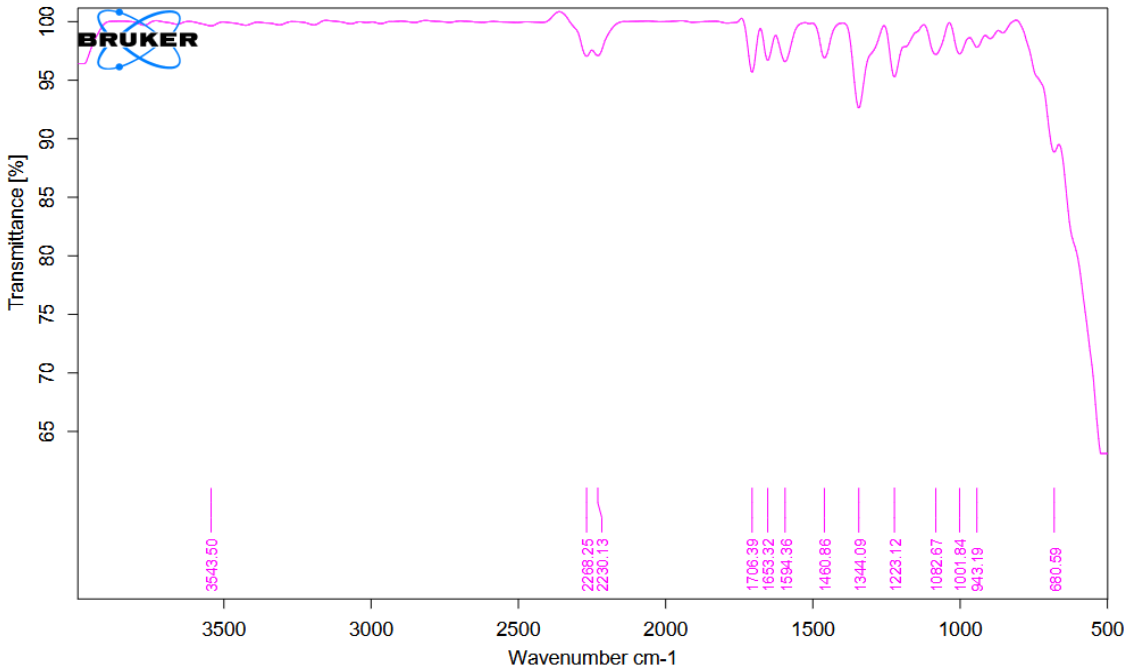


Figure 3.3 FT-IR Spectra of 3-methyleneoxindole **1a**

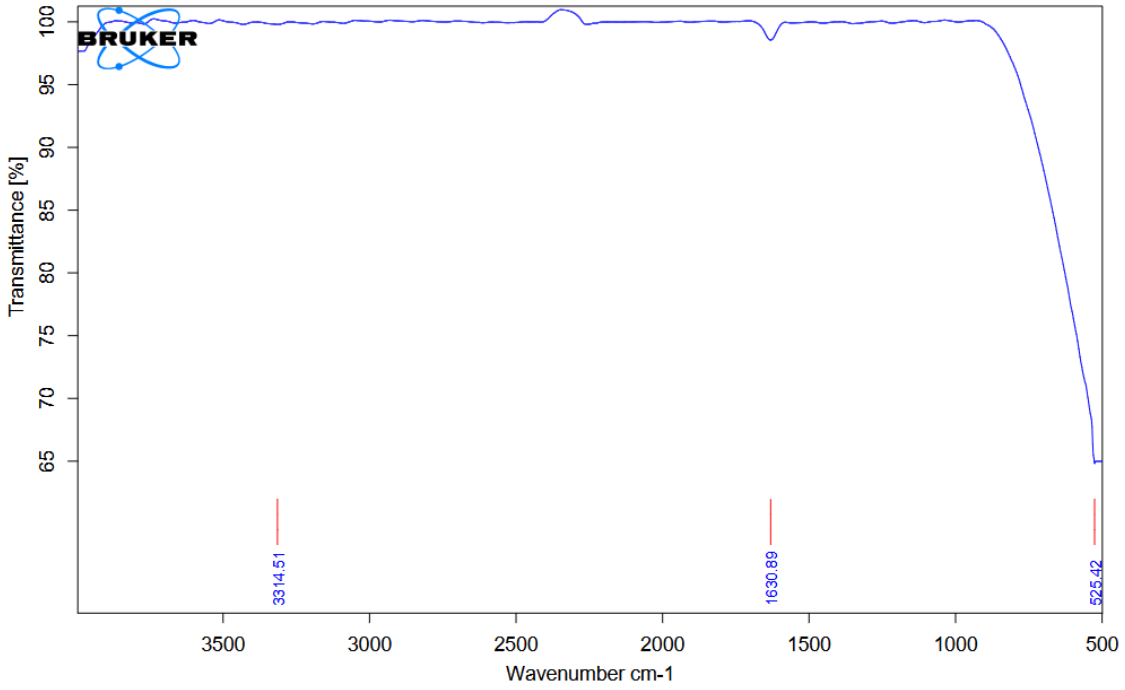


Figure 3.4 FT-IR Spectra of $CeCl_3$

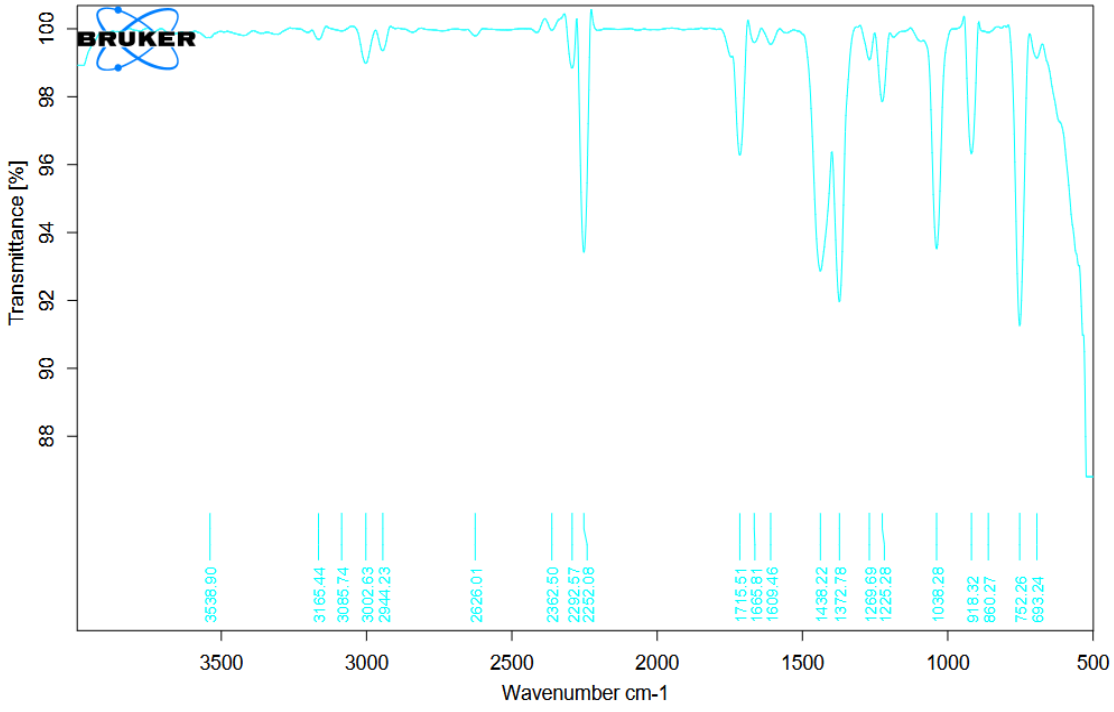
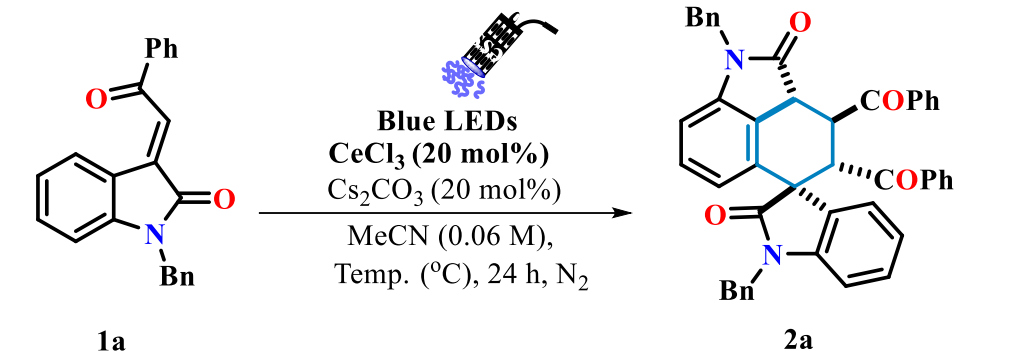


Figure 3.5 FT-IR Spectra of 3-methyleneoxindole **1a** + $CeCl_3$

Table 3.2 Evaluation of various light sources was conducted for the formal [4+2] cycloaddition reaction.[a]



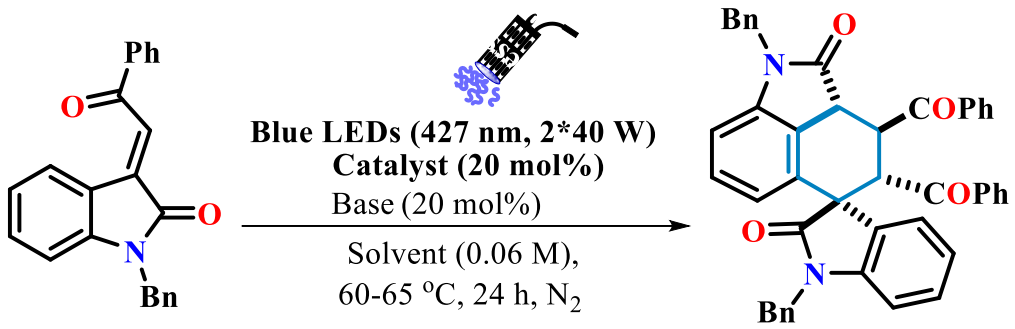
1a **2a**

Entry	1a	Light (nm)	Light Intensity	Temp. (°C)	Yield (%)[b]	*dr.*[c]
1	1 equiv.	456	50	25	11	>20:1
2	1 equiv.	440	50	28	15	>20:1
3	1 equiv.	427	50	30	20	>20:1
4	1 equiv.	405	50	32	12	>20:1
5	1 equiv.	2* 456	100	40-45	30	>20:1
6	1 equiv.	2* 440	100	50-55	59	>20:1
7	1 equiv.	2* 427	100	60-65	70	>20:1
8	1 equiv.	2* 405	100	70-75	49	>20:1

Reaction conditions: [a]3-Methyleneoxindole **1a** (0.2 mmol, 1 equiv), $CeCl_3$ (20 mol%), Cs_2CO_3 (20 mol%), in MeCN (0.06 M), using Kessil Blue LED (nm, % intensity, temperature °C with fan off). [b]Yields were determined after column chromatography purification. [c]Diastereomeric ratio was determined.

To confirm this, a variety of Lewis acids were screened (see Tables 3.3, entries 1–7). Among them, $CeCl_3$ exhibited the highest efficiency in affording the desired product **2a** in the highest yield (Table 3.1, entry 1). Later, we also evaluated both organic and inorganic bases. Among all, Cs_2CO_3 proved to be the most effective in affording the desired product **2a** efficiently. Conversely, the use of alternative bases significantly diminished the yield of the product **2a** (see Tables 3.3, entries 8–13).

Table 3.3 Investigation of acid catalyst, base additive, and solvent for the formal [4+2] cycloaddition reaction.[a]



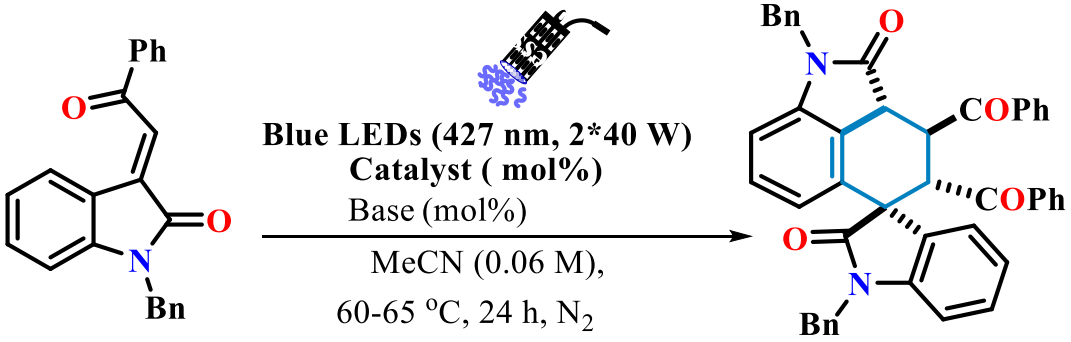
1a **2a**

Entry	Acidic Catalyst	Basic Additives	Solvent	Yield(%)[b]	*dr.*[c]
1	$CeCl_3$	Cs_2CO_3	MeCN	70	>20:1
2	$Sc(OTf)_3$	Cs_2CO_3	MeCN	42	>20:1
3	$In(OTf)_3$	Cs_2CO_3	MeCN	48	>20:1
4	$FeCl_3$	Cs_2CO_3	MeCN	36	>20:1
5	CuCl	Cs_2CO_3	MeCN	20	>20:1
6	$CuCl_2$	Cs_2CO_3	MeCN	NR	-
7	$CeCl_3$ ($7H_2O$)	Cs_2CO_3	MeCN	44	>20:1
8	$CeCl_3$	K_2CO_3	MeCN	59	>20:1
9	$CeCl_3$	Na_2CO_3	MeCN	63	>20:1
10	$CeCl_3$	$NaHCO_3$	MeCN	67	>20:1
11	$CeCl_3$	DABCO	MeCN	49	>20:1
12	$CeCl_3$	DMAP	MeCN	NR	-
13	$CeCl_3$	DBU	MeCN	NR	-
14	$CeCl_3$	Cs_2CO_3	DCM	56	>20:1

15	$CeCl_3$	Cs_2CO_3	Toluene	48	>20:1
16	$CeCl_3$	Cs_2CO_3	$CHCl_3$	60	>20:1
17	$CeCl_3$	Cs_2CO_3	THF	62	>20:1
18	$CeCl_3$	Cs_2CO_3	MeOH	30	>20:1
19	$CeCl_3$	Cs_2CO_3	DMSO	58	>20:1
20	$CeCl_3$	Cs_2CO_3	EtOAc	55	>20:1
21	$CeCl_3$	Cs_2CO_3	Benzene	60	>20:1
22	$CeCl_3$	Cs_2CO_3	H_2O	NR	-
23[d]	$CeCl_3$	Cs_2CO_3	MeCN	42	>20:1
24[d]	$CeCl_3$	-	MeCN	26	>20:1

Reaction conditions: [a]3-Methyleneoxindole **1a** (0.2 mmol, 1 equiv), $CeCl_3$ (20 mol%), Cs_3CO_3 (20 mol%) in solvent (0.06 M), with Kessil Blue LED (427 nm, 100% intensity, 60–65 °C, fan off, 2*40 W) under a nitrogen atmosphere. [b]Yields were determined after column chromatography. [c]Diastereomeric ratio analyzed by ^1H NMR spectroscopy. [d] dry MeCN. NR= No Reaction.

Table 3.4 Investigation of reactant ratio for the formal [4+2] cycloaddition reaction[a]



1a **2a**

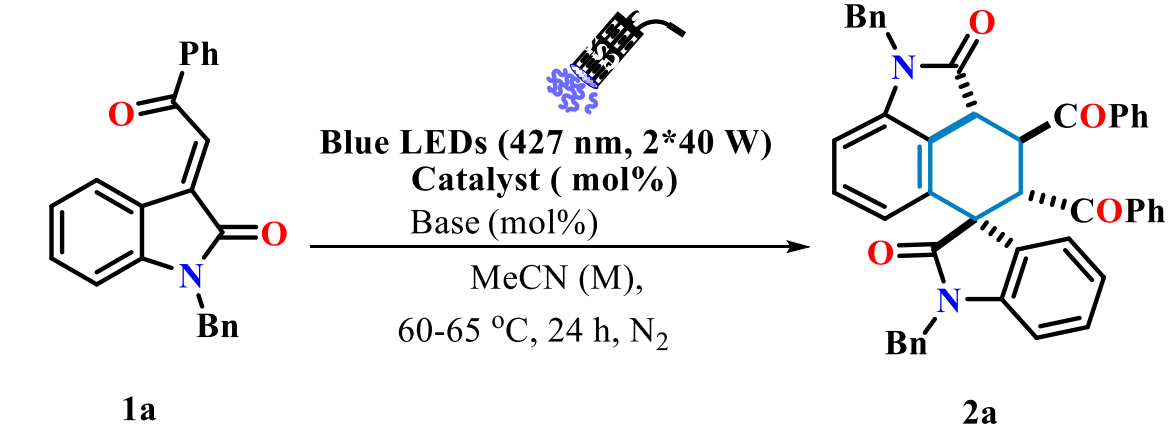
Entry	1a	$CeCl_3$	Cs_2CO_3	Yield (%)[b]	*dr.*[c]
1	1 equiv	20 mol%	20 mol%	70	>20:1
2	1 equiv	30 mol%	20 mol%	46	>20:1
3	1 equiv	10 mol%	20 mol%	36	>20:1

4	1 equiv	05 mol%	20 mol%	26	>20:1
5	1 equiv	20 mol%	10 mol%	30	>20:1
6	1 equiv	20 mol%	30 mol%	62	>20:1

Reaction conditions: [a]3-Methyleneoxindole **1a** (2 mmol, 1 equiv), $CeCl_3$ (20 mol%), Cs_2CO_3 (20 mol%), in MeCN (0.06 M) under Kessil Blue LED light (427 nm, 100% intensity, 60–65 °C, fan off, 2*40 W) in a nitrogen atmosphere. [b]Yields were measured following purification by column chromatography. [c]Diastereomeric ratio was determined using ^1H NMR spectroscopy.

Additionally, in order to evaluate the influence solvent, we screened various solvents and among all, acetonitrile proved to be efficient in affording the desired product **2a** in the highest yield (see Table 3.3, entries 14-24). Later, we also investigated the effect of solvent concentration on the outcome of the desired product **2a**. The results revealed that both lower and higher concentrations adversely affected the yield of **2a**. The optimum result was obtained in 0.06 M acetonitrile, leading to the highest yield of **2a** (see Table 3.5, entries 1–4).

Table 3.5 Evaluation of solvent Ratio for the formal [4+2] cycloaddition reaction: [a]



1a **2a**

Entry	1a	MeCN (M)	Yield (%)[b]	*dr.*[c]
1	1 equiv	0.2	49	>20:1
2	1 equiv	0.1	45	>20:1
3	1 equiv	0.06	70	>20:1
4	1 equiv	0.05	50	>20:1

Reaction conditions: [a]3-Methyleneoxindole **1a** (2 mmol, 1 equiv.), $CeCl_3$ (20 mol%), Cs_3CO_3 (20 mol%), in MeCN (varied concentration), under Kessil Blue LED (427 nm, 100% intensity, 60–65 °C, fan off, 2*40 W) in a nitrogen atmosphere. [b]Yields were assessed after purification via column chromatography. [c]Diastereomeric ratio was analyzed using ^{1}H NMR spectroscopy.

Furthermore, we varied the loading of both Lewis acid ($CeCl_3$) and base (Cs_2CO_3) to study the impact on the overall transformation. We observed that 20 mol% is optimum to obtain the desired product **2a** in the highest yield with very high diastereoselectivity (see Table 3.4, entries 1–6). Interestingly, when the reaction was performed under atmospheric air, the desired product **2a** was obtained in modest yield (Table 3.1, entry 6). However, the reaction under molecular oxygen, no product formation was observed (Table 3.1, entry 7).

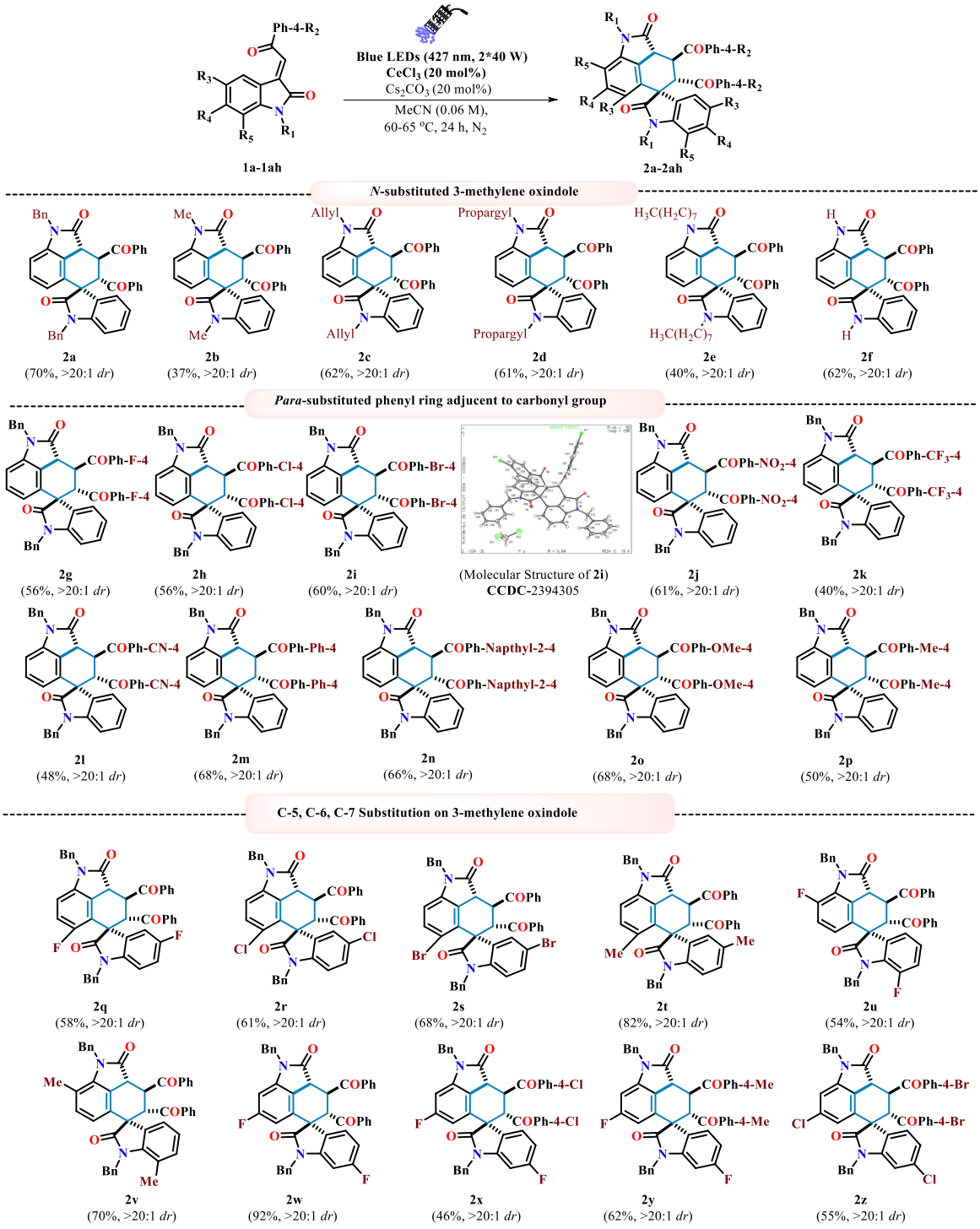
Based on these extensive optimizations, the ideal reaction conditions were identified as 3-methyleneoxindole **1a** (0.2 mmol, 1 equiv), $CeCl_3$ (20 mol%), and Cs_2CO_3 (20 mol%) in acetonitrile under blue LED irradiation (427 nm, 2*40 W) in a nitrogen atmosphere, resulting in the highest yield of **2a**.

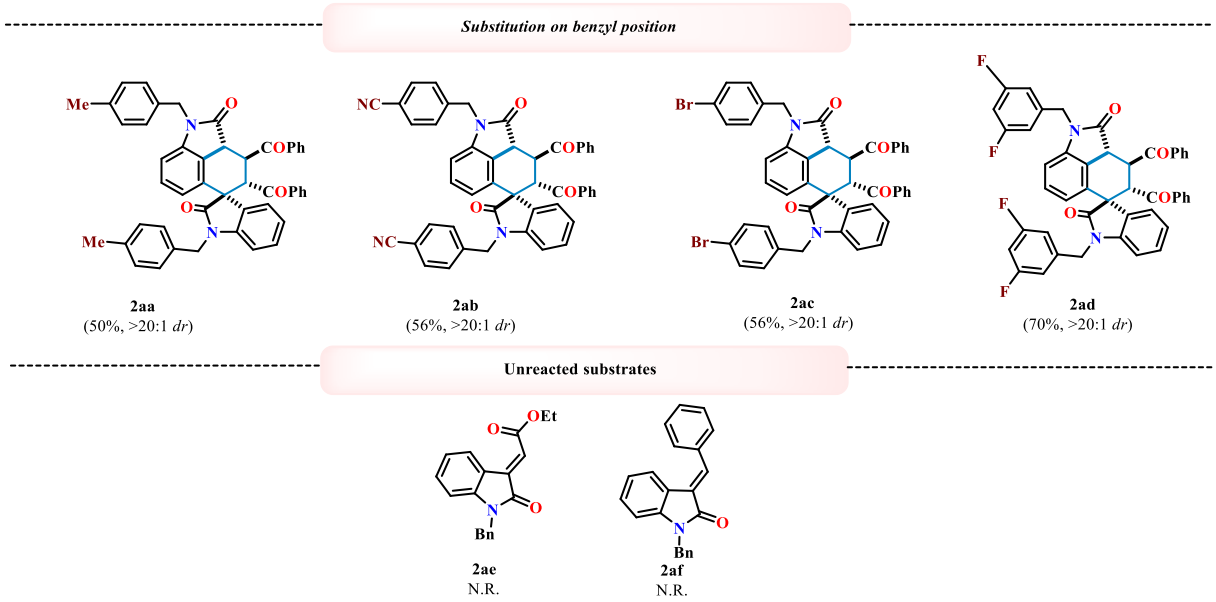
Having obtained the optimized reaction condition, we further investigated the substrate scope of different 3-methyleneoxindole derivatives **1b**–**1af** for the [4+2] cycloaddition. Various *N*-protected 3-methyleneoxindole derivatives **1b**–**1e**, as well as unprotected 3-methyleneoxindole **1f**, underwent the reaction efficiently under the established reaction conditions to afford the corresponding products **2b**–**2f** in moderate to good yields in excellent diastereoselectivity (see Scheme 3.7). Later, we explored the reaction with *N*-benzyl 3-methyleneoxindole derivatives with various substituents on the *para*- position of the phenyl ring adjacent to carbonyl moiety (**1g**–**1p)**. These substrates successfully furnished the corresponding desired products **2g**–**2p** in moderate to good yields in excellent diastereoselectivity (see Scheme 3.7). Notably, the nature of substituents on the phenyl group, including electron-donating, and electron-withdrawing groups, significantly influenced the yield of **2a** (see Scheme 3.7).

Substrates featuring electron-withdrawing and electron-donating groups at the C-5, C-6, and C-7 positions of 3-methyleneoxindoles underwent reactions smoothly by giving the corresponding products **2q**–**2z** in moderate to excellent yields with a high degree of diastereoselectivity (up to 92%, >20:1 *dr*) (see Scheme 3.7). *N*-benzyl 3-methyleneoxindole derivatives with *ortho-, meta-, and para*-substituents on the benzyl ring also provided the desired products **2aa**–**2ad** in moderate yields while maintaining excellent diastereoselectivity (see Scheme 3.7).

However, it was observed that certain *N*-benzyl 3-alkylidene/arylidene oxindole derivatives **1ae-1af** did not react under the standard conditions and expected desired products **2ae**–**2af** did not form (see Scheme 3.7).

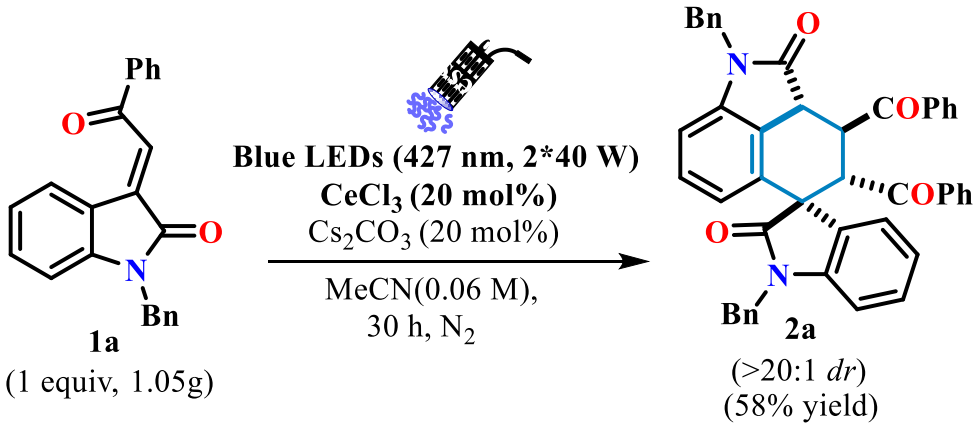
Scheme 3.7 The substrate scope of 3-methyleneoxindole derivatives was explored [a]



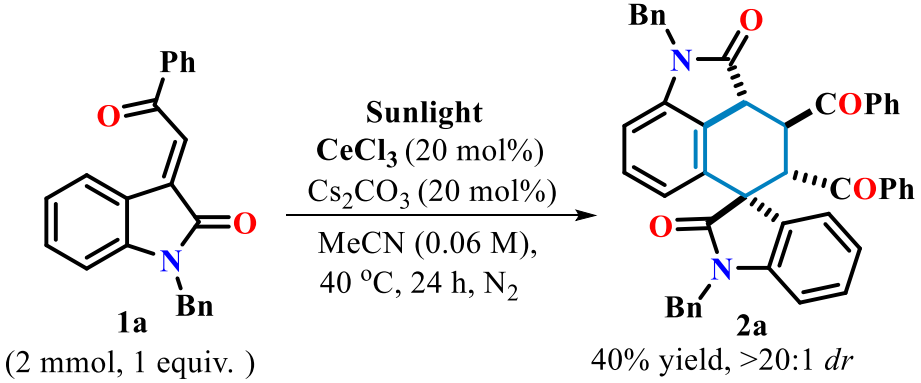


Standard reaction conditions: [a]3-Methyleneoxindole **1a** (0.2 mmol, 1 equiv), $CeCl_3$ (20 mol%), Cs_2CO_3 (20 mol%) in MeCN (0.06 M), irradiated with Kessil Blue LED (427 nm, 100% intensity, 60–65 °C, fan off, 2*40 W) under a nitrogen atmosphere. Diastereomeric ratio (>20:1 *dr*) was determined using ^1H NMR spectroscopy.

A. Scale-up synthesis of 3,4-fused spirooxindole



B. Sunlight-Mediated Synthesis of 3,4-Fused Spirooxindole



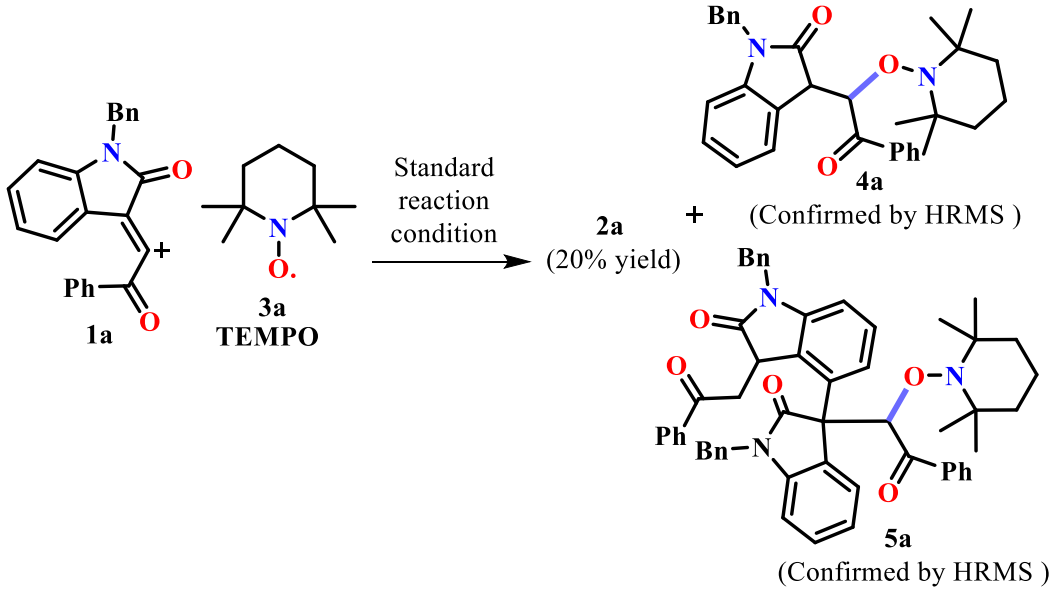
Scheme 3.8 Post synthetic transformations of 3,4-fused spirooxindoles

To evaluate the practicality of the developed protocol, we successfully carried out the scale-up reaction of **1a** (1.05 g, 3 mmol) to afford the desired product **2a,** in moderate yield with excellent diastereoselectivity (see Scheme 3.8A).

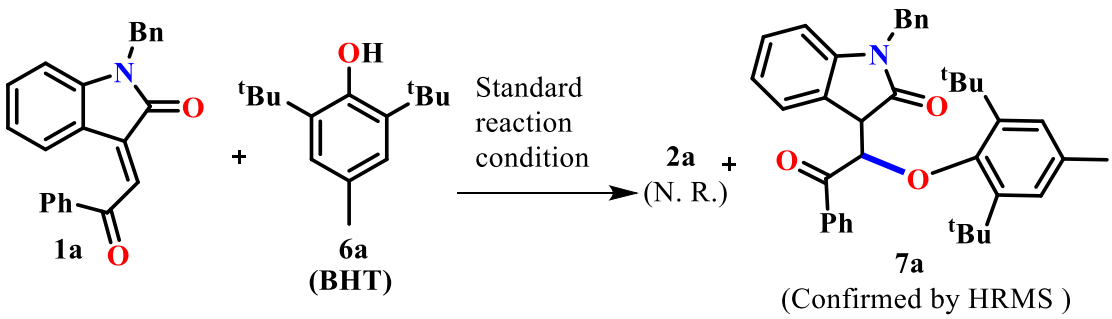
The reaction of **1a** was further investigated under the direct exposure of sunlight, leading to the formation of the desired product **2a**, albeit in modest yield, but with excellent diastereoselectivity (40%, see Scheme 3.8B). This demonstrates the potential of sunlight as a natural energy source for this transformation though with limited efficiency.

Further to gain the mechanistic insights, we carried out few control experiments. The radical trapping experiments were conducted using TEMPO and BHT as radical scavengers under standard reaction conditions (Scheme 3.9).

A. Radical trapping using TEMPO



B. Radical trapping using BHT



Scheme 3.9 Control experiments

In the presence of TEMPO, the desired product **2a** was obtained in low yield (20%) along with TEMPO-trapped radical intermediates **4a** and **5a**. Conversely, using BHT, not the desired product **2a** was formed, but the radical-trapped intermediate **7a** was formed, as confirmed by HRMS analysis (see Scheme 3.9A and 3.9B).

The radical trapping experiments strongly suggest the involvement of a radical during the course of the reaction. To further investigate, UV-visible spectroscopy was employed.

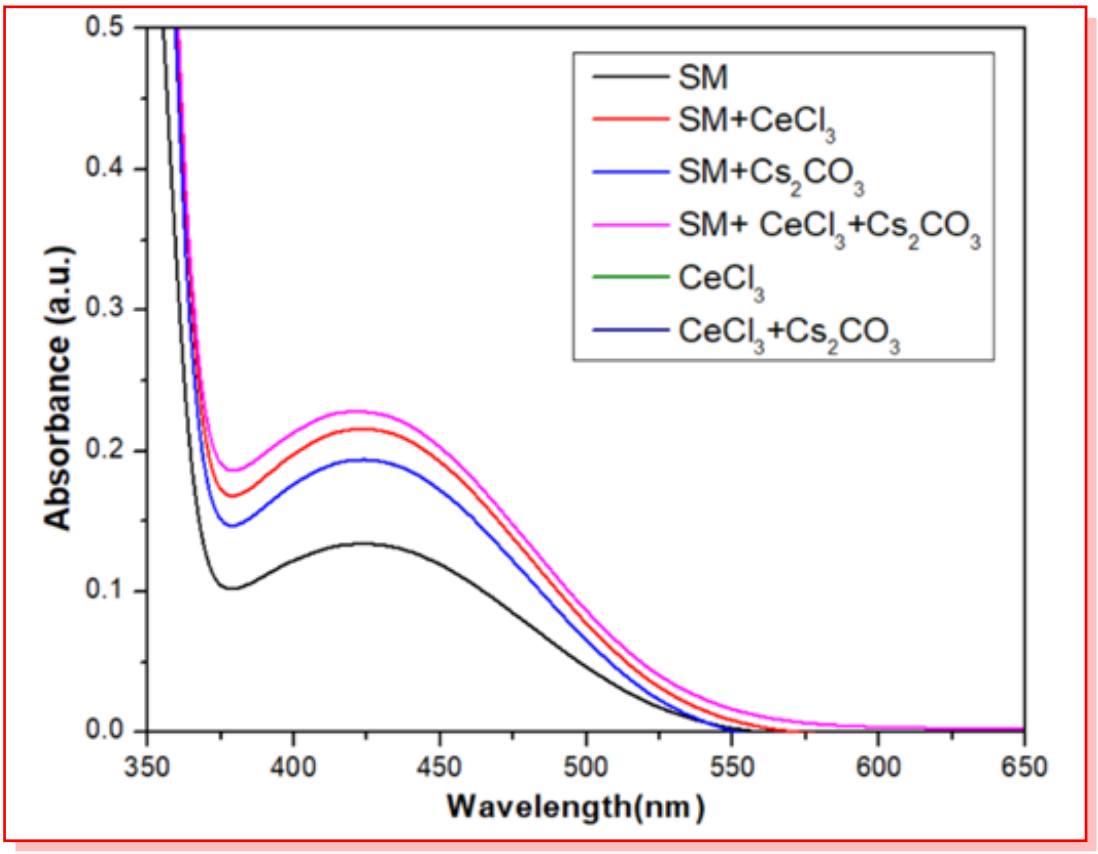
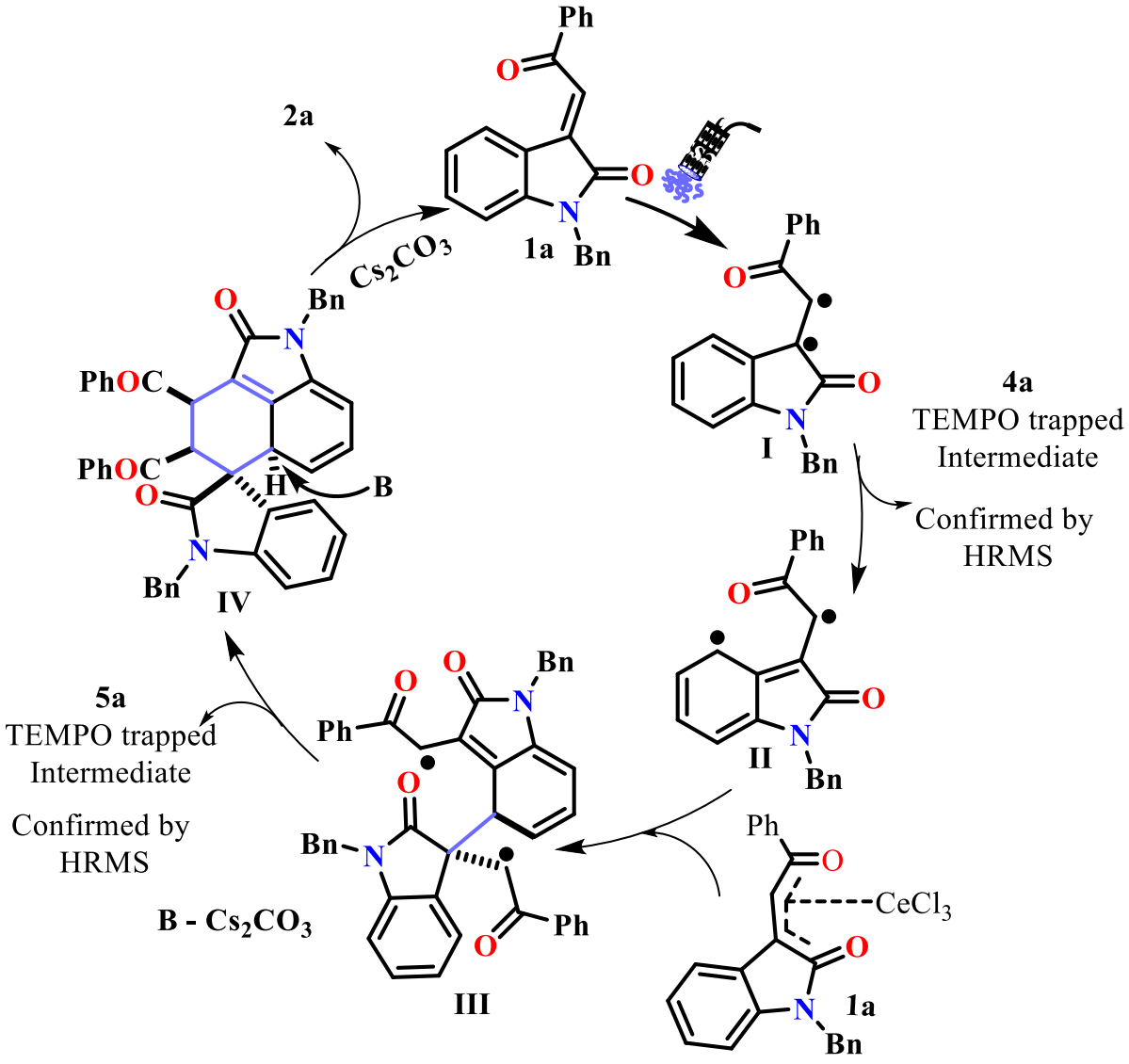


Figure 3.6 UV-visible absorption spectra of various forms of the starting material (3-methyleneoxindole) **1a** in acetonitrile (MeCN). The analysis includes: 20 µM starting material alone, 20 µM starting material with $CeCl_3$, 20 µM starting material with both $CeCl_3$ and Cs_2CO_3, 20 µM $CeCl_3$ alone, and 20 µM $CeCl_3$ combined with Cs_2CO_3.

The UV-visible absorption spectrum of the starting material, 3-methyleneoxindole **1a**, revealed absorption within the visible range (370-500 nm), providing additional insights into the reaction mechanism (Figure 3.6). The UV-visible absorption spectrum of the mixture containing 3-methyleneoxindole **2a** and $CeCl_3$ displayed absorption within the visible range. Subsequently, the spectrum was recorded for a mixture of 3-methyleneoxindole **2a**, $CeCl_3$, and Cs_2CO_3. Notably, no significant change or even slight shift in the absorption maxima (370–

500 nm) was observed (Figure 3.6). These findings suggest that 3-methyleneoxindole **2a** and $CeCl_3$ likely do not interact via a charge transfer pathway (see Figure 3.6).

These comparisons provide mechanistic insights into the interaction of the starting material with the catalyst and base under reaction conditions.



Scheme 3.10 Proposed plausible mechanism for the [4+2] cycloaddition reaction

Based on the control experiments, spectroscopic studies and literature precedence,[15] a plausible reaction mechanism has been proposed (see Scheme 3.10). This mechanistic pathway aims to rationalize the observed transformation, integrating key steps supported by experimental evidence and established precedents.

Under photoirradiation, 3-methyleneoxindole **1a** generates a radical intermediate **I**, as confirmed by HRMS (Scheme 3.9). This intermediate **I** may equilibrate with an unstable

intermediate **II** due to the heat generated by light exposure. The intermediate **II** further interacts with $CeCl_3$-activated 3-methyleneoxindole **1a (**see Figure 3.3, 3.4,.3.5**)**, forming a diradical intermediate **III**, which is validated by HRMS (Scheme 3.9). Subsequently, intermediate **III** undergoes cyclization, leading to another intermediate **IV**, which eventually undergoes aromatization via deprotonation to afford the target product **2a**.

3.4 Conclusions

In summary, we have established an efficient visible light-mediated approach for direct C4-H functionalization, enabling the synthesis of 3,4-fused spirooxindoles through a formal [4+2] cycloaddition of unactivated C4-H 3-methyleneoxindoles. This methodology employs a catalytic amount of $CeCl_3$ under basic conditions to afford 3,4-fused spirooxindoles with moderate to good yields and exceptional chemo- and regio-selectivity. The protocol proved to be scalable and also works under direct sunlight exposure. This straightforward and practical strategy holds potential for constructing complex molecular frameworks.

3.5 Experimental Section

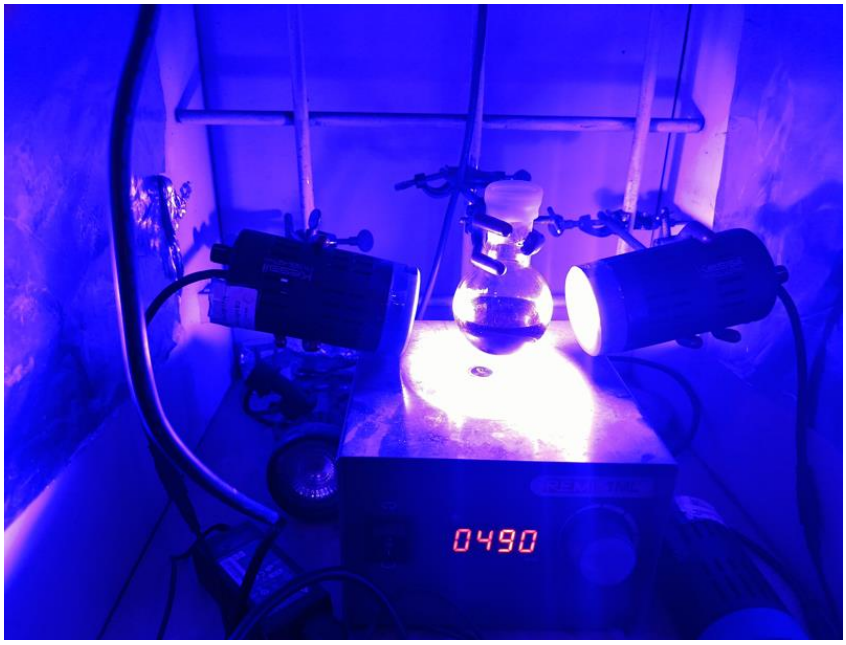
3.5.1 General

Unless specified otherwise, all starting materials and reagents were procured from commercial sources (Aldrich, TCI, and Alfa Aesar) and utilized without further purification. Thin-layer chromatography (TLC) was conducted on silica gel 60 GF254 pre-coated aluminum-backed plates (2.5 mm), with visualization achieved under UV light irradiation at 254 nm. Column chromatography employed silica gel (100–200 mesh) with a mixture of petroleum ether and ethyl acetate as the eluent. NMR spectra were recorded using tetramethylsilane (TMS) as the internal reference. Proton NMR (^{1}H NMR) spectra were acquired at 400 MHz, and carbon NMR (^{13}C{^{1}H} NMR) spectra at 100 MHz, utilizing Bruker and Jeol instruments unless stated otherwise. Chemical shifts (δ) are reported in parts per million (ppm), relative to $CDCl_3$ for ^{1}H NMR (δ = 7.26 ppm) and for ^{13}C{^{1}H} NMR (δ = 77.16 ppm). For ^{1}H NMR, data include chemical shifts, multiplicity (s = singlet, d = doublet, dd = double doublet, t = triplet, q = quartet, br = broad, m = multiplet), coupling constants (J) in Hz, and integration values. Carbon NMR spectra were recorded with full proton decoupling, and ^{19}F NMR spectra were acquired at 377 MHz. High-resolution mass spectrometry (HRMS) analyses were performed using an ESI-TOF mass analyzer. UV-Visible absorption studies were carried out using a Shimadzu UV-2600 spectrophotometer. All photocatalytic reactions were conducted under blue light illumination using Kessil PR160L series Blue LEDs.

3.5.2 General procedure for the synthesis of 2a (GP1)

In a dried 10 mL crimp-capped vial equipped with a magnetic stir bar, 3-methyleneoxindole **1a** (0.2 mmol, 1 equiv.), $CeCl_3$ (20 mol%, 0.2 equiv.), and Cs_2CO_3 (20 mol%, 0.2 equiv.) were combined at room temperature. Acetonitrile (0.06 M) was added, and the reaction mixture was degassed under a nitrogen atmosphere for 15 minutes with continuous purging. The mixture was then exposed to two 427 nm Kessil Blue LED lights (2*40 W, 100% intensity) without external cooling, allowing the temperature to stabilize at 60–65 °C as measured by an infrared thermometer. Stirring continued under irradiation for 24 hours. Upon completion, confirmed by TLC, the solvent was removed under reduced pressure, and the crude product **2a** was purified via silica gel column chromatography using a gradient of ethyl acetate and petroleum ether as the eluent.

Reaction setup under visible light (Kessil lamp)



3.5.3 General procedure for the synthesis of 2a under sunlight

In a dried 10 mL crimp-capped vial equipped with a magnetic stir bar, 3-methyleneoxindole **1a** (0.2 mmol, 1 equiv), $CeCl_3$ (20 mol%, 0.2 equiv), and Cs_2CO_3 (20 mol%, 0.2 equiv) were combined at room temperature. Acetonitrile (0.06 M) was then added to the mixture, followed by degassing under a nitrogen atmosphere with continuous purging for 15 minutes. The reaction vial was placed under direct sunlight (approximately 40 °C) for 24 hours, spread over

three days (8 hours/day). Upon reaction completion, as monitored by TLC, the solvent was removed under reduced pressure, and the resulting crude product was purified by silica gel column chromatography using a gradient eluent system of ethyl acetate and petroleum ether.

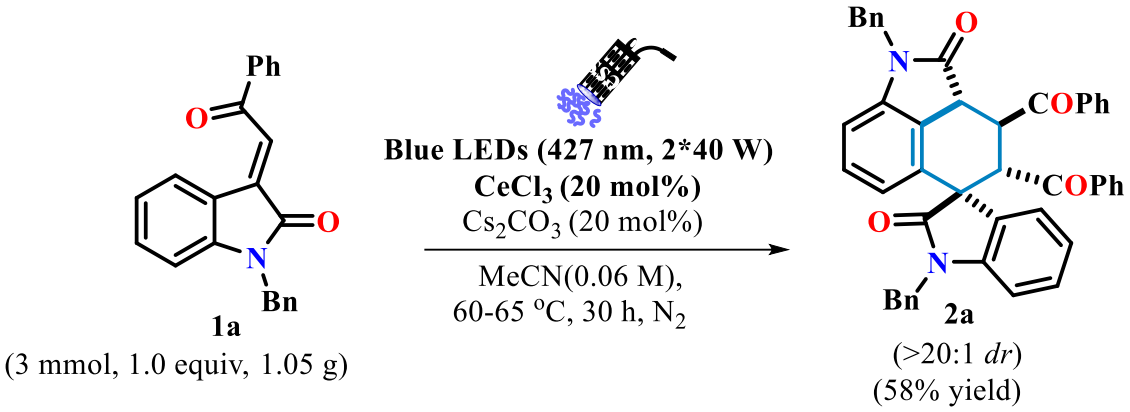
Reaction setup under sunlight



Atmospheric Temperature (40 ^{o}C)

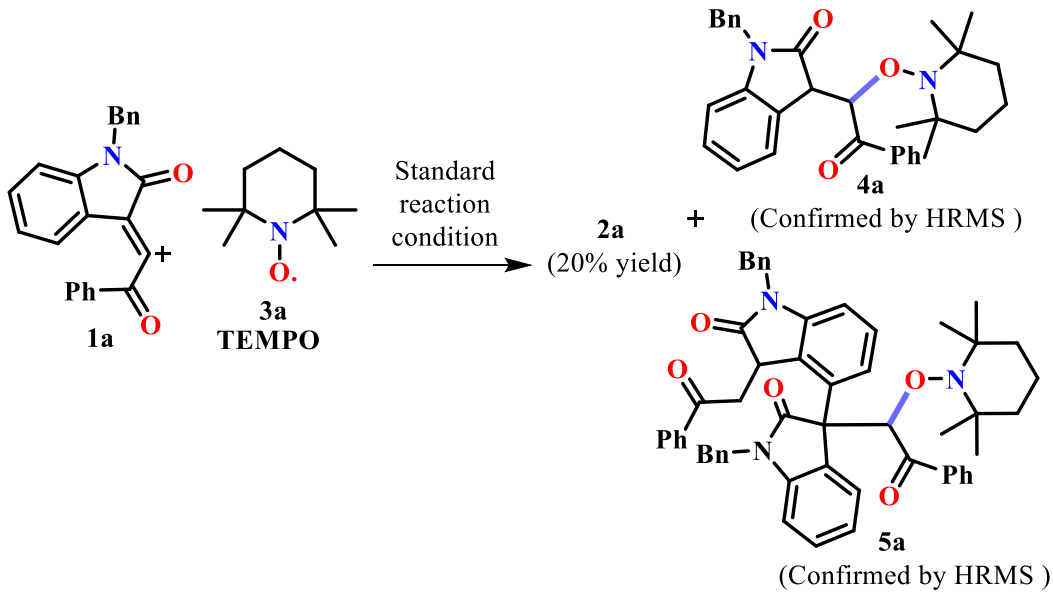
3.5.4 Procedure for the synthesis of 2a on mmol scale

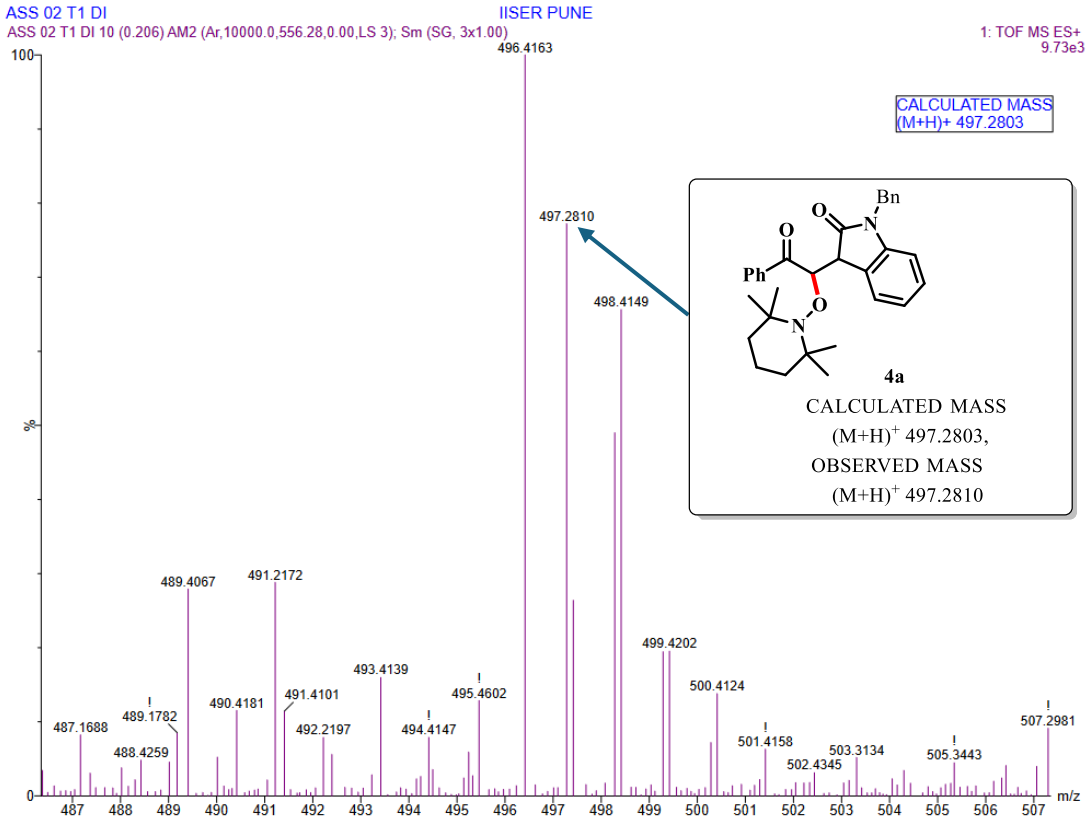
In a 100 mL oven-dried round-bottom flask equipped with a magnetic stir bar, 3-methyleneoxindole **1a** (3 mmol, 1.05 g, 1 equiv), $CeCl_3$ (20 mol%, 0.2 equiv), and Cs_2CO_3 (20 mol%, 0.2 equiv) were added at ambient temperature. MeCN (0.06 M) was introduced as the solvent, and the reaction mixture was thoroughly degassed under a nitrogen atmosphere for 1 hour with continuous purging. The mixture was then irradiated using two 427 nm Kessil Blue LED lamps (2*40 W, 100% intensity), maintaining a reaction temperature of 60–65 °C (monitored via IR thermometer) without external heating (fan turned off). The reaction proceeded for 30 hours, after which completion was confirmed by TLC analysis. The solvent was evaporated under reduced pressure, and the crude product was subjected to column chromatography on silica gel (100–200 mesh) using petroleum ether/ethyl acetate as the eluent to isolate the purified product.



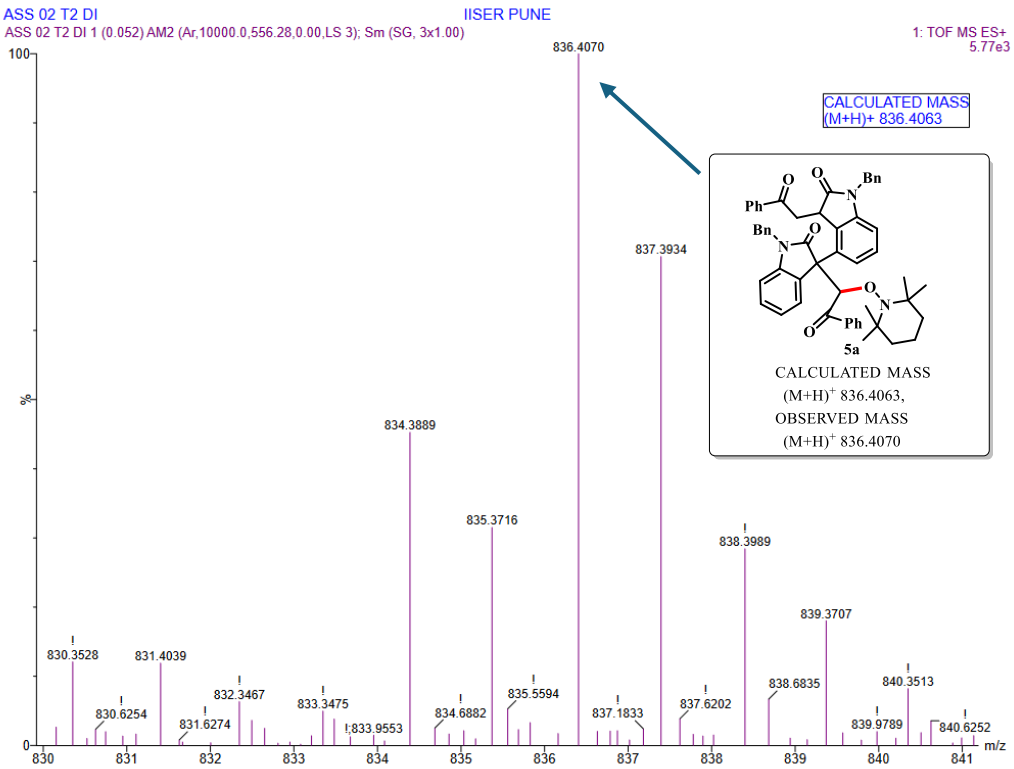
3.5.5 Procedure for the reaction using TEMPO

In an oven-dried 10 mL crimp-capped vial equipped with a magnetic stir bar, 3-methyleneoxindole **1a** (0.2 mmol, 1 equiv), $CeCl_3$ (20 mol%, 0.2 equiv), Cs_2CO_3 (20 mol%, 0.2 equiv), and TEMPO (2 equiv.) were combined at ambient temperature. MeCN (0.06 M) was added as the reaction medium, and the mixture was degassed under a nitrogen atmosphere for 15 minutes with continuous purging. The reaction mixture was then irradiated with two 427 nm Kessil Blue LED lamps (40 W, 100% intensity), maintaining a reaction temperature of 60–65 °C (monitored using an IR thermometer) without external heating (fan turned off). Despite stirring for 24 hours under these conditions, the desired product **2a** was obtained with only a 20% yield, even with an extended reaction time.





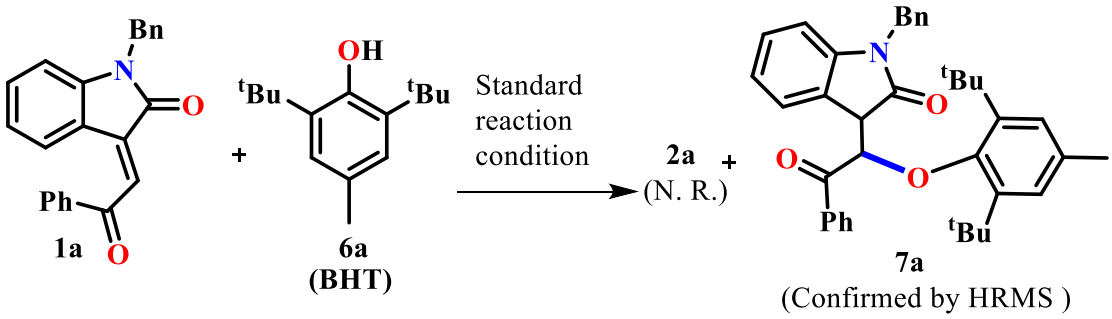
HRMS spectrum of **4a**



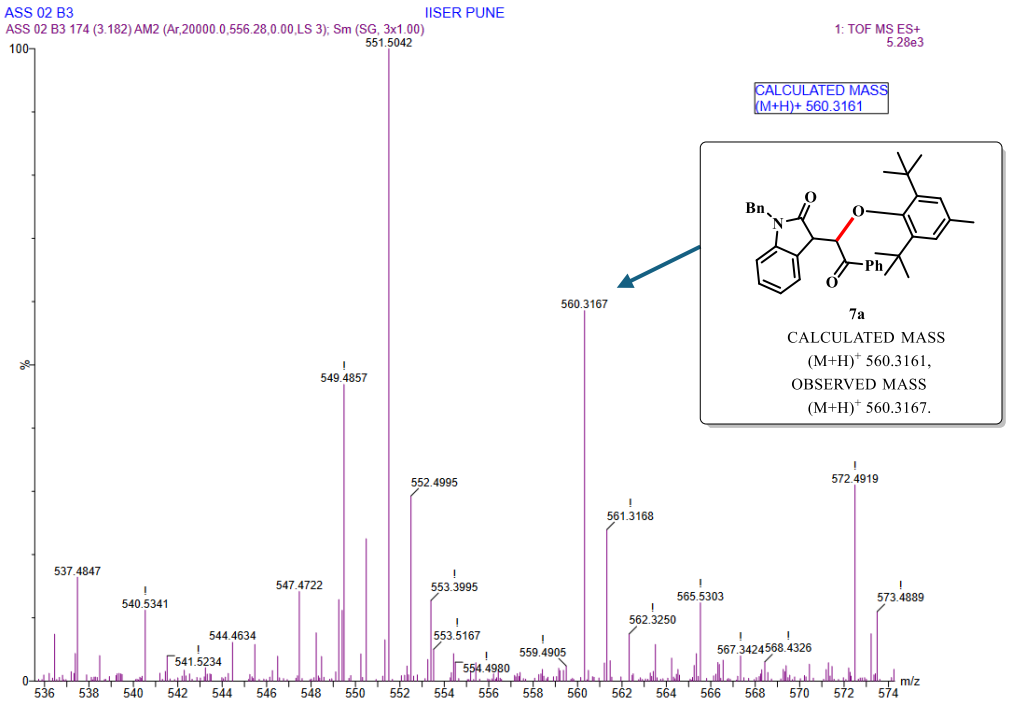
HRMS spectrum of **5a**

3.5.6 Procedure for the reaction using BHT

In a 10 mL oven-dried crimp-capped vial equipped with a magnetic stir bar, 3-methyleneoxindole **1a** (0.2 mmol, 1 equiv), $CeCl_3$ (20 mol%, 0.2 equiv), Cs_2CO_3 (20 mol%, 0.2 equiv), and BHT (2 equiv) were added at room temperature. MeCN (0.06 M) was introduced as the solvent, and the reaction mixture was thoroughly degassed under a nitrogen atmosphere for 15 minutes with continuous purging. The reaction was then irradiated using two 427 nm Kessil Blue LED lamps (40 W, 100% intensity), maintaining a temperature range of 60–65 °C (monitored via IR thermometer) without external heating (fan switched off). Despite stirring for 24 hours under these conditions, no formation of the desired product **2a** was observed, even with prolonged reaction time.



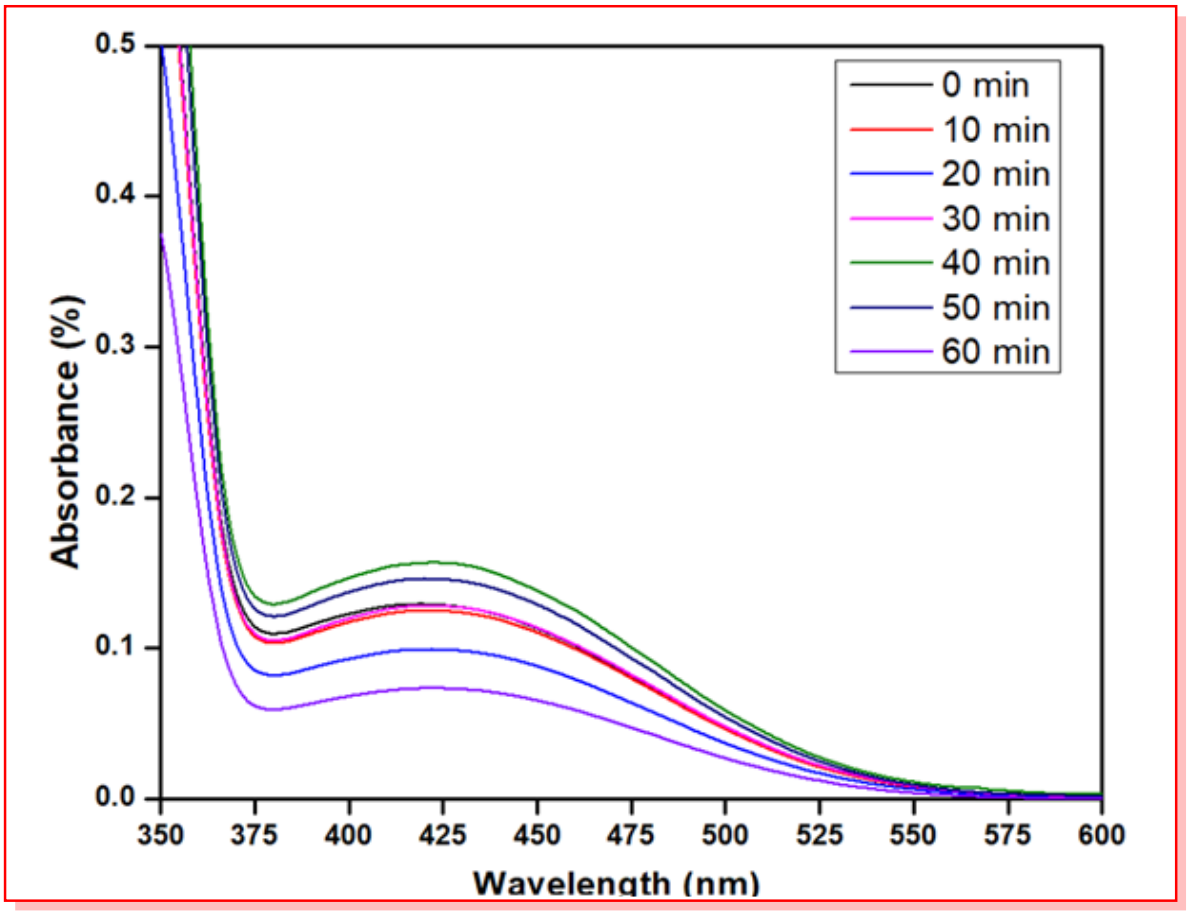
(Confirmed by HRMS)



HRMS spectrum of **7a**

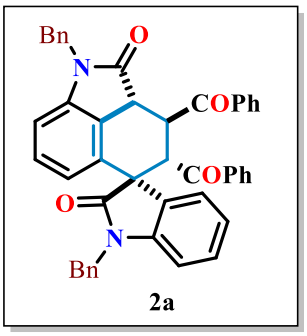
3.5.7 Procedure for UV-Visible absorption spectra without light

In an oven-dried 10 mL round-bottom flask equipped with a magnetic stir bar, 3-methyleneoxindole **1a** (0.2 mmol, 0.2 equiv), $CeCl_3$ (20 mol%, 0.2 equiv), and Cs_2CO_3 (20 mol%, 0.2 equiv) were added at room temperature. MeCN (0.06 M) was introduced, and the reaction mixture was degassed under a nitrogen atmosphere for 15 minutes with continuous purging. Subsequently, the mixture was stirred while UV-visible absorption spectra were recorded at intervals (every 10 minutes) from the initial time point (0 min) up to 1 hour. The spectra were captured using a Shimadzu UV-2600 spectrophotometer, ensuring consistent reaction progress monitoring.



3.6 Experimental Data

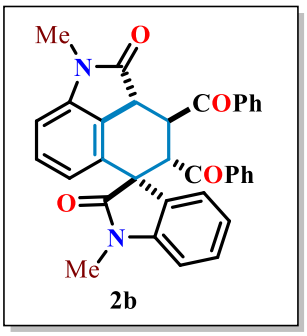
***(2aR,3S,4S,5R)*-3,4-Dibenzoyl-1,1'-dibenzyl-1,2a,3,4-tetrahydro-2H-spiro[benzo[cd]indole-5,3'-indoline]-2,2'-dione (2a)**



2a

The compound **2a** was prepared following the general procedure GP-1. White solid (95 mg, 70% yield, *dr* >20:1), R_f = 0.5 (petroleum ether/EtOAc 75:25), MP: 208-210 °C. ^{1}H NMR (400 MHz, $CDCl_3$): δ 8.2 (d, *J* = 7.6 Hz, 2H), 7.6 – 7.6 (m, 1H), 7.5 (dd, *J* = 8.3, 6.7 Hz, 2H), 7.5 – 7.4 (m, 1H), 7.3 – 7.3 (m, 7H), 7.3 – 7.2 (m, 5H), 7.1 (dd, *J* = 7.3, 2.3 Hz, 2H), 7.1 (td, *J* = 7.6, 1.5 Hz, 1H), 7.0 – 6.9 (m, 2H), 6.9 (dd, *J* = 7.5, 1.5 Hz, 1H), 6.6 (d, *J* = 7.7 Hz, 1H), 6.3 (d, *J* = 7.8 Hz, 1H), 6.0 (d, *J* = 8.1 Hz, 1H), 5.4 (d, *J* = 10.8 Hz, 1H), 5.1 (d, *J* = 15.4 Hz, 1H), 5.0 (d, *J* = 15.5 Hz, 1H), 4.5 – 4.4 (m, 1H), 4.4 (d, *J* = 11.3 Hz, 1H), 4.3 (s, 1H), 3.7 (d, *J* = 15.5 Hz, 1H). ^{13}C{^{1}H} NMR (100 MHz, $CDCl_3$): δ 201.9, 200.4, 178.2, 175.3, 142.6, 142.4, 138.0, 137.3, 135.7, 135.5, 133.2, 132.9, 132.8, 131.3, 129.3, 128.8, 128.8, 128.8, 128.8, 128.4, 128.2, 128.0, 127.8, 127.7, 127.6, 127.3, 126.5, 126.2, 123.4, 119.2, 108.9, 107.5, 56.9, 54.6, 46.6, 44.0, 43.9, 42.0. HRMS (ESI TOF) *m/z* calcd. For $C_{46}H_{35}N_2O_4$ $[M+H]^+$ 679.2597 found 679.2608.

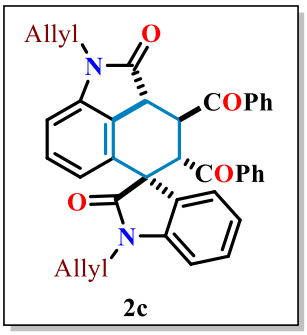
(*2aR,3S,4S,5R*)-3,4-Dibenzoyl-1,1'-dimethyl-1,2a,3,4-tetrahydro-2H-spiro[benzo[cd]indole-5,3'-indoline]-2,2'-dione (2b)



2b

The compound **2b** was prepared following the general procedure GP-1. White solid (39 mg, 37% yield, *dr* >20:1), R_f = 0.4 (petroleum ether/EtOAc 75:25), MP: 269-271 °C. ^{1}H NMR (400 MHz, $CDCl_3$): δ 8.2 – 8.1 (m, 2H), 7.7 – 7.6 (m, 1H), 7.5 (s, 2H), 7.5 – 7.4 (m, 1H), 7.3 (s, 1H), 7.3 – 7.2 (m, 4H), 7.1 – 7.0 (m, 2H), 7.0 – 6.9 (m, 1H), 6.7 (d, *J* = 7.6 Hz, 1H), 6.5 – 6.4 (m, 1H), 6.1 (d, *J* = 8.0 Hz, 1H), 5.3 (d, *J* = 10.9 Hz, 1H), 4.4 (dd, *J* = 11.9, 10.9 Hz, 1H), 4.2 (d, *J* = 11.8 Hz, 1H), 3.2 (s, 3H), 2.8 (s, 3H). ^{13}C{^{1}H} NMR (100 MHz, $CDCl_3$): δ 202.2, 200.7, 178.1, 175.6, 143.5, 143.3, 138.2, 137.4, 133.2, 132.7, 132.7, 131.5, 129.4, 129.0, 128.9, 128.5, 128.2, 127.9, 126.6, 126.0, 123.5, 119.4, 108.0, 106.5, 57.3, 54.7, 46.6, 41.8, 26.5, 26.4. HRMS (ESI TOF) *m/z* calcd. For $C_{46}H_{35}N_2O_4$ $[M+H]^+$ 527.1971 found 527.1974.

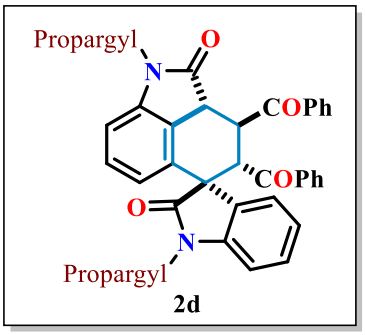
(*2aR,3S,4S,5R*)-1,1'-Diallyl-3,4-dibenzoyl-1,2a,3,4-tetrahydro-2H-spiro[benzo[cd]indole-5,3'-indoline]-2,2'-dione (2c)



2c

The compound **2c** was prepared following the general procedure GP-1. White solid (72 mg, 62% yield, *dr* >20:1), R_f = 0.45 (petroleum ether/EtOAc 75:25), MP: 154-156 °C. ^{1}H NMR (400 MHz, $CDCl_3$): δ 8.2 – 8.0 (m, 2H), 7.6 – 7.5 (m, 1H), 7.5 (dd, *J* = 8.3, 6.8 Hz, 2H), 7.4 – 7.4 (m, 1H), 7.3 – 7.3 (m, 1H), 7.3 (d, *J* = 1.6 Hz, 1H), 7.2 (dd, *J* = 8.2, 7.0 Hz, 2H), 7.1 (d, *J* = 1.4 Hz, 1H), 7.0 (ddd, *J* = 16.1, 7.8, 1.0 Hz, 2H), 6.9 (dd, *J* = 7.6, 1.3 Hz, 1H), 6.7 (d, *J* = 7.7 Hz, 1H), 6.5 (d, *J* = 7.8 Hz, 1H), 6.1 (d, *J* = 8.0 Hz, 1H), 5.8 (ddt, *J* = 17.2, 10.8, 5.5 Hz, 1H), 5.4 (ddt, *J* = 17.4, 10.6, 5.5 Hz, 1H), 5.3 – 5.2 (m, 3H), 5.1 (dd, *J* = 13.7, 2.4 Hz, 2H), 4.5 (d, *J* = 5.4 Hz, 1H), 4.4 (dd, *J* = 11.9, 10.9 Hz, 1H), 4.2 – 4.1 (m, 2H), 4.0 (ddt, *J* = 16.0, 5.6, 1.5 Hz, 1H), 3.5 – 3.4 (m, 1H). ^{13}C{^{1}H} NMR (100 MHz, $CDCl_3$): δ 202.0, 200.5, 177.6, 175.1, 142.6, 142.5, 138.1, 137.4, 133.2, 132.8, 132.8, 131.4, 131.4, 131.1, 129.3, 128.8, 128.8, 128.4, 128.2, 128.0, 126.4, 126.2, 123.4, 119.1, 117.9, 117.9, 108.8, 107.4, 56.7, 54.6, 46.5, 42.7, 42.6, 42.0. HRMS (ESI TOF) *m/z* calcd. For $C_{38}H_{30}N_2O_4$ $[M+H]^+$ 579.2283 found 679.2281.

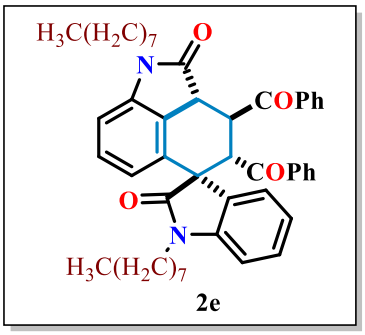
(*2aR,3S,4S,5R*)-3,4-Dibenzoyl-1,1'-di(prop-2-yn-1-yl)-1,2a,3,4-tetrahydro-2H-spiro[benzo[cd]indole-5,3'-indoline]-2,2'-dione (2d)



2d

The compound **2d** was prepared following the general procedure GP-1. White solid (70 mg, 61% yield, *dr* >20:1), R_f = 0.45 (petroleum ether/EtOAc 75:25), MP: 194-196 °C. ^{1}H NMR (400 MHz, $CDCl_3$): δ 8.2 – 8.0 (m, 2H), 7.6 – 7.5 (m, 1H), 7.5 (dd, *J* = 8.3, 6.8 Hz, 2H), 7.4 – 7.4 (m, 1H), 7.2 – 7.2 (m, 5H), 7.1 (td, *J* = 7.9, 1.0 Hz, 1H), 7.0 (td, *J* = 7.6, 1.0 Hz, 1H), 7.0 – 6.9 (m, 2H), 6.7 (d, *J* = 7.8 Hz, 1H), 6.1 (d, *J* = 8.1 Hz, 1H), 5.3 (d, *J* = 10.8 Hz, 1H), 4.6 (dd, *J* = 17.6, 2.6 Hz, 1H), 4.5 – 4.4 (m, 2H), 4.3 – 4.2 (m, 1H), 4.2 – 4.1 (m, 1H), 3.4 (dd, *J* = 17.7, 2.5 Hz, 1H), 2.3 (q, *J* = 2.6, 2.1 Hz, 1H), 2.1 (t, *J* = 2.5 Hz, 1H). ^{13}C{^{1}H} NMR (100 MHz, $CDCl_3$): δ 201.8, 200.3, 176.9, 174.2, 141.5, 141.2, 137.9, 137.2, 133.2, 132.9, 132.6, 131.1, 129.4, 128.9, 128.8, 128.4, 128.1, 128.0, 126.2, 126.0, 123.8, 119.7, 109.0, 107.8, 76.2, 76.2, 72.6, 72.6, 56.7, 54.5, 46.4, 41.7, 29.5, 29.5. HRMS (ESI TOF) *m/z* calcd. For $C_{38}H_{27}N_2O_4$ $[M+H]^+$ 575.1971 found 575.1977.

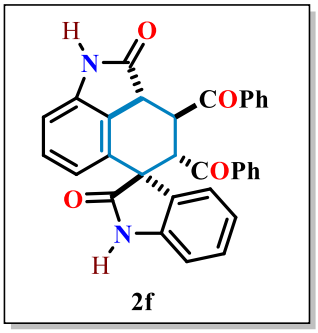
(*2aR,3S,4S,5R*)-3,4-Dibenzoyl-1,1'-dioctyl-1,2a,3,4-tetrahydro-2H spiro[benzo[cd]indole-5,3'-indoline]-2,2'-dione (2e)



2e

The compound **2e** was prepared following the general procedure GP-1. Yellow solid (58 mg, 40% yield, *dr* >20:1), R_f = 0.4 (petroleum ether/EtOAc 75:25), MP: 117-119 °C. ^{1}H NMR (400 MHz, Chloroform-*d*): δ 8.2 – 8.0 (m, 2H), 7.6 – 7.5 (m, 1H), 7.5 (dd, *J* = 8.3, 6.7 Hz, 2H), 7.4 (t, *J* = 7.2 Hz, 1H), 7.3 – 7.1 (m, 5H), 7.0 (dtd, *J* = 23.6, 7.7, 1.0 Hz, 2H), 6.9 (dd, *J* = 7.6, 1.3 Hz, 1H), 6.7 (d, *J* = 7.7 Hz, 1H), 6.5 (d, *J* = 7.8 Hz, 1H), 6.0 (d, *J* = 8.1 Hz, 1H), 5.3 (d, *J* = 10.9 Hz, 1H), 4.4 (dd, *J* = 11.9, 10.9 Hz, 1H), 4.1 (d, *J* = 11.8 Hz, 1H), 3.8 (dt, *J* = 14.4, 7.5 Hz, 1H), 3.5 (s, 1H), 3.4 – 3.3 (m, 1H), 2.9 (s, 1H), 1.6 (t, *J* = 7.0 Hz, 2H), 1.4 – 1.1 (m, 22H), 0.9 (td, *J* = 6.9, 1.4 Hz, 6H). ^{13}C{^{1}H} NMR (100 MHz, $CDCl_3$): δ 202.1, 200.7, 177.8, 175.3, 143.0, 142.8, 138.1, 137.4, 133.1, 133.0, 132.7, 131.6, 129.2, 128.8, 128.8, 128.4, 128.2, 127.9, 126.6, 126.3, 123.1, 118.8, 108.1, 106.6, 56.7, 54.6, 46.6, 41.9, 40.3, 40.2, 31.8, 31.7, 29.3, 29.3, 29.2, 29.2, 29.1, 29.1, 27.6, 27.1, 26.9, 26.8, 22.6, 14.1. HRMS (ESI TOF) *m/z* calcd. For $C_{48}H_{54}N_2O_4$ $[M+H]^+$ 723.4162 found 723.4165.

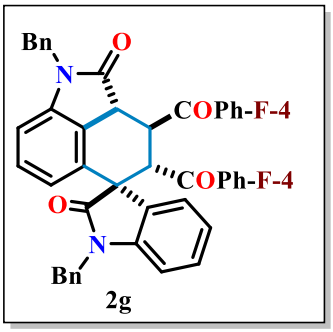
(*2aR,3S,4S,5R*)-3,4-Dibenzoyl-1,2a,3,4-tetrahydro-2H-spiro[benzo[cd]indole-5,3'-indoline]-2,2'-dione (2f)



2f

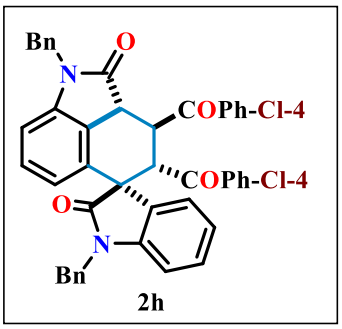
The compound **2f** was prepared following the general procedure GP-1. White solid (62 mg, 62% yield, *dr* >20:1), R_f = 0.35 (petroleum ether/EtOAc 75:25), MP: 220-222 °C. ^{1}H NMR (400 MHz, $CDCl_3$): δ 8.1 – 8.1 (m, 2H), 8.1 – 8.0 (m, 1H), 7.7 (s, 1H), 7.6 – 7.5 (m, 1H), 7.5 (dd, *J* = 8.3, 6.9 Hz, 2H), 7.4 – 7.3 (m, 3H), 7.2 – 7.0 (m, 4H), 7.0 (d, *J* = 1.0 Hz, 1H), 6.9 – 6.9 (m, 1H), 6.7 (d, *J* = 7.6 Hz, 1H), 6.5 (d, *J* = 7.8 Hz, 1H), 6.2 (d, *J* = 8.1 Hz, 1H), 5.3 (d, *J* = 10.8 Hz, 1H), 4.4 (dd, *J* = 11.9, 10.9 Hz, 1H), 4.2 (d, *J* = 7.5 Hz, 1H). ^{13}C{^{1}H} NMR (100 MHz, $CDCl_3$): δ 201.8, 200.4, 179.9, 177.3, 140.4, 140.2, 138.0, 137.2, 133.2, 132.9, 131.7, 129.4, 128.9, 128.9, 128.8, 128.4, 128.2, 128.0, 127.2, 126.4, 123.5, 119.3, 109.5, 108.2, 56.7, 54.9, 46.7, 42.0. HRMS (ESI TOF) *m/z* calcd. For $C_{32}H_{23}N_2O_4$ $[M+H]^+$ 499.1658 found 499.1657.

(*2aR,3S,4S,5R*)-1,1'-Dibenzyl-3,4-bis(4-fluorobenzoyl)-1,2a,3,4-tetrahydro-2H-spiro[benzo[cd]indole-5,3'-indoline]-2,2'-dione (2g)



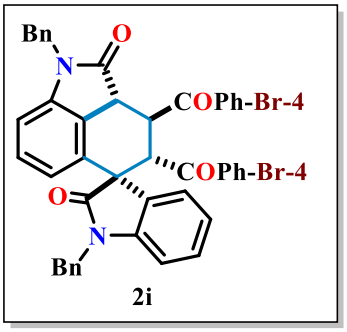
The compound **2g** was prepared following the general procedure GP-1. White solid (80 mg, 56% yield, *dr* >20:1), R_f = 0.5 (petroleum ether/EtOAc 75:25), MP: 238-240 °C. ^{1}H NMR (400 MHz, $CDCl_3$): δ 8.2 – 8.1 (m, 2H), 7.4 – 7.3 (m, 8H), 7.3 (s, 2H), 7.2 – 7.1 (m, 4H), 7.1 (td, *J* = 7.7, 1.3 Hz, 1H), 7.0 (tdd, *J* = 7.6, 4.7, 1.0 Hz, 2H), 6.9 – 6.8 (m, 3H), 6.6 (d, *J* = 7.7 Hz, 1H), 6.4 (d, *J* = 7.8 Hz, 1H), 6.0 (d, *J* = 8.0 Hz, 1H), 5.3 (d, *J* = 10.6 Hz, 1H), 5.1 (d, *J* = 15.4 Hz, 1H), 5.0 (d, *J* = 15.4 Hz, 1H), 4.5 (d, *J* = 15.4 Hz, 1H), 4.4 (dd, *J* = 11.9, 10.7 Hz, 1H), 4.2 (d, *J* = 11.8 Hz, 1H), 3.9 (d, *J* = 15.4 Hz, 1H). ^{13}C{^{1}H} NMR (100 MHz, $CDCl_3$): δ 200.3, 198.8, 178.1, 175.3, 167.0 (d, $J_{(C-F)}$ = 38.4 Hz), 164.5 (d, $J_{(C-F)}$ = 38.7 Hz), 142.5, 142.4, 135.6, 135.3, 134.4 (d, $J_{(C-F)}$ = 2.9 Hz), 133.5 (d, $J_{(C-F)}$ = 2.9 Hz), 132.8, 131.5 (d, $J_{(C-F)}$ = 9.5 Hz), 131.1, 130.9 (d, $J_{(C-F)}$ = 9.4 Hz), 129.4, 128.9, 128.9, 128.8, 127.9, 127.9, 127.6, 127.4, 126.4, 126.2, 123.5, 119.2, 115.6 (d, $J_{(C-F)}$ = 22.0 Hz), 115.2 (d, $J_{(C-F)}$ = 21.9 Hz), 108.9, 107.6, 56.5, 54.5, 46.5, 44.2, 44.0, 42.1. ^{19}F NMR (377 MHz, $CDCl_3$): δ -104.5, -105.1. HRMS (ESI TOF) *m/z* calcd. For $C_{46}H_{32}F_2N_2O_4$ $[M+H]^+$ 715.2408 found 715.2411.

(*2aR,3S,4S,5R*)-1,1'-Dibenzyl-3,4-bis(4-chlorobenzoyl)-1,2a,3,4-tetrahydro-2H-spiro[benzo[cd]indole-5,3'-indoline]-2,2'-dione (2h)



The compound **2h** was prepared following the general procedure GP-1. Orange solid (84 mg, 56% yield, *dr* >20:1), R_f = 0.50 (petroleum ether/EtOAc 75:25), MP: 199-201 °C. ^{1}H NMR (400 MHz, $CDCl_3$): δ 8.1 – 7.9 (m, 2H), 7.5 – 7.4 (m, 2H), 7.4 – 7.3 (m, 8H), 7.2 (s, 1H), 7.2 – 7.2 (m, 3H), 7.2 – 7.1 (m, 2H), 7.1 (td, *J* = 7.8, 1.3 Hz, 1H), 7.0 (tdd, *J* = 7.6, 5.5, 1.0 Hz, 2H), 6.9 (dd, *J* = 7.4, 1.3 Hz, 1H), 6.6 (d, *J* = 7.7 Hz, 1H), 6.4 (d, *J* = 7.8 Hz, 1H), 6.0 (d, *J* = 8.0 Hz, 1H), 5.3 (d, *J* = 10.6 Hz, 1H), 5.1 (d, *J* = 15.4 Hz, 1H), 5.0 (d, *J* = 15.4 Hz, 1H), 4.5 (d, *J* = 15.4 Hz, 1H), 4.4 – 4.3 (m, 1H), 4.2 (d, *J* = 11.9 Hz, 1H), 3.8 (d, *J* = 15.4 Hz, 1H). ^{13}C{^{1}H} NMR (100 MHz, $CDCl_3$): δ 200.7, 199.3, 178.1, 175.3, 142.5, 142.5, 139.8, 139.4, 136.3, 135.6, 135.4, 135.3, 132.8, 131.0, 130.2, 129.6, 129.5, 129.0, 128.9, 128.9, 128.8, 128.3, 127.9, 127.9, 127.6, 127.4, 126.3, 126.2, 123.5, 119.2, 109.0, 107.7, 56.7, 54.5, 46.5, 44.2, 44.0, 42.1. HRMS (ESI TOF) *m/z* calcd. For $C_{46}H_{32}Cl_2N_2O_4$ $[M+H]^+$ 747.1817 found 747.1824.

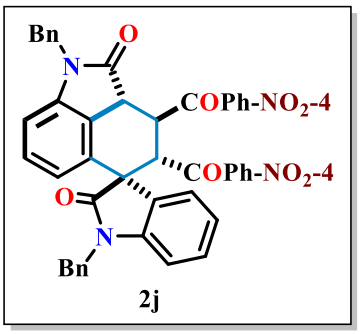
(*2aR,3S,4S,5R*)-1,1'-Dibenzyl-3,4-bis(4-bromobenzoyl)-1,2a,3,4-tetrahydro-2H-spiro[benzo[cd]indole-5,3'-indoline]-2,2'-dione (2i)



2i

The compound **2i** was prepared following the general procedure GP-1. Orange solid (100 mg, 60% yield, *dr* >20:1), R_f = 0.50 (petroleum ether/EtOAc 75:25), MP: 188-190 °C. ^{1}H NMR (400 MHz, $CDCl_3$): δ 8.0 – 7.9 (m, 2H), 7.7 – 7.5 (m, 2H), 7.4 – 7.3 (m, 10H), 7.2 – 7.1 (m, 4H), 7.1 (s, 1H), 7.0 (dd, *J* = 6.3, 1.1 Hz, 2H), 6.9 (dd, *J* = 7.5, 1.3 Hz, 1H), 6.6 (d, *J* = 7.7 Hz, 1H), 6.4 (d, *J* = 7.8 Hz, 1H), 6.0 (d, *J* = 8.0 Hz, 1H), 5.3 (d, *J* = 10.5 Hz, 1H), 5.1 (d, *J* = 15.4 Hz, 1H), 5.0 (d, *J* = 15.4 Hz, 1H), 4.5 (d, *J* = 15.4 Hz, 1H), 4.4 – 4.2 (m, 2H), 3.8 (d, *J* = 15.4 Hz, 1H); ^{13}C{^{1}H} NMR (100 MHz, $CDCl_3$): δ 200.9, 199.5, 178.0, 175.3, 142.5, 142.4, 136.6, 135.8, 135.6, 135.2, 132.7, 131.8, 131.3, 131.0, 130.3, 129.7, 129.5, 129.0, 128.9, 128.9, 128.6, 128.1, 127.9, 127.9, 127.6, 127.4, 126.3, 126.1, 123.5, 119.2, 109.1, 107.7, 56.7, 54.5, 46.5, 44.2, 44.0, 42.1. HRMS (ESI TOF) *m/z* calcd. For $C_{46}H_{32}Br_2N_2O_4$ $[M+H]^+$ 837.0787 found 837.0827.

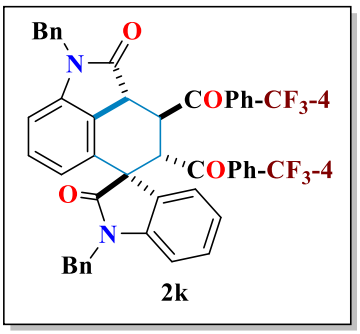
(*2aR,3S,4S,5R*)-1,1'-Dibenzyl-3,4-bis(4-nitrobenzoyl)-1,2a,3,4-tetrahydro-2H-spiro[benzo [cd]indole-5,3'-indoline]-2,2'-dione (2j)



2j

The compound **2j** was prepared following the general procedure GP-1. Light Yellowish solid (77 mg, 50% yield, *dr* >20:1), R_f = 0.35 (petroleum ether/EtOAc 75:25), MP: 238-240 °C. ^{1}H NMR (400 MHz, $CDCl_3$): δ 8.4 – 8.3 (m, 2H), 8.3 – 8.2 (m, 2H), 8.0 – 7.9 (m, 2H), 7.3 (ddd, *J* = 23.3, 9.3, 7.1 Hz, 8H), 7.3 (s, 1H), 7.3 (s, 1H), 7.2 – 7.1 (m, 3H), 7.0 (tdd, *J* = 7.9, 3.4, 1.0 Hz, 2H), 6.9 (dd, *J* = 7.5, 1.3 Hz, 1H), 6.6 (d, *J* = 7.8 Hz, 1H), 6.5(d, *J* = 7.8 Hz, 1H), 6.0 (d, *J* = 8.0 Hz, 1H), 5.4 (d, *J* = 10.7 Hz, 1H), 5.1 (d, *J* = 15.4 Hz, 1H), 4.9 (d, *J* = 15.2 Hz, 1H), 4.5 (s, 1H), 4.4 (s, 1H), 4.3 (s, 1H), 3.9 (d, *J* = 15.1 Hz, 1H). ^{13}C{^{1}H} NMR (100 MHz, $CDCl_3$): δ 200.9, 199.5, 177.8, 175.1, 150.4, 150.0, 142.6, 142.5, 142.4, 141.5, 135.4, 134.8, 132.5, 130.5, 129.8, 129.8, 129.5, 129.0, 128.9, 128.9, 128.2, 128.0, 127.7, 127.6, 126.2, 125.9, 123.8, 123.8, 123.1, 119.2, 109.1, 108.0, 57.3, 54.2, 46.6, 44.3, 44.1, 42.8. HRMS (ESI TOF) *m/z* calcd. For $C_{46}H_{32}N_4O_8$ $[M+H]^+$ 769.2298 found 769.2296.

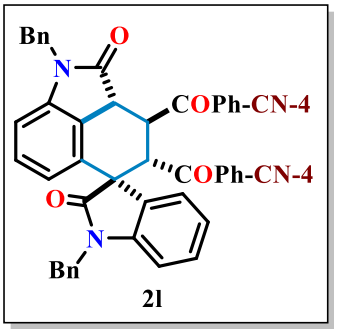
(*2aR,3S,4S,5R*)-1,1'-Dibenzyl-3,4-bis(4-(trifluoromethyl)benzoyl)-1,2a,3,4-tetrahydro-2H-spiro[benzo[cd]indole-5,3'-indoline]-2,2'-dione (2k)



2k

The compound **2k** was prepared following the general procedure GP-1. Yellow solid (50 mg, 81% yield, *dr* >20:1), R_f = 0.35 (petroleum ether/EtOAc 75:25), MP: 230-232 °C.^{1}H NMR (400 MHz, $CDCl_3$): δ 8.2 (d, *J* = 8.1 Hz, 2H), 7.8 (d, *J* = 8.2 Hz, 2H), 7.5 (d, *J* = 8.2 Hz, 2H), 7.4 – 7.3 (m, 8H), 7.3 (d, *J* = 1.9 Hz, 2H), 7.1 (ddd, *J* = 24.4, 7.7, 2.1 Hz, 3H), 7.0 – 6.9 (m, 2H), 6.9 – 6.8 (m, 1H), 6.6 (d, *J* = 7.7 Hz, 1H), 6.4 (d, *J* = 7.8 Hz, 1H), 6.0 (d, *J* = 8.1 Hz, 1H), 5.4 (d, *J* = 10.6 Hz, 1H), 5.1 (d, *J* = 15.4 Hz, 1H), 5.0 (d, *J* = 15.4 Hz, 1H), 4.5 (d, *J* = 15.4 Hz, 1H), 4.4 (dd, *J* = 11.7, 10.7 Hz, 1H), 4.3 (d, *J* = 11.9 Hz, 1H), 3.6 (d, *J* = 15.3 Hz, 1H). ^{13}C{^{1}H} NMR (100 MHz, $CDCl_3$): δ 201.2, 200.0, 177.9, 175.2, 142.5, 142.5, 140.5, 139.9, 135.5, 135.1, 134.9 – 134.2 (m), 133.9 (dd, $J_{(C-F)}$ = 32.5, 22.0 Hz), 132.5, 130.9, 129.7, 129.2, 129.1, 128.9, 128.5, 128.0 (d, *J* = 5.4 Hz), 127.6, 127.4, 126.0, 126.0, 125.6 (q, $J_{(C-F)}$ = 3.6 Hz), 125.2 – 124.7 (m), 123.7, 122.4, 122.1, 119.2, 109.1, 107.8, 57.6, 54.4, 46.6, 44.1, 44.0, 42.3. ^{19}F NMR (377 MHz, $CDCl_3$): δ -63.1, -63.1. HRMS (ESI TOF) *m/z* calcd. For $C_{48}H_{32}F_6N_2O_4$ $[M+H]^+$ 815.2344 found 815.2338.

(*2aR,3S,4S,5R*)-4,4'-(1,1'-Dibenzyl-2,2'-dioxo-2,2a,3,4-tetrahydro-1H-spiro[benzo[cd]indole-5,3'-indoline]-3,4-dicarbonyl)dibenzonitrile (2l)

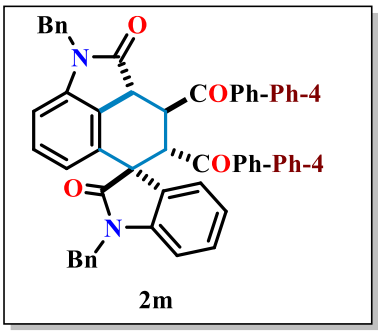


2l

The compound **2l** was prepared following the general procedure GP-1. White solid (70 mg, 48% yield, *dr* >20:1), R_f = 0.35 (petroleum ether/EtOAc 75:25), MP: 238-240 °C.^{1}H NMR (400 MHz, $CDCl_3$): δ 8.2 – 8.1 (m, 2H), 7.8 (d, *J* = 8.5 Hz, 2H), 7.5 – 7.4 (m, 2H), 7.4 – 7.3 (m, 10H), 7.2 (dd, *J* = 6.7, 2.9 Hz, 2H), 7.1 (dd, *J* = 7.8, 1.3 Hz, 1H), 7.0 (tdd, *J* = 7.6, 2.7, 1.0 Hz, 2H), 6.9 (dd, *J* = 7.5, 1.2 Hz, 1H), 6.6 (d, *J* = 7.7 Hz, 1H), 6.5 (d, *J* = 7.9 Hz, 1H), 6.0 (d, *J* = 8.0 Hz, 1H), 5.3 (d, *J* = 10.5 Hz, 1H), 5.1 (d, *J* = 15.4 Hz, 1H), 4.9 (d, *J* = 15.2 Hz, 1H), 4.5 (d, *J* = 15.4 Hz, 1H), 4.4 – 4.1 (m, 2H), 3.8 (d, *J* = 15.2 Hz, 1H). ^{13}C{^{1}H} NMR (100 MHz, $CDCl_3$): δ 201.0, 199.5, 177.8, 175.1, 142.6, 142.5, 140.9, 140.0, 135.4, 134.9, 132.5, 132.4, 131.8, 130.6, 129.8, 129.4, 129.2, 129.0, 128.9, 128.4, 128.2, 128.0, 127.7, 127.6, 126.1, 125.9, 123.8, 119.1, 118.1, 117.7, 116.5, 116.1, 109.0, 108.0, 57.1, 54.2, 46.6,

44.3, 44.1, 42.5. HRMS (ESI TOF) *m/z* calcd. For $C_{48}H_{32}N_4O_4$ $[M+H]^+$ 729.2502 found 729.2495.

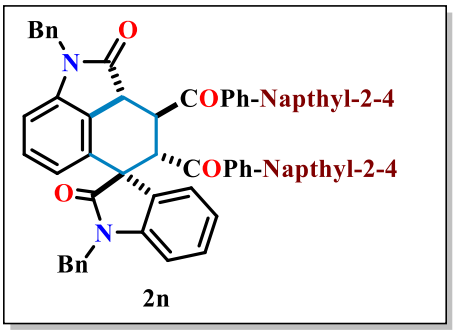
(*2aR,3S,4S,5R*)-3,4-Di([1,1'-biphenyl]-4-carbonyl)-1,1'-dibenzyl-1,2a,3,4-tetrahydro-2H-spiro[benzo[cd]indole-5,3'-indoline]-2,2'-dione (2m)



2m

The compound **2m** was prepared following the general procedure GP-1. White solid (113 mg, 68% yield, *dr* >20:1), R_f = 0.40 (petroleum ether/EtOAc 75:25), MP: 265-267 °C. 1H NMR (400 MHz, $CDCl_3$): δ 8.3 – 8.2 (m, 2H), 7.7 (d, *J* = 8.7 Hz, 2H), 7.7 – 7.6 (m, 2H), 7.6 – 7.5 (m, 2H), 7.5 – 7.4 (m, 11H), 7.3 (d, *J* = 5.3 Hz, 4H), 7.2 – 7.2 (m, 3H), 7.1 – 7.0 (m, 3H), 7.0 – 6.9 (m, 3H), 6.6 (d, *J* = 7.7 Hz, 1H), 6.3 (d, *J* = 7.8 Hz, 1H), 6.0 (dd, *J* = 8.1, 0.6 Hz, 1H), 5.4 (d, *J* = 10.9 Hz, 1H), 5.2 (d, *J* = 15.4 Hz, 1H), 5.0 – 4.9 (m, 1H), 4.6 – 4.4 (m, 2H), 4.3 (s, 1H), 3.7 (d, *J* = 15.5 Hz, 1H). $^{13}C\{^1H\}$ NMR (100 MHz, $CDCl_3$): δ 201.5, 200.0, 178.4, 175.6, 145.9, 145.6, 142.7, 142.6, 140.4, 139.8, 136.8, 136.0, 135.8, 135.5, 133.1, 131.4, 129.5, 129.4, 129.2, 129.0, 128.9, 128.9, 128.9, 128.5, 128.1, 127.9, 127.8, 127.7, 127.5, 127.4, 127.4, 127.4, 127.3, 126.7, 126.6, 126.3, 123.6, 119.4, 109.0, 107.6, 57.1, 54.8, 46.7, 44.2, 44.0, 42.1. HRMS (ESI TOF) *m/z* calcd. For $C_{58}H_{42}N_2O_4$ $[M+H]^+$ 831.3223 found 831.3229.

(*2aR,3S,4S,5R*)-3,4-Di(2-naphthoyl)-1,1'-dibenzyl-1,2a,3,4-tetrahydro-2H-spiro[benzo[cd]indole-5,3'-indoline]-2,2'-dione (2n)

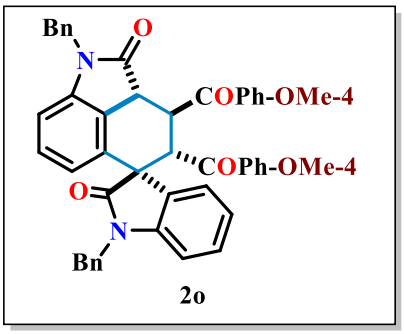


2n

The compound **2n** was prepared following the general procedure GP-1. White solid (123 mg, 66% yield, *dr* >20:1), R_f = 0.40 (petroleum ether/EtOAc 75:25), MP: 227-229 °C. ^1H NMR (400 MHz, $CDCl_3$): δ 8.9 – 8.6 (m, 1H), 8.2 (dd, *J* = 8.6, 1.8 Hz, 1H), 8.1 (d, *J* = 1.8 Hz, 1H), 8.0 (dd, *J* = 8.1, 1.5 Hz, 1H), 8.0 (s, 2H), 7.9 – 7.8 (m, 1H), 7.8 (dd, *J* = 8.2, 1.3 Hz, 1H), 7.6 – 7.5 (m, 5H), 7.3 – 7.3 (m, 5H), 7.2 – 7.1 (m, 4H), 7.0 – 7.0 (m, 3H), 6.9 (s, 3H), 6.6 (d, *J* = 7.6 Hz, 1H), 6.3 – 6.1 (m, 1H), 6.0 (d, *J* = 8.1 Hz, 1H), 5.6 (d, *J* = 10.9 Hz, 1H), 5.1 (d, *J* = 15.4 Hz, 1H), 4.7 (s, 1H), 4.6 (d, *J* = 1.0 Hz, 1H), 4.5 (d, *J* = 15.4 Hz, 1H), 4.4 (d, *J* = 11.8 Hz, 1H), 3.2 (d, *J* = 15.5 Hz, 1H). $^{13}C\{^1H\}$ NMR (100 MHz, $CDCl_3$): δ 201.7, 200.2, 178.4, 175.4, 142.5, 142.5, 135.9, 135.8, 135.4, 135.3, 135.2, 134.4, 133.1, 132.6, 131.9, 131.3, 130.6, 130.2, 130.0, 129.7, 129.3, 128.8, 128.8, 128.6, 128.5, 128.3, 128.3, 127.8, 127.8, 127.8, 127.7, 127.6, 127.6, 127.1,

126.8, 126.7, 126.4, 126.2, 124.6, 123.7, 123.4, 119.3, 108.8, 107.5, 57.0, 54.7, 46.7, 43.9, 43.9, 42.3. HRMS (ESI TOF) *m/z* calcd. For $C_{54}H_{39}N_2O_4$ $[M+H]^+$ 779.2910 found 779.2905.

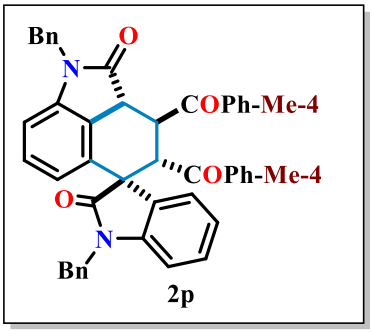
(*2aR,3S,4S,5R*)-1,1'-Dibenzyl-3,4-bis(4-methoxybenzoyl)-1,2a,3,4-tetrahydro-2H-spiro[benzo[cd]indole-5,3'-indoline]-2,2'-dione (2o)



2o

The compound **2o** was prepared following the general procedure GP-2. Light Yellow solid (101 mg, 68% yield, *dr* >20:1), R_f = 0.50 (petroleum ether/EtOAc 75:25), MP: 166-168 °C. ^{1}H NMR (400 MHz, $CDCl_3$): δ 8.1 (d, *J* = 9.0 Hz, 2H), 7.4 (d, *J* = 8.8 Hz, 2H), 7.3 – 7.3 (m, 5H), 7.2 (dd, *J* = 5.0, 1.8 Hz, 3H), 7.1 – 7.0 (m, 3H), 7.0 – 6.9 (m, 5H), 6.7 (d, *J* = 9.0 Hz, 2H), 6.6 (d, *J* = 7.7 Hz, 1H), 6.4 (d, *J* = 7.9 Hz, 1H), 6.0 (d, *J* = 8.0 Hz, 1H), 5.3 (d, *J* = 10.8 Hz, 1H), 5.2 (d, *J* = 15.4 Hz, 1H), 5.0 (d, *J* = 15.5 Hz, 1H), 4.5 – 4.4 (m, 2H), 4.3 (d, *J* = 11.8 Hz, 1H), 4.0 (s, 1H), 3.9 (s, 3H), 3.8 (s, 3H); $^{13}C\{^1H\}$ NMR (100 MHz, $CDCl_3$): δ 199.9, 198.2, 178.4, 175.5, 163.6, 163.4, 142.4, 142.4, 135.8, 135.5, 133.1, 131.4, 131.1, 131.1, 130.7, 130.2, 129.2, 128.8, 128.8, 128.6, 127.8, 127.7, 127.6, 127.3, 126.7, 126.4, 123.3, 119.2, 113.7, 113.2, 108.8, 107.4, 55.8, 55.5, 55.4, 54.8, 46.5, 44.1, 43.9, 41.8. HRMS (ESI TOF) *m/z* calcd. For $C_{48}H_{38}N_2O_6$ $[M+H]^+$ 739.2808 found 739.2801.

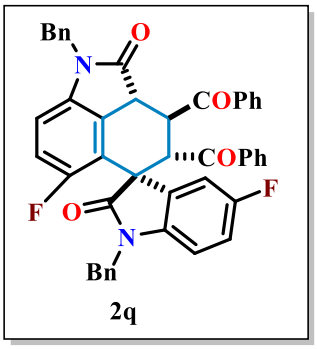
(*2aR,3S,4S,5R*)-1,1'-Dibenzyl-3,4-bis(4-methylbenzoyl)-1,2a,3,4-tetrahydro-2H-spiro[benzo[cd]indole-5,3'-indoline]-2,2'-dione (2p)



2p

The compound **2p** was prepared following the general procedure GP-1. White solid (71 mg, 50% yield, *dr* >20:1), R_f = 0.50 (petroleum ether/EtOAc 75:25), MP: 137-139 °C. ^{1}H NMR (400 MHz, $CDCl_3$): δ 8.1 – 8.0 (m, 2H), 7.3 – 7.3 (m, 7H), 7.2 (td, *J* = 4.2, 1.9 Hz, 5H), 7.1 (dd, *J* = 6.9, 2.7 Hz, 2H), 7.1 – 7.0 (m, 3H), 6.9 (s, 3H), 6.6 (d, *J* = 7.7 Hz, 1H), 6.4 (d, *J* = 7.8 Hz, 1H), 6.0 (d, *J* = 8.0 Hz, 1H), 5.3 (d, *J* = 10.8 Hz, 1H), 5.2 (d, *J* = 15.4 Hz, 1H), 4.9 (d, *J* = 15.5 Hz, 1H), 4.5 – 4.4 (m, 2H), 4.3 (s, 1H), 3.7 (d, *J* = 15.5 Hz, 1H), 2.4 (s, 3H), 2.3 (s, 3H). $^{13}C\{^1H\}$ NMR (100 MHz, $CDCl_3$): δ 201.3, 199.7, 178.3, 175.5, 144.0, 143.6, 142.5, 142.4, 135.8, 135.6, 135.5, 134.8, 133.1, 131.4, 129.2, 129.2, 128.9, 128.8, 128.8, 128.6, 128.4, 127.8, 127.7, 127.6, 127.3, 127.3, 126.7, 126.3, 123.4, 119.3, 108.9, 107.4, 56.4, 54.7, 46.6, 44.1, 43.9, 41.9, 21.8, 21.7. HRMS (ESI TOF) *m/z* calcd. For $C_{48}H_{38}N_2O_4$ $[M+H]^+$ 707.2910 found 707.2905.

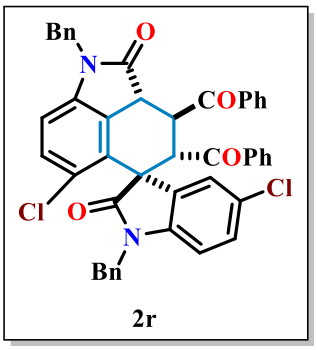
(*2aR,3S,4S,5R*)-3,4-Dibenzoyl-1,1'-dibenzyl-5',7-difluoro-1,2a,3,4-tetrahydro-2H-spiro[benzo[cd]indole-5,3'-indoline]-2,2'-dione (2q)



2q

The compound **2q** was prepared following the general procedure GP-1. Yellow solid (83 mg, 58% yield, *dr* >20:1), R_f = 0.50 (petroleum ether/EtOAc 75:25), MP: 211-213 °C. ^{1}H NMR (400 MHz, $CDCl_3$): δ 8.2 – 8.1 (m, 2H), 7.6 – 7.4 (m, 6H), 7.4 – 7.3 (m, 7H), 7.2 (dd, *J* = 6.0, 1.4 Hz, 3H), 7.1 (dd, *J* = 7.3, 2.3 Hz, 2H), 6.8 – 6.7 (m, 3H), 6.6 (dd, *J* = 8.4, 3.3 Hz, 1H), 6.2 (dd, *J* = 8.6, 4.1 Hz, 1H), 5.3 – 5.1 (m, 2H), 4.8 (d, *J* = 15.9 Hz, 1H), 4.6 – 4.4 (m, 2H), 4.3 – 4.2 (m, 1H), 3.3 (d, *J* = 16.0 Hz, 1H). ^{13}C{^{1}H} NMR (100 MHz, $CDCl_3$): δ 201.5, 199.2, 176.4, 174.8, 159.2 (d, $J_{(C-F)}$ = 242.6 Hz), 155.2 (d, $J_{(C-F)}$ = 170.6 Hz), 138.5, 138.5, 138.4, 138.0, 137.9, 137.6 (d, $J_{(C-F)}$ = 37.7 Hz), 135.0 (d, $J_{(C-F)}$ = 73.1 Hz), 133.5, 131.0 (d, $J_{(C-F)}$ = 7.8 Hz), 129.5, 128.9, 128.9, 128.7, 128.6, 128.3, 128.3, 128.3, 127.6, 127.5, 127.0 (d, $J_{(C-F)}$ = 2.8 Hz), 120.4 (d, $J_{(C-F)}$ = 12.9 Hz), 115.6 (d, $J_{(C-F)}$ = 12.1 Hz), 115.4 (d, $J_{(C-F)}$ = 11.6 Hz), 113.2 (d, $J_{(C-F)}$ = 25.0 Hz), 110.0 (d, $J_{(C-F)}$ = 8.0 Hz), 108.9 (d, $J_{(C-F)}$ = 8.1 Hz), 56.6, 53.1, 46.9, 44.1, 44.0, 41.2. ^{19}F NMR (377 MHz, $CDCl_3$): δ -118.8, -124.5. HRMS (ESI TOF) *m/z* calcd. For $C_{46}H_{32}F_2N_2O_4$ $[M+H]^+$ 715.2408 found 715.2427.

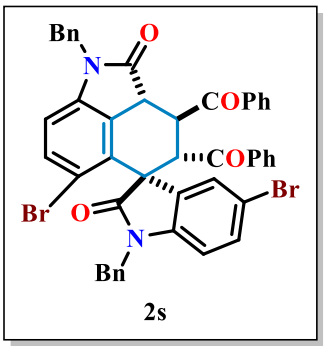
(*2aR,3S,4S,5R*)-3,4-Dibenzoyl-1,1'-dibenzyl-5',7-dichloro-1,2a,3,4-tetrahydro-2H-spiro[benzo[cd]indole-5,3'-indoline]-2,2'-dione (2r)



2r

The compound **2r** was prepared following the general procedure GP-1. Orange solid (52 mg, 61% yield, *dr* >20:1), R_f = 0.50 (petroleum ether/EtOAc 75:25) MP: 201-203 °C. ^{1}H NMR (400 MHz, $CDCl_3$): δ 8.3 – 7.8 (m, 2H), 7.6 – 7.5 (m, 4H), 7.5 (dd, *J* = 8.3, 6.8 Hz, 2H), 7.4 (t, *J* = 7.6 Hz, 2H), 7.4 – 7.3 (m, 2H), 7.3 (td, *J* = 6.5, 1.7 Hz, 3H), 7.2 – 7.2 (m, 3H), 7.1 (dq, *J* = 7.0, 2.4 Hz, 3H), 7.0 (dd, *J* = 8.2, 1.0 Hz, 1H), 6.8 (d, *J* = 2.1 Hz, 1H), 6.6 (d, *J* = 8.2 Hz, 1H), 6.4 (d, *J* = 8.4 Hz, 1H), 5.2 – 5.1 (m, 2H), 4.5 – 4.4 (m, 3H), 4.3 – 4.2 (m, 1H), 3.3 (d, *J* = 15.3 Hz, 1H). ^{13}C{^{1}H} NMR (100 MHz, $CDCl_3$): δ 201.6, 198.7, 175.9, 174.5, 141.6, 140.7, 137.7, 137.6, 135.2, 134.3, 133.7, 133.5, 131.1, 130.7, 129.3, 129.0, 129.0, 128.9, 128.9, 128.6, 128.6, 128.5, 128.5, 128.3, 128.2, 128.0, 127.9, 127.5, 126.0, 125.2, 110.2, 109.4, 56.9, 55.9, 47.4, 44.3, 44.0, 40.9. HRMS (ESI TOF) *m/z* calcd. For $C_{46}H_{32}Cl_2N_2O_4$ $[M+H]^+$ 747.1817 found 747.1823.

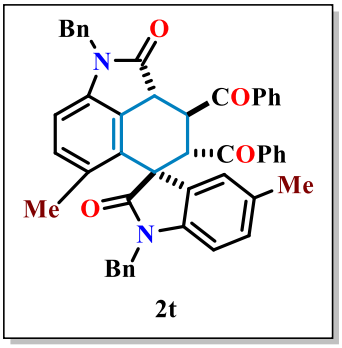
(*2aR,3S,4S,5R*)-3,4-Dibenzoyl-1,1'-dibenzyl-5',7-dibromo-1,2a,3,4-tetrahydro-2H-spiro[benzo[cd]indole-5,3'-indoline]-2,2'-dione (2s)



2s

The compound **2s** was prepared following the general procedure GP-1. Orange solid (114 mg, 68% yield, *dr* >20:1), R_f = 0.50 (petroleum ether/EtOAc 75:25), MP: 210-212 °C. ^{1}H NMR (400 MHz, $CDCl_3$): δ 8.1 – 7.9 (m, 2H), 7.7 – 7.6 (m, 2H), 7.4 – 7.3 (m, 8H), 7.3 (s, 2H), 7.2 – 7.0 (m, 5H), 7.0 (tdd, *J* = 7.5, 6.4, 1.0 Hz, 2H), 6.9 (dd, *J* = 7.5, 1.3 Hz, 1H), 6.6 (d, *J* = 7.7 Hz, 1H), 6.4 (d, *J* = 7.8 Hz, 1H), 6.0 (d, *J* = 8.0 Hz, 1H), 5.3 (d, *J* = 10.5 Hz, 1H), 5.1 (d, *J* = 15.4 Hz, 1H), 5.0 (d, *J* = 15.4 Hz, 1H), 4.5 (d, *J* = 15.4 Hz, 1H), 4.3 (d, *J* = 10.5 Hz, 1H), 4.2 (d, *J* = 11.9 Hz, 1H), 3.8 (d, *J* = 15.4 Hz, 1H). ^{13}C{^{1}H} NMR (100 MHz, $CDCl_3$): δ 200.9, 199.5, 178.0, 175.3, 142.5, 142.4, 136.7, 135.8, 135.6, 135.2, 132.7, 131.8, 131.3, 131.0, 130.3, 129.7, 129.5, 129.0, 128.9, 128.9, 128.6, 128.1, 127.9, 127.9, 127.6, 127.4, 126.2, 126.1, 123.5, 119.2, 109.1, 107.7, 56.7, 54.5, 46.5, 44.2, 44.0, 42.1. HRMS (ESI TOF) *m/z* calcd. For $C_{46}H_{32}Br_2N_2O_4$ $[M+H]^+$ 837.0786 found 837.0768.

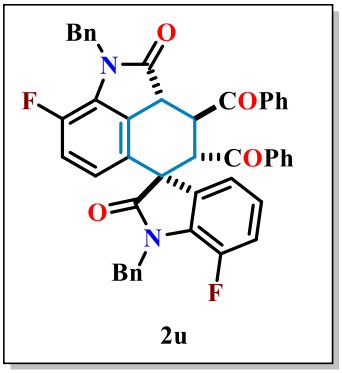
(*2aR,3S,4S,5R*)-1,1'-Dibenzyl-3,4-bis(4-methylbenzoyl)-1,2a,3,4-tetrahydro-2H-spiro[benzo[cd]indole-5,3'-indoline]-2,2'-dione (2t)



2t

The compound **2t** was prepared following the general procedure GP-1. Orange solid (116 mg, 82% yield, *dr* >20:1), R_f = 0.50 (petroleum ether/EtOAc 75:25), MP: 207-209 °C. ^{1}H NMR (400 MHz, CDCl3): δ 8.1 – 8.0 (m, 2H), 7.5 (d, *J* = 12.4 Hz, 6H), 7.4 (s, 2H), 7.3 (d, *J* = 3.1 Hz, 5H), 7.2 – 7.1 (m, 5H), 7.0 – 6.9 (m, 1H), 6.8 – 6.7 (m, 1H), 6.7 (d, *J* = 1.7 Hz, 1H), 6.5 (s, 1H), 6.4 (d, *J* = 8.0 Hz, 1H), 5.2 – 5.1 (m, 2H), 4.5 (d, *J* = 1.2 Hz, 1H), 4.5 – 4.4 (m, 2H), 4.3 (d, *J* = 12.0 Hz, 1H), 3.3 (d, *J* = 15.1 Hz, 1H), 2.3 (s, 3H), 1.3 (s, 3H). ^{13}C{^{1}H} NMR (100 MHz, CDCl3): δ 202.5, 199.8, 177.0, 175.2, 140.1, 140.1, 138.2, 138.1, 135.9, 135.2, 133.3, 133.3, 133.1, 131.5, 130.7, 130.4, 130.1, 129.4, 128.9, 128.9, 128.6, 128.5, 128.5, 128.4, 128.2, 127.9, 127.8, 127.6, 127.2, 126.2, 108.9, 107.9, 57.9, 56.2, 47.8, 44.1, 43.8, 41.1, 21.4, 18.1. HRMS (ESI TOF) *m/z* calcd. For $C_{48}H_{38}N_2O_4$ $[M+H]^+$ 707.2910 found 707.2921.

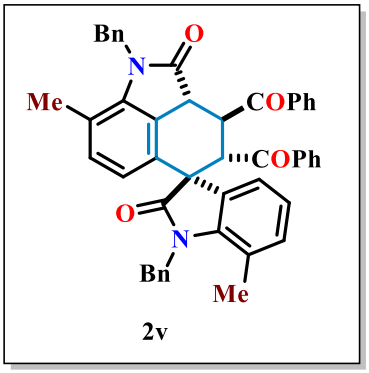
(*2aR,3S,4S,5R*)-3,4-Dibenzoyl-1,1'-dibenzyl-7',8-difluoro-1,2a,3,4-tetrahydro-2H-spiro[benzo[cd]indole-5,3'-indoline]-2,2'-dione (2u)



2u

The compound **2u** was prepared following the general procedure GP-1. White solid (86 mg, 54% yield, *dr* >20:1), R_f = 0.50 (petroleum ether/EtOAc 75:25), MP: 210-212 °C. ^{1}H NMR (400 MHz, $CDCl_3$): δ 8.2 – 8.1 (m, 2H), 7.6 (d, *J* = 7.4 Hz, 1H), 7.5 – 7.4 (m, 3H), 7.4 – 7.3 (m, 7H), 7.2 (dd, *J* = 4.6, 2.4 Hz, 5H), 7.2 – 7.2 (m, 2H), 7.0 – 6.8 (m, 2H), 6.7 (ddd, *J* = 11.2, 8.8, 1.0 Hz, 1H), 6.7 (d, *J* = 1.2 Hz, 1H), 5.9 (dd, *J* = 8.8, 3.5 Hz, 1H), 5.3 (d, *J* = 10.8 Hz, 1H), 5.1 (d, *J* = 15.0 Hz, 1H), 4.9 (d, *J* = 15.0 Hz, 1H), 4.8 (d, *J* = 15.0 Hz, 1H), 4.3 (d, *J* = 11.1 Hz, 1H), 4.2 (d, *J* = 11.8 Hz, 1H), 4.0 (dd, *J* = 14.9, 1.6 Hz, 1H). ^{13}C{^{1}H} NMR (100 MHz, $CDCl_3$): δ 201.1, 200.0, 177.8, 174.4, 147.8 (d, $J_{(C-F)}$ = 69.4 Hz), 145.4 (d, $J_{(C-F)}$ = 69.2 Hz), 137.4 (d, $J_{(C-F)}$ = 77.2 Hz), 136.7 (d, $J_{(C-F)}$ = 20.4 Hz), 133.8 (d, $J_{(C-F)}$ = 2.8 Hz), 133.3 (d, $J_{(C-F)}$ = 23.2 Hz), 129.4, 129.3, 129.1, 129.1, 128.8, 128.7, 128.6, 128.5, 128.4, 128.3, 128.1 (d, $J_{(C-F)}$ = 1.3 Hz), 128.0, 128.0, 127.8, 127.8, 127.7, 127.7, 124.1 (d, $J_{(C-F)}$ = 6.4 Hz), 122.1 (d, $J_{(C-F)}$ = 3.2 Hz), 120.3 (d, $J_{(C-F)}$ = 6.4 Hz), 117.9 (d, $J_{(C-F)}$ = 20.9 Hz), 116.9 (d, $J_{(C-F)}$ = 19.5 Hz), 57.1, 54.2, 46.9, 45.5 (d, $J_{(C-F)}$ = 4.9 Hz), 45.2 (d, $J_{(C-F)}$ = 3.4 Hz), 41.8; ^{19}F NMR (377 MHz, $CDCl_3$): δ -133.5, -135.3. HRMS (ESI TOF) *m/z* calcd. For $C_{46}H_{32}F_2N_2O_4$ $[M+H]^+$ 715.2408 found 715.2404.

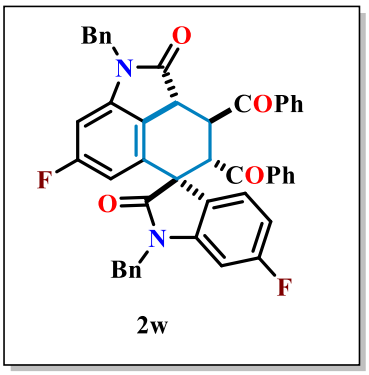
(*2aR,3S,4S,5R*)-3,4-Dibenzoyl-1,1'-dibenzyl-7',8-dimethyl-1,2a,3,4-tetrahydro-2H-spiro[benzo[cd]indole-5,3'-indoline]-2,2'-dione (2v)



2v

The compound **2v** was prepared following the general procedure GP-1. Light Yellowish solid (99 mg, 70% yield, *dr* >20:1), R_f = 0.50 (petroleum ether/EtOAc 75:25), MP: 282-284 °C. ^{1}H NMR (400 MHz, Chloroform-*d*) δ 8.1 – 8.0 (m, 2H), 7.4 – 7.3 (m, 7H), 7.2 (td, *J* = 4.2, 1.9 Hz, 5H), 7.2 – 7.1 (m, 2H), 7.1 – 7.0 (m, 3H), 7.0 – 6.9 (m, 3H), 6.6 (d, *J* = 7.7 Hz, 1H), 6.4 (d, *J* = 7.8 Hz, 1H), 6.0 (d, *J* = 8.0 Hz, 1H), 5.3 (d, *J* = 10.8 Hz, 1H), 5.2 (d, *J* = 15.4 Hz, 1H), 4.9 (d, *J* = 15.5 Hz, 1H), 4.5 – 4.3 (m, 2H), 4.3 (d, *J* = 11.9 Hz, 1H), 3.7 (d, *J* = 15.5 Hz, 1H), 2.4 (s, 3H), 2.3 (s, 3H). ^{13}C{^{1}H} NMR (100 MHz, $CDCl_3$): δ 201.9, 200.7, 179.6, 175.9, 140.9, 140.2, 138.1, 137.7, 137.5, 137.5, 133.1, 133.1, 132.6, 132.6, 132.3, 131.0, 128.8, 128.8, 128.8, 128.4, 128.2, 127.8, 127.3, 127.3, 126.9, 125.9, 125.9, 124.3, 123.5, 119.6, 119.6, 118.6, 57.6, 53.8, 46.4, 45.1, 44.6, 42.0, 18.6, 18.0. HRMS (ESI TOF) *m/z* calcd. For $C_{48}H_{38}N_2O_4$ $[M+H]^+$ 707.2910 found 707.2909.

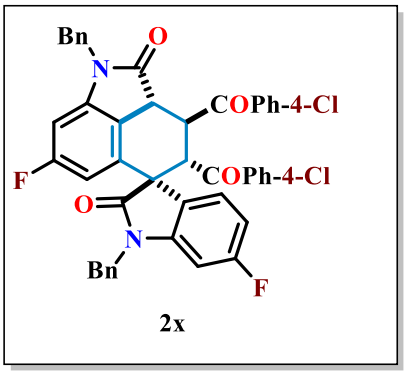
(*2aR,3S,4S,5R*)-3,4-Dibenzoyl-1,1'-dibenzyl-6',7-difluoro-1,2a,3,4-tetrahydro-2H-spiro[benzo[cd]indole-5,3'-indoline]-2,2'-dione (2w)



2w

The compound **2w** was prepared following the general procedure GP-1. White solid (132 mg, 92% yield, dr >20:1), R_f = 0.50 (petroleum ether/EtOAc 75:25), MP: 255-257 °C.^{1}H NMR (400 MHz, $CDCl_3$): δ 8.2 – 8.1 (m, 2H), 7.6 (d, *J* = 7.4 Hz, 1H), 7.5 – 7.4 (m, 3H), 7.4 – 7.3 (m, 11H), 7.2 (d, *J* = 1.9 Hz, 1H), 7.1 – 7.0 (m, 2H), 6.9 (dd, *J* = 8.3, 5.2 Hz, 1H), 6.7 (ddd, *J* = 9.3, 8.3, 2.4 Hz, 1H), 6.4 (dd, *J* = 8.6, 2.0 Hz, 1H), 6.1 (dd, *J* = 8.8, 2.3 Hz, 1H), 5.7 (dd, *J* = 10.1, 2.0 Hz, 1H), 5.3 (d, *J* = 10.8 Hz, 1H), 5.1 (d, *J* = 15.4 Hz, 1H), 4.9 (d, *J* = 15.5 Hz, 1H), 4.5 – 4.3 (m, 2H), 4.2 (dd, *J* = 11.8, 2.0 Hz, 1H), 3.6 (d, *J* = 15.5 Hz, 1H). ^{13}C{^{1}H} NMR (100 MHz, $CDCl_3$): δ 201.4, 200.0, 178.1, 175.3, 164.7 (d, $J_{(C-F)}$ = 64.3 Hz), 162.2 (d, $J_{(C-F)}$ = 65.9 Hz), 144.1 (d, $J_{(C-F)}$ = 11.7 Hz), 143.6 (d, $J_{(C-F)}$ = 12.4 Hz), 137.4 (d, $J_{(C-F)}$ = 76.0 Hz), 135.0 (d, $J_{(C-F)}$ = 44.9 Hz), 133.8, 133.7, 133.4, 133.2, 129.0, 129.0, 128.8, 128.5, 128.2, 128.2, 128.1, 128.1, 127.7, 127.5, 127.4, 127.2, 126.0 (d, $J_{(C-F)}$ = 3.1 Hz), 121.9 (d, $J_{(C-F)}$ = 2.3 Hz), 110.0 (d, $J_{(C-F)}$ = 22.6 Hz), 105.1 (d, $J_{(C-F)}$ = 24.5 Hz), 97.8 (d, $J_{(C-F)}$ = 27.7 Hz), 97.2 (d, $J_{(C-F)}$ = 28.9 Hz), 56.5, 54.1, 46.0, 44.3, 44.1, 42.1. ^{19}F NMR (377 MHz, $CDCl_3$): δ -109.5, -109.7. HRMS (ESI TOF) *m/z* calcd. For $C_{46}H_{32}F_2N_2O_4$ $[M+H]^+$ 715.2408 found 715.2411.

(*2aR,3S,4S,5R*)-1,1'-Dibenzyl-3,4-bis(4-chlorobenzoyl)-6',7-difluoro-1,2a,3,4-tetrahydro-2H-spiro[benzo[cd]indole-5,3'-indoline]-2,2'-dione (2x)

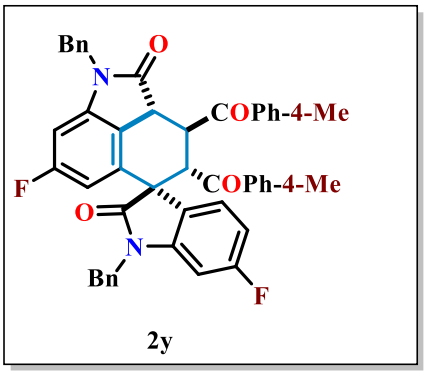


2x

The compound **2x** was prepared following the general procedure GP-2. White solid (72 mg, 46% yield, *dr* >20:1), R_f = 0.50 (petroleum ether/EtOAc 75:25), MP: 230-232 °C.^{1}H NMR (400 MHz, $CDCl_3$): δ 8.1 – 7.9 (m, 2H), 7.5 – 7.4 (m, 2H), 7.4 – 7.3 (m, 3H), 7.3 – 7.3 (m, 7H), 7.2 (d, *J* = 8.7 Hz, 2H), 7.1 – 7.1 (m, 2H), 6.8 (dd, *J* = 8.3, 5.2 Hz, 1H), 6.7 (ddd, *J* = 10.7, 8.5, 2.4 Hz, 1H), 6.4 (dd, *J* = 8.6, 2.0 Hz, 1H), 6.2 (dd, *J* = 8.6, 2.3 Hz, 1H), 5.7 (dd, *J* = 10.1, 1.9 Hz, 1H), 5.3 (d, *J* = 10.7 Hz, 1H), 5.1 (d, *J* = 15.4 Hz, 1H), 4.9 (d, *J* = 15.4 Hz, 1H), 4.4 (d, *J* = 15.4 Hz, 1H), 4.3 (t, *J* = 11.3 Hz, 1H), 4.2 (dd, *J* = 11.8, 2.0 Hz, 1H), 3.9 (d, *J* = 15.4 Hz, 1H). ^{13}C{^{1}H} NMR (100 MHz, $CDCl_3$): δ 200.2, 198.8, 177.9, 175.2, 164.8 (d, $J_{(C-F)}$ = 64.4 Hz), 162.3 (d, $J_{(C-F)}$ = 66.4 Hz), 144.0 (d, $J_{(C-F)}$ = 13.2 Hz), 143.7 (d, $J_{(C-F)}$ = 12.5 Hz), 140.0, 139.9, 136.0, 135.1 (d, $J_{(C-F)}$ = 7.9 Hz), 134.5,

133.6 (d, $J_{(C-F)}$ = 9.0 Hz), 130.2, 129.6, 129.1, 129.0, 128.9, 128.6, 128.3, 128.2, 127.7, 127.6, 127.5, 127.3, 125.7 (d, $J_{(C-F)}$ = 3.1 Hz), 121.6 (d, $J_{(C-F)}$ = 2.3 Hz), 110.2 (d, $J_{(C-F)}$ = 22.6 Hz), 105.1 (d, $J_{(C-F)}$ = 24.7 Hz), 98.0 (d, $J_{(C-F)}$ = 27.7 Hz), 97.4 (d, $J_{(C-F)}$ = 28.8 Hz), 56.2, 54.1, 46.0, 44.5, 44.2, 42.2. ^{19}F NMR (377 MHz, $CDCl_3$): δ -108.8, -109.3. HRMS (ESI TOF) *m/z* calcd. For $C_{46}H_{30}Cl_2F_2N_2O_4$ $[M+H]^+$ 783.1629 found 783.1628.

(*2aR,3S,4S,5R*)-1,1'-Dibenzyl-6',7-difluoro-3,4-bis(4-methylbenzoyl)-1,2a,3,4-tetrahydro-2H-spiro[benzo[cd]indole-5,3'-indoline]-2,2'-dione (2y)

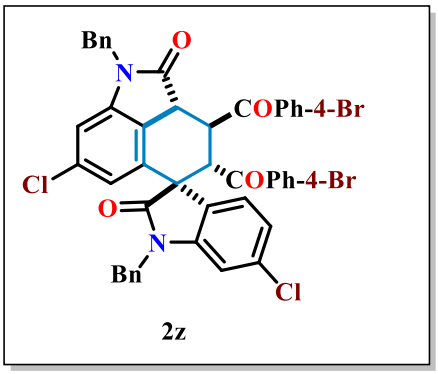


2y

The compound **2y** was prepared following the general procedure GP-1. White solid (94 mg, 62% yield, *dr* >20:1), R_f = 0.50 (petroleum ether/EtOAc 75:25), MP: 235-237 °C.^{1}H NMR (400 MHz, $CDCl_3$): δ 8.1 – 8.0 (m, 2H), 7.4 – 7.3 (m, 10H), 7.3 (d, *J* = 2.9 Hz, 2H), 7.1 – 7.0 (m, 4H), 6.9 (dd, *J* = 8.3, 5.3 Hz, 1H), 6.7 – 6.6 (m, 1H), 6.3 (dd, *J* = 8.7, 2.0 Hz, 1H), 6.1 (dd, *J* = 8.7, 2.3 Hz, 1H), 5.7 (dd, *J* = 10.2, 2.0 Hz, 1H), 5.3 (d, *J* = 10.8 Hz, 1H), 5.1 (d, *J* = 15.4 Hz, 1H), 4.9 (d, *J* = 15.5 Hz, 1H), 4.5 – 4.3 (m, 2H), 4.2 (d, *J* = 2.0 Hz, 1H), 3.8 (d, *J* = 15.5 Hz, 1H), 2.4 (s, 3H), 2.4 (s, 3H). ^{13}C{^{1}H} NMR (100 MHz, $CDCl_3$): δ 200.7, 199.2, 178.2, 175.4, 164.6 (d, $J_{(C-F)}$ = 67.2 Hz), 162.2 (d, $J_{(C-F)}$ = 68.7 Hz), 144.2, 144.1, 144.0, 143.9, 143.6 (d, $J_{(C-F)}$ = 12.5 Hz), 135.3 (d, $J_{(C-F)}$ = 6.3 Hz), 134.8, 134.5, 133.9 (d, $J_{(C-F)}$ = 9.9 Hz), 129.3, 129.1, 129.0, 129.0, 128.9, 128.9, 128.4, 128.1 (d, $J_{(C-F)}$ = 2.6 Hz), 127.6, 127.6, 127.3, 126.1 (d, $J_{(C-F)}$ = 3.1 Hz), 122.0 (d, $J_{(C-F)}$ = 2.2 Hz), 109.9 (d, $J_{(C-F)}$ = 22.6 Hz), 105.1 (d, $J_{(C-F)}$ = 24.4 Hz), 97.8 (d, $J_{(C-F)}$ = 27.7 Hz), 97.2 (d, $J_{(C-F)}$ = 28.8 Hz), 56.0, 54.2, 46.0, 44.4, 44.1, 42.0, 21.8, 21.7. ^{19}F NMR (377 MHz, $CDCl_3$): δ -109.8, -109.9. HRMS (ESI TOF) *m/z* calcd. For $C_{48}H_{36}F_2N_2O_4$ $[M+H]^+$ 743.2721 found 743.2713.

(*2aR,3S,4S,5R*)-1,1'-Dibenzyl-3,4-bis(4-bromobenzoyl)-5',7-dichloro-1,2a,3,4-tetrahydro-2H-spiro[benzo[cd]indole-5,3'-indoline]-2,2'-dione (2z)

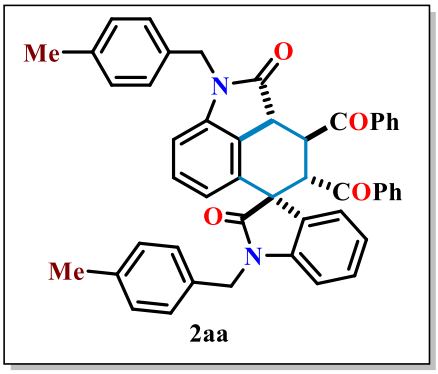
The compound **2z** was prepared following the general procedure GP-1. Orange solid (100 mg, 55% yield, *dr* >20:1), R_f = 0.50 (petroleum ether/EtOAc 75:25), MP: 240-242 °C.^{1}H NMR (400 MHz, $CDCl_3$): ^{1}H NMR (400 MHz, Chloroform-*d*) δ 7.9 – 7.8 (m, 2H), 7.7 – 7.6 (m, 2H), 7.6 – 7.5 (m, 2H), 7.4 (d, *J* = 8.5 Hz, 2H), 7.4 – 7.3 (m, 5H), 7.2 (dd, *J* = 5.0, 1.9 Hz, 3H), 7.2 – 7.1 (m, 3H), 7.1 – 7.0 (m, 1H), 6.8 (d, *J* = 2.1 Hz, 1H), 6.6 (d, *J* = 8.2 Hz, 1H), 6.5 (d, *J* = 8.4



2z

Hz, 1H), 5.2 (d, *J* = 15.5 Hz, 1H), 5.1 (d, *J* = 10.5 Hz, 1H), 4.5 (d, *J* = 15.3 Hz, 1H), 4.4 (d, *J* = 15.5 Hz, 1H), 4.4 – 4.3 (m, 1H), 4.3 (d, *J* = 1.0 Hz,1H), 3.5 (d, *J* = 15.2 Hz, 1H); $^{13}C\{^{1}H\}$ NMR (100 MHz, $CDCl_3$): δ 200.7, 197.7, 175.9, 174.4, 141.6, 140.7, 136.3, 136.0, 135.1, 134.0, 132.0, 131.9, 130.9, 130.8, 130.3, 129.7, 129.2, 129.2, 129.1, 129.1, 129.0, 128.7, 128.6, 128.5, 128.3, 128.1, 128.0, 127.5, 126.1, 125.2, 110.2, 109.6, 56.7, 55.8, 47.3, 44.5, 44.0, 41.0. HRMS (ESI TOF) *m/z* calcd. For $C_{46}H_{30}Br_2N_2O_4$ $[M+H]^+$ 905.0007 found 905.0015.

(*2aR,3S,4S,5R*)-3,4-Dibenzoyl-1,1'-bis(4-methylbenzyl)-1,2a,3,4-tetrahydro-2H-spiro[benzo[cd]indole-5,3'-indoline]-2,2'-dione (2aa)

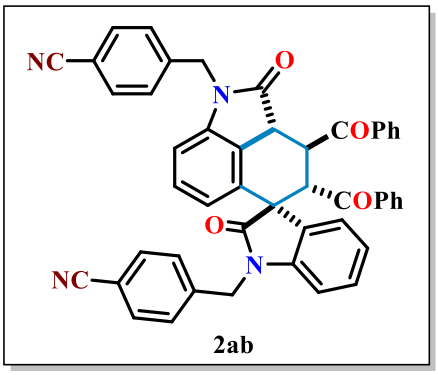


2aa

The compound **2aa** was prepared following the general procedure GP-1. Yellow solid (71 mg, 50% yield, *dr* >20:1), R_f = 0.50 (petroleum ether/EtOAc 75:25), MP: 209-211 °C.^{1}H NMR (400 MHz, $CDCl_3$): δ 8.2 – 8.1 (m, 2H), 7.6 (d, *J* = 7.3 Hz, 1H), 7.5 (dd, *J* = 8.3, 6.7 Hz, 2H), 7.5 – 7.4 (m, 1H), 7.3 – 7.3 (m, 2H), 7.2 – 7.2 (m, 4H), 7.1 (d, *J* = 7.8 Hz, 2H), 7.0 (dd, *J* = 8.4, 7.0 Hz, 5H), 7.0–6.9 (m, 3H), 6.6 (d, *J* = 7.7 Hz, 1H), 6.3 (d, *J* = 7.8 Hz, 1H), 6.0 (d, *J* = 8.1 Hz, 1H),5.4 (d, *J* = 10.8 Hz, 1H), 5.1 (d, *J* = 15.3 Hz, 1H), 4.9 (d, *J* = 15.4 Hz, 1H), 4.5 – 4.4 (m, 2H), 4.3 (d, *J* = 11.8 Hz, 1H), 3.6 (d, *J* = 15.4 Hz, 1H), 2.3 (s, 3H), 2.3 (s, 3H). $^{13}C\{^{1}H\}$ NMR (100 MHz, $CDCl_3$): δ 201.9, 200.5, 178.2, 175.3, 142.6, 142.5, 138.0, 137.5, 137.5, 137.3, 133.2, 133.0, 132.8, 132.8, 132.5, 131.4, 129.5, 129.5, 129.3, 128.8, 128.7, 128.5, 128.2, 128.0, 127.6, 127.3, 126.6, 126.1, 123.4, 119.2, 108.9, 107.5, 56.9, 54.6, 46.6, 43.8, 43.7, 42.1, 21.1, 21.1. HRMS (ESI TOF) *m/z* calcd. For $C_{48}H_{38}N_2O_4$ $[M+H]^+$ 707.2910 found 707.2907.

(2aR,3S,4S,5R)-4,4'-((3,4-Dibenzoyl-2,2'-dioxo-2,2a,3,4-tetrahydro-1H-spiro[benzo[cd]indole-5,3'-indoline]-1,1'-diyl)bis(methylene))dibenzonitrile (2ab)

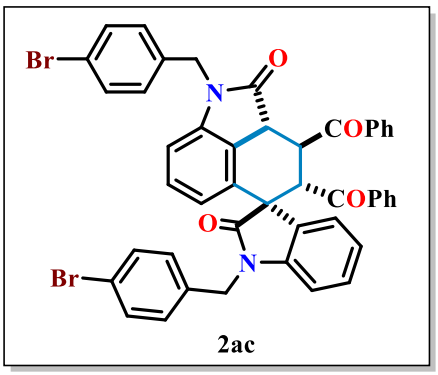
The compound **2ab** was prepared following the general procedure GP-1. White solid (82 mg, 56% yield, dr >20:1), R_f = 0.50 (petroleum ether/EtOAc 75:25), MP: 196-198 °C.^{1}H NMR (400 MHz, $CDCl_3$): δ 7.7 – 7.6 (m, 7H), 7.6 – 7.6 (m, 3H), 7.4 (dt, *J* = 13.3, 7.6 Hz, 3H), 7.3



2ab

(d, *J* = 8.2 Hz, 2H), 7.2 (s, 2H), 7.1 – 7.0 (m, 3H), 7.0 (s, 2H), 6.5 (d, *J* = 7.8 Hz, 1H), 6.3 – 6.1 (m, 2H), 5.3 (d, *J* =1.4 Hz, 1H), 5.2 (d, *J* = 16.5 Hz, 1H), 5.1 (s, 1H), 5.0 – 4.9 (m, 2H), 4.1 (q, *J* = 7.1 Hz, 1H), 3.8 (d, *J* = 15.8 Hz, 1H). $^{13}C\{^{1}H\}$ NMR (100 MHz, $CDCl_3$): δ 201.3, 197.3, 178.6, 177.5, 143.4, 141.6, 141.3, 140.6, 136.9, 134.5, 134.2, 133.9, 133.3, 132.8, 132.7, 131.4, 130.5, 129.2, 128.6, 128.6, 128.3, 128.2, 128.1, 128.0, 127.9, 126.8, 124.1, 118.7, 118.2, 118.0, 112.1, 111.6, 108.3, 108.3, 70.7, 54.1, 53.5, 50.5, 44.2, 43.9. HRMS (ESI TOF) *m/z* calcd. For $C_{48}H_{32}N_4O_4$ $[M+H]^+$ 729.2502 found 729.2507.

(*2aR,3S,4S,5R*)-3,4-Dibenzoyl-1,1'-bis(4-bromobenzyl)-1,2a,3,4-tetrahydro-2H-spiro[benzo[cd]indole-5,3'-indoline]-2,2'-dione (2ac)

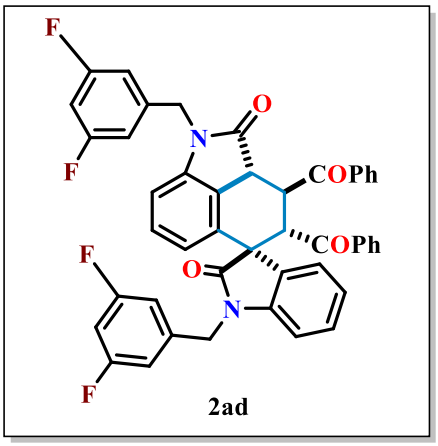


2ac

The compound **2ac** was prepared following the general procedure GP-1. White solid (94 mg, 56% yield, dr >20:1), Rf = 0.50 (petroleum ether/EtOAc 75:25), MP: 208-210 °C.^{1}H NMR (400 MHz, $CDCl_3$): δ 8.2 – 8.1 (m, 2H), 7.6 – 7.6 (m, 1H), 7.5 (ddd, *J* = 21.6, 7.6, 5.9 Hz, 5H), 7.4 – 7.3 (m, 2H), 7.3 (d, *J* = 6.9 Hz, 1H), 7.2 – 7.2(m, 4H), 7.1 (td, *J* = 7.7, 1.4 Hz, 1H), 7.0 – 6.9 (m, 4H), 6.9 (dd, *J* = 7.5, 1.4 Hz, 1H), 6.6 (d, *J* = 7.7 Hz, 1H), 6.3 (d, *J* = 7.8 Hz, 1H), 6.0 (d, *J* = 8.0 Hz, 1H), 5.3 (d, *J* = 10.8 Hz, 1H), 5.1 (d, *J* = 15.5 Hz, 1H), 4.9 (d, *J* = 15.6 Hz, 1H), 4.5 – 4.4 (m, 2H), 4.3 (s, 1H), 4.1 (d, *J* = 7.1 Hz, 1H), 3.6 (d, *J* = 15.6 Hz, 1H). $^{13}C\{^{1}H\}$ NMR (100 MHz, $CDCl_3$): δ 201.7, 200.3, 178.2, 175.3, 142.3, 142.2, 137.9, 137.3, 134.8, 134.6, 133.3, 133.0, 132.9, 132.0, 131.2, 129.4, 129.3, 129.0, 129.0, 128.9, 128.8, 128.5, 128.2, 128.0, 126.5, 126.3, 123.7, 121.8, 121.8, 119.3, 108.7, 107.4, 56.7, 54.5, 46.5, 43.5, 43.4, 42.0. HRMS (ESI TOF) *m/z* calcd. For $C_{46}H_{32}Br_2N_2O_4$ $[M+H]^+$ 837.0786 found 837.0786.

(*2aR,3S,4S,5R*)-3,4-Dibenzoyl-1,1'-bis(3,5-difluorobenzyl)-1,2a,3,4-tetrahydro-2H-spiro[benzo[cd]indole-5,3'-indoline]-2,2'-dione (2ad)

The compound **2ad** was prepared following the general procedure GP-1. White solid (69 mg, 48% yield, *dr* >20:1), R_f = 0.50 (petroleum ether/EtOAc 75:25), MP: 205-207 °C.^{1}H NMR (400 MHz, $CDCl_3$): δ 8.2 – 8.0 (m, 2H), 7.6 (d, *J* = 7.4 Hz, 1H), 7.5 (dd, *J* = 8.3, 6.8 Hz, 2H),



2ad

7.4 (s, 1H), 7.3 (d, J = 7.5 Hz, 2H), 7.3 – 7.2 (m, 2H), 7.1 (dd, J = 7.7, 1.5 Hz, 1H), 7.1 – 7.0 (m, 2H), 6.9 (d, J = 1.3 Hz, 1H), 6.8 (dt, J = 6.2, 2.0 Hz, 2H), 6.8 – 6.6 (m, 4H), 6.6 (d, J = 7.7 Hz, 1H), 6.3 (d, J = 7.8 Hz, 1H), 6.0 (d, J = 8.0 Hz, 1H), 5.4 (d, J = 10.8 Hz, 1H), 5.0 (d, J = 15.7 Hz, 1H), 4.9 (d, J = 15.8 Hz, 1H), 4.5 (d, J = 15.7 Hz, 1H), 4.4 (dd, J = 11.8, 10.8 Hz, 1H), 4.3 (d, J = 11.8 Hz, 1H), 3.6 (d, J = 15.8 Hz, 1H). $^{13}C\{^{1}H\}$ NMR (100 MHz, $CDCl_3$): δ 201.5, 200.2, 178.2, 175.3, 164.6 (d, $J_{(C-F)}$ = 4.8 Hz), 164.4 (d, $J_{(C-F)}$ = 5.0 Hz), s162.0, 161.9 (d, $J_{(C-F)}$ = 5.9 Hz), 142.1, 142.0, 139.6 (t, $J_{(C-F)}$ = 8.8 Hz), 139.4 (t, $J_{(C-F)}$ = 8.8 Hz), 137.8, 137.2, 133.4, 133.0, 132.9, 131.1, 129.6, 129.0, 128.8, 128.5, 128.2, 128.0, 126.5, 126.5, 123.9, 119.5, 110.7 – 110.2 (m), 110.4 – 108.5 (m), 107.4, 103.5 (t, $J_{(C-F)}$ = 25.2 Hz), 56.8, 54.5, 46.4, 43.4, 43.3, 42.0. ^{19}F NMR (377 MHz, $CDCl_3$): δ -108.4 (t, J = 7.9 Hz), -108.6 (t, J = 7.8 Hz). HRMS (ESI TOF) *m/z* calcd. For $C_{46}H_{30}F_4N_2O_4$ $[M+H]^+$ 751.2220 found 751.2212.

3.7 Appendix III ^{1}H, ^{13}C spectral data of representative compounds

Compound No.	Figure AIII.X	Data	Page No
2a	Figure AIII.1 and AIII.2	^{1}H and ^{13}C	107
2h	Figure AIII.3 and AIII.4	^{1}H and ^{13}C	108
2r	Figure AIII.5 and AIII.6	^{1}H and ^{13}C	109
2aa	Figure AIII.7 and AIII.8	^{1}H and ^{13}C	110
3i	Figure AIII.9	ORTEP plot	111

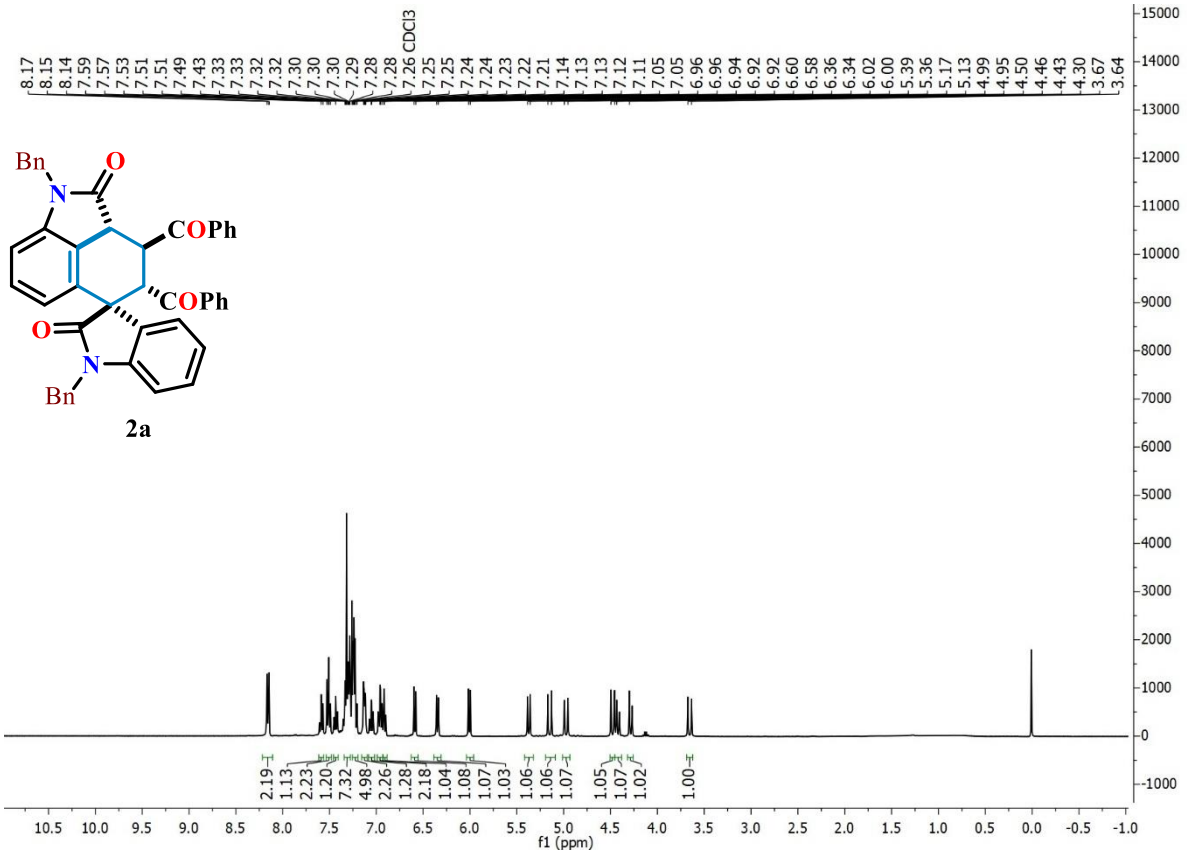


Figure AIII.1 ^{1}H NMR (400 MHz, $CDCl_3$) spectrum of compound **2a**

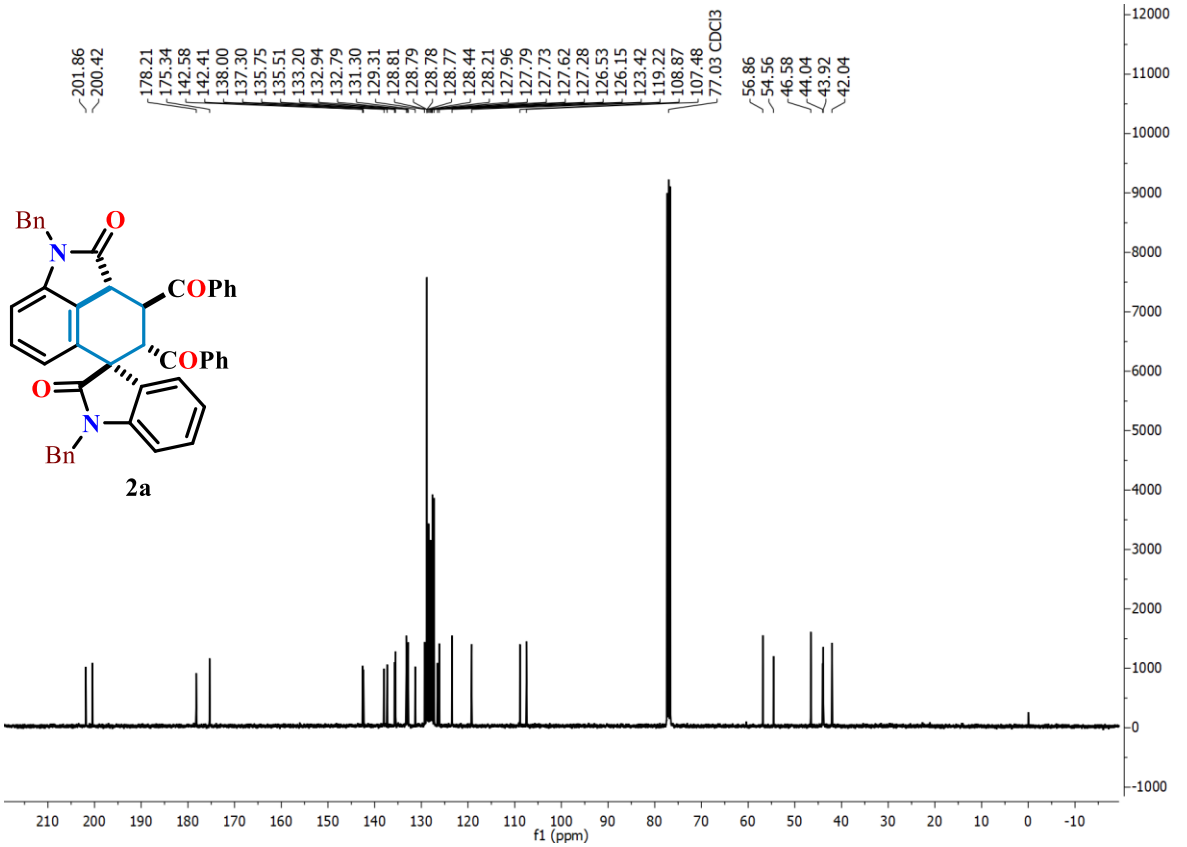


Figure AIII.2 $^{13}C\{^{1}H\}$ NMR (100 MHz, $CDCl_3$) spectrum of compound **2a**

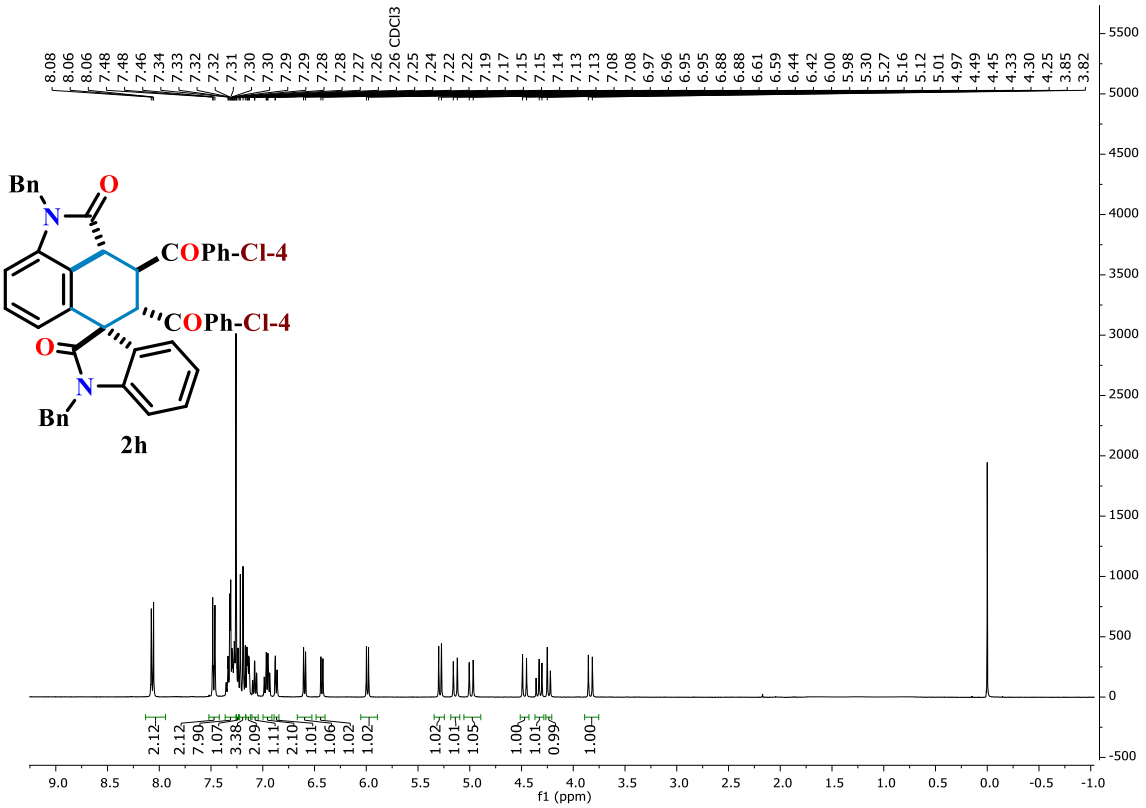


Figure AIII.3 ^{1}H NMR (400 MHz, $CDCl_3$) spectrum of compound **2h**

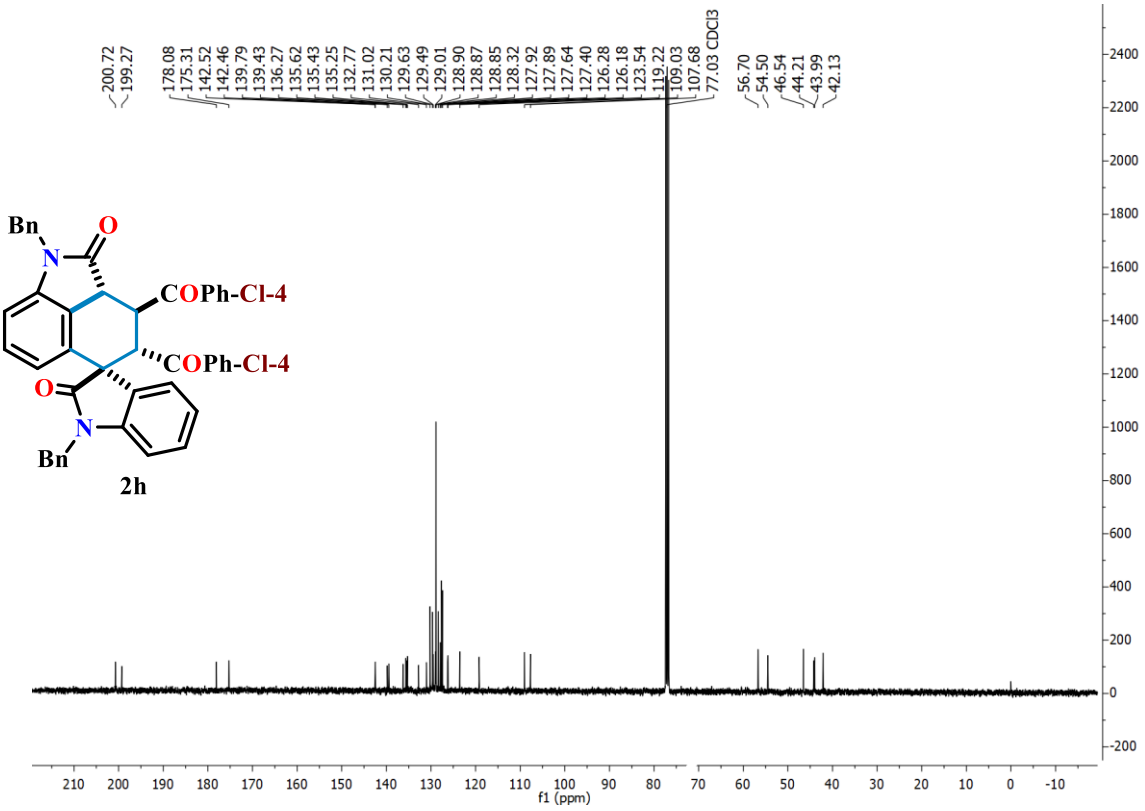


Figure AIII.4 $^{13}C\{^{1}H\}$ NMR (100 MHz, $CDCl_3$) spectrum of compound **2h**

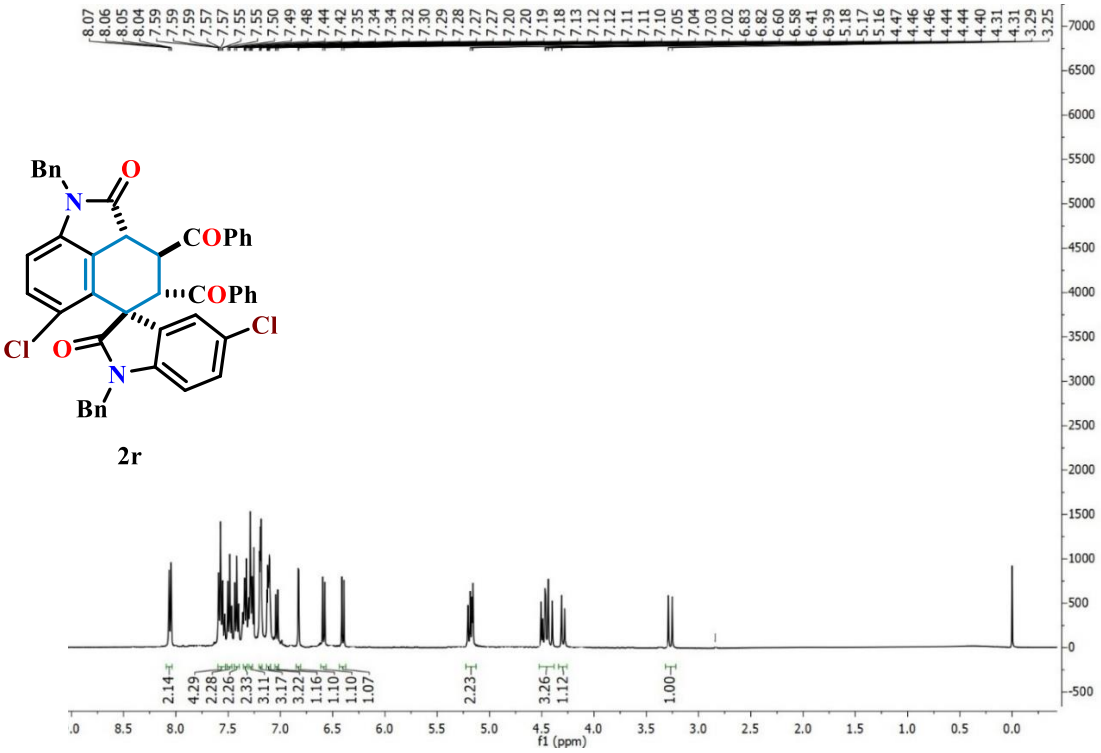


Figure AIII.5 ^{1}H NMR (400 MHz, $CDCl_3$) spectrum of compound **2r**

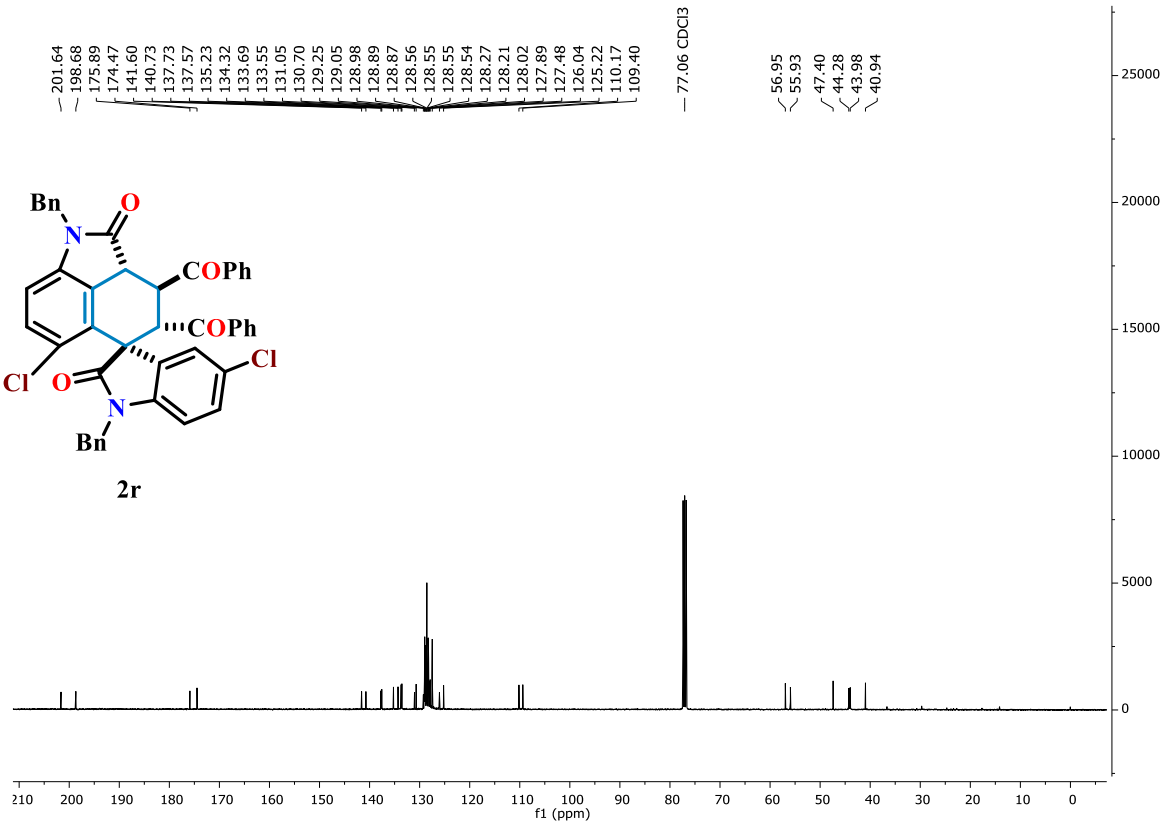


Figure AIII.6 ^{13}C{^{1}H} NMR (100 MHz, $CDCl_3$) spectrum of compound **2r**

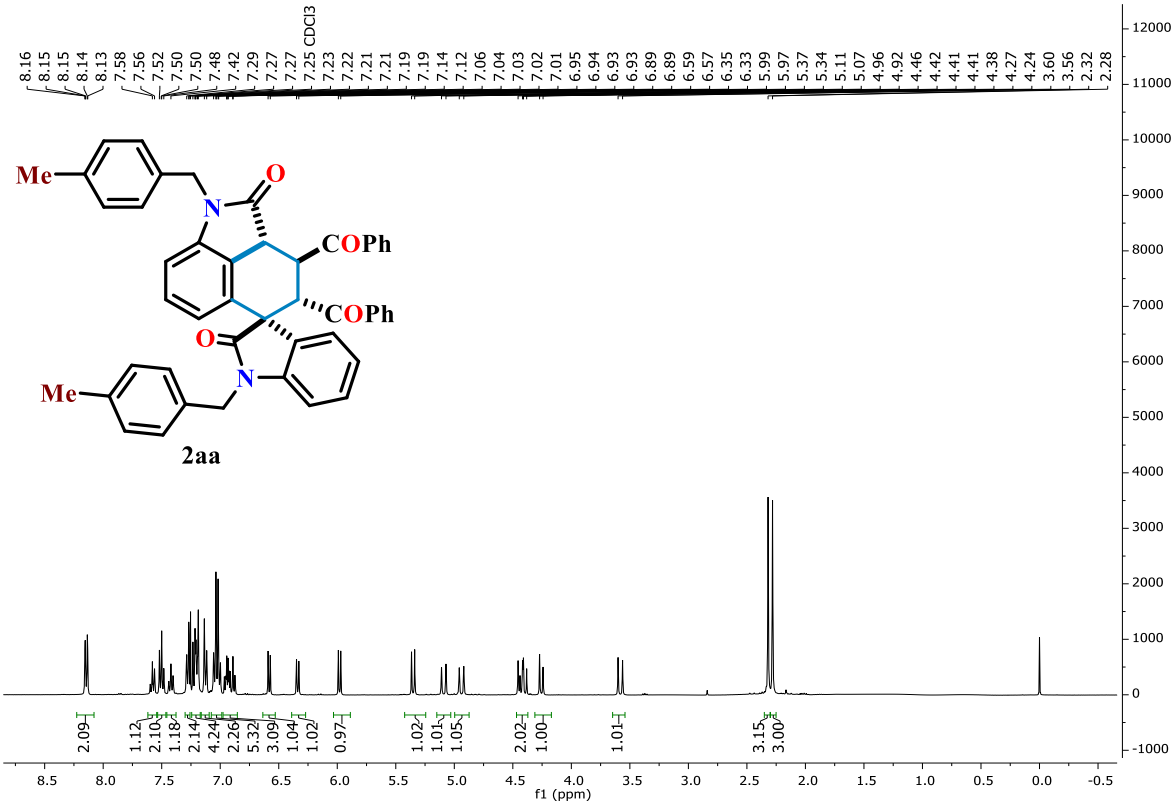


Figure AIII.7 ^{1}H NMR (400 MHz, $CDCl_3$) spectrum of compound **2aa**

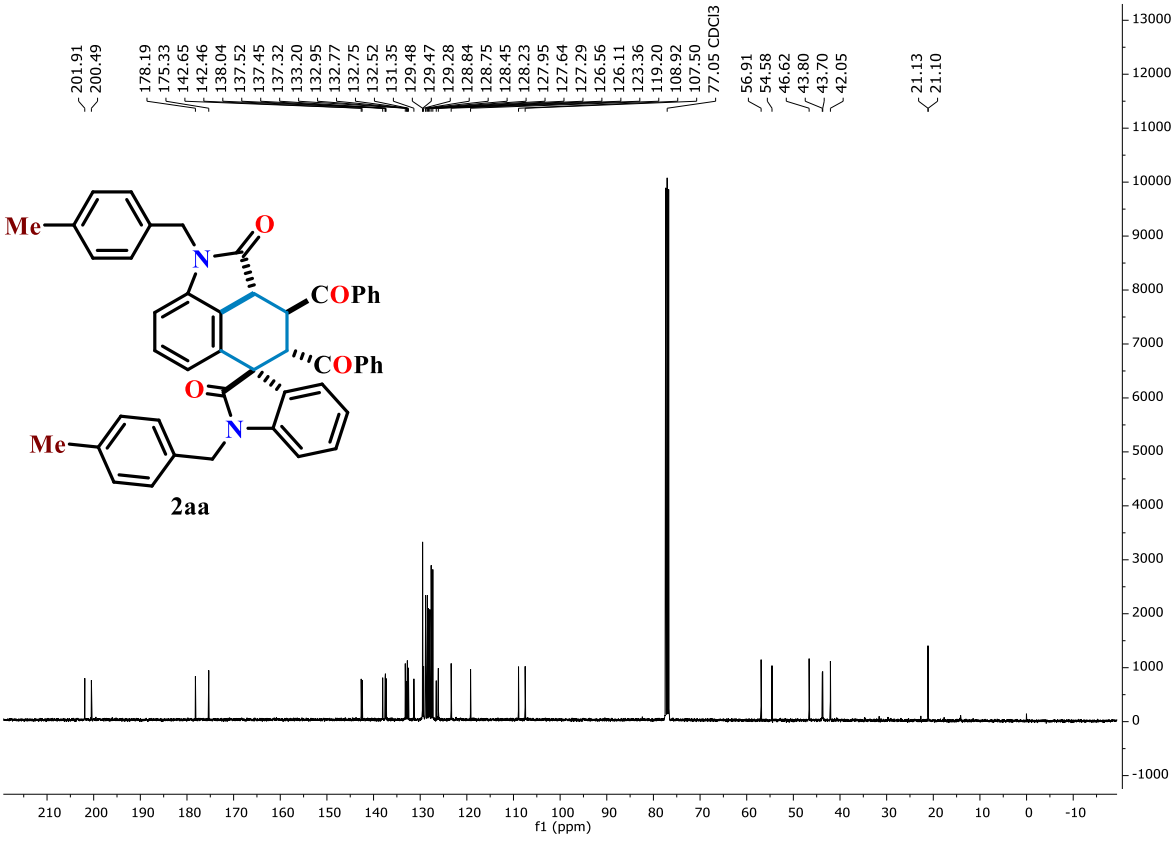


Figure AIII.8 $^{13}C\{^{1}H\}$ NMR (100 MHz, $CDCl_3$) spectrum of compound **2aa**

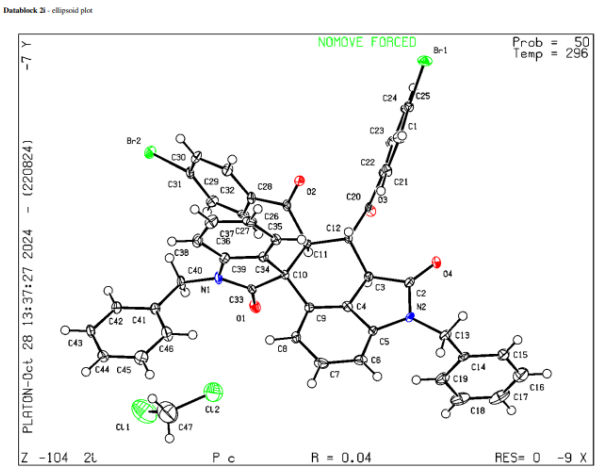


Figure AIII.9 An ORTEP diagram showing thermal ellipsoids at a 50% probability level was created to represent the structures determined by single-crystal X-ray diffraction analysis of compound **2i**

3.8 References

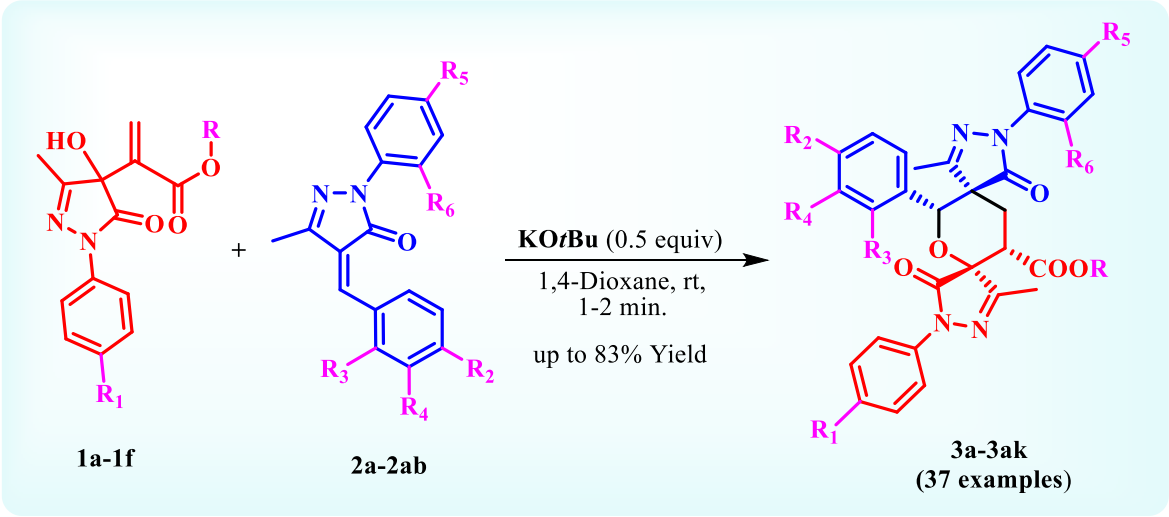
1. (a) Peat, A. J.; Buchwald, S. L. *J. Am. Chem. Soc.* **1996**, *118*, 1028. (b) Canan, S. S.; Koch, L.; Thoresen, H.; Tikhe, J. G.; Maegley, K. A.; Almassy, R. J.; Li, J.; Yu, X. H.; Zook, S. E.; Kumpf, R. A.; Zhang, C.; Boritzki, T. J.; Mansour, R. N.; Zhang, K. E.; Ekker, A.; Calabrese, C. R.; Curtin, N. J.; Kyle, S.; Thomas, H. D.; Wang, L. Z.; Calvert, A. H.; Golding, B. T.; Griffin, R. J.; Newell, D. R.; Webber, S. E.; Hostom- sky, Z.. *J. Med. Chem.* **2002**, *45*, 4961. (c) Koizumi, Y.; Kobayashi, H.; Wakimoto, T.; Furuta, T.; Fukuyama, T.; Kan, T. *J. Am. Chem. Soc.* **2008**, *130*, 16854. (d) Hughes, C. C.; Fenical, W. *J. Am. Chem. Soc.* **2010**, *132*, 2528. (e) Qin, H.; Xu, Z.; Cui, Y.; Jia, Y.*Angew. Chem., Int. Ed.* **2011**, *50*, 4447. (f) Bronner, S. M.; Goetz, A. E.; Garg, N. K. *J. Am. Chem. Soc.* **2011**, *133*, 3832. (g) Yang, S. W.; Wang, C. M.; Tang, K. X.; Wang, J. X.; Sun, L. P. *Eur. J. Org. Chem.* **2016**, 2016, 1050. (h) Alluri, S. R.; Riss, P. J. *ACS Chem. Neurosci.* **2018**, *9*, 1259. (i) Chaudhuri, S.; Bhunia, S.; Roy, A.; Das, M. K.; Bisai, A. *Org. Lett.* **2018**, *20*, 288.
2. (a) Umezaki, S.; Yokoshima, S.; Fukuyama, T. *Org. Lett.* **2013**, *15*, 4230. (b) Liu, Q.; Zhang, Y.-A.; Xu, P.; Jia, Y. *J. Org. Chem.* **2013**, *78*, 10885.
3. (a) Zhang, Y. A.; Iiu, Q.; Wang, C.; Jia, Y. *Org. Lett.* **2013**, *15*, 3662. (b) Bartoccini, F.; Regni, A.; Retini, M.; Prof. Piersanti, G. *E. J. Org. Chem.* **2022**, *17*, 2022.
4. Yokoyama, Y.; Kondo, K.; Mitsuhashi, M.; Murakami, Y. *Tetrahedron Lett.* **1996**, *37*, 9309.

5. (a) Peat, A. J.; Buchwald, S. L. *J. Am. Chem. Soc.* **1996**, *118*, 1028. (b) Stoffman, E. J. L.; Clive, D. L. J. *Tetrahedron* **2010**, *66*, 4452.
6. Kato, K.; Ono, M.; Akita, H. *Tetrahedron* **2001**, *57*, 10055.
7. (a) Baran, P. S.; Maimone, T. J.; Richter, J. M. *Nature* **2007**, *446*, 404. (b) Rafferty, R. J.; Williams, R. M. *J. Org. Chem.* **2012**, *77*, 519.
8. Yang, S.; An, X. D.; Qiu, B.; Liu, R. B.; Xiao, J. *Org. Lett.* **2021**, *23*, 9100.
9. Inuki, S.; Iwata, A.; Oishi, S.; Fujii, N.; and Ohno, H. *J. Org. Chem.* **2011**, *76*, 2072.
10. Nemoto, T.; Harada, S.; and Nakajima, M. *Asian J. Org. Chem.* **2018**, *7*, 1730.
11. (a) Kubo, A.; Nakai, T.; Nozoye, T.; Itai, A.; Iitaka, Y. *Heterocycles*, **1978**, *9*, 1051. (b) Osman, F. H.; EI-Samahy, F. A. *Heterocycl. Commun.* **2000**, *6*, 175. (c) Kozminykh, V. O.; Lomidze, K. Sh.; Kozminykh, E. N.; Berezin, A. N. *Chem. Heterocycl. Compd.* **2004**, *40*, 521. (d) Paponov, B. V.; Shishkin, O. V.; Shishkina, S. V.; Zubatyuk, R. I.; Kalyuzhny, A. L.; Musatov, V. I. *Russ. Chem. Bull.* **2008**, *57*, 622.
12. (a) Chen, Y.; Cui, B. D.; Wang, Y.; Han, W. Y.; Wan, N. W.; Bai, M.; Yuan, W. C.; and Chen, Y. Z. *J. Org. Chem.* **2018**, *83*, 10465. (b) Warghude, P. K.; Sabale, A. S.; and Bhat, R. G. *Org. Biomol. Chem.* **2020**, *18*, 1794. (c) Warghude, P. K.; Sabale, A. S.; Dixit, R.; Vanka, R.; Bhat, R. G. *Org. Biomol. Chem.* **2021**, *19*, 4338. (d) Sabale, A. S.; Warghude, P. K.; Bhat, R. G. *Synlett.* **2023**, *34*, 1732. (e) Warghude, P. K.; Sabale, A. S.; Bhat, R. G. *Elsevier* **2024**, 309.
13. An earlier version of this manuscript was filed on the preprint server ChemRxiv: Sabale, A. S.; Bhowmick, A.; Bankar, O. S.; Bhat, R. G. *ChemRxiv*, **2024**, DOI:10.26434/chemrxiv-2024-xhpj4
14. (a) Cao, S. H.; Zhang, X.-C.; Wei, Y.; Shi, M. *Eur. J. Org. Chem.* **2011**, *2011*, 2668. (b) Reddy, C. N.; Nayak, V. L.; Mani, G. S.; Kapure, J. S.; Adiyala, P. R.; Maurya, R. A.; Kamal, A. *Bioorg. Med. Chem. Lett.* **2015**, *25*, 4580. (c) Massari, S.; Desantis, J.; Nannetti, G.; Sabatini, S.; Tortorella, S.; Goracci, L.; Cecchetti, V.; Loregian, A.; Tabarrini, O. *Org. Biomol. Chem.* **2017**, *15*, 7944. (d) Warghude, P. K.; Dharpure, P. D.; Bhat, R. G. *Tetrahedron Lett.* **2018**, *59*, 4076. (e) Bhowmick, A.; Warghude, P. K.; Bhat, R. G. Asian J. Org. Chem. **2022**, *11*, e202200205 DOI: 10.1002/ajoc.202200205.
15. (a) Dhara, D.; Gayen, K. S.; Khamarui, S.; Pandit, P.; Ghosh, S.; and Maiti D. K. *J. Org. Chem.* **2012**, *77*, 10441. (b) Feng, C.; Yan, Y.; Zhang, Z.; Xu, K. and Wang, Z. *Org. Biomol. Chem.* **2014**, *12*, 4837.

4 One-Pot Oxa-Michael-Initiated [4+2] Cycloaddition Cascade Between Pyrazoledione-Based Morita–Baylis–Hillman Alcohols and Arylidene Pyrazolones: A Concise Route to Dispiropyrazolone Fused Tetrahydropyrans

Abstract

An expedient transition metal-free oxa-Michael cascade [4+2] annulation has been developed for the efficient synthesis of dispiropyrazolone fused tetrahydropyran framework. This atom-economical method leverages pyrazolonedione-based Morita−Baylis−Hillman (Pyro-MBH) alcohol as unique oxa-Michael donors. The reaction enables the rapid assembly of complex spiroheterocyclic compounds with two tertiary and two quaternary stereocenters in excellent yields in very rapid reaction times (1–2 minute). The protocol also proved to be scalable, and the compounds synthesized were utilized for the successful Suzuki coupling reactions, showcasing its practicality of the method.



Sabale, A. S.; Khandeparkar, M.; Bankar, O. S.; Bhat. R. G. One-Pot Oxa-Michael-Initiated [4+2] Cycloaddition Cascade Between Pyrazoledione-Based Morita–Baylis–Hillman Alcohols and Arylidene Pyrazolones: A Concise Route to Dispiropyrazolone Fused Tetrahydropyrans, *Manuscript is ready to be communicated.*

4 One-Pot Oxa-Michael-Initiated [4+2] Cycloaddition Cascade Between Pyrazoledione-Based Morita–Baylis–Hillman Alcohols and Arylidene Pyrazolones: A Concise Route to Dispiropyrazolone Fused Tetrahydropyrans

4.1 Introduction

The efficient synthesis of spiropyrazolone frameworks, particularly those bearing tertiary and quaternary carbon stereocenters, remains a significant challenge in synthetic organic chemistry due to the inherent steric hindrance associated with such structures. Achieving precise stereochemical control at spirocyclic junctions and adjacent tertiary and secondary carbon centers further complicates their construction, necessitating sophisticated and highly controlled synthetic approaches. Morita−Baylis−Hillman (MBH) adducts and their derivatives have established themselves as versatile intermediates, widely employed in annulation reactions to assemble structurally diverse and intricate spirocyclic architectures.[1] Morita−Baylis−Hillman (Pyro-MBH) carbonates hold particular importance among MBH adducts due to their reactivity in diverse [3+2] annulation reactions. Despite their versatility, these annulations generally demand prolonged reaction times, spanning anywhere between 12 to 72 h. The underlying mechanism involves the in-situ formation of electrophilic salts and zwitterionic allylic ylides, driven by Lewis base catalysis, which facilitates the efficient construction of complex molecular frameworks.[2]

The six-membered dispiropyrazolone frameworks represent key structural motifs prevalent in a variety of bioactive compounds (Fig. 4.1b).[3] Their unique architecture, featuring heteroatoms (Fig. 1b),[4] two pyrazolone units (Fig. 4.1b),[5] and two spiropyrazolone moieties (Fig. 4.1a)[4], in addition to dispirocyclic scaffolds (Fig. 4.1a),[6] significantly amplifies the biological activity of the resulting molecules (Fig. 4.1b). These distinctive features underscore their importance in medicinal chemistry as well as their potential for diverse therapeutic applications.

The deliberate incorporation of pharmacologically relevant scaffolds is a recognized strategy in the discovery and design of novel lead compounds. Specifically, the fusion of two spiro-pyrazolone frameworks to form dispiro cyclic structures presents a promising approach for creating architecturally sophisticated and biologically significant molecules. This strategy

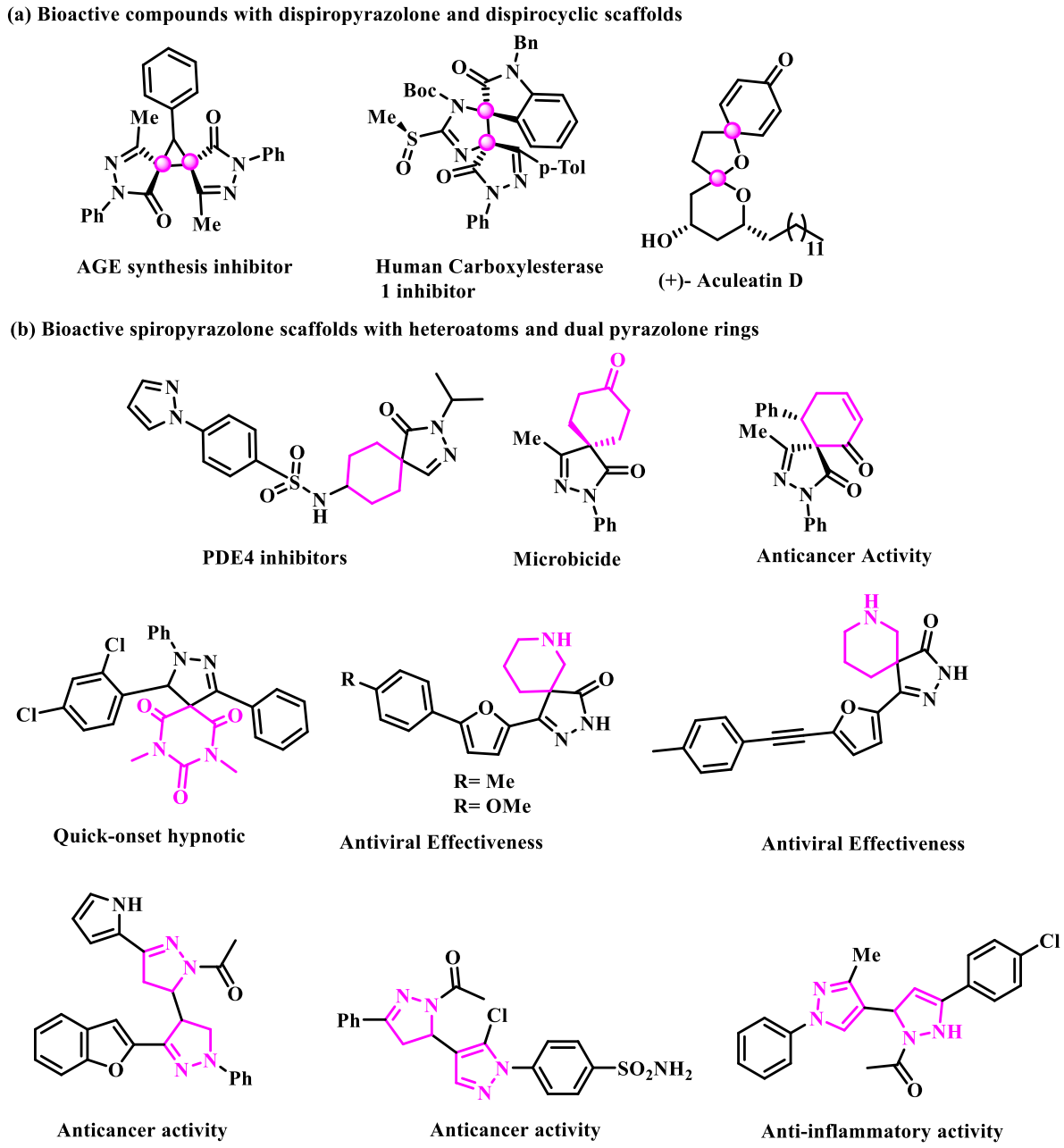


Figure 4.1 Biologically active compounds and proposed hybrid structures: innovative scaffolds for drug development

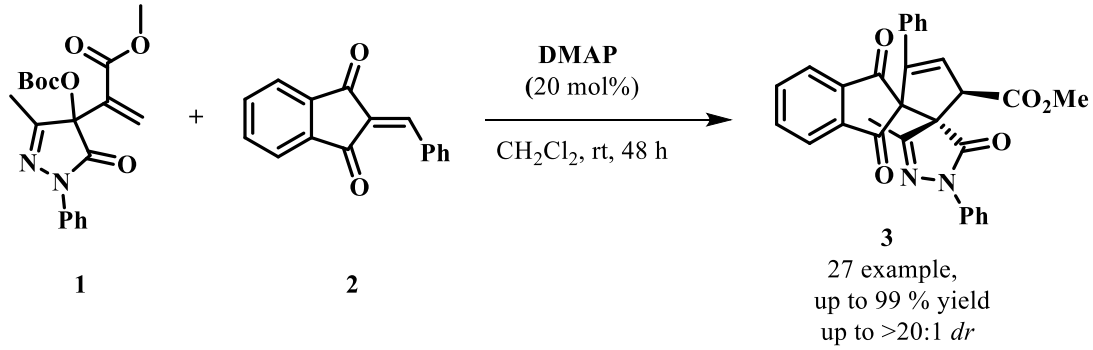
offer a compelling pathway for the identification of possibly new bioactive entities, showcasing their potential in advancing therapeutic development (Fig. 4.1c).[7]

The synthesis of spiropyrazole and dispiropyrazole frameworks has become a central area of focus in contemporary synthetic chemistry owing to their exceptional structural diversity and significant biological relevance. Recent progress in this field highlights the development of novel and efficient synthetic methodologies, particularly catalytic strategies, and multicomponent reaction systems. These innovative approaches aim to enhance synthetic versatility and applicability of spiropyrazole frameworks, thereby unlocking their full potential in drug discovery and materials science.[8]

4.2 Recent developments in the synthesis of dispiropyrazolone

Several studies have been reported in the literature regarding the synthesis of dispiro pyrazolone derivatives through a [3+2] cycloaddition of pyrazolonedione-based Morita−Baylis−Hillman (Pyro-MBH) carbonates with various dienophiles. This approach facilitates the efficient construction of dispirocyclic frameworks, demonstrating significant versatility and applicability in synthetic chemistry. Some of the representative reports have been highlighted.

Guo and co-workers[2a] have explored a novel approach utilizing 4-(dimethylamino) pyridine (DMAP) as a catalyst to achieve [3+2] annulation reaction. This process involves the reaction of pyrazoledione-derived Morita–Baylis–Hillman (MBH) carbonates **1** with 2-arylideneindane-1,3-diones **2**, leading to the formation of a diverse array of multifunctional

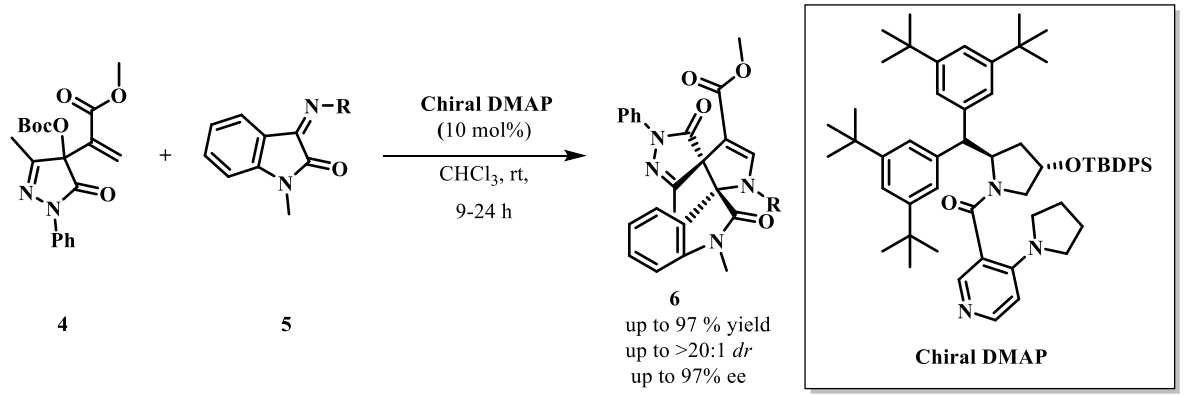


Scheme 4.1 Synthesis of multifunctional spiropyrazole via DMAP catalyzed [3+2] cycloaddition

spiropyrazole derivatives **3** in modest to excellent yields with a varied diastereoselectivities (16 to 99%, 3:2 to 20:1 *dr*). The pyrazoledione-derived Morita–Baylis–Hillman (MBH) carbonates **1** act as essential substrates in this organocatalyzed transformation, paving the way for the synthesis of complex pyrazolinone-containing dispirocyclic compounds **3**, which may have

potential applications in medicinal chemistry and material science. This work underscores the versatility of organocatalysis in constructing intricate molecular architectures (see Scheme 4.1).

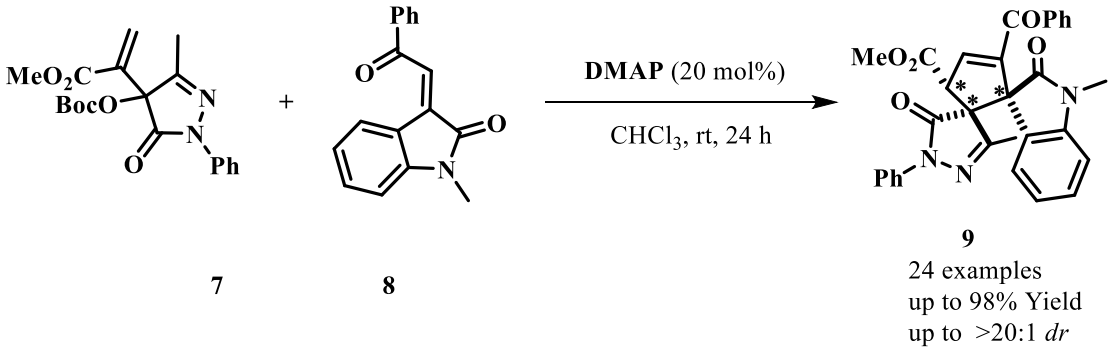
Han and coworkers[2b] have successfully synthesized a catalytic asymmetric dispiro[pyrazolone–dihydropyrrole–oxindole] framework **6** using a DMAP-derived chiral catalyst. This innovative approach utilized a recently developed pyrazolonedione-based Morita−Baylis−Hillman (Pyro-MBH) carbonates **4** to afford the desired spirocyclic product **6** in excellent yields with exceptional stereoselectivities. The proposed transition state analysis suggested that intermolecular hydrogen bonding and π–π stacking interactions are critical in facilitating the stereoselective transformation. This work highlights the efficiency of the DMAP-derived chiral catalysts in asymmetric catalysis and underscores the importance of non-covalent interactions in directing stereochemical outcome in complex organic transformations. Further exploration of these interactions could pave the way for developing more efficient catalytic systems in asymmetric synthesis (see Scheme 4.2).



Scheme 4.2 Synthesis of dispiro[pyrazolone–dihydropyrrole–oxindole] via chiral DMAP catalyzed [3+2] cycloaddition

Our research group reported[2c] a DMAP-catalyzed, highly diastereoselective [3+2] cycloaddition utilizing pyrazolonedione-based Morita−Baylis−Hillman (Pyro-MBH) carbonates **7** and 3-methyleneoxindole **8** as key substrates (Scheme 4.4). This strategy enables the efficient construction of structurally intricate spiropyrazolone-fused oxindoles **9**, incorporating three contiguous stereocenters with remarkable precision. The methodology afforded the spirocyclic frameworks in exceptional yields (up to 98%) with outstanding diastereoselectivity (up to 99:1). Furthermore, the synthetic utility of this approach has been

demonstrated through subsequent transformations, including Suzuki cross-coupling and hydrolysis reactions, thereby expanding the applicability of this protocol (see scheme 4.3).

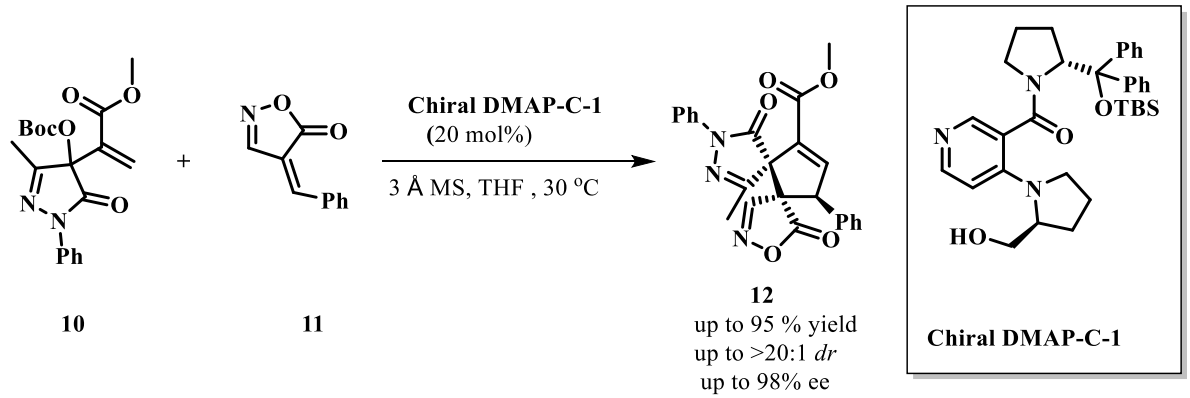


7 8

Scheme 4.3 Synthesis of spiropyrazolone-fused oxindoles via DMAP catalyzed [3+2] cycloaddition

Wang and coworkers[2d] have developed a catalytic asymmetric [3+2] cyclization reaction of pyrazolonedione-based Morita−Baylis−Hillman (Pyro-MBH) carbonates **10** with arylidenyl isoxazolones **11**, using a DMAP-derived chiral catalyst. This innovative approach has led to the synthesis of dispirocyclic pyrazolones **12** bearing vicinal all-carbon quaternary stereocenters within an embedded cyclopentene ring scaffold. Notably, this reaction affords the desired products **12** in very good yields (up to 85%) with an excellent stereoselectivity (up to 20:1 *dr*) under mild reaction conditions (room temperature, 1 atm). The DMAP-derived chiral catalyst used in this reaction is a key component in achieving high levels of stereoselectivity. The unique structure and properties of the catalyst enabled the asymmetric [3+2] cyclization reaction, resulting in the formation of complex dispirocyclic pyrazolones **12** with high levels of stereocontrol.

This work represents an important advancement in asymmetric catalysis, providing a new and efficient method for synthesizing complex molecules with quaternary stereocenters. The mild



10 11

12
up to 95 % yield
up to >20:1 *dr*
up to 98% ee

Scheme 4.4 Synthesis of dispiro[pyrazolone–dihydropyrrole–oxindole] via chiral DMAP catalyzed [3+2] cycloaddition

reaction conditions and excellent stereoselectivities make this method attractive for synthesizing complex natural products and biologically active molecules (Scheme 4.4).

In line with our ongoing efforts to develop novel spirocyclic frameworks, we focused on establishing an efficient, atom-economical, and stereoselective strategy for constructing spirocyclic architectures via an oxa-Michael-initiated [4+2] annulation cascade. Drawing from our extensive experience in the chemistry of pyrazolone-derived Morita–Baylis–Hillman (Pyro-MBH) carbonates and alcohols, we identified a significant gap in the literature, specifically, the uncharted potential of Pyro-MBH alcohols in cycloaddition reactions. To date, no direct application of unprotected Pyro-MBH alcohols in such annulation strategies has been reported, highlighting a valuable opportunity for methodological innovation.

Motivated by this unexplored synthetic route, we investigated the direct [4+2] cycloaddition of Pyro-MBH alcohols with arylidene pyrazolones. This chapter presents, for the first time, a metal-free and rapid protocol for accessing dispiropyrazolone-fused tetrahydropyrans using this novel approach. Remarkably, the reaction proceeds cleanly under mild conditions and completes within 1–2 minute, showcasing excellent efficiency and environmental compatibility. This methodology represents a significant advancement in the synthesis of oxygen-containing spirocyclic systems and opens new avenues for utilizing Pyro-MBH alcohols in complex molecule construction.

4.3 Results and Discussion

In order to realize the proposed synthetic pathway, oxa-Michael cascade [4+2] annulation reaction for accessing the hybrid structure, we commenced with the model optimization reaction. In this regard, we commenced with Pyro-MBH alcohol **1a** and arylidene pyrazolone **2a** as model substrates. The reaction of compounds **1a** and **2a** in presence of 1,8-diazabicyclo[5.4.0]undec-7-ene (DBU) as the base (50 mol%) in 1,4-Dioxane at room temperature underwent very sluggishly by affording the desired product **3a** in poor yield in spite of the prolonged reaction time (24 h, 10%, Table 4.1, entry 1). Interestingly, the reaction in the presence of other bases such as DMAP, DABCO, PPh_3, and Et_3N did not facilitate the formation of **3a** (Table 4.1, entries 2−5).

Later, we screened various inorganic bases (50 mol%) to drive this reaction. Notably, $NaHCO_3$ and Na_2CO_3 proved ineffective for driving this annulation reaction between **1a** and **2a** (Table 4.1, entries 6 and 7). Interestingly, the reaction worked smoothly in the presence of bases such as K_2CO_3, K_3PO_4, Cs_2CO_3, and KOt-Bu to afford the desired product **3a** in relatively better

yields than organic bases such as DBU (31% to 68%, Table 4.1, entries 8−11). Among all the bases screened, potassium *tert*-butoxide worked more efficiently in forming the desired product **3a** in the highest yield in an extremely rapid time of 1 min. with a very high diastereoselectivity (68%, Table 4.1, entry 11). These results indicate that the choice of base plays a crucial role in modulating the reaction outcome.

Encouraged by this initial success, we further screened the reaction by varying the loading of KOt-Bu. Interestingly, further increase as well as decrease in the loading of KOt-Bu (100 mol% and 20 mol%) furnished the desired product **3a** in lower yields, 40% and 54% respectively, and also the reaction took more time to complete when compared with 50 mol% of KOt-Bu (Table 4.1, entries 12−13). These findings indicate that the optimum concentration of the base is very important to have a pronounced impact on reaction efficiency and overall yield of the desired product **3a**.

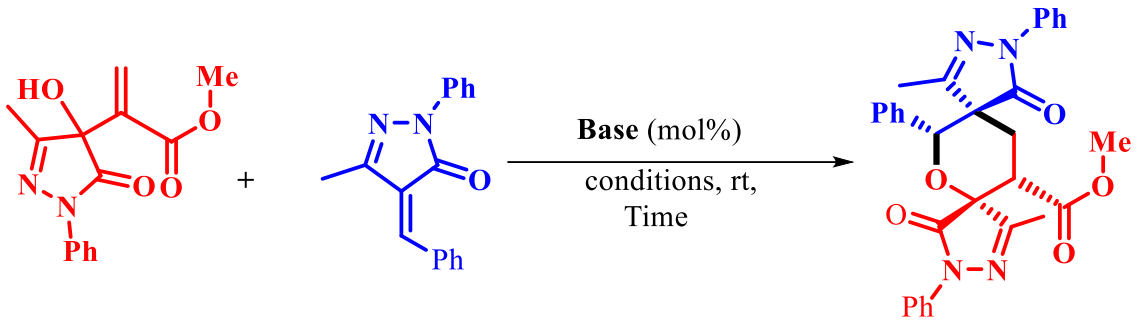
Later, we carried out the reaction by screening various solvents while using the KOt-Bu (50 mol%). Though reaction worked in all solvents screened, however, 1,4-Dioxane proved to be most efficient in affording the desired product **3a** in the highest yield (Table 4.1, entries 11, 14−20).

Later, we carried out the reaction of **1a** and **2a** in 1,4-Dioxane containing the molecular sieves (4Å), and we observed that yield of the desired product dropped significantly (50%, Table 4.1, entry 21). This result suggests that moisture (present in the solvent) is critical in influencing the overall reaction efficiency.

Based on the detailed screening, Pyro-MBH alcohol **1a** (1 equiv) and arylidene pyrazolone **2a** (1 equiv), KOt-Bu (50 mol%) in 1,4-Dioxane at room temperature proved to be the optimum reaction conditions to access the desired spirocyclic compound **3a** via oxa-Michael cascade [4+2] annulation reaction (Table 4.1, entry 11).

Along with spectroscopic analysis, the molecular structure of the desired spirocyclic compound **3a** was unambiguously confirmed by the single-crystal X-ray diffraction analysis.[9] Additionally, the stereochemistry of the major diastereomer (isolated as a single diastereomer) was determined to be *R, R, R, S*, as supported by further analysis (See Scheme 4.5, also see Appendix Page-174).

Table 2.1 Screening of catalysts and solvents for cycloaddition reaction[a-c]



1a **2a** **3a**

Entry	Base (mol%)	solvent	time	Yield[b] (%)
1	DBU (50)	1,4-Dioxane	24 h	10
2	DMAP (50)	1,4-Dioxane	24 h	NR
3	DABCO (50)	1,4-Dioxane	24 h	NR
4	PPh_3 (50)	1,4-Dioxane	24 h	NR
5	Et_3N (50)	1,4-Dioxane	24 h	NR
6	$NaHCO_3$ (50)	1,4-Dioxane	24 h	NR
7	Na_2CO_3 (50)	1,4-Dioxane	24 h	NR
8	K_3PO_4 (50)	1,4-Dioxane	24 h	31
9	K_2CO_3 (50)	1,4-Dioxane	24 h	33
10	Cs_2CO_3 (50)	1,4-Dioxane	40 min.	50
11	**KOt-Bu (50)**	1,4-Dioxane	**1 min.**	**68**
12	KOt-Bu (100)	1,4-Dioxane	5 min.	40
13	KOt-Bu (20)	1,4-Dioxane	10 min.	52
14	KOt-Bu (50)	MeCN	1 min.	48
15	KOt-Bu (50)	Toluene	1 min.	40
16	KOt-Bu (50)	THF	1 min.	58
17	KOt-Bu (50)	CH_2Cl_2	1 min.	65
18	KOt-Bu (50)	$CHCl_3$	1 min.	56
19	KOt-Bu (50)	$ClCH_2CH_2Cl$	1 min.	56
20	KOt-Bu (50)	EtOAC	1 min.	57
21[c]	KOt-Bu (50)	1,4-Dioxane	15 min.	50

[a]**Reaction Conditions:** Unless stated otherwise, reactions were performed using **1a** (0.2 mmol), **2a** (0.2 mmol), and the catalyst [50 mol%] in 1.0 mL of the specified solvent at room temperature for min. [b]Isolated yields of **3a**. [C]Control experiment (MS-4 Å used). NR- No Reaction

Further, explored the substrate scope of this cascade annulation reaction under the optimized conditions. In this regard, we synthesized starting materials Pyro-MBH alcohols (**1b**–**1f**) and arylidene pyrazolones (**2a**–**2af**) to assess their reactivity and compatibility in accessing the desired annulated products (**3a**–**3ak**, Scheme 4.5).

Various substituted Pyro-MBH alcohols (**1b-1f**), encompassing ethyl, propargyl, tert-butyl, methyl, and chloro derivatives, exhibited exceptional reactivity with **2a** under the optimized reaction conditions by affording the corresponding annulated products (**3b**–**3f**) in moderate to very good yields (up to 83%, Scheme 4.5). Remarkably, all these transformations were accomplished in a rapid reaction time of just 1 minute, thus underscoring the remarkable efficiency of the catalytic system (Scheme 4.5). Also, in all the cases, the desired products were obtained in very high diastereoselectivity and were isolated as single diastereomers, mostly.

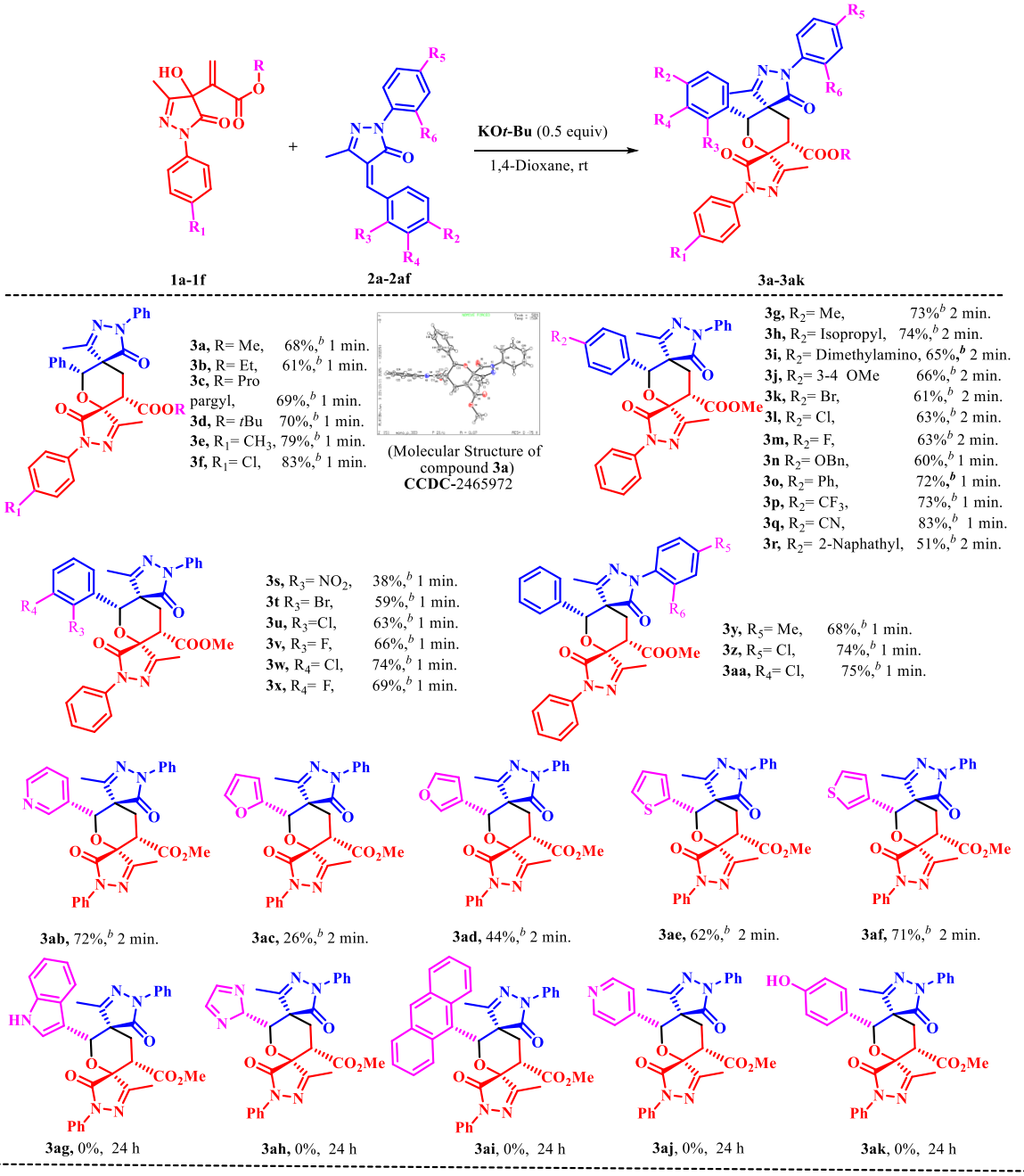
Later, substituted arylidene pyrazolones (**2b**–**2ab**) were explored by treating with the Pyro-MBH alcohol (**1a**). Initially, the impact of *para*-substituents on the phenyl ring of arylidene pyrazolones was systematically investigated. Electron-donating *para*-substituents, including 4-methyl, 4-isopropyl, 4-(diethylamino), and 3,4-dimethoxy groups (**2b-2e**), exhibited excellent reactivity with **1a**, furnishing the corresponding desired products (**3g**–**3j**) in moderate to very

good yields within 2 minute reaction time (up to 74%, Scheme 4.5). Likewise, *para*-halogen substituted derivatives, such as 4-bromo, 4-chloro, and 4-fluoro arylidene pyrazolones (**2f-2h**), reacted efficiently with Pyro-MBH alcohol **1a**, to furnish the desired dispiropyrazolone products (**3k**–**3m**) in moderate yields (61%–63%) in rapid reaction time. Furthermore, arylidene pyrazolones having electron-deactivating and electron-withdrawing substituents such as benzyloxy (OBn), phenyl (Ph), trifluoromethyl (CF_3), cyano (CN), and 2-naphthyl groups (**2i-2m**) at *para* position of the phenyl ring exhibited excellent reactivity with **1a** to afford the corresponding annulated products (**3n**–**3r**) in moderate to very good yields (up to 83%, within 1–2 minute, Scheme 4.5).

Additionally, substrates featuring *ortho*- and *meta*-substituents on the phenyl ring, including 2-nitro, 2-bromo, 2-chloro, 2-fluoro, 3-chloro, and 3-fluoro derivatives (**2n-2s**), efficiently

participated in the reaction, affording the respective desired products (**3s**–**3x**) in modest to good yields in rapid time (up to 74%, Scheme 4.5).

Scheme 4.5 Exploration of substrate scope for the [4+2] annulation reaction[a]



[a]**Reaction conditions:** Unless stated otherwise, reactions were performed using Pyro-MBH Alcohol **1a-1f** (1 equiv, 0.2 mmol), **2a-2af** (1 equiv, 0.2 mmol) and KOt-Bu (50 mol%, 0.1 mmol) in 1,4-Dioxane (1.0 mL) at room temperature for 1–2 min. isolated yields. [b] Single diastereomer. [c]Thermal ellipsoids at the 50% probability level.

Moreover, arylidene pyrazolones featuring phenyl substitutions at the nitrogen atom, including 4-methyl, 4-chloro, and 2-chloro derivatives (**2t-2v**), underwent efficient transformation under

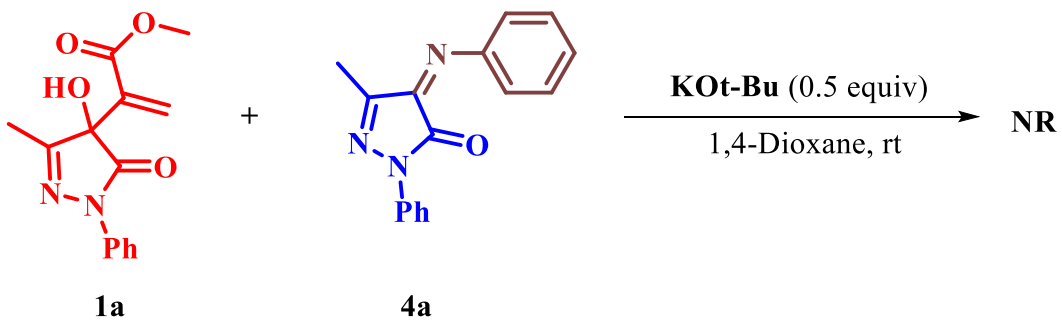
the optimized conditions to afford the corresponding products (**3y**–**3aa**) in moderate to good yields in rapid reaction time 1 min (up to 74%, Scheme 4.5).

Later, we explored the reactions of hetreoarylidene pyrazolones (**2w-2aa**) having heteroaromatic moieties such as 3-pyridyl, 2-furyl, 3-furyl, 2-thienyl, and 3-thienyl, with Pyro-MBH alcohol **1a** successfully afforded the corresponding annulated products (**3ab**–**3af**) in modest to good yields in just 2 minute (72%, Scheme 4.5). In contrast, substrates containing 3-indolyl, imidazolyl, anthracenyl, 4-pyridyl, and 4-hydroxy functionalities (**2ab-2af**) exhibited no reactivity under the annulation conditions, and the expected products (**3ag–3ak**) were not formed (Scheme 4.5).

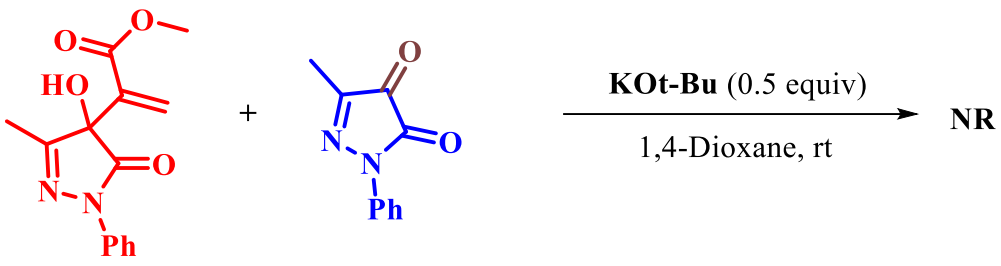
These findings underscore the extensive substrate compatibility and the remarkable efficiency of the optimized cascade annulation methodology in the stereoselective synthesis of dispiropyrazolone derivatives. The resulting dispiropyrazolone fused tetrahydropyran derivatives, incorporating a 2-oxane-fused pyrazolone framework (compounds **3a**–**3ak**), were successfully synthesized and isolated as single diastereomeric entities (Scheme 4.5). Notably, these compounds feature quaternary carbon stereocenters, thus highlighting the precision and stereoselectivity of the protocol, that too in a rapid reaction time. The exceptional diastereomeric purity observed further highlights the robustness of this approach.

Subsequently, we explored the reactivity of Pyro-MBH alcohol **1a** with structurally diverse substrates, including imino-pyrazolone **4a** and pyrazolidinedione **5a**, under the previously optimized reaction conditions. Unfortunately, these transformations were unsuccessful, as no conversion was observed and the starting materials were recovered intact, indicating a lack of reactivity under the applied conditions (Scheme 4.6).

Scheme 4.6 Attempts on other alkenes and MBH alcohol[a]



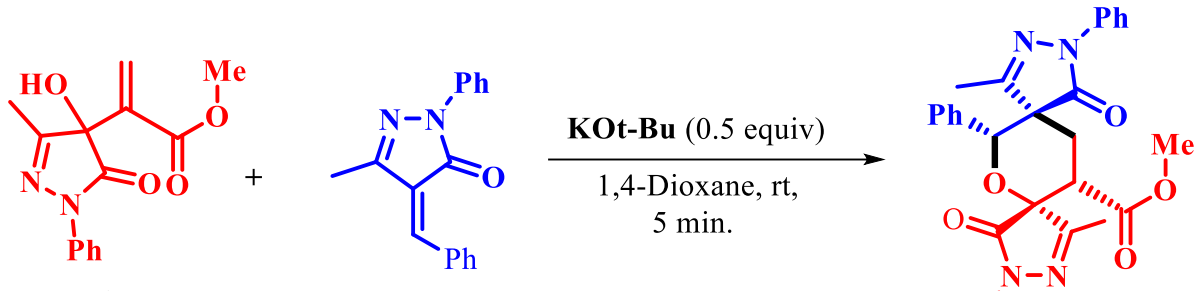
1a **4a**



1a **5a**

[a]**Reaction conditions:** Unless stated otherwise, reactions were performed using Pyro-MBH Alcohol **1a** (1 equiv, 0.2 mmol), Alkenes **4a** and **5a** (1 equiv, 0.2 mmol) and KOt-Bu (50 mol%, 0.1 mmol) in 1,4-Dioxane (1.0 mL) at room temperature for 24 h.

To assess the scalability and practicality of this protocol, a gram-scale reaction was performed using **1a** (1.0 g, 3.65 mmol), potassium tert-butoxide (50 mol%, 1.82 mmol) and **2a** (3.65 mmol) were added at ambient temperature. Remarkably, the transformation was completed within 5 minute, affording the desired product **3a** (1.28 g, 2.39 mmol) with a consistent yield (65%, Scheme 4.7).



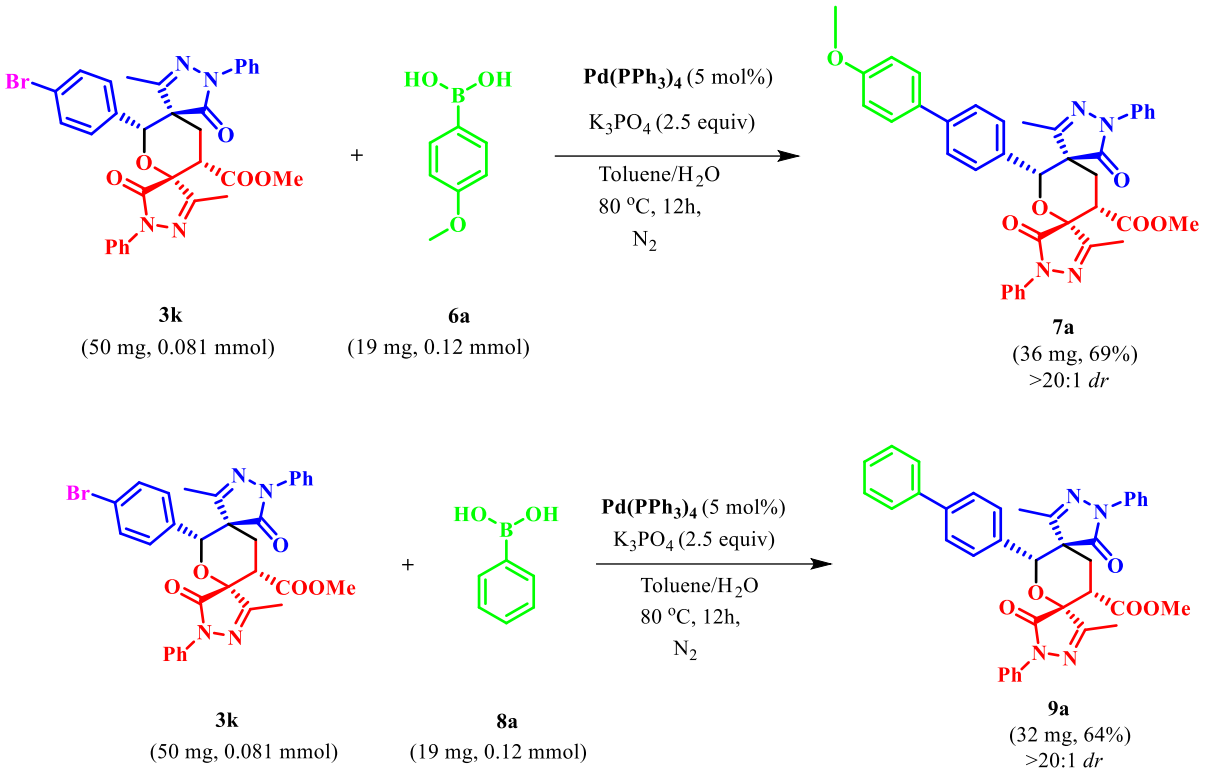
1a
(1. g, 3.65 mmol)

2a
(3.65 mmol)

3a
(1.28 g, 2.39 mmol)

Scheme 4.7 Large-scale synthesis

The synthetic versatility of the cycloaddition product was further demonstrated through a Suzuki coupling reaction. Specifically, the reaction of dispiropyrazolone fused tetrahydropyran **3k** with 4-methoxyphenyl boronic acid (**6a**) and phenylboronic acid (**8a**) was successfully carried out in the presence of $Pd(PPh_3)_4$ and K_3PO_4 at 80 °C. This transformation afforded the corresponding products **7a** and **9a** in good yields of 69% and 64% respectively with excellent diastereoselectivity (Scheme 4.8).

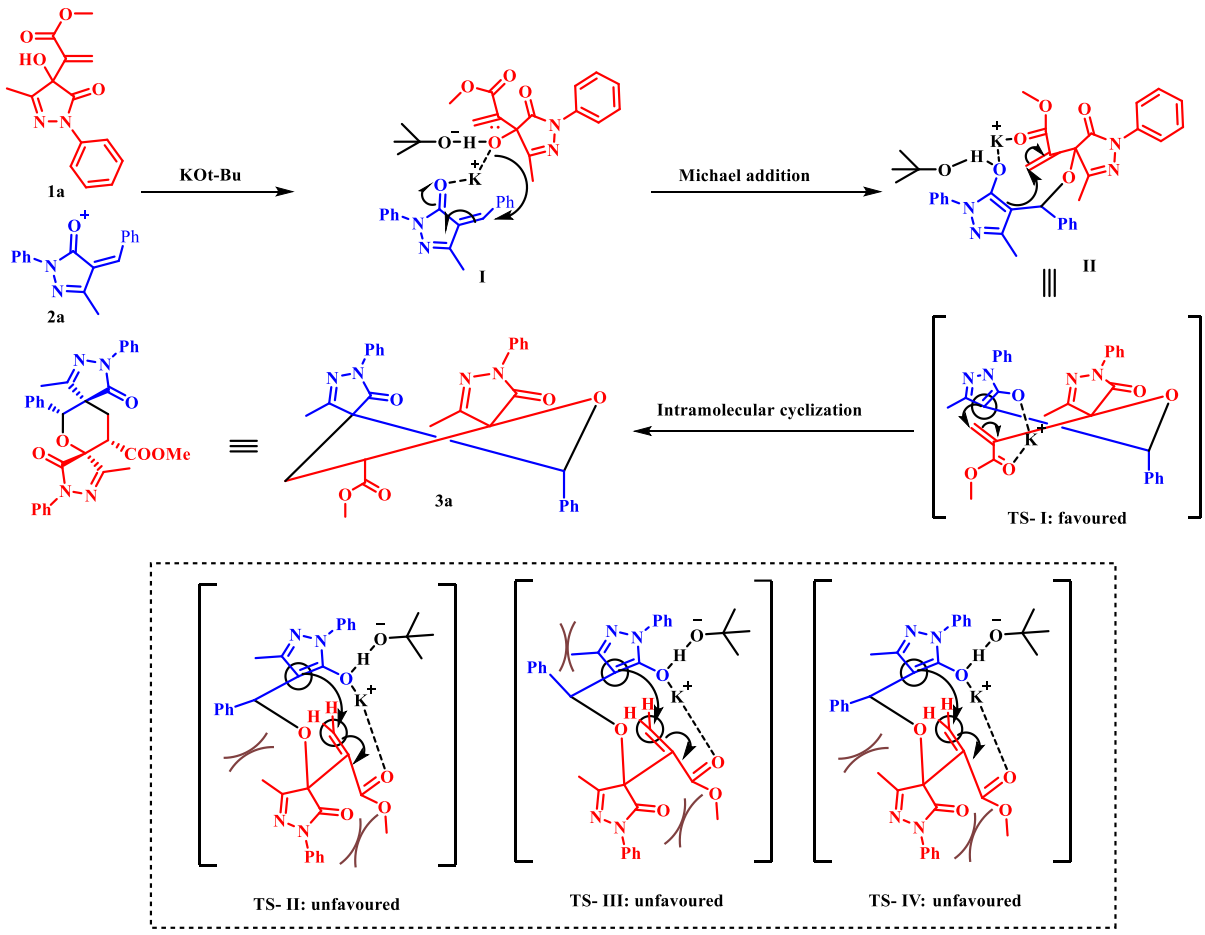


Scheme 4.8 Synthetic modifications

A plausible mechanistic pathway has been proposed based on comprehensive literature precedents, our experimental data, and corroborative single-crystal X-ray crystallographic analysis.[9, 10] The catalytic cycle is initiated by the deprotonation of the Michael donor, Pyro-MBH alcohol **1a**, in the presence of KOt-Bu as a base, generating a reactive nucleophilic species **I**. This intermediate subsequently engages in a Michael addition with arylidene pyrazolone **2a**, leading to the formation of intermediate **II**.

X-ray diffraction data suggest that the Michael addition may proceed via a more energetically favored transition state (**TS-1**), characterized by an unexpected half-chair-like conformation. This transition state then undergoes intramolecular cyclization, furnishing the final spirocyclic product **3a**. The proposed mechanism is consistent with established catalytic paradigms and offers a coherent explanation for the observed reactivity and stereochemical outcome.

Overall, the protocol proved to be operating under mild basic conditions and allowed easy access to the formation of complex molecules that contain two tertiary and two quaternary stereocenters, which are often challenging to synthesize using traditional methods. The reaction showcases remarkable efficiency, allowing for the rapid construction of diverse spirocyclic



Scheme 4.9 Proposed reaction mechanism for the [4+2] annulation

frameworks, which can have significant implications in the fields of medicinal chemistry and drug development. Notably, this work marks the first reported synthesis of a spiropyrazolone fused 2-oxane scaffold, expanding the repertoire of pyrazolone derivatives available to researchers.

4.4 Conclusions

In summary, expedient transition metal-free oxa-Michael cascade [4+2] annulation has been developed to construct the structurally intricate dispiropyrazolone fused tetrahydropyran framework. By employing pyrazolone-derived Morita–Baylis–Hillman alcohols (Pyro-MBH alcohol) as innovative oxa-Michael donors, this methodology exhibits remarkable atom economy, enabling the simultaneous formation of two tertiary and two quaternary stereocenters within an exceptionally short reaction time. It's very important to highlight that Pyro-MBH alcohols were directly used (without protection) for the very first time for accessing pyrazolone-based spirocyclic compounds. Moreover, the method proved to be scalable on a

gram scale, and the synthesized compounds have been explored for post-synthetic modifications by exploring the Suzuki coupling reaction. The protocol avoids the use of any expensive reagents or catalysts and efficiently constructs the complex spirohetreocyclic scaffold with high diastereoselectivity.

4.5 Experimental Section

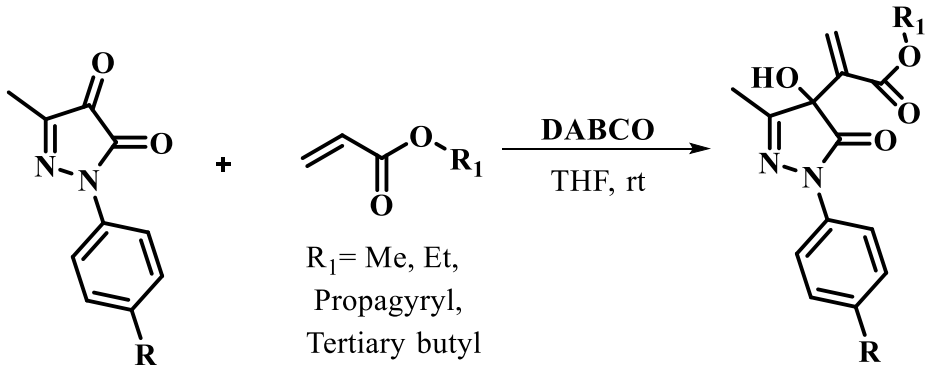
4.5.1 General

All starting materials and reagents were procured from commercial vendors (Aldrich, TCI, and Alfa Aesar) and utilized as received without additional purification unless stated otherwise. Reactions were carried out in flame-dried reaction vessels. Commercial-grade solvents were employed for the reaction. Analytical Reagent grade (AR)-grade 1,4-Dioxane was used. Thin-layer chromatography (TLC) was performed on silica gel 60 GF254 aluminum-backed plates (2.5 mm thickness), and compounds were visualized under ultraviolet (UV) light at a wavelength of 254 nm. Column chromatography utilized silica gel (100–200 mesh), with petroleum ether and ethyl acetate as the mobile phase. Nuclear magnetic resonance (NMR) spectra were recorded using tetramethylsilane (TMS) as an internal standard. For ^{1}H NMR, spectra were acquired at 400 MHz, while $^{13}C\{^{1}H\}$ NMR spectra were recorded at 100 MHz using Bruker or Neo instruments unless otherwise noted. Chemical shifts (δ) are reported in parts per million (ppm) relative to the residual solvent peak of $CDCl_3$ (δ = 7.26 ppm for ^{1}H NMR, δ = 77.16 ppm for $^{13}C\{^{1}H\}$ NMR). The multiplicity of ^{1}H NMR signals is described as follows: singlet (s), doublet (d), double doublet (dd), triplet (t), quartet (q), broad (br), or multiplet (m), with coupling constants (J) reported in hertz (Hz) alongside integration values. $^{13}C\{^{1}H\}$ NMR spectra were fully proton decoupled. ^{19}F NMR spectra were acquired at 377 MHz. High-resolution mass spectrometry (HRMS) analyses were performed using an electrospray ionization time-of-flight (ESI-TOF) instrument. Single-crystal X-ray diffraction data were collected using Enraf-Nonius CAD4-MV31 and Bruker Kappa APEXII diffractometers. Crystal structure **3a** was obtained by slow evaporation of a 9:1 dichloromethane and ethyl acetate mixture.

4.5.2 General procedure for the synthesis of Pyro-MBH alcohols 1a−1f

A mixture of pyrazolodione (1 mmol) and methyl acrylate (1.1 mmol) in tetrahydrofuran (THF, 3 mL) was introduced to 1,4-diazabicyclo[2.2.2]octane (DABCO, 2 mmol) at ambient temperature. Upon completion of the reaction, the solvent was removed under reduced pressure. The resulting crude product was purified via column chromatography on silica gel,

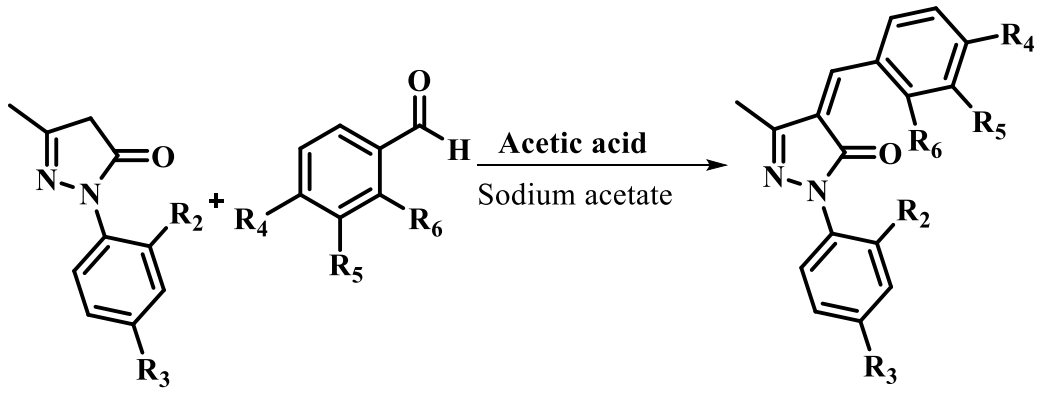
employing a gradient of ethyl acetate and hexanes as the eluent, to yield the MBH alcohol as the purified product.



Pyrazoledione **Pyrazoledione-Derived Morita-Baylis-Hillman (Pyro-MBH) Alcohols**

4.5.3 General procedure for the synthesis of arylidene pyrazolone derivatives 2a–2af

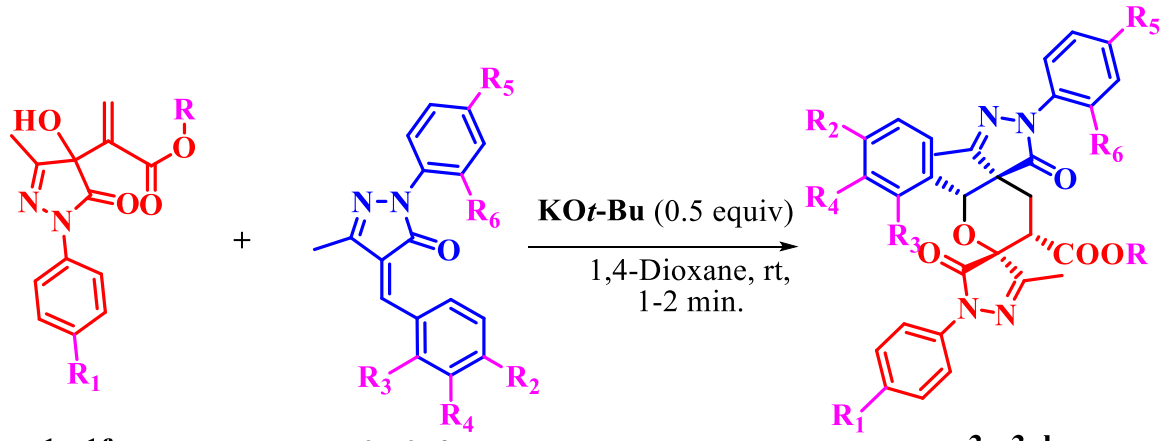
A solution of pyrazolones (1.1 equiv) in acetic acid (20 mL) was combined with benzaldehydes (1.0 equiv) and sodium acetate (1.1 equiv). The reaction mixture was heated under reflux for 30 minute, followed by dilution with ethyl acetate (20 mL). The resulting mixture was extracted with ethyl acetate (3 × 20 mL), and the combined organic layers were dried over anhydrous sodium sulfate (Na_2SO_4). After removing the solvent under reduced pressure, the crude product was purified via column chromatography on silica gel using a 98:2 hexane/ethyl acetate eluent, yielding the target compounds **2a**–**2af** in quantitative yields.



Pyrazolones **Benzaldehydes** **Arylidene pyrazonoles**

4.5.4 General procedure for the synthesis of Tetrahydro-dispiro[indolinone-3,2′-pyran-5′,4″-pyrazolone] scaffolds (3a–3ak)

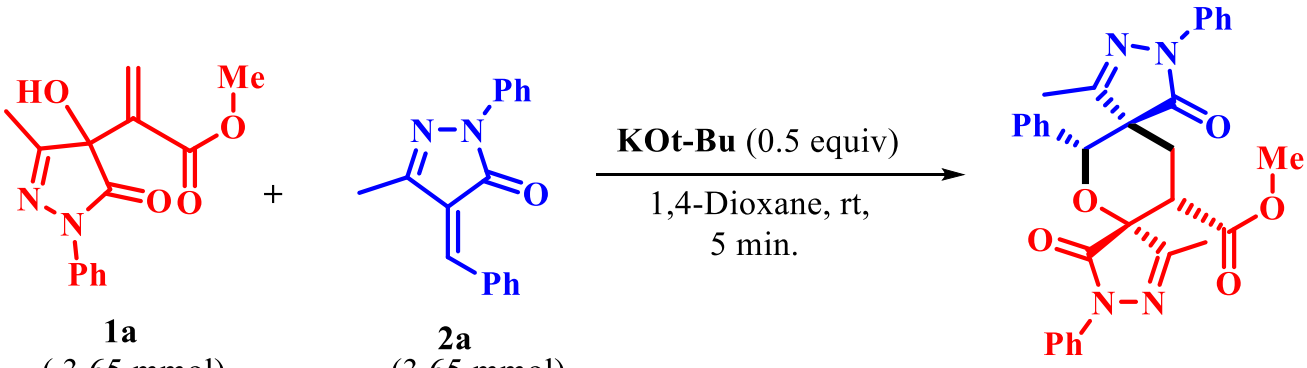
An oven-dried 10 mL glass reaction vessel was loaded with Pyrazoledione-derived Morita–Baylis–Hillman (Pyro-MBH) alcohol (**1a**–**1f**, 1 equiv, 0.2 mmol), potassium tert-butoxide (50 mol%, 0.1 mmol), and arylidene pyrazolones (**2a**–**2af**, 1 equiv, 0.2 mmol). 1,4-Dioxane (1 mL) was then added to the reaction mixture. The reaction was stirred at ambient temperaturefor 1–2 minute. Upon completion, the solvent was removed under reduced pressure. The resulting residue was purified by silica gel column chromatography using a hexane/ethyl acetate gradient, yielding the desired products (**3a**–**3ak**).



1a-1f **2a-2af** **3a-3ak**

4.5.5 Procedure for the synthesis of 3a on mmol scale

A solution of Morita-Baylis-Hillman alcohol **1a** (1 equiv, 3.65 mmol) in 20 mL of 1,4-Dioxane was prepared, to which arylidene pyrazolone **2a** (1 equiv, 3.65 mmol) and potassium tert-butoxide (50 mol%, 1.82 mmol) were added at ambient temperature. The reaction mixture was stirred for 5 minute, with progress monitored by thin-layer chromatography (TLC). Upon completion, the solvent was removed under reduced pressure. The resulting residue was



1a
(3.65 mmol)

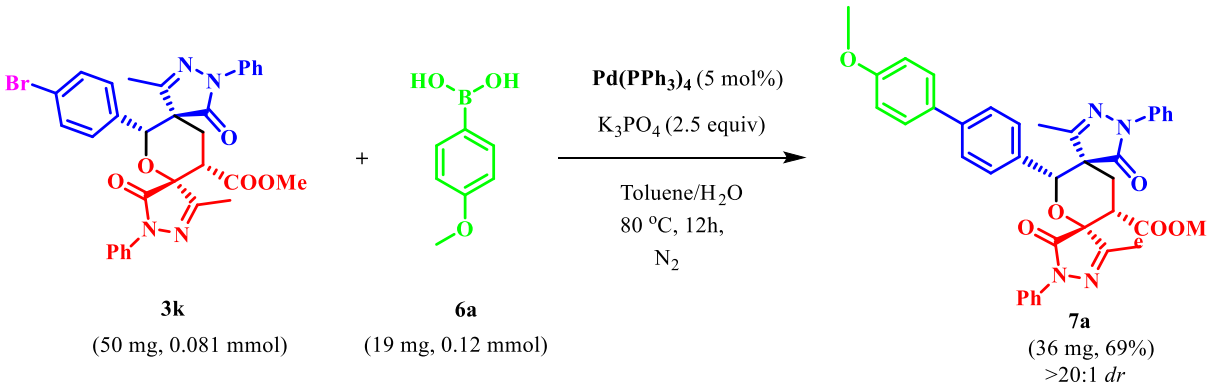
2a
(3.65 mmol)

3a
(1.28 g, 2.39 mmol)

purified by silica gel column chromatography, using a 20% ethyl acetate/hexane eluent, to yield the desired product **3a** as a white solid in 65% yield (1.28 g, 2.39 mmol).

4.5.6 Procedure for the Synthesis of 7a

A solution of **3k** (1.0 equiv, 0.081 mmol) in toluene (1 mL) and water (0.3 mL) was prepared at room temperature. To this mixture, methoxyphenylboronic acid **6a** (1.5 equiv, 0.12 mmol), $Pd(PPh_3)_4$ (0.06 equiv, 0.005 mmol), and K_3PO_4 (2.5 equiv, 0.20 mmol) were added sequentially under a nitrogen atmosphere. The reaction was heated to 80 °C and stirred for 12 hours. After completion, the mixture was cooled to room temperature, filtered through a Celite bed, and the solvent was removed under reduced pressure. The crude product was purified by column chromatography on silica gel using a 78:22 hexane/ethyl acetate mixture, yielding product **7a**.



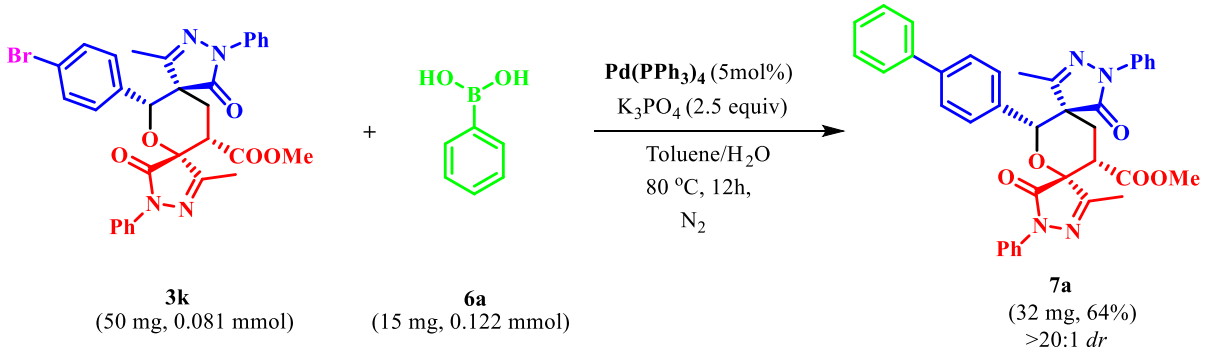
3k
(50 mg, 0.081 mmol)

6a
(19 mg, 0.12 mmol)

7a
(36 mg, 69%)
>20:1 *dr*

4.5.7 Procedure for the Synthesis of 9a

A solution of **3k** (1.0 equiv, 0.081 mmol) in toluene (1 mL) and water (0.3 mL) was prepared at room temperature. To this, phenylboronic acid **8a** (1.5 equiv, 0.122 mmol), $Pd(PPh_3)_4$ (0.06 equiv, 0.005 mmol), and K_3PO_4 (2.5 equiv, 0.20 mmol) were added sequentially under a nitrogen atmosphere. The reaction mixture was heated to 80 °C and stirred for 12 hours. Upon completion, the reaction was cooled to room temperature, filtered through a Celite bed, and the solvent was removed under reduced pressure. The resulting residue was purified by column



3k
(50 mg, 0.081 mmol)

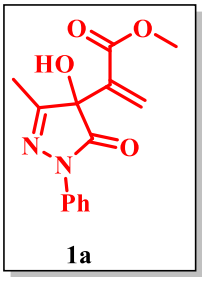
6a
(15 mg, 0.122 mmol)

7a
(32 mg, 64%)
>20:1 *dr*

chromatography (silica gel 100–200 mesh), yielding the desired compound **9a** as a white solid (32 mg, 64% isolated yield, >20:1 *dr*).

4.6 Experimental Data

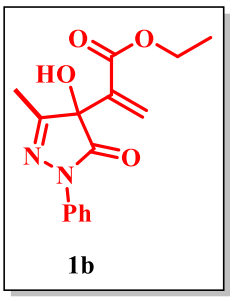
Methyl 2-(4-hydroxy-3-methyl-5-oxo-1-phenyl-4,5-dihydro-1H-pyrazol-4-yl)acrylate (1a)



1a

The compound **1a** was synthesized following the standard procedure outlined in Section **4.5.2**, with a reaction duration of 6 hours, resulting in an 82% yield (225 mg). Purification was achieved via column chromatography on silica gel (SiO_2) using a solvent mixture of 25% ethyl acetate in hexanes. The product was obtained as a white solid. Its identity was confirmed by ^{1}H and $^{13}C\{^{1}H\}$ NMR spectroscopy and high-resolution mass spectrometry (HRMS). The melting point was determined to be 161–163 °C. ^{1}H NMR (400 MHz, $CDCl_3$): δ 7.9 – 7.8 (m, 2H), 7.5 – 7.3 (m, 2H), 7.2 (t, J = 7.4 Hz, 1H), 6.6 (s, 1H), 6.4 (s, 1H), 4.2 (s, 1H), 3.7 (s, 3H), 2.0 (s, 3H). $^{13}C\{^{1}H\}$ NMR (100 MHz, $CDCl_3$): δ 171.9, 164.5, 159.1, 137.7, 136.0, 130.0, 128.9, 125.4, 119.1, 79.2, 52.5, 13.0. HRMS (ESI TOF) *m/z* calcd. For $C_{14}H_{14}N_2O_4$ $[M+Na]^+$ 297.0851 found 297.0850.

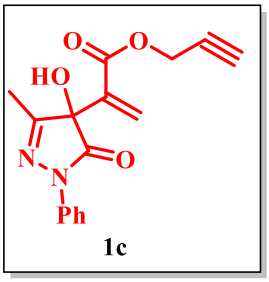
Ethyl 2-(4-hydroxy-3-methyl-5-oxo-1-phenyl-4,5-dihydro-1H-pyrazol-4-yl)acrylate (1b)



1b

The compound **1b** was synthesized following the standard procedure outlined in Section **4.5.2**, with a reaction duration of 6 hours, resulting in a 71% yield (205 mg). Purification was achieved via column chromatography on silica gel (SiO_2) using a solvent mixture of 25% ethyl acetate in hexanes. The product was obtained as a white solid. Its identity was confirmed by ^{1}H and $^{13}C\{^{1}H\}$ NMR spectroscopy and high-resolution mass spectrometry (HRMS). The melting point was determined to be 107–109 °C. ^{1}H NMR (400 MHz, $CDCl_3$): δ 7.9 – 7.8 (m, 2H), 7.4 – 7.3 (m, 2H), 7.2 (td, *J* = 7.4, 1.2 Hz, 1H), 6.6 (d, *J* = 1.8 Hz, 1H), 6.4 (d, *J* = 1.5 Hz, 1H), 4.6 (s, 1H), 4.3 – 3.9 (m, 2H), 2.1 – 2.0 (m, 3H), 1.2 – 1.1 (m, 3H). $^{13}C\{^{1}H\}$ NMR (100 MHz, $CDCl_3$): δ 172.1, 163.9, 159.5, 137.7, 136.2, 130.2, 128.9, 125.3, 118.9, 79.3, 61.6, 13.9, 12.9. HRMS (ESI TOF) *m/z* calcd. For $C_{15}H_{16}N_2O_4$ $[M+H]^+$ 311.1007 found 311.1009.

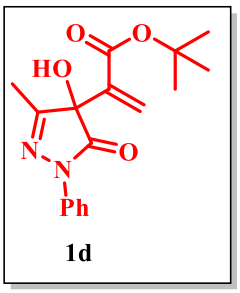
Prop-2-yn-1-yl 2-(4-hydroxy-3-methyl-5-oxo-1-phenyl-4,5-dihydro-1H-pyrazol-4-yl)acrylate (1c)



1c

The compound **1c** was synthesized following the standard procedure outlined in Section **4.5.2**, with a reaction duration of 6 hours, resulting in a 74% yield (220 mg). Purification was achieved via column chromatography on silica gel (SiO_2) using a solvent mixture of 25% ethyl acetate in hexanes. The product was obtained as a brown sticky solid. Its identity was confirmed by ^{1}H and $^{13}C\{^{1}H\}$ NMR spectroscopy and high-resolution mass spectrometry (HRMS). ^{1}H NMR (400 MHz, DMSO-d_6): δ 7.8 – 7.7 (m, 2H), 7.5 – 7.4 (m, 2H), 7.2 – 7.2 (m, 1H), 6.1 (s, 1H), 5.7 (s, 1H), 4.6 – 4.5 (m, 2H), 3.6 (t, J = 2.5 Hz, 1H), 3.4 (s, 1H), 2.1 (s, 3H). $^{13}C\{^{1}H\}$ NMR (100 MHz, DMSO-d_6): δ 171.5, 169.9, 165.4, 161.3, 138.0, 136.5, 129.4, 125.4, 118.8, 78.7 (d, J = 2.0 Hz), 78.4 – 78.2 (m), 77.8, 52.8, 13.8. HRMS (ESI TOF) *m/z* calcd. For $C_{14}H_{14}N_2O_4$ $[M+H]^+$ 299.1032 found 299.1034.

Tert-butyl 2-(4-hydroxy-3-methyl-5-oxo-1-phenyl-4,5-dihydro-1H-pyrazol-4-yl)acrylate (1d)

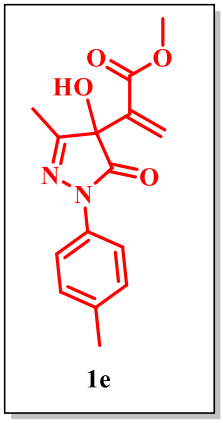


1d

The compound **1d** was synthesized following the standard procedure outlined in Section **4.5.2**, with a reaction duration of 6 hours, resulting in a 73% yield (230 mg). Purification was achieved via column chromatography on silica gel (SiO_2) using a solvent mixture of 25% ethyl acetate in hexanes. The product was obtained as a white solid. Its identity was confirmed by ^{1}H and $^{13}C\{^{1}H\}$ NMR spectroscopy and high-resolution mass spectrometry (HRMS). The melting point was determined to be 116–118 °C. ^{1}H NMR (400 MHz, $CDCl_3$): δ 7.9 – 7.8 (m, 2H), 7.4 – 7.3 (m, 2H), 7.2 – 7.1 (m, 1H), 6.6 (d, J = 0.8 Hz, 1H), 6.3 (d, J = 0.8 Hz, 1H), 5.2 (s, 1H), 2.0 (s, 3H), 1.3 (s, 9H). $^{13}C\{^{1}H\}$ NMR (100 MHz, $CDCl_3$): δ 172.3, 163.0, 160.2, 137.9, 137.1, 130.0, 128.8, 125.1, 118.7, 82.9, 79.3, 27.9, 12.9. HRMS (ESI TOF) *m/z* calcd. For $C_{17}H_{20}N_2O_4$ $[M+Na]^+$ 339.1320 found 339.1320.

Methyl 2-(4-hydroxy-3-methyl-5-oxo-1-(p-tolyl)-4,5-dihydro-1H-pyrazol-4-yl)acrylate (1e)

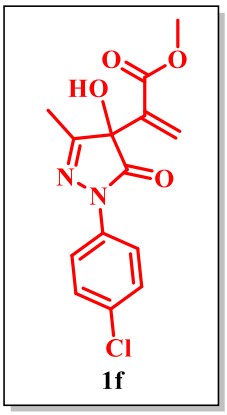
The compound **1e** was synthesized following the standard procedure outlined in Section **4.5.2**, with a reaction duration of 6 hours, resulting in a 78% yield (225 mg). Purification was



1e

achieved via column chromatography on silica gel (SiO_2) using a solvent mixture of 25% ethyl acetate in hexanes. The product was obtained as a white solid. Its identity was confirmed by ^{1}H and $^{13}C\{^{1}H\}$ NMR spectroscopy and high-resolution mass spectrometry (HRMS). The melting point was determined to be 188–190 °C. ^{1}H NMR (400 MHz, $CDCl_3$): δ 7.7 – 7.6 (m, 2H), 7.2 – 7.1 (m, 2H), 6.6 (s, 1H), 6.4 (s, 1H), 4.9 (s, 1H), 3.7 (s, 3H), 2.3 (s, 3H), 2.0 (s, 3H). $^{13}C\{^{1}H\}$ NMR (100 MHz, $CDCl_3$): δ 172.0, 164.5, 159.4, 136.0, 135.2, 135.2, 130.3, 129.4, 119.3, 79.3, 52.4, 21.0, 12.9. HRMS (ESI TOF) *m/z* calcd. For $C_{15}H_{16}N_2O_4$ $[M+Na]^+$ 311.1007 found 311.1032.

Methyl 2-(1-(4-chlorophenyl)-4-hydroxy-3-methyl-5-oxo-4,5-dihydro-1H-pyrazol-4-yl)acrylate (1f)

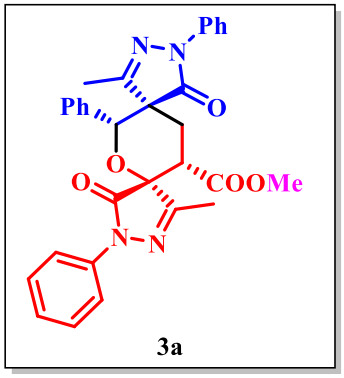


1f

The compound **1f** was synthesized following the standard procedure outlined in Section **4.5.2**, with a reaction duration of 6 hours, resulting in a 75% yield (230 mg). Purification was achieved via column chromatography on silica gel (SiO_2) using a solvent mixture of 25% ethyl acetate in hexanes. The product was obtained as a white solid. Its identity was confirmed by ^{1}H and $^{13}C\{^{1}H\}$ NMR spectroscopy and high-resolution mass spectrometry (HRMS). The melting point was determined to be 115–117 °C. ^{1}H NMR (400 MHz, $CDCl_3$): δ 7.8 (dd, J = 8.8, 1.6 Hz, 2H), 7.5 – 7.3 (m, 2H), 6.6 (d, J = 1.2 Hz, 1H), 6.4 (s, 1H), 4.2 (s, 1H), 3.7 (s, 3H), 2.0 (s, 3H). $^{13}C\{^{1}H\}$ NMR (100 MHz, $CDCl_3$)) δ 170.6, 163.1, 158.1, 134.9, 134.5, 129.1, 128.8, 127.6, 118.7, 77.8, 51.1, 11.6. HRMS (ESI TOF) *m/z* calcd. For $C_{15}H_{16}N_2O_4$ $[M+Na]^+$ 331.0461 found 331.0456.

Methyl (*5R,7R,8R,14S*)-1,12-dimethyl-4,9-dioxo-3,7,10 triphenyl-6-oxa-2,3,10,11-tetraazadispiro[4.2.48.25]tetradeca-1,11-diene-14-carboxylate (3a)

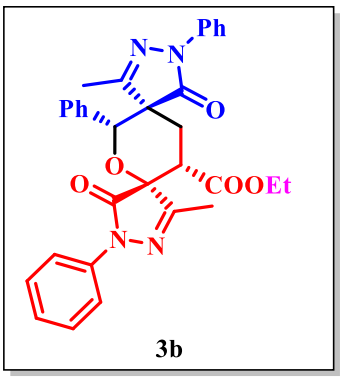
Product **3a** was synthesized following the general experimental procedure **4.5.4**. An oven-dried 10 mL glass reaction tube was charged with pyrazoledione-derived Morita–Baylis–Hillman (Pyro-MBH) Alcohol **1a** (1.0 equiv, 0.2 mmol), potassium tert-butoxide (50 mol%, 0.1 mmol), and arylidene pyrazolone **2a** (1.0 equiv, 0.2 mmol). Subsequently, 1,4-Dioxane (1 mL) was added to the tube. The reaction mixture was stirred at ambient temperature for 1 minute. Upon



3a

completion, the solvent was removed under reduced pressure, and the residue was purified by column chromatography on silica gel using 20% ethyl acetate in hexanes as the eluent. The purified product, **3a**, identified as Methyl (*5R,7R,8R,14S*)-1,12-dimethyl-4,9-dioxo-3,7,10-triphenyl-6-oxa-2,3,10,11-tetraazadispiro[4.2.48.25]tetradeca-1,11-diene-14-carboxylate, was obtained as a white solid in a yield of 73 mg (68%) as a single diastereomer. The structure was confirmed through spectroscopic methods, including ^{1}H NMR, ^{13}C{^{1}H} NMR, HRMS, and X-ray crystallographic analysis. The compound displayed a melting point of 185–188 °C and a TLC retention factor (R_f) of 0.5 (silica gel, 30% ethyl acetate/hexanes). ^{1}H NMR (400 MHz, $CDCl_3$): δ 8.0 – 7.9 (m, 2H), 7.9 – 7.8 (m, 2H), 7.4 (dt, *J* = 8.7, 7.6 Hz, 4H), 7.3 – 7.1 (m, 5H), 7.1 – 7.1 (m, 2H), 6.1 (s, 1H), 4.2 (dd, *J* = 13.1, 4.3 Hz, 1H), 2.4 (d, *J* = 10.3 Hz, 1H), 2.3 (s, 3H), 2.3 (d, *J* = 14.4 Hz, 1H), 2.0 (s, 3H), 1.3 (s, 3H). ^{13}C{^{1}H} NMR (100 MHz, $CDCl_3$): δ 174.0, 170.7, 168.4, 161.1, 156.9, 137.7, 137.6, 135.7, 128.9, 128.9, 128.4, 128.3, 125.4, 125.0, 124.2, 119.1, 118.1, 83.2, 80.0, 74.7, 58.0, 38.6, 27.5, 25.5, 15.0, 14.7. HRMS (ESI TOF) *m/z* calcd. For $C_{31}H_{28}N_4O_5$ $[M+H]^+$ 537.2138 found 537.2140.

Ethyl (*5R,7R,8R,14S*)-1,12-dimethyl-4,9-dioxo-3,7,10-triphenyl-6-oxa-2,3,10,11-tetraazadispiro[4.2.48.25]tetradeca-1,11-diene-14-carboxylate (3b)

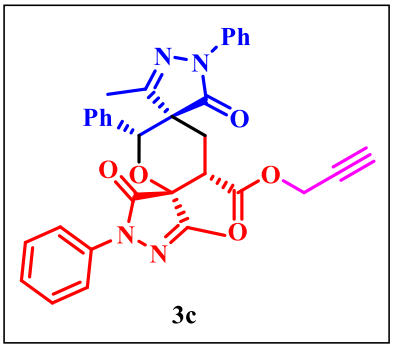


3b

Product **3b** was synthesized following the general experimental procedure **4.5.4**. An oven-dried 10 mL glass reaction tube was charged with pyrazoledione-derived Morita–Baylis–Hillman (Pyro-MBH) alcohol **1b** (1.0 equiv, 0.2 mmol), potassium tert-butoxide (50 mol%, 0.1 mmol), and arylidene pyrazolone **2a** (1.0 equiv, 0.2 mmol). Subsequently, 1,4-Dioxane (1 mL) was added to the tube. The reaction mixture was stirred at ambient temperature for 1 minute. Upon completion, the solvent was removed under reduced pressure, and the residue was purified by column chromatography on silica gel using 20% ethyl acetate in hexanes as the eluent. The purified product, **3b**, identified as Methyl (Ethyl (*5R,7R,8R,14S*)-1,12-dimethyl-4,9-dioxo-3,7,10-triphenyl-6-oxa-2,3,10,11-tetraazadispiro [4.2.48.25] tetradeca-1,11-diene-14-carboxylate, was obtained as a light yellow solid in a yield of 67 mg (61%) as a single diastereomer. The structure was confirmed through spectroscopic methods,

including ^{1}H NMR, $^{13}C\{^{1}H\}$ NMR, HRMS, and X-ray crystallographic analysis. The compound displayed a melting point of 167–169 °C and a TLC retention factor (R_f) of 0.5 (silica gel, 30% ethyl acetate/hexanes). ^{1}H NMR (400 MHz, $CDCl_3$): δ 7.9 – 7.9 (m, 2H), 7.9 – 7.8 (m, 2H), 7.4 (ddd, *J* = 8.7, 7.3, 5.0 Hz, 4H), 7.2 – 7.2 (m, 5H), 7.2 – 7.1 (m, 2H), 6.1 (s, 1H), 4.3 (dd, *J* = 11.6, 5.7 Hz, 1H), 4.2 – 4.0 (m, 2H), 2.4 – 2.4 (m, 2H), 2.3 (s, 3H), 2.0 (s, 3H), 1.0 (t, *J* = 7.1 Hz, 3H). $^{13}C\{^{1}H\}$ NMR (100 MHz, $CDCl_3$): δ 173.9, 170.6, 169.3, 160.9, 156.9, 137.6, 137.6, 135.5, 128.9, 128.9, 128.4, 128.3, 125.5, 125.3, 124.2, 119.1, 118.4, 79.9, 75.0, 62.0, 57.9, 38.4, 25.5, 15.0, 14.7, 13.7. HRMS (ESI TOF) *m/z* calcd. For $C_{32}H_{30}N_4O_5$ $[M+H]^+$ 551.2294 found 551.2299.

Prop-2-yn-1-yl (*5R,7R,8R,14S*)-1,12-dimethyl-4,9-dioxo-3,7,10-triphenyl-6-oxa-2,3,10,11-tetraazadispiro[4.2.48.25]tetradeca-1,11-diene-14-carboxylate (3c)

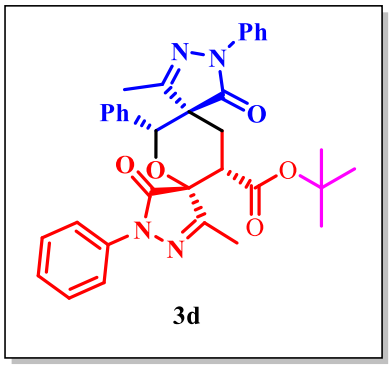


3c

Product **3c** was synthesized following the general experimental procedure **4.5.4**. An oven-dried 10 mL glass reaction tube was charged with pyrazoledione-derived Morita–Baylis–Hillman (Pyro-MBH) alcohol **1c** (1.0 equiv, 0.2 mmol), potassium tert-butoxide (50 mol%, 0.1 mmol), and arylidene pyrazolone **2a** (1.0 equiv, 0.2 mmol). Subsequently, 1,4-Dioxane (1 mL) was added to the tube. The reaction mixture was stirred at ambient temperature for 1 minute. Upon completion, the solvent was removed under reduced pressure, and the residue was purified by column chromatography on silica gel using 20% ethyl acetate in hexanes as the eluent. The purified product, **3c**, identified as Prop-2-yn-1-yl (*5R,7R,8R,14S*)-1,12-dimethyl-4,9-dioxo-3,7,10-triphenyl-6-oxa-2,3,10,11 tetraazadispiro [4.2.48.25] tetradeca-1,11-diene-14-carboxylate, was obtained as a gray sticky solid in a yield of 77 mg (69%) as a single diastereomer. The structure was confirmed through spectroscopic methods, including ^{1}H NMR, $^{13}C\{^{1}H\}$ NMR, HRMS, and X-ray crystallographic analysis. The compound displayed a TLC retention factor (R_f) of 0.5 (silica gel, 30% ethyl acetate/hexanes). ^{1}H NMR (400 MHz, $CDCl_3$): δ 7.9 – 7.9 (m, 2H), 7.8 – 7.8 (m, 2H), 7.4 (dt, *J* = 8.7, 7.7 Hz, 4H), 7.2 – 7.2 (m, 5H), 7.2 – 7.1 (m, 2H), 6.1 (s, 1H), 4.7 (dd, *J* = 15.4, 2.5 Hz, 1H), 4.5 (dd, *J* = 15.4, 2.5 Hz, 1H), 4.4 (dd, *J* = 12.0, 5.4 Hz, 1H), 2.5 – 2.4 (m, 2H), 2.3 (s, 3H), 2.3 (t, *J* = 2.5 Hz, 1H), 2.0 (s, 3H). $^{13}C\{^{1}H\}$ NMR (100 MHz, $CDCl_3$): δ 173.8, 170.3, 168.6, 160.8, 156.4, 137.6, 137.4, 135.4, 129.0, 128.8, 128.4, 128.4, 125.5, 125.3, 124.2, 119.1,

118.9, 79.7, 76.0, 75.9, 75.0, 57.8, 53.2, 38.2, 25.5, 15.0, 14.7. HRMS (ESI TOF) *m/z* calcd. For $C_{33}H_{28}N_4O_5$ $[M+Na]^+$ 583.1957 found 583.1943.

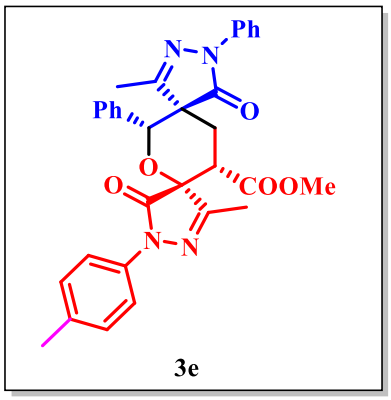
Tert-butyl (*5R,7R,8R,14S*)-1,12-dimethyl-4,9-dioxo-3,7,10-triphenyl-6-oxa-2,3,10,11-tetraazadispiro[4.2.48.25]tetradeca-1,11-diene-14-carboxylate (3d)



Product **3d** was synthesized following the general experimental procedure **4.5.4**. An oven-dried 10 mL glass reaction tube was charged with pyrazoledione-derived Morita–Baylis–Hillman (Pyro-MBH) alcohol **1d** (1.0 equiv, 0.2 mmol), potassium tert-butoxide (50 mol%, 0.1 mmol), and arylidene pyrazolone **2a** (1.0 equiv, 0.2 mmol). Subsequently, 1,4-Dioxane (1 mL) was added to the tube. The reaction mixture was stirred at ambient temperature for 1 minute. Upon completion, the solvent was removed under reduced pressure, and the residue was purified by column chromatography on silica gel using 20% ethyl acetate in hexanes as the eluent. The purified product, **3d**, identified as Tert-butyl (*5R,7R,8R,14S*)-1,12-dimethyl-4,9-dioxo-3,7,10-triphenyl-6-oxa-2,3,10,11-tetraazadispiro [4.2.48.25]tetradeca-1,11-diene-14-carboxylate, was obtained as a light yellow solid in a yield of 81 mg (70%) as a single diastereomer. The structure was confirmed through spectroscopic methods, including ^{1}H NMR, ^{13}C{^{1}H} NMR, HRMS, and X-ray crystallographic analysis. The compound displayed a melting point of 185–187 °C and a TLC retention factor (R_f) 0.5 (silica gel, 30% ethyl acetate/hexanes). ^{1}H NMR (400 MHz, $CDCl_3$): δ 8.0 – 7.9 (m, 2H), 7.9 – 7.8 (m, 2H), 7.4 (dt, *J* = 8.7, 7.6 Hz, 4H), 7.3 – 7.1 (m, 5H), 7.1 – 7.1 (m, 2H), 6.1 (s, 1H), 4.2 (dd, *J* = 13.1, 4.3 Hz, 1H), 2.4 (d, *J* = 10.3 Hz, 1H), 2.3 (s, 3H), 2.3 (d, *J* = 14.4 Hz, 1H), 2.0 (s, 3H), 1.3 (s, 9H). ^{13}C{^{1}H} NMR (100 MHz, $CDCl_3$): δ 174.0, 170.7, 168.4, 161.1, 156.9, 137.7, 137.6, 135.7, 128.9, 128.9, 128.4, 128.3, 125.4, 125.0, 124.2, 119.1, 118.1, 83.2, 80.0, 74.7, 58.0, 38.6, 27.5, 25.5, 15.0, 14.7. HRMS (ESI TOF) *m/z* calcd. For $C_{34}H_{34}N_4O_5$ $[M+H]^+$ 579.2607 found 579.2600.

Methyl (*5R,7R,8R,14S*)-1,12-dimethyl-4,9-dioxo-7,10-diphenyl-3-(p-tolyl)-6-oxa-2,3,10,11-tetraazadispiro[4.2.48.25]tetradeca-1,11-diene-14-carboxylate (3e)

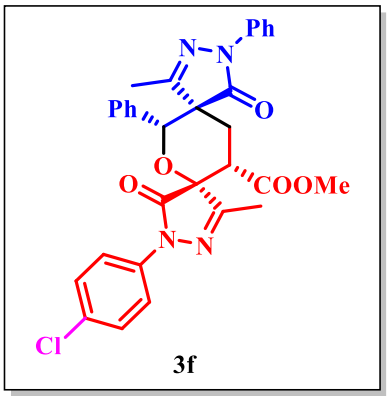
Product **3e** was synthesized following the general experimental procedure **4.5.4**. An oven-dried 10 mL glass reaction tube was charged with pyrazoledione-derived Morita–Baylis–Hillman (Pyro-MBH) alcohol **1e** (1.0 equiv, 0.2 mmol), potassium tert-butoxide (50 mol%, 0.1 mmol),



3e

and arylidene pyrazolone **2a** (1.0 equiv, 0.2 mmol). Subsequently, 1,4-Dioxane (1 mL) was added to the tube. The reaction mixture was stirred at ambient temperature for 1 minute. Upon completion, the solvent was removed under reduced pressure, and the residue was purified by column chromatography on silica gel using 20% ethyl acetate in hexanes as the eluent. The purified product, **3e**, identified as purified by column chromatography (SiO2, 20% EtOAc /hexanes) to afford **3e**, Methyl (*5R,7R,8R,14S*)-1,12-dimethyl-4,9-dioxo-7,10-diphenyl-3-(p-tolyl)-6-oxa-2,3,10,11-tetraazadispiro [4.2.48.25]tetradeca-1,11-diene-14-carboxylate, was obtained as a light yellow solid in a yield of 87 mg (79%) as a single diastereomer. The structure was confirmed through spectroscopic methods, including ^{1}H NMR, ^{13}C{^{1}H} NMR, HRMS, and X-ray crystallographic analysis. The compound displayed a melting point of 194–196 °C and a TLC retention factor (R_f) of 0.5 (silica gel, 30% ethyl acetate/hexanes). ^{1}H NMR (400 MHz, $CDCl_3$): δ 7.8 (dd, *J* = 8.5, 1.4 Hz, 2H), 7.8 – 7.7 (m, 2H), 7.5 – 7.3 (m, 2H), 7.2 (td, *J* = 6.5, 5.5, 2.4 Hz, 6H), 7.1 – 7.1 (m, 2H), 6.1 (s, 1H), 4.3 (dd, *J* = 10.1, 7.3 Hz, 1H), 3.6 (s, 3H), 2.4 – 2.4 (m, 2H), 2.3 (s, 3H), 2.3 (s, 3H), 2.0 (s, 3H). ^{13}C{^{1}H} NMR (100 MHz, $CDCl_3$): δ 173.9, 170.4, 169.8, 160.8, 156.9, 137.6, 135.5, 135.1, 135.1, 129.5, 129.0, 128.4, 128.3, 125.4, 124.2, 119.0, 118.8, 79.8, 75.0, 57.9, 52.8, 38.8, 25.6, 21.0, 15.0, 14.7. HRMS (ESI TOF) *m/z* calcd. For $C_{32}H_{30}N_4O_5$ $[M+Na]^+$ 573.2114 found 573.2113.

Methyl (*5R,7R,8R,14S*)-3-(4-chlorophenyl)-1,12-dimethyl-4,9-dioxo-7,10-diphenyl-6-oxa-2,3,10,11-tetraazadispiro[4.2.48.25]tetradeca-1,11-diene-14-carboxylate (3f)

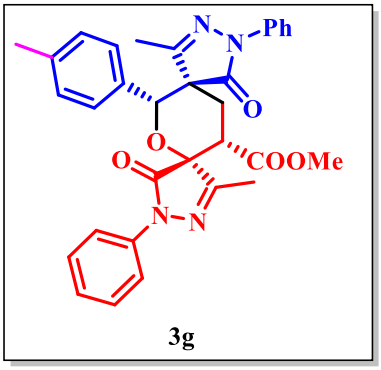


3f

Product **3f** was synthesized following the general experimental procedure **4.5.4**. An oven-dried 10 mL glass reaction tube was charged with pyrazoledione-derived Morita–Baylis–Hillman (Pyro-MBH) alcohol **1f** (1.0 equiv, 0.2 mmol), potassium tert-butoxide (50 mol%, 0.1 mmol), and arylidene pyrazolone **2a** (1.0 equiv, 0.2 mmol). Subsequently, 1,4-Dioxane (1 mL) was added to the tube. The reaction mixture was stirred at ambient temperature for 1 minute. Upon completion, the solvent was removed under reduced pressure, and the residue was purified by column chromatography on silica gel using 20% ethyl acetate in hexanes as the

eluent. The purified product, **3f**, identified as Methyl (*5R,7R,8R,14S*)-3-(4-chlorophenyl)-1,12-dimethyl-4,9-dioxo-7,10-diphenyl-6-oxa-2,3,10,11 tetraazadispiro [4.2.48.25] tetradeca-1,11-diene-14-carboxylate, was obtained as a light red solid in a yield of 95 mg (83%) as a single diastereomer. The structure was confirmed through spectroscopic methods, including ^{1}H NMR, ^{13}C{^{1}H} NMR, HRMS, and X-ray crystallographic analysis. The compound displayed a melting point of 211–213 °C and a TLC retention factor (R_f) of 0.5 (silica gel, 30% ethyl acetate/hexanes). ^{1}H NMR (400 MHz, $CDCl_3$): δ 7.9 – 7.8 (m, 4H), 7.4 – 7.3 (m, 4H), 7.2 – 7.2 (m, 4H), 7.2 – 7.1 (m, 2H), 6.1 (s, 1H), 4.3 (dd, *J* = 12.0, 5.3 Hz, 1H), 3.6 (s, 3H), 2.4 – 2.4 (m, 2H), 2.3 (s, 3H), 2.0 (s, 3H). ^{13}C{^{1}H} NMR (100 MHz, $CDCl_3$): δ 173.8, 170.5, 169.7, 160.7, 157.3, 137.5, 136.1, 135.4, 130.5, 129.0, 129.0, 128.4, 128.4, 125.5, 124.2, 119.7, 119.0, 79.9, 75.1, 57.8, 52.8, 38.8, 25.5, 15.0, 14.7. HRMS (ESI TOF) *m/z* calcd. For $C_{31}H_{27}ClN_4O_5$ $[M+Na]^+$ 593.1568 found 593.1568.

Methyl (*5R,7R,8R,14S*)-1,12-dimethyl-4,9-dioxo-3,10-diphenyl-7-(p-tolyl)-6-oxa-2,3,10,11-tetraazadispiro[4.2.48.25]tetradeca-1,11-diene-14-carboxylate (3g)

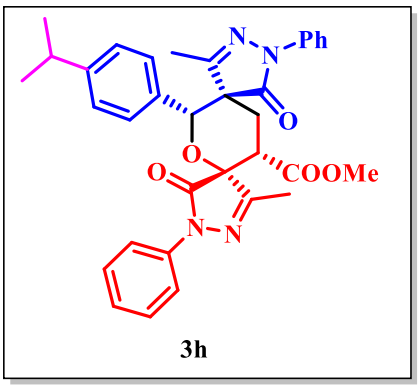


3g

Product **3g** was synthesized following the general experimental procedure **4.5.4**. An oven-dried 10 mL glass reaction tube was charged with pyrazoledione-derived Morita–Baylis–Hillman (Pyro-MBH) alcohol **1a** (1.0 equiv, 0.2 mmol), potassium tert-butoxide (50 mol%, 0.1 mmol), and arylidene pyrazolone **2b** (1.0 equiv, 0.2 mmol). Subsequently, 1,4-Dioxane (1 mL) was added to the tube. The reaction mixture was stirred at ambient temperature for 2 minute. Upon completion, the solvent was removed under reduced pressure, and the residue was purified by column chromatography on silica gel using 20% ethyl acetate in hexanes as the eluent. The purified product, **3g**, identified as Methyl (*5R,7R,8R,14S*)-1,12-dimethyl-4,9-dioxo-3,10-diphenyl-7-(p-tolyl)-6-oxa-2,3,10,11-tetraazadispiro [4.2.48.25]tetradeca-1,11-diene-14-carboxylate, was obtained as a light yellow solid in a yield of 80 mg (73%) as a single diastereomer. The structure was confirmed through spectroscopic methods, including ^{1}H NMR, ^{13}C{^{1}H} NMR, HRMS, and X-ray crystallographic analysis. The compound displayed a melting point of 165-167 °C and a TLC retention factor (R_f) of 0.5 (silica gel, 30% ethyl acetate/hexanes). ^{1}H NMR (400 MHz, $CDCl_3$): δ 7.8 (ddd, *J* = 10.9, 8.8, 1.2 Hz, 4H), 7.4 (ddd, *J* = 8.6, 7.4, 3.6 Hz, 4H), 7.2 – 7.1 (m, 2H), 7.0 (s, 4H), 6.1 (s, 1H), 4.3 (dd, *J* = 10.4, 6.9 Hz, 1H), 3.6 (s, 3H), 2.4 – 2.3 (m, 2H), 2.3

(s, 3H), 2.3 (s, 3H), 2.0 (s, 3H). $^{13}C\{^{1}H\}$ NMR (100 MHz, $CDCl_3$): δ 173.9, 170.5, 169.8, 161.0, 157.0, 138.0, 137.6, 137.5, 132.4, 129.0, 129.0, 128.9, 125.4, 125.4, 124.1, 119.1, 118.7, 79.9, 75.0, 57.9, 52.8, 38.7, 25.5, 21.1, 15.0, 14.7. HRMS (ESI TOF) *m/z* calcd. For $C_{32}H_{30}N_4O_5$ $[M+H]^+$ 551.2293 found 551.2292.

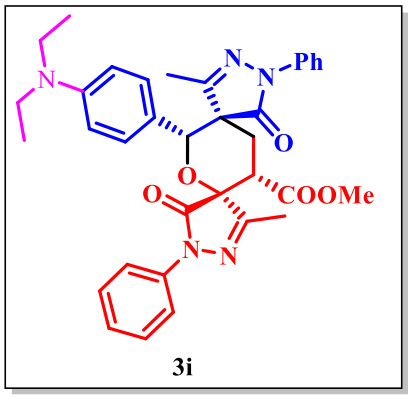
Methyl (*5R,7R,8R,14S*)-7-(4-isopropylphenyl)-1,12-dimethyl-4,9-dioxo-3,10-diphenyl-6-oxa-2,3,10,11-tetraazadispiro[4.2.48.25]tetradeca-1,11-diene-14-carboxylate (3h)



3h

Product **3h** was synthesized following the general experimental procedure **4.5.4**. An oven-dried 10 mL glass reaction tube was charged with pyrazoledione-derived Morita–Baylis–Hillman (Pyro-MBH) alcohol **1a** (1.0 equiv, 0.2 mmol), potassium tert-butoxide (50 mol%, 0.1 mmol), and arylidene pyrazolones **2c** (1.0 equiv, 0.2 mmol). Subsequently, 1,4-Dioxane (1 mL) was added to the tube. The reaction mixture was stirred at ambient temperature for 2 minute. Upon completion, the solvent was removed under reduced pressure, and the residue was purified by column chromatography on silica gel using 20% ethyl acetate in hexanes as the eluent. The purified product, **3h**, identified as Methyl (*5R,7R,8R,14S*)-7-(4-isopropylphenyl)-1,12-dimethyl-4,9-dioxo-3,10-diphenyl-6-oxa-2,3,10,11-tetraazadispiro[4.2.48.25]tetradeca-1,11-diene-14-carboxylate, was obtained as a yellow solid in a yield of 86 mg (74%) as a single diastereomer. The structure was confirmed through spectroscopic methods, including ^{1}H NMR, $^{13}C\{^{1}H\}$ NMR, HRMS, and X-ray crystallographic analysis. The compound displayed a melting point of 173-175 °C and a TLC retention factor (R_f) of 0.5 (silica gel, 30% ethyl acetate/hexanes). ^{1}H NMR (400 MHz, $CDCl_3$): δ 7.9 – 7.7 (m, 4H), 7.4 (ddd, *J* = 8.6, 7.4, 5.7 Hz, 4H), 7.2 – 7.2 (m, 2H), 7.1 – 7.0 (m, 4H), 6.1 (s, 1H), 4.3 (dd, *J* = 9.8, 7.5 Hz, 1H), 3.6 (s, 3H), 2.9 – 2.7 (m, 1H), 2.4 – 2.4 (m, 2H), 2.3 (s, 3H), 2.0 (s, 3H), 1.2 (dd, *J* = 6.9, 1.9 Hz, 6H). $^{13}C\{^{1}H\}$ NMR (100 MHz, $CDCl_3$): δ 173.9, 170.5, 169.9, 161.0, 157.0, 149.0, 137.6, 137.5, 132.8, 128.9, 128.9, 126.4, 125.4, 125.3, 124.2, 119.1, 118.7, 79.9, 75.0, 57.8, 52.8, 38.7, 33.7, 25.6, 23.8, 15.0, 14.7. HRMS (ESI TOF) *m/z* calcd. For $C_{34}H_{34}N_4O_5$ $[M+Na]^+$ 601.2426 found 601.2424.

Methyl (*5R,7R,8R,14S*)-7-(4-(diethylamino)phenyl)-1,12-dimethyl-4,9-dioxo-3,10-diphenyl-6-oxa-2,3,10,11-tetraazadispiro[4.2.48.25]tetradeca-1,11-diene-14-carboxylate (3i)

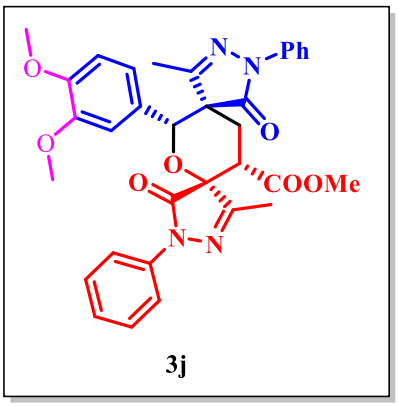


3i

Product **3i** was synthesized following the general experimental procedure **4.5.4**. An oven-dried 10 mL glass reaction tube was charged with pyrazoledione-derived Morita–Baylis–Hillman (Pyro-MBH) alcohol **1a** (1.0 equiv, 0.2 mmol), potassium tert-butoxide (50 mol%, 0.1 mmol), and arylidene pyrazolones **2d** (1.0 equiv, 0.2 mmol). Subsequently, 1,4-Dioxane (1 mL) was added to the tube. The reaction mixture was stirred at ambient temperature for 2 minute. Upon completion, the solvent was removed under reduced pressure, and the residue was purified by column chromatography on silica gel using 30% ethyl acetate in hexanes as the eluent. The purified product, **3i**, identified as Methyl (*5R,7R,8R,14S*)-7-(4-(diethylamino)phenyl)-1,12-dimethyl-4,9-dioxo-3,10-diphenyl-6-oxa-2,3,10,11-tetraazadispiro[4.2.48.25]tetradeca-1,11-diene-14-carboxylate, was obtained as a sticky red solid in a yield of 78 mg (65%) as a single diastereomer. The structure was confirmed through spectroscopic methods, including ^{1}H NMR, ^{13}C{^{1}H} NMR, HRMS, and X-ray crystallographic analysis. The compound displayed a TLC retention factor (R_f) of 0.3 (silica gel, 30% ethyl acetate/hexanes). ^{1}H NMR (400 MHz, $CDCl_3$): δ 7.9 – 7.8 (m, 2H), 7.7 – 7.6 (m, 2H), 7.4 (t, *J* = 7.9 Hz, 2H), 7.3 (t, *J* = 7.9 Hz, 2H), 7.2 (dt, *J* = 14.6, 7.4 Hz, 2H), 7.1 (d, *J* = 8.7 Hz, 2H), 6.5 (d, *J* = 8.8 Hz, 2H), 6.0 (s, 1H), 3.7 (s, 3H), 3.5 (d, *J* = 7.5 Hz, 2H), 3.2 (ddt, *J* = 18.4, 14.8, 7.4 Hz, 4H), 2.5 (s, 3H), 2.3 (s, 3H), 2.3 – 2.2 (m, 1H), 1.0 (t, *J* = 7.0 Hz, 6H). ^{13}C{^{1}H} NMR (100 MHz, $CDCl_3$): δ 172.1, 169.3, 168.9, 159.8, 157.0, 147.8, 137.5, 128.8, 128.7, 126.8, 126.8, 125.3, 125.3, 121.1, 119.5, 119.0, 111.3, 77.6, 74.9, 58.2, 52.8, 44.2, 39.7, 26.7, 19.3, 13.1, 12.4. HRMS (ESI TOF) *m/z* calcd. For $C_{35}H_{37}N_5O_5$ $C_{35}H_{37}N_5O_5$ $[M+H]^+$ 608.2873 found 608.2875.

Methyl (*5R,7R,8R,14S*)-7-(3,4-dimethoxyphenyl)-1,12-dimethyl-4,9-dioxo-3,10-diphenyl-6-oxa-2,3,10,11-tetraazadispiro[4.2.48.25]tetradeca-1,11-diene-14-carboxylate (3j)

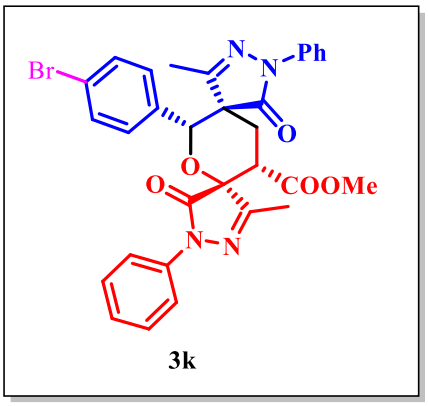
Product **3j** was synthesized following the general experimental procedure **4.5.4**. An oven-dried 10 mL glass reaction tube was charged with pyrazoledione-derived Morita–Baylis–Hillman (Pyro-MBH) alcohol **1a** (1.0 equiv, 0.2 mmol), potassium tert-butoxide (50 mol%, 0.1 mmol), and arylidene pyrazolones **2e** (1.0 equiv, 0.2 mmol). Subsequently, 1,4-Dioxane (1 mL) was added to the tube. The reaction mixture was stirred at ambient temperature for 2 minute. Upon completion, the solvent was removed under reduced pressure, and the residue was purified by



3j

column chromatography on silica gel using 20% ethyl acetate in hexanes as the eluent. The purified product, **3j**, identified as Methyl (*5R,7R,8R,14S*)-7-(3,4-dimethoxyphenyl)-1,12-dimethyl-4,9-dioxo-3,10-diphenyl-6-oxa-2,3,10,11-tetraazadispiro[4.2.48.25]tetradeca-1,11-diene-14-carboxylate, was obtained as a red solid in a yield of 80 mg (66%) as a single diastereomer. The structure was confirmed through spectroscopic methods, including ^{1}H NMR, ^{13}C{^{1}H} NMR, HRMS, and X-ray crystallographic analysis. The compound displayed a melting point of 179-181 °C and a TLC retention factor (R_f) of 0.5 (silica gel, 30% ethyl acetate/hexanes). ^{1}H NMR (400 MHz, $CDCl_3$): δ 7.9 (td, *J* = 8.2, 1.2 Hz, 4H), 7.4 (ddd, *J* = 8.6, 7.4, 5.7 Hz, 4H), 7.2 (d, *J* = 3.3 Hz, 2H), 6.8 (s, 1H), 6.7 (d, *J* = 8.4 Hz, 1H), 6.5 (d, *J* = 2.0 Hz, 1H), 6.0 (s, 1H), 4.3 (dd, *J* = 12.3, 5.1 Hz, 1H), 3.8 (s, 3H), 3.6 (s, 3H), 3.5 (s, 3H), 2.5 – 2.4 (m, 2H), 2.3 (s, 3H), 2.0 (s, 3H). ^{13}C{^{1}H} NMR (100 MHz, $CDCl_3$): δ 174.0, 170.5, 169.8, 161.1, 157.0, 148.8, 148.7, 137.6, 137.5, 129.0, 129.0, 127.7, 125.4, 125.3, 118.7, 118.7, 116.4, 110.7, 107.2, 80.0, 75.2, 58.0, 55.8, 55.5, 52.8, 38.8, 25.3, 15.1, 14.7. HRMS (ESI TOF) *m/z* calcd. For $C_{33}H_{32}N_4O_7$ $[M+H]^+$ 597.2349 found 597.2352.

Methyl (*5R,7R,8R,14S*)-7-(4-bromophenyl)-1,12-dimethyl-4,9-dioxo-3,10-diphenyl-6-oxa-2,3,10,11-tetraazadispiro[4.2.48.25]tetradeca-1,11-diene-14-carboxylate (3k)

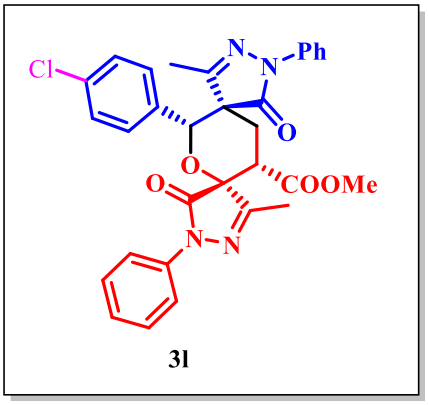


3k

Product **3k** was synthesized following the general experimental procedure **4.5.4**. An oven-dried 10 mL glass reaction tube was charged with pyrazoledione-derived Morita–Baylis–Hillman (Pyro-MBH) alcohol **1a** (1.0 equiv, 0.2 mmol), potassium tert-butoxide (50 mol%, 0.1 mmol), and arylidene pyrazolones **2f** (1.0 equiv, 0.2 mmol). Subsequently, 1,4-Dioxane (1 mL) was added to the tube. The reaction mixture was stirred at ambient temperature for 2 minute. Upon completion, the solvent was removed under reduced pressure, and the residue was purified by column chromatography on silica gel using 20% ethyl acetate in hexanes as the eluent. The purified product, **3k**, identified as purified by column chromatography (SiO2, 20% EtOAc /hexanes) to afford **3k**, Methyl (*5R,7R,8R,14S*)-7-(4-bromophenyl)-1,12-dimethyl-4,9-dioxo-3,10-diphenyl-6-oxa-2,3,10,11-tetraazadispiro

[4.2.48.25] tetradeca-1,11-diene-14-carboxylate, was obtained as a light yellow solid in a yield of 75 mg (61%) as a single diastereomer. The structure was confirmed through spectroscopic methods, including ^{1}H NMR, ^{13}C{^{1}H} NMR, HRMS, and X-ray crystallographic analysis. The compound displayed a melting point of 173-175 °C and a TLC retention factor (R_f) of 0.5 (silica gel, 30% ethyl acetate/hexanes). ^{1}H NMR (400 MHz, $CDCl_3$): δ 7.8 (ddt, J = 11.1, 8.6, 1.2 Hz, 4H), 7.4 (ddd, J = 8.6, 7.3, 4.6 Hz, 4H), 7.4 (d, J = 8.6 Hz, 2H), 7.2 (d, J = 7.7 Hz, 2H), 7.1 – 6.9 (m, 2H), 6.0 (s, 1H), 4.3 (dd, J = 12.2, 5.2 Hz, 1H), 3.6 (s, 3H), 2.4 – 2.3 (m, 2H), 2.3 (s, 3H), 2.0 (s, 3H). ^{13}C{^{1}H} NMR (100 MHz, $CDCl_3$): δ 173.6, 170.4, 169.6, 160.5, 156.8, 137.4, 134.6, 131.6, 129.0, 129.0, 129.0, 125.9, 125.6, 125.5, 122.4, 119.0, 118.7, 79.9, 74.6, 57.7, 52.8, 38.7, 25.5, 15.0, 14.7. HRMS (ESI TOF) *m/z* calcd. For $C_{31}H_{27}BrN_4O_5$ $[M+H]^+$ 615.1243 found 615.1248.

Methyl (*5R,7R,8R,14S*)-7-(4-chlorophenyl)-1,12-dimethyl-4,9-dioxo-3,10-diphenyl-6-oxa-2,3,10,11-tetraazadispiro[4.2.48.25]tetradeca-1,11-diene-14-carboxylate (3l)

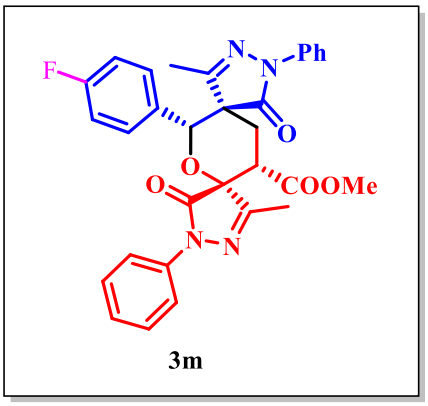


3l

Product **3l** was synthesized following the general experimental procedure **4.5.4**. An oven-dried 10 mL glass reaction tube was charged with pyrazoledione-derived Morita–Baylis–Hillman (Pyro-MBH) alcohol **1a** (1.0 equiv, 0.2 mmol), potassium tert-butoxide (50 mol%, 0.1 mmol), and arylidene pyrazolones **2g** (1.0 equiv, 0.2 mmol). Subsequently, 1,4-Dioxane (1 mL) was added to the tube. The reaction mixture was stirred at ambient temperature for 2 minute. Upon completion, the solvent was removed under reduced pressure, and the residue was purified by column chromatography on silica gel using 20% ethyl acetate in hexanes as the eluent. The purified product, **3l**, identified as Methyl (*5R,7R,8R,14S*)-7-(4-chlorophenyl)-1,12-dimethyl-4,9-dioxo-3,10-diphenyl-6-oxa-2,3,10,11-tetraazadispiro [4.2.48.25] tetradeca-1,11-diene-14-carboxylate, was obtained as a light yellow solid in a yield of 78 mg (63%) as a single diastereomer. The structure was confirmed through spectroscopic methods, including ^{1}H NMR, ^{13}C{^{1}H} NMR, HRMS, and X-ray crystallographic analysis. The compound displayed a melting point of 173-175 °C and a TLC retention factor (R_f) of 0.5 (silica gel, 30% ethyl acetate/hexanes). ^{1}H NMR (400 MHz, $CDCl_3$): δ 7.9 – 7.8 (m, 4H), 7.4 (ddd, *J* = 8.6, 7.4, 4.2 Hz, 4H), 7.2 (dd, *J* = 8.0, 6.1 Hz, 4H), 7.1 – 7.0 (m, 2H), 6.1 (s, 1H), 4.3 (dd, *J* = 12.3, 5.1 Hz, 1H), 3.6 (s, 3H), 2.4 – 2.3 (m, 2H), 2.3 (s, 3H), 2.0 (s, 3H). ^{13}C{^{1}H} NMR

(100 MHz, $CDCl_3$): δ 173.6, 170.4, 169.6, 160.5, 156.8, 137.4, 134.2, 134.0, 129.0, 129.0, 129.0, 128.7, 125.7, 125.6, 125.5, 119.0, 118.7, 79.9, 74.6, 57.7, 52.8, 38.7, 25.5, 15.0, 14.7. HRMS (ESI TOF) *m/z* calcd. For $C_{31}H_{27}ClN_4O_5$ $[M+H]^+$ 571.1748 found 571.1748.

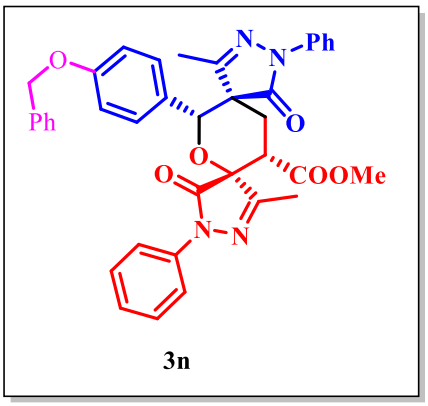
Methyl (*5R,7R,8R,14S*)-7-(4-fluorophenyl)-1,12-dimethyl-4,9-dioxo-3,10-diphenyl-6-oxa-2,3,10,11-tetraazadispiro[4.2.48.25]tetradeca-1,11-diene-14-carboxylate (3m)



3m

Product **3m** was synthesized following the general experimental procedure **4.5.4**. An oven-dried 10 mL glass reaction tube was charged with pyrazoledione-derived Morita–Baylis–Hillman (Pyro-MBH) alcohol **1a** (1.0 equiv, 0.2 mmol), potassium tert-butoxide (50 mol%, 0.1 mmol), and arylidene pyrazolones **2h** (1.0 equiv, 0.2 mmol). Subsequently, 1,4-Dioxane (1 mL) was added to the tube. The reaction mixture was stirred at ambient temperature for 2 minute. Upon completion, the solvent was removed under reduced pressure, and the residue was purified by column chromatography on silica gel using 20% ethyl acetate in hexanes as the eluent. The purified product, **3m**, identified as Methyl (*5R,7R,8R,14S*)-7-(4-fluorophenyl)-1,12-dimethyl-4,9-dioxo-3,10-diphenyl-6-oxa-2,3,10,11-tetraazadispiro [4.2.48.25] tetradeca-1,11-diene-14-carboxylate, was obtained as a light yellow solid in a yield of 80 mg (63%) as a single diastereomer. The structure was confirmed through spectroscopic methods, including ^1H NMR, $^{13}C\{^1H\}$ NMR, HRMS, and X-ray crystallographic analysis. The compound displayed a melting point of 172-174 °C and a TLC retention factor (R_f) of 0.5 (silica gel, 30% ethyl acetate/hexanes). ^1H NMR (400 MHz, $CDCl_3$): δ 7.9 – 7.8 (m, 4H), 7.4 (ddd, *J* = 8.5, 7.3, 2.6 Hz, 4H), 7.3 – 7.2 (m, 2H), 7.1 – 7.1 (m, 2H), 7.0 – 6.9 (m, 2H), 6.1 (s, 1H), 4.3 (dd, *J* = 12.1, 5.3 Hz, 1H), 3.6 (s, 3H), 2.5 – 2.4 (m, 2H), 2.3 (s, 3H), 2.0 (s, 3H). $^{13}C\{^1H\}$ NMR (100 MHz, $CDCl_3$): δ 173.7, 170.5, 169.7, 160.6, 156.9, 137.5, 137.4, 129.0 (d, $J_{(C-F)}$ = 1.1 Hz), 129.0 (d, $J_{(C-F)}$ = 0.8 Hz), 126.1, 126.0, 125.6, 125.5, 119.0 (d, $J_{(C-F)}$ = 1.0 Hz), 118.7 (d, $J_{(C-F)}$ = 0.6 Hz), 115.6, 115.3, 79.9, 74.7, 57.8, 52.8, 38.7, 25.4, 15.0, 14.7. ^{19}F NMR (377 MHz, $CDCl_3$): δ -113.1. HRMS (ESI TOF) *m/z* calcd. For $C_{31}H_{27}FN_4O_5$ $[M+H]^+$ 555.2043 found 555.2041.

Methyl (*5R,7S,8R,14R*)-7-(4-(benzyloxy)phenyl)-1,12-dimethyl-4,9-dioxo-3,10-diphenyl-6-oxa-2,3,10,11-tetraazadispiro[4.2.48.25]tetradeca-1,11-diene-14-carboxylate (3n)

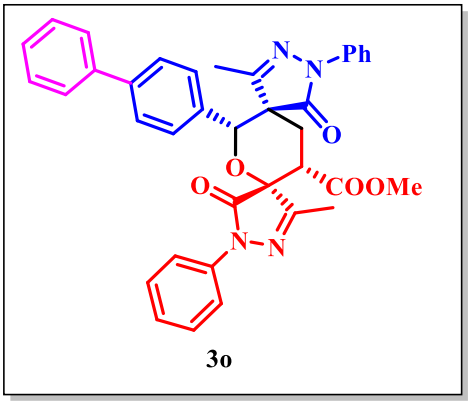


3n

Product **3n** was synthesized following the general experimental procedure **4.5.4**. An oven-dried 10 mL glass reaction tube was charged with pyrazoledione-derived Morita–Baylis–Hillman (Pyro-MBH) alcohol **1a** (1.0 equiv, 0.2 mmol), potassium tert-butoxide (50 mol%, 0.1 mmol), and arylidene pyrazolones **2i** (1.0 equiv, 0.2 mmol). Subsequently, 1,4-Dioxane (1 mL) was added to the tube. The reaction mixture was stirred at ambient temperature for 1 minute. Upon completion, the solvent was removed under reduced pressure, and the residue was purified by column chromatography on silica gel using 25% ethyl acetate in hexanes as the eluent. The purified product, **3n**, identified as Methyl (*5R,7S,8R,14R*)-7-(4-(benzyloxy)phenyl)-1,12-dimethyl-4,9-dioxo-3,10-diphenyl-6-oxa-2,3,10,11-tetraazadispiro[4.2.48.25]tetradeca-1,11-diene-14-carboxylate, was obtained as a light yellow solid in a yield of 77 mg (60%) as a single diastereomer. The structure was confirmed through spectroscopic methods, including ^{1}H NMR, ^{13}C{^{1}H} NMR, HRMS, and X-ray crystallographic analysis. The compound displayed a melting point of 172-174 °C and a TLC retention factor (R_f) 0.4 (silica gel, 30% ethyl acetate/hexanes). ^{1}H NMR (400 MHz, $CDCl_3$): δ 7.9 – 7.8 (m, 4H), 7.5 – 7.3 (m, 9H), 7.2 – 7.1 (m, 2H), 7.1 – 7.0 (m, 2H), 6.9 – 6.8 (m, 2H), 6.0 (s, 1H), 5.0 (s, 2H), 4.3 (dd, *J* = 11.0, 6.4 Hz, 1H), 3.6 (s, 3H), 2.4 – 2.3 (m, 2H), 2.3 (s, 3H), 2.0 (s, 3H). ^{13}C{^{1}H} NMR (100 MHz, $CDCl_3$): δ 173.9, 170.6, 169.8, 161.0, 158.6, 157.0, 137.6, 137.5, 136.7, 129.0, 128.9, 128.6, 128.0, 127.7, 127.5, 125.5, 125.4, 125.4, 119.0, 118.7, 114.7, 79.9, 75.0, 70.0, 57.9, 52.8, 38.7, 29.7, 15.1, 14.7. HRMS (ESI TOF) *m/z* calcd. For $C_{38}H_{34}N_4O_6$ $[M+Na]^+$ 665.2375 found 665.2374.

Methyl (*5R,7R,8R,14S*)-7-([1,1'-biphenyl]-4-yl)-1,12-dimethyl-4,9-dioxo-3,10-diphenyl-6-oxa-2,3,10,11-tetraazadispiro[4.2.48.25]tetradeca-1,11-diene-14-carboxylate (3o)

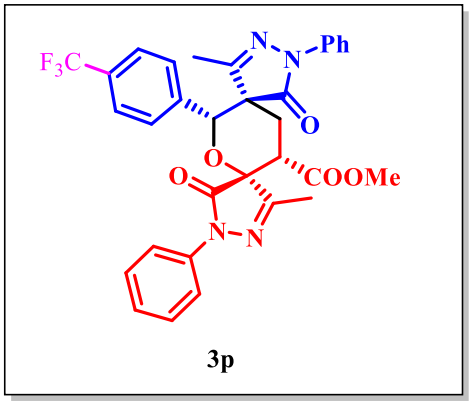
Product **3o** was synthesized following the general experimental procedure **4.5.4**. An oven-dried 10 mL glass reaction tube was charged with pyrazoledione-derived Morita–Baylis–Hillman (Pyro-MBH) alcohol **1a** (1.0 equiv, 0.2 mmol), potassium tert-butoxide (50 mol%, 0.1 mmol), and arylidene pyrazolones **2j** (1.0 equiv, 0.2 mmol). Subsequently, 1,4-Dioxane (1 mL) was added to the tube. The reaction mixture was stirred at ambient temperature for 1 minute. Upon



3o

completion, the solvent was removed under reduced pressure, and the residue was purified by column chromatography on silica gel using 25% ethyl acetate in hexanes as the eluent. The purified product, **3o**, identified as Methyl (*5R,7R,8R,14S*)-7-([1,1'-biphenyl]-4-yl)-1,12-dimethyl-4,9-dioxo-3,10-diphenyl-6-oxa-2,3,10,11-tetraazadispiro [4.2.48.25]tetradeca-1,11-diene-14-carboxylate, was obtained as a light yellow solid in a yield of 88 mg (72%) as a single diastereomer. The structure was confirmed through spectroscopic methods, including ^{1}H NMR, ^{13}C{^{1}H} NMR, HRMS, and X-ray crystallographic analysis. The compound displayed a melting point of 223-225 °C and a TLC retention factor (R_f) of 0.4 (silica gel, 30% ethyl acetate/hexanes). ^{1}H NMR (400 MHz, $CDCl_3$): δ 7.9 (tt, *J* = 8.6, 1.2 Hz, 4H), 7.5 – 7.5 (m, 2H), 7.5 – 7.4 (m, 8H), 7.3 (d, *J* = 7.3 Hz, 1H), 7.2 – 7.2 (m, 4H), 6.1 (s, 1H), 4.3 (dd, *J* = 10.7, 6.7 Hz, 1H), 3.6 (s, 3H), 2.5 – 2.4 (m, 2H), 2.3 (s, 3H), 2.0 (s, 3H). ^{13}C{^{1}H} NMR (100 MHz, $CDCl_3$): δ 173.9, 170.5, 169.8, 160.8, 157.0, 141.1, 140.3, 137.6, 137.5, 134.5, 129.0, 129.0, 128.8, 127.5, 127.0, 127.0, 125.5, 125.4, 124.7, 119.1, 118.7, 79.9, 74.9, 57.9, 52.8, 38.8, 25.6, 15.1, 14.7. HRMS (ESI TOF) *m/z* calcd. For $C_{37}H_{32}N_4O_5$ $[M+Na]^+$ 635.2270 found 635.2263.

Methyl (*5R,7R,8R,14S*)-1,12-dimethyl-4,9-dioxo-3,10-diphenyl-7-(4-(trifluoromethyl)phenyl)-6-oxa-2,3,10,11-tetraazadispiro[4.2.48.25]tetradeca-1,11-diene-14-carboxylate (3p)

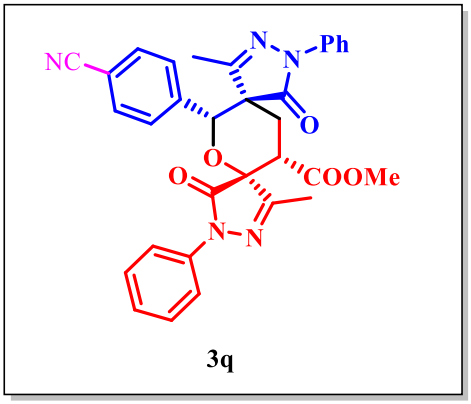


3p

Product **3p** was synthesized following the general experimental procedure **4.5.4**. An oven-dried 10 mL glass reaction tube was charged with pyrazoledione-derived Morita–Baylis–Hillman (Pyro-MBH) alcohol **1a** (1.0 equiv, 0.2 mmol), potassium tert-butoxide (50 mol%, 0.1 mmol), and arylidene pyrazolones **2k** (1.0 equiv, 0.2 mmol). Subsequently, 1,4-Dioxane (1 mL) was added to the tube. The reaction mixture was stirred at ambient temperature for 1 minute. Upon completion, the solvent was removed under reduced pressure, and the residue was purified by column chromatography on silica gel using 25% ethyl acetate in hexanes as the eluent. The purified product, **3p**, identified Methyl (*5R,7R,8R,14S*)-1,12-dimethyl-4,9-dioxo-

3,10-diphenyl-7-(4-(trifluoromethyl)phenyl)-6-oxa 2,3,10, 11 - tetraazadispiro[4.2.48.25]tetradeca-1,11-diene-14-carboxylate, was obtained as a light yellow solid in a yield of 88 mg (73%) as a single diastereomer. The structure was confirmed through spectroscopic methods including ^{1}H NMR, ^{13}C{^{1}H} NMR, HRMS, and X-ray crystallographic analysis. The compound displayed a melting point of 122-124 °C and a TLC retention factor (R_f) 0.4 (silica gel, 30% ethyl acetate/hexanes). ^{1}H NMR (400 MHz, $CDCl_3$): δ 7.8 (ddd, *J* = 10.5, 8.1, 1.2 Hz, 4H), 7.5 (d, *J* = 8.2 Hz, 2H), 7.5 – 7.4 (m, 4H), 7.3 – 7.2 (m, 4H), 6.1 (s, 1H), 4.3 (dd, *J* = 12.5, 4.9 Hz, 1H), 3.6 (s, 3H), 2.5 – 2.4 (m, 2H), 2.3 (s, 3H), 2.0 (s, 3H). ^{13}C{^{1}H} NMR (100 MHz, $CDCl_3$): δ 173.5, 170.4, 169.5, 160.3, 156.7, 139.6 – 139.4 (m), 137.5 – 137.3 (m), 130.6 (d, $J_{(C-F)}$ = 32.8 Hz), 129.1, 129.0, 129.0, 128.9, 125.7, 125.6 – 125.4 (m), 124.8 – 124.6 (m), 119.0, 118.9, 118.7, 79.9, 74.5, 57.7, 52.9, 38.7, 25.6, 14.9, 14.7. ^{19}F NMR (377 MHz, $CDCl_3$): δ -62.7. HRMS (ESI TOF) *m/z* calcd. For $C_{32}H_{27}F_3N_4O_5$ $[M+Na]^+$ 627.1831 found 627.1815.

Methyl (*5R,7R,8R,14S*)-7-(4-cyanophenyl)-1,12-dimethyl-4,9-dioxo-3,10-diphenyl-6-oxa-2,3,10,11-tetraazadispiro[4.2.48.25]tetradeca-1,11-diene-14-carboxylate (3q)

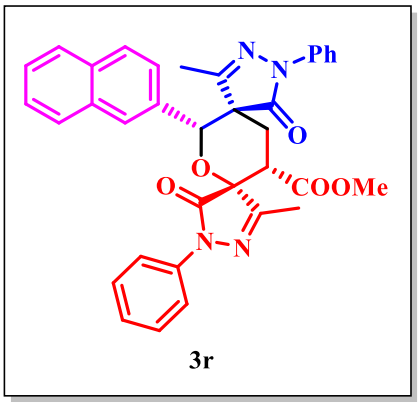


3q

Product **3q** was synthesized following the general experimental procedure **4.5.4**. An oven-dried 10 mL glass reaction tube was charged with pyrazoledione-derived Morita–Baylis–Hillman (Pyro-MBH) alcohol **1a** (1.0 equiv, 0.2 mmol), potassium tert-butoxide (50 mol%, 0.1 mmol), and arylidene pyrazolones **2l** (1.0 equiv, 0.2 mmol). Subsequently, 1,4-Dioxane (1 mL) was added to the tube. The reaction mixture was stirred at ambient temperature for 1 minute. Upon completion, the solvent was removed under reduced pressure, and the residue was purified by column chromatography on silica gel using 25% ethyl acetate in hexanes as the eluent. The purified product, **3q**, identified as Methyl (*5R,7R,8R,14S*)-7-(4-cyanophenyl)-1,12-dimethyl-4,9-dioxo-3,10-diphenyl-6-oxa-2,3,10,11-tetraazadispiro [4.2.48.25] tetradeca-1,11-diene-14-carboxylate, was obtained as a white solid in a yield of 93 mg (83%) as a single diastereomer. The structure was confirmed through spectroscopic methods including ^{1}H NMR, ^{13}C{^{1}H} NMR, HRMS, and X-ray crystallographic analysis. The compound displayed a melting point of 213-215 °C and a TLC retention factor (R_f) of 0.4 (silica gel, 30% ethyl acetate/hexanes). ^{1}H NMR (400 MHz, $CDCl_3$): δ 7.9 – 7.8 (m, 4H), 7.6

– 7.5 (m, 2H), 7.5 – 7.4 (m, 4H), 7.3 – 7.2 (m, 4H), 6.1 (s, 1H), 4.3 (dd, J = 13.1, 4.2 Hz, 1H), 3.6 (s, 3H), 2.5 – 2.3 (m, 2H), 2.3 (s, 3H), 2.0 (s, 3H). $^{13}C\{^{1}H\}$ NMR (100 MHz, $CDCl_3$): δ 173.3, 170.3, 169.4, 160.0, 156.6, 140.7, 137.3, 137.3, 132.3, 129.1, 129.0, 125.8, 125.6, 125.1, 118.9, 118.7, 118.2, 112.5, 79.9, 74.4, 57.7, 52.9, 38.7, 25.5, 15.0, 14.7. HRMS (ESI TOF) *m/z* calcd. For $C_{32}H_{27}N_5O_5$ $[M+H]^+$ 562.2090 found 562.2098.

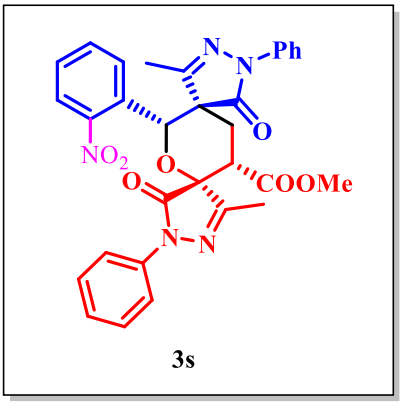
Methyl (*5R,7R,8R,14S*)-1,12-dimethyl-7-(naphthalen-2-yl)-4,9-dioxo-3,10-diphenyl-6-oxa-2,3,10,11-tetraazadispiro[4.2.48.25]tetradeca-1,11-diene-14-carboxylate (3r)



3r

Product **3r** was synthesized following the general experimental procedure **4.5.4**. An oven-dried 10 mL glass reaction tube was charged with pyrazoledione-derived Morita–Baylis–Hillman (Pyro-MBH) alcohol **1a** (1.0 equiv, 0.2 mmol), potassium tert-butoxide (50 mol%, 0.1 mmol), and arylidene pyrazolones **2m** (1.0 equiv, 0.2 mmol). Subsequently, 1,4-Dioxane (1 mL) was added to the tube. The reaction mixture was stirred at ambient temperature for 2 minute. Upon completion, the solvent was removed under reduced pressure, and the residue was purified by column chromatography on silica gel using 25% ethyl acetate in hexanes as the eluent. The purified product, **3r**, identified as Methyl (*5R,7R,8R,14S*)-1,12-dimethyl-7-(naphthalen-2-yl)-4,9-dioxo-3,10-diphenyl-6-oxa-2,3,10,11-tetraazadispiro [4.2.48.25] tetradeca-1,11-diene-14-carboxylate, was obtained as a white solid in a yield of 60 mg (51%) as a single diastereomer. The structure was confirmed through spectroscopic methods, including ^{1}H NMR, $^{13}C\{^{1}H\}$ NMR, HRMS, and X-ray crystallographic analysis. The compound displayed a melting point of 246-248 °C and a TLC retention factor (R_f) of 0.4 (silica gel, 30% ethyl acetate/hexanes). ^{1}H NMR (400 MHz, $CDCl_3$): δ 7.9 – 7.7 (m, 6H), 7.6 – 7.5 (m, 2H), 7.5 – 7.4 (m, 3H), 7.3 (tdd, *J* = 8.2, 3.2, 1.6 Hz, 3H), 7.2 – 7.1 (m, 3H), 6.8 (s, 1H), 4.7 (dd, *J* = 13.6, 3.1 Hz, 1H), 3.6 (s, 3H), 2.5 (t, *J* = 13.8 Hz, 1H), 2.4 (s, 3H), 2.4 (d, *J* = 3.1 Hz, 1H), 1.9 (s, 3H). $^{13}C\{^{1}H\}$ NMR (100 MHz, $CDCl_3$): δ 174.2, 170.6, 170.1, 160.4, 157.1, 137.5, 137.3, 133.4, 132.0, 129.2, 129.2, 128.9, 128.9, 128.7, 128.6, 126.4, 125.9, 125.3, 124.2, 123.4, 123.0, 119.1, 118.7, 79.8, 72.1, 58.1, 52.8, 38.3, 26.3, 15.2, 14.6. HRMS (ESI TOF) *m/z* calcd. For $C_{35}H_{30}N_4O_5$ $[M+H]^+$ 587.2294 found 587.2288.

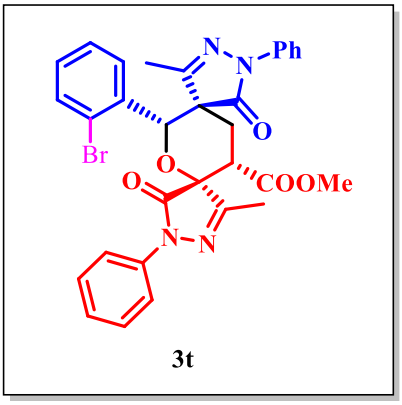
Methyl (*5R,7R,8R,14S*)-1,12-dimethyl-7-(2-nitrophenyl)-4,9-dioxo-3,10-diphenyl-6-oxa-2,3,10,11-tetraazadispiro[4.2.48.25]tetradeca-1,11-diene-14-carboxylate (3s)



3s

Product **3s** was synthesized following the general experimental procedure **4.5.4**. An oven-dried 10 mL glass reaction tube was charged with pyrazoledione-derived Morita–Baylis–Hillman (Pyro-MBH) alcohol **1a** (1.0 equiv, 0.2 mmol), potassium tert-butoxide (50 mol%, 0.1 mmol), and arylidene pyrazolones **2n** (1.0 equiv, 0.2 mmol). Subsequently, 1,4-Dioxane (1 mL) was added to the tube. The reaction mixture was stirred at ambient temperature for 1 minute. Upon completion, the solvent was removed under reduced pressure, and the residue was purified by column chromatography on silica gel using 25% ethyl acetate in hexanes as the eluent. The purified product, **3s**, identified as Methyl (*5R,7R,8R,14S*)-1,12-dimethyl-7-(2-nitrophenyl)-4,9-dioxo-3,10-diphenyl-6-oxa-2,3,10,11-tetraazadispiro [4.2.48.25] tetradeca-1,11-diene-14-carboxylate, was obtained as a light yellow solid in a yield of 44 mg (38%) as a single diastereomer. The structure was confirmed through spectroscopic methods, including ^{1}H NMR, ^{13}C{^{1}H} NMR, HRMS, and X-ray crystallographic analysis. The compound displayed a melting point of 235-237 °C and a TLC retention factor (R_f) of 0.4 (silica gel, 30% ethyl acetate/hexanes). ^{1}H NMR (400 MHz, $CDCl_3$): δ 7.9 (ddt, *J* = 14.8, 8.1, 1.1 Hz, 4H), 7.8 (dd, *J* = 8.1, 1.4 Hz, 1H), 7.7 (dt, *J* = 8.0, 1.1 Hz, 1H), 7.6 (d, *J* = 1.4 Hz, 1H), 7.5 – 7.3 (m, 5H), 7.2 (dd, *J* = 7.4, 3.3 Hz, 2H), 6.7 (s, 1H), 4.7 (dd, *J* = 13.5, 2.9 Hz, 1H), 3.6 (s, 3H), 2.5 (t, *J* = 13.8 Hz, 1H), 2.3 (s, 3H), 2.3 – 2.2 (m, 1H), 1.8 (s, 3H). ^{13}C{^{1}H} NMR (100 MHz, $CDCl_3$): δ 173.3, 170.1, 169.9, 159.2, 156.6, 147.4, 147.4, 137.5, 132.4, 130.6, 129.5, 128.9, 128.9, 127.9, 125.5, 125.4, 125.0, 119.1, 118.7, 79.3, 70.9, 57.5, 52.8, 37.5, 26.8, 15.2, 14.4. HRMS (ESI TOF) *m/z* calcd. For $C_{31}H_{27}N_5O_7$ $[M+H]^+$ 582.1988 found 582.1982.

Methyl (*5R,7S,8R,14S*)-7-(2-bromophenyl)-1,12-dimethyl-4,9-dioxo-3,10-diphenyl-6-oxa-2,3,10,11-tetraazadispiro[4.2.48.25]tetradeca-1,11-diene-14-carboxylate (3t)

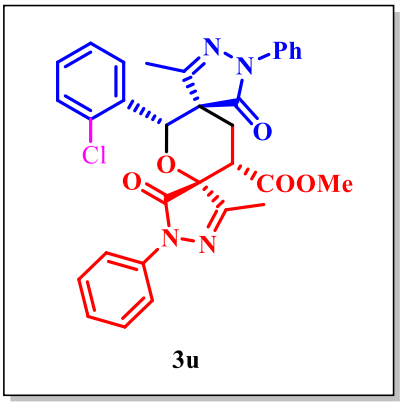


3t

Product **3t** was synthesized following the general experimental procedure **4.5.4**. An oven-dried 10 mL glass reaction tube was charged with pyrazoledione-derived Morita–Baylis–Hillman (Pyro-MBH) alcohol **1a** (1.0 equiv, 0.2 mmol), potassium tert-butoxide (50 mol%, 0.1 mmol), and arylidene pyrazolones **2o** (1.0 equiv, 0.2 mmol). Subsequently, 1,4-Dioxane (1 mL) was added to the tube.

The reaction mixture was stirred at ambient temperature for 1 minute. Upon completion, the solvent was removed under reduced pressure, and the residue was purified by column chromatography on silica gel using 20% ethyl acetate in hexanes as the eluent. The purified product, **3t**, identified as Methyl (*5R,7S,8R,14S*)-7-(2-bromophenyl)-1,12-dimethyl-4,9-dioxo-3,10-diphenyl-6-oxa-2,3,10,11-tetraazadispiro [4.2.48.25] tetradeca-1,11-diene-14-carboxylate, was obtained as a white solid in a yield of 73 mg (59%) as a single diastereomer. The structure was confirmed through spectroscopic methods, including ^{1}H NMR, ^{13}C{^{1}H} NMR, HRMS, and X-ray crystallographic analysis. The compound displayed a melting point of 258-260 °C and a TLC retention factor (R_f) of 0.5 (silica gel, 30% ethyl acetate/hexanes). ^{1}H NMR (400 MHz, $CDCl_3$): δ 7.9 – 7.8 (m, 4H), 7.6 (dd, *J* = 7.9, 1.7 Hz, 1H), 7.5 – 7.3 (m, 5H), 7.3 – 7.3 (m, 1H), 7.2 – 7.1 (m, 3H), 6.3 (s, 1H), 4.7 (dd, *J* = 13.5, 2.8 Hz, 1H), 3.6 (s, 3H), 2.5 (t, *J* = 13.7 Hz, 1H), 2.3 (s, 3H), 2.3 (dd, *J* = 13.9, 2.8 Hz, 1H), 1.9 (s, 3H). ^{13}C{^{1}H} NMR (100 MHz, $CDCl_3$): δ 173.8, 170.4, 170.1, 159.3, 156.9, 137.9, 137.5, 136.4, 133.4, 129.9, 128.9, 128.9, 128.3, 126.7, 125.3, 125.2, 120.7, 118.8, 118.7, 79.3, 73.4, 57.2, 52.7, 37.5, 26.9, 15.4, 14.4. HRMS (ESI TOF) *m/z* calcd. For $C_{31}H_{27}BrN_4O_5$ $[M+H]^+$ 615.1243 found 615.1243.

Methyl (*5R,7S,8R,14S*)-7-(2-chlorophenyl)-1,12-dimethyl-4,9-dioxo-3,10-diphenyl-6-oxa-2,3,10,11-tetraazadispiro[4.2.48.25]tetradeca-1,11-diene-14-carboxylate (3u)

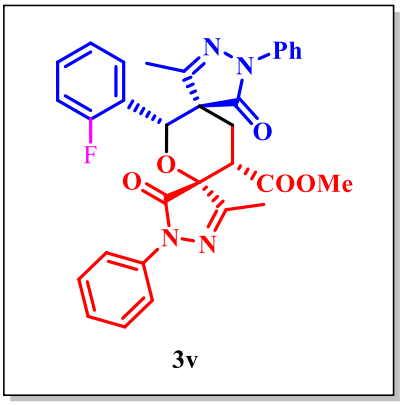


3u

Product **3u** was synthesized following the general experimental procedure **4.5.4**. An oven-dried 10 mL glass reaction tube was charged with pyrazoledione-derived Morita–Baylis–Hillman (Pyro-MBH) alcohol **1a** (1.0 equiv, 0.2 mmol), potassium tert-butoxide (50 mol%, 0.1 mmol), and arylidene pyrazolones **2p** (1.0 equiv, 0.2 mmol). Subsequently, 1,4-Dioxane (1 mL) was added to the tube. The reaction mixture was stirred at ambient temperature for 1 minute. Upon completion, the solvent was removed under reduced pressure, and the residue was purified by column chromatography on silica gel using 20% ethyl acetate in hexanes as the eluent. The purified product, **3u**, identified as Methyl (*5R,7S,8R,14S*)-7-(2-chlorophenyl)-1,12-dimethyl-4,9-dioxo-3,10-diphenyl-6-oxa-2,3,10,11-tetraazadispiro [4.2.48.25]tetradeca-1,11-diene-14-carboxylate, was obtained as a white solid in a yield of 72 mg (63%) as a single diastereomer. The structure was confirmed through spectroscopic methods, including ^{1}H NMR,

$^{13}C\{^{1}H\}$ NMR, HRMS, and X-ray crystallographic analysis. The compound displayed a melting point of 229-231 °C and a TLC retention factor (R_f) of 0.5 (silica gel, 30% ethyl acetate/hexanes). ^{1}H NMR (400 MHz, $CDCl_3$): δ 7.9 – 7.8 (m, 4H), 7.6 (dd, *J* = 7.6, 1.7 Hz, 1H), 7.4 (tt, *J* = 7.3, 1.7 Hz, 4H), 7.3 – 7.1 (m, 5H), 6.3 (s, 1H), 4.6 (dd, *J* = 13.5, 2.8 Hz, 1H), 3.6 (s, 3H), 2.5 (t, *J* = 13.7 Hz, 1H), 2.3 (s, 3H), 2.3 (dd, *J* = 14.0, 2.9 Hz, 1H), 1.8 (s, 3H). $^{13}C\{^{1}H\}$ NMR (100 MHz, $CDCl_3$): δ 173.8, 170.4, 170.1, 159.4, 156.9, 137.8, 137.5, 134.6, 131.3, 129.9, 129.6, 128.9, 128.9, 127.8, 126.2, 125.3, 125.2, 118.8, 118.6, 79.4, 71.7, 57.1, 52.8, 37.6, 26.8, 15.2, 14.4. HRMS (ESI TOF) *m/z* calcd. For $C_{31}H_{27}ClN_4O_5$ $[M+H]^+$ 571.1748 found 571.1743.

Methyl (*5R,7S,8R,14S*)-7-(2-fluorophenyl)-1,12-dimethyl-4,9-dioxo-3,10-diphenyl-6-oxa-2,3,10,11-tetraazadispiro[4.2.48.25]tetradeca-1,11-diene-14-carboxylate (3v)

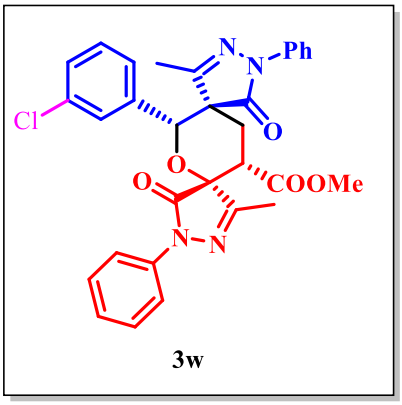


3v

Product **3v** was synthesized following the general experimental procedure **4.5.4**. An oven-dried 10 mL glass reaction tube was charged with pyrazoledione-derived Morita–Baylis–Hillman (Pyro-MBH) alcohol **1a** (1.0 equiv, 0.2 mmol), potassium tert-butoxide (50 mol%, 0.1 mmol), and arylidene pyrazolones **2q** (1.0 equiv, 0.200 mmol). Subsequently, 1,4-Dioxane (1 mL) was added to the tube. The reaction mixture was stirred at ambient temperature for 1 minute. Upon completion, the solvent was removed under reduced pressure, and the residue was purified by column chromatography on silica gel using 20% ethyl acetate in hexanes as the eluent. The purified product, **3v**, identified as Methyl (*5R,7S,8R,14S*)-7-(2-fluorophenyl)-1,12-dimethyl-4,9-dioxo-3,10-diphenyl-6-oxa-2,3,10,11-tetraazadispiro [4.2.48.25] tetradeca-1,11-diene-14-carboxylate, was obtained as a white solid in a yield of 73 mg (66%) as a single diastereomer. The structure was confirmed through spectroscopic methods, including ^{1}H NMR, $^{113}C\{^{1}H\}$ NMR, HRMS, and X-ray crystallographic analysis. The compound displayed a melting point of 213-215 °C and a TLC retention factor (R_f) of 0.5 (silica gel, 30% ethyl acetate/hexanes). ^{1}H NMR (400 MHz, $CDCl_3$): δ 7.9 – 7.8 (m, 4H), 7.5 – 7.5 (m, 1H), 7.4 – 7.3 (m, 4H), 7.3 – 7.2 (m, 3H), 7.1 (td, J = 7.6, 1.2 Hz, 1H), 6.9 (ddd, J = 10.7, 8.2, 1.2 Hz, 1H), 6.3 (s, 1H), 4.5 (dd, J = 12.8, 3.9 Hz, 1H), 3.6 (s, 3H), 2.5 – 2.3 (m, 2H), 2.3 (s, 3H), 1.9 (s, 3H). $^{13}C\{^{1}H\}$ NMR (100 MHz, $CDCl_3$): δ 173.5, 170.4, 169.8, 160.0 (d, $J_{(C-F)}$ = 49.3 Hz), 157.3 (d, $J_{(C-F)}$ = 85.6 Hz), 137.7, 137.5, 130.0, 129.9, 129.0, 128.9, 126.8 (d, $J_{(C-F)}$ = 3.8 Hz), 125.4,

125.2, 123.9 (d, $J_{(C-F)}$ = 3.3 Hz), 123.6, 123.5, 118.9 (d, $J_{(C-F)}$ = 41.5 Hz), 115.5 (d, $J_{(C-F)}$ = 21.3 Hz), 79.5, 70.2, 57.1, 52.8, 38.2, 26.2, 14.8, 14.5. HRMS (ESI TOF) *m/z* calcd. For $C_{31}H_{27}FN_4O_5$ $[M+H]^+$ 555.2043 found 555.2038.

Methyl (*5R,7R,8R,14S*)-7-(3-chlorophenyl)-1,12-dimethyl-4,9-dioxo-3,10-diphenyl-6-oxa-2,3,10,11-tetraazadispiro[4.2.48.25]tetradeca-1,11-diene-14-carboxylate (3w)

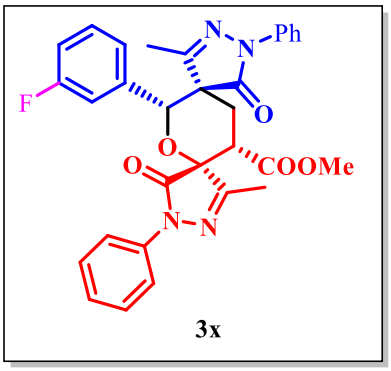


3w

Product **3w** was synthesized following the general experimental procedure **4.5.4**. An oven-dried 10 mL glass reaction tube was charged with pyrazoledione-derived Morita–Baylis–Hillman (Pyro-MBH) alcohol **1a** (1.0 equiv, 0.2 mmol), potassium tert-butoxide (50 mol%, 0.1 mmol), and arylidene pyrazolones **2r** (1.0 equiv, 0.2 mmol). Subsequently, 1,4-Dioxane (1 mL) was added to the tube. The reaction mixture was stirred at ambient temperature for 1 minute. Upon completion, the solvent was removed under reduced pressure, and the residue was purified by column chromatography on silica gel using 20% ethyl acetate in hexanes as the eluent. The purified product, **3w**, identified as Methyl (*5R,7R,8R,14S*)-7-(3-chlorophenyl)-1,12-dimethyl-4,9-dioxo-3,10-diphenyl-6-oxa-2,3,10,11-tetraazadispiro [4.2.48.25] tetradeca-1,11-diene-14-carboxylate, was obtained as a light yellow solid in a yield of 84 mg (74%) as a single diastereomer. The structure was confirmed through spectroscopic methods, including ^{1}H NMR, ^{13}C{^{1}H} NMR, HRMS, and X-ray crystallographic analysis. The compound displayed a melting point of 229-231 °C and a TLC retention factor (R_f) of 0.5 (silica gel, 30% ethyl acetate/hexanes). ^{1}H NMR (400 MHz, $CDCl_3$): δ 7.9 – 7.8 (m, 4H), 7.4 (ddd, J = 8.5, 7.3, 2.8 Hz, 4H), 7.2 – 7.2 (m, 4H), 7.1 (d, J = 7.8 Hz, 1H), 6.9 (d, J = 0.9 Hz, 1H), 6.1 (s, 1H), 4.3 (dd, J = 12.4, 4.9 Hz, 1H), 3.6 (s, 3H), 2.5 – 2.4 (m, 2H), 2.3 (s, 3H), 2.0 (s, 3H). ^{13}C{^{1}H} NMR (100 MHz, $CDCl_3$): δ 173.6, 170.4, 169.6, 160.5, 156.8, 137.5, 137.4, 137.4, 134.6, 129.8, 129.0, 129.0, 128.6, 125.7, 125.5, 124.6, 122.4, 119.2, 118.7, 79.9, 74.4, 57.7, 52.9, 38.8, 25.5, 15.0, 14.7. HRMS (ESI TOF) *m/z* calcd. For $C_{31}H_{27}ClN_4O_5$ $[M+H]^+$ 571.1748 found 571.1751.

Methyl (*5R,7R,8R,14S*)-7-(3-fluorophenyl)-1,12-dimethyl-4,9-dioxo-3,10-diphenyl-6-oxa-2,3,10,11-tetraazadispiro[4.2.48.25]tetradeca-1,11-diene-14-carboxylate (3x)

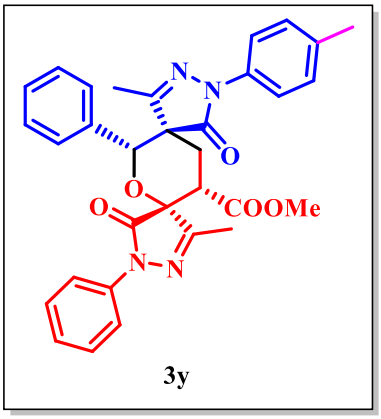
Product **3x** was synthesized following the general experimental procedure **4.5.4**. An oven-dried 10 mL glass reaction tube was charged with pyrazoledione-derived Morita–Baylis–Hillman



3x

(Pyro-MBH) alcohol **1a** (1.0 equiv, 0.2 mmol), potassium tert-butoxide (50 mol%, 0.1 mmol), and arylidene pyrazolones **2s** (1.0 equiv, 0.200 mmol). Subsequently, 1,4-Dioxane (1 mL) was added to the tube. The reaction mixture was stirred at ambient temperature for 1 minute. Upon completion, the solvent was removed under reduced pressure, and the residue was purified by column chromatography on silica gel using 20% ethyl acetate in hexanes as the eluent. The purified product, **3x**, identified as Methyl (*5R,7R,8R,14S*)-7-(3-fluorophenyl)-1,12-dimethyl-4,9-dioxo-3,10-diphenyl-6-oxa-2,3,10,11-tetraazadispiro [4.2.48.25] tetradeca-1,11-diene-14-carboxylate , was obtained as a light yellow solid in a yield of 77 mg (69%) as a single diastereomer. The structure was confirmed through spectroscopic methods, including ^{1}H NMR, ^{13}C{^{1}H} NMR, HRMS, and X-ray crystallographic analysis. The compound displayed a melting point of 204-06 °C and a TLC retention factor (R_f) of 0.5 (silica gel, 30% ethyl acetate/hexanes). ^{1}H NMR (400 MHz, $CDCl_3$): δ 7.9 – 7.8 (m, 4H), 7.5 – 7.4 (m, 4H), 7.3 – 7.1 (m, 3H), 6.9 (dd, J = 5.4, 3.6 Hz, 2H), 6.8 – 6.8 (m, 1H), 6.1 (s, 1H), 4.3 (dd, J = 11.8, 5.5 Hz, 1H), 3.6 (s, 3H), 2.5 – 2.4 (m, 2H), 2.3 (s, 3H), 2.0 (s, 3H). ^{13}C{^{1}H} NMR (100 MHz, $CDCl_3$): δ 173.6, 170.4, 169.6, 162.7 (d, $J_{(C-F)}$ = 246.9 Hz), 160.5, 156.8, 138.0 (d, $J_{(C-F)}$ = 7.5 Hz), 137.4, 130.2 (d, $J_{(C-F)}$ = 8.2 Hz), 129.0, 129.0, 129.0, 125.6, 125.5, 119.9 (d, $J_{(C-F)}$ = 3.1 Hz), 119.1, 118.7, 115.3 (d, $J_{(C-F)}$ = 21.0 Hz), 111.7 (d, $J_{(C-F)}$ = 23.5 Hz), 79.9, 74.3, 57.7, 52.8, 38.7, 25.6, 15.0, 14.7. ^{19}F NMR (377 MHz, $CDCl_3$): δ -111.7. HRMS (ESI TOF) *m/z* calcd. For $C_{31}H_{27}FN_4O_5$ $[M+H]^+$ 555.2043 found 555.2042.

Methyl (*5R,7R,8R,14S*)-1,12-dimethyl-4,9-dioxo-3,7-diphenyl-10-(p-tolyl)-6-oxa-2,3,10,11-tetraazadispiro[4.2.48.25]tetradeca-1,11-diene-14-carboxylate (3y)

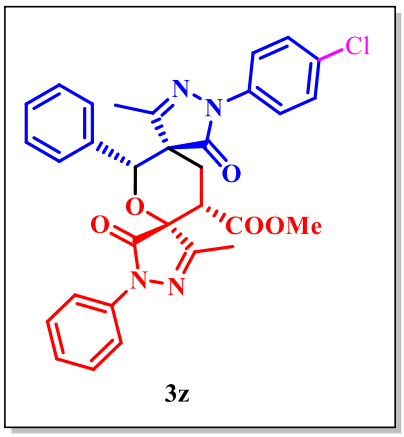


3y

Product **3y** was synthesized following the general experimental procedure **4.5.4**. An oven-dried 10 mL glass reaction tube was charged with pyrazoledione-derived Morita–Baylis–Hillman (Pyro-MBH) alcohol **1a** (1.0 equiv, 0.2 mmol), potassium tert-butoxide (50 mol%, 0.1 mmol), and arylidene pyrazolones **2t** (1.0 equiv, 0.2 mmol). Subsequently, 1,4-Dioxane (1 mL) was added to the tube. The reaction mixture was stirred at ambient temperature for 1 minute. Upon

completion, the solvent was removed under reduced pressure and the residue was purified by column chromatography on silica gel using 20% ethyl acetate in hexanes as the eluent. The purified product, **3y**, identified as Methyl (*5R,7R,8R,14S*)-1,12-dimethyl-4,9-dioxo-3,7-diphenyl-10-(p-tolyl)-6-oxa-2,3,10,11-tetraazadispiro [4.2.48.25]tetradeca-1,11-diene-14-carboxylate, was obtained as a light yellow solid in a yield of 75 mg (68%) as a single diastereomer. The structure was confirmed through spectroscopic methods, including ^{1}H NMR, ^{13}C{^{1}H} NMR, HRMS, and X-ray crystallographic analysis. The compound displayed a melting point of 192-194 °C and a TLC retention factor (R_f) of 0.5 (silica gel, 30% ethyl acetate/hexanes). ^{1}H NMR (400 MHz, $CDCl_3$): δ 7.9 – 7.8 (m, 2H), 7.7 – 7.6 (m, 2H), 7.4 – 7.4 (m, 2H), 7.2 – 7.2 (m, 6H), 7.1 – 7.1 (m, 2H), 6.1 (s, 1H), 4.3 (dd, *J* = 11.1, 6.2 Hz, 1H), 3.6 (s, 3H), 2.4 – 2.4 (m, 2H), 2.4 (s, 3H), 2.3 (s, 3H), 2.0 (s, 3H). ^{13}C{^{1}H} NMR (100 MHz, $CDCl_3$): δ 173.7, 170.6, 169.8, 160.7, 157.0, 137.5, 135.5, 135.2, 135.1, 129.5, 129.0, 128.4, 128.3, 125.4, 124.2, 119.1, 118.7, 79.9, 75.0, 57.8, 52.8, 38.8, 25.5, 21.0, 15.0, 14.7. HRMS (ESI TOF) *m/z* calcd. For $C_{32}H_{30}N_4O_5$ $[M+H]^+$ 551.2294 found 551.2294.

Methyl (*5R,7R,8R,14S*)-10-(4-chlorophenyl)-1,12-dimethyl-4,9-dioxo-3,7-diphenyl-6-oxa-2,3,10,11-tetraazadispiro[4.2.48.25]tetradeca-1,11-diene-14-carboxylate (3z)

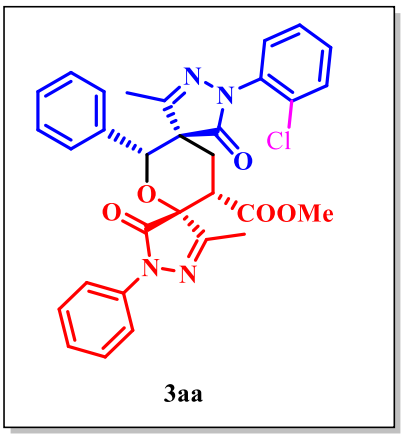


3z

Product **3z** was synthesized following the general experimental procedure **4.5.4**. An oven-dried 10 mL glass reaction tube was charged with pyrazoledione-derived Morita–Baylis–Hillman (Pyro-MBH) alcohol **1a** (1.0 equiv, 0.2 mmol), potassium tert-butoxide (50 mol%, 0.1 mmol), and arylidene pyrazolones **2u** (1.0 equiv, 0.2 mmol). Subsequently, 1,4-Dioxane (1 mL) was added to the tube. The reaction mixture was stirred at ambient temperature for 1 minute. Upon completion, the solvent was removed under reduced pressure, and the residue was purified by column chromatography on silica gel using 20% ethyl acetate in hexanes as the eluent. The purified product, **3z**, identified as Methyl (*5R,7R,8R,14S*)-10-(4-chlorophenyl)-1,12-dimethyl-4,9-dioxo-3,7-diphenyl-6-oxa-2,3,10,11-tetraazadispiro [4.2.48.25] tetradeca-1,11-diene-14-carboxylate, was obtained as a light yellow solid in a yield of 84 mg (74%) as a single diastereomer. The structure was confirmed through spectroscopic methods, including ^{1}H NMR, ^{13}C{^{1}H} NMR, HRMS, and X-ray crystallographic analysis. The compound displayed a melting point of 192-194 °C and a TLC retention factor

(R_f) of 0.5 (silica gel, 30% ethyl acetate/hexanes). ^{1}H NMR (400 MHz, $CDCl_3$): δ 7.9 – 7.7 (m, 4H), 7.4 – 7.3 (m, 4H), 7.2 – 7.2 (m, 4H), 7.1 – 7.1 (m, 2H), 6.1 (s, 1H), 4.3 (dd, J = 10.8, 6.6 Hz, 1H), 3.6 (s, 3H), 2.4 – 2.4 (m, 2H), 2.3 (s, 3H), 2.0 (s, 3H). ^{13}C{^{1}H} NMR (100 MHz, $CDCl_3$): δ 173.8, 170.5, 169.7, 161.1, 156.9, 137.5, 136.2, 135.1, 130.5, 129.0, 129.0, 128.4, 128.4, 125.4, 124.1, 120.0, 118.7, 79.8, 75.0, 58.0, 52.8, 38.7, 25.5, 15.0, 14.7. HRMS (ESI TOF) *m/z* calcd. For $C_{31}H_{27}ClN_4O_5$ $[M+H]^+$ 571.1748 found 571.1747.

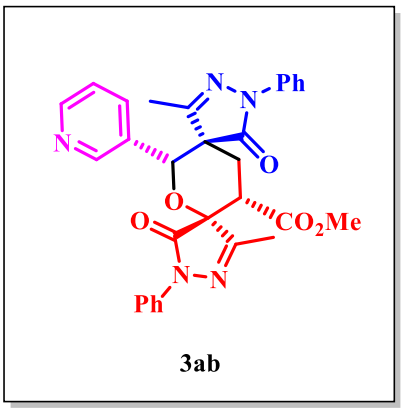
Methyl (*5R,7R,8R,14S*)-10-(2-chlorophenyl)-1,12-dimethyl-4,9-dioxo-3,7-diphenyl-6-oxa-2,3,10,11-tetraazadispiro[4.2.48.25]tetradeca-1,11-diene-14-carboxylate (3aa)



3aa

Product **3aa** was synthesized following the general experimental procedure **4.5.4**. An oven-dried 10 mL glass reaction tube was charged with pyrazoledione-derived Morita–Baylis–Hillman (Pyro-MBH) alcohol **1a** (1.0 equiv, 0.2 mmol), potassium tert-butoxide (50 mol%, 0.1 mmol), and arylidene pyrazolones **2v** (1.0 equiv, 0.2 mmol). Subsequently, 1,4-Dioxane (1 mL) was added to the tube. The reaction mixture was stirred at ambient temperature for 1 minute. Upon completion, the solvent was removed under reduced pressure, and the residue was purified by column chromatography on silica gel using 20% ethyl acetate in hexanes as the eluent. The purified product, **3aa**, identified as the mixture was purified by column chromatography (SiO2, 20% EtOAc /hexanes) to afford **3aa**, Methyl (*5R,7R,8R,14S*)-10-(2-chlorophenyl)-1,12-dimethyl-4,9-dioxo-3,7-diphenyl-6-oxa-2,3,10,11-tetraazadispiro [4.2.48.25] tetradeca-1,11-diene-14-carboxylate, was obtained as a light yellow solid in a yield of 86 mg (75%) as a single diastereomer. The structure was confirmed through spectroscopic methods, including ^{1}H NMR, ^{13}C{^{1}H} NMR, HRMS, and X-ray crystallographic analysis. The compound displayed a melting point of 203-205 °C and a TLC retention factor (R_f) of 0.5 (silica gel, 30% ethyl acetate/hexanes). ^{1}H NMR (400 MHz, $CDCl_3$): δ 7.9 – 7.8 (m, 2H), 7.5 – 7.5 (m, 1H), 7.4 – 7.3 (m, 9H), 7.2 (d, *J* = 3.2 Hz, 1H), 7.2 (d, *J* = 7.4 Hz, 1H), 6.1 (s, 1H), 4.3 (dd, *J* = 12.1, 5.3 Hz, 1H), 3.6 (s, 3H), 2.5 – 2.4 (m, 2H), 2.3 (s, 3H), 2.0 (s, 3H). ^{13}C{^{1}H} NMR (100 MHz, $CDCl_3$): δ 174.3, 170.5, 169.8, 160.9, 157.0, 137.5, 135.6, 134.0, 131.9, 130.6, 130.0, 129.0, 128.5, 128.5, 128.4, 127.6, 125.4, 124.6, 118.7, 79.9, 74.7, 56.5, 52.8, 38.7, 25.6, 15.0, 14.7. HRMS (ESI TOF) *m/z* calcd. For $C_{31}H_{27}ClN_4O_5$ $[M+H]^+$ 571.1748 found 571.1743.

Methyl (*5R,7R,8R,14S*)-1,12-dimethyl-4,9-dioxo-3,10-diphenyl-7-(pyridin-3-yl)-6-oxa-2,3,10,11-tetraazadispiro[4.2.48.25]tetradeca-1,11-diene-14-carboxylate (3ab)

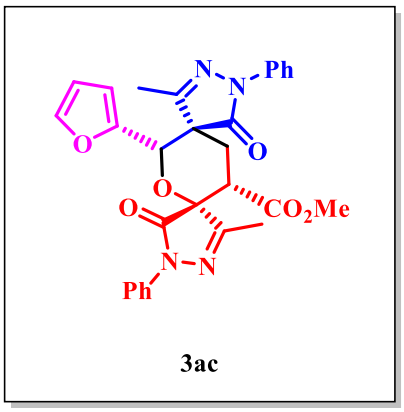


3ab

Product **3ab** was synthesized following the general experimental procedure **4.5.4**. An oven-dried 10 mL glass reaction tube was charged with pyrazoledione-derived Morita–Baylis–Hillman (Pyro-MBH) alcohol **1a** (1.0 equiv, 0.2 mmol), potassium tert-butoxide (50 mol%, 0.1 mmol), and arylidene pyrazolones **2w** (1.0 equiv, 0.2 mmol). Subsequently, 1,4-Dioxane (1 mL) was added to the tube. The reaction mixture was stirred at ambient temperature for 2 minute. Upon completion, the solvent was removed under reduced pressure, and the residue was purified by column chromatography on silica gel using 20% ethyl acetate in hexanes as the eluent. The purified product, **3ab**, identified as mixture was purified by column chromatography (SiO2, 25% EtOAc /hexanes) to afford **3ab**, Methyl (*5R,7R,8R,14S*)-1,12-dimethyl-4,9-dioxo-3,10-diphenyl-7-(pyridin-3-yl)-6-oxa-2,3,10,11-tetraazadispiro [4.2.48.25] tetradeca-1,11-diene-14-carboxylate, was obtained as a red solid in a yield of 77 mg (72%) as a single diastereomer. The structure was confirmed through spectroscopic methods, including ^{1}H NMR, ^{13}C{^{1}H} NMR, HRMS, and X-ray crystallographic analysis. The compound displayed a melting point of 197-199 °C and a TLC retention factor (R_f) of 0.4 (silica gel, 30% ethyl acetate/hexanes). ^{1}H NMR (400 MHz, $CDCl_3$): δ 8.6 – 8.4 (m, 2H), 7.9 – 7.8 (m, 4H), 7.4 – 7.3 (m, 5H), 7.2 – 7.1 (m, 3H), 6.1 (s, 1H), 4.3 (dd, *J* = 12.7, 4.7 Hz, 1H), 3.6 (s, 3H), 2.5 – 2.4 (m, 2H), 2.3 (s, 3H), 2.0 (s, 3H). ^{13}C{^{1}H} NMR (100 MHz, $CDCl_3$): δ 173.3, 170.4, 169.5, 160.2, 156.7, 149.9, 145.9, 137.4, 137.3, 132.1, 131.2, 129.0, 129.0, 125.7, 125.6, 123.1, 119.0, 118.7, 79.9, 73.6, 57.6, 52.9, 38.7, 25.4, 15.0, 14.7. HRMS (ESI TOF) *m/z* calcd. For $C_{30}H_{27}N_5O_5$ $[M+H]^+$ 538.2090 found 538.2089.

Methyl (*5R,7S,8R,14S*)-7-(furan-2-yl)-1,12-dimethyl-4,9-dioxo-3,10-diphenyl-6-oxa-2,3,10,11-tetraazadispiro[4.2.48.25]tetradeca-1,11-diene-14-carboxylate (3ac)

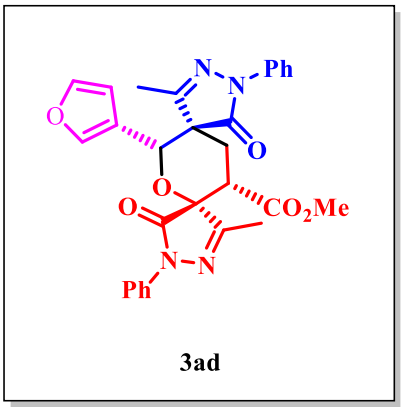
Product **3ac** was synthesized following the general experimental procedure **4.5.4**. An oven-dried 10 mL glass reaction tube was charged with pyrazoledione-derived Morita–Baylis–Hillman (Pyro-MBH) alcohol **1a** (1.0 equiv, 0.2 mmol), potassium tert-butoxide (50 mol%, 0.1 mmol), and arylidene pyrazolones **2x** (1.0 equiv, 0.2 mmol). Subsequently, 1,4-Dioxane (1 mL) was added to the tube. The reaction mixture was stirred at ambient temperature for 2 minute.



3ac

Upon completion, the solvent was removed under reduced pressure, and the residue was purified by column chromatography on silica gel using 25% ethyl acetate in hexanes as the eluent. The purified product, **3ac**, identified as Methyl (*5R,7S,8R,14S*)-7-(furan-2-yl)-1,12-dimethyl-4,9-dioxo-3,10-diphenyl-6-oxa-2,3,10,11-tetraazadispiro [4.2.48.25] tetradeca-1,11-diene-14-carboxylate, was obtained as a white solid in a yield of 27 mg (26%) as a single diastereomer. The structure was confirmed through spectroscopic methods including ^{1}H NMR, ^{13}C{^{1}H} NMR, HRMS, and X-ray crystallographic analysis. The compound displayed a melting point of 260-262 °C and a TLC retention factor (R_f) of 0.4 (silica gel, 30% ethyl acetate/hexanes). ^{1}H NMR (400 MHz, $CDCl_3$): δ 7.8 (ddd, J = 10.0, 8.7, 1.2 Hz, 4H), 7.4 (dt, J = 8.6, 7.2 Hz, 4H), 7.3 (s, 1H), 7.3 – 7.2 (m, 2H), 6.3 – 6.2 (m, 2H), 6.1 (d, J = 0.9 Hz, 1H), 4.2 (dd, J = 12.1, 5.4 Hz, 1H), 3.6 (s, 3H), 2.4 – 2.3 (m, 2H), 2.3 (s, 3H), 2.2 (s, 3H). ^{13}C{^{1}H} NMR (100 MHz, $CDCl_3$): δ 173.0, 169.5, 169.5, 161.0, 156.7, 147.8, 143.2, 137.4, 129.0, 128.9, 128.9, 125.5, 125.3, 119.0, 118.8, 110.3, 108.5, 79.8, 71.0, 56.0, 52.8, 38.8, 25.4, 15.0, 14.6. HRMS (ESI TOF) *m/z* calcd. For $C_{29}H_{26}N_4O_6$ $[M+Na]^+$ 549.1749 found 549.1752.

Methyl (*5R,7R,8R,14S*)-7-(furan-3-yl)-1,12-dimethyl-4,9-dioxo-3,10-diphenyl-6-oxa-2,3,10,11-tetraazadispiro[4.2.48.25]tetradeca-1,11-diene-14-carboxylate (3ad)

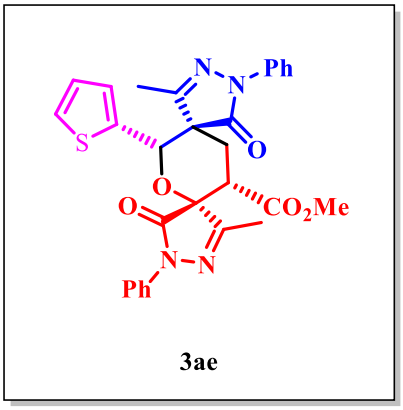


3ad

Product **3ad** was synthesized following the general experimental procedure **4.5.4**. An oven-dried 10 mL glass reaction tube was charged with pyrazoledione-derived Morita–Baylis–Hillman (Pyro-MBH) alcohol **1a** (1.0 equiv, 0.2 mmol), potassium tert-butoxide (50 mol%, 0.1 mmol), and arylidene pyrazolones **2y** (1.0 equiv, 0.2 mmol). Subsequently, 1,4-Dioxane (1 mL) was added to the tube. The reaction mixture was stirred at ambient temperature for 2 minute. Upon completion, the solvent was removed under reduced pressure, and the resulting crude product was subjected to extraction using dichloromethane (DCM). The organic layer was concentrated under reduced pressure, and the residue was purified by column chromatography on silica gel using 25% ethyl acetate in hexanes as the eluent. The purified product, **3ad**, identified as Methyl (*5R,7R,8R,14S*)-7-(furan-3-yl)-1,12-dimethyl-4,9-dioxo-

3,10-diphenyl-6-oxa-2,3,10,11-tetraazadispiro [4.2.48.25] tetradeca-1,11-diene-14-carboxylate, was obtained as a light yellow solid in a yield of 46 mg (44%) as a single diastereomer. The structure was confirmed through spectroscopic methods, including ^{1}H NMR, ^{13}C{^{1}H} NMR, HRMS, and X-ray crystallographic analysis. The compound displayed a melting point of 242-244 °C and a TLC retention factor (R_f) of 0.4 (silica gel, 30% ethyl acetate/hexanes). ^{1}H NMR (400 MHz, $CDCl_3$): δ 7.9 – 7.8 (m, 4H), 7.4 (ddd, *J* = 8.6, 7.4, 1.3 Hz, 4H), 7.3 – 7.3 (m, 2H), 7.2 (dd, *J* = 7.4, 2.1 Hz, 2H), 6.0 (d, *J* = 2.0 Hz, 1H), 6.0 (s, 1H), 4.2 (dd, *J* = 13.1, 4.5 Hz, 1H), 3.6 (s, 3H), 2.5 – 2.3 (m, 2H), 2.3 (s, 3H), 2.1 (s, 3H). ^{13}C{^{1}H} NMR (100 MHz, $CDCl_3$): δ 173.3, 170.6, 169.6, 161.2, 156.9, 143.8, 139.0, 137.6, 137.5, 129.0, 129.0, 125.5, 125.4, 120.6, 118.9, 118.7, 107.2, 79.9, 70.8, 56.8, 52.8, 38.8, 25.2, 15.0, 14.7. HRMS (ESI TOF) *m/z* calcd. For $C_{29}H_{26}N_4O_6$ $[M+Na]^+$ 549.1749 found 549.1751.

Methyl (*5R,7S,8R,14S*)-1,12-dimethyl-4,9-dioxo-3,10-diphenyl-7-(thiophen-2-yl)-6-oxa-2,3,10,11-tetraazadispiro[4.2.48.25]tetradeca-1,11-diene-14-carboxylate (3ae)

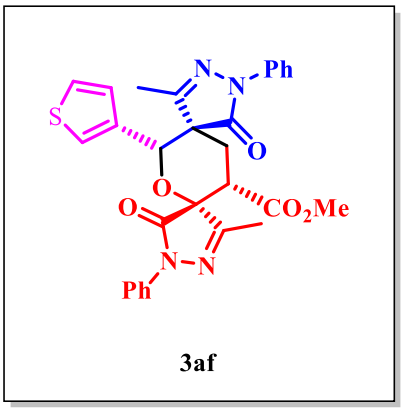


3ae

Product **3ae** was synthesized following the general experimental procedure **4.5.4**. An oven-dried 10 mL glass reaction tube was charged with pyrazoledione-derived Morita–Baylis–Hillman (Pyro-MBH) alcohol **1a** (1.0 equiv, 0.2 mmol), potassium tert-butoxide (50 mol%, 0.1 mmol), and arylidene pyrazolones **2z** (1.0 equiv, 0.2 mmol). Subsequently, 1,4-Dioxane (1 mL) was added to the tube. The reaction mixture was stirred at ambient temperature for 2 minute. Upon completion, the solvent was removed under reduced pressure, and the residue was purified by column chromatography on silica gel using 25% ethyl acetate in hexanes as the eluent. The purified product, **3ae**, identified as Methyl (*5R,7S,8R,14S*)-1,12-dimethyl-4,9-dioxo-3,10-diphenyl-7-(thiophen-2-yl)-6-oxa-2,3,10,11-tetraazadispiro [4.2.48.25] tetradeca-1,11-diene-14-carboxylate, was obtained as a light yellow solid in a yield of 67 mg (62%) as a single diastereomer. The structure was confirmed through spectroscopic methods, including ^{1}H NMR, ^{13}C{^{1}H} NMR, HRMS, and X-ray crystallographic analysis. The compound displayed a melting point of 222-224 °C and a TLC retention factor (R_f) of 0.4 (silica gel, 30% ethyl acetate/hexanes). ^{1}H NMR (400 MHz, $CDCl_3$): δ 7.9 – 7.8 (m, 2H), 7.8 – 7.7 (m, 2H), 7.4 (dtd, *J* = 14.5, 7.4, 1.9 Hz, 4H), 7.2 – 7.1 (m, 3H), 6.9 – 6.8 (m, 2H), 6.4 (d, *J* = 0.9 Hz, 1H), 3.7 (s, 3H), 3.5 – 3.4 (m, 2H), 2.5 (s, 3H), 2.3 (s, 3H), 2.3 – 2.2 (m, 1H). ^{13}C{^{1}H} NMR (100 MHz,

$CDCl_3$): δ 171.5, 169.0, 168.7, 159.4, 156.7, 137.5, 137.4, 137.3, 128.9, 128.9, 126.8, 125.4, 125.4, 125.3, 125.0, 119.1, 119.0, 77.7, 72.2, 57.9, 52.9, 39.6, 26.8, 19.3, 13.0. HRMS (ESI TOF) *m/z* calcd. For $C_{29}H_{26}N_4O_5S$ $[M+H]^+$ 543.1702 found 543.1700.

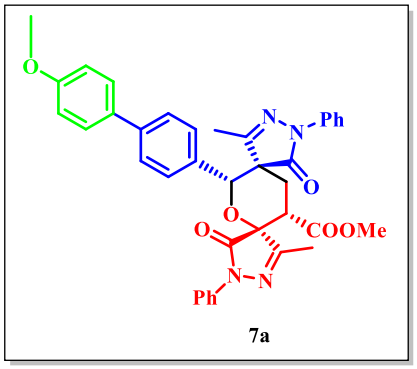
Methyl (*5R,7S,8R,14S*)-1,12-dimethyl-4,9-dioxo-3,10-diphenyl-7-(thiophen-3-yl)-6-oxa-2,3,10,11-tetraazadispiro[4.2.48.25]tetradeca-1,11-diene-14-carboxylate (3af)



3af

Product **3af** was synthesized following the general experimental procedure **4.5.4**. An oven-dried 10 mL glass reaction tube was charged with pyrazoledione-derived Morita–Baylis–Hillman (Pyro-MBH) alcohol **1a** (1.0 equiv, 0.2 mmol) potassium tert-butoxide (50 mol%, 0.1 mmol), and arylidene pyrazolones **2aa** (1.0 equiv, 0.2 mmol). Subsequently, 1,4-Dioxane (1 mL) was added to the tube. The reaction mixture was stirred at ambient temperature for 2 minute. Upon completion, the solvent was removed under reduced pressure, and the residue was purified by column chromatography on silica gel using 25% ethyl acetate in hexanes as the eluent. The purified product, **3af**, identified as Methyl (*5R,7S,8R,14S*)-1,12-dimethyl-4,9-dioxo-3,10-diphenyl-7-(thiophen-3-yl)-6-oxa-2,3,10,11-tetraazadispiro [4.2.48.25] tetradeca-1,11-diene-14-carboxylate, was obtained as a white solid in a yield of 77 mg (71%) as a single diastereomer. The structure was confirmed through spectroscopic methods, including ^{1}H NMR, $^{13}C\{^1H\}$ NMR, HRMS, and X-ray crystallographic analysis. The compound displayed a melting point of 228-230 °C and a TLC retention factor (R_f) of 0.4 (silica gel, 30% ethyl acetate/hexanes). ^{1}H NMR (400 MHz, $CDCl_3$): δ 7.9 (dt, *J* = 8.7, 1.2 Hz, 4H), 7.5 – 7.4 (m, 4H), 7.3 – 7.2 (m, 3H), 7.1 (dt, *J* = 2.8, 1.2 Hz, 1H), 6.7 (dd, *J* = 5.1, 1.4 Hz, 1H), 6.1 (d, *J* = 1.1 Hz, 1H), 4.3 (dd, *J* = 12.2, 5.2 Hz, 1H), 3.6 (s, 3H), 2.5 – 2.3 (m, 2H), 2.3 (s, 3H), 2.0 (s, 3H). $^{13}C\{^1H\}$ NMR (100 MHz, $CDCl_3$): δ 173.6, 170.6, 169.7, 161.1, 156.9, 137.6, 137.5, 136.2, 129.0, 129.0, 126.7, 125.5, 125.4, 123.7, 120.8, 118.9, 118.7, 79.9, 73.4, 57.2, 52.8, 38.8, 25.4, 14.8, 14.7. HRMS (ESI TOF) *m/z* calcd. For $C_{29}H_{26}N_4O_5S$ $[M+H]^+$ 543.1702 found 543.1710.

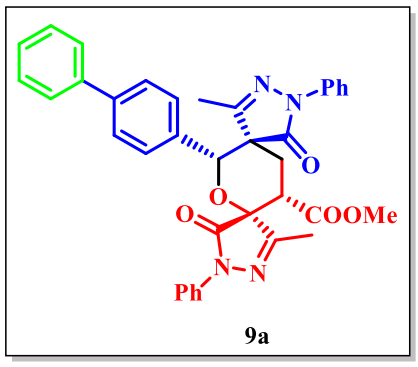
Methyl (*5R,7R,8R,14S*)-7-(4'-methoxy-[1,1'-biphenyl]-4-yl)-1,12-dimethyl-4,9-dioxo-3,10-diphenyl-6-oxa-2,3,10,11-tetraazadispiro[4.2.48.25]tetradeca-1,11-diene-14-carboxylate (7a)



7a

Product **7a** was synthesized following the general procedure **4.5.6** A solution of compound **3k** (1.0 equiv, 0.81 mmol) in a mixture of toluene (1 mL) and water (0.3 mL) was prepared at room temperature. Methoxy phenylboronic acid **6a** (1.5 equivs, 0.12 mmol), $Pd(PPh_3)_4$ (0.06 equiv, 0.005 mmol), and K_3PO_4 (2.5 equiv, 0.20 mmol) were added sequentially under a nitrogen atmosphere. The reaction mixture was heated to 80 °C and stirred at this temperature for 12 hours. Upon completion, the reaction was cooled to room temperature and passed through a Celite bed for filtration. The filtrate was concentrated under reduced pressure to remove the solvent. The resulting crude product was purified by column chromatography on silica gel using 22% ethyl acetate in hexanes as the eluent, affording product **7a** as a white solid (36 mg, 69% yield, single diastereomer). The structure of **7a**, identified as methyl (*5R,7R,8R,14S*)-7-(4'-methoxy-[1,1'-biphenyl]-4-yl)-1,12-dimethyl-4,9-dioxo-3,10-diphenyl-6-oxa-2,3,10,11-tetraazadispiro[4.2.4^2.2^5]tetradeca-1,11-diene-14-carboxylate, was confirmed by ^{1}H NMR, $^{13}C\{^1H\}$ NMR, and HRMS analyses. The compound exhibited a melting point of 178–180 °C and a TLC retention factor (R_f) value of 0.4 (30% ethyl acetate in hexanes on silica gel). ^{1}H NMR (400 MHz, $CDCl_3$): δ 7.9 – 7.8 (m, 4H), 7.5 – 7.4 (m, 8H), 7.2 – 7.1 (m, 4H), 7.0 – 6.9 (m, 2H), 6.1 (s, 1H), 4.3 (dd, *J* = 10.5, 6.8 Hz, 1H), 3.8 (s, 3H), 3.6 (s, 3H), 2.5 – 2.4 (m, 2H), 2.3 (s, 3H), 2.0 (s, 3H). $^{13}C\{^1H\}$ NMR (100 MHz, $CDCl_3$): δ 173.9, 170.5, 169.8, 160.9, 159.3, 157.0, 140.7, 137.6, 137.5, 133.8, 132.8, 129.0, 129.0, 128.0, 126.6, 125.5, 125.4, 124.6, 119.1, 118.7, 114.2, 79.9, 75.0, 57.9, 55.4, 52.8, 38.8, 25.6, 15.1, 14.7. HRMS (ESI TOF) *m/z* calcd. For $C_{38}H_{34}N_4O_6$ $[M+Na]^+$ 665.2375 found 665.2374.

Methyl (*5R,7R,8R,14S*)-7-([1,1'-biphenyl]-4-yl)-1,12-dimethyl-4,9-dioxo-3,10-diphenyl-6-oxa-2,3,10,11-tetraazadispiro[4.2.48.25]tetradeca-1,11-diene-14-carboxylate (9a)



9a

Product **9a** was synthesized following the general procedure **4.5.7** A solution of compound **3k** (1.0 equiv, 0.81 mmol) in a mixture of toluene (1 mL) and water (0.3 mL) was prepared at room temperature. phenylboronic acid **8a** (1.5 equiv, 0.12 mmol), $Pd(PPh_3)_4$ (0.06 equivs, 0.005 mmol), and K_3PO_4 (2.5 equivs, 0.20 mmol) were added sequentially under a nitrogen atmosphere. The reaction

mixture was heated to 80 °C and stirred at this temperature for 12 hours. Upon completion, the reaction was cooled to room temperature and passed through a Celite bed for filtration. The filtrate was concentrated under reduced pressure to remove the solvent. The resulting crude product was purified by column chromatography on silica gel using 18% ethyl acetate in hexanes as the eluent, affording product **9a** as a white solid (32 mg, 64% yield, single diastereomer). The structure of **9a**, identified as Methyl (*5R,7R,8R,14S*)-7-([1,1'-biphenyl]-4-yl)-1,12-dimethyl-4,9-dioxo-3,10-diphenyl-6-oxa-2,3,10,11 tetraazadispiro[4.2.48.25]tetradeca-1,11-diene-14-carboxylate, was confirmed by ^{1}H NMR, ^{13}C{^{1}H} NMR, and HRMS analyses. The compound exhibited a melting point of 222–224 °C and a TLC retention factor (R_f) value of 0.5 (30% ethyl acetate in hexanes on silica gel). ^{1}H NMR (400 MHz, $CDCl_3$): δ 7.9 (tt, *J* = 8.6, 1.2 Hz, 4H), 7.6 – 7.5 (m, 2H), 7.5 – 7.4 (m, 8H), 7.3 (s, 1H), 7.2 – 7.1 (m, 4H), 6.1 (s, 1H), 4.3 (dd, *J* = 10.7, 6.7 Hz, 1H), 3.6 (s, 3H), 2.5 – 2.4 (m, 2H), 2.3 (s, 3H), 2.0 (s, 3H). ^{13}C{^{1}H} NMR (100 MHz, $CDCl_3$): δ 173.9, 170.5, 169.8, 160.8, 157.0, 141.1, 140.3, 137.6, 137.5, 134.5, 129.0, 129.0, 128.8, 127.5, 127.0, 127.0, 125.5, 125.4, 124.7, 119.1, 118.7, 79.9, 74.9, 57.9, 52.8, 38.8, 25.6, 15.1, 14.7. HRMS (ESI TOF) *m/z* calcd. For $C_{37}H_{32}N_4O_5$ $[M+Na]^+$ 635.2270 found 635.2269.

4.7 Appendix IV ^{1}H, ^{13}C spectral data of representative compounds

Compound No.	Figure AII.X	Data	Page No
1a	Figure AIV.1 and AIV.2	^{1}H and ^{13}C	163
3a	Figure AIV.3 and AIV.4	^{1}H and ^{13}C	164
3e	Figure AIV.5 and AIV.6	^{1}H and ^{13}C	165
3aa	Figure AIV.7 and AIV.8	^{1}H and ^{13}C	166
3ab	Figure AIV.9 and AIV.10	^{1}H and ^{13}C	167
7a	Figure AIV.11 and AIV.12	ORTEP plot	168
3a	Figure AII.13	ORTEP plot	169

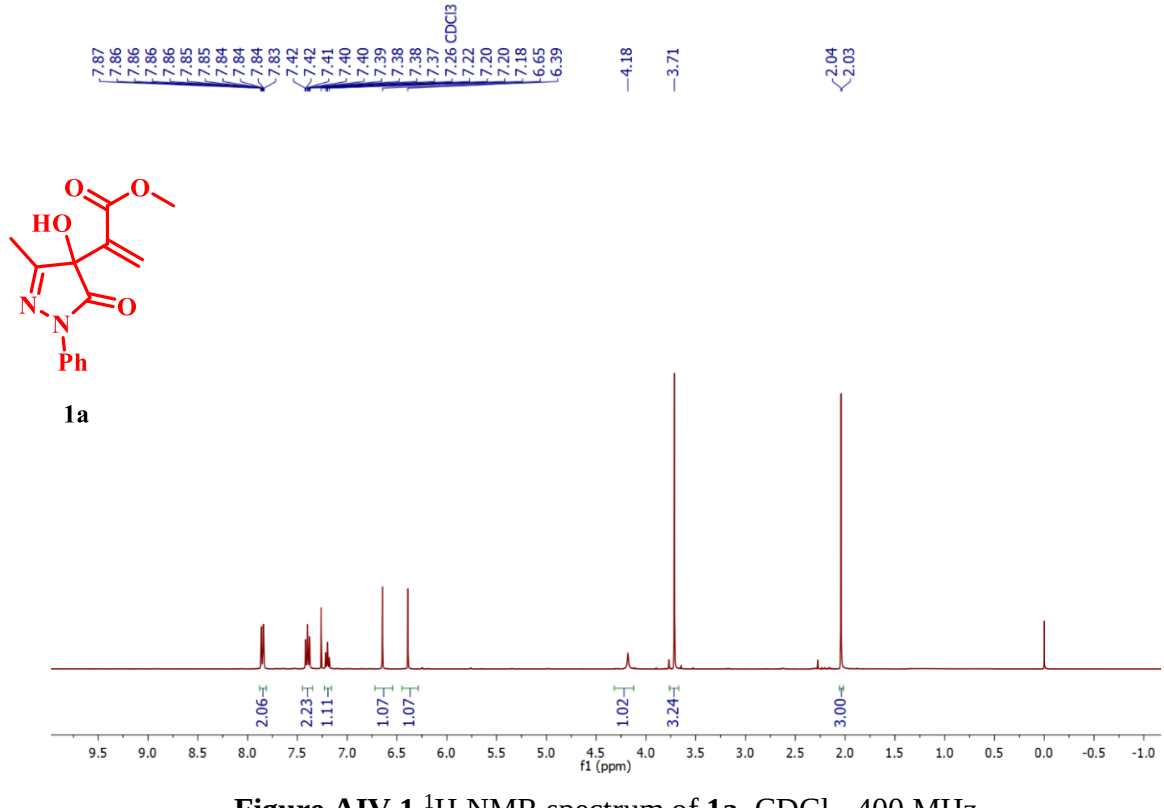


Figure AIV.1 ^{1}H NMR spectrum of **1a**, $CDCl_3$, 400 MHz

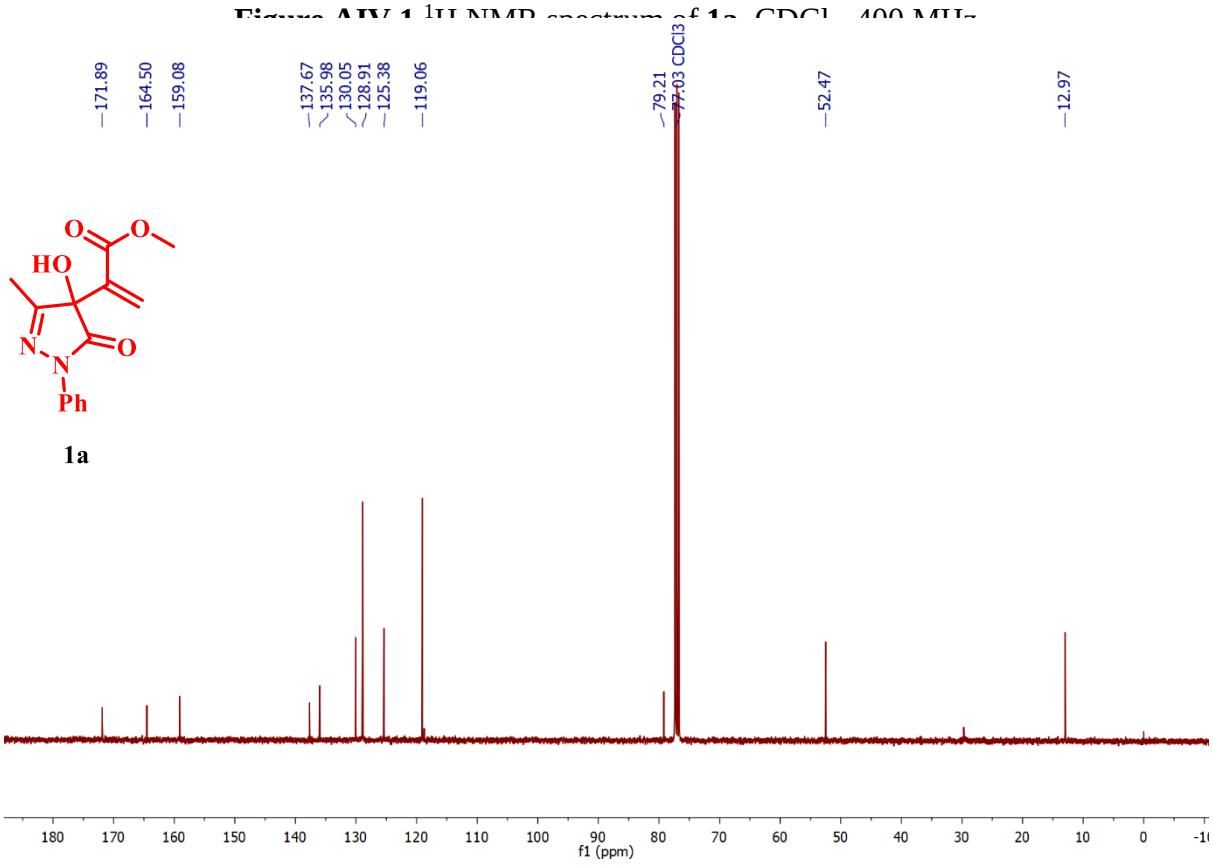


Figure AIV.2 $^{13}C\{^{1}H\}$ NMR spectrum of **1a**, $CDCl_3$, 100 MHz

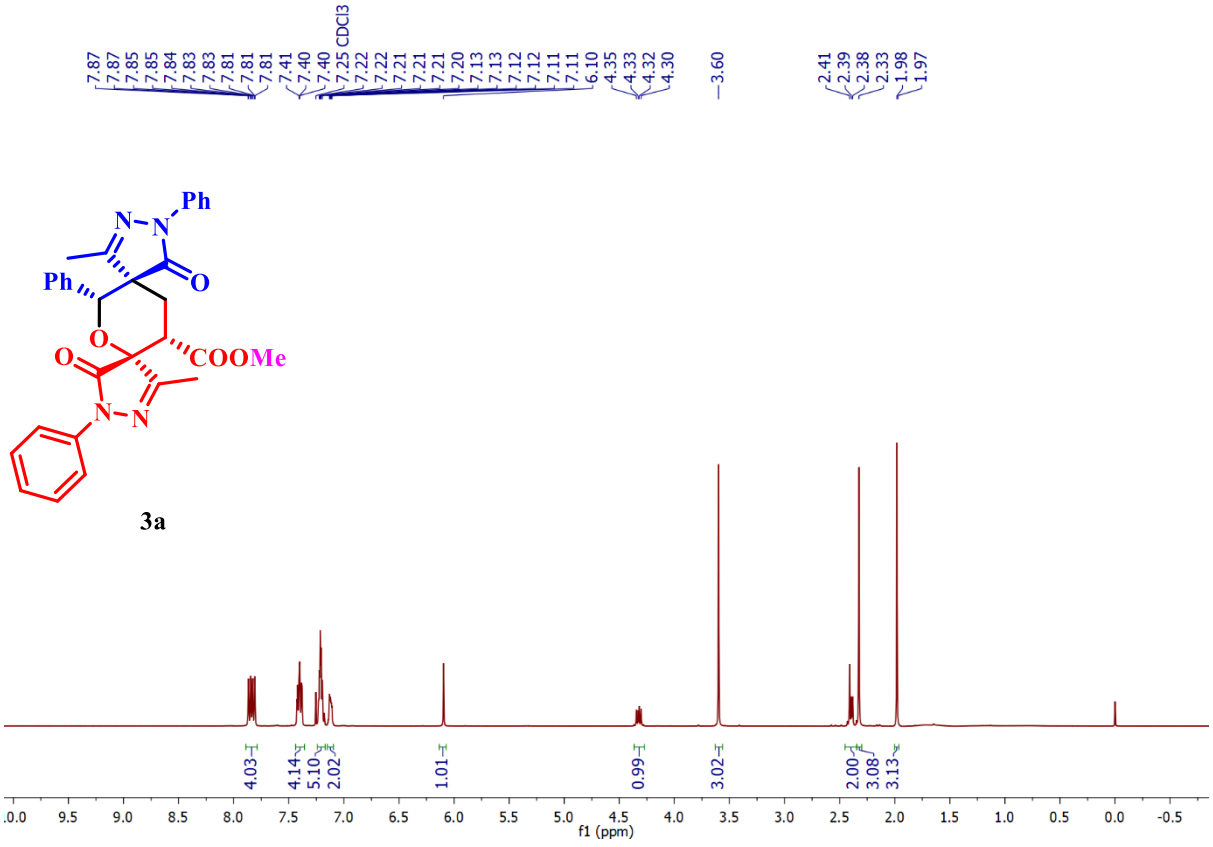


Figure AIV.3 ^{1}H NMR spectrum of **3a**, $CDCl_3$, 400 MHz

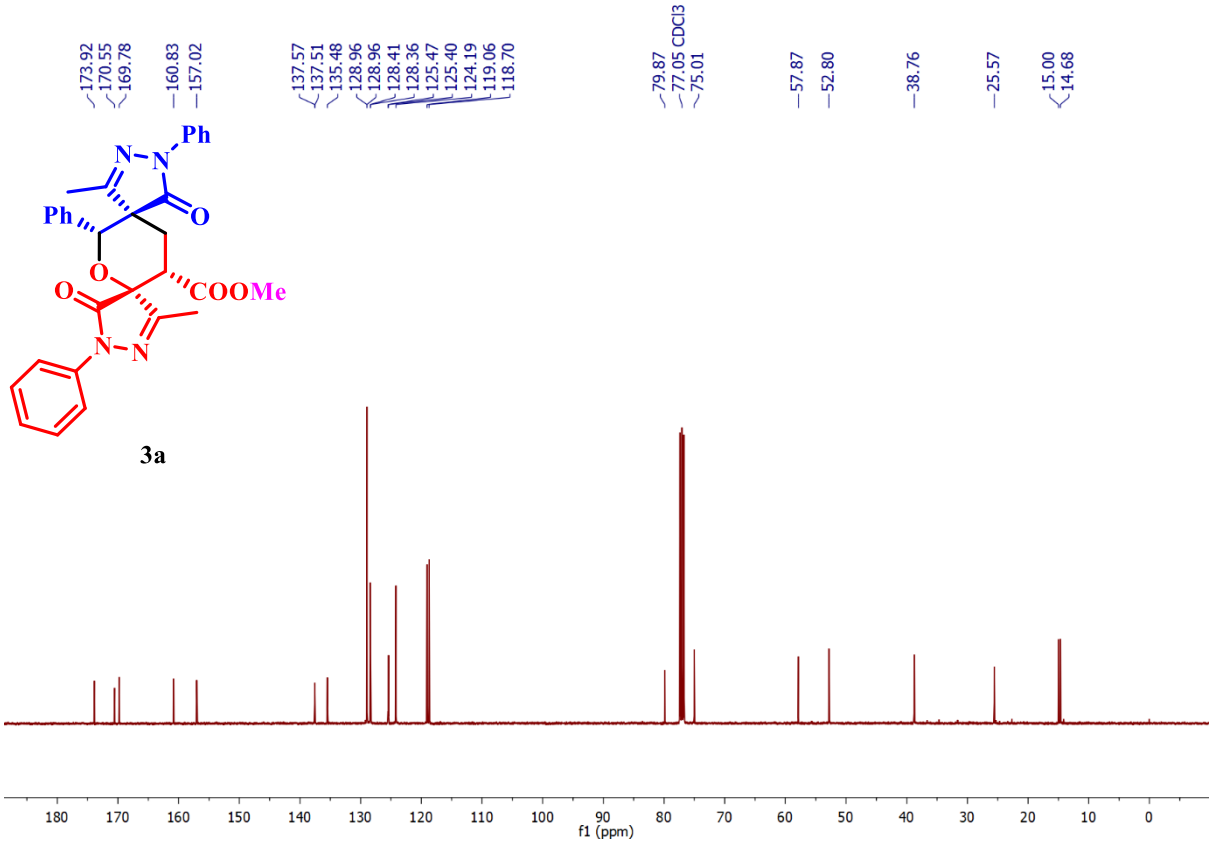


Figure AIV.4 $^{13}C\{^{1}H\}$ NMR spectrum of **3a**, $CDCl_3$, 100 MHz

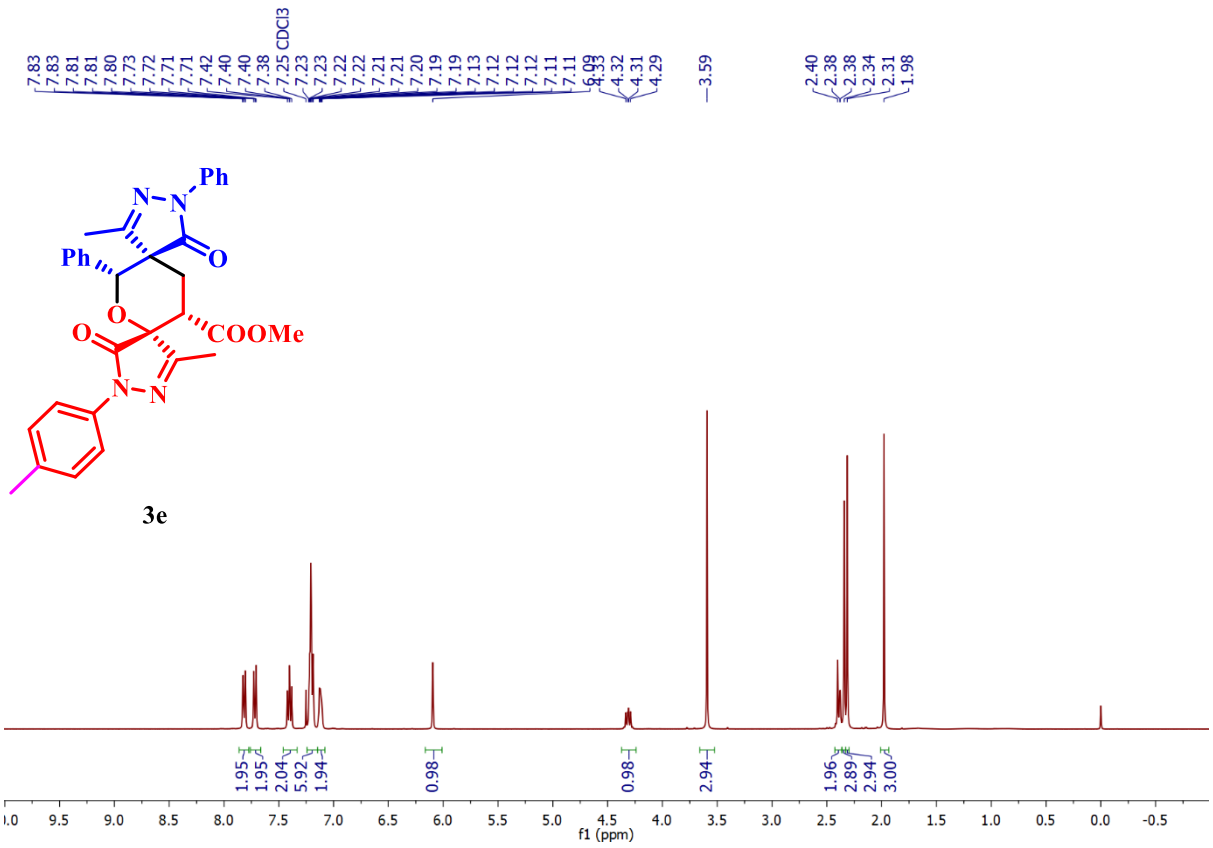


Figure AIV.5 ^{1}H NMR spectrum of **3e**, $CDCl_3$, 400 MHz

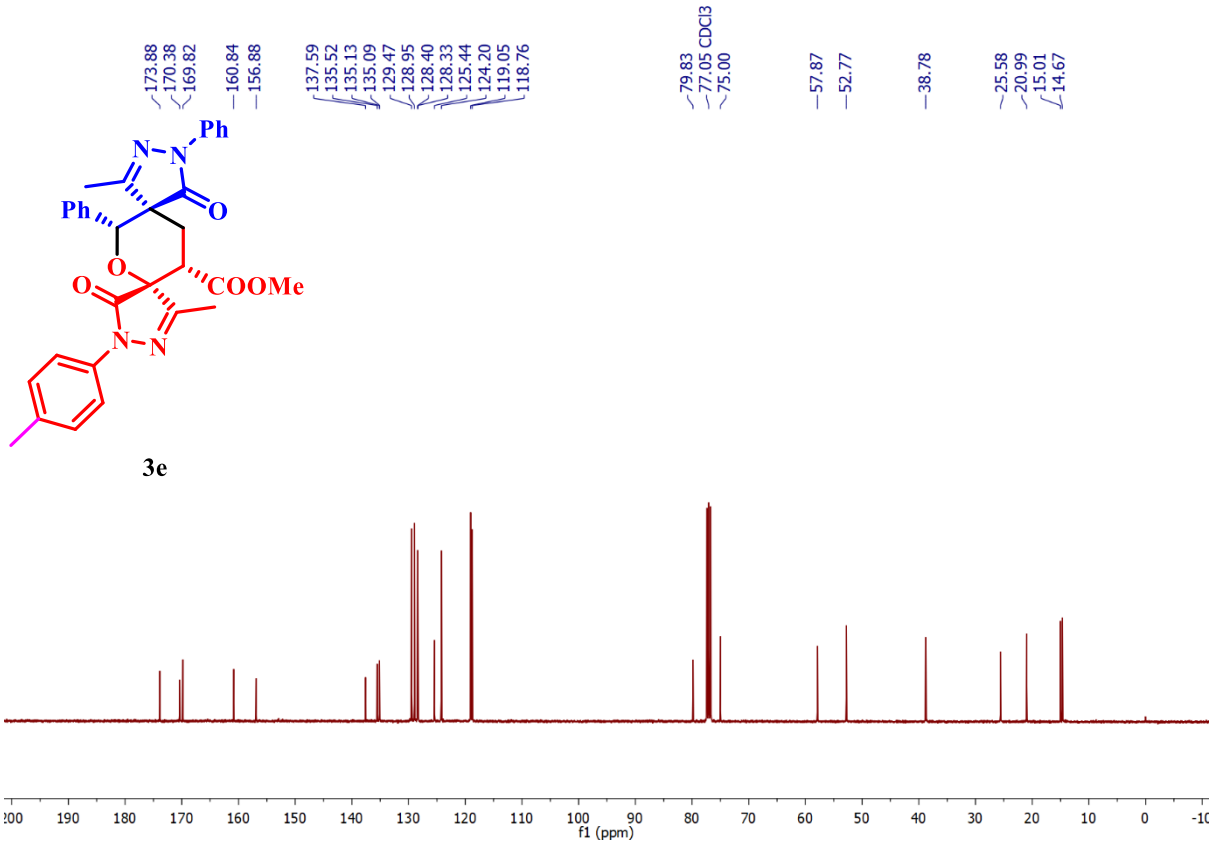


Figure AIV.6 ^{13}C{^{1}H} NMR spectrum of **3e**, $CDCl_3$, 100 MHz

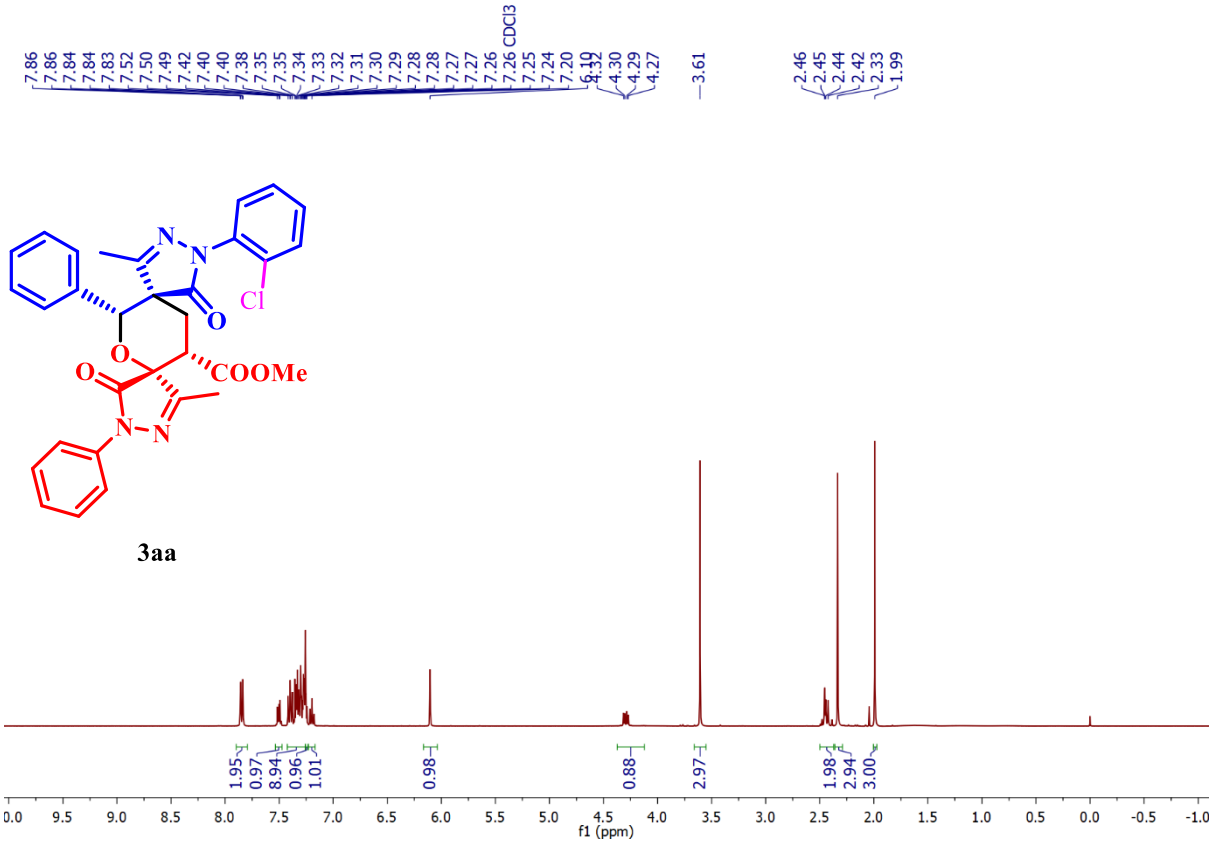


Figure AIV.7 ^{1}H NMR spectrum of **3aa**, $CDCl_3$, 400 MHz

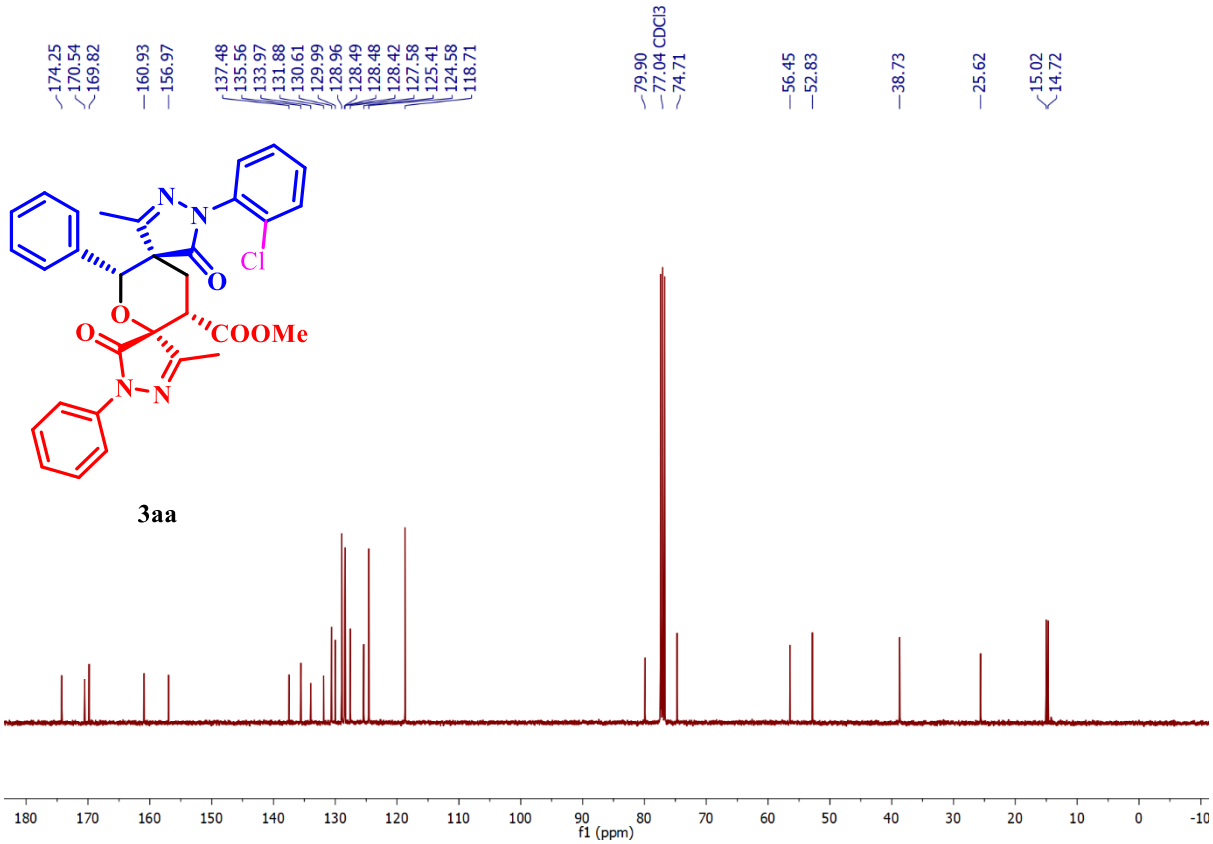


Figure AIV.8 $^{13}C\{^{1}H\}$ NMR spectrum of **3aa**, $CDCl_3$, 100 MHz

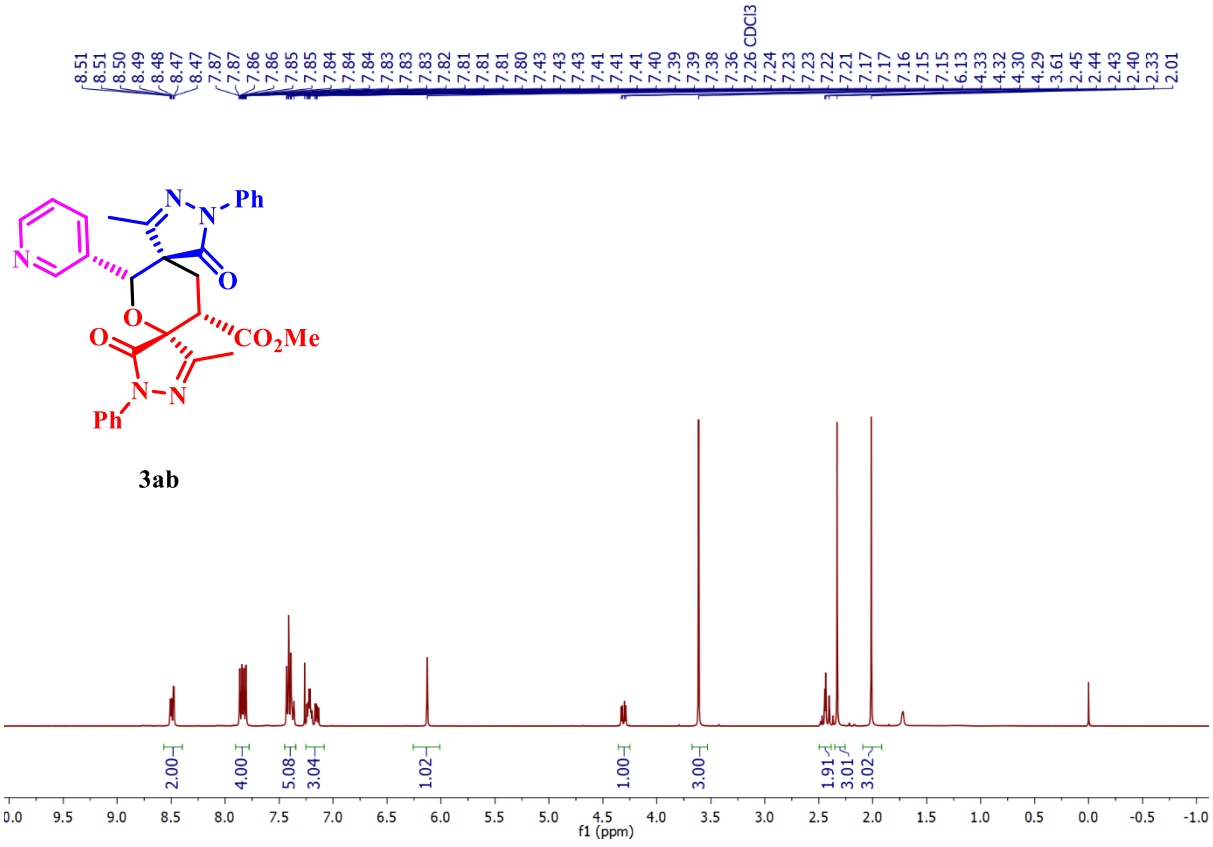


Figure AIV.9 ^{1}H NMR spectrum of **3ab**, $CDCl_3$, 400 MHz

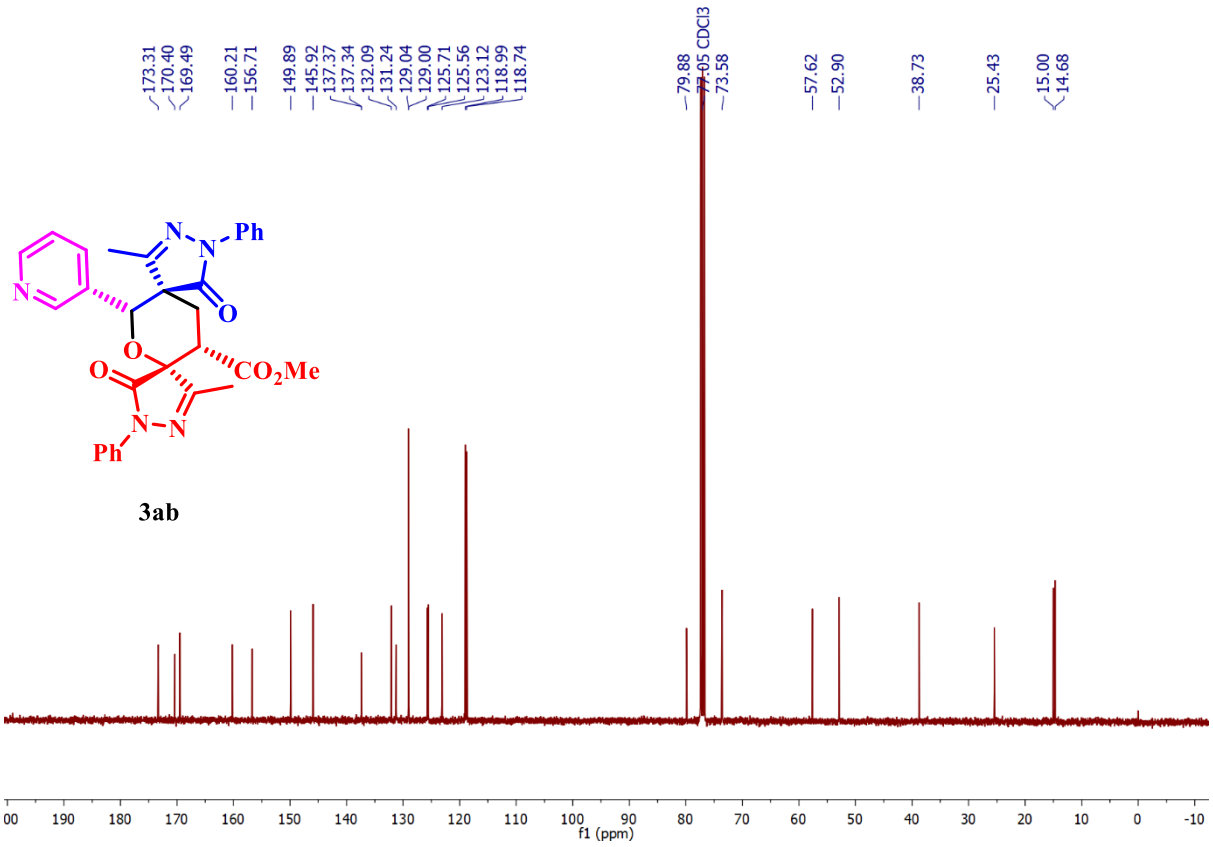


Figure AIV.10 $^{13}C\{^{1}H\}$ NMR spectrum of **3ab**, $CDCl_3$, 100 MHz

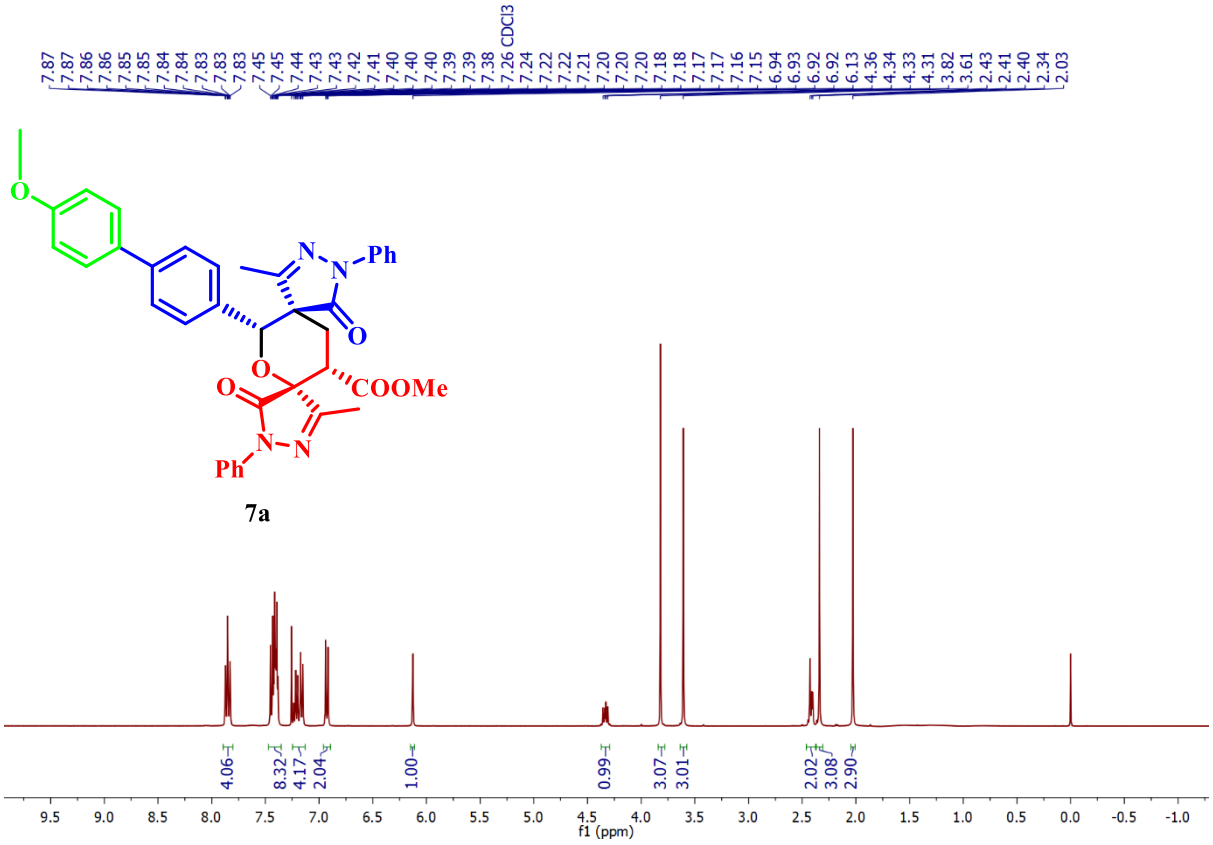


Figure AIV.11 ^{1}H NMR spectrum of **7a**, $CDCl_3$, 400 MHz

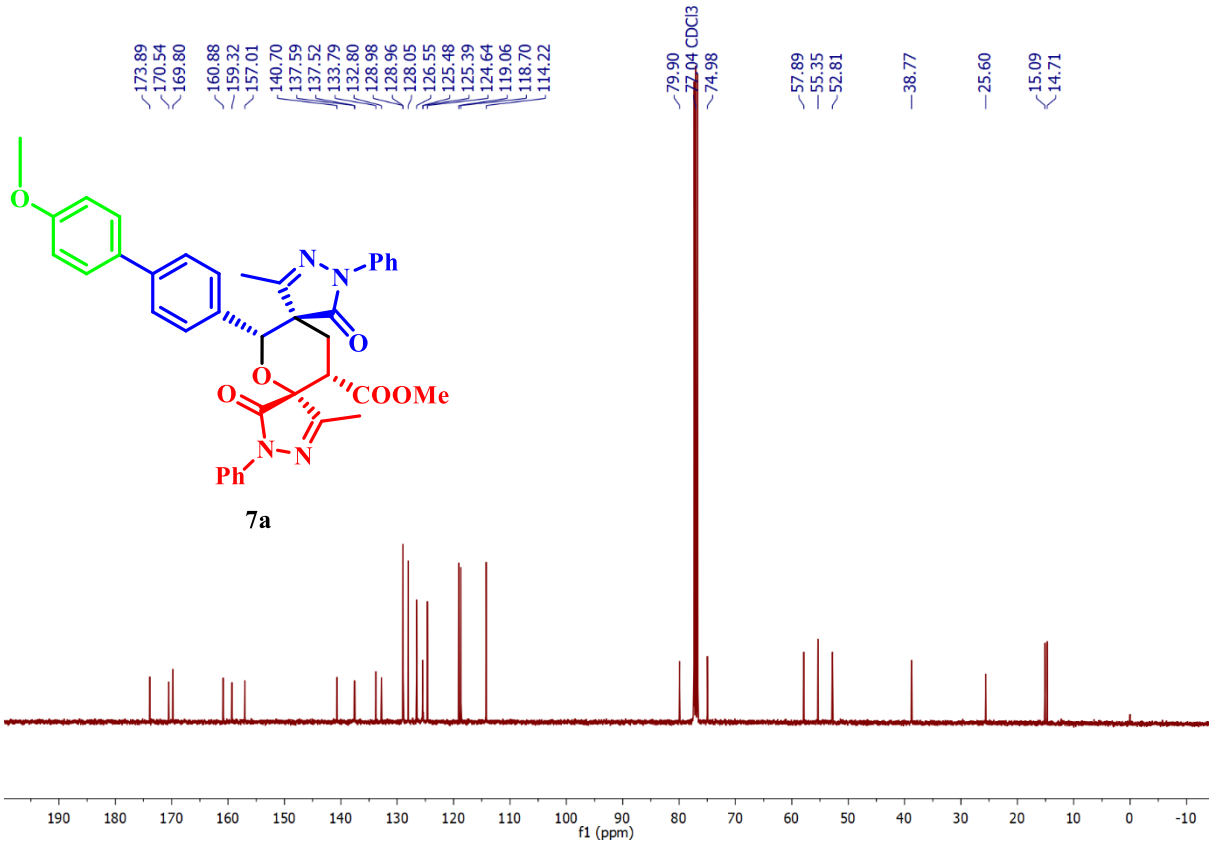


Figure AIV.12 $^{13}C\{^{1}H\}$ NMR spectrum of **7a**, $CDCl_3$, 100 MHz

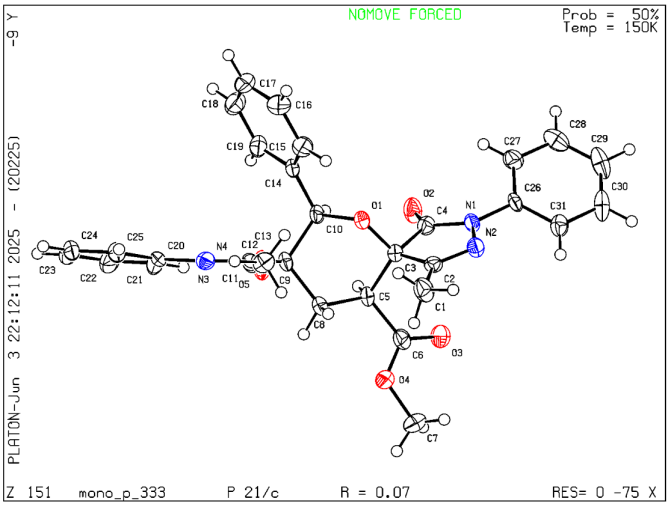


Figure AIV.13 An ORTEP diagram showing thermal ellipsoids at a 50% probability level was created to represent the structures determined by single-crystal X-ray diffraction analysis of compound **3a**.

4.8 References

1. (a) Basavaiah, D.; Rao, A. J.; Satyanarayana, T. *Chem. Rev.* **2003**, *103*, 811. (b) Ma, G.-N.; Jiang, J.-J.; Shi, M.; Wei, Y. *Chem. Commun.* **2009**, *37*, 5496. (c) Basavaiah, D.; Reddy, B. S.; Badsara, S. S. *Chem. Rev.* **2010**, *110*, 5447.
2. (a) Liao, J.; Xu, J.; Wu, Y.; Hou, Y.; Guoa, H. *Adv. Synth. Catal*. **2022**, *364*, 1074. (b) Tian, Z.; Jiang, J.; Yan, Z.-H.; Luo, Q.-Q.; Zhan, G.; Huang, W.; Li, X.; Han, B. *Chem. Commun.* **2022**, *58*, 5363. (c) Sabale, A. S.; Warghude, P. K.; Bhat, R. G. *Synlett* **2023**, *34*, 1732. (d) Yang, M.; Xue, A.; Wei, X.; Huang, Y.; Qu, J.; Wang, B. *Eur. J. Org. Chem.* **2024**, *27*, e202400305.
3. (a) Pavankumar, Y.; Anwar, S. *RSC Adv.* **2022**, *12*, 34634. (b) Li, G.; Zhang, H.; Zhang, G.; Wei, B.; Liu, B.; Song, H.; Li, Q.; Ban, S. *J. Org. Chem.* **2023**, *88*, 4809. (c) Gond, M. R. Maddani, K. K. *New J. Chem.* **2024**, *48*, 8667.
4. Zhao, Z.; Dai, X.; Li, C.; Wang, X.; Tian, J.; Feng, Y.; Xie, J.; Ma, C.; Nie, Z.; Fan, P.; Qian, M. He, X.; Wu, S.; Zhang, Y.; Zheng, X. *Eur. J. Med. Chem.* **2020**, *186*, 111893.
5. Karrouchi, K.; Radi, S.; Ramli, Y.; Taoufik, J.; Mabkhot, Y. N.; Al-aizari, F. A.; Ansar, M. *Molecules*, **2018**, *23*, 134.
6. (a) Li, Q.-M.; Luo, J.-G.; Zhao, H.-J.; Yu, W.-Y.; Wang, X.-B.; Yang, M.-H.; Luo, J.; Sun, H.-B.; Chen, Y.-J.; Guo, Q.-L.; Kong, L.-Y. *Asian J. Org. Chem.* **2015**, *4*, 1366.

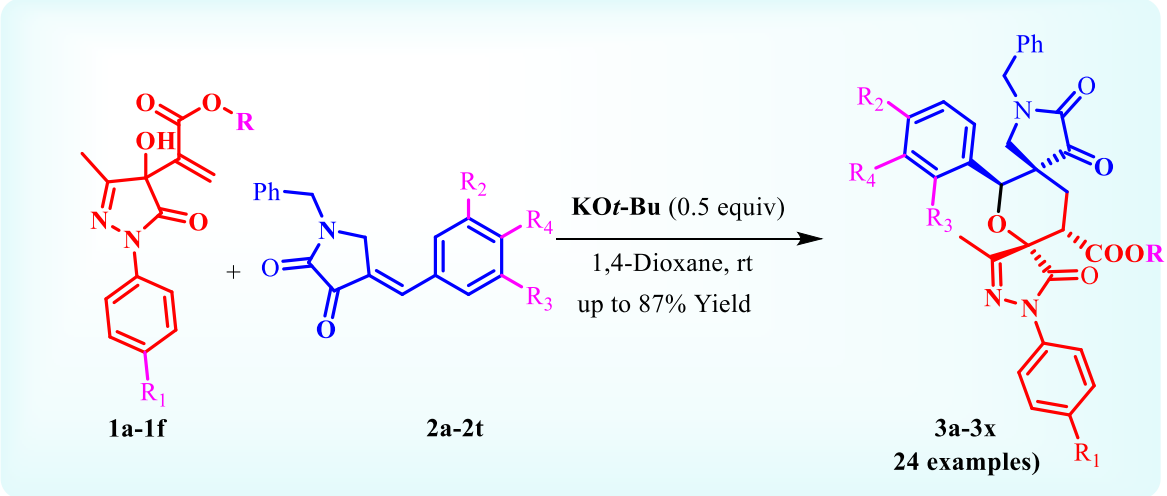
(b) Chen, N.; Zhu, L.; Gan, L.; Liu, Z.; Wang, R.; Cai X.; Jiang, X. *Eur. J. Org. Chem.* **2018**, *23*, 2939. (c) Warghude, P. K.; Sabale, A. S.; Dixit, R.; Vanka, R.; Bhat, R. G. *Org. Biomol. Chem.* **2021**, *19*, 4338. (d) Warghude, P. K.; Sabale, A. S.; Bhat, R. G. *Org. Biomol. Chem.* **2020**, *18*, 1794.

7. Wang, B.; Peng, F.; Huang, W.; Zhou, J.; Zhang, N.; Sheng, J.; Haruehanroengra, P.; He, G.; Han, B. *Acta Pharm. Sin. B* **2020**, *10*, 1492.
8. Cui, B.-D.; Li, S.-W.; Zuo, J.; Wu, Z.-J.; Zhang X.-M.; Yuan, W.-C. *Tetrahedron*, **2014**, *70*, 1895.
9. CCDC 2465972 (Compound **3a**) contains the crystallographic data. The Cambridge Crystallographic Data Centre can obtain these data free of charge.
10. (a) Pearson, D. E.; Buehler, C. A. *Chem. Rev.* **1974**, *74*, 45. (b) Madasu, J.; Shinde, S.; Das, R.; Patel, S.; Shard, A. *Org. Biomol. Chem.* **2020**, *18*, 8346. (c) Dub, P. A.; Tkachenko, N. V. *J. Phys. Chem. A.* **2021**, *125*, 5726.

5 Efficient Synthesis of Spiropyrazolone Pyrrolidinediones Fused Tetrahydropyran via Base-Induced [4+2] Cycloaddition

Abstract

A novel and efficient metal-free oxa-Michael cascade [4+2] annulation strategy has been established for the direct synthesis of spiropyrazolone pyrrolidinedione fused tetrahydropyran framework. This atom-economic transformation utilizes pyrazoledione-derived Morita–Baylis–Hillman (Pyro-MBH) alcohol as specialized oxa-Michael donors, facilitating the construction of structurally complex spiroheterocyclic products with remarkable stereocontrol. Notably, the reaction generates two contiguous tertiary and two quaternary stereocenters in a single step, delivering the desired products in excellent yields of up to 87%. The protocol exhibits a rapid conversion rate, completing in a very short reaction time (5–20 min) under mild reaction conditions.



Sabale, A. S.; Khandeparkar, M.; Pattanaik, S.; Bhat. R. G Efficient Synthesis of Spiropyrazolone Pyrrolidinediones Fused Tetrahydropyran via Base-Induced [4+2] Cycloaddition, *Manuscript under preparation.*

5 Efficient Synthesis of Spiropyrazolone Pyrrolidinediones Fused Tetrahydropyran via Base-Induced [4+2] Cycloaddition

5.1 Introduction

Spiropyrazolone is a significant structural motif that has garnered attention in pharmaceutical and medicinal chemistry due to its diverse range of applications in drug development. Characterized by its unique bicyclic structure, spiropyrazolone has become integral to the design of various biologically active compounds. This structural framework is frequently found in various therapeutic agents, particularly those targeting cancer, where it demonstrates potential as an anti-tumor agent.[1] Additionally, spiropyrazolone derivatives have shown efficacy as inhibitors against specific phosphodiesterases, including type-4 phosphodiesterases, which are crucial in regulating cellular signalling pathways.[2] Moreover, some spiropyrazolone compounds have been identified as inhibitors of TbrPDEB1, an enzyme implicated in the pathology of certain diseases.[3] The ability of spiropyrazolone to interact with biological systems underscores its versatility and importance in developing novel therapeutic strategies. Its presence in drugs that combat a range of conditions highlights the significance of this structural motif in contemporary medicinal chemistry.[4]

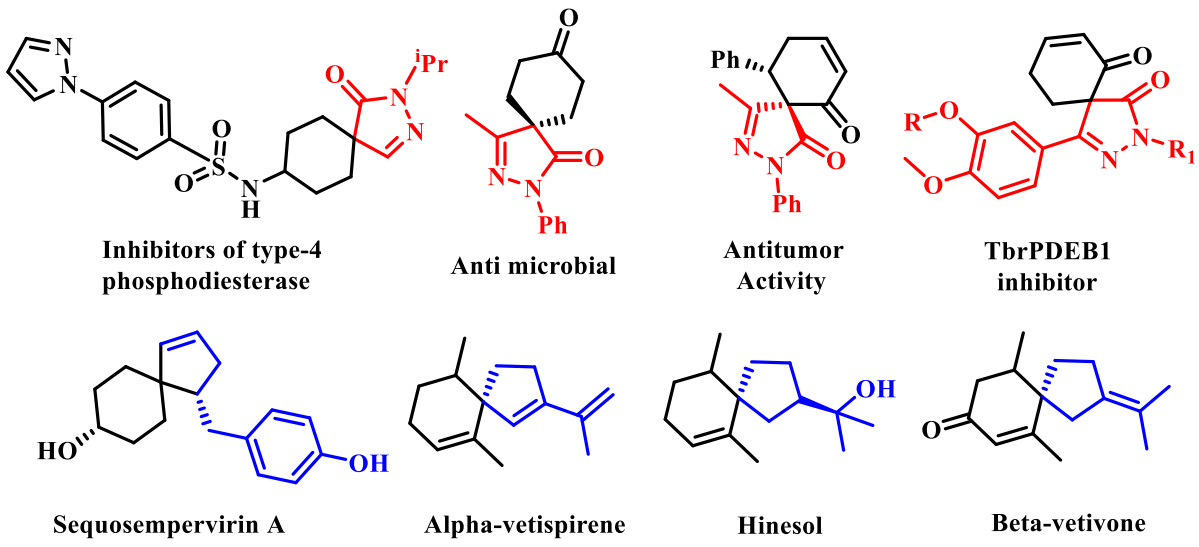


Figure 5.1 Bioactive molecules containing spiropyrazolone and spiropyrrolidinediones skeletone

Likewise, the spiropyrrolidinediones scaffold is a prominent structural motif frequently encountered in biologically active molecules. Based on the available literature, its presence

imparts significant pharmacological properties due to its rigid, cyclic framework, which facilitates selective interactions with biological targets. Spiropyrrolidinediones-containing compounds exhibit a broad spectrum of bioactivities, including anticancer, antimicrobial, antiviral, and anti-inflammatory effects. Furthermore, the scaffold's conformational restriction often enhances receptor binding affinity and metabolic stability. As a result, spiropyrrolidinediones derivatives serve as essential building blocks in the design and development of therapeutic agents across various therapeutic domains (see Figure 5.1).[5] As a result, the design and development of novel synthetic methods for constructing spiro-pyrazolone fused pyrrolidinediones frameworks has emerged as a highly appealing and useful topic within the synthetic research community.

Base-mediated annulation reactions serve as highly efficient synthetic methodologies for the construction of spiropyrazole scaffolds. These transformations facilitate the formation of structurally intricate frameworks through regioselective and stereoselective bond-forming processes. Their utility in modern organic synthesis is underscored by their ability to generate complex molecular architectures with significant pharmaceutical and biological relevance.[2, 6]

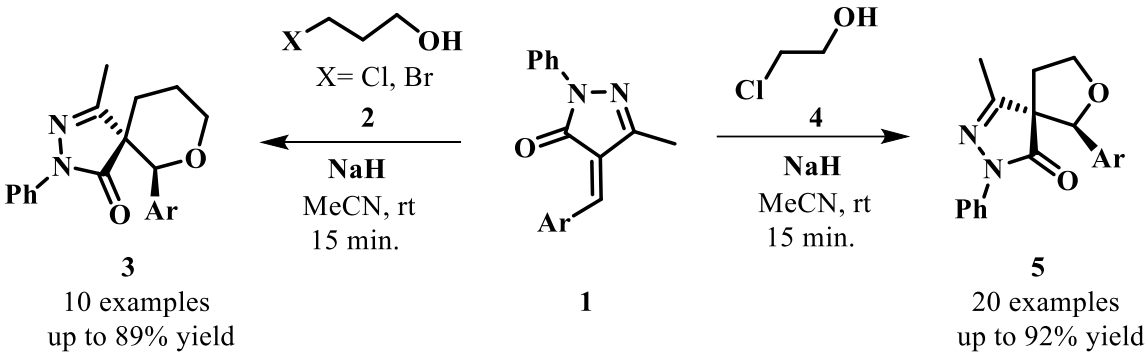
The incorporation of a spiropyrazolone moiety into a spiropyrrolidinediones framework represents a compelling synthetic approach, given the increasing interest in hybrid molecular architectures. In recent years, the fusion of distinct pharmacologically significant scaffolds has emerged as a highly effective strategy for the rational design and development of novel bioactive compounds. This approach leverages individual core structures' synergistic biological properties, enhancing their therapeutic potential and broadening their applicability in drug discovery.[7] Considering this perspective, the integration of spiropyrazolones and spiropyrrolidinones frameworks presents a highly promising strategy for synthesizing structurally diverse and architecturally intriguing spiro-heterocyclic compounds. This approach holds significant potential for discovering novel bioactive molecules, as these hybrid structures may exhibit enhanced pharmacological properties. The rational design of these fused scaffolds not only expands the chemical space of spirocyclic systems but also facilitates the identification of lead compounds with improved therapeutic efficiency.

5.2 Recent advances in the synthesis of spiropyrazolone and spiropyrrolidinediones scaffolds

Spiropyrazolone and spiropyrrolidinediones, both naturally derived and synthetically engineered, exhibit a broad spectrum of significant biological activities. Due to their

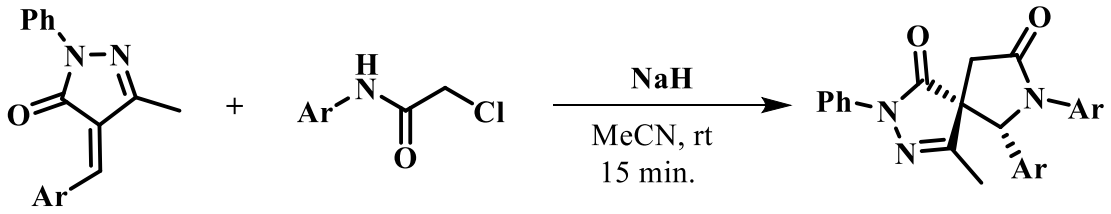
pharmacological relevance, extensive research efforts have been directed toward the construction of these spirocyclic frameworks with high regio-, diastereo-, and enantioselectivity over the past few decades. Various advanced methodologies have been developed for the efficient synthesis of spiropyrazolone and spiropyrrolidinones; some of the representative examples are highlighted.

In 2024, Maddani and coworkers[8] introduced an efficient approach for the synthesis of spiropyrazolone-tetrahydrofurans **3** and spiropyrazolone-tetrahydropyrans **5** through a base-mediated cascade *ipso*-cyclization of unsaturated pyrazolones **1** with haloalcohols **2** and **4** (Scheme 5.1). This strategy is distinguished by its rapid reaction kinetics, broad substrate scope, excellent product yields, and mild reaction conditions, eliminating the requirement for any transition metal catalysts. Furthermore, the synthetic utility of this methodology was validated on a gram scale, demonstrating its practicality while maintaining high product yields.



Scheme 5.1 Synthesis of spiropyrazolone-tetrahydrofurans and spiropyrazolone-tetrahydropyrans via base-mediated cyclization reaction

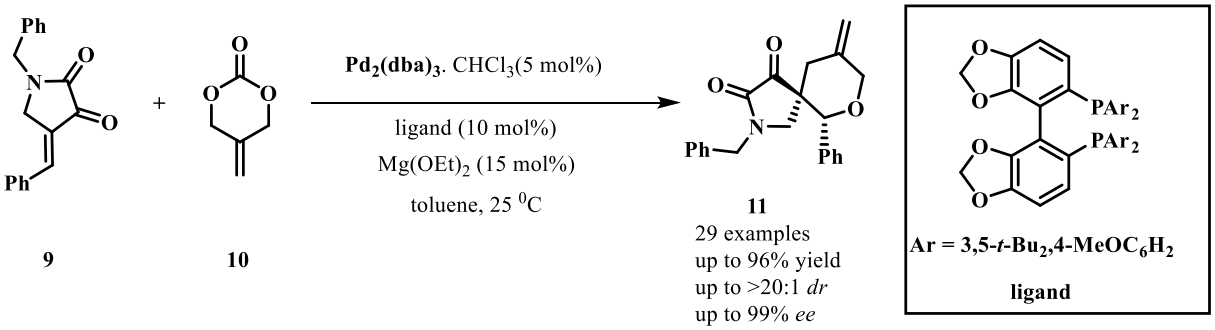
In 2024, Maddani and coworkers[9] developed an efficient and practical strategy for the synthesis of spiropyrazolone–pyrrolidinones **8** through a NaH-mediated cascade *ipso*-cyclization of unsaturated pyrazolones **6** with 2-chloro-N-phenylacetamides **7**. This transition metal-free approach enables the construction of highly functionalized spiropyrazolone–pyrrolidinones in good yields. The methodology is distinguished by several key advantages, including the use of stable substrates, operational simplicity, and enhanced atom and step economy. Moreover, its synthetic applicability has been successfully validated on a gram scale, ensuring high product yields and demonstrating its practical utility (Scheme 5.2).



6 **7** **8**
24 examples
up to 76% yield

Scheme 5.2 Synthesis of spiropyrazolone-tetrahydrofurans via base-mediated cyclization reaction between unsaturated pyrazolones with 2-chloro-N-phenylacetamides

In 2023, Chen and coworkers[10] reported an innovative asymmetric [4+2] cycloaddition of 2-methylidenetrimethylene carbonate **10** with pyrrolidinedione-derived substrates **9**, enabling the synthesis of functionalized tetrahydropyran-fused spirocyclic framework **11** via palladium catalysis. This methodology facilitates the formation of enantioenriched spiropyrrolidinedione featuring adjacent quaternary and tertiary stereocenters with remarkable efficiency, achieving yields of desired products up to 96% and enantiomeric excesses (*ee*) as high as 99%. Furthermore, the synthetic utility of the obtained products has been demonstrated through subsequent transformations, leading to the construction of pharmaceutically relevant $\beta_{2,2}$-amino acids and β-lactams. Additionally, a comprehensive mechanistic investigation has been conducted to elucidate the underlying reaction pathways.



9 **10**
11
29 examples
up to 96% yield
up to >20:1 *dr*
up to 99% *ee*

Scheme 5.3 Synthesis of spiropyrrolidinediones via Pd-mediated cyclization reaction between 2-methylidenetrimethylene carbonate with pyrrolidone-derived substrates

Nonetheless, several existing synthetic approaches for constructing spiropyrazolone and spiropyrrolidinone frameworks depend on transition metal catalysts and stoichiometric bases. These requirements pose limitations in terms of cost, sustainability, and operational simplicity. Consequently, the development of a transition metal-free, highly efficient, and more practical

synthetic strategy for accessing structurally diverse spiropyrazolones and spiropyrrolidinones remains a highly desirable objective and a significant synthetic challenge as well.

Based on our continuous interest in spiroheterocycles and experience in constructing the spiroheterocyclic compounds, we hypothesized that Pyro-MBH alcohol and arylidene pyrrolidinediones may undergo [4+2] annulation in the presence of a suitable base and reaction conditions to afford the spiropyrazolone pyrrolidinediones fused tetrahydropyran as a hybrid molecule.

In this chapter, we have disclosed an expedient transition metal-free oxa-Michael cascade [4+2] annulation strategy to directly construct the spiropyrazolone pyrrolidinediones fused tetrahydropyran framework using commercially viable and easily available potassium tert-butoxide.

5.3 Results and Discussion

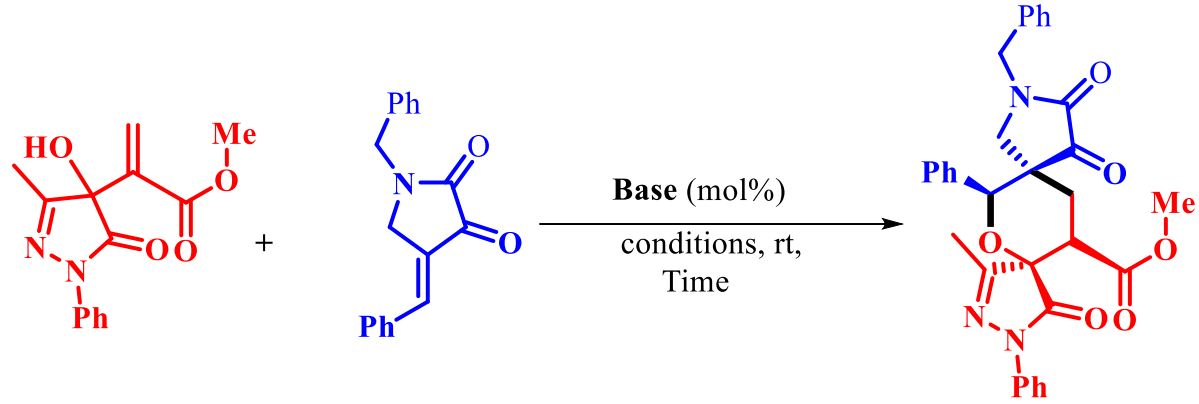
To validate the proposed synthetic route to access a hybrid molecule via oxa-Michael cascade [4+2] annulation, we commenced with Pyro-MBH alcohol **1a** and arylidene pyrrolidinediones **2a** as model substrates. To begin with, we carried out the reaction of **1a** and **2a** using 1,8-diazabicyclo[5.4.0]undec-7-ene (DBU, 50 mol%) as the base in 1,4-Dioxane as the solvent under ambient reaction conditions. However, even after prolonged reaction time (24 h), the reaction progressed very sluggishly to afford the desired product **3a** in very poor yield (5%, Table 5.1, entry 1).

Later, we screened different organic bases such as DMAP, DABCO, PPh_3, and Et_3N, and all them were not successful in affording the desired products (Table 5.1 entries 2–5). Though the reaction worked in the presence of DMAP, it afforded the product **3a** in very poor or negligible yield (5%, Table 5.1 entry 2), while the other organic bases did not even promote the formation of **3a**.

We switched our focus to evaluating a few inorganic bases. The reaction of **1a** and **2a** in 1,4-Dioxane using bases (50 mol%) such as K_2CO_3, K_3PO_4, Cs_2CO_3, and KOt-Bu proved to be promising by affording the desired product **3a** in modest to very good yields (40% to 86%, Table 5.1, entries 6–9). Among all the inorganic bases screened, KOt-Bu proved to be most efficient in terms of affording **3a** in the highest yield in a very rapid time of 5 min (Table 5.1, entry 9). These findings highlight the pivotal role of base and their selection in governing the efficiency and outcome of the transformation. Further, increasing the loading of KOt-Bu (100 mol%) resulted in a decreased yield of compound **3a** (68%, Table 5.1, entry 10). Whereas,

lowering the amount of KOt-Bu (20 mol%) led to a reduction in the yield of **3a** in taking relatively longer time for the completion (62%, Table 5.1, entry 11). These observations highlight the critical influence of base concentration on reaction efficiency, where excessive and insufficient amounts adversely affect the yield (Table 5.1, entries 10–11).

Table 5.1 Screening of catalysts and solvents for cycloaddition reaction[a-b]



1a **2a** **3a**

Entry	Base (mol%)	Solvent	Time	Yield[b] (%)
1	DBU (0.5)	1,4-Dioxane	24 h	5
2	DMAP (0.5)	1,4-Dioxane	24 h	5
3	DABCO (0.5)	1,4-Dioxane	24 h	NR
4	Et_3N (0.5)	1,4-Dioxane	24 h	NR
5	PPh_3 (0.5)	1,4-Dioxane	24 h	NR
6	K_2CO_3 (0.5)	1,4-Dioxane	24 h	40
7	K_3PO_4	1,4-Dioxane	4 h	55
8	Cs_2CO_3	1,4-Dioxane	4 h	60
9	KOt-Bu (0.5)	1,4-Dioxane	5 min.	86
10	KOt-Bu (0.2)	1,4-Dioxane	20 min.	62
11	KOt-Bu (1.0)	1,4-Dioxane	5 min.	68
12	KOt-Bu (0.5)	MeCN	5 min.	72
13	KOt-Bu (0.5)	CH_2Cl_2	5 min.	72
14	KOt-Bu (0.5)	$CHCl_3$	5 min.	67
15	KOt-Bu (0.5)	Toluene	5 min.	62
16	KOt-Bu (0.5)	EtOAC	5 min.	64

17	KOt-Bu (0.5)	$ClCH_2CH_2Cl$	5 min.	70
18	KOt-Bu (0.5)	THF	5 min.	68
19	KOt-Bu (0.5)	DMF	5 min.	64

[a]**Reaction Conditions:** Unless stated otherwise, reactions were performed using **1a** (0.2 mmol), **2a** (0.2 mmol), and the catalyst [50 mol%] in 1.0 mL of the specified solvent at room temperature for min. [b]Isolated yields of **3a**.

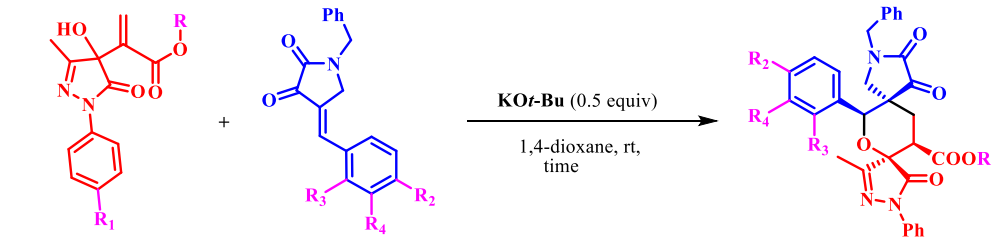
Later, we carried out a comprehensive investigation solvent effect by screening different solvents while maintaining KOt-Bu as base (50 mol%). Though reactions in all the solvents such as MeCN, DCM, $CHCl_3$, toluene, ethyl acetate, DCE, THF, DMF worked, however, 1,4-Dioxane proved to be most advantageous in affording the desired product **3a** in the highest yield (Table 5.1, entries 9, 12–19). Building upon these results, the optimal reaction conditions were determined to be 50 mol% KOt-Bu in 1,4-Dioxane at ambient temperature, offering the most suitable environment for investigating the substrate scope of the oxa-Michael cascade [4+2] annulation reaction (Table 1, entry 9).

Based on the systematic screening, Pyro-MBH alcohol **1a** (1 equiv) and arylidene pyrrolidinediones **2a** (1 equiv), KOt-Bu (50 mol%) in 1,4-Dioxane at ambient temperature proved to be optimized reaction conditions for oxa-Michael cascade [4+2] annulation to obtain the desired product **3a** (Table 1, entry 9).

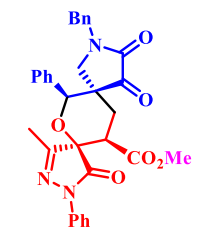
Having obtained the optimized reaction conditions, we further explored the substrate scope of the [4+2] cascade annulation reaction. In this regard, we synthesized a diverse range of substituted Pyro-MBH alcohols (**1b**–**1e**) and arylidene pyrazolones (**2a**–**2t**) to evaluate their reactivity and compatibility in forming the desired annulated frameworks. A diverse array of substituted Pyro-MBH alcohols having including ethyl, tert-butyl, methyl, and chloro moieties (**1b-1e**) reacted smoothly with **2a** under the optimized conditions to afford the corresponding annulated products (**3b**–**3e**) in modest to moderate yields (up to 59%, Scheme 5.4). Remarkably, these transformations were completed in a very short time of 5-20 minutes, highlighting the exceptional catalytic efficiency of the system (Scheme 5.4).

The optimized reaction conditions were further applied to a broad range of substituted arylidene pyrrolidinediones (**2b**–**2t**). A systematic investigation was conducted to assess the electronic influence of *para*-substituents on the phenyl ring. arylidene pyrrolidinediones having electron-donating substituents at the *para*-position of the phenyl ring (4-methyl and 4-dimethoxy groups, **2b-2c**) displayed excellent reactivity with **1a** under the optimized reaction condition to

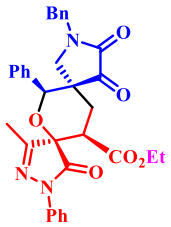
Scheme 5.4 Investigation of Substrate Scope for the [4+2] Annulation Reaction[a]



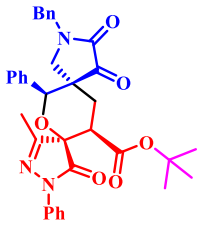
1a-1e **2a-2t** **3a-3x**



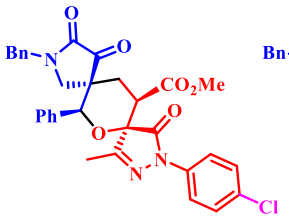
3a, 86%,[b] 5 min.



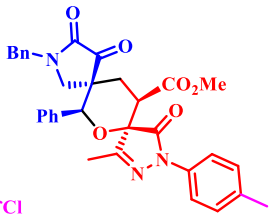
3b, 27%,[b] 20 min.



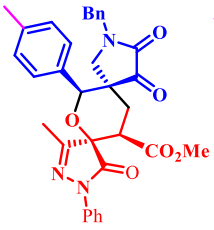
3c, 59%,[b] 5 min.



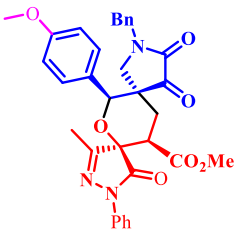
3d, 57%,[b] 5 min.



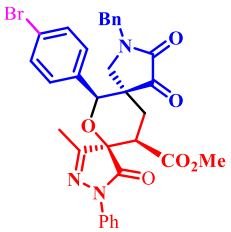
3e, 53%,[b] 5 min.



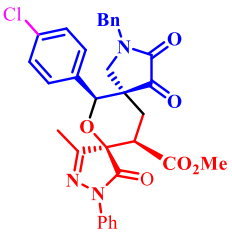
3f, 71%,[b] 5 min.



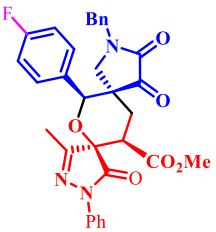
3g, 62%,[b] 5 min.



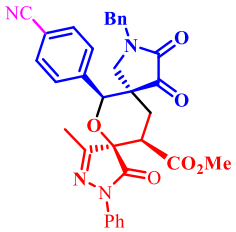
3h, 61%,[b] 5 min.



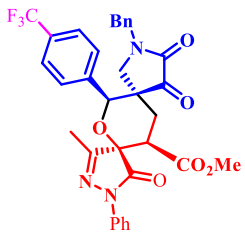
3i, 65%,[b] 5 min.



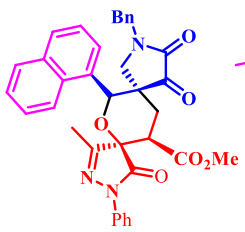
3j, 80%,[b] 5 min.



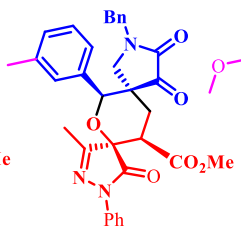
3k, 76%,[b] 10 min.



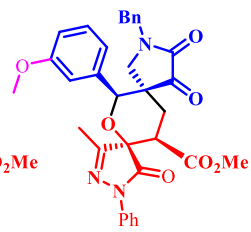
3l, 83%,[b] 20 min.



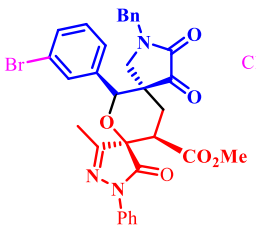
3m, 53%,[b] 5 min.



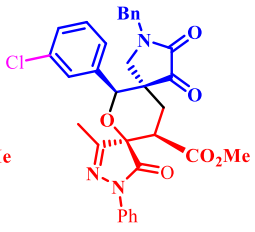
3n, 62%,[b] 5 min.



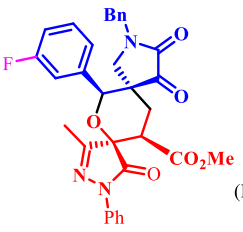
3o, 76%,[b] 5 min.



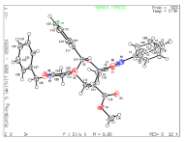
3p, 36%,[b] 5 min.



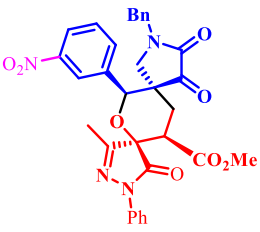
3q, 45%,[b] 5 min.



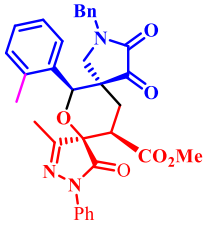
3r, 87%,[b] 5 min.



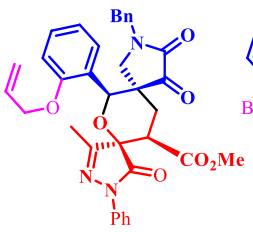
(Molecular Structure of compound **3r**)[c]
CCDC-2465733



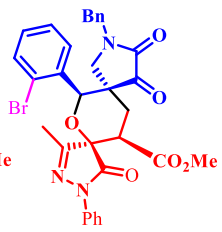
3s, 64%,[b] 20 min.



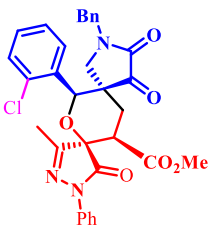
3t, 50%,[b] 5 min.



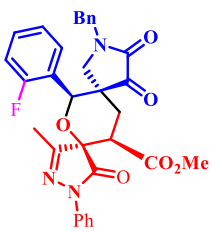
3u, 59%,[b] 5 min.



3v, 67%,[b] 5 min.



3w, 45%,[b] 5 min.



3x, 72%,[b] 20 min.

[a]**Reaction conditions:** Unless stated otherwise, reactions were performed using Pyro-MBH Alcohol **1a-1e** (1 equiv, 0.2 mmol), **2a-2t** (1 equiv, 0.2 mmol) and KOt-Bu (50 mol%, 0.1 mmol) in 1,4-Dioxane (1.0 mL) at room temperature for 5-20 min. isolated yields. [b] Single diastereomer. [c]Thermal ellipsoids at the 50% probability level.

afford the corresponding products (**3f**–**3g**) in moderate to very good yields in very short reaction time in 5 mins (up to 71%, Scheme 5.4). Similarly, arylidene pyrrolidinediones having *para*-halogens (4-bromo, 4-chloro, and 4-fluoro, **2d-2f**) efficiently underwent annulation with Pyro-MBH alcohol **1a**, affording the desired dispiropyrazolone products (**3h**–**3j**) in moderate to very yields in short reaction time and were isolated as as a single diastereomer (up to 80%, Scheme 5.4).

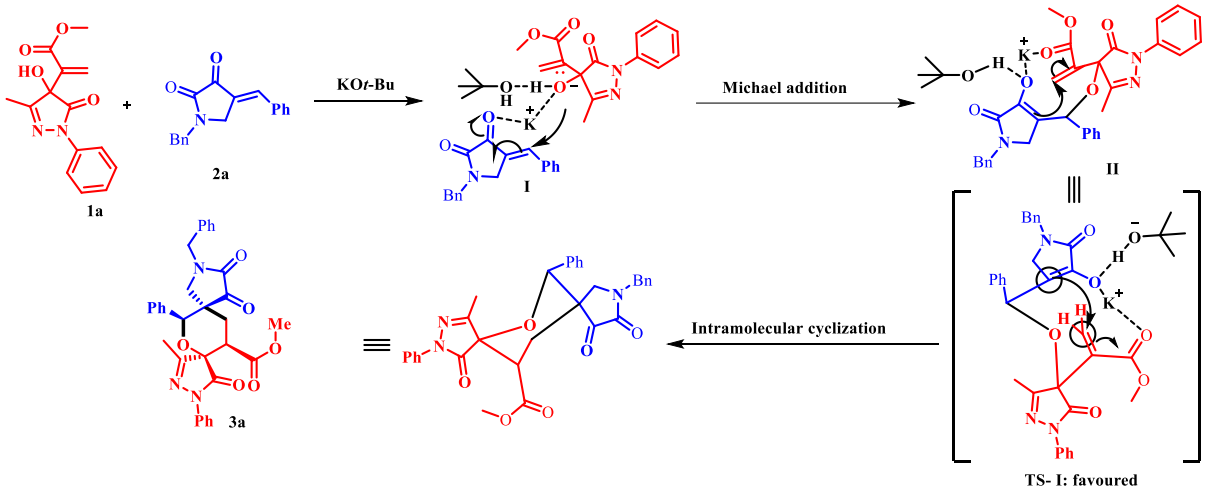
Moreover, arylidene pyrrolidinediones (**2g-2i**) featuring electron-deficient *para*-substituents, such as cyano (CN), trifluoromethyl (CF_3), and 1-naphthyl groups, exhibited exceptional reactivity with **1a**, affording the corresponding annulated products (**3k**–**3m**) in moderate to very good yields in 5-20 minutes and were isolated as a single diastereomer (up to 83%, Scheme 5.4). Furthermore, substrates bearing *ortho*- and *meta*-substituents (3-methyl, 3-methoxy, 3-bromo, 3-chloro, 3-fluoro, 3-nitro, 2-methyl, 2-methoxy 2-o-allyl, 2-bromo, 2-chloro, and 2-fluoro) on the phenyl ring (**2j-2t**) reacted smoothly with **1a** and demonstrated excellent compatibility under the optimized reaction conditions to afford the desired corresponding products (**3n–3x**) in modest to very good yields and they were isolated as a single diastereomer (up to 87%, Scheme 5.4).

The structural identity of the target compound **3r** was unequivocally confirmed through single-crystal X-ray diffraction analysis. Furthermore, detailed stereochemical investigation established the configuration of the predominant diastereomer as *R, S, R, R,* corroborated by comprehensive analytical studies (Scheme 5.4). Based on analogy stereochemistry of the other compounds was proposed.[11]

These results highlight the broad substrate scope and outstanding efficiency of the optimized cascade [4+2] annulation strategy for the stereoselective synthesis of spiropyrazolone pyrrolidinediones fused tetrahydropyran derivatives. The synthesized spiropyrazolone pyrrolidinediones fused tetrahydropyran incorporating a 2-oxane-fused pyrazolone core (compounds **3a**–**3x**), were successfully obtained and isolated as single diastereomeric entities (Scheme 5.4). Notably, these compounds possess quaternary carbon stereocenters, demonstrating the exceptional precision and stereoselectivity of this synthetic methodology.

Furthermore, the high diastereomeric purity observed underscores the robustness of this approach in maintaining strict stereochemical control throughout the transformation.

Based on the literature precedents and experimental observations,[11, 12] a plausible mechanistic pathway has been proposed (Scheme 5.5). The reaction commences with the deprotonation of the Pyro-MBH alcohol **1a**, facilitated by KOt-Bu, generating a highly reactive nucleophilic species **I** that acts as a Michael donor. This nucleophile subsequently engages in a Michael addition with arylidene pyrrolidinediones **2a**, proceeding through a transition state



Scheme 5.5 Proposed reaction mechanism for the [4+2] annulation

characterized by an expectedly chair conformation (Transition State I), as corroborated by single-crystal X-ray diffraction analysis. The subsequent intramolecular cyclization event leads to the formation of the annulated product **3a**. This mechanistic proposal is in accordance with established catalytic cycles and offers a coherent explanation for the observed experimental outcomes.

5.4 Conclusion

In summary, an expedient protocol for the oxa-Michael cascade [4+2] annulation has been developed for the synthesis of structurally complex spiropyrazolone pyrrolidinedione fused tetrahydropyran derivatives. Utilizing pyrazolone-derived Morita–Baylis–Hillman (Pyro-MBH) Alcohols as oxa-Michael donors, this strategy demonstrates exceptional atom economy, facilitating the concurrent formation of two tertiary and two quaternary stereocenters within a

remarkably short reaction time of 5–20 minutes. Also, the protocol utilized the Pyro-MBH alcohols has been successfully utilized without the need for any protection or deprotection.

5.5 Experimental Section

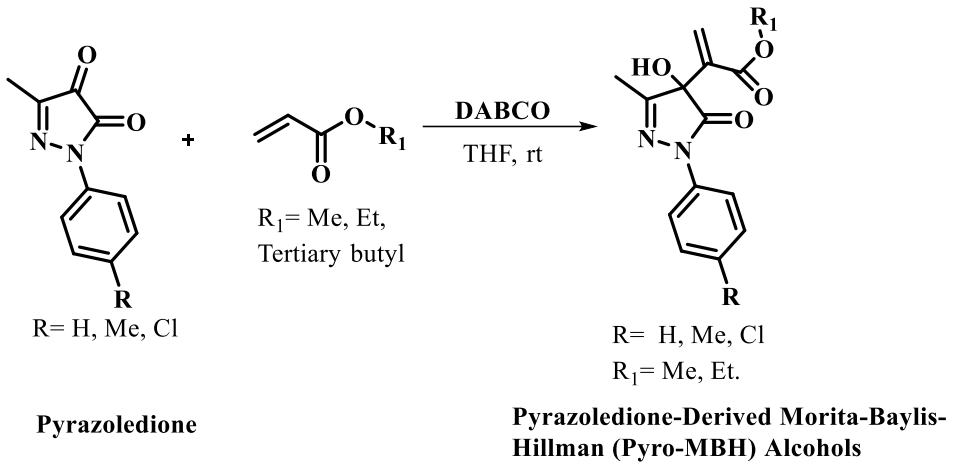
5.5.1 General

All starting materials and reagents were procured from commercial vendors (Aldrich, TCI, and Alfa Aesar) and utilized as received without additional purification unless stated otherwise. Reactions were carried out in flame-dried reaction vessels. Commercial-grade solvents were employed for the reaction. Analytical Reagent grade (AR)-grade 1,4-Dioxane was used. Thin-layer chromatography (TLC) was performed on silica gel 60 GF254 aluminum-backed plates (2.5 mm thickness), and compounds were visualized under ultraviolet (UV) light at a wavelength of 254 nm. Column chromatography utilized silica gel (100–200 mesh), with petroleum ether and ethyl acetate as the mobile phase. Nuclear magnetic resonance (NMR) spectra were recorded using tetramethylsilane (TMS) as an internal standard. For ^{1}H NMR, spectra were acquired at 400 MHz, while $^{13}C\{^{1}H\}$ NMR spectra were recorded at 100 MHz using Bruker or Neo instruments unless otherwise noted. Chemical shifts (δ) are reported in parts per million (ppm) relative to the residual solvent peak of $CDCl_3$ (δ = 7.26 ppm for ^{1}H NMR, δ = 77.16 ppm for $^{13}C\{^{1}H\}$ NMR). The multiplicity of ^{1}H NMR signals is described as follows: singlet (s), doublet (d), double doublet (dd), triplet (t), quartet (q), broad (br), or multiplet (m), with coupling constants (J) reported in hertz (Hz) alongside integration values. $^{13}C\{^{1}H\}$ NMR spectra were fully proton decoupled. ^{19}F NMR spectra were acquired at 377 MHz. High-resolution mass spectrometry (HRMS) analyses were performed using an electrospray ionization time-of-flight (ESI-TOF) instrument. Single-crystal X-ray diffraction data were collected using Enraf-Nonius CAD4-MV31 and Bruker Kappa APEXII diffractometers. Crystal structure **3r** was obtained by slow evaporation of a 1:1 dichloromethane and ethyl acetate mixture.

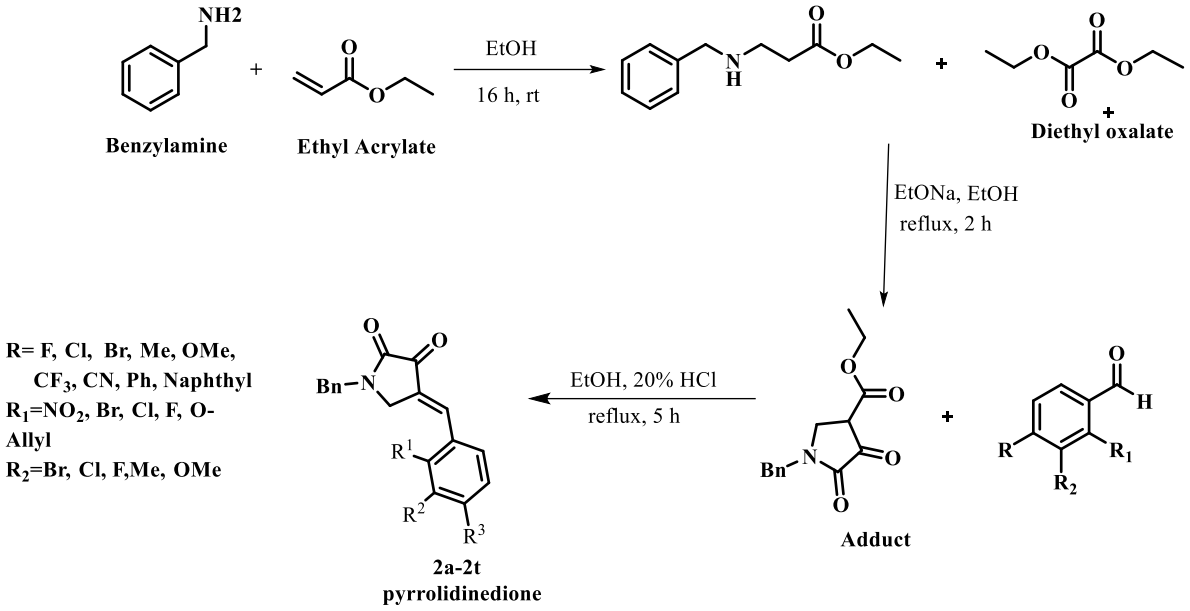
5.5.2 General procedure for the synthesis of Pyro-MBH alcohols 1a−1e

A mixture of pyrazolodione (1 mmol) and methyl acrylate (1.1 mmol) in tetrahydrofuran (THF, 3 mL) was introduced to 1,4-diazabicyclo[2.2.2]octane (DABCO, 2 mmol) at ambient temperature. Upon completion of the reaction, the solvent was removed under reduced pressure. The resulting crude product was purified via column chromatography on silica gel,

employing a gradient of ethyl acetate and hexanes as the eluent, to yield the MBH alcohol as the purified product.



5.5.3 General procedure for the synthesis of pyrrolidinediones derivatives 2a-2t [13]

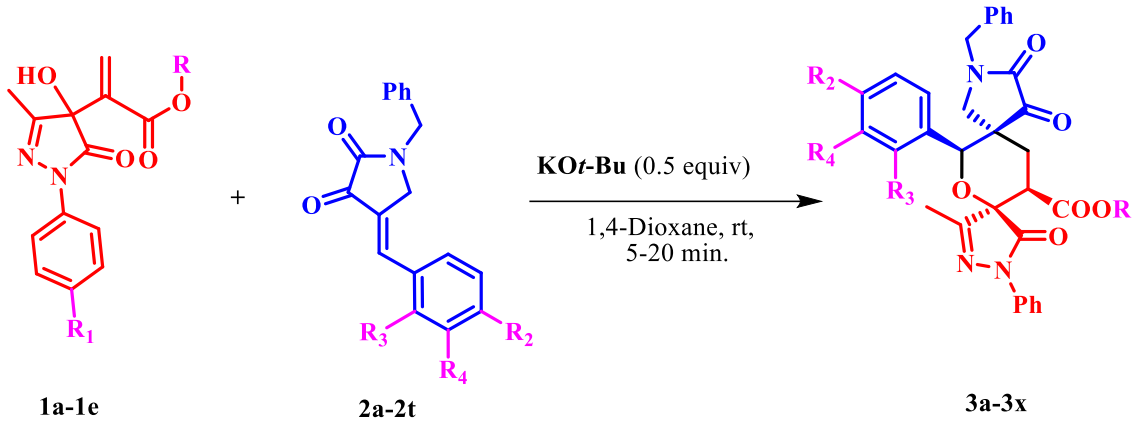


Step 1: A mixture of benzylamine (660.0 mmol, 70.7 g, 1.0 equiv), ethyl acrylate (660.0 mmol, 70.3 mL, 1.0 equiv) in EtOH (150 mL) was stirred at room temperature for 16 h. Diethyl oxalate (66.0 mmol, 90 mL, 0.1 equiv) and freshly-made sodium ethoxide solution in EtOH (generated from 20.0 g of sodium metal, 880.0 mmol, in 300 mL EtOH, 1.3 equiv) were added. The mixture was heated at 80 °C for 2 hours and then cooled to solidify. The volatiles were removed in vacuo. The crude product was diluted with H_2O (600 mL) and the pH of the mixture to 1 by

adding conc. HCl. The mixture was subjected to filtration to afford Adduct as a white solid (135 g, yield 78%).

Step 2: To a solution of the above Adduct (2.0 g, 7.7 mmol, 1.0 equiv) in 20 mL EtOH / 20% HCl, 60 mL was added corresponding benzaldehyde (8.5 mmol, 1.1 equiv). The mixture was stirred at 110 ºC for 5 hours. After cooling down to ambient temperature, the aqueous layer was decanted. The obtained chunky solid was collected and further recrystallized from EtOAc to generate enones **2a-2t** as a yellow solid.

5.5.4 General procedure for the synthesis of spiropyrazolone pyrrolidinediones fused tetrahydropyran scaffolds (3a–3x)

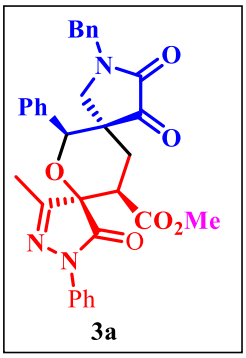


1a-1e **2a-2t** **3a-3x**

An oven-dried 10 mL glass reaction vessel was loaded with pyrazoledione-derived Morita–Baylis–Hillman (Pyro-MBH) alcohol (**1a**–**1e**, 1 equiv, 0.2 mmol), potassium tert-butoxide (50 mol%, 0.1 mmol), and arylidene pyrrolidinediones (**2a**–**2t**, 1 equiv, 0.2 mmol). 1,4-Dioxane (1 mL) was then added to the reaction mixture. The reaction was stirred at ambient temperature for 5–20 minutes. Upon completion, the solvent was removed under reduced pressure. The resulting residue was purified by silica gel column chromatography using a hexane/ethyl acetate gradient, yielding the desired products (**3a**–**3x**).

5.6 Experimental Data

Methyl (*5R,7S,8R,14R*)-10-benzyl-1-methyl-4,11,12-trioxo-3,7-diphenyl-6-oxa-2,3,10-triazadispiro[4.2.48.25]tetradec-1-ene-14-carboxylate (3a)

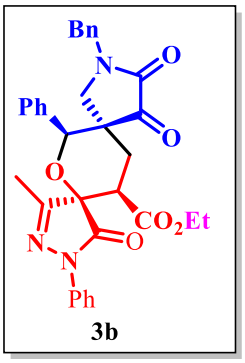


3a

Product **3a** was synthesized following the general experimental procedure **5.5.4**. An oven-dried 10 mL glass reaction tube was charged with pyrazoledione-derived Morita–Baylis–Hillman (Pyro-MBH) alcohol **1a** (1.0 equiv, 0.2 mmol), potassium tert-butoxide (50 mol%, 0.1 mmol), and arylidene pyrrolidinediones **2a** (1.0 equiv, 0.2 mmol). Subsequently, 1,4-Dioxane (1 mL) was added to the tube. The reaction mixture was stirred at ambient temperature for 5 minute. Upon completion, the solvent was removed under reduced pressure, and the residue was purified by column chromatography on silica gel using 50% ethyl acetate in hexanes as the eluent. The purified product **3a**, identified as Methyl (*5R,7S,8R,14R*)-10-benzyl-1-methyl-4,11,12-trioxo-3,7-diphenyl-6-oxa-2,3,10-triazadispiro[4.2.48.25]tetradec-1-ene-14-carboxylate, was obtained as a white solid in a yield of 95 mg (86%) as a single diastereomer. The structure was confirmed through spectroscopic methods, including ^{1}H NMR, ^{13}C{^{1}H} NMR, HRMS, and X-ray crystallographic analysis. The compound displayed a melting point of 232–234 °C and a TLC retention factor (R_f) 0.5 (silica gel, 50% ethyl acetate/hexanes). ^{1}H NMR (400 MHz, $CDCl_3$): δ 7.8 – 7.7 (m, 2H), 7.4 – 7.3 (m, 2H), 7.3 – 7.3 (m, 2H), 7.3 – 7.1 (m, 5H), 7.1 (dt, *J* = 7.3, 1.5 Hz, 2H), 6.9 – 6.8 (m, 2H), 6.1 (s, 1H), 4.5 – 4.2 (m, 2H), 3.7 (d, *J* = 11.2 Hz, 1H), 3.6 (s, 3H), 3.5 (t, *J* = 13.6 Hz, 1H), 3.3 (d, *J* = 11.2 Hz, 1H), 2.9 (dd, *J* = 13.6, 4.2 Hz, 1H), 2.2 (s, 3H), 2.1 – 2.0 (m, 1H). ^{13}C{^{1}H} NMR (100 MHz, $CDCl_3$): δ 200.1, 169.0, 168.8, 158.6, 156.9, 137.4, 135.1, 133.9, 129.1, 128.9,128.8, 128.8, 128.1, 128.0, 125.6, 125.4, 118.9, 77.1, 73.5, 52.9, 48.3, 47.5, 47.0, 40.7, 29.0, 13.0. HRMS (ESI TOF) *m/z* calcd. For $C_{32}H_{29}N_3O_6$ $[M+Na]^+$ 574.1953 found 574.1958.

Ethyl (*5R,7S,8R,14R*)-10-benzyl-1-methyl-4,11,12-trioxo-3,7-diphenyl-6-oxa-2,3,10-triazadispiro[4.2.48.25]tetradec-1-ene-14-carboxylate (3b)

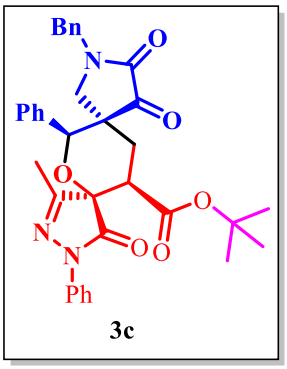
Product **3b** was synthesized following the general experimental procedure **5.5.4**. An oven-dried 10 mL glass reaction tube was charged with pyrazoledione-derived Morita–Baylis–Hillman (Pyro-MBH) alcohol **1b** (1.0 equiv, 0.2 mmol), potassium tert-butoxide (50 mol%, 0.1 mmol), and arylidene pyrrolidinediones **2a** (1.0 equiv, 0.2 mmol). Subsequently, 1,4-Dioxane (1 mL) was added to the tube. The reaction mixture was stirred at ambient temperature for 20 minute.



3b

Upon completion, the solvent was removed under reduced pressure, and the residue was purified by column chromatography on silica gel using 50% ethyl acetate in hexanes as the eluent. The purified product **3b**, identified as Ethyl (*5R,7S,8R,14R*)-10-benzyl-1-methyl-4,11,12-trioxo-3,7-diphenyl-6-oxa-2,3,10-triazadispiro[4.2.48.25]tetradec-1-ene-14-carboxylate, was obtained as a sticky white solid in a yield of 31 mg (27%) as a single diastereomer. The structure was confirmed through spectroscopic methods including ^{1}H NMR, ^{13}C{^{1}H} NMR, HRMS, and X-ray crystallographic analysis. The compound displayed a TLC retention factor (R_f) 0.5 (silica gel, 50% ethyl acetate/hexanes). ^{1}H NMR (400 MHz, $CDCl_3$): δ 7.8 (d, *J* = 8.1 Hz, 2H), 7.5 – 7.3 (m, 5H), 7.2 – 7.1 (m, 4H), 7.1 (d, *J* = 7.5 Hz, 2H), 6.8 (d, *J* = 7.2 Hz, 2H), 6.1 (s, 1H), 4.5 – 4.2 (m, 2H), 4.1 – 4.0 (m, 2H), 3.7 (d, *J* = 11.1 Hz, 1H), 3.5 (t, *J* = 13.7 Hz, 1H), 3.3 (d, *J* = 11.2 Hz, 1H), 2.9 (dd, *J* = 13.6, 4.2 Hz, 1H), 2.2 (s, 3H), 2.1 (dd, *J* = 13.7, 4.1 Hz, 1H), 1.1 (t, *J* = 7.1 Hz, 3H). ^{13}C{^{1}H} NMR (100 MHz, $CDCl_3$): δ 200.1, 168.7, 168.5, 158.6, 157.0, 137.4, 135.2, 133.9, 129.1, 128.9, 128.8, 128.8, 128.1, 128.0, 125.6, 125.3, 118.7, 77.1, 73.5, 62.2, 48.3, 47.6, 47.0, 40.7, 29.0, 13.8, 13.0. HRMS (ESI TOF) *m/z* calcd. For $C_{33}H_{31}N_3O_6$ $[M+H]^+$ 566.2291 found 566.2292.

Tert-butyl (*5R,7S,8R,14R*)-10-benzyl-1-methyl-4,11,12-trioxo-3,7-diphenyl-6-oxa-2,3,10-triazadispiro[4.2.48.25]tetradec-1-ene-14-carboxylate (3c)

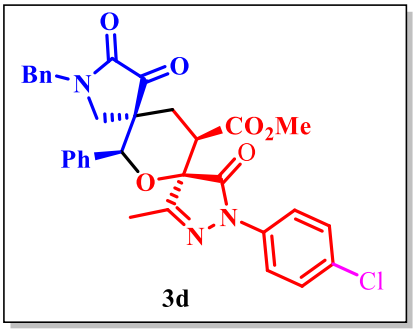


3c

Product **3c** was synthesized following the general experimental procedure **5.5.4**. An oven-dried 10 mL glass reaction tube was charged with pyrazoledione-derived Morita–Baylis–Hillman (Pyro-MBH) alcohol **1c** (1.0 equiv, 0.2 mmol), potassium tert-butoxide (50 mol%, 0.1 mmol), and arylidene pyrrolidinediones **2a** (1.0 equiv, 0.2 mmol). Subsequently, 1,4-Dioxane (1 mL) was added to the tube. The reaction mixture was stirred at ambient temperature for 5 minute. Upon completion, the solvent was removed under reduced pressure, and the residue was purified by column chromatography on silica gel using 50% ethyl acetate in hexanes as the eluent. The purified product **3c**, identified as Tert-butyl (*5R,7S,8R,14R*)-10-benzyl-1-methyl-4,11,12-trioxo-3,7-diphenyl-6-oxa-2,3,10-triazadispiro[4.2.48.25]tetradec-1-ene-14-carboxylate **(3c)** was obtained as a white solid in a yield of 70 mg (59%) as a single diastereomer. The structure was confirmed through spectroscopic methods including ^{1}H NMR, ^{13}C{^{1}H} NMR, HRMS, and X-ray crystallographic analysis. The compound displayed a

melting point of 249-251 °C and a TLC retention factor (R_f) 0.5 (silica gel, 50% ethyl acetate/hexanes). ^{1}H NMR (400 MHz, $CDCl_3$): δ 7.9 – 7.8 (m, 2H), 7.4 (td, *J* = 7.3, 1.8 Hz, 3H), 7.3 – 7.3 (m, 2H), 7.3 – 7.1 (m, 4H), 7.1 – 7.0 (m, 2H), 6.9 – 6.7 (m, 2H), 6.1 (s, 1H), 4.5 – 4.3 (m, 2H), 3.7 (d, *J* = 11.2 Hz, 1H), 3.5 (t, *J* = 13.7 Hz, 1H), 3.3 (d, *J* = 11.2 Hz, 1H), 2.8 (dd, *J* = 13.5, 4.1 Hz, 1H), 2.2 (s, 3H), 2.0 (dd, *J* = 13.8, 4.2 Hz, 1H), 1.3 (s, 9H). ^{13}C{^{1}H} NMR (100 MHz, $CDCl_3$): δ 200.3, 168.6, 167.3, 158.7, 157.5, 137.5, 135.3, 133.9, 129.1, 128.9, 128.8, 128.7, 128.1, 128.0, 125.6, 125.2, 118.5, 83.8, 77.4, 73.5, 48.3, 47.7, 47.0, 41.3, 28.9, 27.6, 13.0. HRMS (ESI TOF) *m/z* calcd. For $C_{35}H_{35}N_3O_6$ $[M+H]^+$ 594.2604 found 594.2606.

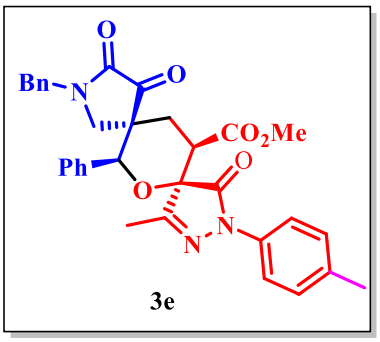
Methyl (*5R,7S,8R,14R*)-10-benzyl-3-(4-chlorophenyl)-1-methyl-4,11,12-trioxo-7-phenyl-6-oxa-2,3,10-triazadispiro[4.2.48.25]tetradec-1-ene-14-carboxylate (3d)



3d

Product **3d** was synthesized following the general experimental procedure **5.5.4**. An oven-dried 10 mL glass reaction tube was charged with pyrazoledione-derived Morita–Baylis–Hillman (Pyro-MBH) alcohol **1d** (1.0 equiv, 0.2 mmol), potassium tert-butoxide (50 mol%, 0.1 mmol), and arylidene pyrrolidinediones **2a** (1.0 equiv, 0.2 mmol). Subsequently, 1,4-Dioxane (1 mL) was added to the tube. The reaction mixture was stirred at ambient temperature for 5 minute. Upon completion, the solvent was removed under reduced pressure, and the residue was purified by column chromatography on silica gel using 50% ethyl acetate in hexanes as the eluent. The purified product, **3d**, identified as Methyl (*5R,7S,8R,14R*)-10-benzyl-3-(4-chlorophenyl)-1-methyl-4,11,12-trioxo-7-phenyl-6-oxa-2,3,10-triazadispiro[4.2.48.25]tetradec-1-ene-14-carboxylate **(3d)**, was obtained as a white solid in a yield of 67 mg (57%) as a single diastereomer. The structure was confirmed through spectroscopic methods, including ^{1}H NMR, ^{13}C{^{1}H} NMR, HRMS, and X-ray crystallographic analysis. The compound displayed a melting point of 265–267 °C and a TLC retention factor (R_f) 0.5 (silica gel, 50% ethyl acetate/hexanes). ^{1}H NMR (400 MHz, $CDCl_3$): δ 7.8 – 7.7 (m, 2H), 7.4 – 7.3 (m, 4H), 7.3 – 7.2 (m, 4H), 7.1 (dd, *J* = 7.2, 1.9 Hz, 2H), 6.8 (dt, *J* = 6.7, 1.5 Hz, 2H), 6.1 (s, 1H), 4.5 – 4.2 (m, 2H), 3.7 (d, *J* = 11.2 Hz, 1H), 3.6 (s, 3H), 3.5 (t, *J* = 13.7 Hz, 1H), 3.3 (d, *J* = 11.2 Hz, 1H), 2.9 (dd, *J* = 13.6, 4.2 Hz, 1H), 2.2 (s, 3H), 2.1 (dd, *J* = 13.7, 4.2 Hz, 1H). ^{13}C{^{1}H} NMR (100 MHz, $CDCl_3$): δ 200.0, 169.0, 168.7, 158.5, 157.1, 136.0, 135.0, 133.8, 130.5, 129.1, 128.9, 128.9, 128.9, 128.1, 128.0, 125.6, 119.9, 77.1, 73.6, 52.9, 48.4, 47.5, 47.0, 40.7, 29.0, 13.0. HRMS (ESI TOF) *m/z* calcd. For $C_{32}H_{28}ClN_3O_6$ $[M+H]^+$ 586.1745 found 586.1744.

Methyl (*5R,7S,8R,14R*)-10-benzyl-1-methyl-4,11,12-trioxo-7-phenyl-3-(p-tolyl)-6-oxa-2,3,10-triazadispiro[4.2.48.25]tetradec-1-ene-14-carboxylate (3e)

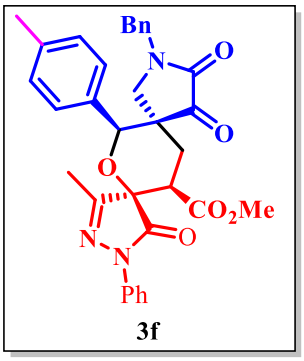


3e

Product **3e** was synthesized following the general experimental procedure **5.5.4**. An oven-dried 10 mL glass reaction tube was charged with pyrazoledione-derived Morita–Baylis–Hillman (Pyro-MBH) alcohol **1d** (1.0 equiv, 0.2 mmol), potassium tert-butoxide (50 mol%, 0.1 mmol), and arylidene pyrrolidinediones **2a** (1.0 equiv, 0.2 mmol). Subsequently, 1,4-Dioxane (1 mL) was added to the tube. The reaction mixture was stirred at ambient temperature for 5 minute. Upon completion, the solvent was removed under reduced pressure, and the residue was purified by column chromatography on silica gel using 50% ethyl acetate in hexanes as the eluent. The purified product, **3e**, identified as Methyl (*5R,7S,8R,14R*)-10-benzyl-1-methyl-4,11,12-trioxo-7-phenyl-3-(p-tolyl)-6-oxa-2,3,10 triazadispiro[4.2.48.25]tetradec-1-ene-14-carboxylate **(3e),** was obtained as a white solid in a yield of 61 mg (53%) as a single diastereomer. The structure was confirmed through spectroscopic methods, including ^{1}H NMR, ^{13}C{^{1}H} NMR, HRMS, and X-ray crystallographic analysis. The compound displayed a melting point of 233–235 °C and a TLC retention factor (R_f) 0.5 (silica gel, 50% ethyl acetate/hexanes). ^{1}H NMR (400 MHz, $CDCl_3$): δ 7.7 – 7.6 (m, 2H), 7.3 – 7.3 (m, 2H), 7.3 – 7.1 (m, 6H), 7.1 (dt, *J* = 7.1, 1.5 Hz, 2H), 6.8 (dt, *J* = 6.7, 1.6 Hz, 2H), 6.1 (s, 1H), 4.4 (d, *J* = 14.8 Hz, 1H), 4.3 (d, *J* = 14.7 Hz, 1H), 3.7 (d, *J* = 11.2 Hz, 1H), 3.6 (s, 3H), 3.5 (t, *J* = 13.6 Hz, 1H), 3.3 (d, *J* = 11.2 Hz, 1H), 2.9 (dd, *J* = 13.6, 4.2 Hz, 1H), 2.3 (s, 3H), 2.2 (s, 3H), 2.1 (dd, *J* = 13.7, 4.2 Hz, 1H). ^{13}C{^{1}H} NMR (100 MHz, $CDCl_3$): δ 200.1, 169.0, 168.6, 158.6, 156.8, 135.2, 135.2, 134.9, 133.9, 129.4, 129.1, 128.8, 128.8, 128.1, 128.0, 125.6, 119.0, 77.2, 73.5, 52.9, 48.3, 47.5, 47.0, 40.7, 29.0, 21.0, 12.9. HRMS (ESI TOF) *m/z* calcd. For $C_{33}H_{31}N_3O_6$ $[M+H]^+$ 566.2291 found 566.2293.

Methyl (*5R,7S,8R,14R*)-10-benzyl-1-methyl-4,11,12-trioxo-3-phenyl-7-(p-tolyl)-6-oxa-2,3,10-triazadispiro[4.2.48.25]tetradec-1-ene-14-carboxylate (3f)

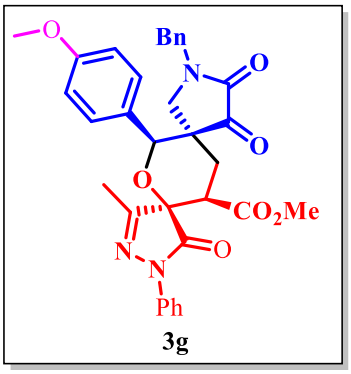
Product **3e** was synthesized following the general experimental procedure **5.5.4**. An oven-dried 10 mL glass reaction tube was charged with pyrazoledione-derived Morita–Baylis–Hillman (Pyro-MBH) alcohol **1a** (1.0 equiv, 0.2 mmol), potassium tert-butoxide (50 mol%, 0.1 mmol), and arylidene pyrrolidinediones **2b** (1.0 equiv, 0.2 mmol). Subsequently, 1,4-Dioxane (1 mL)



3f

was added to the tube. The reaction mixture was stirred at ambient temperature for 5 minute. Upon completion, the solvent was removed under reduced pressure, and the residue was purified by column chromatography on silica gel using 50% ethyl acetate in hexanes as the eluent. The purified product **3f**, identified as Methyl (*5R,7S,8R,14R*)-10-benzyl-1-methyl-4,11,12-trioxo-3-phenyl-7-(p-tolyl)-6-oxa-2,3,10-triazadispiro[4.2.48.25]tetradec-1-ene-14-carboxylate **(3f)** was obtained as a white solid in a yield of 80 mg (71%) as a single diastereomer. The structure was confirmed through spectroscopic methods including ^{1}H NMR, ^{13}C{^{1}H} NMR, HRMS, and X-ray crystallographic analysis. The compound displayed a melting point of 233–235 °C and a TLC retention factor (R_f) 0.5 (silica gel, 50% ethyl acetate/hexanes). ^{1}H NMR (400 MHz, $CDCl_3$): δ 7.9 – 7.7 (m, 2H), 7.4 – 7.3 (m, 2H), 7.3 – 7.3 (m, 1H), 7.3 (s, 2H), 7.2 – 7.1 (m, 1H), 7.0 (d, *J* = 8.0 Hz, 2H), 6.9 (d, *J* = 8.2 Hz, 2H), 6.9 – 6.8 (m, 2H), 6.1 (s, 1H), 4.4 (d, *J* = 14.7 Hz, 1H), 4.3 (d, *J* = 14.7 Hz, 1H), 3.8 (d, *J* = 11.1 Hz, 1H), 3.6 (s, 3H), 3.5 (t, *J* = 13.6 Hz, 1H), 3.3 (d, *J* = 11.1 Hz, 1H), 2.9 (dd, *J* = 13.6, 4.2 Hz, 1H), 2.3 (s, 3H), 2.2 (s, 3H), 2.1 (dd, *J* = 13.6, 4.2 Hz, 1H). ^{13}C{^{1}H} NMR (100 MHz, $CDCl_3$): δ 200.1, 169.1, 168.8, 158.6, 156.9, 138.4, 137.4, 133.9, 132.1, 129.5, 128.9, 128.9, 128.1, 128.1, 125.5, 125.4, 119.0, 77.1, 73.5, 52.9, 48.4, 47.5, 47.0, 40.7, 29.0, 21.2, 12.9. HRMS (ESI TOF) *m/z* calcd. For $C_{33}H_{31}N_3O_6$ $[M+H]^+$ 566.2291 found 566.2295.

Methyl (*5R,7S,8R,14R*)-10-benzyl-7-(4-methoxyphenyl)-1-methyl-4,11,12-trioxo-3-phenyl-6-oxa-2,3,10-triazadispiro[4.2.48.25]tetradec-1-ene-14-carboxylate (3g)

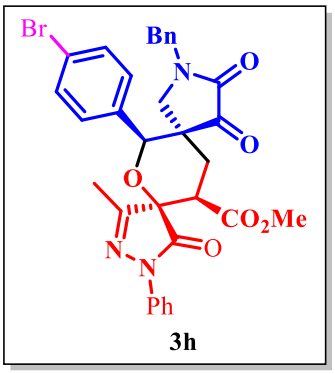


3g

Product **3g** was synthesized following the general experimental procedure **5.5.4**. An oven-dried 10 mL glass reaction tube was charged with pyrazoledione-derived Morita–Baylis–Hillman (Pyro-MBH) alcohol **1a** (1.0 equiv, 0.2 mmol), potassium tert-butoxide (50 mol%, 0.1 mmol), and arylidene pyrrolidinediones **2c** (1.0 equiv, 0.2 mmol). Subsequently, 1,4-Dioxane (1 mL) was added to the tube. The reaction mixture was stirred at ambient temperature for 5 minute. Upon completion, the solvent was removed under reduced pressure, and the residue was purified by column chromatography on silica gel using 50% ethyl acetate in hexanes as the eluent. The purified product, **3g**, Methyl (5R,7S,8R,14R)-10-benzyl-7-(4-methoxyphenyl)-1-methyl-4,11,12-trioxo-3-phenyl-6-oxa-

2,3,10-triazadispiro[4.2.48.25]tetradec-1-ene-14-carboxylate (**3g**), was obtained as a white solid in a yield of 72 mg (62%) as a single diastereomer. The structure was confirmed through spectroscopic methods including ^{1}H NMR, ^{13}C{^{1}H} NMR, HRMS, and X-ray crystallographic analysis. The compound displayed a melting point of 214–216 °C and a TLC retention factor (R_f) 0.5 (silica gel, 50% ethyl acetate/hexanes). ^{1}H NMR (400 MHz, $CDCl_3$): δ 7.8 (dd, *J* = 8.8, 1.2 Hz, 2H), 7.4 – 7.3 (m, 2H), 7.3 (d, *J* = 4.3 Hz, 2H), 7.2 (d, *J* = 2.0 Hz, 1H), 7.2 – 7.1 (m, 1H), 7.0 – 6.9 (m, 2H), 6.9 – 6.8 (m, 2H), 6.8 – 6.7 (m, 2H), 6.1 (s, 1H), 4.5 (d, *J* = 14.7 Hz, 1H), 4.3 (d, *J* = 14.7 Hz, 1H), 3.8 (s, 3H), 3.7 (d, *J* = 11.2 Hz, 1H), 3.6 (s, 3H), 3.5 (t, *J* = 13.6 Hz, 1H), 3.3 (d, *J* = 11.2 Hz, 1H), 2.9 (dd, *J* = 13.6, 4.2 Hz, 1H), 2.2 (s, 3H), 2.1 (dd, *J* = 13.6, 4.2 Hz, 1H). ^{13}C{^{1}H} NMR (100 MHz, $CDCl_3$): δ 200.2, 169.0, 168.8, 159.7, 158.6, 156.9, 137.4, 133.9, 129.0, 128.9, 128.1, 128.0, 127.1, 126.8, 125.4, 119.0, 114.2, 77.2, 73.3, 55.2, 52.9, 48.4, 47.6, 47.0, 40.7, 29.0, 12.9. HRMS (ESI TOF) *m/z* calcd. For $C_{33}H_{31}N_3O_7$ $[M+H]^+$ 582.2240 found 582.2242.

Methyl (*5R,7S,8R,14R*)-10-benzyl-7-(4-bromophenyl)-1-methyl-4,11,12-trioxo-3-phenyl-6-oxa-2,3,10-triazadispiro[4.2.48.25]tetradec-1-ene-14-carboxylate (3h)

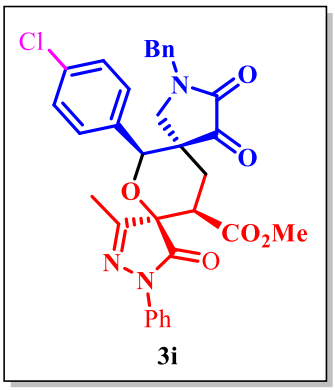


3h

Product **3h** was synthesized following the general experimental procedure **5.5.4**. An oven-dried 10 mL glass reaction tube was charged with pyrazoledione-derived Morita–Baylis–Hillman (Pyro-MBH) alcohol **1a** (1.0 equiv, 0.2 mmol), potassium tert-butoxide (50 mol%, 0.1 mmol), and arylidene pyrrolidinediones **2d** (1.0 equiv, 0.2 mmol). Subsequently, 1,4-Dioxane (1 mL) was added to the tube. The reaction mixture was stirred at ambient temperature for 5 minute. Upon completion, the solvent was removed under reduced pressure, and the residue was purified by column chromatography on silica gel using 50% ethyl acetate in hexanes as the eluent. The purified product **3h**, Methyl (*5R,7S,8R,14R*)-10-benzyl-7-(4-bromophenyl)-1-methyl-4,11,12-trioxo-3-phenyl-6-oxa-2,3,10-triazadispiro[4.2.48.25]tetradec-1-ene-14-carboxylate **(3h),** was obtained as a white solid in a yield of 77 mg (61%) as a single diastereomer. The structure was confirmed through spectroscopic methods, including ^{1}H NMR, ^{13}C{^{1}H} NMR, HRMS, and X-ray crystallographic analysis. The compound displayed a melting point of 234–236 °C and a TLC retention factor (R_f) 0.5 (silica gel, 50% ethyl acetate/hexanes). ^{1}H NMR (400 MHz, $CDCl_3$): δ 7.9 – 7.7 (m, 2H), 7.4 – 7.3 (m, 5H), 7.3 – 7.2 (m, 2H), 7.2 (s, 1H), 6.9 – 6.8 (m, 4H), 6.1 (s, 1H), 4.7 (d, *J*

= 14.5 Hz, 1H), 4.1 (d, *J* = 14.6 Hz, 1H), 3.7 (d, *J* = 11.6 Hz, 1H), 3.6 (s, 3H), 3.5 (t, *J* = 13.6 Hz, 1H), 3.3 (d, *J* = 11.3 Hz, 1H), 2.9 (dd, *J* = 13.6, 4.2 Hz, 1H), 2.2 (s, 3H), 2.1 (dd, *J* = 13.7, 4.2 Hz, 1H). $^{13}C\{^1H\}$ NMR (100 MHz, $CDCl_3$) δ 200.1, 168.9, 168.7, 158.4, 156.7, 137.3, 134.1, 133.7, 131.9, 129.1, 128.9, 128.3, 128.0, 127.2, 125.5, 122.8, 118.9, 77.3, 73.0, 52.9, 48.5, 47.1, 46.7, 40.7, 29.1, 13.0. HRMS (ESI TOF) *m/*calcd. For $C_{32}H_{28}BrN_3O_6$ $[M+H]^+$ 630.1240 found 630.1242.

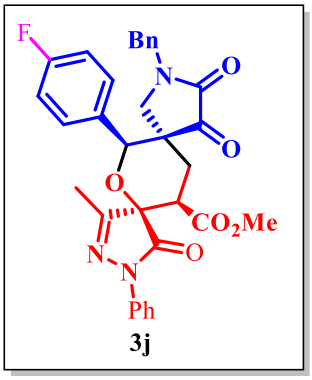
Methyl (*5R,7S,8R,14R*)-10-benzyl-7-(4-chlorophenyl)-1-methyl-4,11,12-trioxo-3-phenyl-6-oxa-2,3,10-triazadispiro[4.2.48.25]tetradec-1-ene-14-carboxylate (3i)



3i

Product **3i** was synthesized following the general experimental procedure **5.5.4**. An oven-dried 10 mL glass reaction tube was charged with pyrazoledione-derived Morita–Baylis–Hillman (Pyro-MBH) alcohol **1a** (1.0 equiv, 0.2 mmol), potassium tert-butoxide (50 mol%, 0.1 mmol), and arylidene pyrrolidinediones **2e** (1.0 equiv, 0.2 mmol). Subsequently, 1,4-Dioxane (1 mL) was added to the tube. The reaction mixture was stirred at ambient temperature for 5 minute. Upon completion, the solvent was removed under reduced pressure, and the residue was purified by column chromatography on silica gel using 50% ethyl acetate in hexanes as the eluent. The purified product **3i**, Methyl (*5R,7S,8R,14R*)-10-benzyl-7-(4-chlorophenyl)-1-methyl-4,11,12-trioxo-3-phenyl-6-oxa-2,3,10-triazadispiro[4.2.48.25]tetradec-1-ene-14-carboxylate **(3i),** was obtained as a white solid in a yield of 76 mg (65%) as a single diastereomer. The structure was confirmed through spectroscopic methods including ^1H NMR, $^{13}C\{^1H\}$ NMR, HRMS, and X-ray crystallographic analysis. The compound displayed a melting point of 231–233 °C and a TLC retention factor (R_f) 0.5 (silica gel, 50% ethyl acetate/hexanes). ^1H NMR (400 MHz, $CDCl_3$): δ 7.8 – 7.7 (m, 2H), 7.4 – 7.3 (m, 5H), 7.2 (d, *J* = 7.4 Hz, 1H), 7.1 – 7.1 (m, 2H), 7.0 – 6.9 (m, 2H), 6.9 – 6.8 (m, 2H), 6.1 (s, 1H), 4.7 (d, *J* = 14.5 Hz, 1H), 4.1 (d, *J* = 14.6 Hz, 1H), 3.7 (d, *J* = 12.0 Hz, 1H), 3.6 (s, 3H), 3.5 (s, 1H), 3.3 (d, *J* = 11.3 Hz, 1H), 2.9 (s, 1H), 2.2 (s, 3H), 2.1 (dd, *J* = 13.7, 4.2 Hz, 1H). $^{13}C\{^1H\}$ NMR (100 MHz, $CDCl_3$): δ 200.0, 168.9, 168.7, 158.4, 156.7, 137.3, 134.6, 133.8, 133.5, 129.1, 129.0, 128.9, 128.3, 128.0, 126.9, 125.5, 118.9, 77.2, 72.9, 52.9, 48.5, 47.2, 46.8, 40.7, 29.1, 13.0. HRMS (ESI TOF) *m/z* calcd. For $C_{32}H_{28}ClN_3O_6$ $[M+H]^+$ 586.1745 found 586.1747.

Methyl (*5R,7S,8R,14R*)-10-benzyl-7-(4-fluorophenyl)-1-methyl-4,11,12-trioxo-3-phenyl-6-oxa-2,3,10-triazadispiro[4.2.48.25]tetradec-1-ene-14-carboxylate (3j)

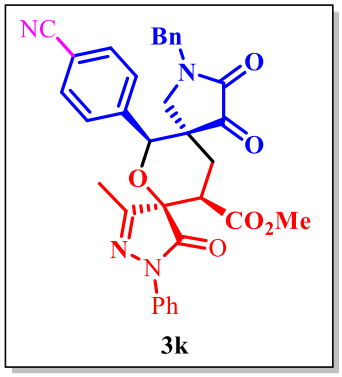


3j

Product **3j** was synthesized following the general experimental procedure **5.5.4**. An oven-dried 10 mL glass reaction tube was charged with pyrazoledione-derived Morita–Baylis–Hillman (Pyro-MBH) alcohol **1a** (1.0 equiv, 0.2 mmol), potassium tert-butoxide (50 mol%, 0.1 mmol), and arylidene pyrrolidinediones **2f** (1.0 equiv, 0.2 mmol). Subsequently, 1,4-Dioxane (1 mL) was added to the tube. The reaction mixture was stirred at ambient temperature for 5 minute. Upon completion, the solvent was removed under reduced pressure, and the residue was purified by column chromatography on silica gel using 50% ethyl acetate in hexanes as the eluent. The purified product **3j**, Methyl (*5R,7S,8R,14R*)-10-benzyl-7-(4-fluorophenyl)-1-methyl-4,11,12-trioxo-3-phenyl-6-oxa-2,3,10-triazadispiro[4.2.48.25]tetradec-1-ene-14-carboxylate **(3j),** was obtained as a white solid in a yield of 91 mg (80%) as a single diastereomer. The structure was confirmed through spectroscopic methods, including ^{1}H NMR, ^{13}C{^{1}H} NMR, HRMS, and X-ray crystallographic analysis. The compound displayed a melting point of 247–249 °C and a TLC retention factor (R_f) 0.5 (silica gel, 50% ethyl acetate/hexanes). ^{1}H NMR (400 MHz, $CDCl_3$): δ 7.9 – 7.8 (m, 2H), 7.4 – 7.3 (m, 2H), 7.3 – 7.2 (m, 3H), 7.2 (s, 1H), 7.0 (dd, *J* = 8.7, 5.2 Hz, 2H), 6.9 – 6.8 (m, 4H), 6.1 (s, 1H), 4.6 (d, *J* = 14.5 Hz, 1H), 4.2 (d, *J* = 14.6 Hz, 1H), 3.7 (d, *J* = 11.2 Hz, 1H), 3.6 (s, 3H), 3.5 (t, *J* = 13.6 Hz, 1H), 3.3 (d, *J* = 11.2 Hz, 1H), 2.9 (dd, *J* = 13.6, 4.2 Hz, 1H), 2.2 (s, 3H), 2.1 (dd, *J* = 13.7, 4.2 Hz, 1H). ^{13}C{^{1}H} NMR (100 MHz, $CDCl_3$): δ 200.1, 168.9, 168.7, 162.5 (d, $J_{(C-F)}$ = 248.2 Hz), 158.4, 156.7, 137.3, 133.9, 130.8 (d, $J_{(C-F)}$ = 3.3 Hz), 129.1, 128.9, 128.3, 128.1, 127.4 (d, $J_{(C-F)}$ = 8.2 Hz), 125.5, 118.9, 115.8 (d, $J_{(C-F)}$ = 21.6 Hz), 77.1, 73.0, 52.9, 48.4, 47.4, 46.8, 40.7, 29.0, 12.9. ^{19}F NMR (377 MHz, $CDCl_3$): δ -112.2. HRMS (ESI TOF) *m/z* calcd. For $C_{32}H_{28}FN_3O_6$ $[M+H]^+$ 570.2040 found 570.2044.

Methyl (*5R,7S,8R,14R*)-10-benzyl-7-(4-cyanophenyl)-1-methyl-4,11,12-trioxo-3-phenyl-6-oxa-2,3,10-triazadispiro[4.2.48.25]tetradec-1-ene-14-carboxylate (3k)

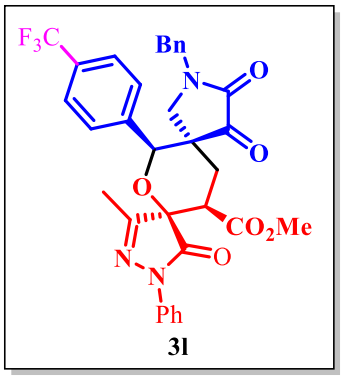
Product **3k** was synthesized following the general experimental procedure **5.5.4**. An oven-dried 10 mL glass reaction tube was charged with pyrazoledione-derived Morita–Baylis–Hillman (Pyro-MBH) alcohol **1a** (1.0 equiv, 0.2 mmol), potassium tert-butoxide (50 mol%, 0.1 mmol), and arylidene pyrrolidinediones **2g** (1.0 equiv, 0.2 mmol). Subsequently, 1,4-Dioxane (1 mL)



3k

was added to the tube. The reaction mixture was stirred at ambient temperature for 10 minute. Upon completion, the solvent was removed under reduced pressure, and the residue was purified by column chromatography on silica gel using 50% ethyl acetate in hexanes as the eluent. The purified product **3k**, Methyl (*5R,7S,8R,14R*)-10-benzyl-7-(4-cyanophenyl)-1-methyl-4,11,12-trioxo-3-phenyl-6-oxa-2,3,10-triazadispiro[4.2.48.25]tetradec-1-ene-14-carboxylate **(3k)** was obtained as a white solid in a yield of 88 mg (76%) as a single diastereomer. The structure was confirmed through spectroscopic methods, including ^{1}H NMR, ^{13}C{^{1}H} NMR, HRMS, and X-ray crystallographic analysis. The compound displayed a melting point of 143–145 °C and a TLC retention factor (R_f) 0.5 (silica gel, 50% ethyl acetate/hexanes). ^{1}H NMR (400 MHz, $CDCl_3$): δ 7.8 – 7.8 (m, 2H), 7.4 – 7.3 (m, 4H), 7.3 – 7.3 (m, 3H), 7.2 (d, *J* = 7.5 Hz, 1H), 7.1 – 7.0 (m, 2H), 6.9 – 6.8 (m, 2H), 6.1 (s, 1H), 4.7 (d, *J* = 14.3 Hz, 1H), 4.0 (d, *J* = 14.3 Hz, 1H), 3.6 (s, 3H), 3.6 (d, *J* = 11.3 Hz, 1H), 3.5 (t, *J* = 13.7 Hz, 1H), 3.4 (d, *J* = 11.4 Hz, 1H), 2.9 (dd, *J* = 13.6, 4.2 Hz, 1H), 2.2 (s, 3H), 2.1 (dd, *J* = 13.7, 4.2 Hz, 1H). ^{13}C{^{1}H} NMR (100 MHz, $CDCl_3$): δ 199.7, 168.7, 168.5, 158.1, 156.5, 140.0, 137.2, 133.8, 132.3, 129.2, 128.9, 128.6, 128.3, 126.3, 125.6, 118.9, 118.1, 112.7, 77.2, 72.8, 53.0, 48.5, 47.1, 46.6, 40.6, 29.1, 13.0. HRMS (ESI TOF) *m/z* calcd. For $C_{33}H_{28}N_4O_6$ $[M+H]^+$ 577.2087 found 577.2089.

Methyl (*5R,7S,8R,14R*)-10-benzyl-1-methyl-4,11,12-trioxo-3-phenyl-7-(4-(trifluoromethyl)phenyl)-6-oxa-2,3,10-triazadispiro[4.2.48.25]tetradec-1-ene-14-carboxylate (3l)

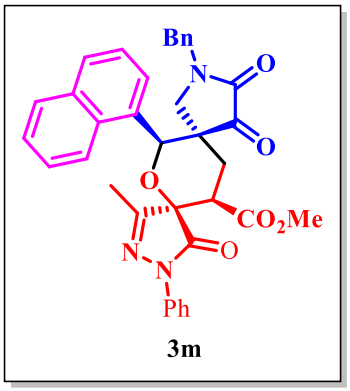


3l

Product **3l** was synthesized following the general experimental procedure **5.5.4**. An oven-dried 10 mL glass reaction tube was charged with pyrazoledione-derived Morita–Baylis–Hillman (Pyro-MBH) alcohol **1a** (1.0 equiv, 0.2 mmol), potassium tert-butoxide (50 mol%, 0.1 mmol), and arylidene pyrrolidinediones **2h** (1.0 equiv, 0.2 mmol). Subsequently, 1,4-Dioxane (1 mL) was added to the tube. The reaction mixture was stirred at ambient temperature for 20 minute. Upon completion, the solvent was removed under reduced pressure, and the residue was purified by column chromatography on silica gel using 50% ethyl acetate in hexanes as the eluent. The purified product **3l**, Methyl (*5R,7S,8R,14R*)-10-benzyl-1-methyl-

4,11,12-trioxo-3-phenyl-7-(4-(trifluoromethyl)phenyl)-6-oxa-2,3,10-triazadispiro[4.2.48.25]tetradec-1-ene-14-carboxylate **(3l)** was obtained as a white solid in a yield of 103 mg (83%) as a single diastereomer. The structure was confirmed through spectroscopic methods, including ^{1}H NMR, ^{13}C{^{1}H} NMR, HRMS, and X-ray crystallographic analysis. The compound displayed a melting point of 192–194 °C and a TLC retention factor (R_f) 0.5 (silica gel, 50% ethyl acetate/hexanes). ^{1}H NMR (400 MHz, $CDCl_3$): δ 7.9 – 7.7 (m, 2H), 7.5 – 7.3 (m, 4H), 7.3 – 7.3 (m, 1H), 7.3 – 7.2 (m, 3H), 7.1 (d, J = 8.1 Hz, 2H), 6.9 – 6.8 (m, 2H), 6.2 (s, 1H), 4.7 (d, J = 14.5 Hz, 1H), 4.1 (d, J = 14.5 Hz, 1H), 3.6 (s, 3H), 3.6 (s, 1H), 3.5 (t, J = 13.6 Hz, 1H), 3.3 (d, J = 11.3 Hz, 1H), 2.9 (dd, J = 13.6, 4.2 Hz, 1H), 2.2 (s, 3H), 2.1 (dd, J = 13.7, 4.2 Hz, 1H). ^{13}C{^{1}H} NMR (100 MHz, $CDCl_3$): δ 199.8, 168.8, 168.6, 158.2, 156.6, 139.2 – 138.9 (m), 133.6, 131.0, 130.6, 129.1, 128.9, 128.9, 128.4, 128.1, 126.3, 125.7 (q, $J_{(C-F)}$ = 3.5 Hz), 125.6, 119.0, 77.1, 73.0, 53.0, 48.4, 47.2, 46.6, 40.7, 29.3, 13.0. ^{19}F NMR (377 MHz, $CDCl_3$): δ -62.6. HRMS (ESI TOF) *m/z* calcd. For $C_{33}H_{28}F_3N_3O_6$ $[M+H]^+$ 619.1930 found 619.1932.

Methyl (5R,7R,8R,14R)-10-benzyl-1-methyl-7-(naphthalen-1-yl)-4,11,12-trioxo-3-phenyl-6-oxa-2,3,10-triazadispiro[4.2.48.25]tetradec-1-ene-14-carboxylate (3m)

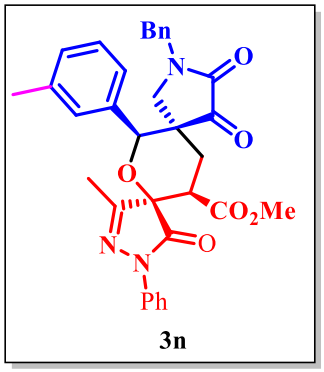


3m

Product **3m** was synthesized following the general experimental procedure **5.5.4**. An oven-dried 10 mL glass reaction tube was charged with pyrazoledione-derived Morita–Baylis–Hillman (Pyro-MBH) alcohol **1a** (1.0 equiv, 0.2 mmol), potassium tert-butoxide (50 mol%, 0.1 mmol), and arylidene pyrrolidinediones **2i** (1.0 equiv, 0.2 mmol). Subsequently, 1,4-Dioxane (1 mL) was added to the tube. The reaction mixture was stirred at ambient temperature for 5 minute. Upon completion, the solvent was removed under reduced pressure, and the residue was purified by column chromatography on silica gel using 50% ethyl acetate in hexanes as the eluent. The purified product **3m**, Methyl (5R,7R,8R,14R)-10-benzyl-1-methyl-7-(naphthalen-1-yl)-4,11,12-trioxo-3-phenyl-6-oxa-2,3,10-triazadispiro[4.2.48.25]tetradec-1-ene-14-carboxylate **(3m)** was obtained as a white solid in a yield of 64 mg (53%) as a single diastereomer. The structure was confirmed through spectroscopic methods including ^{1}H NMR, ^{13}C{^{1}H} NMR, HRMS, and X-ray crystallographic analysis. The compound displayed a melting point of 256–258 °C and a TLC retention factor (R^f) 0.5 (silica gel, 50% ethyl acetate/hexanes). ^{1}H NMR (400 MHz, $CDCl_3$): δ 7.9 (d, *J* = 8.5

Hz, 1H), 7.9 – 7.7 (m, 4H), 7.6 – 7.4 (m, 3H), 7.4 – 7.3 (m, 6H), 7.2 – 7.1 (m, 1H), 7.0 (s, 1H), 7.0 – 6.9 (m, 2H), 4.3 (d, *J* = 14.6 Hz, 1H), 4.1 – 3.9 (m, 2H), 3.7 (t, *J* = 13.8 Hz, 1H), 3.7 (s, 3H), 3.3 (d, *J* = 11.1 Hz, 1H), 3.0 (dd, *J* = 13.7, 4.2 Hz, 1H), 2.2 (s, 3H), 2.1 (dd, *J* = 13.8, 4.2 Hz, 1H). $^{13}C\{^1H\}$ NMR (100 MHz, $CDCl_3$): δ 199.3, 169.1, 169.0, 158.2, 156.8, 137.3, 134.0, 133.7, 131.1, 129.8, 129.3, 129.1, 128.9, 128.8, 128.4, 128.3, 127.1, 126.4, 125.5, 124.5, 123.7, 123.6, 119.1, 77.5, 69.1, 52.9, 48.4, 48.3, 47.3, 41.0, 29.4, 13.1. HRMS (ESI TOF) *m/z* calcd. For $C_{36}H_{31}N_3O_6$ $[M+H]^+$ 602.2291 found 602.2293.

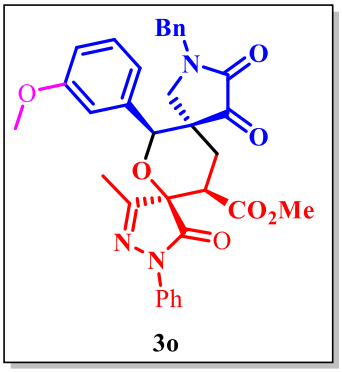
Methyl (*5R,7S,8R,14R*)-10-benzyl-1-methyl-4,11,12-trioxo-3-phenyl-7-(m-tolyl)-6-oxa-2,3,10-triazadispiro[4.2.48.25]tetradec-1-ene-14-carboxylate (3n)



3n

Product **3n** was synthesized following the general experimental procedure **5.5.4**. An oven-dried 10 mL glass reaction tube was charged with pyrazoledione-derived Morita–Baylis–Hillman (Pyro-MBH) alcohol **1a** (1.0 equiv, 0.2 mmol), potassium tert-butoxide (50 mol%, 0.1 mmol), and arylidene pyrrolidinediones **2j** (1.0 equiv, 0.2 mmol). Subsequently, 1,4-Dioxane (1 mL) was added to the tube. The reaction mixture was stirred at ambient temperature for 5 minute. Upon completion, the solvent was removed under reduced pressure, and the residue was purified by column chromatography on silica gel using 50% ethyl acetate in hexanes as the eluent. The purified product **3n**, Methyl (*5R,7S,8R,14R*)-10-benzyl-1-methyl-4,11,12-trioxo-3-phenyl-7-(m-tolyl)-6-oxa-2,3,10-triazadispiro[4.2.48.25]tetradec-1-ene-14-carboxylate **(3n),** was obtained as a white solid in a yield of 70 mg (62%) as a single diastereomer. The structure was confirmed through spectroscopic methods, including ^1H NMR, $^{13}C\{^1H\}$ NMR, HRMS, and X-ray crystallographic analysis. The compound displayed a melting point of 234–236 °C and a TLC retention factor (R_f) 0.5 (silica gel, 50% ethyl acetate/hexanes). ^1H NMR (400 MHz, $CDCl_3$): δ 7.7 – 7.6 (m, 2H), 7.3 – 7.3 (m, 2H), 7.3 – 7.2 (m, 4H), 7.2 – 7.1 (m, 2H), 7.1 (dt, *J* = 7.1, 1.5 Hz, 2H), 6.8 (dt, *J* = 6.7, 1.6 Hz, 2H), 6.1 (s, 1H), 4.4 (d, *J* = 14.7 Hz, 1H), 4.3 (d, *J* = 14.7 Hz, 1H), 3.7 (d, *J* = 11.2 Hz, 1H), 3.6 (s, 3H), 3.5 (t, *J* = 13.6 Hz, 1H), 3.3 (d, *J* = 11.2 Hz, 1H), 2.9 (dd, *J* = 13.6, 4.2 Hz, 1H), 2.3 (s, 3H), 2.2 (s, 3H), 2.1 (dd, *J* = 13.7, 4.2 Hz, 1H). $^{13}C\{^1H\}$ NMR (100 MHz, $CDCl_3$): δ 199.1, 169.1, 169.0, 158.7, 156.8, 137.4, 135.6, 134.1, 133.3, 131.9, 129.1, 128.9, 128.9, 128.5, 128.4, 125.9, 125.5, 125.4, 119.1, 77.4, 69.3, 52.9, 48.5, 48.2, 47.0, 40.9, 29.4, 19.8, 12.9. HRMS: (ESI TOF) *m/z* calcd for $C_{33}H_{31}N_3O_6$ $[M + H]^+$ 566.2291, found 566.2293.

Methyl (*5R,7S,8R,14R*)-10-benzyl-7-(3-methoxyphenyl)-1-methyl-4,11,12-trioxo-3-phenyl-6-oxa-2,3,10-triazadispiro[4.2.48.25]tetradec-1-ene-14-carboxylate (3o)

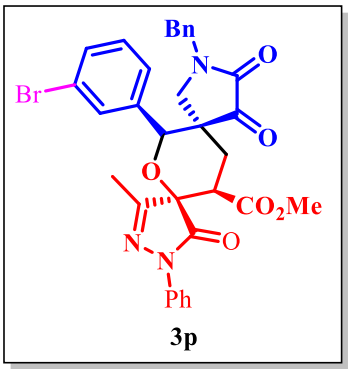


3o

Product **3o** was synthesized following the general experimental procedure **5.5.4**. An oven-dried 10 mL glass reaction tube was charged with pyrazoledione-derived Morita–Baylis–Hillman (Pyro-MBH) alcohol **1a** (1.0 equiv, 0.2 mmol), potassium tert-butoxide (50 mol%, 0.1 mmol), and arylidene pyrrolidinediones **2k** (1.0 equiv, 0.2 mmol). Subsequently, 1,4-Dioxane (1 mL) was added to the tube. The reaction mixture was stirred at ambient temperature for 5 minute. Upon completion, the solvent was removed under reduced pressure, and the residue was purified by column chromatography on silica gel using 50% ethyl acetate in hexanes as the eluent. The purified product **3o**, Methyl (*5R,7S,8R,14R*)-10-benzyl-7-(3-methoxyphenyl) 1-methyl-4,11,12-trioxo-3-phenyl-6-oxa-2,3,10-triazadispiro[4.2.48.25]tetradec-1-ene-14-carboxylate **(3o),** was obtained as a white solid in a yield of 88 mg (76%) as a single diastereomer. The structure was confirmed through spectroscopic methods, including ^{1}H NMR, ^{13}C{^{1}H} NMR, HRMS, and X-ray crystallographic analysis. The compound displayed a melting point of 234–236 °C and a TLC retention factor (R^f) 0.5 (silica gel, 50% ethyl acetate/hexanes). ^{1}H NMR (400 MHz, $CDCl_3$): δ 7.9 – 7.8 (m, 2H), 7.4 – 7.3 (m, 2H), 7.3 (ddd, *J* = 10.5, 7.6, 5.9 Hz, 3H), 7.2 (dt, *J* = 14.2, 7.7 Hz, 2H), 6.8 (ddd, *J* = 24.6, 7.9, 2.0 Hz, 3H), 6.7 – 6.5 (m, 2H), 6.1 (s, 1H), 4.5 (d, *J* = 14.7 Hz, 1H), 4.3 (d, *J* = 14.7 Hz, 1H), 3.7 (d, *J* = 11.2 Hz, 1H), 3.7 (s, 3H), 3.6 (s, 3H), 3.5 (t, *J* = 13.6 Hz, 1H), 3.3 (d, *J* = 11.2 Hz, 1H), 2.9 (dd, *J* = 13.6, 4.2 Hz, 1H), 2.2 (s, 3H), 2.1 (dd, *J* = 13.7, 4.2 Hz, 1H). ^{13}C{^{1}H} NMR (100 MHz, $CDCl_3$): δ 200.3, 169.0, 168.8, 159.7, 158.7, 156.9, 137.4, 136.7, 133.9, 130.0, 129.0, 128.9, 128.1, 128.0, 125.4, 119.0, 117.8, 114.4, 111.1, 77.1, 73.4, 55.2, 52.9, 48.4, 47.5, 47.1, 40.7, 29.0, 13.0. HRMS: (ESI TOF) *m/z* calcd for $C_{33}H_{31}N_3O_7$ $[M + H]^+$ 582.2040, found 582.2044.

Methyl (5R,7R,8R,14R)-10-benzyl-7-(3-bromophenyl)-1-methyl-4,11,12-trioxo-3-phenyl-6-oxa-2,3,10-triazadispiro[4.2.48.25]tetradec-1-ene-14-carboxylate (3p)

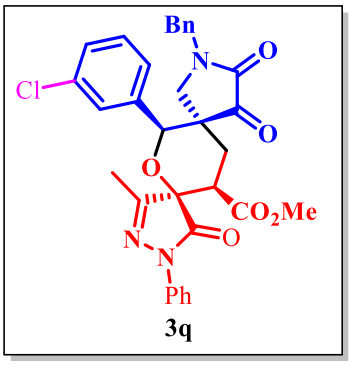
Product **3p** was synthesized following the general experimental procedure **5.5.4**. An oven-dried 10 mL glass reaction tube was charged with pyrazoledione-derived Morita–Baylis–Hillman (Pyro-MBH) alcohol **1a** (1.0 equiv, 0.2 mmol), potassium tert-butoxide (50 mol%, 0.1 mmol), and arylidene pyrrolidinediones **2l** (1.0 equiv, 0.2 mmol). Subsequently, 1,4-Dioxane (1 mL)



3p

was added to the tube. The reaction mixture was stirred at ambient temperature for 5 minute. Upon completion, the solvent was removed under reduced pressure, and the residue was purified by column chromatography on silica gel using 50% ethyl acetate in hexanes as the eluent. The purified product **3p**, Methyl (5R,7R,8R,14R)-10-benzyl-7-(3-bromophenyl)-1-methyl-4,11,12-trioxo-3-phenyl-6-oxa-2,3,10-triazadispiro[4.2.48.25]tetradec-1-ene-14-carboxylate **(3p),** was obtained as a white solid in a yield of 45 mg (36%) as a single diastereomer. The structure was confirmed through spectroscopic methods, including ^{1}H NMR, ^{13}C{^{1}H} NMR, HRMS, and X-ray crystallographic analysis. The compound displayed a melting point of 252–254 °C and a TLC retention factor (R_f) 0.5 (silica gel, 50% ethyl acetate/hexanes).^{1}H NMR (400 MHz, $CDCl_3$): δ 7.9 – 7.8 (m, 2H), 7.4 – 7.4 (m, 3H), 7.3 – 7.3 (m, 4H), 7.2 – 7.1 (m, 1H), 7.1 (t, *J* = 7.9 Hz, 1H), 6.9 – 6.8 (m, 3H), 6.1 (s, 1H), 4.5 (d, *J* = 14.7 Hz, 1H), 4.3 (d, *J* = 14.7 Hz, 1H), 3.7 (s, 1H), 3.6 (s, 3H), 3.5 (t, *J* = 13.7 Hz, 1H), 3.3 (d, *J* = 11.3 Hz, 1H), 2.9 (dd, *J* = 13.6, 4.2 Hz, 1H), 2.2 (s, 3H), 2.1 (dd, *J* = 13.7, 4.2 Hz, 1H). ^{13}C{^{1}H} NMR (100 MHz, $CDCl_3$): δ 199.9, 168.8, 168.6, 158.5, 156.7, 137.5, 137.3, 133.8, 132.0, 130.4, 129.2, 128.9, 128.4, 128.4, 127.8, 125.5, 124.8, 123.1, 119.0, 77.2, 72.8, 52.9, 48.5, 47.4, 46.9, 40.7, 29.1, 13.0. HRMS (ESI TOF) *m/z* calcd. For $C_{32}H_{28}BrN_3O_6$ $[M+H]^+$ 630.1240 found 630.1244.

Methyl (*5R,7S,8R,14R*)-10-benzyl-7-(3-chlorophenyl)-1-methyl-4,11,12-trioxo-3-phenyl-6-oxa-2,3,10-triazadispiro[4.2.48.25]tetradec-1-ene-14-carboxylate (3q)

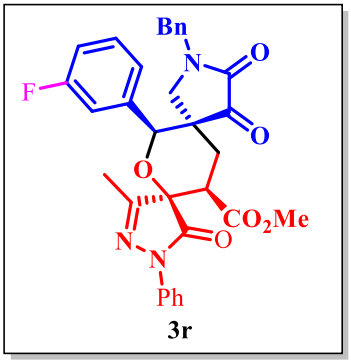


3q

Product **3q** was synthesized following the general experimental procedure **5.5.4**. An oven-dried 10 mL glass reaction tube was charged with pyrazoledione-derived Morita–Baylis–Hillman (Pyro-MBH) alcohol **1a** (1.0 equiv, 0.2 mmol), potassium tert-butoxide (50 mol%, 0.1 mmol), and arylidene pyrrolidinediones **2m** (1.0 equiv, 0.2 mmol). Subsequently, 1,4-Dioxane (1 mL) was added to the tube. The reaction mixture was stirred at ambient temperature for 5 minute. Upon completion, the solvent was removed under reduced pressure, and the residue was purified by column chromatography on silica gel using 50% ethyl acetate in hexanes as the eluent. The purified product **3q**, Methyl (*5R,7S,8R,14R*)-10-benzyl-7-(3-chlorophenyl)-1-methyl-4,11,12-trioxo-3-phenyl-6-oxa-2,3,10-

triazadispiro[4.2.48.25]tetradec-1-ene-14-carboxylate **(3q),** was obtained as a white solid in a yield of 53 mg (45%) as a single diastereomer. The structure was confirmed through spectroscopic methods, including ^{1}H NMR, ^{13}C{^{1}H} NMR, HRMS, and X-ray crystallographic analysis. The compound displayed a melting point of 228–230 °C and a TLC retention factor (R^f) 0.5 (silica gel, 50% ethyl acetate/hexanes).^{1}H NMR (400 MHz, $CDCl_3$): δ 7.9 – 7.7 (m, 2H), 7.4 – 7.3 (m, 5H), 7.3 – 7.1 (m, 4H), 6.9 – 6.8 (m, 3H), 6.1 (s, 1H), 4.5 (d, J = 14.7 Hz, 1H), 4.3 (d, J = 14.7 Hz, 1H), 3.7 (s, 1H), 3.6 (s, 3H), 3.5 (t, J = 13.7 Hz, 1H), 3.3 (d, J = 11.3 Hz, 1H), 2.9 (dd, J = 13.6, 4.2 Hz, 1H), 2.2 (s, 3H), 2.1 (dd, J = 13.7, 4.2 Hz, 1H).^{13}C{^{1}H} NMR (100 MHz, $CDCl_3$): δ 199.9, 168.8, 168.6, 158.5, 156.7, 137.3, 137.3, 134.9, 133.8, 130.1, 129.1, 129.1, 129.0, 128.9, 128.4, 127.8, 125.5, 124.3, 119.0, 77.1, 72.8, 52.9, 48.5, 47.3, 46.9, 40.7, 29.1, 13.0. HRMS (ESI TOF) *m/z* calcd. For $C_{32}H_{28}ClN_3O_6$ $[M+H]^+$ 586.1745 found 586.1749.

Methyl (*5R,7S,8R,14R*)-10-benzyl-7-(3-fluorophenyl)-1-methyl-4,11,12-trioxo-3-phenyl-6-oxa-2,3,10-triazadispiro[4.2.48.25]tetradec-1-ene-14-carboxylate (3r)

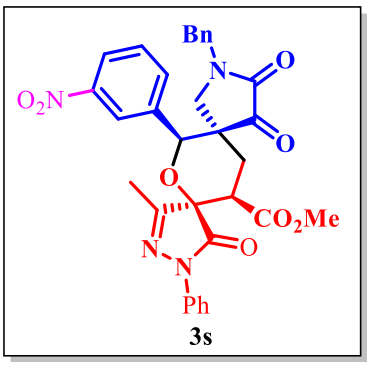


3r

Product **3r** was synthesized following the general experimental procedure **5.5.4**. An oven-dried 10 mL glass reaction tube was charged with pyrazoledione-derived Morita–Baylis–Hillman (Pyro-MBH) alcohol **1a** (1.0 equiv, 0.2 mmol), potassium tert-butoxide (50 mol%, 0.1 mmol), and arylidene pyrrolidinediones **2n** (1.0 equiv, 0.2 mmol). Subsequently, 1,4-Dioxane (1 mL) was added to the tube. The reaction mixture was stirred at ambient temperature for 5 minute. Upon completion, the solvent was removed under reduced pressure, and the residue was purified by column chromatography on silica gel using 50% ethyl acetate in hexanes as the eluent. The purified product **3r,** Methyl (*5R,7S,8R,14R*)-10-benzyl-7-(3-fluorophenyl)-1-methyl-4,11,12-trioxo-3-phenyl-6-oxa-2,3,10-triazadispiro[4.2.48.25]tetradec-1-ene-14-carboxylate **(3r),** was obtained as a white solid in a yield of 99 mg (87%) as a single diastereomer. The structure was confirmed through spectroscopic methods, including ^{1}H NMR, ^{13}C{^{1}H} NMR, HRMS, and X-ray crystallographic analysis. The compound displayed a melting point of 250–252 °C and a TLC retention factor (R^f) 0.5 (silica gel, 50% ethyl acetate/hexanes).^{1}H NMR (400 MHz, $CDCl_3$): δ 7.9 – 7.7 (m, 2H), 7.4 – 7.3 (m, 2H), 7.3 (dtd, *J* = 14.4, 5.5, 2.2 Hz, 3H), 7.2 – 7.1 (m, 2H), 6.9 (td, *J* = 8.4, 2.6 Hz, 1H), 6.9 – 6.7 (m, 4H), 6.1 (s, 1H), 4.6 (d, *J* = 14.7 Hz, 1H), 4.2 (d, *J* = 14.6 Hz, 1H),

3.7 (d, *J* = 11.3 Hz, 1H), 3.6 (s, 3H), 3.5 (s, 1H), 3.3 (d, *J* = 11.3 Hz, 1H), 2.9 (dd, *J* = 13.6, 4.2 Hz, 1H), 2.2 (s, 3H), 2.1 (dd, *J* = 13.7, 4.2 Hz, 1H). $^{13}C\{^1H\}$ NMR (100 MHz, $CDCl_3$): δ 199.9, 168.9, 168.6, 162.7 (d, $J_{(C-F)}$ = 247.6 Hz), 157.6 (d, $J_{(C-F)}$ = 173.6 Hz), 137.8, 137.7, 137.3, 133.8, 130.5 (d, $J_{(C-F)}$ = 8.3 Hz), 129.1, 128.9, 128.3, 128.0, 125.5, 121.7 (d, $J_{(C-F)}$ = 3.0 Hz), 118.9, 115.8 (d, $J_{(C-F)}$ = 20.9 Hz), 112.7 (d, $J_{(C-F)}$ = 23.0 Hz), 72.8, 72.8, 52.9, 48.4, 47.3, 46.8, 40.7, 29.1, 13.0. ^{19}F NMR (377 MHz, $CDCl_3$): δ -110.4. HRMS: (ESI TOF) *m/z* calcd for $C_{32}H_{28}FN_3O_6$ $[M + H]^+$ 570.2040, found 570.2042.

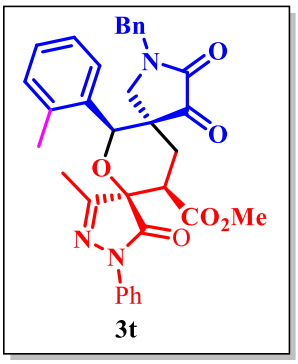
Methyl (*5R,7S,8R,14R*)-10-benzyl-1-methyl-7-(3-nitrophenyl)-4,11,12-trioxo-3-phenyl-6-oxa-2,3,10-triazadispiro[4.2.48.25]tetradec-1-ene-14-carboxylate (3s)



3s

Product **3s** was synthesized following the general experimental procedure **5.5.4**. An oven-dried 10 mL glass reaction tube was charged with pyrazoledione-derived Morita–Baylis–Hillman (Pyro-MBH) alcohol **1a** (1.0 equiv, 0.2 mmol), potassium tert-butoxide (50 mol%, 0.1 mmol), and arylidene pyrrolidinediones **2o** (1.0 equiv, 0.2 mmol). Subsequently, 1,4-Dioxane (1 mL) was added to the tube. The reaction mixture was stirred at ambient temperature for 20 minute. Upon completion, the solvent was removed under reduced pressure, and the residue was purified by column chromatography on silica gel using 50% ethyl acetate in hexanes as the eluent. The purified product **3s**, Methyl (*5R,7S,8R,14R*)-10-benzyl-1-methyl-7-(3-nitrophenyl)-4,11,12-trioxo-3-phenyl-6-oxa-2,3,10-triazadispiro[4.2.48.25]tetradec-1-ene-14-carboxylate **(3s),** was obtained as a white solid in a yield of 76 mg (64%) as a single diastereomer. The structure was confirmed through spectroscopic methods, including ^1H NMR, $^{13}C\{^1H\}$ NMR, HRMS, and X-ray crystallographic analysis. The compound displayed a melting point of 192–194 °C and a TLC retention factor (R_f) 0.5 (silica gel, 50% ethyl acetate/hexanes).^1H NMR (400 MHz, $CDCl_3$): δ 8.1 – 8.0 (m, 1H), 7.9 (t, *J* = 2.0 Hz, 1H), 7.9 – 7.7 (m, 2H), 7.4 – 7.3 (m, 3H), 7.3 – 7.1 (m, 5H), 6.9 – 6.8 (m, 2H), 6.2 (s, 1H), 4.8 (d, *J* = 14.3 Hz, 1H), 4.0 (d, *J* = 14.3 Hz, 1H), 3.7 (d, *J* = 1.7 Hz, 3H), 3.6 (s, 1H), 3.6 – 3.4 (m, 2H), 3.0 (dd, *J* = 13.6, 3.9 Hz, 1H), 2.3 (s, 3H), 2.2 (dd, *J* = 13.8, 4.1 Hz, 1H). $^{13}C\{^1H\}$ NMR (100 MHz, $CDCl_3$): δ 199.9, 168.7, 168.6, 158.1, 156.7, 148.1, 137.2, 137.2, 133.8, 132.4, 129.6, 128.9, 128.9, 128.5, 128.1, 125.6, 123.8, 120.3, 119.0, 77.2, 72.4, 53.0, 48.5, 47.1, 46.5, 40.6, 29.1, 13.1. HRMS: (ESI TOF) *m/z* calcd for $C_{32}H_{28}N_4O_8$ $[M + H]^+$ 597.1985, found 597.1989.

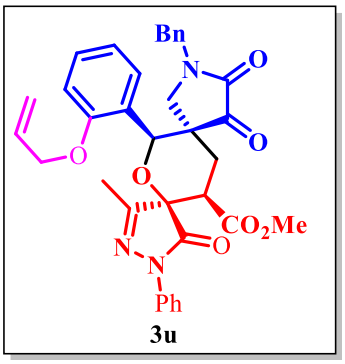
Methyl (*5R,7S,8R,14R*)-10-benzyl-1-methyl-4,11,12-trioxo-3-phenyl-7-(o-tolyl)-6-oxa-2,3,10-triazadispiro[4.2.48.25]tetradec-1-ene-14-carboxylate (3t)



3t

Product **3t** was synthesized following the general experimental procedure **5.5.4**. An oven-dried 10 mL glass reaction tube was charged with pyrazoledione-derived Morita–Baylis–Hillman (Pyro-MBH) alcohol **1a** (1.0 equiv, 0.2 mmol), potassium tert-butoxide (50 mol%, 0.1 mmol), and arylidene pyrrolidinediones **2p** (1.0 equiv, 0.2 mmol). Subsequently, 1,4-Dioxane (1 mL) was added to the tube. The reaction mixture was stirred at ambient temperature for 5 minute. Upon completion, the solvent was removed under reduced pressure, and the residue was purified by column chromatography on silica gel using 50% ethyl acetate in hexanes as the eluent. The purified product **3t**, Methyl (*5R,7S,8R,14R*)-10-benzyl-1-methyl-4,11,12-trioxo-3-phenyl-7-(o-tolyl)-6-oxa-2,3,10-triazadispiro[4.2.48.25]tetradec-1-ene-14-carboxylate **(3t),** was obtained as a white solid in a yield of 56 mg (50%) as a single diastereomer. The structure was confirmed through spectroscopic methods, including ^{1}H NMR, ^{13}C{^{1}H} NMR, HRMS, and X-ray crystallographic analysis. The compound displayed a melting point of 255–257 °C and a TLC retention factor (R_f) 0.5 (silica gel, 50% ethyl acetate/hexanes).^{1}H NMR (400 MHz, $CDCl_3$): δ 7.8 – 7.7 (m, 2H), 7.4 – 7.3 (m, 5H), 7.2 – 7.1 (m, 3H), 7.1 (ddd, *J* = 7.5, 4.8, 2.0 Hz, 3H), 7.0 (d, *J* = 1.5 Hz, 1H), 6.4 (s, 1H), 4.5 (d, *J* = 14.5 Hz, 1H), 4.2 (d, *J* = 14.6 Hz, 1H), 4.1 (d, *J* = 11.1 Hz, 1H), 3.6 (s, 3H), 3.6 (s, 1H), 3.3 (d, *J* = 11.2 Hz, 1H), 2.9 (dd, *J* = 13.6, 4.2 Hz, 1H), 2.2 (s, 6H), 2.0 (dd, *J* = 13.7, 4.2 Hz, 1H). ^{13}C{^{1}H} NMR (100 MHz, $CDCl_3$): δ 199.1, 169.1, 169.0, 158.7, 156.8, 137.4, 135.6, 134.1, 133.3, 131.9, 129.1, 128.9, 128.9, 128.5, 128.4, 125.9, 125.5, 125.3, 119.1, 77.4, 69.3, 52.9, 48.5, 48.2, 47.0, 40.9, 29.4, 19.8, 12.9. HRMS: (ESI TOF) *m/z* calcd for $C_{33}H_{31}N_3O_6$ $[M + H]^+$ 566.2291, found 566.2293.

Methyl (*5R,7S,8R,14R*)-7-(2-(allyloxy)phenyl)-10-benzyl-1-methyl-4,11,12-trioxo-3-phenyl-6-oxa-2,3,10-triazadispiro[4.2.48.25]tetradec-1-ene-14-carboxylate (3u)

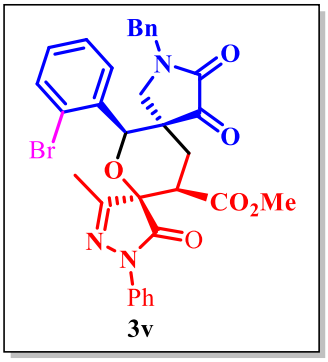


3u

Product **3u** was synthesized following general experimental procedure **5.5.4**. An oven-dried 10 mL glass reaction tube was charged with pyrazoledione-derived Morita–Baylis–Hillman (Pyro-MBH) alcohol **1a** (1.0 equiv, 0.2 mmol), potassium tert-butoxide (50 mol%, 0.1 mmol), and arylidene pyrrolidinediones **2q** (1.0 equiv, 0.2 mmol). Subsequently, 1,4-Dioxane (1 mL) was

added to the tube. The reaction mixture was stirred at ambient temperature for 5 minute. Upon completion, the solvent was removed under reduced pressure, and the residue was purified by column chromatography on silica gel using 50% ethyl acetate in hexanes as the eluent. The purified product **3u**, Methyl (*5R,7S,8R,14R*)-7-(2-(allyloxy)phenyl)-10-benzyl-1-methyl-4,11,12-trioxo-3-phenyl-6-oxa-2,3,10-triazadispiro[4.2.48.25]tetradec-1-ene-14-carboxylate **(3u),** was obtained as a white solid in a yield of 72 mg (59%) as a single diastereomer. The structure was confirmed through spectroscopic methods, including ^{1}H NMR, ^{13}C{^{1}H} NMR, HRMS, and X-ray crystallographic analysis. The compound displayed a melting point of 152–154 °C and a TLC retention factor (R_f) 0.5 (silica gel, 50% ethyl acetate/hexanes).^{1}H NMR (400 MHz, $CDCl_3$): δ 7.8 – 7.8 (m, 2H), 7.4 – 7.3 (m, 3H), 7.3 – 7.3 (m, 4H), 7.2 (dd, *J* = 7.7, 1.7 Hz, 1H), 7.2 – 7.1 (m, 1H), 7.0 (dd, *J* = 6.5, 2.8 Hz, 2H), 6.9 (t, *J* = 7.5 Hz, 1H), 6.8 (d, *J* = 8.3 Hz, 1H), 6.2 (s, 1H), 6.1 (dddd, *J* = 16.8, 10.6, 6.0, 4.7 Hz, 1H), 5.4 – 5.2 (m, 2H), 4.6 – 4.4 (m, 3H), 3.7 – 3.6 (m, 2H), 3.6 (s, 3H), 3.6 (s, 1H), 3.1 (d, *J* = 10.5 Hz, 1H), 2.9 (dd, *J* = 13.9, 4.1 Hz, 1H), 2.2 (s, 3H), 2.0 (dd, *J* = 14.0, 4.2 Hz, 1H). ^{13}C NMR (100 MHz, $CDCl_3$): δ 197.3, 169.3, 168.6, 159.5, 156.9, 154.6, 137.5, 134.2, 133.0, 129.7, 129.0, 128.8, 128.4, 128.1, 126.1, 125.3, 124.1, 120.4, 119.0, 117.7, 111.3, 69.0, 68.5, 52.8, 48.1, 48.0, 47.9, 41.2, 31.6, 27.6, 13.0. HRMS: (ESI TOF) *m/z* calcd for $C_{35}H_{33}N_3O_7$ $[M + H]^+$ 608.2397, found 608.2399.

Methyl (*5R,7R,8R,14R*)-10-benzyl-7-(2-bromophenyl)-1-methyl-4,11,12-trioxo-3-phenyl-6-oxa-2,3,10-triazadispiro[4.2.48.25]tetradec-1-ene-14-carboxylate (3v)

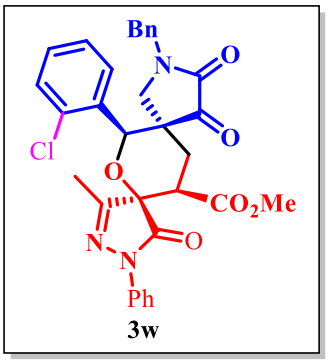


3v

Product **3v** was synthesized following the general experimental procedure **5.5.4**. An oven-dried 10 mL glass reaction tube was charged with pyrazoledione-derived Morita–Baylis–Hillman (Pyro-MBH) alcohol **1a** (1.0 equiv, 0.2 mmol), potassium tert-butoxide (50 mol%, 0.1 mmol), and arylidene pyrrolidinediones **2r** (1.0 equiv, 0.2 mmol). Subsequently, 1,4-Dioxane (1 mL) was added to the tube. The reaction mixture was stirred at ambient temperature for 5 minute. Upon completion, the solvent was removed under reduced pressure, and the residue was purified by column chromatography on silica gel using 50% ethyl acetate in hexanes as the eluent. The purified product **3u**, Methyl (5R,7R,8R,14R)-10-benzyl-7-(2-bromophenyl)-1-methyl-4,11,12-trioxo-3-phenyl-6-oxa-2,3,10-triazadispiro[4.2.48.25]tetradec-1-ene-14-carboxylate **(3v)**, was obtained as a white solid in a yield of 84 mg (67%) as a single diastereomer. The structure was confirmed through spectroscopic methods, including ^{1}H NMR, ^{13}C{^{1}H} NMR, HRMS, and X-ray crystallographic

analysis. The compound displayed a melting point of 249–251 °C and a TLC retention factor (R_f) 0.5 (silica gel, 50% ethyl acetate/hexanes).^{1}H NMR (400 MHz, $CDCl_3$): δ 7.9 – 7.8 (m, 2H), 7.5 – 7.5 (m, 1H), 7.4 – 7.3 (m, 5H), 7.3 (s, 1H), 7.2 – 7.2 (m, 2H), 7.1 (ddd, *J* = 9.9, 6.8, 3.0 Hz, 4H), 6.5 (s, 1H), 4.5 (d, *J* = 14.4 Hz, 1H), 4.2 – 3.9 (m, 2H), 3.6 (s, 1H), 3.6 (s, 3H), 3.3 (d, *J* = 11.1 Hz, 1H), 2.9 (s, 1H), 2.2 (s, 3H), 2.0 (dd, *J* = 13.8, 4.2 Hz, 1H). ^{13}C{^{1}H} NMR (100 MHz, $CDCl_3$): δ 197.9, 169.0, 168.6, 158.8, 156.6, 137.4, 134.6, 134.3, 134.1, 130.5, 129.1, 128.9, 128.6, 128.4, 127.7, 127.3, 125.4, 122.2, 119.0, 77.3, 71.7, 52.9, 48.5, 48.3, 47.2, 40.9, 28.9, 13.0. HRMS (ESI TOF) *m/z* calcd. For $C_{32}H_{28}BrN_3O_6$ $[M+H]^+$ 630.1240 found 630.1240.

Methyl (*5R,7R,8R,14R*)-10-benzyl-7-(2-chlorophenyl)-1-methyl-4,11,12-trioxo-3-phenyl-6-oxa-2,3,10-triazadispiro[4.2.48.25]tetradec-1-ene-14-carboxylate (3w)

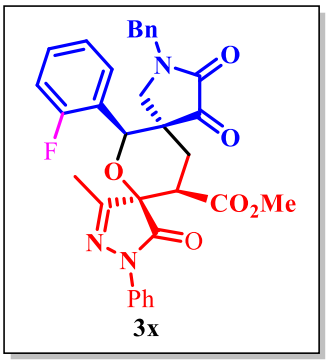


3w

Product **3w** was synthesized following the general experimental procedure **5.5.4**. An oven-dried 10 mL glass reaction tube was charged with pyrazoledione-derived Morita–Baylis–Hillman (Pyro-MBH) alcohol **1a** (1.0 equiv, 0.2 mmol), potassium tert-butoxide (50 mol%, 0.1 mmol), and arylidene pyrrolidinediones **2s** (1.0 equiv, 0.2 mmol). Subsequently, 1,4-Dioxane (1 mL) was added to the tube. The reaction mixture was stirred at ambient temperature for 5 minute. Upon completion, the solvent was removed under reduced pressure, and the residue was purified by column chromatography on silica gel using 50% ethyl acetate in hexanes as the eluent. The purified product **3w**, Methyl (5R,7R,8R,14R)-10-benzyl-7-(2-chlorophenyl)-1-methyl-4,11,12-trioxo-3-phenyl-6-oxa-2,3,10-triazadispiro[4.2.48.25]tetradec-1-ene-14-carboxylate **(3w),** was obtained as a white solid in a yield of 53 mg (45%) as a single diastereomer. The structure was confirmed through spectroscopic methods, including ^{1}H NMR, ^{13}C{^{1}H} NMR, HRMS, and X-ray crystallographic analysis. The compound displayed a melting point of 295–297 °C and a TLC retention factor (R_f) 0.5 (silica gel, 50% ethyl acetate/hexanes).^{1}H NMR (400 MHz, $CDCl_3$): δ 7.9 – 7.8 (m, 2H), 7.4 – 7.3 (m, 6H), 7.3 (d, *J* = 3.2 Hz, 1H), 7.2 – 7.2 (m, 2H), 7.1 – 7.0 (m, 3H), 6.5 (s, 1H), 4.5 (d, *J* = 14.5 Hz, 1H), 4.1 (d, *J* = 14.5 Hz, 1H), 4.0 (d, *J* = 11.1 Hz, 1H), 3.7 (d, *J* = 13.8 Hz, 1H), 3.6 (s, 3H), 3.3 (d, *J* = 11.1 Hz, 1H), 2.9 (dd, *J* = 13.8, 4.2 Hz, 1H), 2.2 (s, 3H), 2.1 – 2.0 (m, 1H). ^{13}C{^{1}H} NMR (100 MHz, $CDCl_3$): δ 197.9, 169.0, 168.6, 158.8, 156.6, 137.3, 134.1, 133.0, 132.3, 130.8, 130.1, 129.1, 128.9, 128.6, 128.4, 127.4, 126.8, 125.4, 119.0, 77.2,

69.9, 52.9, 48.4, 48.1, 47.2, 40.9, 28.8, 13.0. HRMS (ESI TOF) *m/z* calcd. For $C_{32}H_{28}ClN_3O_6$ $[M+H]^+$ 586.1745 found 586.1747.

Methyl (*5R,7R,8R,14R*)-10-benzyl-7-(2-fluorophenyl)-1-methyl-4,11,12-trioxo-3-phenyl-6-oxa-2,3,10-triazadispiro[4.2.48.25]tetradec-1-ene-14-carboxylate (3x)



3x

Product **3x** was synthesized following the general experimental procedure **5.5.4**. An oven-dried 10 mL glass reaction tube was charged with pyrazoledione-derived Morita–Baylis–Hillman (Pyro-MBH) alcohol **1a** (1.0 equiv, 0.2 mmol), potassium tert-butoxide (50 mol%, 0.1 mmol), and arylidene pyrrolidinediones **2t** (1.0 equiv, 0.2 mmol). Subsequently, 1,4-Dioxane (1 mL) was added to the tube. The reaction mixture was stirred at ambient temperature for 20 minute. Upon completion, the solvent was removed under reduced pressure, and the residue was purified by column chromatography on silica gel using 50% ethyl acetate in hexanes as the eluent. The purified product **3x**, Methyl (5R,7R,8R,14R)-10-benzyl-7-(2-fluorophenyl)-1-methyl-4,11,12-trioxo-3-phenyl-6-oxa-2,3,10-triazadispiro[4.2.48.25]tetradec-1-ene-14-carboxylate **(3x),** was obtained as a white solid in a yield of 82 mg (72%) as a single diastereomer. The structure was confirmed through spectroscopic methods, including ^{1}H NMR, ^{13}C{^{1}H} NMR, HRMS, and X-ray crystallographic analysis. The compound displayed a melting point of 274–276 °C and a TLC retention factor (R_f) 0.5 (silica gel, 50% ethyl acetate/hexanes).^{1}H NMR (400 MHz, $CDCl_3$): δ 7.9 – 7.7 (m, 2H), 7.4 – 7.3 (m, 5H), 7.3 (d, *J* = 2.7 Hz, 2H), 7.2 – 7.1 (m, 2H), 7.1 – 6.9 (m, 4H), 6.2 (s, 1H), 4.5 – 4.2 (m, 2H), 3.9 (d, *J* = 11.2 Hz, 1H), 3.6 (s, 3H), 3.6 (s, 1H), 3.3 (d, *J* = 11.2 Hz, 1H), 2.9 (dd, *J* = 13.7, 4.1 Hz, 1H), 2.2 (s, 3H), 2.1 (dd, *J* = 13.8, 4.2 Hz, 1H). ^{13}C{^{1}H} NMR (100 MHz, $CDCl_3$): δ 197.9, 169.0, 168.6, 159.0 (d, $J_{(C-F)}$ = 249.7 Hz), 157.7 (d, $J_{(C-F)}$ = 181.1 Hz), 137.4, 134.0, 130.6 (d, $J_{(C-F)}$ = 8.5 Hz), 129.1, 128.9, 128.4, 128.3, 127.7 (d, $J_{(C-F)}$ = 3.5 Hz), 125.4, 124.4 (d, $J_{(C-F)}$ = 3.5 Hz), 122.4, 122.3, 118.9, 116.3 (d, $J_{(C-F)}$ = 22.1 Hz), 69.5, 52.9, 48.4, 47.7, 47.4, 47.4, 40.7, 28.7, 12.9. ^{19}F NMR (377 MHz, $CDCl_3$): δ -109.4 – -113.3 (m). HRMS: (ESI TOF) *m/z* calcd for $C_{32}H_{28}FN_3O_6$ $[M + H]^+$ 570.2040, found 570.2046.

5.7 Appendix V ^{1}H, ^{13}C, ^{19}F spectral data of representative compounds

Compound No.	Figure AII.X	Data	Page No
3a	Figure AV.1 and AV.2	^{1}H and ^{13}C	205
3e	Figure AIV.3 and AIV.4	^{1}H and ^{13}C	206
3f	Figure AIV.5 and AIV.6	^{1}H and ^{13}C	207
3n	Figure AIV.7 and AIV.8	^{1}H and ^{13}C	208
3u	Figure AIV.9 and AIV.10	^{1}H and ^{13}C	209
3v	Figure AIV.11, AIV.12 and AIV.13	^{1}H, ^{13}C and ^{19}F	210
3a	Figure AII.14	ORTEP plot	211

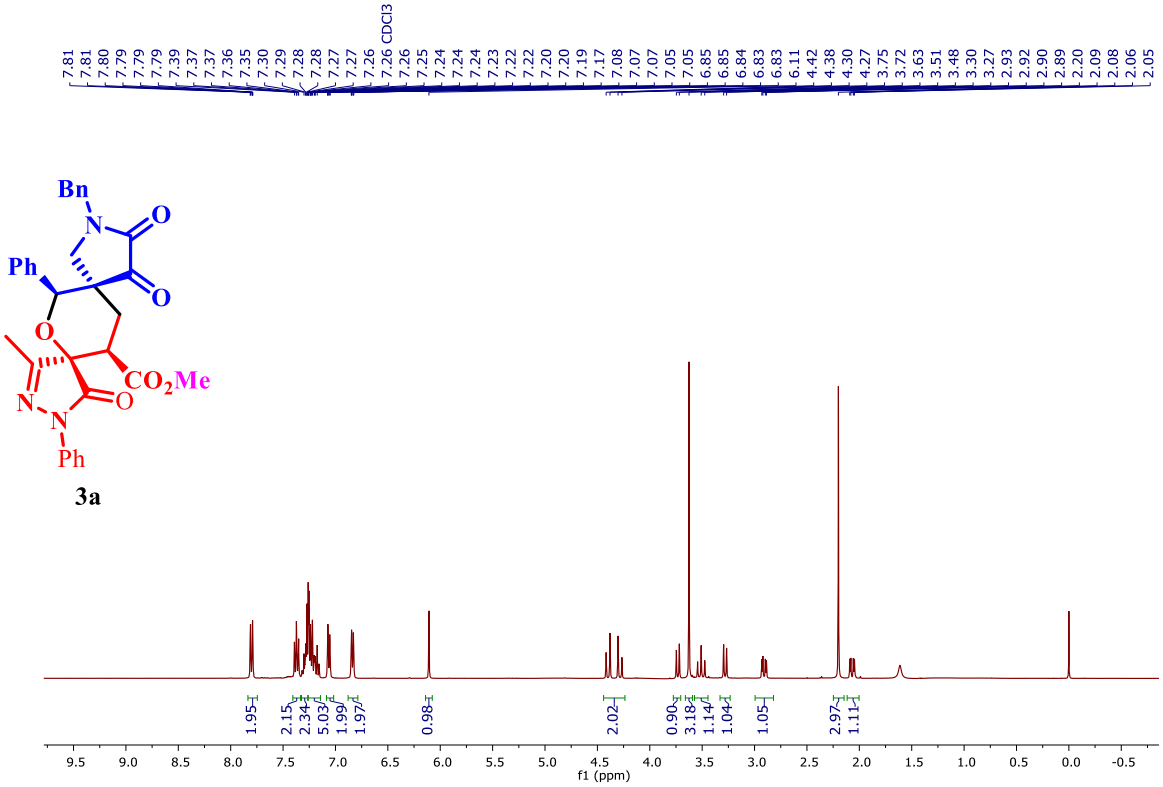


Figure AV.1 ^{1}H NMR spectrum of **3a**, $CDCl_3$, 400 MHz

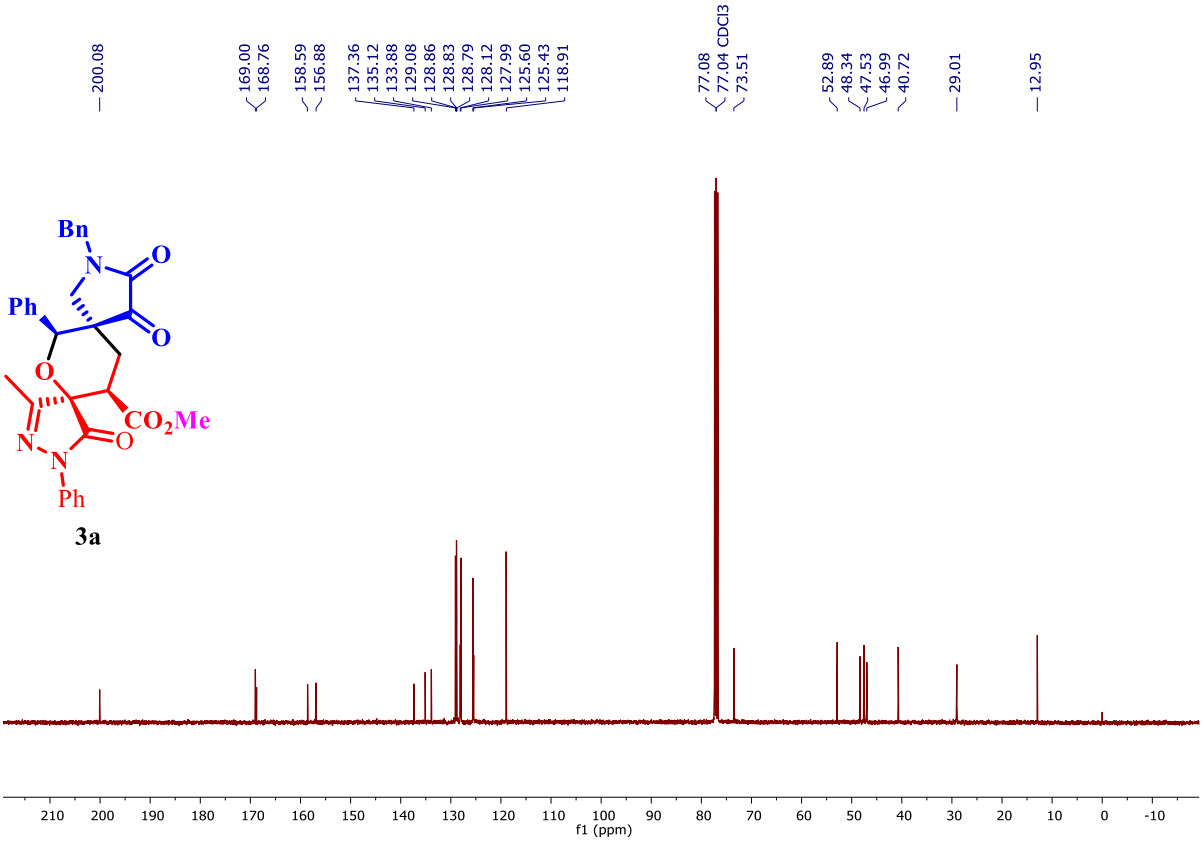


Figure AV.2 $^{13}C\{^{1}H\}$ NMR spectrum of **3a**, $CDCl_3$, 100 MHz

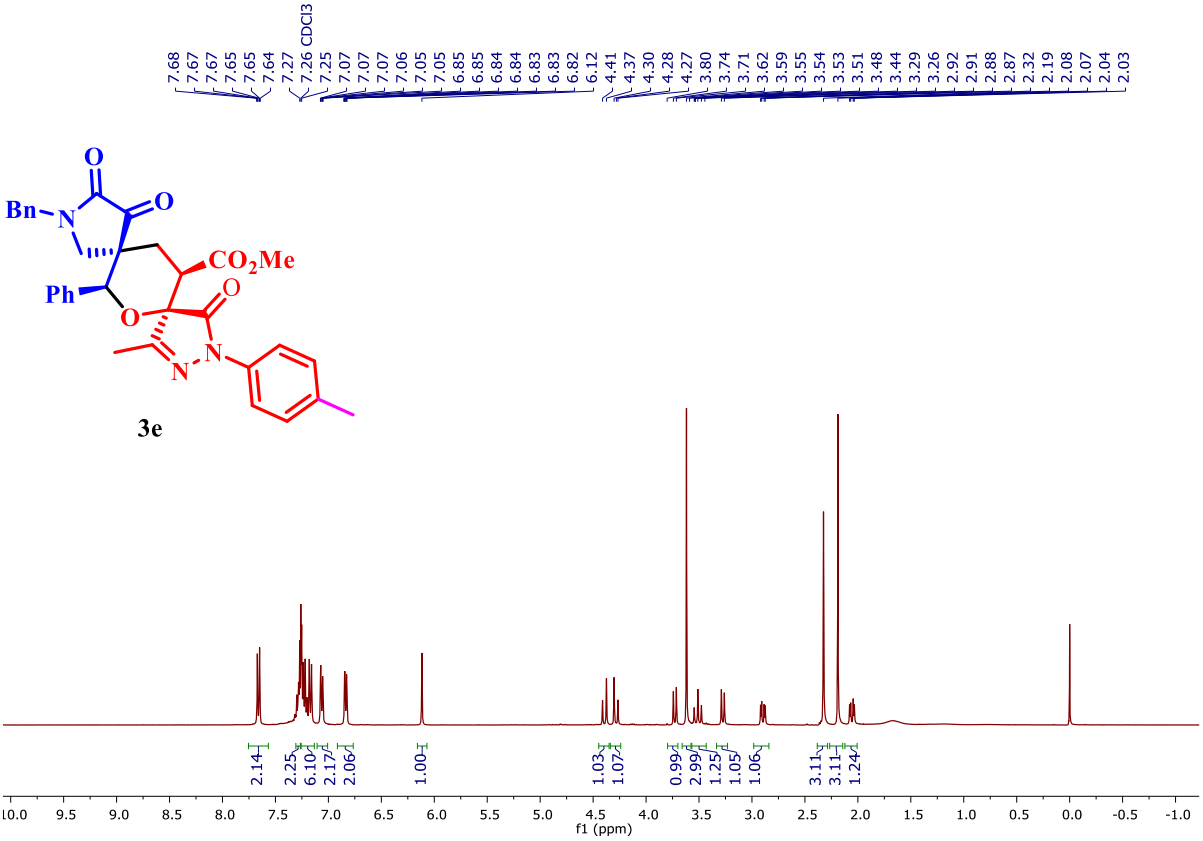


Figure AV.3 ^{1}H NMR spectr um of **3e**, $CDCl_3$, 400 MHz

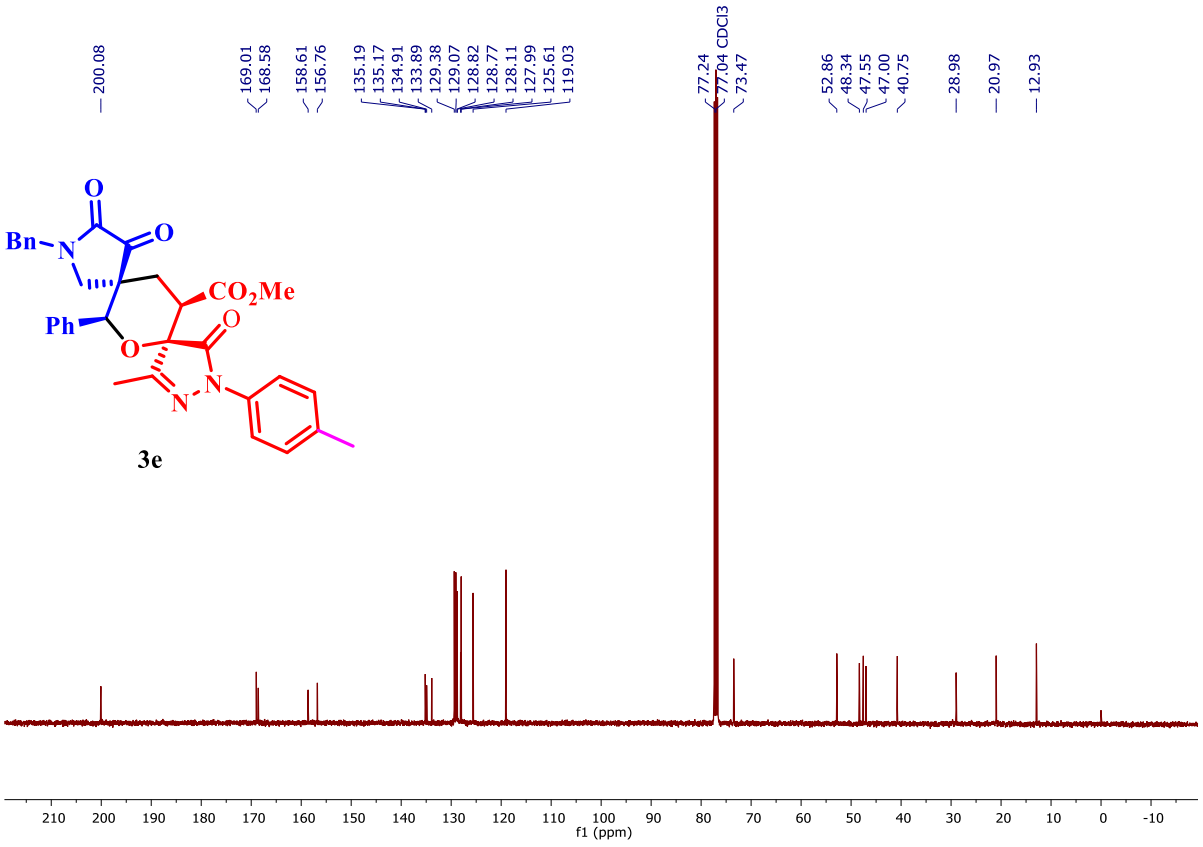


Figure AV.4 $^{13}C\{^{1}H\}$ NMR spectrum of **3e**, $CDCl_3$, 100 MHz

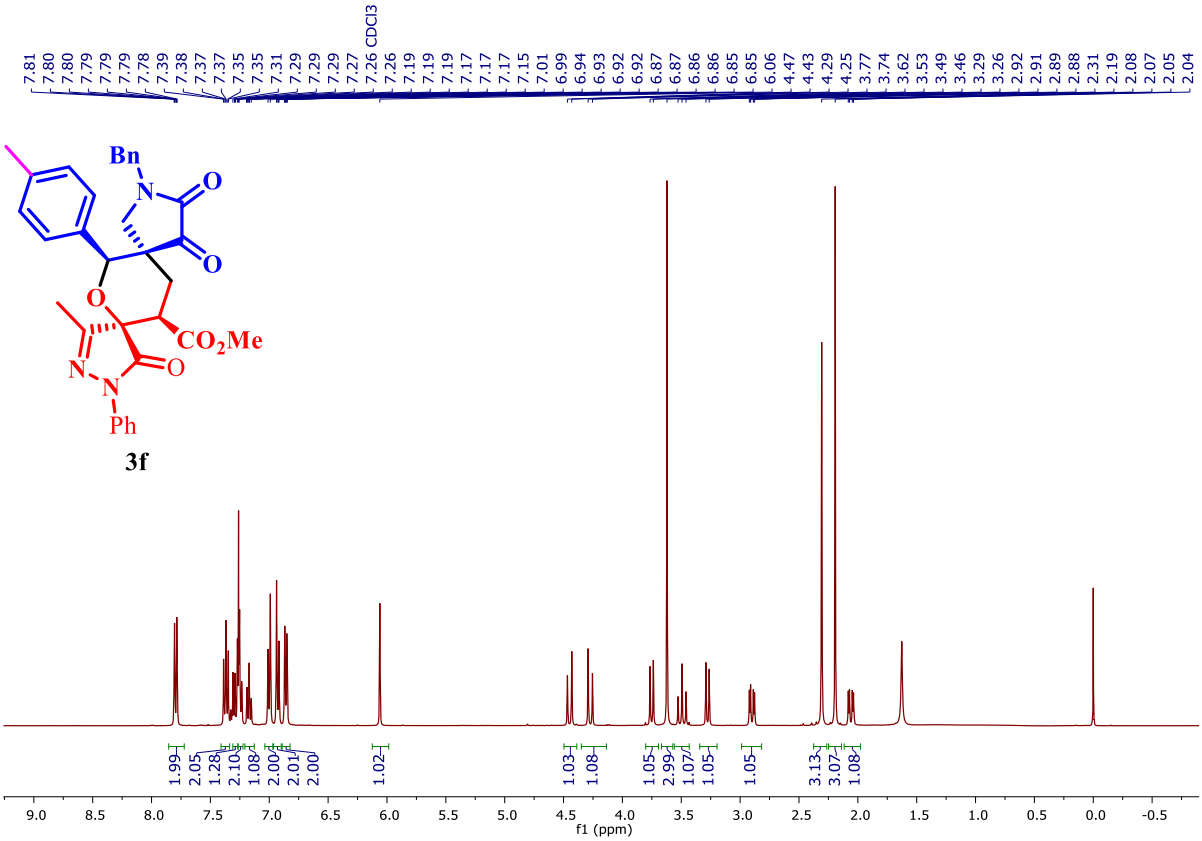


Figure AV.5 ^{1}H NMR spectrum of **3f**, $CDCl_3$, 400 MHz

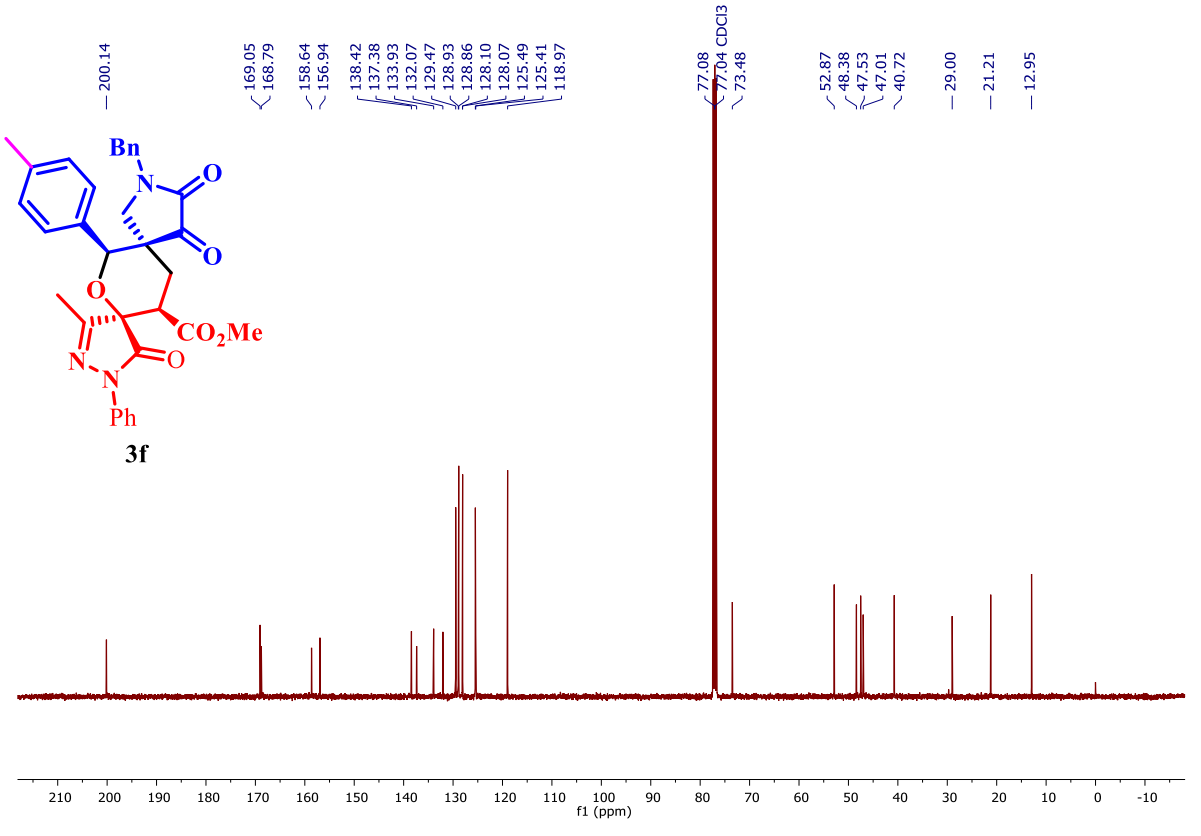


Figure AV.6 $^{13}C\{^{1}H\}$ NMR spectrum of **3f**, $CDCl_3$, MHz

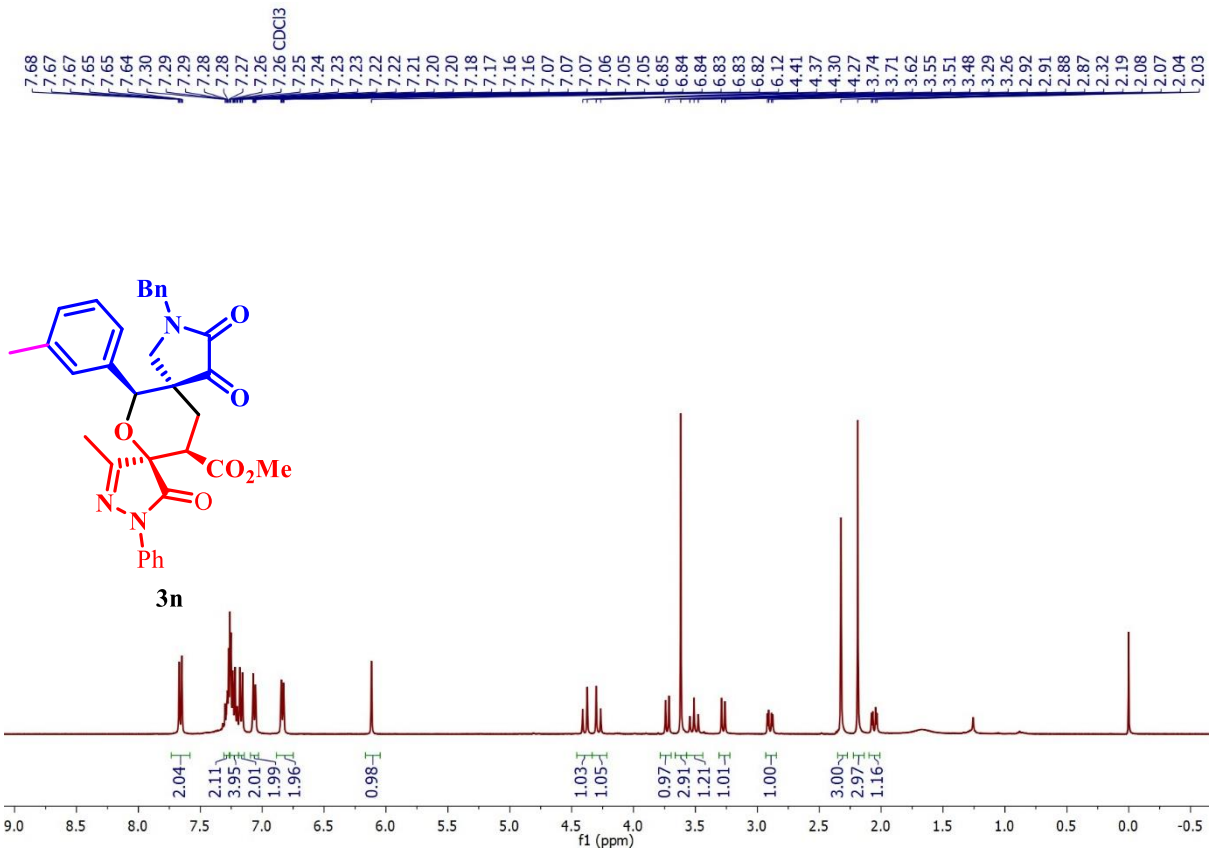


Figure AV.7 ^{1}H NMR spectrum of **3n**, $CDCl_3$, 400 MHz

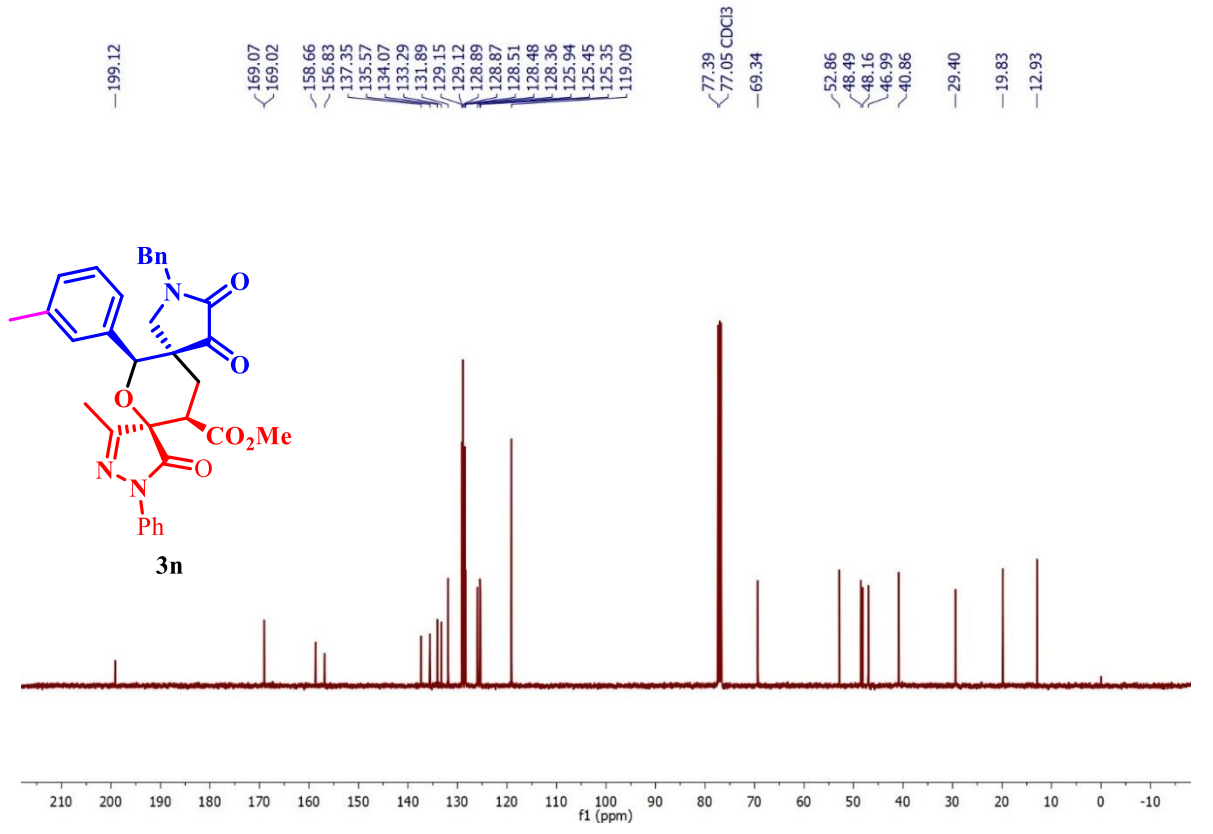


Figure AV.8 $^{13}C\{^{1}H\}$ NMR spectrum of **3n**, $CDCl_3$, MHz

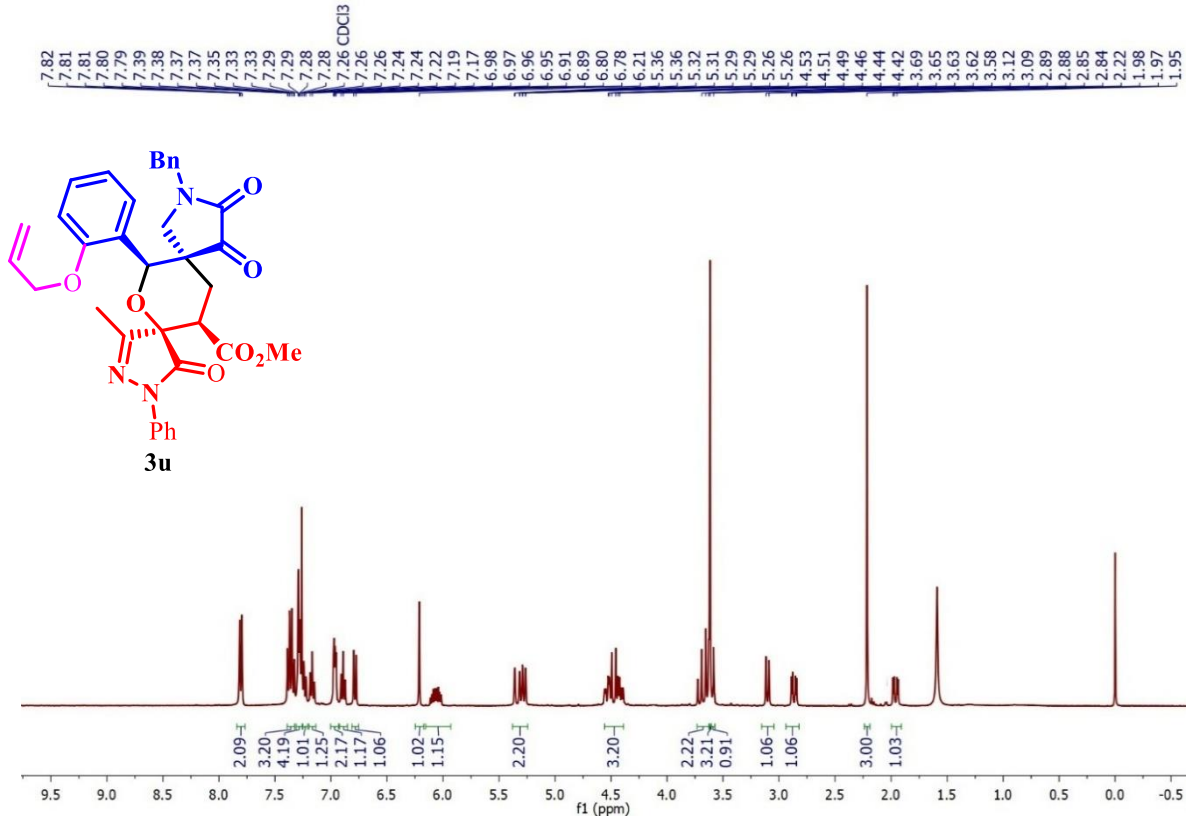


Figure AV.9 ^{1}H NMR spectrum of **3u**, $CDCl_3$, 400 MHz

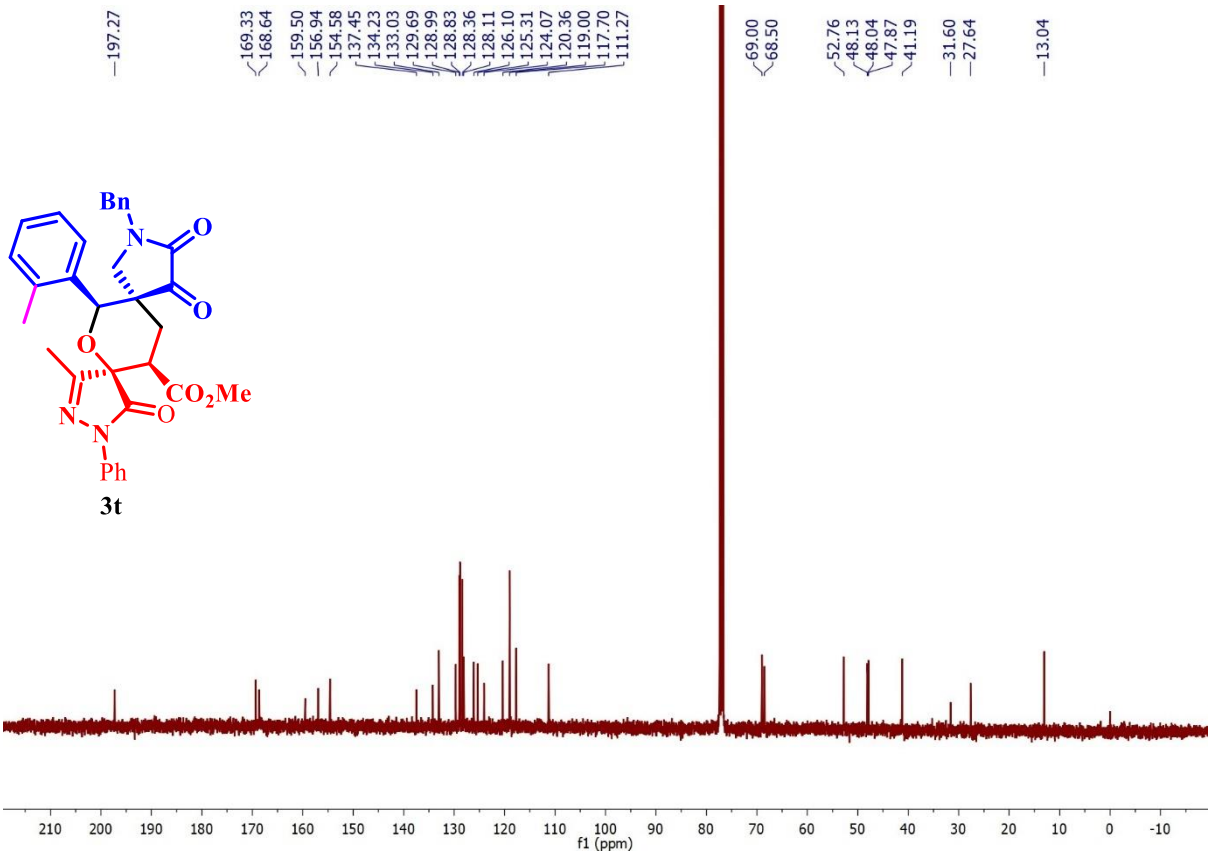


Figure AV.10 $^{13}C\{^{1}H\}$ NMR spectrum of **3u**, $CDCl_3$, MHz

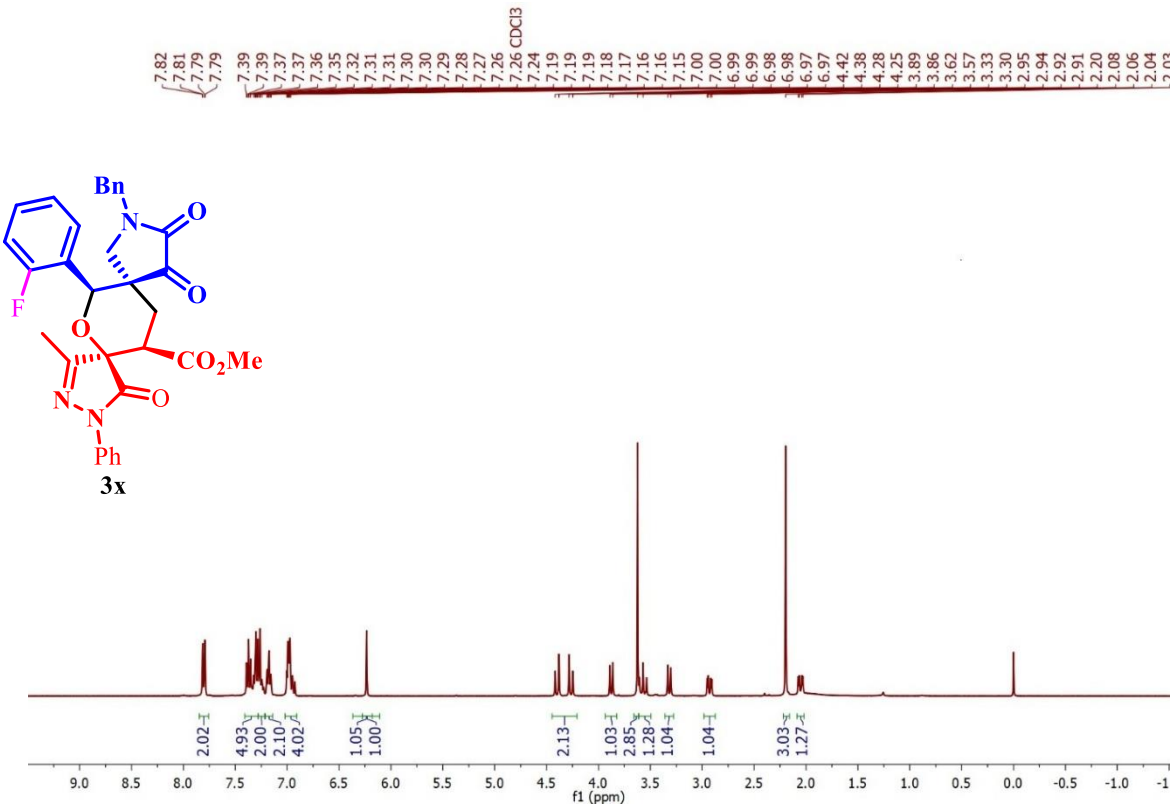


Figure AV.11 ^{1}H NMR spectrum of **3x**, $CDCl_3$, 400 MHz

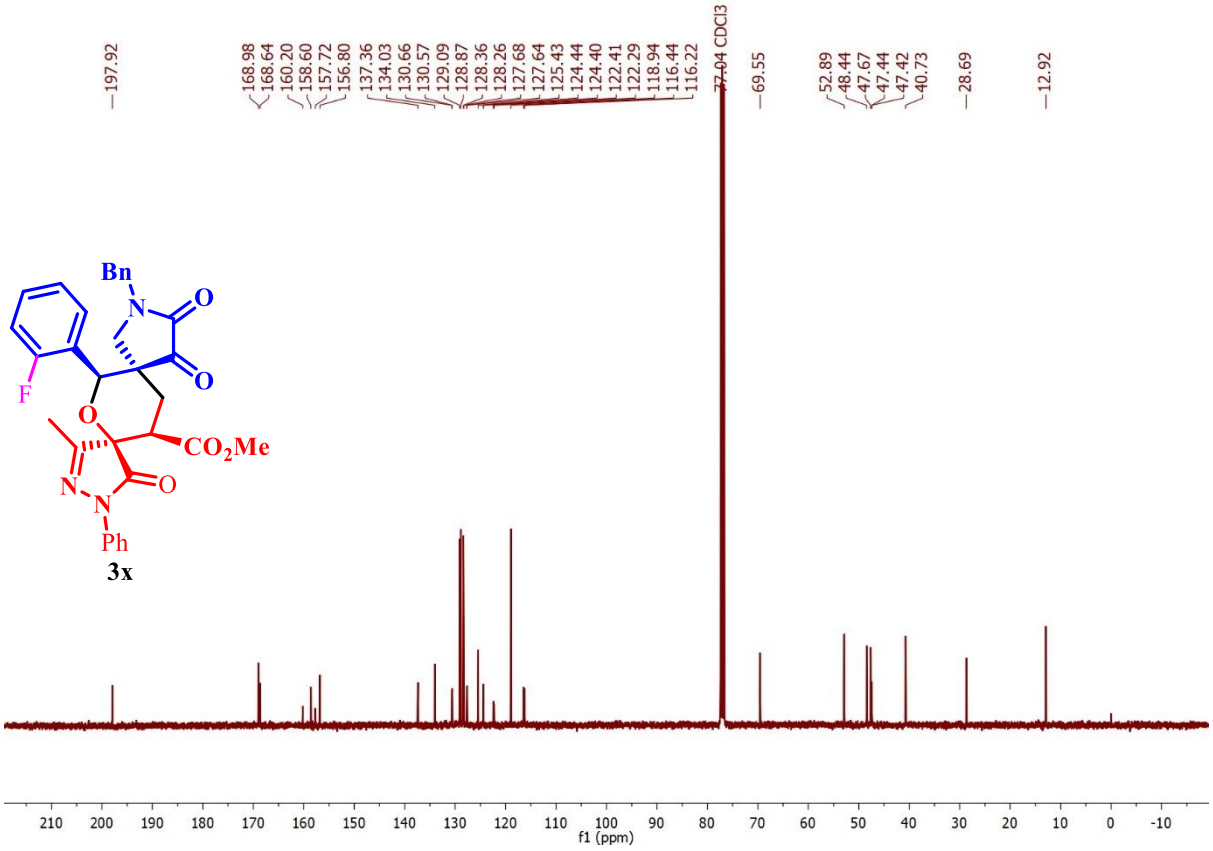


Figure AV.12 $^{13}C\{^{1}H\}$ NMR spectrum of **3x**, $CDCl_3$, MHz

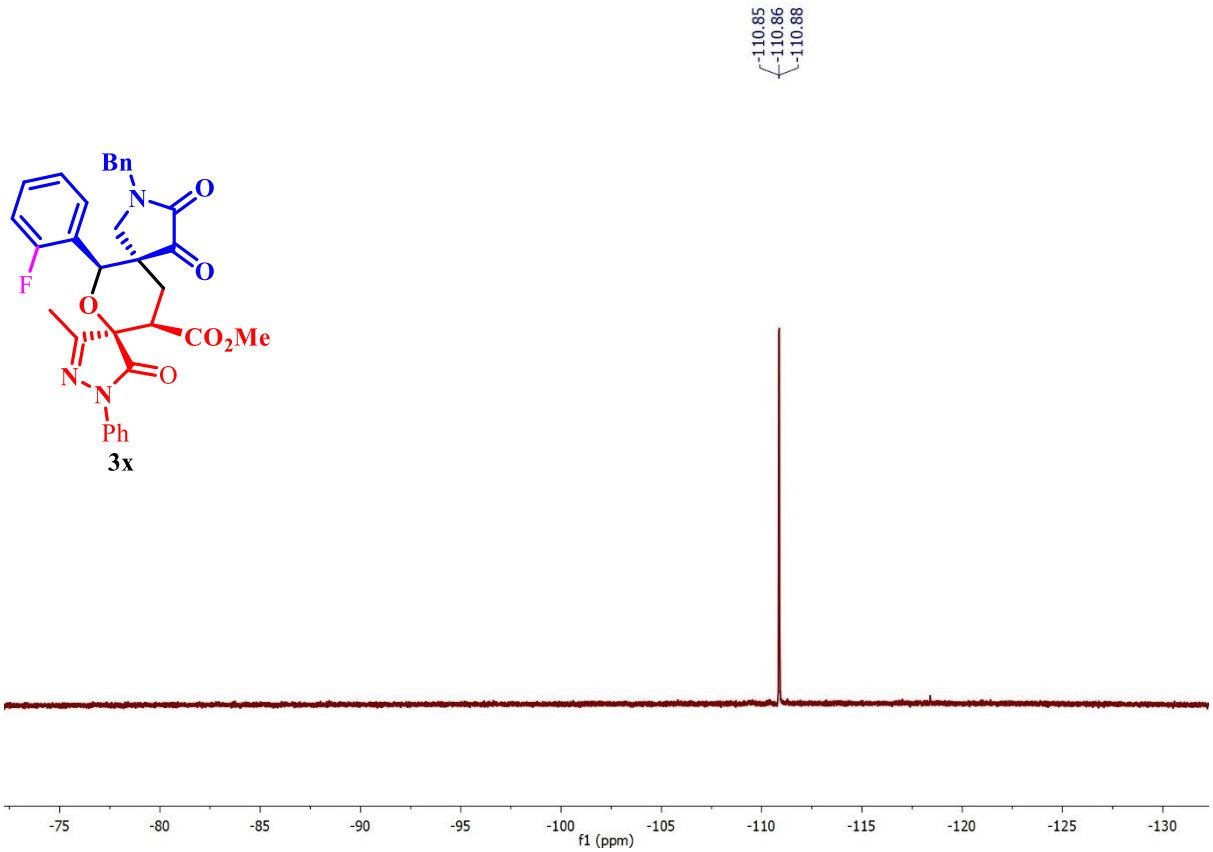


Figure AV.13 ^{19}F NMR spectrum of **3x**, $CDCl_3$, 377 MHz

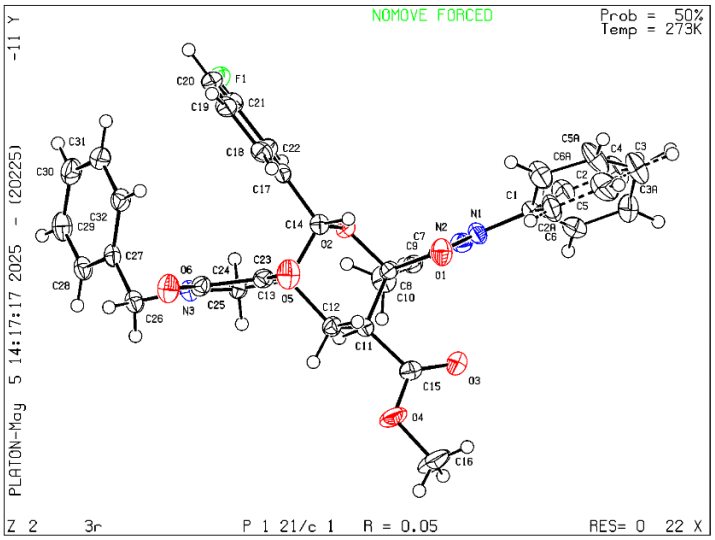


Figure AV.14 An ORTEP diagram showing thermal ellipsoids at a 50% probability level was created to represent the structures determined by single-crystal X-ray diffraction analysis of compound **3r**

5.8 References

1. Chauhan, P.; Mahajan, S.; Loh, C. C. J.; Raabe, G.; Enders, D. *Org. Lett*. **2014**, *16*, 2954.
2. Reddy, Y. P.; Anwar, S. *RSC Adv.* **2022**, *12*, 34634.
3. Amata, E.; Bland, N. D.; Campbell, R. K.; Pollastri, M. P. *Tetrahedron Lett.* **2015**, *56*, 2832.
4. (a) Li, Q.-M.; Luo, J.-G.; Zhao, H.-J.; Yu, W.-Y.; Wang, X.-B.; Yang, M.-H.; Luo, J.; Sun, H.-B.; Chen, Y.-J.; Guo, Q.-L.; Kong, L.-Y. *Asian J. Org. Chem.* **2015**, *4*, 1366. (b) Karrouchi, K.; Radi, S.; Ramli, Y.; Taoufik, J.; Mabkhot, Y. N.; Al-aizari, F. A.; Ansar, M. *Molecules* **2018**, *23*, 134. (c) Chen, N.; Zhu, L.; Gan, L.; Liu, Z.; Wang, R.; Cai, X.; and Jiang, X. *Eur. J. Org. Chem.* **2018**, *23*, 2939. (d) Warghude, P. K.; Sabale, A. S.; Bhat, R. G. *Org. Biomol. Chem.* **2020**, *18*, 1794. (e) Zhao, Z.; Dai, X.; Li, C.; Wang, X.; Tian, J.; Feng, Y.; Xie, J.; Ma, C.; Nie, Z.; Fan, P.; Qian, M. He, X.; Wu, S.; Zhang, Y.; and Zheng, X. *Eur J Med Chem.* **2020**, *186*, 111893. (f) Warghude, P. K.; Sabale, A. S.; Dixit, R.; Vanka, V.; Bhat, R. G. *Org. Biomol. Chem.*, **2021**, *19*, 4338. (g) Pavankumar, Y.; and Anwar, S. *RSC Adv.* **2022**, *12*, 34634. (h) Li, G.; Zhang, H.; Zhang, G.; Wei, B.; Liu, B.; Song, H.; Li, Q.; and Ban, S. *J. Org. Chem.* **2023**, *88*, 4809.
5. (a) Nakazaki, A.; Era, T.; Numada, Y.; Kobayashi, S. *Tetrahedron Lett.* **2006**, *62*, 6264. (b) Maity, S.; Ghosh, S. *Tetrahedron Lett.* **2007**, *48*, 3355.
6. (a) Han, X.; Yao, W.; Wang, T.; Tan, Y. R.; Yan, Z.; Kwiatkowski, J.; Lu, Y. *Angew. Chem. Int. Ed.* **2014**, *53*, 5643. (b) Li, J. H.; Feng, T. F.; Du, D. M.; J. Org. Chem. **2015**, *80*, 11369. (c) Lin, Y.; Zhao, B. L.; Du, D. M. *J. Org. Chem.* **2019**, *84*, 10209.
7. Wang, B.; Peng, F.; Huang, W.; Zhou, J.; Zhang, N.; Sheng, J.; Haruehanroengra, P.; He, G.; and Han, B. *Acta Pharm. Sin. B* **2020**, *10*, 1492.
8. Gond, K. K.; Maddani, M. R. *New J. Chem.* **2024**, *48*, 8667.
9. Gond, K. K.; Maddani, M. R. *New J. Chem.* **2024**, *48*, 15866.
10. Zhang, K.; Zuo, S.; You, P.; Ru, T.; Chen, F. E. *Chin. Chem. Lett.* **2024**, *35*, 109157.
11. CCDC 2465733 (Compound **3r**) contains the crystallographic data. The Cambridge Crystallographic Data Centre can obtain these data free of charge.
12. (a) Pearson, D. E.; Buehler, C. A. **1974**, *74*, 45. (b) Madasu, J.; Shinde, S.; Das, R.; Patel, S.; Shard, A. *Org. Biomol. Chem.* **2020**, *18*, 8346. (c) Dub, P. A.; Tkachenko, N. V. *J. Phys. Chem. A,* **2021**, *125*, 5726. (b) Madasu, J.; Shinde, S.; Das, R.; Patel, S.; Shard, A. *Org. Biomol. Chem.* **2020**, *18*, 8346.

13. (a) Liu, L.; Guo, D. H., Wang, J. *Org. Lett.* **2020**, *22*, 7025. (b) Wang, H. K.; Zeng, T. L.; Chang, W.; Liu, L.; Li, J. *Org. Lett*. **2021**, *23*, 3573.

Summary

Spiroheterocycles consisting of pyrazolone and isatin scaffolds represent a pivotal class of molecular architecture, and they are prevalent in many known bioactive compounds. These intricate frameworks have captured the attention of synthetic organic as well as medicinal chemists due to their pronounced pharmacological profiles, including antimicrobial, anticancer, antiviral, and anti-inflammatory activities. The strategic construction of such complex spirocyclic systems hinges fundamentally on carbon–carbon bond-forming transformations that constitute the bedrock of modern organic synthesis. Through meticulous tuning as well as modulating the reactivity and selectivity, these bond-forming reactions enable the elegant fusion of pyrazolone and isatin cores into architecturally sophisticated spiroheterocyclic frameworks. These structurally novel and functionally potent molecular entities will be of great interest. Among the numerous methodologies available, the Morita–Baylis–Hillman (MBH) reaction stands out as an exceptionally powerful tool due to its ability to generate densely functionalized compounds with broad synthetic utility and versatility. These MBH adducts are uniquely positioned as synthetic intermediates, offering rich functionality and reactivity, making them ideal precursors for the development of a wide array of biologically relevant molecules, including carbocyclic and heterocyclic structures.

In recent years, a new class of MBH-derived intermediates has emerged, pyrazolonedione-derived MBH carbonates. These entities have demonstrated remarkable synthetic potential, particularly in the realm of organocatalytic and base-catalyzed transformations. This thesis greatly focuses on harnessing the reactivity of MBH derivatives to develop novel, efficient pathways to synthesize spiropyrazolone-based frameworks with structural complexity and potential biological relevance.

A series of spiroheterocycles has been synthesized using the MBH carbonates by exploring both tertiary amine catalysis and base-mediated strategies. The synthesis of some of the following spiroheterocycles has been achieved.

- Spirooxindole-pyrazolone fused cyclopentenes, constructed through a highly efficient [3+2] annulation between pyrazolonedione-derived MBH carbonates and 3-methyleneoxindoles under organocatalytic conditions.
- Dispiropyrazolone fused tetrahydropyrans and spiropyrazolone pyrrolidinediones

fused tetrahydropyran, achieved via [4+2] annulation reactions using pyrazoledione-derived Morita–Baylis–Hillman (Pyro-MBH) alcohol and arylidenepyrazolones or arylidenepyrrolidinediones under base catalysis.

Furthermore, an innovative visible-light-promoted [4+2] cycloaddition was explored to directly functionalize the inert C4 position of 3-methyleneoxindoles. This method allowed for the successful construction of 3,4-fused spirooxindole systems, adding a new dimension to the synthetic utility of these substrates under mild and environmentally benign conditions. The thesis mainly exploited the untapped potential of pyrazolonedione-derived MBH carbonates as multi-faceted building blocks. These designed catalytic protocols -both thermal and photochemical pathways led to a diverse collection of highly functionalized spirocyclic compounds. These complex structures hold a great promise for future applications in medicinal chemistry and materials science.

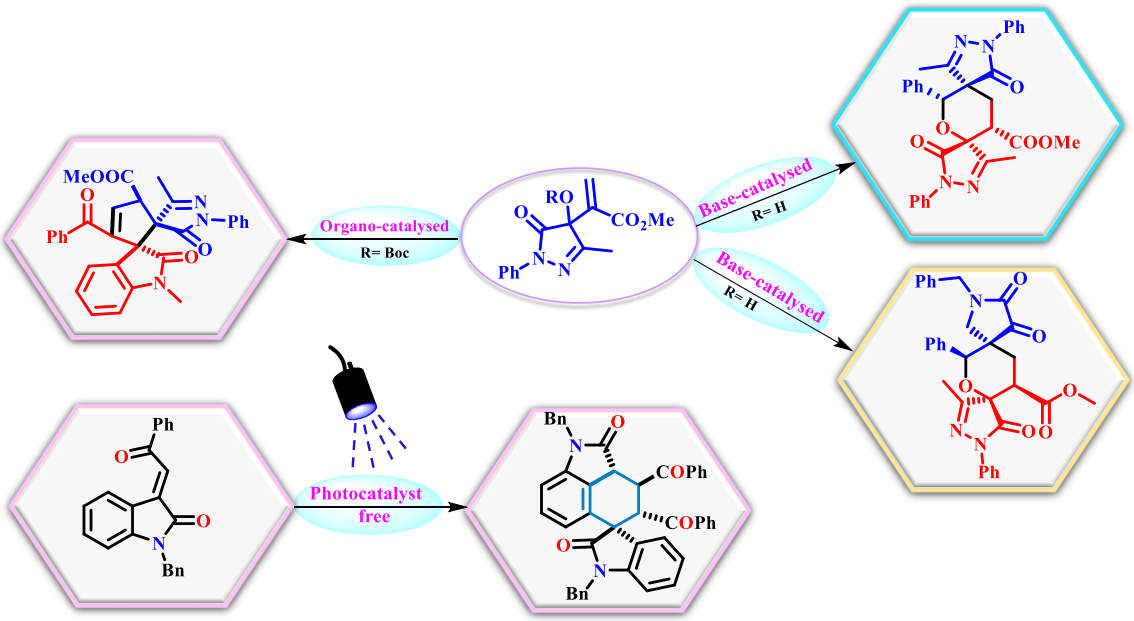


Figure: An exploration of spiroheterocycle synthesis through the reaction between Pyro-MBH adducts and 3-methyleneoxindole under various conditions

Rights and Permission

List of research publications included in the thesis

Chapter 2

"Reprinted from Ref. **Sabale, A. S**.; Warghude, P. K.; Bhat, R. G. An Efficient Route to Access Spirooxindole Pyrazolone Fused Cyclopentene via Diastereoselective [3+2] Annulation, *Synlett* **2023**, 34, 1732–1738, with permission from Thieme Publishers"

Chapter 3

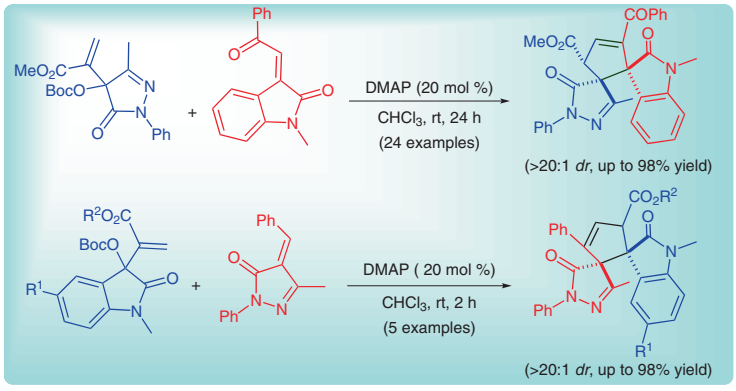
Reproduced from Ref. **Sabale, A. S**.; Bhowmick, A.; Pattanaik, S.; Bankar, O. S.; Bhat, R. G. "Direct Access to 3,4-Fused Spirooxindoles Through Visible-Light-Driven Diasterioselective [4+2] Cyclization of 3-Methylene Oxindoles''. *Asian J. Org. Chem.* **2025**, *11*, https://doi.org/10.1002/ajoc.202500424, With permission from Wiley.

Synlett A. S. Sabale et al. Letter

An Efficient Route to Access Spirooxindole–Pyrazolone-Fused Cyclopentenes by a Diastereoselective [3+2] Annulation

Abhijeet S. Sabale
Prakash K. Warghude
Ramakrishna G. Bhat*

Department of Chemistry, Indian Institute of Science Education and Research (IISER)-Pune, Dr. Homi Bhabha Road, Pashan, Pune, 411008, Maharashtra, India
rgb@iiserpune.ac.in



Received: 05.11.2022
Accepted after revision: 16.01.2023
Published online: 16.01.2023 (Accepted Manuscript), 11.05.2023 (Version of Record)
DOI: 10.1055/a-2014-2813; Art ID: ST-2022-11-0476-L

Abstract A DMAP-catalyzed, highly diastereoselective, [3+2] cycloaddition of pyrazolone-derived Morita–Baylis–Hillman carbonates to 3-methyleneoxindoles has been developed. A variety of structurally diverse and complex spiropyrazolone-fused oxindoles bearing three contiguous chiral centers have been synthesized in high yields (up to 98%) and with excellent diastereoselectivities (up to 99:1). Moreover, the synthetic potential of this protocol has been demonstrated by performing a Suzuki coupling reaction.

Key words annulation, spiropyrazolones, diastereoselectivity, Morita–Baylis–Hillman carbonates, spirooxindoles

The construction of spiro carbocyclic/heterocyclic structures has received enormous attention from synthetic and medicinal-chemistry researchers in recent decades.[1] The three-dimensional complex structures of spirocyclic frameworks help to improve their physicochemical properties, such as their metabolic stability, aqueous solubility, and lipophilicity, compared with the corresponding monocyclic structures.[2] Among the polyfunctional spirocyclic compounds, spirocyclopentane–pyrazolones and spirocyclopentane–oxindoles have attracted considerable interest in the area of organosynthetic and pharmaceutical research, due to their varied biological activities (Figure 1). For example, the spiropyrazolone–cyclopentane compound **I** acts as a peroxisome proliferator-activated receptor α antagonist.[3] In addition, spiro compound **II** and **III** show inhibitory activities against type-4 phosphodiesterases.[4] The spirocyclopentane–oxindoles citrinadin A (**IV**) and spirotryprostatin B (**V**) have been reported as natural products.[5] Moreover, the spirooxindole compound **VI** exhibits p53/Mdm2-inhibitory activity.[6]

Merging or combining various pharmacologically relevant scaffolds is emerging as one of the most popular and effective strategies for designing and developing new biologically active compounds.[7] In view of this, a merger of spiropyrazolone and spirooxindole skeletons to construct structurally diverse and interesting spiroheterocyclic compounds might be an effective approach for producing promising compounds. Recently, compound VII, which exhibits human liver carboxylestarase-inhibitory activity, has been successfully synthesized by using this combinatorial approach.[8]

The synthesis of spirocyclic compounds bearing heterocyclic frameworks such as an oxindole or pyrazolone scaffold is of great importance, especially in modern drug-discovery research programs. Owing to the importance of these frameworks, many elegant protocols have been developed for the construction of spirooxindole–pyrazolone molecules under organocatalytic conditions.[9] In 2013, the Wang group developed a bifunctional thiourea-catalyzed asymmetric [3+2] annulation of 3-isothiocyanatooxindoles with unsaturated pyrazolones to synthesize spiropyrazolone–oxindole molecules.[10] In the following year, Yuan and co-workers reported a similar strategy for the synthesis of spirooxindole–pyrazolones derivatives under quinine catalysis.[11] In 2015, the Du group reported a Michael/alkylation cascade reaction of arylidenepyrazolones with 3-chlorooxindoles for the construction of spiropyrazolone–cyclopropane–oxindole scaffolds.[12] In 2018, Wang and Zou collaboratively developed an asymmetric [3+2] cycloaddition protocol for the synthesis of spiropyrazolone-fused oxindole compounds by using 4-isothiocyanatopyrazolones and isatin-derived ketimines substrates.[8] Recently, several organocatalytic transformations that use various isatin-based scaffolds and novel pyrazolones or unsaturated pyra-

© 2023. Thieme. All rights reserved.
Georg Thieme Verlag KG, Rüdigerstraße 14, 70469 Stuttgart, Germany

Downloaded by: Ind Inst of Science Edu & Res PUNE. Copyrighted material.

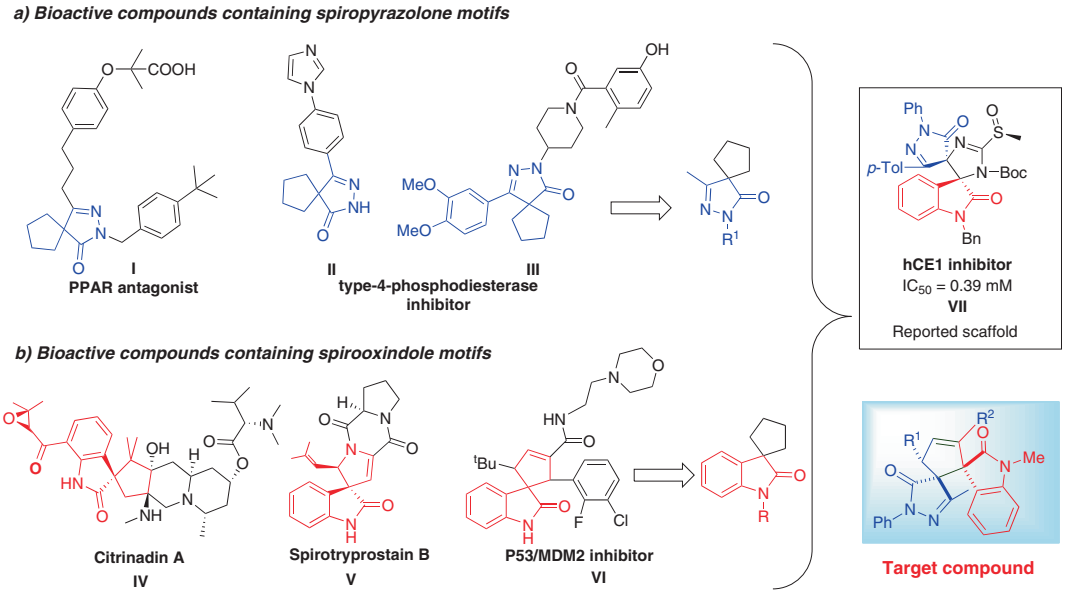


Figure 1 Representative examples of bioactive compounds with spirooxindole and spiropyrazolone scaffolds

zolones derivatives as synthons for the synthesis of spiropyrazolones-fused spirooxindoles have been successfully developed by the research groups of Liu and Zhou;[13] Du;[14] Wang and Yuan;[15] Zhong;[16] Zhan, Li, and Han;[17] and Chen,[18] as well as by ourselves.[19]

Despite these recent advances in synthesizing spiropyrazolone-fused oxindole derivatives, few methods have been described for the synthesis of a spirocyclic molecule bearing three different scaffolds, such as pyrazolone, oxindole, and cyclopentene, in a diastereoselective manner.[16] In this regard, there is a high demand for the development of an effective one-pot protocol to access polyfunctionalized spirocyclic pyrazolones and oxindoles, a challenging task from the point of view of synthetic organic chemistry.

As part of our continuing interest in the synthesis of spirocyclic compound and our ongoing research on cycloaddition reactions of isatin-based Morita–Baylis–Hillman (MBH) carbonates,[19a,b,20] we became interested in the synthesis of spirooxindole-fused pyrazolone molecules.

In recent years, isatin-derived MBH carbonates have been effectively used as three-carbon synthons to synthesize polyfunctional heterospirocyclic compounds.[21] Recently, pyrazolone-based MBH carbonates have emerged as versatile precursors to access spiropyrazolone scaffolds.[17,22] Similarly, 3-methyleneoxindole derivatives have proven to be valuable synthons in cycloaddition reactions for constructing the structurally diverse spirocyclic oxindole moieties. The versatile reactivity of these compounds has provided a new platform for developing a wide range of synthetic compounds and building blocks, including bioactive molecules.[23]

In this regard, we hypothesized that a spiropyrazolone–oxindole scaffold could be obtained by the cycloaddition reaction of a pyrazolone-based Morita-Baylis-Hillman carbonate and a 3-methyleneoxindole in the presence of a suitable Lewis base catalyst. Here, we report a DMAP-catalyzed, highly diastereoselective, [3+2] annulation of pyrazolone-based MBH carbonates with a 3-methyleneoxindole to give diverse spiropyrazolone–oxindole derivatives bearing vicinal quaternary spirocenters.

To validate our hypothesis, we performed a model reaction of the pyrazolone-derived MBH carbonate **1a** with (3*E*)-1-methyl-3-(2-oxo-2-phenylethylidene)indolin-2-one (**2a**) in the presence of DABCO (20 mol%) as a catalyst in dichloromethane (DCM) at room temperature. To our delight, the reaction delivered the α-regioselective [3+2] annulation product **3a** in 30% yield and with excellent diastereoselectivity (>20:1 dr; Table 1, entry 1).

To enhance the yield of **3a**, we treated **1a** and **2a** independently with PPh_3 (20 mol%) or DBU (20 mol%) as a catalyst (, entries 2 and 3); surprisingly, we did not observe any product formation, even after a prolonged reaction time. Interestingly, in the presence of 20 mol% of DMAP as a catalyst, the expected [3+2] annulation product **3a** was obtained in 90% yield with an excellent diastereoselectivity (entry 4). Encouraged by this result, we focused on achieving an asymmetric version of this α-regioselective [3+2] annulation reaction. In this regard, we screened several chiral tertiary amine catalysts (entries 5–8). We did not observe any product formation in the presence of the cinchona-derived catalyst **C1**, even after prolonged reaction time (entry 5). Next, we employed the chiral DMAP-derived catalysts **C2**–**C4** to obtain the corresponding optically pure product

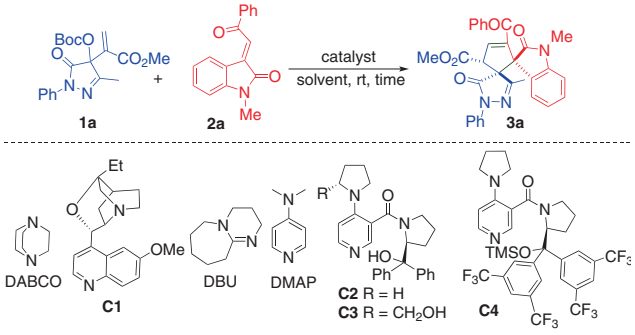
© 2023. Thieme. All rights reserved.

Downloaded by: Ind Inst of Science Edu & Res PUNE. Copyrighted material.

3a. Pleasingly, the [3+2] annulation product **3a** was formed with all these catalysts; however, the enantioselectivity was poor in all cases (ee = 15–23%; entries 6–8).

Unfortunately, our various attempts to achieve enantioselectivity did not succeed despite screening the reaction with various chiral catalysts under a range of reaction conditions [see the Supporting Information (SI) for more details]. Considering the importance of the spiropyrazolone and spirooxindole scaffolds, we decided to explore a diastereoselective version of this α-regioselective [3+2] annulation reaction. Furthermore, to optimize the reaction conditions, we screened various solvents (chloroform, acetonitrile, tetrahydrofuran, *N*,*N*-dimethylformamide, ethyl acetate, toluene, chlorobenzene, methanol, ethanol, and propanol) (Table 1, entries 9–18). Among the solvents screened, chloroform was found to be advantageous for the desired transformation, affording the spirooxindole–pyrazolone **3a** in 92% yield and with an excellent diastereoselectivity (>20:1 dr; entry 9). A reduction in the catalyst loading furnished compound **3a** in 78% yield, but the diastereoselectivity remained unchanged (entry 19). Based on the catalyst and solvent screening, the MBH carbonate of pyrazolone **1a** (1 equiv), (3*E*)-1-methyl-3-(2-oxo-2-phenylethylidene)indolin-2-one (**2a**; 1.2 equiv), and DMAP (20

Table 1 Optimization of the Reaction Conditions[a]



Entry	Catalyst (mol%)	Solvent	Time (h)	Yield[b] (%)	dr[c]	ee[d] (%)
1	DABCO (20)	DCM	36	30	>20:1	–
2	PPh_3 (20)	DCM	72	NR[e]	–	–
3	DBU (20)	DCM	72	NR	–	–
4	DMAP (20)	DCM	24	90	>20:1	–
5	**C1** (20)	DCM	72	NR	–	–
6	**C2**(20)	DCM	24	65	>20:1	15
7	**C3** (20)	DCM	24	68	>20:1	21
8	**C4** (20)	DCM	24	73	>20:1	23
9	DMAP (20)	DCM	24	92	>20:1	–
10	DMAP (20)	MeCN	24	81	>20:1	–
11	DMAP (20)	THF	24	80	>20:1	–
12	DMAP (20)	DMF	24	82	>20:1	–
13	DMAP (20)	EtOAc	24	85	>20:1	–
14	DMAP (20)	toluene	24	87	>20:1	–
15	DMAP (20)	PhCl	24	89	>20:1	–
16	DMAP (20)	MeOH	24	85	>20:1	–
17	DMAP (20)	EtOH	24	78	>20:1	–
18	DMAP (20)	PrOH	24	84	>20:1	–
19	DMAP (15)	$CHCl_3$	24	78	>20:1	–

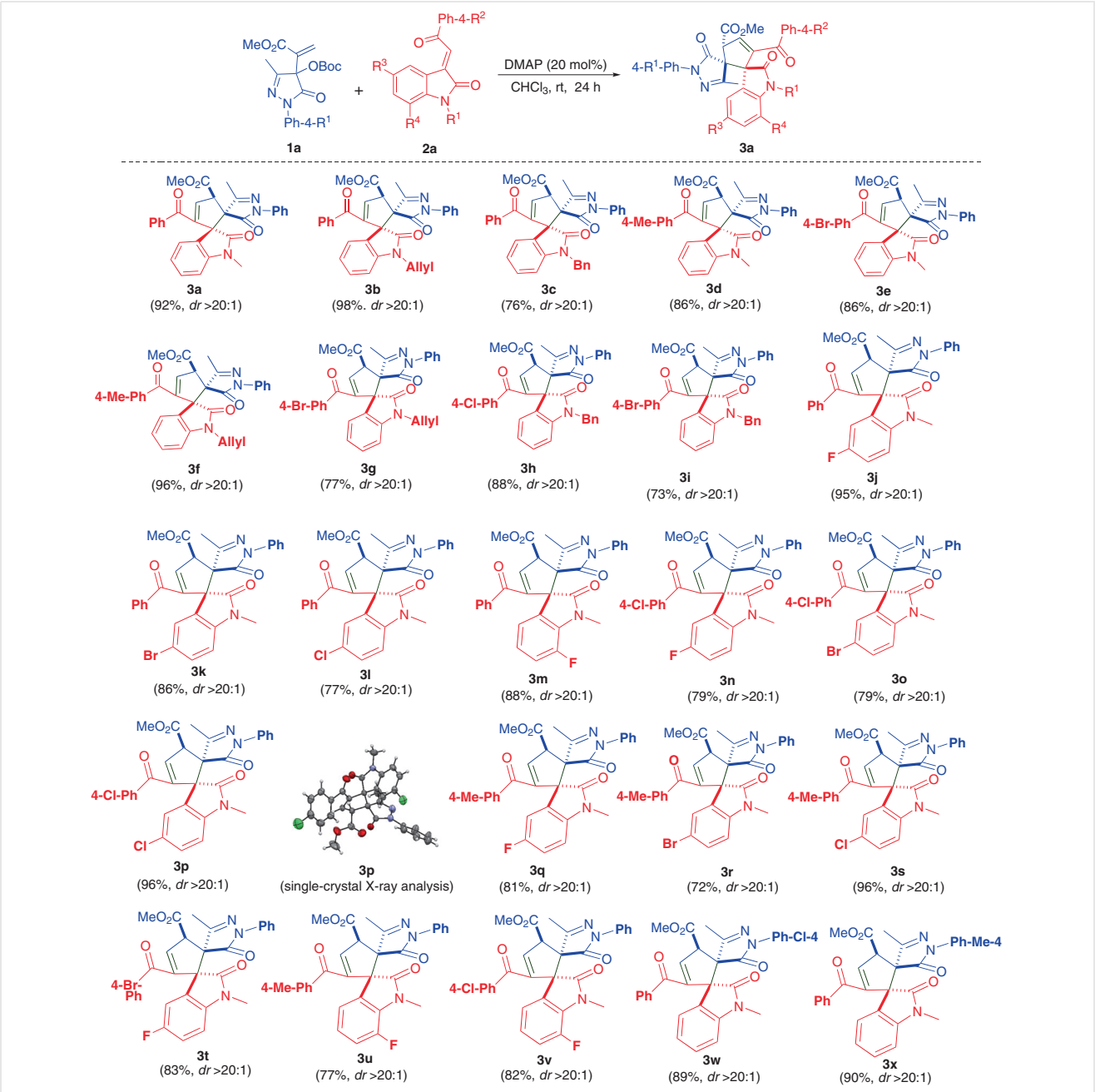
[a] Reaction conditions: **1a** (0.094 mmol), **2a** (0.112 mmol), catalyst, solvent (2.0 mL).
[b] Isolated yield after column chromatography.
[c] Determined by ^{1}H NMR.
[d] Determined by HPLC with a chiral stationary phase.
[e] NR = no reaction.

© 2023. Thieme. All rights reserved.

Downloaded by: Ind Inst of Science Edu & Res PUNE. Copyrighted material.

mol%) in chloroform were found to provide the optimal reaction conditions for the desired [3+2] cycloaddition reaction to give spiropyrazolone-fused oxindole derivatives.

To explore the substrate scope of the [3+2] annulation reaction, we first synthesized various pyrazolone-based MBH carbonates **1a–c** and 3-methyleneoxindoles derivatives **2a–v**. Under the optimized reaction conditions, the pyrazolone MBH carbonates **1a–c** reacted efficiently with the 3-methyleneoxindoles **2a–v** to afford the corresponding spiropyrazolone oxindole derivatives **3a–x** in good to excellent yields (up to 98%) and with very high diastereoselectivities (dr 99:1) (Scheme 1). Note that all the substrates smoothly underwent a [3+2] annulation to afford the corresponding spiropyrazolone–oxindole derivatives bearing vicinal quaternary spirocenters under the optimized reaction conditions. Neither electron-donating nor weakly elec-



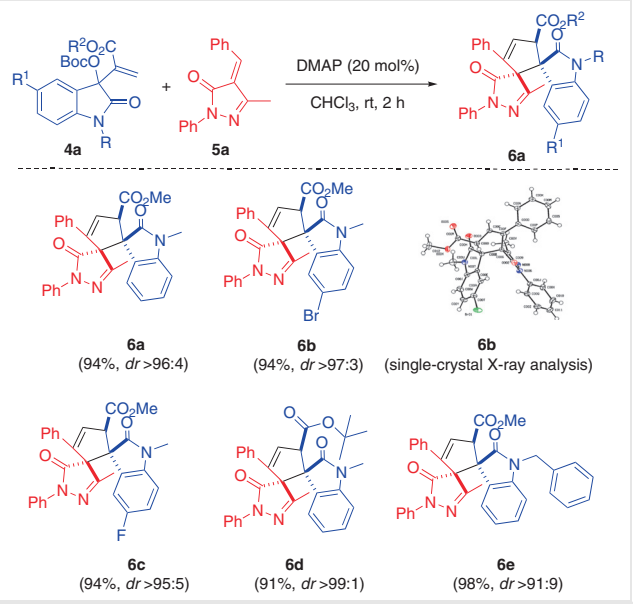
Scheme 1 Substrate scope of pyrazolone-derived MBH carbonates and 3-methyleneoxindoles. *Reaction conditions*: **1a** (0.094 mmol), **2a** (0.112 mmol), DMAP (20 mol%), $CHCl_3$, 24 h, rt. Isolated yields after column chromatograph are reported; the dr values were determined by ^1H NMR.

Downloaded by: Ind Inst of Science Edu & Res PUNE. Copyrighted material.

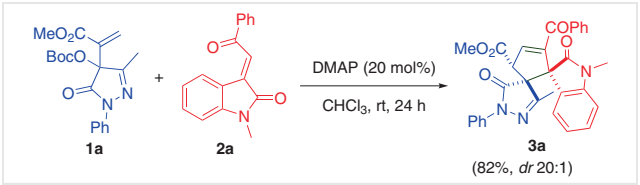
tron-deactivating groups (Br, Cl, F) on the 3-methyleneoxindoles **2** affected the yield and diastereoselectivity of the desired spirooxindole products. Also, *N*-allyl- and *N*-benzyl-protected 3-methyleneoxindoles reacted smoothly to furnish the spirooxindole-fused pyrazolones in high yields and with high diastereoselectivities. Furthermore, the molecular structure of product **3p** was unambiguously established by single-crystal X-ray diffraction analysis (see SI).[24]

Encouraged by these results, we planned to employ MBH carbonates of isatin to construct spirooxindole–pyrazolone derivatives through a [3+2] cycloaddition reaction. To the best of our knowledge, till date there is no report on the use of arylidene pyrazolone for the synthesis of spirooxindole fused pyrazolone compounds bearing adjacent quaternary spirocenters. In this regard, we synthesized the MBH carbonates of isatin **4a–e**. Next, we treated these isatin-based MBH carbonates with the arylidene pyrazolone **5a** under similar reaction conditions (Scheme 2). To our delight, all the reactions proceeded smoothly to afford the corresponding highly functionalized spiropyrazolone-fused oxindoles **6a–e** in excellent yields (up to 98%) and with high diastereoselectivities (dr 91:9 to 99:1). The molecular structure of compound **6b** was established unambiguously by single-crystal X-ray diffraction analysis.[24] The structures of all other products were deduced by analogy and from spectroscopic data.

To demonstrate the practicality of this [3+2] annulation protocol, a millimolar-scale reaction was performed by using pyrazolone-derived MBH carbonate **1a** and the 3-methyleneoxindole **2a** under the optimal conditions. Gratifyingly, the reaction afforded the corresponding spirooxindole **3a** in 82% yield (Scheme 3).

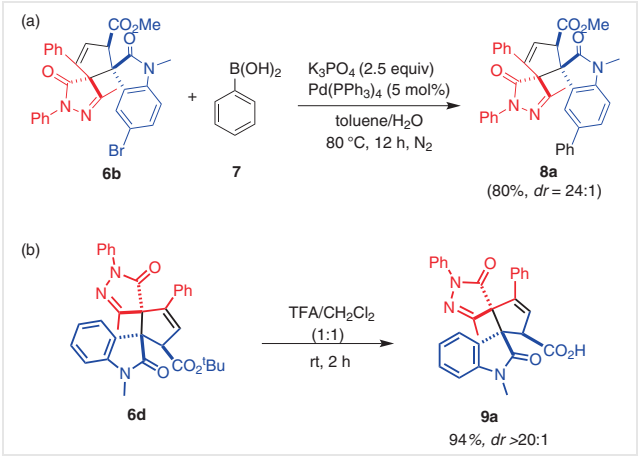


Scheme 2 Substrate scope of isatin-derived MBH carbonates and unsaturated pyrazolones. *Reaction conditions*: **4** (0.115 mmol), **5a** (0.138 mmol), DMAP (20 mol%), $CHCl_3$, 2 h, rt. Isolated yields after column chromatography are reported. The dr values were determined by ^1H NMR.



Scheme 3 Scaled-up synthesis

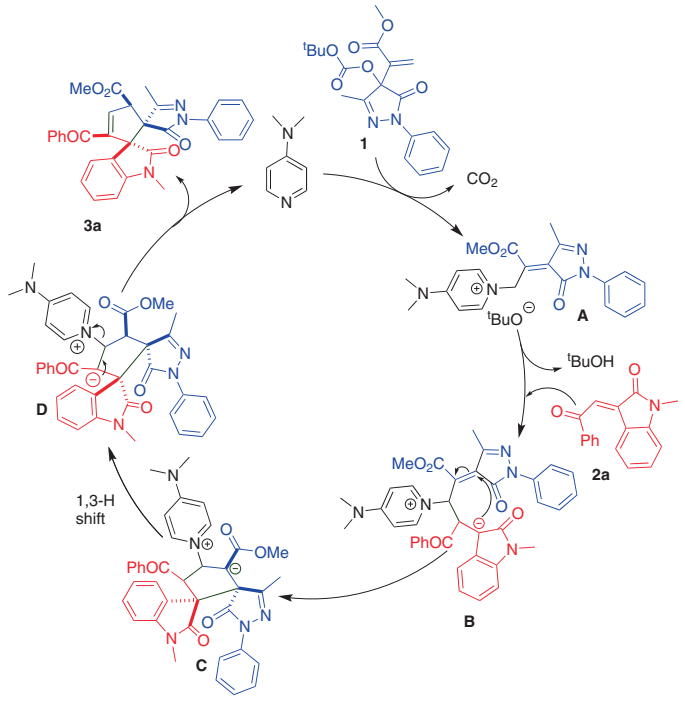
Next, a Suzuki coupling was performed with compound **6b** to demonstrate the synthetic potential of the cycloaddition reaction. The reaction of phenylboronic acid (**7**) with the spirooxindole-fused pyrazolone **6b** in the presence of $Pd(PPh_3)_4$ and K_3PO_4 at 80 °C furnished the product **8a** in 80% yield and with a high diastereoselectivity (Scheme 4a). Next, treatment of compound **6d** with 1:1 v/v TFA–DCM afforded the corresponding carboxylic acid derivative **9a** in 94% yield (Scheme 4b).



Scheme 4 Synthetic transformations

On the basis of our experimental results and previous reports in the literature,[17,19b,d,20,22,26] a plausible catalytic cycle for [3+2] cycloaddition reaction is proposed (Scheme 5). Nucleophilic attack by DMAP on the pyrazolone-derived MBH carbonate **1a** generates the corresponding quaternary ammonium salt **A** together with a *tert*-butoxide anion and carbon dioxide. Next, the Brønsted base (*tert*-butoxide) abstracts an acidic proton to generate an allylic nitrogen ylide. Subsequently, this reacts with the 3-methyleneoxindole **2a** through the α-position to form the corresponding intermediate **B**, which undergoes an intramolecular Michael addition to afford the corresponding cyclic intermediate **C**. Finally, a 1,3-proton shift delivers intermediate **D**, which subsequently forms the spirooxindole product **3a** with regeneration of the catalyst.

Downloaded by: Ind Inst of Science Edu & Res PUNE. Copyrighted material.



Scheme 5 Plausible reaction mechanism for the [3+2] annulation

In summary, we have developed a highly efficient [3+2] annulation reaction between MBH carbonates of pyrazolones with 3-methyleneoxindoles under mild conditions.[26] DMAP served as an effective catalyst for the construction of highly functionalized and medicinally relevant spiroheterocyclic compounds. Spirooxindole–pyrazolone-fused cyclopentene derivatives containing two vicinal spiro quaternary centers have been successfully synthesized in high yields and with excellent diastereoselectivities.

Conflict of Interest

The authors declare no conflict of interest.

Funding Information

R.G.B. thanks DST-SERB (CRG/2019/005753), Government of India, for the generous research grant. The authors also thank IISER Pune for the financial assistance. A.S.S. and P.K.W. thank UGC New Delhi, Government of India, for providing fellowships.

Supporting Information

Supporting information for this article is available online at https://doi.org/10.1055/a-2014-2813.

References and Notes

(1) (a) Kotha, S.; Panguluri, N. R.; Ali, R. *Eur. J. Org. Chem.* **2017**, 5316. (b) Reddy, C. R.; Prajapti, S. K.; Warudikar, K.; Ranjan, R.; Rao, B. B. *Org. Biomol. Chem.* **2017**, *15*, 3130. (c) James, M. J.; O'Brien, P.; Taylor, R. J. K.; Unsworth, W. P. *Chem. Eur. J.* **2016**, *22*, 2856. (d) Cao, Z.-Y.; Zhou, J. *Org. Chem. Front.* **2015**, 849. (e) Carreira, E. M.; Fessard, T. C. *Chem. Rev.* **2014**, *114*, 8257. (f) Rios, R. *Chem. Soc. Rev.* **2012**, *41*, 1060.

(2) (a) Degorce, S. L.; Bodnarchuk, M. S.; Scott, J. S. *ACS Med. Chem. Lett.* **2019**, *48*, 1198. (b) Müller, G.; Berkenbosch, T.; Benningshof, J. C. J.; Stumpfe, D.; Bajorath, J. *Chem. Eur. J.* **2017**, *23*, 703. (c) Ritchie, T. J.; MacDonald, S. J. F. *Drug Discovery Today* **2009**, *14*, 1011. (d) Ritchie, T. J.; MacDonald, S. J. F.; Young, R. J.; Pickett, S. D. *Drug Discovery Today* **2011**, *16*, 164.

(3) Tada, I.; Motoki, M.; Takahashi, N.; Miyata, T.; Takechi, T.; Uchida, T.; Takagi, Y. *Pestic. Sci.* **1996**, *48*, 165.

(4) (a) Schlemminger, I.; Schmidt, B.; Flockerzi, D.; Tenor, H.; Zitt, C.; Hatzelmann, A.; Marx, D.; Braun, C.; Külzer, R.; Heuser, A.; Kley, H.-P.; Sterk, G. J. WO 2010055083, **2010**. (b) Schmidt, B.; Scheufler, C.; Volz, J.; Feth, M.-P.; Hummel, R.-P.; Hatzeimann, A.; Zitt, C.; Wohlsen, A.; Marx, D.; Kley, H.-P.; Marx, D.; Ockert, D.; Heuser, A.; Christiaans, J.-A. M.; Sterk, G.-J.; Menge, W. M. P. B. WO 2008138939, **2008**.

(5) (a) Mugishima, T.; Tsuda, M.; Kasai, Y.; Ishiyama, H.; Fukushi, E.; Kawabata, J.; Watanabe, M.; Akao, K.; Kobayashi, J. *J. Org. Chem.* **2005**, *70*, 9430. (b) Mercado-Marin, E.; Garcia-Reynaga, P.; Romminger, S.; Pimenta, E. F.; Romney, D. K.; Lodewyk, M. W.; Williams, D. E.; Andersen, R. J.; Miller, S. J.; Tantillo, D. J.; Berlinck, R. G. S.; Sarpong, R. *Nature* **2014**, *509*, 318. (c) Cui, C. B.; Kakeya, H.; Osada, H. *J. Antibiot.* **1996**, *49*, 832.

© 2023. Thieme. All rights reserved.

Downloaded by: Ind Inst of Science Edu & Res PUNE. Copyrighted material.

(6) Gicquel, M.; Gomez, C.; Garcia Alvarez, M. C.; Pamlard, O.; Guérineau, V.; Jacquet, E.; Bignon, J.; Voituriez, A.; Marinetti, A. *J. Med. Chem.* **2018**, *61*, 9386.
(7) Wang, B.; Peng, F.; Huang, W.; Zhou, J.; Zhang, N.; Sheng, J.; Haruehanroengra, P.; He, G.; Han, B. *Acta Pharm. Sin. B* **2020**, *10*, 1492.
(8) Bao, X.; Wei, S.; Qian, X.; Qu, J.; Wang, B.; Zou, L.; Ge, G. *Org. Lett.* **2018**, *20*, 3394.
(9) (a) Boddy, A. J.; Bull, J. A. *Org. Chem. Front.* **2021**, *8*, 1026. (b) Zhou, L.-M.; Qu, R.-Y.; Yang, G.-F. *Expert Opin. Drug Discovery* **2020**, *15*, 603. (c) Liu, S.; Bao, X.; Wang, B. *Chem. Commun.* **2018**, *54*, 11515. (d) Carceller-Ferrer, L.; Blay, G.; Pedro, J. R.; Vila, C. *Synthesis* **2021**, *53*, 215. (e) Han, X.; Yao, W.; Wang, T.; Tan, Y. R.; Yan, Z.; Kwiatkowski, J.; Lu, Y. *Angew. Chem. Int. Ed.* **2014**, *53*, 5643. (f) Zhong, F.; Luo, J.; Chen, G.-Y.; Dou, X.; Lu, Y. *J. Am. Chem. Soc.* **2012**, *134*, 10222. (g) Guo, X.; Shen, Z.-A.; Zhou, X.; Dai, L.; Lu, Y. *Sci. China Chem.* **2023**, *66*, 127.
(10) Chen, Q.; Liang, J.; Wang, S.; Wang, D.; Wang, R. *Chem. Commun.* **2013**, *49*, 1657.
(11) Cui, B.-D.; Li, S.-W.; Zuo, J.; Wu, Z.-J.; Zhang, X.-M.; Yuan, W.-C. *Tetrahedron* **2014**, *70*, 1895.
(12) Li, J.-H.; Feng, T.-F.; Du, D.-M. *J. Org. Chem.* **2015**, *80*, 11369.
(13) Liu, X.-L.; Zuo, X.; Wang, J.-X.; Chang, S.-Q.; Wei, Q.-D.; Zhou, Y. *Org. Chem. Front.* **2019**, *6*, 1485.
(14) Lin, Y.; Zhao, B.-L.; Du, D.-M. *J. Org. Chem.* **2019**, *84*, 10209.
(15) Wang, C.; Wen, D.; Chen, H.; Deng, Y.; Liu, X.; Liu, X.; Wang, L.; Gao, F.; Guo, Y.; Sun, M.; Wang, K.; Yan, W. *Org. Biomol. Chem.* **2019**, *17*, 5514.
(16) Luo, W.; Shao, B.; Li, J.; Xiao, X.; Song, D.; Ling, F.; Zhong, W. *Org. Chem. Front.* **2020**, *7*, 1016.
(17) Tian, Z.; Jiang, J.; Yan, Z.-H.; Luo, Q.-Q.; Zhan, G.; Huang, W.; Li, X.; Han, B. *Chem. Commun.* **2022**, *58*, 5363.
(18) Chen, Y.; Cui, B.-D.; Wang, Y.; Hang, W.-Y.; Wan, N.-W.; Bai, M.; Yuan, W.-C.; Chen, Y.-Z. **2018**, *83*, 10465.
(19) (a) Warghude, P. K.; Sabale, A. S.; Bhat, R. G. *Org. Biomol. Chem.* **2020**, *18*, 1794. (b) Warghude, P. K.; Bhowmick, A.; Bhat, R. G. *Tetrahedron Lett.* **2022**, *97*, 153791.
(20) (a) Warghude, P. K.; Dharpure, P. D.; Bhat, R. G. *Tetrahedron Lett.* **2018**, *59*, 4076. (b) Warghude, P. K.; Sabale, A. S.; Dixit, R.; Vanka, K.; Bhat, R. G. *Org. Biomol. Chem.* **2021**, *19*, 4338.
(21) Chen, Z.-C.; Chen, Z.; Du, W.; Chen, Y.-C. *Chem. Rec.* **2020**, *20*, 541.
(22) (a) Huang, S.; Wen, H.; Tian, Y.; Wang, P.; Qin, W.; Yan, H. *Angew. Chem. Int. Ed.* **2021**, *60*, 21486. (b) Liao, J.; Xu, J.; Wu, Y.; Hou, Y.; Guo, H. *Adv. Synth. Catal.* **2022**, *364*, 1074. (c) Wei, X.; Huang, Y.; Wang, W.; Wei, S.; Qu, J.; Wang, B. *Chem. Commun.* **2022**, *58*, 9504. (d) Luo, Q.; Tian, Z.; Tang, J.; Wang, Y.; Tian, Y.; Peng, C.; Zhan, G.; Han, B. *ACS Catal.* **2022**, *12*, 7221. (e) Yang, Z.-H.; Chen, P.; Chen, Z.-C.; Chen, Z.; Du, W.; Chen, Y.-C. *Angew. Chem. Int. Ed.* **2021**, *60*, 13913.
(23) (a) Saeed, R.; Sakla, A. P.; Shankaraiah, N. *Org. Biomol. Chem.* **2021**, *19*, 7768. (b) Cao, Y.; Jiang, X.; Liu, L.; Shen, F.; Zhang, F.; Wang, R. *Angew. Chem. Int. Ed.* **2011**, *50*, 9124. (c) Tan, Y.; Feng, E.-L.; Sun, Q.-S.; Lin, H.; Sun, X.; Lin, G.-Q.; Sun, X.-W. *Org. Biomol. Chem.* **2017**, *15*, 778. (d) Zhou, Y.-H.; Lu, Y.; Hu, X.-Y.; Mei, H.-J.; Lin, L.-L.; Liu, X.-H.; Feng, X.-M. *Chem. Commun.* **2017**, *53*, 2060.
(24) CCDC 2189452 and CCDC 2183100 contains the supplementary crystallographic data for compounds **3p** and **6b**, respectively. The data can be obtained free of charge from The Cambridge Crystallographic Data Centre via www.ccdc.cam.ac.uk/structures
(25) (a) Peng, J.; Huang, X.; Jiang, L.; Cui, H.-L.; Chen, Y.-C. *Org. Lett.* **2011**, *13*, 4584. (b) Wei, F.; Huang, H.-Y.; Zhong, N.-J.; Gu, C.-L.; Wang, D.; Liu, L. *Org. Lett.* **2015**, *17*, 1688.
(26) **Product 3a; Typical Procedure**
An oven-dried round-bottomed flask was charged with the MBH carbonate **1a** (35 mg, 0.094 mmol), the indolinone **2a** (24 mg, 0.112 mmol), DMAP (2.28 mg, 0.019 mmol), and $CHCl_3$ (2 mL), and the mixture was stirred at rt for 12 h. When the reaction was complete (TLC), the solvent was evaporated under reduced pressure and the crude product was directly purified by column chromatography [silica gel (100–200 mesh), PE–EtOAc (70:30)] to give a brown solid; yield: 45 mg (92%, 99:1 dr); mp 78–80 °C. R_f = 0.3 (PE–EtOAc, 70:30).
^{1}H NMR (400 MHz, $CDCl_3$): δ = 8.0 (d, *J* = 7.0 Hz, 2 H), 7.6 (m, 3 H), 7.5–7.4 (m, 2 H), 7.4–7.3 (m, 3 H), 7.2–7.1 (m, 2 H), 7.1 (d, *J* = 2.2 Hz, 1 H), 6.8 (d, *J* = 25.2 Hz, 2 H), 4.9 (d, *J* = 2.3 Hz, 1 H), 3.7 (s, 3 H), 3.3 (s, 3 H), 2.2 (s, 3 H). ^{13}C {^{1}H} NMR (100 MHz, $CDCl_3$): δ = 190.9, 174.1, 172.5, 169.1, 156.5, 144.7, 143.3, 142.8, 137.3, 136.8, 133.6, 130.1, 129.9, 128.9, 128.8, 125.9, 125.0, 124.0, 123.4, 119.7, 108.6, 67.2, 65.0, 53.8, 53.0, 26.9, 15.9. HRMS (ESI TOF): *m/z* [M + H]$^+$ calcd for $C_{31}H_{26}N_3O_5$: 520.1872; found: 520.1876.

Downloaded by: Ind Inst of Science Edu & Res PUNE. Copyrighted material.

Check for updates

ACES Asian Chemical Editorial Society

doi.org/10.1002/ajoc.202500424

ASIAN JOURNAL OF ORGANIC CHEMISTRY
Research Article

www.asianjoc.org

Direct Access to 3,4-Fused Spirooxindoles Through Visible-Light-Driven Diasterioselective [4+2] Cyclization of 3-Methylene Oxindoles

Abhijeet S. Sabale,[a] Anindita Bhowmick,[a] Saswata Pattanaik,[a] Onkar S. Bankar,[a] and Ramakrishna G Bhat*[a]

A visible light-mediated strategy has been developed to synthesize diastereoselective 3,4-fused spirooxindoles via formal [4+2] cycloaddition of 3-methylene oxindoles without the need of pre-functionalization. The 3-methylene oxindoles, when exposed to visible light in the presence of catalytic amount of $CeCl_3$ under alkaline conditions, afforded the complex 3,4-fused spirooxindole framework with four contiguous chiral centers. The protocol proved to be highly chemo- and regio-selective by affording 3,4-fused spirooxindoles in moderatetogood yields. The protocol also works smoothly under the direct exposure of sunlight. It has been demonstrated that the method is also scalable on gram quantity.

1. Introduction

The 3,4-fused indole and oxindole skeleton is a common structural motif in many drugs, natural products, and pharmaceuticals.[1] This specific arrangement of atoms within the fused indole and oxindole scaffold is known to exhibit significant biological activity. Notable compounds featuring this structural framework include lysergic acid,[2] rugulovasine A,[3] chanoclavine-I,[4] dehydrobufotenine,[5] chuangxinmycin,[6] hapalindole U,[7] ammosamide B, and its analogs[1d,g] (see Figure 1). Given the biological importance of this scaffold, considerable efforts have been directed towards the construction of this scaffold and also compounds derived from this framework have been utilized in drug discovery process.[8] Consequently, the development of novel synthetic methods to access intricate 3,4-fused indole and oxindole frameworks remains highly desirable.[9]

Various strategies have been employed to synthesize biologically important molecules containing 3,4-fused indole and oxindole frameworks with six-membered ring. Fujii, Ohno and co-workers reported an efficient one-step total synthesis of (+)-lysergic acid using a palladium-catalyzed domino cyclization of 4-halo indole derivatives of allenic amides (Scheme 1A).[10] Similarly, Fukuyama and co-workers achieved the total synthesis of lysergic acid through a palladium-catalyzed cyclization at an elevated temperature (100 °C) to access 3,4-substituted indoline.[2a] Murakami and co-workers accomplished the enantioselective total synthesis of optically active chanoclavine-I, an ergot alkaloid, using a palladium-catalyzed intramolecular cyclization (Heck reaction) at an elevated temperature (100 °C) (Scheme 1B).[4] Buchwald and co-worker disclosed the synthesis of tetrahydropyrroloquinolines via a palladium-catalyzed intramolecular cyclization at 200 °C to construct the 3,4-fused indoline core (Scheme 1C).[5a] Fenical and co-worker reported the total synthesis of ammosamide B, which required pre-functionalization at the C4 position at an elevated temperature (100 °C) (Scheme 1D).[1d] Similarly, Sun, Wang and co-workers accomplished the total synthesis of ammosamide B using a palladium-catalyzed cyclization at 110 °C to access 3,4-substituted oxindoles (Scheme 1E).[1g]

All these methods involve the initial activation of the 4-halo group by palladium, followed by its subsequent addition to the double bond to achieve the desired 3,4-indole or oxindole skeleton. However, these approaches mostly rely on pre-functionalized substrates to facilitate cyclization at the C4 position. Furthermore, to our knowledge, no existing methods enable the direct C–H functionalization of the unactivated C4 position at room temperature without pre-functionalization. This challenge arises primarily from the low reactivity of the C4–H bond toward electrophiles, thus making it difficult for the efficient cyclization.[11]

Additionally, some of the earlier methods reported for synthesizing 3,4-fused oxindoles using the 3-methylene oxindole as a model substrate present notable limitation. These methods rely on traditional [4+2] cycloaddition, and they often require high temperatures, also exhibit a limited substrate scope, require environmentally hazardous solvents like acetic anhydride/DMF, and also afforded the products in lower yields.[12] Some of these drawbacks underscore the need to develop alternative, sustainable, more efficient, and versatile synthetic approaches.

Starting from a single substrate, constructing a complex molecule such as a 3,4-fused spirooxindole has not yet been explored, particularly under visible light. Developing a more straightforward approach to construct the 3,4-fused spirooxin-

[a] A. S. Sabale, A. Bhowmick, S. Pattanaik, O. S. Bankar, R. G Bhat
Department of Chemistry, Indian Institute of Science Education and Research (IISER) Pune, Dr. Homi Bhabha Road, Pashan, Pune, Maharashtra 411008, India
E-mail: rgb@iiserpune.ac.in

Supporting information for this article is available on the WWW under https://doi.org/10.1002/ajoc.202500424

© 2025 Wiley-VCH GmbH

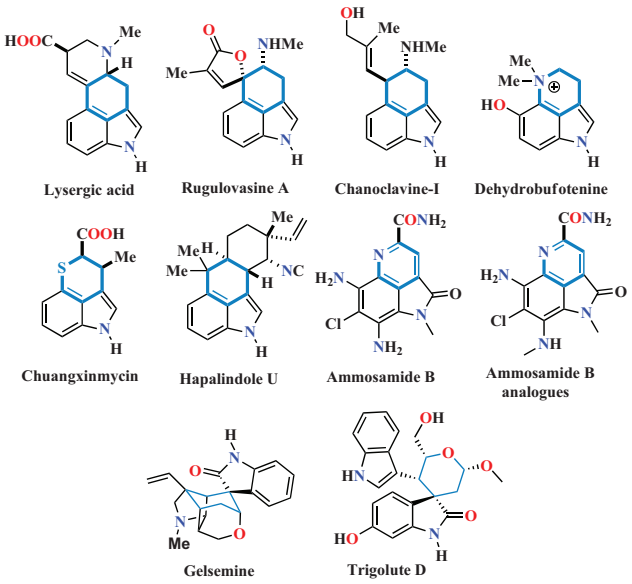


Figure 1. Natural products with 3,4-fused indole, oxindole, and spirooxindole skeletons

dole framework at room temperature remains highly desirable and challenging. Additionally, 3,3-substituted spirooxindole frameworks have been extensively synthesized due to their significant biological activity (Figure 1).[13]

Herein, we report a visible light-mediated direct synthesis of a 3,4-fused spirooxindole framework featuring a six-membered ring using the 3-methylene oxindole as the key substrate (Scheme 1F).[14]

2. Results and Discussion

Based on the available literature, we planned to explore a visible-light-driven approach using a ligand-to-metal charge transfer (LMCT) complex to construct a 3,4-fused spirooxindole framework. We hypothesized that the 3-methylene oxindole could interact with cerium chloride ($CeCl_3$) to facilitate LMCT-driven cyclization under visible light, involving an electron transfer from Ce(III) to Ce(IV). To investigate this, we began with N-benzyl 3-methylene oxindole **1a** as a model substrate, synthesized according to a reported procedure.[15] The reaction of **1a** in the presence of $CeCl_3$ (20 mol%) and cesium carbonate in acetonitrile, when exposed to 456 nm blue LED light (Kessil lamp) under an inert atmosphere, afforded the desired product **2a**, albeit in very low yield of 11% (see Supporting Information S11; Table S1, entry 1).

We then screened various LEDs with different wavelengths and intensities (see Supporting Information S11; Table S1, entries 2–4). Among them, the blue LED (427 nm, 50% intensity, 20 W) proved more efficient, affording the desired product **2a** in a moderate yield (20%). Interestingly, when the reaction of **1a** was conducted under the illumination of two blue LEDs (2 × 427 nm, 2* 40W) while maintaining the other optimized conditions, the yield of **2a** significantly increased (70%, Table 1, entry 1; see also Supporting Information S11;Table S1, entries 5–8).

However, under these conditions, the reaction temperature raised to 60–65 °C. To investigate whether the temperature influenced the reaction outcome, we performed the reaction of **1a** at elevated temperature (up to 70 °C) in the absence of light (Table 1, entry 3). Surprisingly, no desired product **2a** was obtained, even after a prolonged reaction time. This result clearly indicates that temperature alone does not drive the reaction, and light is essential for the transformation. We strongly believe that the increase in the reaction temperature due to the high intensity of the LEDs may have enhanced the reaction rate, thereby contributing to the improved yield of **2a**.

Interestingly, when the reaction was carried out in the absence of Cs_2CO_3 while maintaining the other conditions, the desired product **2a** was obtained in moderate yield, indicating the essential role of the base (see Table 1, entry 4). Surprisingly, the reaction in the absence of both $CeCl_3$ and Cs_2CO_3 still afforded the product **2a**, albeit in moderate yield (see Table 1, entry 5). This observation raised concerns regarding the role of $CeCl_3$ and the earlier presumed LMCT pathway.

To gain further mechanistic insights, we conducted systematic UV–visible absorption studies. The UV–visible absorption spectra of the reaction mixture were recorded at 10-min intervals over a period of one hour in the absence of light. Notably, no change was observed in the absorption maxima of the 3-methylene oxindole **1a**, and no new absorption peaks appeared (see Figure 2B; Supporting Information S8–S9; Figure S2). This suggests that a single-electron transfer (SET) process may not be occurring from $CeCl_3$ to **1a** via the oxidation of Ce(III) to Ce(IV).

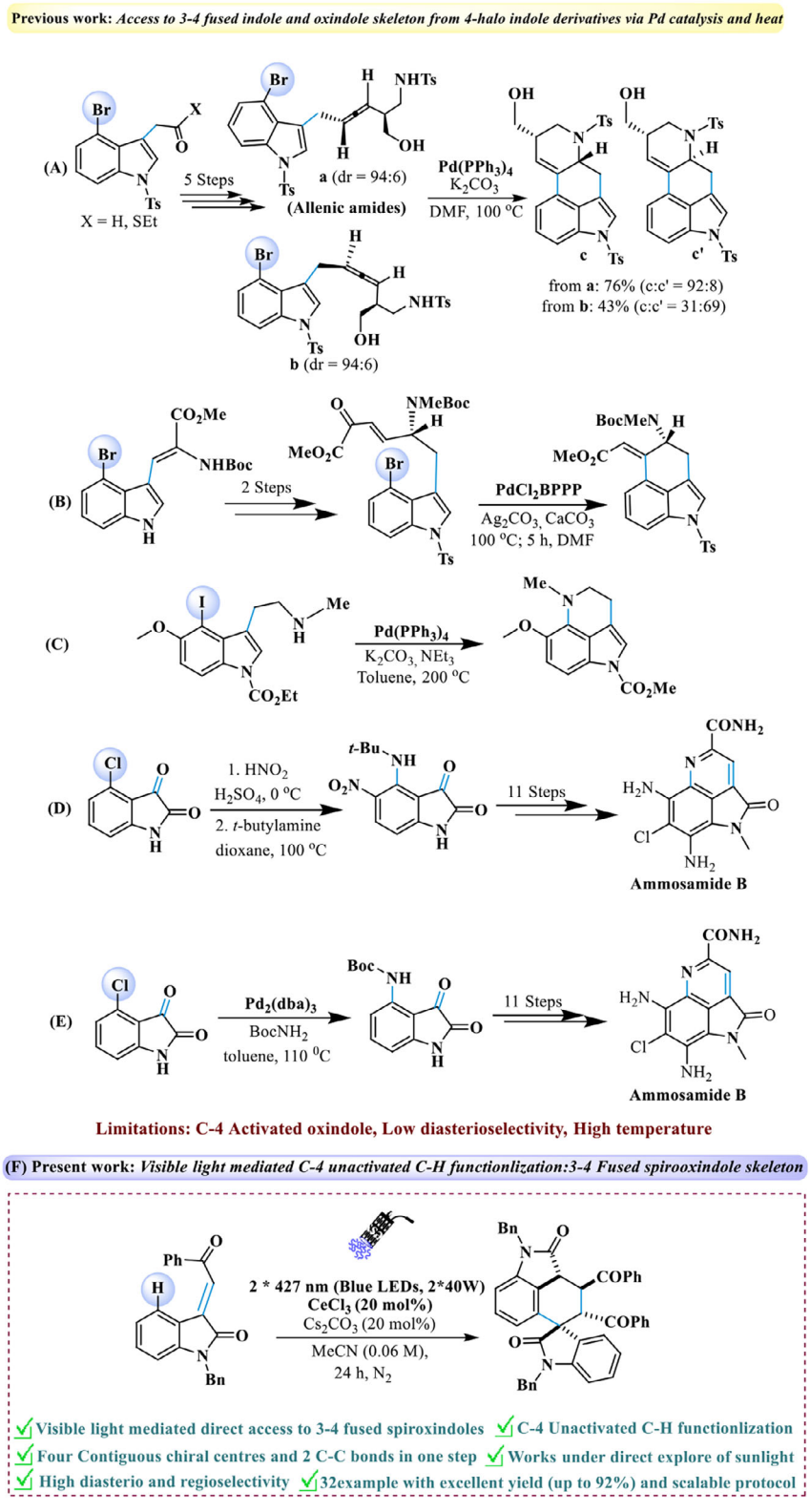
Additionally, FT-IR spectroscopic analysis revealed significant changes in the vibrational frequencies, indicating possible interactions or structural modifications. These findings provide valuable insights into the reaction mechanism and the nature of the intermediates formed (see Supporting Information S9 and S10; S3–S5). Based on these results and our previous observation regarding the necessity of $CeCl_3$, we proposed that $CeCl_3$ likely functions as a Lewis acid additive.[16]

To validate this assumption, we screened various Lewis acids (see Supporting Information S11–S12; Table S2, entries 1–7). Among them, $CeCl_3$ proved to be the most effective catalyst by affording the desired product **2a** in the highest yield (Table 1, entry 1). Subsequently, we evaluated both organic and inorganic bases, among all Cs_2CO_3 emerged as the most efficient base, providing **2a** in a higher yield. In contrast, other bases significantly reduced the yield of the product **2a** (see Supporting Information S11–S12; Table S2, entries 8–13).

Furthermore, we investigated the effect of different solvents, and among all, acetonitrile proved to be most advantageous by furnishing the **2a** in higher yield (see Supporting Information S11–S12; Table S2, entries 14–24). We also assessed the influence of solvent concentration on the reaction outcome. Both lower and higher concentrations led to a decline in the

© 2025 Wiley-VCH GmbH

21935815, 0, Downloaded from https://acses.onlinelibrary.wiley.com/doi/10.1002/ajoc.202500424 by Indian Institute Of Science Education And Research Pune, Wiley Online Library on [20/06/2025]. See the Terms and Conditions (https://onlinelibrary.wiley.com/terms-and-conditions) on Wiley Online Library for rules of use; OA articles are governed by the applicable Creative Commons License



Scheme 1. Visible light-mediated direct access to biologically important compounds containing 3,4-fused spirooxindoles.

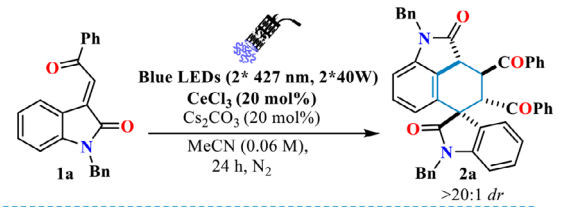
yield of **2a**. Notably, the reaction proceeded most efficiently at a concentration of 0.06 M in acetonitrile, by providing **2a** in highest yield (see Supporting Information S13; Table S4, entries 1–4).

We also investigated the effect of acidic and basic additives loading on the outcome of the yield of **2a** (see Supporting Information S12 and S13; Table S3, entries 1–6). Interestingly, when the reaction was conducted in the presence of atmospheric

© 2025 Wiley-VCH GmbH

21935815, 0, Downloaded from https://aces.onlinelibrary.wiley.com/doi/10.1002/ajoc.202500424 by Indian Institute Of Science Education And Research Pune, Wiley Online Library on [20/06/2025]. See the Terms and Conditions (https://onlinelibrary.wiley.com/terms-and-conditions) on Wiley Online Library for rules of use; OA articles are governed by the applicable Creative Commons License

Table 1. Optimization studies of the visible light-mediated C-4 unactivated C–H functionalization to synthesize 3,4-fused spirooxindole skeleton.[a]



Entry	Variation from the Optimized Condition[a)]	Yield[b)] %2a
1[d)]	**None**	**70**
2[d)]	No light	NR
3[d)]	Reaction in the absence of light at 70 °C.	NR
4[d)]	Absence of Cs_2CO_3	48
5[d)]	Absence of $CeCl_3$ and Cs_2CO_3	35
6[d)]	Open air instead of inert atmosphere	36
7[d)]	Presence of molecular oxygen	ND

Reaction conditions: [a)] 3-Methylene oxindole **1a** (0.2 mmol, 1 equiv.), $CeCl_3$ (20 mol %), Cs_2CO_3 (20 mol%), in MeCN (0.06 M), Kessil Blue LED (427 nm with 100% intensity temperature around 60–65 °C, switching the fan off, 2* 40W), nitrogen atmosphere. [b)] Yields are obtained after purification over column chromatography. [c)] Diastereomeric ratio determined by ^{1}H NMR spectroscopy (we observed > 20:1 dr). [d)] A.R. grade ACN was used. NR = No reaction. ND = Not detected.

air, the desired product **2a** was obtained in modest yield (see Table 1, entry 6). In contrast, the reaction did not proceed in the presence of molecular oxygen (see Table 1, entry 7). Based on comprehensive screening, the optimal reaction conditions were determined to be the 3-methylene oxindole **1a** (0.2 mmol, 1 equiv.), $CeCl_3$ (20 mol%), and Cs_2CO_3 (20 mol%) in acetonitrile under the irradiation of blue LEDs (2 × 427 nm, 2* 40W) in an inert atmosphere, affording the desired product **2a** in the highest yield.

After determining the optimum reaction conditions, we explored the substrate scope for the [4+2] cycloaddition of the 3-methylene oxindole derivatives **1b**–**1ad**. Various N-protected 3-methylene oxindole derivatives (**1b**–**1e**), as well as the unprotected 3-methylene oxindole **1f**, reacted under the optimized conditions to afford the corresponding products (**2b**–**2f**) in moderate to good yields with excellent diastereoselectivity (see Scheme 2). Next, we examined N-benzyl 3-methylene oxindole derivatives with different substituents on the phenyl ring of the arylethylidene moiety (**1g**–**1p**). These reactions furnished the desired products (**2g**–**2p**) in moderate to good yields, also with excellent diastereoselectivity (see Scheme 2). Notably, the presence of electron-donating, electron-withdrawing, and deactivating groups on the phenyl ring significantly influenced the yield of **2a**. Furthermore, the 3-methylene oxindoles with substituents at the C-5, C-6, and C-7 positions reacted smoothly, delivering the corresponding products (**2q**–**2z**) in moderate to excellent yields with a high degree of diastereoselectivity (up to 92%, >20:1 dr) (see Scheme 2). Additionally, *ortho*-, *meta*-, and *para*-substituted N-benzyl 3-methylene oxindole derivatives (**2aa**–**2ad**) provided the desired products in moderate yields with excellent diastereoselectivity (Scheme 2).

However, a few N-benzyl 3-alkylidene/arylidene oxindole derivatives did not react under the standard reaction condition and the desired products (**2ae**–**2af**) were not obtained. This lack of reactivity is likely due to the low stability of the radicals formed during the course of the reaction, which may have hindered the reaction progress and prevented the formation of the cyclized products (see Scheme 2).

To evaluate the practicality of the protocol, we conducted the reaction of **1a** on a larger scale (1.05 g) under the standard conditions to obtain the desired product **2a** in a moderate yield with excellent diastereoselectivity (58% yield; see Scheme 3A; Supporting Information S7–S8). Furthermore, we explored the reaction of **1a** under the direct exposure of sunlight to obtain the desired product **2a**, albeit in a lower yield (40%; see Scheme 3B; Supporting Information S3).

To gain mechanistic insights into the transformation, we conducted radical trapping experiments using TEMPO and BHT as radical scavengers while maintaining the standard reaction conditions. In the presence of TEMPO, the desired product **2a** was obtained in a poor yield (20%) along with the formation of TEMPO-trapped radical intermediates (**5a**, **6a**) (confirmed by HRMS, see Scheme 4A). When BHT was used as a radical scavenger, the desired product **2a** was not obtained, and the

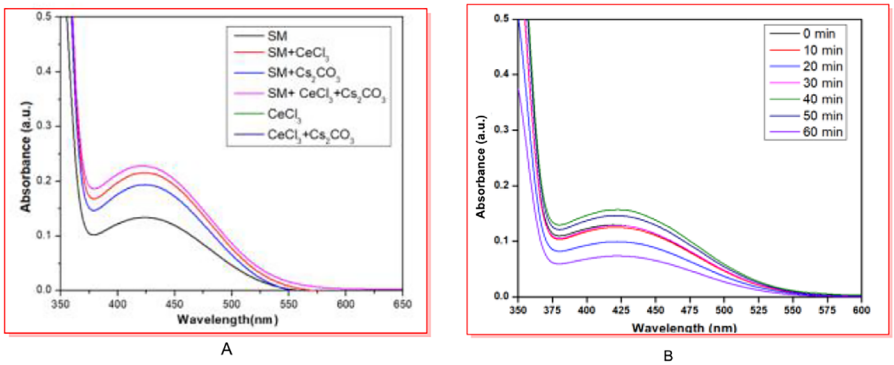
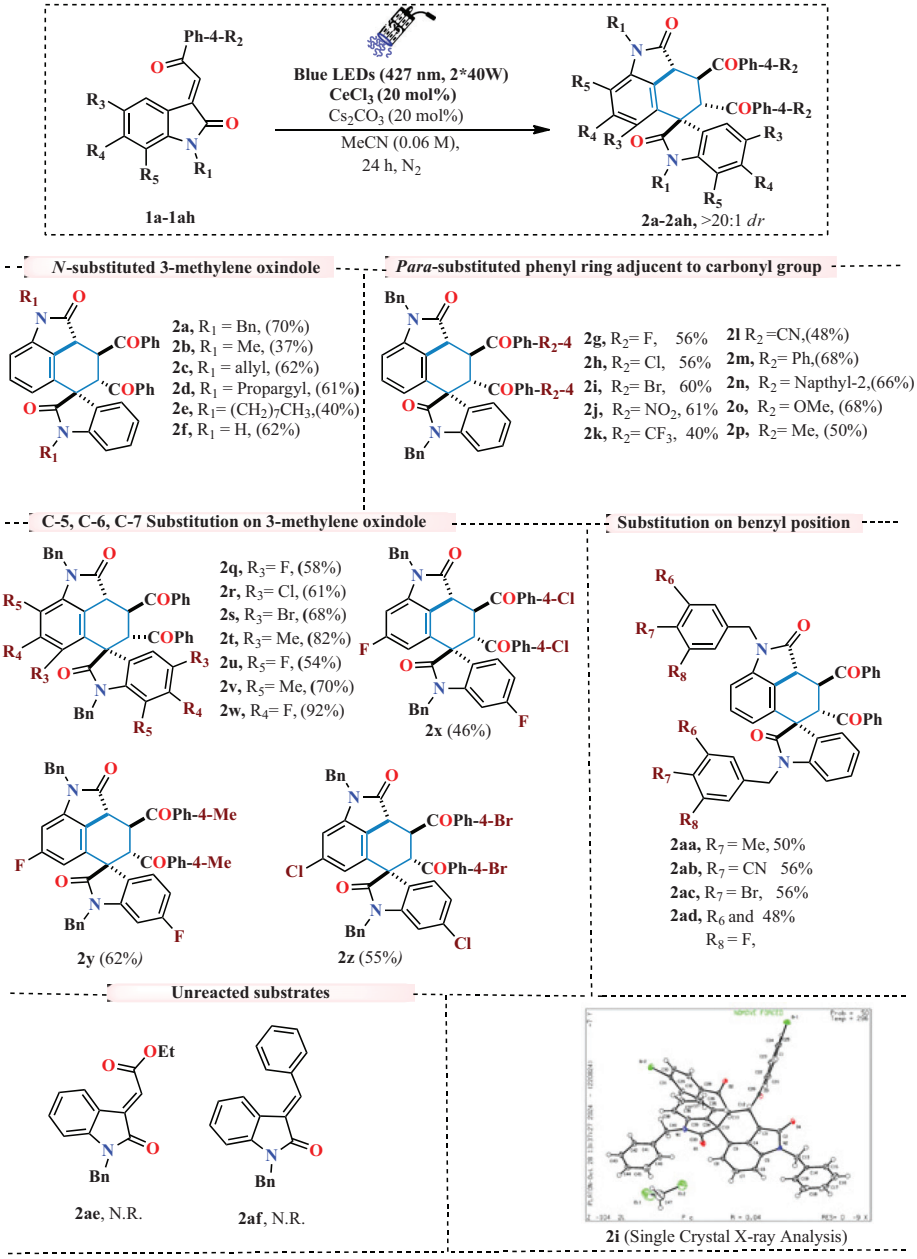


Figure 2. UV–visible absorption spectra of starting material and reaction mixture: (A) UV–visible absorption of different forms of starting material (SM) 3-methylene oxindole in ACN. 20 μM starting material (SM) 3-methylene oxindole+$CeCl_3$, 20 μM starting material (SM) 3-methylene oxindole+$CeCl_3$+Cs_2CO_3, 20μM only $CeCl_3$, 20μM $CeCl_3$+Cs_2CO_3 (B) UV–visible absorption spectra of the reaction mixture without light.

© 2025 Wiley-VCH GmbH

21935815, 0, Downloaded from https://acses.onlinelibrary.wiley.com/doi/10.1002/ajoc.202500424 by Indian Institute Of Science Education And Research Pune, Wiley Online Library on [20/06/2025]. See the Terms and Conditions (https://onlinelibrary.wiley.com/terms-and-conditions) on Wiley Online Library for rules of use; OA articles are governed by the applicable Creative Commons License



Scheme 2. The substrate scope of 3-methylene oxindoles derivatives[a] Standard reaction conditions: [a]3-Methylene oxindole **1** (0.2 mmol, 1 equiv.), $CeCl_3$ (20 mol%), Cs_2CO_3 (20 mol%), in MeCN (0.06 M), Kessil Blue LED (427 nm with 100% intensity temperature around 60–65 °C, switching the fan off, 2*40W), nitrogen atmosphere, diastereomeric ratio determined by ^1H NMR spectroscopy (we observed > 20:1 dr).

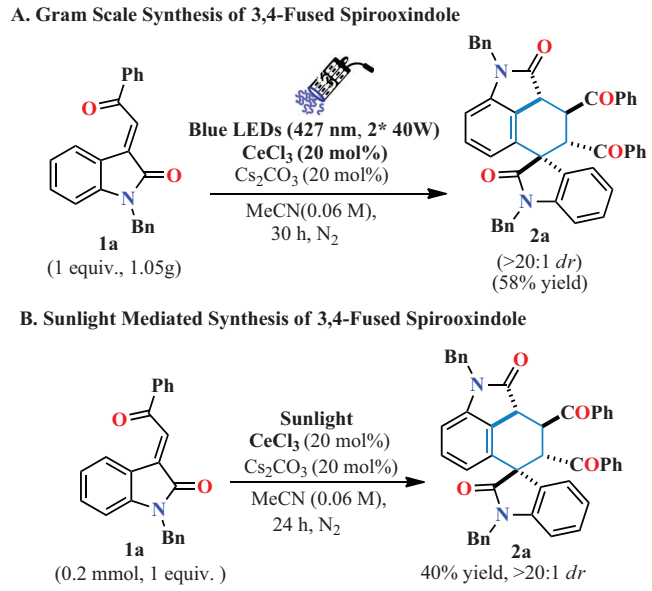
radical-trapped intermediate **8a** was detected (confirmed by HRMS; see Scheme 4B).

These radical trapping experiments indicate a radical pathway in this reaction (see Scheme 4; Supporting Information S4–S7). To gain further insights into the reaction mechanism, we conducted UV–visible spectroscopic studies. The UV–visible absorption spectrum of the starting material, the 3-methylene oxindole **1a**, showed absorption within the visible region (370–500 nm). Similarly, the UV–visible absorption of a mixture of the 3-methylene oxindole and $CeCl_3$ also remained within the visible range (Figure 2A).

Subsequently, we recorded the UV–visible absorption spectrum of a mixture containing the 3-methylene oxindole **1a**, $CeCl_3$, and Cs_2CO_3. Interestingly, no significant change or a slight shift in the absorption maxima (370–500 nm) was observed. These results indicate that the 3-methylene oxindole and $CeCl_3$ likely do not interact with each other through any charge transfer pathway (see Figure 2A; Supporting Information S8; Figure S1). The UV visible absorption spectra of the reaction mixture were recorded (10 min interval over 1 h, in the absence of light) and we did not see any changes in the absorption maxima of 3-methylene

© 2025 Wiley-VCH GmbH

21935815, 0, Downloaded from https://aces.onlinelibrary.wiley.com/doi/10.1002/ajoc.202500424 by Indian Institute Of Science Education And Research Pune, Wiley Online Library on [20/06/2025]. See the Terms and Conditions (https://onlinelibrary.wiley.com/terms-and-conditions) on Wiley Online Library for rules of use; OA articles are governed by the applicable Creative Commons License

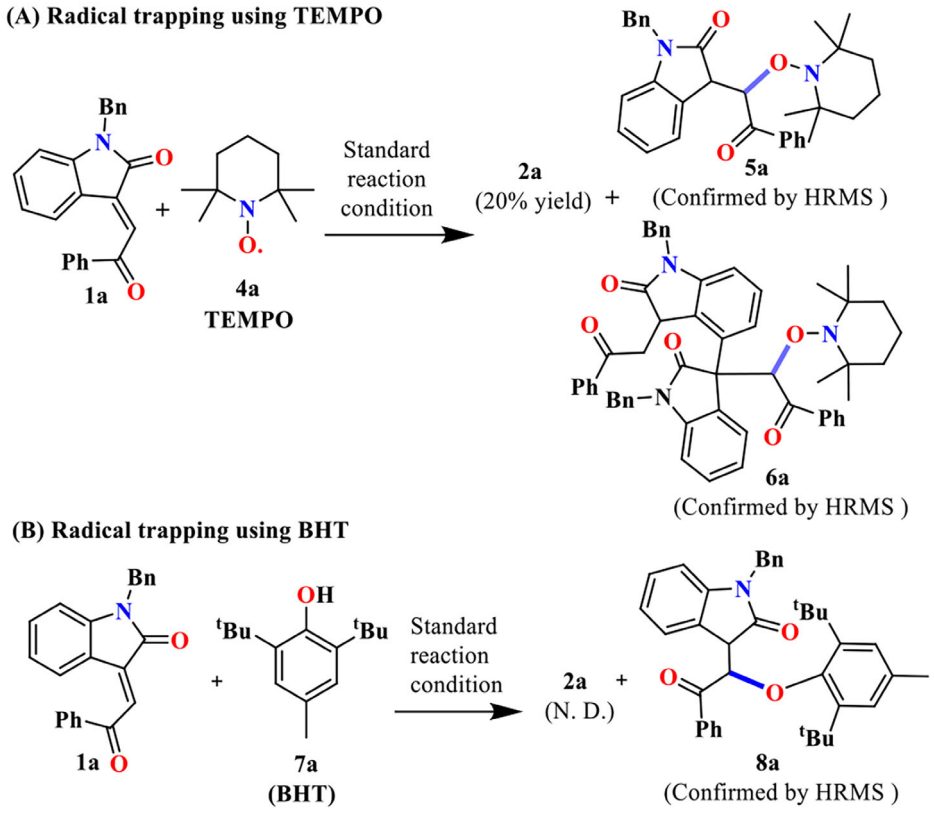


Scheme 3. Gramscale and sunlightmediated synthesis of 3–4 Fused Spirooxindoles

oxindole **1a** thus indicating that SET single-electron transfer (SET) process may not be occurring between $CeCl_3$_and **1a** (Figure 2B, see Supporting Information S8-S9; Figure S2 for details).

A plausiblecatalytic cycle has been proposed based on prior literature as well as on our experimental findings (Scheme 5). Upon photoirradiation, the 3-methylene oxindole **1a** generates a radical intermediate **I**, as confirmed by HRMS (see Supporting Information S4–S7; Scheme 4). Due to the heat generated from light exposure, intermediate **I** may exist in equilibrium with a relatively unstable intermediate **II**. Subsequently, this intermediate undergoes a radical-mediated C–H functionalization with the $CeCl_3$-activated 3-methylene oxindole **1a**, an interaction further corroborated by FT-IR analysis (see Supporting Information S9–S10; Figure S3–S5). This step leads to the formation of a diradical intermediate **III**, further validated by HRMS (see Supporting Information S4–S7; Scheme 4). Further, intermediate **III** undergoes cyclization to afford an intermediate **IV**. Eventually, the intermediate **IV** undergoes aromatization via deprotonation to afford the desired product **2a**.

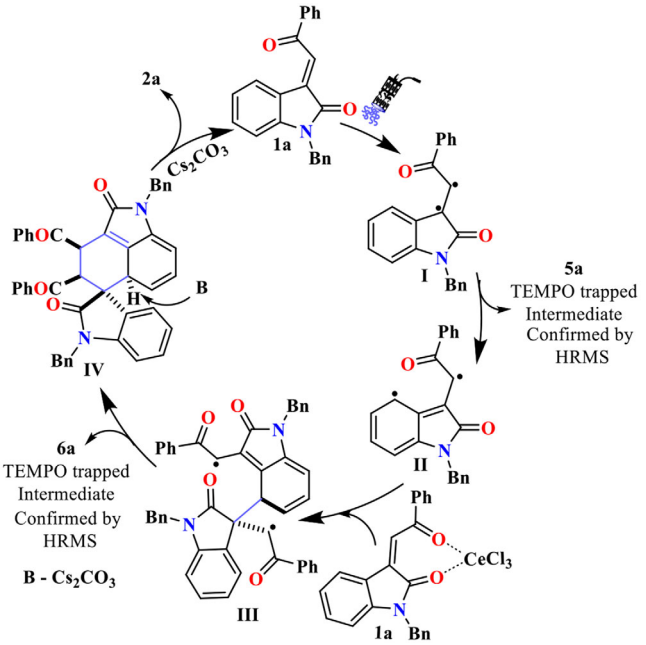
In summary, we have developed a visible light-mediated direct C4–H functionalization strategy to access 3,4-fused spirooxindoles via a formal [4+2] cycloaddition of unactivated C4–H 3-methylene oxindoles. This approach employed a catalytic amount of $CeCl_3$ under alkaline conditions to access the 3,4-fused spirooxindole with contiguous chiral centers in, moderate to good yields with excellent chemo- and regio-selectivity. The protocol proved to be scalable on a gram quantity and is also effective under the direct exposure of sunlight. This simple and practical strategy offers potential application for constructing complex molecular architectures.



Scheme 4. Radical Trapping experiments Standard reaction conditions: [a]3-Methylene oxindole **1a** (0.2 mmol, 1 equiv.), $CeCl_3$ (20 mol%), Cs_2CO_3 (20 mol%), in MeCN (0.06 M), Kessil Blue LED (427 nm with 100% intensity temperature around 60–65 °C, switching the fan off, 2* 40W), nitrogen atmosphere, diastereomeric ratio determined by ^1H NMR spectroscopy (we observed > 20:1 dr). ND = Not detected.

© 2025 Wiley-VCH GmbH

21935815, 0, Downloaded from https://acsjournals.onlinelibrary.wiley.com/doi/10.1002/ajoc.202500424 by Indian Institute Of Science Education And Research Pune, Wiley Online Library on [20/06/2025]. See the Terms and Conditions (https://onlinelibrary.wiley.com/terms-and-conditions) on Wiley Online Library for rules of use; OA articles are governed by the applicable Creative Commons License



Scheme 5. Plausible Mechanism of the transformation

Supporting Information

The reaction optimization tables, the procedure for the reaction, the series of control experiments, the Sunlight synthesis procedure, characterization data for all new compounds, and copies of ^{1}H, $^{13}C\{^{1}H\}$, and $^{19}F\{^{1}H\}$ NMR spectra (PDF). Data for the crystal structure reported in this manuscript have been deposited at the Cambridge Crystallographic Data Centre (CCDC) under the deposition number CCDC 2394305 (compound **2i**).

Acknowledgements

Ramakrishna G. Bhat thanks the Science and Engineering Research Board, Department of Science and Technology (SERB-DST), New Delhi, Government of India (File no: CRG/2023/004226), for the generous research grant. The authors also thank IISER Pune for financial assistance. Abhijeet S. Sabale, Anindita Bhowmick, Saswata Pattanaik, and Onkar S. Bankar thank UGC New Delhi, the Government of India for providing fellowship.

Conflict of Interests

The authors declare no conflict of interest.

Data Availability Statement

The data that support the findings of this study are available in the Supporting Information of this article.

Keywords: 3,4-Fused Spirooxindoles · C4–H Functionalization · Diastereoselective · Sunlight · Visible light [4+2] cycloaddition

[1] a) A. J. Peat, S. L. Buchwald, *J. Am. Chem. Soc.* **1996**, *118*, 1028–1030; b) S. S. Canan, L. Koch, J. G. Tikhe H Thoresen, K. A. Maegley, R. J. Almassy, J. Li, X. H. Yu, S. E. Zook, R. A. Kumpf, C. Zhang, T. J. Boritzki, R. N. Mansour, K. E. Zhang, A. Ekker, C. R. Calabrese, N. J. Curtin, S. Kyle, H. D. Thomas, L. Z. Wang, A. H. Calvert, B. T. Gold-ing, R. J. Griffin, D. R. Newell, S. E. Webber, H.-Z. sky, *J. Med. Chem.* **2002**, *45*, 4961–4974; c) Y. Koizumi, H. Kobayashi, T. Wakimoto, T. Furuta, T. Fukuyama, T. Kan, *J. Am. Chem. Soc.* **2008**, *130*, 16854–16855; d) C. C. Hughes, W. Fenical, *J. Am. Chem. Soc.* **2010**, *132*, 2528–2529; e) H. Qin, Z. Xu, Y. Cui, Y. Jia, *Angew. Chem. Int. Ed.* **2011**, *50*, 4447–4449; f) S. M. Bronner, A. E. Goetz, N. K. Garg, *J. Am. Chem. Soc.* **2011**, *133*, 3832–3835; g) S. W. Yang, C. M. Wang, K. X. Tang, J. X. Wang, L. P. Sun, *Eur. J. Org. Chem.* **2016**, *2016*, 1050–1053; h) S. R. Alluri JP, ACS Chem. Neurosci **2018**, *9*, 1259–1263; i) S. Chaudhuri, S. Bhunia, A. Roy, M. K. Das, A. Bisai, *Org. Lett.* **2018**, *20*, 288–291.

[2] a) S. Umezaki, S. Yokoshima, T. Fukuyama, *Org. Lett.* **2013**, *15*, 4230–4233; b) Q. Liu, Y.-A. Zhang, P. Xu, Y. Jia, *J. Org. Chem.* **2013**, *78*, 10885–10893.

[3] a) Y. A. Zhang, Q. liu, C. Wang, Y. Jia, *Org. Lett.* **2013**, *15*, 3662–3665; b) F. Bartoccini, A. Regni, M. Retini, G. Piersanti, *E. J. Org. Chem.* **2022**, *17*, 2022–2027.

[4] Y. Yokoyama, K. Kondo, M. Mitsuhashi, Y. Murakami, *Tetrahedron Lett.* **1996**, *37*, 9309–9312.

[5] a) A. J. Peat, S. L. Buchwald, *J. Am. Chem. Soc.* **1996**, *118*, 1028–1030; b) E. J. L. Stoffman, D. L. J. Clive, *Tetrahedron* **2010**, *66*, 4452–4461.

[6] K. Kato, M. Ono, H. Akita, *Tetrahedron* **2001**, *57*, 10055–10062.

[7] a) P. S. Baran, T. J. Maimone, J. M. Richter, *Nature* **2007**, *446*, 404–408; b) R. J. Rafferty, R. M. Williams, *J. Org. Chem.* **2012**, *77*, 519–524.

[8] a) L. M. Zhou, R. Y. Qu, G.F. Yang, *Expert Opin. Drug Discov.* **2020**, *15*, 603–625; b) G. Pradhan, K. Juvale, *Bioorg. Chem.* **2025**, *154*, 107975–108000.

[9] S. Yang, X. D. An, B. Qiu, R. B. Liu, J. Xiao, *Org. Lett.* **2021**, *23*, 9100–9105.

[10] S. Inuki, A. Iwata, S. Oishi, N. Fujii, H. Ohno, *J. Org. Chem.* **2011**, *76*, 2072–2083.

[11] T. Nemoto, S. Harada, M. Nakajima, *Asian J. Org. Chem.* **2018**, *7*, 1730–1742.

[12] a) A. Kubo, T. Nakai, T. Nozoye, A. Itai, Y. Iitaka, *Heterocycles* **1978**, *9*, 1051; b) F. H. Osman, F. A. El-Samahy, *Heterocycl. Commun.* **2000**, *6*, 175–180; c) V. O. Kozminykh, K. S. Lomidze, E. N. Kozminykh, A. N. Berezin, *Chem. Heterocycl. Compd.* **2004**, *40*, 521–522; d) B. V. Paponov, O. V. Shishkin, S. V. Shishkina, R. I. Zubatyuk, A. L. Kalyuzhny, V. I. Musatov, *Russ. Chem. Bull.* **2008**, *57*, 622–631.

[13] a) Y. Chen, B. D. Cui, Y. Wang, W. Y. Han, N. W. Wan, M. Bai, W. C. Yuan, Y. Z. Chen, *J. Org. Chem.* **2018**, *83*, 10465–10475; b) P. K. Warghude, A. S. Sabale, R. G. Bhat, *Org. Biomol. Chem.* **2020**, *18*, 1794–1799; c) P. K. Warghude, A. S. Sabale, R. Dixit, R. Vanka, R. G. Bhat, *Org. Biomol. Chem.* **2021**, *19*, 4338–4345; d) A. S. Sabale, P. K. Warghude, R. G. Bhat, *Synlett* **2023**, *34*, 1732–1738; e) P. K. Warghude, A. S. Sabale, R. G. Bhat, *Synthesis of Spirooxindoles*, Elsevier, **2024**, 309–331.

[14] An earlier version of this manuscript was filed on the pre-print server ChemRxiv: A. S. Sabale, A. Bhowmick, S. Pattanaik, O. S. Bankar, R. G. Bhat, *ChemRxiv* **2024**, https://doi.org/10.26434/chemrxiv-2024-xhpj4.

[15] a) S. H. Cao, X. C. Zhang, Y. Shi, M. Wei, *Eur. J. Org. Chem.* **2011**, *2011*, 2668–2672; b) C. N. Reddy, V. L. Nayak, G. S. Mani, J. S. Kapure, P. R. Adiyala, R. A. Maurya, A. Kamal, *Bioorg. Med. Chem. Lett.* **2015**, *25*, 4580–4586; c) S. Massari, J. Desantis, G. Nannetti, S. Sabatini, S. Tortorella, L. Goracci, V. Cecchetti, A. Loregian, O. Tabarrini, *Org. Biomol. Chem.* **2017**, *15*, 7944–7955; d) P. K. Warghude, P. D. Dharpure, R. G. Bhat, *Tetrahedron Lett.* **2018**, *59*, 4076–4079; e) A. Bhowmick, P. K. Warghude, R. G. Bhat, *Asian J. Org. Chem.* **2022**, *11*, e202200205.

[16] a) D. Dhara, K. S. Gayen, S. Khamarui, P. Pandit, S. Ghosh, D. K. Maiti, *J. Org. Chem.* **2012**, *77*, 10441–10449; b) C. Feng, Y. Yan, Z. Zhang, K. Xu, Z. Wang, *Org. Biomol. Chem.* **2014**, *12*, 4837–4840.

Manuscript received: April 3, 2025
Revised manuscript received: April 8, 2025
Version of record online: ■■, ■■

© 2025 Wiley-VCH GmbH

21935815, 0, Downloaded from https://aces.onlinelibrary.wiley.com/doi/10.1002/ajoc.202500424 by Indian Institute Of Science Education And Research Pune, Wiley Online Library on [20/06/2025]. See the Terms and Conditions (https://onlinelibrary.wiley.com/terms-and-conditions) on Wiley Online Library for rules of use; OA articles are governed by the applicable Creative Commons License

Publications not included in the thesis

Published on 11 February 2020. Downloaded by Indian Institute of Science Education & Research Pune on 6/20/2025 12:51:47 PM.

Organic & Biomolecular Chemistry

ROYAL SOCIETY OF CHEMISTRY

PAPER

View Article Online
View Journal | View Issue

Check for updates

Cite this: *Org. Biomol. Chem.*, 2020, **18**, 1794

Access to highly enantioselective and diastereoselective spirooxindole dihydrofuran fused pyrazolones†

Prakash K. Warghude, Abhijeet S. Sabale and Ramakrishna G. Bhat *

Received 2nd January 2020,
Accepted 7th February 2020

DOI: 10.1039/d0ob00007h

rsc.li/obc

A tertiary amine catalyzed highly diastereoselective and enantioselective [3 + 2] annulation between Morita–Baylis–Hillman (MBH) carbonates derived from isatin and pyrazolone 4,5-diones has been developed. A series of structurally diverse and multifunctional spirooxindole dihydrofuran fused pyrazolone derivatives with two adjacent quaternary spirocenters has been achieved in excellent yields with good to excellent enantioselectivity. Further synthetic utility of this protocol has been successfully demonstrated by employing the bromo derivative of spirooxindole dihydrofuran fused pyrazolone to Suzuki coupling.

Introduction

Among the various spirocyclic compounds,[1] heterocyclic spirooxindole is an important structural scaffold, widely present in numerous natural products and clinical pharmaceuticals. Compounds containing this scaffold exhibit a wide range of biological activities.[2] Particularly, spirooxindole containing two vicinal quaternary spirocenters is known to exhibit notable biological activities.[3] Therefore, considerable efforts have been focused on the development of highly efficient and practical methods for the synthesis of various carbocyclic and heterocyclic spirooxindole architectures with structural diversity and complexity.[4] Among the various heterocyclic spirooxindoles, spirooxindolyl five-membered oxaheterocycles have drawn attention in asymmetric synthesis due to their presence in a variety of natural and synthetic bioactive compounds (Fig. 1a).[5] There are a few elegant methods available in the literature for the preparation of the spirooxindole-dihydrofuran framework.[6] Some of the methods include transition-metal mediated cyclization,[6a–c] ceric ammonium nitrate catalyzed [3 + 2] oxidative cycloaddition,[6d] intramolecular Friedel–Crafts reaction,[6e] dimethyl sulfide catalyzed Baylis–Hillman annulation,[6f] reductive [1 + 4] annulation,[6g] iodide-mediated reaction,[6h] and tandem Michael-cyclization.[6i] However, the number of protocols to access spirooxindole-dihydrofuran in a catalytic and enantioselective fashion is very limited in the literature.[7] Hence, the development of more effective and catalytic protocols for the enantioselective synthesis of spirooxindole and its derivatives is in high demand and challenging.

On the other hand, pyrazolones and their derivatives represent a unique class of five membered aza-heterocycles. They have attracted the attention of synthetic chemists in recent years due to their potential utility as pharmacologically active agents, photographic couplers, chelating agents and synthetic scaffolds in medicinal chemistry.[8] In particular, spiropyrazolone scaffolds bearing contiguous stereocenters fused with different carbocyclic and heterocyclic units such as cyclohexane, cyclopentane and oxindole exhibit significant biological activity.[9] Compound **I** containing a spirocyclic pyrazolone skeleton is known to act as an antibacterial agent,[9a] whereas the spiropyrazolone derivative **II** and **III** are known inhibitors of type-4-phospodiesterase.[9b,c] In addition, compound **IV** con-

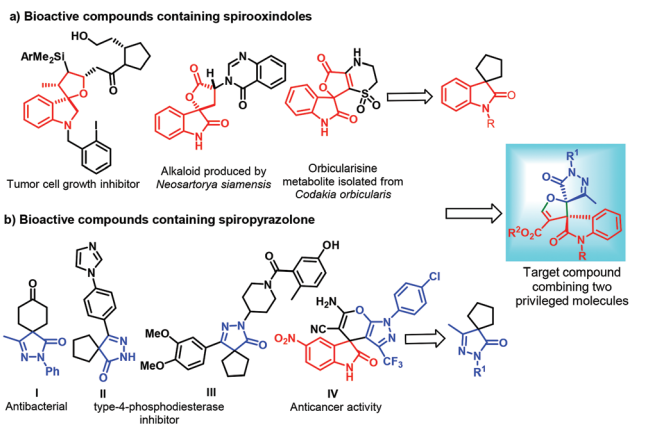


Fig. 1 Natural products containing the spiro-scaffold and precursors to access spirooxindole dihydrofuran pyrazolones.

Department of Chemistry, Main Building, Indian Institute of Science Education and Research (IISER)-Pune, Dr. Homi Bhabha Road, Pashan, Pune, 411008 Maharashtra, India. E-mail: rgb@iiserpune.ac.in

†Electronic supplementary information (ESI) available. CCDC 1967741. For ESI and crystallographic data in CIF or other electronic format see DOI: 10.1039/d0ob00007h

This journal is © The Royal Society of Chemistry 2020

Published on 11 February 2020. Downloaded by Indian Institute of Science Education & Research Pune on 6/20/2025 12:51:47 PM.

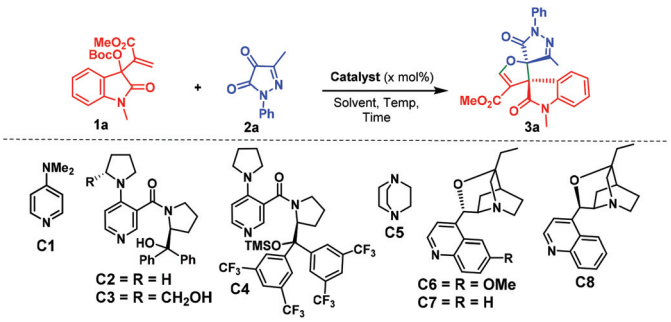
taining both oxindole and pyrazolone scaffolds shows anticancer activity (Fig. 1b).[9d]

As a consequence, great efforts have been devoted to the diastereoselective and enantioselective construction of the spiropyrazolone framework in the last decade.[10] However, the number of reports on the catalytic enantioselective synthesis of bis-spirocyclic compounds containing pyrazolone and oxindole scaffolds are very limited in the literature.[11] Thus, the development of a highly efficient strategy for the construction of structurally diverse spirooxindole fused pyrazolone scaffolds in an enantiomerically pure form is highly desirable (Fig. 1).

Recently, the [3 + 2] cycloaddition reaction of Morita–Baylis–Hillman carbonate (MBH) has emerged as an easy and powerful strategy for building multi-functionalized spirocarbo-/spirohetero-cyclic compounds.[12] In this realm, isatin derived MBH adducts have been successfully employed as three carbon synthons in different annulation reactions for the construction of five membered fused carbo/hetero cyclic spirooxindole molecules.[13] Similarly, pyrazolone 4,5-dione derivatives have been employed for various organocatalytic transformations in recent years.[14]

However, interestingly the cycloaddition of pyrazolone 4,5-dione at the electrophilic C-4 position has not been reported to date. In this context, we envisioned that enantiomerically enriched spirooxindole dihydrofuran fused pyrazolone compounds can be achieved by the organocatalytic asymmetric [3 + 2] cycloaddition reaction. Herein, we wish to report a chiral Lewis base catalyzed [3 + 2] cycloaddition reaction of isatin derived MBH carbonates with pyrazolone 4,5-diones for the construction of biologically relevant novel spirooxindole dihydrofuran pyrazolone derivatives containing two vicinal quaternary spirocenters.

Table 1 Optimization of the reaction conditions[a,b,c,d,e,f]



Entry	Cat.	Solvent	Temp (°C)	Time (h)	Yield[b] (%)	dr[c]	ee[d] (%)
1	C1	CH_2Cl_2	rt	2	95	>20 : 1	—
2	C2	CH_2Cl_2	rt	12	95	>20 : 1	36
3	C3	CH_2Cl_2	rt	12	88	>20 : 1	42
4	C4	CH_2Cl_2	rt	12	75	>20 : 1	40
5	C3	CH_2Cl_2	−20	16	86	>20 : 1	40
6	C5	CH_2Cl_2	rt	12	62	>20 : 1	—
7	C6	CH_2Cl_2	rt	30	58	>20 : 1	70
8	C7	CH_2Cl_2	rt	30	50	>20 : 1	30
9	C8	CH_2Cl_2	rt	30	48	>20 : 1	20
10	C6	CH_2Cl_2	0	30	60	>20 : 1	79
11	C6	CH_2Cl_2	−20	36	66	>20 : 1	89
12	C6	CH_2Cl_2	−40	72	60	>20 : 1	95
13	C6	Toluene	−20	30	58	>20 : 1	86
14	C6	$CHCl_3$	−20	36	52	>20 : 1	75
15	C6	CH_3CN	−20	24	60	>20 : 1	78
16	C6	THF	−20	20	75	>20 : 1	93
17[e]	C6	THF	−20	50	58	>20 : 1	90
18[f]	C6	THF	−20	72	50	>20 : 1	84

[a] Reaction conditions: Unless otherwise noted, the reactions were carried out with **1a** (0.15 mmol, 50 mg), **2a** (0.15 mmol, 22 mg), Cat. (20 mol%) in 1.0 mL of solvent at a specified temperature for the specified time. [b] Isolated yield after column chromatography. [c] Determined by ^{1}H NMR. [d] Enantiomeric excess of the major diastereoisomer was determined by HPLC using the chiral stationary phase. [e] 15 mol% **C6**. [f] 10 mol% **C6**.

Results and discussion

In order to validate the hypothesis, initially we performed a model reaction between isatin derived MBH carbonate **1a** and pyrazolone 4,5-dione **2a** in the presence of the catalyst 4-dimethyl amino pyridine **C1** (20 mol%) (DMAP) in dichloromethane (DCM) at room temperature. To our delight, the reaction was completed within 2 h to furnish the corresponding [3 + 2] cycloaddition product **3a** in excellent yield with excellent diastereoselectivity (Table 1, entry 1). Inspired by this initial result we turned our attention to achieve an enantioselective version of this protocol. In this regard, we synthesized and screened different chiral DMAP based organocatalysts for the desired transformation. We observed that the reactions performed in the presence of catalysts **C2**, **C3** and **C4** at room temperature proceeded smoothly to afford the corresponding [3 + 2] annulation product **3a** in good to excellent yield with very high diastereoselectivity; however, the enantiomeric excess was found to be poor (Table 1, entries 2–4). Further lowering of the reaction temperature (−20 °C) did not have any significant change in the enantioselectivity (Table 1, entry 5). We surmised that the lack of enantioselectivity was probably due to the insufficient spatial interaction between the chiral DMAP derived organocatalyst with either the MBH carbonate or with pyrazolone 4,5-dione. In order to validate this and to establish better stereointeraction, we planned to explore quinine based organocatalysts. Initially, we examined the racemic reaction using 20 mol% of 1,4-diazabicyclo[2.2.2] octane (DABCO) **C5** as a catalyst in DCM at room temperature.

Gratifyingly, the expected [3 + 2] cycloaddition product **3a** was formed in moderate yield with very high diastereoselectivity (Table 1, entry 6). Encouraged by this initial result, we screened different quinine based catalysts β-isoquinidine **C6**, β-isocinchonine **C7** and α-isocinchonidine **C8** to optimize the reaction. The [3 + 2] annulation reaction in the presence of catalyst **C6** proceeded smoothly to afford the desired product **3a** in moderate yield with good enantiomeric excess (Table 1, entry 7), while we observed that the catalysts **C7** and **C8** proved to be not advantageous for the desired transformation (Table 1, entries 8 and 9). In order to investigate the catalytic efficiency, we further screened some more catalysts containing free hydroxyl group and a bi-functional thiourea catalyst (see

Published on 11 February 2020. Downloaded by Indian Institute of Science Education & Research Pune on 6/20/2025 12:51:47 PM.

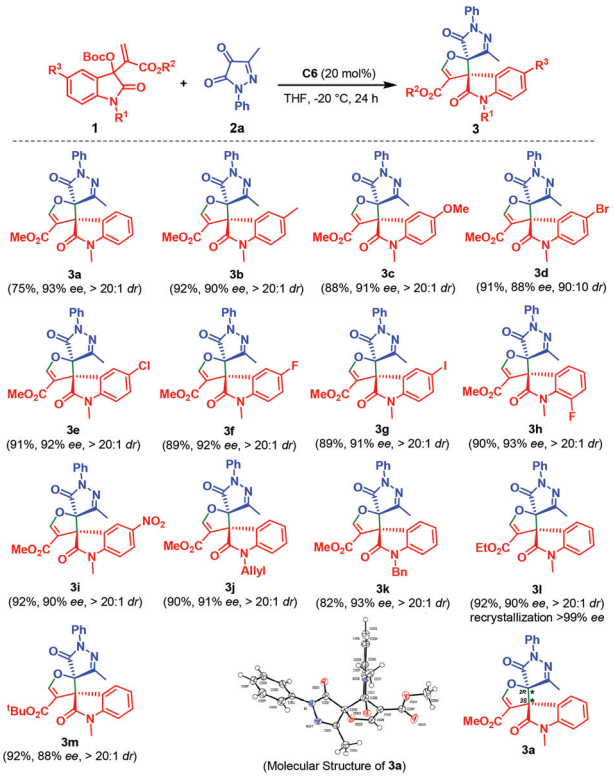
Appendix-I, page S3, ESI†). However, the reactions did not proceed in the presence of any of these catalysts.

Though the catalyst **C6** was found to be satisfactory, further optimization was needed to enhance the enantioselectivity. After various attempts, we planned to lower the reaction temperature as we had obtained good enantioselectivity at room temperature with catalyst **C6**. The reaction at 0 °C resulted in a marginal increase in the yield and enantioselectivity of **3a** (Table 1, entry 10). It is very important to note that further lowering the reaction temperature to −20 °C afforded the corresponding [3 + 2] annulation product **3a** in good yield (66% yield) with very high diastereoselectivity (>20 : 1 dr) and enantioselectivity (>89% ee) (Table 1, entry 11). However, we observed that further reduction in the reaction temperature (−40 °C) proved to be not beneficial as the reaction proceeded sluggishly (Table 1, entry 12). Subsequently, we examined the effects of various solvents such as toluene, $CHCl_3$, acetonitrile and THF to achieve better selectivity and yield (Table 1, entries 13–16). Based on our observation THF was found to be the optimal solvent for the desired transformation to afford the compound **3a** in very good yield with high enantioselectivity (Table 1, entry 16). Later, in order to evaluate the efficiency of the catalyst over the desired transformation, we further lowered the catalyst (**C6**) loading (15 to 10 mol%). This resulted in a significant reduction of the yield **3a** with a marginal reduction in enantioselectivity (Table 1, entries 17 and 18). Based on exhaustive screening, isatin derived MBH carbonate **1a** (1 equiv.), pyrazolone 4,5-dione (1 equiv.) and β-isoquinidine **C6** (20 mol%) in THF at −20 °C proved to be the optimal reaction conditions for the desired [3 + 2] cyclization.

Having obtained the optimum reaction conditions, we then explored the substrate scope for the synthesis of novel spirooxindole dihydrofuran pyrazolone derivatives *via* asymmetric [3 + 2] cycloaddition. To begin with we synthesized various isatin based MBH carbonates (**1a–1m**) and substituted pyrazolone 4,5-diones (**2a–2f**).[14]

Having synthesized different substrates we investigated the substrate scope of various MBH carbonates (**1a–1m**) with pyrazolone 4,5-dione **2a** under the optimized reaction conditions. We observed that all the MBH carbonates (**1a–1m**) reacted smoothly with **2a** to afford the corresponding spirooxindole dihydrofuran pyrazolones (**3a–3m**) in excellent yields (up to 96%) with excellent diastereoselectivity and very high enantioselectivity (>20 : 1 dr, up to 92% ee; see Scheme 1).

We observed that, the electron-donating (CH_3, OCH_3) as well as electron-withdrawing (Br, Cl, F, I, NO_2) substituents at different positions on the aryl ring of MBH carbonates were compatible under the optimum reaction conditions. Also, *N*-protected allyl and benzyl groups on MBH carbonates reacted smoothly to furnish the spirooxindole dihydofuran pyrazolones in excellent yields with high enantioselectivity and diastereoselectivity (Scheme 1). Moreover, different ester-substituted Morita–Baylis–Hillman carbonates underwent the [3 + 2] annulation reaction easily to give the corresponding products (**3l**, **3m**) in excellent yields with high stereoselectivity



Scheme 1 Substrate scope for isatin derived MBH-carbonates.[a–d] Reaction conditions: [a]Unless otherwise mentioned, all the reactions were carried out with **1** (1 equiv.), **2** (1 equiv.), Cat. **C6** (20 mol%) in 1.0 mL of solvent at a specified temperature for the specified time. [b]Isolated yield after column chromatography. [c]Diastereomeric ratio was determined by ^{1}H NMR. [d]Enantiomeric excess was determined by HPLC using the chiral stationary phase.

(Scheme 1). Very importantly, we observed that recrystallization further enhances the optical purity of the product as the recrystallization of compound **3l** enhanced the enantioselectivity from 90% ee to >99% ee (Scheme 1).

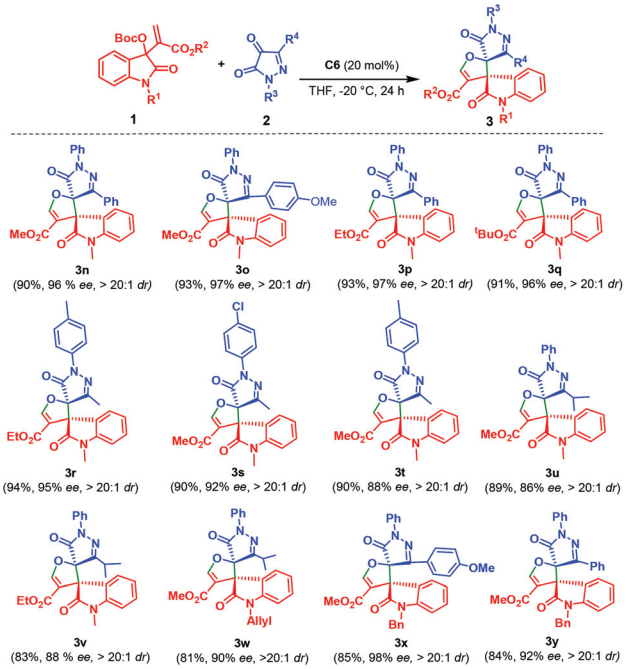
Later, we investigated the substrate scope of various pyrazolone 4,5-diones (**2b–2f**) with a few MBH carbonates (**1a**, **1j**, **1k**, **1l**, **1m**) under the standard optimum reaction conditions (Scheme 2).

Gratifyingly, the reactions proceeded smoothly to afford the corresponding [3 + 2] annulation products **3n–3y** in very good to excellent yields (88–94%) with very high diastereoselectivity (>20 : 1 dr) and good to excellent enantioselectivity (88–98% ee, Scheme 2).

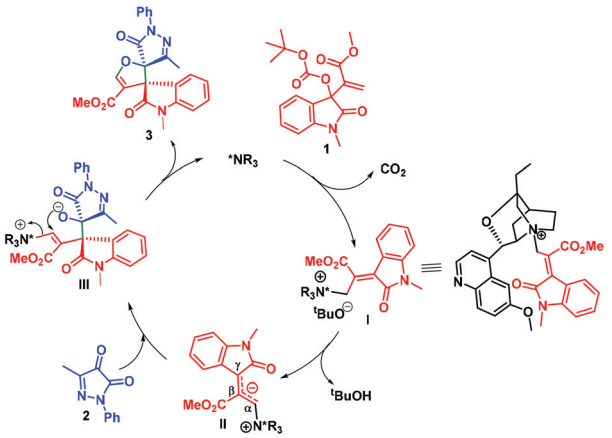
It is very important to note that the reactions of C-3 aryl substituted pyrazolone 4,5-diones (**2b** and **2c**) proceeded smoothly to afford the corresponding desired spirooxindole dihydrofuran pyrazolones (**3n**, **3o**, **3p** and **3q**) in excellent yields (up to 93%) with very high diastereoselectivity (>20 : 1 dr) and enantioselectivity (up to 97% ee), while the reaction of 3-isopropyl-1-phenyl-1*H*-pyrazole-4,5-dione **2f** with MBH carbonates (**1a**, **1j**, **1l**) afforded the corresponding products (**3u**, **3v**, **3w**) in very good yields (up to 90%) with very good stereoselectivity (>20 : 1 dr, up to 88% ee). It is significant to note

This journal is © The Royal Society of Chemistry 2020

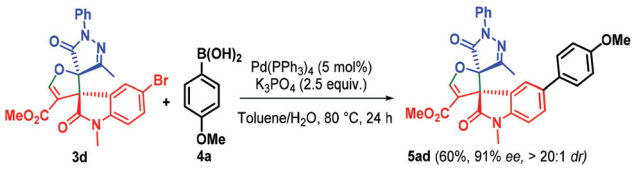
Published on 11 February 2020. Downloaded by Indian Institute of Science Education & Research Pune on 6/20/2025 12:51:47 PM.



Scheme 2 Substrate scope for pyrazolone 4,5-diones.[a–d] Reaction conditions: [a]Unless otherwise mentioned, all the reactions were carried out with **1** (1 equiv.), **2** (1 equiv.), Cat. **C6** (20 mol%) in 1.0 mL of solvent at a specified temperature for the specified time. [b]Isolated yield after column chromatography. [c]Diastereomeric ratio was determined by ^{1}H NMR. [d]Enantiomeric excess was determined by HPLC using the chiral stationary phase.



Scheme 3 Proposed catalytic cycle for the asymmetric [3 + 2] cycloaddition reaction.



Scheme 4 Application-Suzuki coupling reaction.

that the aryl moiety substituted at the C-3 position of pyrazolone 4,5-diones afforded the desired products in higher stereoselectivity in comparison with the aliphatic group substituted at the C-3 position. Our repeated attempts to synthesize *N*-alkyl pyrazolone 4,5-dione derivatives were unsuccessful. The molecular structure of compound **3a** was established unambiguously using single-crystal X-ray diffraction analysis and it was established as 2*R*,3*S* (Scheme 1).[15]

Based on previous literature reports[12,13] and our experimental observation the plausible catalytic cycle for the asymmetric cycloaddition reaction is depicted in Scheme 3.

Initially, the catalytic cycle is initiated by the nucleophilic attack of the chiral tertiary amine catalyst on **1** to form the corresponding quaternary ammonium salt **I** by liberating carbon dioxide and *tert*-butoxide. This intermediate **I** further reacts with the *in situ* generated *tert*-butoxide to form a reactive allylic nitrogen ylide **II** intermediate. Then the C-4 position of pyrazolone 4,5-dione **2** is attacked by the intermediate **II** (*via* γ-position) to give the corresponding intermediate **III**. Subsequently the intermediate **III** undergoes intramolecular cyclization to form compound **3** and regenerates the catalyst to complete the catalytic cycle.

In order to demonstrate the synthetic potential of this protocol, Suzuki coupling was performed on compound **3d** (Scheme 4). The reaction of methoxyphenyl boronic acid **4a** with **3d** in the presence of $Pd(PPh_3)_4$ and K_3PO_4 at 80 °C furnished the corresponding product **5ad** in high enantioselectivity and diastereoselectivity (91% ee, >20 : 1).

Conclusions

In summary, we have developed a highly diastereoselective and enantioselective [3 + 2]-annulation between isatin-derived Morita–Baylis–Hillman adducts and pyrazolone 4,5-diones to access enantiopure spirooxindole dihydrofuran fused pyrazolones. In the presence of a tertiary amine catalyst, a wide range of highly functionalized spirooxindole dihydrofuran fused pyrazolones containing two vicinal spiro-quaternary chiral centers were successfully obtained with excellent stereoselectivity.

Conflicts of interest

There are no conflicts to declare.

Acknowledgements

R. G. B. thanks DST-SERB (CRG/2019/005753), Govt. of India for the generous research grant. The authors also thank IISER Pune for financial assistance. P. K. W and A. S. S. thank UGC-JRF, New Delhi, Government of India for providing fellowship. The authors also thank T. Vijayakanth IISER Pune for obtaining crystal data.

Published on 11 February 2020. Downloaded by Indian Institute of Science Education & Research Pune on 6/20/2025 12:51:47 PM.

Notes and references

1 (*a*) M. Sannigrahi, *Tetrahedron*, 1999, **55**, 9007–9071; (*b*) C. H. Heathcock, S. L. Graham, M. C. Pirrung, F. Plavac and C. T. White, Spirocyclic Systems, in *The Total Synthesis of Natural Products*, ed. J. ApSimon, John Wiley and Sons, New York, 1983, vol. 5, pp. 264–313.

2 (*a*) R. M. Williams and R. J. Cox, *Acc. Chem. Res.*, 2003, **36**, 127–139; (*b*) C. V. Galliford and K. A. Scheidt, *Angew. Chem., Int. Ed.*, 2007, **46**, 8748–8758; (*c*) H. Lin and S. J. Danishefsky, *Angew. Chem., Int. Ed.*, 2003, **42**, 36–51; (*d*) C. Marti and E. M. Carreira, *Eur. J. Org. Chem.*, 2003, 2209–2219; (*e*) J. S. Bindra, in *The Alkaloids*, ed. R. H. F. Manske, Academic Press, New York, 1973, ch. 2, vol. 14; (*f*) R. S. Kumar, A. I. Almansour, N. Arumugam, F. Mohammad, D. Kotresha and J. C. Menéndez, *Bioorg. Med. Chem.*, 2019, **27**, 2487–2498; (*g*) R. S. Kumar, P. Antonisamy, A. I. Almansour, N. Arumugam, G. Periyasami, M. Altaf, H. R. Kim and K. B. Kwon, *Eur. J. Med. Chem.*, 2018, **152**, 417–423.

3 (*a*) Y. Arun, G. Bhaskar, C. Balachandran, S. Ignacimuthu and P. T. Perumal, *Bioorg. Med. Chem. Lett.*, 2013, **23**, 1839–1845; (*b*) A. S. Girgis, *Eur. J. Med. Chem.*, 2009, **44**, 91–100; (*c*) M. A. Ali, R. Ismail, T. S. Choon, Y. K. Yoon, A. C. Wei, S. Pandian, R. S. Kumar, H. Osman and E. Manogaran, *Bioorg. Med. Chem. Lett.*, 2010, **20**, 7064–7066.

4 (*a*) A. K. Franz, N. V. Hanhan and N. R. Ball-Jones, *ACS Catal.*, 2013, **3**, 540–553; (*b*) D. Cheng, Y. Ishihara, B. Tan and C. F. Barbas, *ACS Catal.*, 2014, **4**, 743–762; (*c*) G. S. Singh and Z. Y. Desta, *Chem. Rev.*, 2012, **112**, 6104–6155; (*d*) F. Zhou, Y. L. Liu and J. Zhou, *Adv. Synth. Catal.*, 2010, **352**, 1381–1407; (*e*) L. Hong and R. Wang, *Adv. Synth. Catal.*, 2013, **355**, 1023–1052; (*f*) N. R. Ball-Jones, J. J. Badillo and A. K. Franz, *Org. Biomol. Chem.*, 2012, **10**, 5165–5181; (*g*) R. Rios, *Chem. Soc. Rev.*, 2012, **41**, 1060–1074; (*h*) P. K. Warghude, P. D. Dharpure and R. G. Bhat, *Tetrahedron Lett.*, 2018, **59**, 4076–4079; (*i*) S. Y. Zhu, H. Zhang, Q. W. Ma, D. Liu and X. P. Hui, *Chem. Commun.*, 2019, **55**, 298–301; (*j*) Z. J. Zhang, L. Zhang, R. L. Geng, J. Song, X. H. Chen and L. Z. Gong, *Angew. Chem., Int. Ed.*, 2019, **58**, 12190–12194.

5 (*a*) M. Zhou, M. M. Miao, G. Du, X. N. Li, S. Z. Shang, W. Zhao, Z. H. Liu, G. Y. Yang, C. T. Che, Q. F. Hu and X. M. Gao, *Org. Lett.*, 2014, **16**, 5016–5019; (*b*) M. S. Poslusney, B. J. Melancon, P. R. Gentry, D. J. Sheffler, T. M. Bridges, T. J. Utley, J. S. Daniels, C. M. Niswender, P. J. Conn, C. W. Lindsley and M. R. Wood, *Bioorg. Med. Chem. Lett.*, 2013, **23**, 1860–1864; (*c*) L. Huang, X. Zhang, J. Li, K. Ding, X. Li, W. Zheng and B. Yin, *Eur. J. Org. Chem.*, 2014, 338–349; (*d*) X. Hu, Q. W. Xia, Y. Y. Zhao, Q. H. Zheng, Q. Y. Liu, L. Chen and Q. Q. Zhang, *Chem. Pharm. Bull.*, 2014, **62**, 942; (*e*) X. Xu, X. Zhang, X. Nong, X. Wei and S. Qi, *Tetrahedron*, 2015, **71**, 610–615; (*f*) F. Goudou, P. Petit, C. Moriou, O. Gros and A. J. Al-Mourabit, *Nat. Prod.*, 2017, **80**, 1693–1696.

6 (*a*) S. Muthusamy, C. Gunanathan and M. Nethaji, *J. Org. Chem.*, 2004, **69**, 5631–5637; (*b*) B. Alcaide, P. Almendros and R. J. Rodríguez-Acebes, *J. Org. Chem.*, 2006, **71**, 2346–2351; (*c*) B. Alcaide, P. Almendros and R. J. Rodríguez-Acebes, *Chem. – Eur. J.*, 2005, **11**, 5708–5712; (*d*) G. Savitha, S. K. Niveditha, D. Muralidharan and P. T. Perumal, *Tetrahedron Lett.*, 2007, **48**, 2943–2947; (*e*) B. L. Yin, J. Q. Lai, Z. R. Zhang and H. F. Jiang, *Adv. Synth. Catal.*, 2011, **353**, 1961–1965; (*f*) D. Basavaiah, S. S. Badsara and B. C. Sahu, *Chem. – Eur. J.*, 2013, **19**, 2961–2965; (*g*) R. Zhou, K. Zhang, Y. Chen, Q. Meng, Y. Liu, R. Li and Z. He, *Chem. Commun.*, 2015, **51**, 14663–14666; (*h*) B. A. Laevens, J. Tao and G. K. Murphy, *J. Org. Chem.*, 2017, **82**, 11903–11908; (*i*) N. Gupta, G. Bhojani, R. Tak, A. Jakhar, N. U. H. Khan, S. Chatterjee and R. I. Kureshy, *ChemistrySelect*, 2017, **2**, 10902–10907; (*j*) J. W. Kang, X. Li, F. Y. Chen, Y. Luo, S. C. Zhang, B. Kang, C. Peng, X. Tian and B. Han, *RSC Adv.*, 2019, **9**, 12255–12364; (*k*) T. Shi, S. Teng, Y. Wei, X. Guob and W. Hu, *Green Chem.*, 2019, **21**, 4936–4940; (*l*) Y. H. Miao, Y. Z. Hua and M. C. Wang, *Org. Biomol. Chem.*, 2019, **17**, 7172–7181; (*m*) N. J. Zhong, F. Wei, Q. Q. Xuan, L. Liu, D. Wanga and Y. C. Chena, *Chem. Commun.*, 2013, **49**, 11071–11073; (*n*) X. Q. Zhu, J. S. Wu and J. W. Xie, *Tetrahedron*, 2016, **72**, 8327–8334; (*o*) R. Baharfar, D. Zareyee and S. L. Allahgholipour, *Appl. Organomet. Chem.*, 2019, **33**, e4805.

7 (*a*) Y. L. Liu, X. Wang, Y. L. Zhao, F. Zhu, X. P. Zeng, L. Chen, C. H. Wang, X. L. Zhao and J. Zhou, *Angew. Chem., Int. Ed.*, 2013, **52**, 13735–13739; (*b*) F. L. Hu, Y. Wei and M. Shi, *Chem. Commun.*, 2014, **50**, 8912–8914; (*c*) Y. S. Zhu, W. B. Wang, B. B. Yuan, Y. N. Li, Q. L. Wang and Z. W. Bu, *Org. Biomol. Chem.*, 2017, **15**, 984–990.

8 (*a*) A. Kimata, H. Nakagawa, R. Ohyama, T. Fukuuchi, S. Ohta, T. Suzuki and N. Miyata, *J. Med. Chem.*, 2007, **50**, 5053–5056; (*b*) S. M. Sondhi, M. Dinodia, J. Singh and R. Rani, *Curr. Bioact. Compd.*, 2007, **3**, 91–108; (*c*) G. Varvounis, Pyrazol-3-ones, *Adv. Heterocycl. Chem.*, 2009, **98**, 143–224; (*d*) A. Schmidt and A. Dreger, *Curr. Org. Chem.*, 2011, **15**, 1423–1463; (*e*) S. Fustero, M. Sanchez-Roselló, P. Barrio and A. Simon-Fuentes, *Chem. Rev.*, 2011, **111**, 6984–7034.

9 (*a*) M. S. Chande and P. A. Barve, *J. Heterocycl. Chem.*, 2007, **44**, 49–53; (*b*) B. Schmidt, C. Scheufler, J. Volz, M. P. Feth, R. P. Hummel, A. Hatzelmann, C. Zitt, A. Wohlsen, D. Marx, H. P. Kley, D. Ockert, A. Heuser, J. A. M. Christiaans, G. J. Sterk and W. M. P. B. Menge, Pyrazolone Derivatives as PDE4 Inhibitors, *Germany Patent* WO2008138939, 2008; (*c*) I. Schlemminger, B. Schmidt, D. Flockerzi, H. Tenor, C. Zitt, A. Hatzelmann, D. Marx, C. Braun, R. Kuelzer, A. Heuser, H. P. Kley and G. J. Sterk, Novel Pyrazolone-Derivatives and Their Use as PD4 Inhibitors, *Germany Patent* WO2010055083, 2010; (*d*) D. Das, R. Banerjee and A. Mitra, *J. Chem. Pharm. Res.*, 2014, **6**, 108–116.

 This journal is © The Royal Society of Chemistry 2020

Published on 11 February 2020. Downloaded by Indian Institute of Science Education & Research Pune on 6/20/2025 12:51:47 PM.

10 (*a*) A. Zea, A. N. P. Alba, A. Mazzanti, A. Moyano and R. Rios, *Org. Biomol. Chem.*, 2011, **9**, 6519–6523; (*b*) J. X. Zhang, N. K. Li, Z. M. Liu, X. F. Huang, Z. C. Geng and X. W. Wang, *Adv. Synth. Catal.*, 2013, **355**, 797–808; (*c*) J. Liang, Q. Chen, L. Liu, X. Jiang and R. Wang, *Org. Biomol. Chem.*, 2013, **11**, 1441–1445; (*d*) P. Chauhan, S. Mahajan, C. C. J. Loh, G. Raabe and D. Enders, *Org. Lett.*, 2014, **16**, 2954–2957; (*e*) P. Chauhan, S. Mahajan and D. Enders, *Chem. Commun.*, 2015, **51**, 12890–12907; (*f*) S. Liu, X. Baoa and B. Wang, *Chem. Commun.*, 2018, **54**, 1151–11529; (*g*) L. Liu, Y. Zhong, P. Zhang, X. Jiang and R. Wang, *J. Org. Chem.*, 2012, **77**, 10228–10234.

11 (*a*) Q. Chen, J. Liang, S. Wang, D. Wang and R. Wang, *Chem. Commun.*, 2013, **49**, 1657–1659; (*b*) J. H. Li, T. F. Feng and D. M. Du, *J. Org. Chem.*, 2015, **80**, 11369–11377; (*c*) N. Kumarswamyreddy and V. Kesavan, *Org. Lett.*, 2016, **18**, 1354–1357; (*d*) C. Wang, D. Wen, H. Chen, Y. Deng, X. Liu, X. Liu, L. Wang, F. Gao, Y. Guo, M. Sun, K. Wang and W. Yan, *Org. Biomol. Chem.*, 2019, **17**, 5514–5519; (*e*) Y. Lin, B. L. Zhao and D. M. Du, *J. Org. Chem.*, 2019, **84**, 10209–10220.

12 (*a*) P. Xie and Y. Huang, *Org. Biomol. Chem.*, 2015, **13**, 8578–8595; (*b*) N. J. Zhong, Y. Z. Wang, L. Cheng, D. Wang and L. Liu, *Org. Biomol. Chem.*, 2018, **16**, 5214–5227; (*c*) T. Y. Liu, M. Xie and C. Y. Chen, *Chem. Soc. Rev.*, 2012, **41**, 4101–4112; (*d*) Y. L. Shi and M. Shi, *Eur. J. Org. Chem.*, 2007, 2905–2916; (*e*) Y. Wei and M. Shi, *Chem. Rev.*, 2013, **113**, 6659–6690; (*f*) D. Basavaiah, B. S. Reddy and S. S. Badsara, *Chem. Rev.*, 2010, **110**, 5447–5674.

13 (*a*) J. Peng, X. Huang, L. Jiang, H. L. Cui and Y. C. Chen, *Org. Lett.*, 2011, **13**, 4584–4587; (*b*) Y. Wang, L. Liu, T. Zhang, N. J. Zhong, D. Wang and Y. J. Chen, *J. Org. Chem.*, 2012, **77**, 4143–4147; (*c*) F. Wei, H. Y. Huang, N. J. Zhong, C. L. Gu, D. Wang and L. Liu, *Org. Lett.*, 2015, **17**, 1688–1691; (*d*) G. Zhan, M. L. Shi, Q. He, W. J. Lin, Q. Ouyang, W. Du and Y. C. Chen, *Angew. Chem., Int. Ed.*, 2016, **55**, 2147–2151; (*e*) K. K. Wang, T. Jin, X. Huang, Q. Ouyang, W. Du and Y. C. Chen, *Org. Lett.*, 2016, **18**, 872–875; (*f*) X. Fan, H. Yang and M. Shi, *Adv. Synth. Catal.*, 2017, **359**, 49–57; (*g*) Q. He, W. Du and Y. C. Chen, *Adv. Synth. Catal.*, 2017, **359**, 3782–3791.

14 (*a*) F. Vetica, P. Chauhan, S. Mahajan, G. Raabe and D. Enders, *Synthesis*, 2018, 1039–1046; (*b*) U. Kaya, P. Chauhan, S. Mahajan, K. Deckers, A. Valkonen, K. Rissanen and D. Enders, *Angew. Chem., Int. Ed.*, 2017, **56**, 15358–15362; (*c*) P. Chauhan, S. Mahajan, U. Kaya, A. Peuronen, K. Rissanen and D. Enders, *J. Org. Chem.*, 2017, **82**, 7050–7058; (*d*) S. Mahajan, P. Chauhan, U. Kaya, K. Deckers, K. Rissanen and D. Enders, *Chem. Commun.*, 2017, **53**, 6633–6636; (*e*) B. Ray and S. Mukherjee, *J. Org. Chem.*, 2018, **83**, 10871–10880.

15 CCDC 1967741† contains the supplementary crystallographic data for compound **3(a)**.

Organic & Biomolecular Chemistry

ROYAL SOCIETY OF CHEMISTRY

PAPER

View Article Online
View Journal | View Issue

Published on 21 April 2021. Downloaded by Indian Institute of Science Education & Research Pune on 6/20/2025 12:51:17 PM.

Check for updates

Cite this: *Org. Biomol. Chem.*, 2021, **19**, 4338

An easy and practical approach to access multifunctional cylcopentadiene- and cyclopentene-spirooxindoles *via* [3 + 2] annulation†

Prakash K. Warghude, [a] Abhijeet S. Sabale,[a] Ruchi Dixit,[b,c] Kumar Vanka [b,c] and Ramakrishna G. Bhat *[a]

Received 17th March 2021,
Accepted 20th April 2021

DOI: 10.1039/d1ob00514f

rsc.li/obc

A highly regioselective [3 + 2] annulation of Morita–Baylis–Hillman (MBH) carbonates of isatin with aurone/thioaurone is developed. Spiroheterocycles such as spirooxindole cyclopentadiene and spirooxindole fused hydroxy cyclopentene derivatives are constructed in one pot by exploring the reactivity of Lewis bases. Combined experimental and density functional theory (DFT) calculations offered an insight into the reaction mechanism.

Introduction

The construction of multifunctional spirocyclic frameworks is of great interest in the field of asymmetric synthesis.[1] More importantly, spirooxindole scaffolds have received great attention, due to their presence in numerous natural products and pharmaceutical compounds.[2,3] Their unique three-dimensional structure and potential pharmacological significance has paved the way for the development of effective methods for the synthesis of molecules containing spiro-carbocyclic and spiro-heterocyclic oxindole scaffolds.[4] Among the carbocyclic oxindoles, the spirocyclopentane oxindole skeleton exists in a variety of naturally occurring bioactive compounds such as notoamide A, (−)-paraherquamide A and cyclopiamine B (Fig. 1).[5] Due to their biological significance, enormous efforts have been focused on the racemic and enantioselective synthesis of the spirocyclic architecture.[4] Though there are many elegant reports on the synthesis of spirocarbocylic scaffolds, the synthesis of densely functionalized spirocyclopentadiene oxindole derivatives is rare in the literature.[6] In 2011, Chen and co-workers reported the asymmetric synthesis of spirocyclic 2-oxindoles incorporating a cyclopentadiene motif using Morita–Baylis–Hillman carbonates of isatins with propargyl sulfones under β-ICD catalysis.[6a] Later, the same group developed the chiral tertiary-amine catalyzed enantioselective [3 + 2] annulation of Morita–Baylis–Hillman carbonates of isatins with nitroolefins to construct spirooxindole cyclopentadiene.[6b] In a recent article, Cui and Chen reported the enantioselective synthesis of spiro-cyclopentene/cyclopentadiene-oxindoles through an asymmetric [3 + 2] cycloaddition of isatin-derived MBH carbonates and β,γ-unsaturated α-keto esters.[6c]

Recently, isatin based Morita–Baylis–Hillman (MBH) carbonates have emerged as versatile and useful building blocks for the synthesis of highly functionalized spirocyclic oxindole architectures.[7] The basic approach in this process involved the nucleophilic attack of a Lewis base (tertiary amine or phosphine) on MBH carbonates of isatin to generate a highly reactive 1,3-dipole namely a zwitterionic allylic ylide *in situ*. This allylic ylide further undergoes diverse annulation reactions

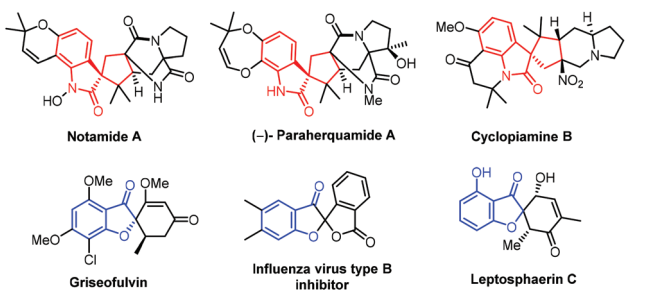


Fig. 1 Natural products containing spirooxindole and spirocyclic benzofuranones.

[a]*Department of Chemistry, Indian Institute of Science Education and Research (IISER)-Pune, Dr Homi Bhabha Road, Pashan, Pune, 411008 Maharashtra, India. E-mail: rgb@iiserpune.ac.in*
[b]*Physical and Materials Chemistry Division, CSIR-National Chemical Laboratory, Dr Homi Bhabha Road, Pune-411008, India*
[c]*Academy of Scientific and Innovative Research (AcSIR), Ghaziabad – 201002, India*
†Electronic supplementary information (ESI) available. CCDC 2067873, 2067874, 2067877 and 2067878. For ESI and crystallographic data in CIF or other electronic format see DOI: 10.1039/d1ob00514f

This journal is © The Royal Society of Chemistry 2021

Published on 21 April 2021. Downloaded by Indian Institute of Science Education & Research Pune on 6/20/2025 12:51:17 PM.

with different electrophilic substrates to give structurally unique spirooxindole derivatives.[8]

Spirocyclic benzofuranones are privileged structural motifs found in natural and synthetic molecules that have remarkable biological properties (Fig. 1).[9] Griseofulvin is an orally active antifungal medication used to treat different types of dermatophytoses.[9a] The spiro[benzofuran-2,1′-isobenzofuran]-3,3-dione is active against type B influenza virus.[9b] In addition, the spirocyclohexane benzofuran-3-one core belongs to the polyketide leptosphaerin C class, exhibiting antifungal activity.[9c] Surprisingly, in spite of high biological significance, the number of reports on the synthesis of spirocyclic benzofuranones are limited in the literature.[10]

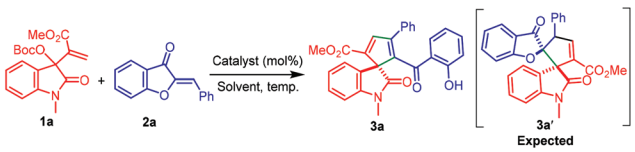
Therefore, the development of an effective and practical method is in high demand. The key precursor for the preparation of spirocyclic benzofuranones is 2-benzylidenebenzofuran-3(2*H*)-one (aurone) that is also present in a number of natural and synthetic products.[11] The class of aurones are easy to prepare and their derivatives have been employed in various cycloaddition reactions to construct complex spiroheterocycles.[12] In 2014, Zhao and co-workers disclosed the NHC catalyzed asymmetric [3 + 2] annulation of aurone and α,β-unsaturated aldehydes to access spiroheterocycles.[12a] Likewise, other research groups have explored similar approaches of [3 + 2] and [3 + 4] cycloaddition reactions of aurones utilizing asymmetric NHC catalysis.[12b,c] Later, Li and Cheng reported the enantioselective [4 + 2] cycloaddition of allenoates with 2-olefinic benzofuran-3-ones in the presence of a chiral Lewis base catalyst.[12d] Recently, Lan, Ullah and Lu developed the regiodivergent [3 + 2] annulation of aurones and allenoates under chiral dipeptide phosphine catalysis.[12e] Despite these recent advances in annulation reactions, the cycloaddition of aurones with MBH carbonates of isatin has rarely been explored.[12f] Similarly, thioaurone, the sulphur analogue of aurone, is also utilized as an excellent electrophilic substrate for various cycloaddition reactions.[13]

In this context, we envisioned that aurones and thioaurones could be employed as suitable C2 synthons in [3 + 2] annulation with MBH carbonates of isatin to construct structurally diverse and multi-functionalized spiro fused carbopentacyclic scaffolds using a suitable Lewis base organocatalyst. Herein, we report the one pot synthesis of spirooxindole cyclopentadiene and spirooxindole fused hydroxy cyclopentene derivatives in a practical manner.

Results and discussion

In order to validate the hypothesis, we commenced with the reaction of MBH carbonate **1a** and aurone **2a** as model substrates in the presence of DMAP (20 mol%) in dichloromethane at room temperature. Interestingly, the reaction afforded the unexpected spiro cyclopentadiene oxindole **3a** in 65% yield and the anticipated compound **3a′** was not obtained (Table 1, entry 1). A literature survey revealed that the synthesis of the spirocyclopentadiene scaffold has been rarely attempted.[6] In this regard, we planned further optimization of reaction conditions. Several attempts of enantioselective synthesis of spiro cyclopentadiene oxindole **3a** using **1a** and **2a** in the presence of a chiral DMAP derived catalyst did not work under various reaction conditions (see the ESI, Appendix I, page S5†). Later, we switched our attention to screen chiral quinine based organocatalysts. Unfortunately, even these catalysts did not afford the desired product (see the ESI, Appendix I, page S5†). After exhaustive screening with various chiral catalysts and reaction conditions we focussed our attention further on optimizing the reaction conditions for the racemic synthesis of spirooxindole cyclopentadiene **3a**. The reaction of **1a** and **2a** in the presence of PPh_3 as a catalyst did not afford the desired product **3a** even after prolonged reaction time (Table 1, entry 2). Later, we turned our attention towards tertiary amine catalysts for the desired transformation. The independent reactions of **1a** and **2a** in the presence of 1,4-diazabicyclo[2.2.2]octane (DABCO) and 1,8-diazabicyclo[5.4.0]undec-7-ene (DBU) afforded the spirooxindole cyclopentadiene **3a** in 40% and 55% yields, respectively (Table 1, entries 3 and 4). Based on the initial results, DMAP proved to be a suitable catalyst for the desired transformation. In order to optimize the reaction conditions further, we screened different solvents such as chloroform, toluene, ethyl acetate, THF and acetonitrile in the presence of 20 mol% of DMAP (Table 1, entries 5–9). Among all, acetonitrile proved to be the optimum solvent by providing the desired product **3a** in 76% yield (Table 1, entry 9). Further reduction in catalyst loading (15 mol% DMAP) drastically lowered the yield of spirooxindole **3a** (40%, Table 1, entry 10). We observed that lowering the reaction temperature to 0 °C significantly lowered the yield of **3a** (30%, Table 1, entry 11). Based on the screening, MBH carbonate **1a** (1 equiv.), aurone (1.2 equiv.) and DMAP (20 mol%) in acetonitrile proved to be

Table 1 Optimization of the reaction conditions[a,b,c]



Entry	Catalyst (mol %)	Solvent	Time (h)	Yield[b] (%)
1	DMAP (20)	CH_2Cl_2	24	65
2	PPh_3 (20)	CH_2Cl_2	48	NR
3	DABCO (20)	CH_2Cl_2	24	40
4	DBU (20)	CH_2Cl_2	24	55
5	DMAP (20)	$CHCl_3$	24	68
6	DMAP (20)	Toluene	24	70
7	DMAP (20)	Ethyl acetate	24	72
8	DMAP (20)	THF	24	68
9	DMAP (20)	CH_3CN	24	76
10	DMAP (15)	CH_3CN	24	40
11[c]	DMAP (20)	CH_3CN	24	30

[a] Reaction conditions: the reactions were carried out with **1a** (0.115 mmol, 40 mg), **2a** (0.138 mmol, 31 mg), and Cat. (20 mol%) in 2.0 mL of solvent at room temperature for the specified time. [b] Isolated yield after purification by column chromatography. [c] Reaction at 0 °C.

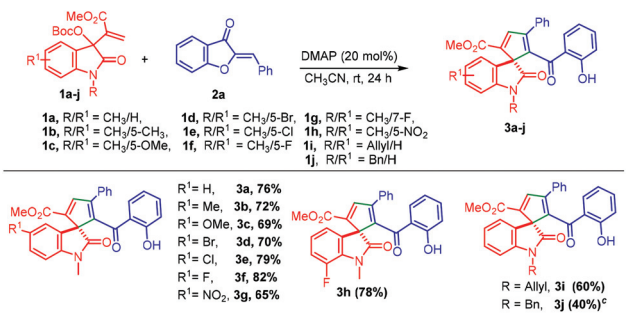
Published on 21 April 2021. Downloaded by Indian Institute of Science Education & Research Pune on 6/20/2025 12:51:17 PM.

the optimum reaction conditions for [3 + 2] annulation followed by ring opening to access the desired product **3a**.

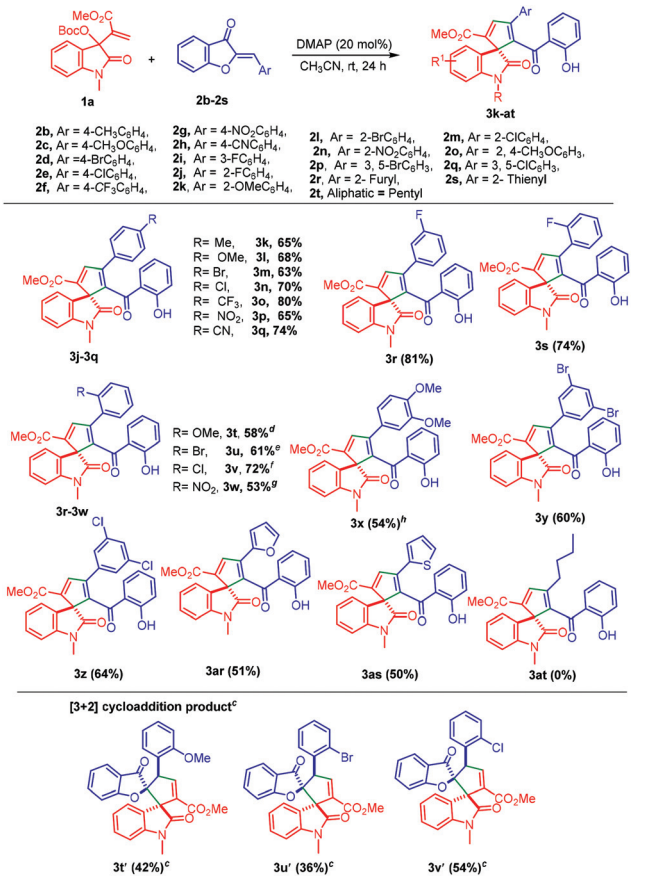
After establishing the optimum reaction conditions, we explored the substrate scope for the synthesis of new spirooxindole cyclopentadiene derivatives *via* [3 + 2] cycloaddition. To begin with, we synthesized various isatin based MBH carbonates[8g] (**1a–1j**) and substituted aurones[10g] (**2a–2t**). Having obtained different substrates, we further investigated the substrate scope of various MBH carbonates (**1a–1j**) with aurone **2a** under the optimized reaction conditions. We observed that all the MBH carbonates (**1a–1j**) reacted smoothly with aurone **2a** to furnish the corresponding spirooxindole cyclopentadienes (**3a–3j**) in very good yields (up to 82%, see Scheme 1). We observed that all the reactions proceeded smoothly irrespective of the electron-donating (CH_3 and OCH_3) and electron-deactivating/withdrawing (Br, Cl, F, and NO_2) nature of substituents at different positions on the aryl ring of MBH carbonates. Likewise, *N*-allyl and *N*-benzyl protected MBH carbonates (**1i** and **1j**) reacted smoothly to furnish the spirooxindole cyclopentadienes **3i** and **3j** in 60% and 40% yield, respectively (Scheme 1). Furthermore, the molecular structure of compound **3a** was established unambiguously using single-crystal X-ray diffraction analysis.[18]

After the initial success, we further investigated the substrate scope of various aurones (**2b–2s**) with MBH carbonate **1a** under the standard reaction conditions (Scheme 2). Gratifyingly, all the reactions proceeded smoothly to afford the corresponding [3 + 2] annulation products **3j–3at** in moderate to good yields (50–81%, Scheme 2). It is important to note that both electron donating (CH_3 and OCH_3) and electron deactivating/withdrawing (F, Cl, Br, CF_3, CN, and NO_2) groups at the *meta* and *para*-positions of aurones were found to be suitable substrates for the desired transformation to afford **3k–3r** in moderate to good yields (63–81%, Scheme 2). To our surprise, *ortho*-substituted aurones (**2k–2m**) furnished the bis-spirocyclic compounds **3t'–3v'** (with the benzofuran-3(2*H*)-one ring intact) in moderate yields (up to 54%) under optimized reaction conditions (Scheme 2). Also, the molecular structure of compound **3v'** was established unambiguously using single-crystal X-ray diffraction analysis.[19] Later, we observed that reaction at elevated temperature (up to 70 °C) delivered the spirocyclopentadienes **3t–3w** (benzofuran-3(2*H*)-one ring opened products) in moderate to good yields (up to 72%). However, the substrate containing a relatively less bulky and more electron deactivating fluoro group (**2i**) at the *ortho* position of aurone furnished the spirooxindole cyclopentadiene product **3s** (benzofuran-3(2*H*)-one ring opened product) in good yield at room temperature (74%, Scheme 2), while the disubstituted aurones reacted smoothly to afford the products (**3x–3z**) in moderate yields (up to 64%, Scheme 2). Moreover, the substrates containing heteroaryl moieties such as furyl and thienyl moieties gave the corresponding products **3ar** and **3as** in satisfactory yields (51% and 50%, Scheme 2). However, the alkyl substituted derivative **2t** did not work under the optimized reaction conditions (Scheme 2).

Based on the experimental results, previous literature reports[7,8] and quantum chemical calculations that we have carried out, the plausible catalytic cycle is depicted in



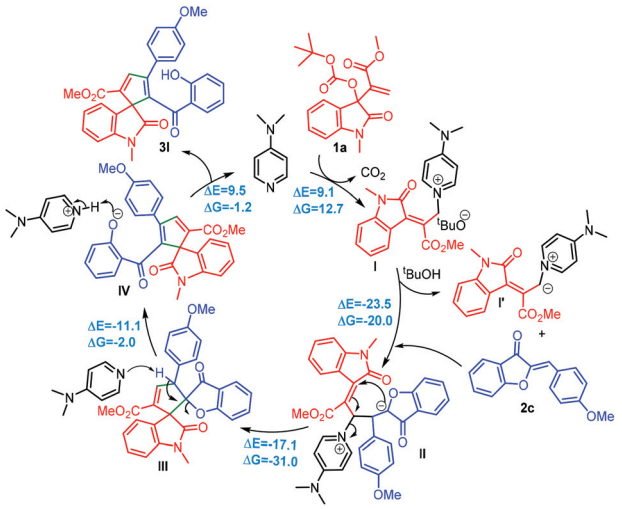
Scheme 1 Substrate scope for isatin derived MBH-carbonates. Reaction conditions: the reactions were carried out with MBH carbonate of isatin **1** (0.115 mmol), aurone **2a** (0.138 mmol), and DMAP (20 mol%) in 2.0 mL of MeCN at room temperature; Isolated yield after column chromatography. 50 mol% DMAP.



Scheme 2 Substrate scope of aurones. Reaction conditions: the reactions were carried out with MBH carbonate of isatin **1a** (0.115 mmol), aurone **2** (0.138 mmol), and DMAP (20 mol%) in 2.0 mL of MeCN at room temperature; isolated yield after column chromatography; spirocyclopentene compounds (benzofuran-3(2*H*)-one ring intact) formed at room temperature; 20 mol% DMAP at 50 °C or 100 mol% DMAP; 100 mol% DMAP at 70 °C; 50 mol% DMAP at 70 °C; 30 mol% DMAP at 70 °C. DMAP: 100 mol%.

This journal is © The Royal Society of Chemistry 2021

Published on 21 April 2021. Downloaded by Indian Institute of Science Education & Research Pune on 6/20/2025 12:51:17 PM.



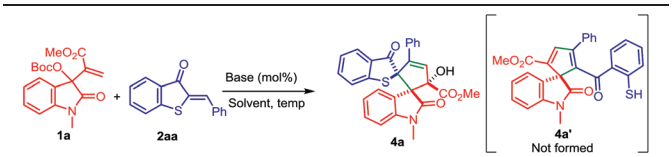
Scheme 3 Proposed reaction mechanism for the formation of spirooxindole cyclopentadiene.

Scheme 3. Computational calculations have been performed using density functional theory (DFT) at the PBE/TZVP level of theory. Based on these findings it is proposed that initially, the nucleophilic DMAP attacks on the MBH carbonate **1a** to form the quaternary ammonium salt **I** with the evolution of carbon dioxide and *tert*-butoxide. This process is found to be thermodynamically unstable (ΔG = 12.7 kcal mol^{-1}). The *in situ* generated *tert*-butoxide in turn abstracts a proton from the quaternary ammonium salt **I** to give an allylic nitrogen ylide **I′**. Subsequently, ylide **I′** reacts with the aurone **2c** to generate an intermediate **II** (reaction free energy ΔG = −20.0 kcal mol^{-1}). This intermediate cyclizes *via* a highly favourable (ΔG = −31.0 kcal mol^{-1}) intramolecular Michael addition to afford the corresponding intermediate **III** by eliminating DMAP. Furthermore, DMAP abstracts the proton from intermediate **III** leading to the formation of the phenoxide intermediate **IV** *via* ring opening. Finally, this intermediate furnishes the desired compound **3l** *via* protonation and regeneration of DMAP to complete the catalytic cycle.

Earlier we had observed that unlike *para*-substituted derivatives, *ortho*-substituted aurones (MeO, Br, and Cl) required an elevated temperature to form the corresponding spirooxindole cyclopentadienes **3t–3v**. In order to understand this observation, we also calculated the transition states and thus the barriers, for both the cases from intermediate **III** to intermediate **IV** (see the ESI, Fig. 4a and 4b, page S13, 14†). It was observed that the *ortho*-substituted aurone has a 1.2 kcal mol^{-1} higher energy barrier than the *para* derivative. Furthermore, the turnover frequency (TOF) values indicate that the mechanism with the *para*-substituted aurone is approximately 6.4 times more efficient than that with the *ortho*-substituted aurone (see the ESI, Appendix II, page S11†).

Thioaurone, 2-arylidenebenzo[*b*]thiophen-3(2*H*)-one, is a sulphur analogue of aurone and its derivatives have been used in photoswitchable materials[14] and dyes,[15] and also thioaurones show cytotoxic activity against the HeLa cell line.[16] In addition, thioaurones have been effectively used as Michael acceptors in different cycloaddition reactions.[13] Interestingly, the application of thioaurone in Morita–Baylis–Hillman chemistry has not been explored yet. Also, the synthesis of sulfur analogues of bioactive spirocyclic aurones may be of great interest due to their biological relevance. In this regard, we became interested in exploring the synthesis of thioaurones (sulfur analogues of aurones) *via* [3 + 2] annulation reaction. In order to explore the synthesis of spirocyclic benzothiofuranones, we prepared a series of (*Z*)-2-benzylidenebenzo[*b*]thiophen-3(2*H*)-ones (**2aa–2ah**) following a reported procedure.[20] Initial attempts to synthesize the desired spirocyclic benzothiofuranones (**4a′**) were unsuccessful under the optimized reaction conditions explored for the synthesis of spirocyclic cyclopentadiene derivatives **3** (Table 2, entry 1). To our dismay, we did not observe any desired product (**4a′**) formation with the increase in DMAP loading (50 mol%) even after prolonged reaction time (Table 2, entry 2). Interestingly, the stoichiometric amount of DMAP (100 mol%) furnished an unanticipated spirooxindole fused benzo[*b*]thiophen-3(2*H*)-one **4a** in 30% yield with high diastereoselectivity (>20 : 1) and we did not observe the target compound **4a′** (Table 2, entry 3). The bis-spiro compound **4a** with three contiguous chiral centres with a tertiary hydroxyl group is an unusual and complex scaffold to build from the synthesis point of view. Also, this non-natural and multifunctional bis-spirocyclic hybrid compound containing a useful skeleton such as cyclopentene, isatin and benzothiofuranone may be of greater biological significance. This result prompted us to take further interest in optimizing the reaction conditions. The reaction in the presence of 1,4-diazabicyclo[2.2.2]octane (DABCO) gave the desired product **4a** in 10% yield (Table 2, entry 4).

Table 2 Optimization of the reaction conditions[a,b,c,d,e]



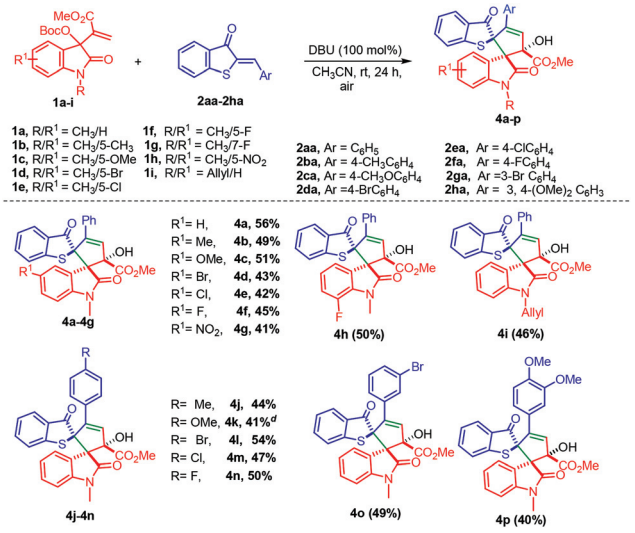
Entry	Base (mol%)	Solvent	Time (h)	dr[c]	Yield[b] (%)
1	DMAP (20)	CH_3CN	72	—	NR
2	DMAP (50)	CH_3CN	72	—	NR
3	DMAP (100)	CH_3CN	48	>20 : 1	30
4	DABCO (100)	CH_3CN	72	>20 : 1	10
5	DBU (100)	CH_3CN	24	>20 : 1	56
6	DBU (100)	$CHCl_3$	24	>20 : 1	40
7	DBU (100)	Toluene	24	>20 : 1	42
8	DBU (100)	THF	48	>20 : 1	20
9	DBU (100)	DMF	36	>20 : 1	50
10[d]	DBU (100)	CH_3CN	24	>20 : 1	52
11[e]	DBU (100)	CH_3CN	48	>20 : 1	20
12	DBU (50)	CH_3CN	72	>20 : 1	30

[a] Reaction conditions: the reactions were carried out with MBH carbonate **1a** (0.115 mmol), thioaurone **2aa** (0.138 mmol), and a base (0.115 mmol) in 2.0 mL of MeCN at room temperature. [b] Isolated yield after column chromatography. [c] Determined by ^{1}H NMR. [d] At 70 °C. [e] At 0 °C.

Published on 21 April 2021. Downloaded by Indian Institute of Science Education & Research Pune on 6/20/2025 12:51:17 PM.

Gratifyingly, 1,8-diazabicyclo (5.4.0)undec-7-ene (DBU) in acetonitrile at room temperature afforded the desired spirooxindole **4a** in 56% yield (Table 2, entry 5). Among all the solvents screened acetonitrile proved to be the optimum solvent for the desired transformation (Table 2, entries 6–9). Further increase in the reaction temperature did not improve the yield of spirooxindole **4a** (Table 2, entry 10), while the lowering of the reaction temperature (0 °C) significantly reduced the yield of **4a** (20%, Table 2, entry 11). We observed that reduction in the loading of DBU (50 mol%) resulted in a lower yield of spirooxindole **4a** (Table 1, entry 12). Based on the screening, MBH carbonate **1a** (1 equiv.), thioaurone (1.2 equiv.) and DBU (100 mol%) in acetonitrile proved to be the optimum reaction conditions for [3 + 2] annulation to access spirooxindole fused benzo[*b*]thiophen-3(2*H*)-one **4a**.

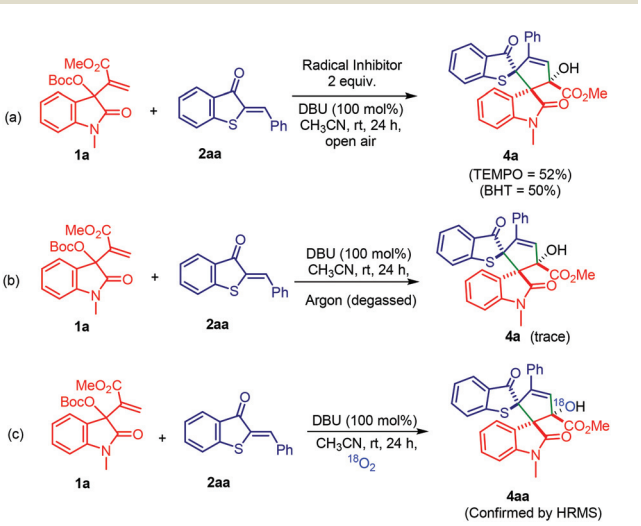
Having standardised the optimum reaction conditions, we explored the substrate scope for the generality of the protocol. The reaction of various MBH carbonates of isatin (**1a–1i**) with different thioaurones (**2aa–2ha**) afforded the corresponding [3 + 2] annulation-hydroxylation products (**4a–4i**) in moderate yields with high diastereoselectivity (up to 56%, >20 : 1, Scheme 4). We observed that, both electron-donating (CH_3, OCH_3) and electron deactivating/withdrawing (Br, Cl, F, and NO_2) substituents at different positions on the aryl ring of MBH carbonates did not have a significant effect on the yield and reaction time. However, the trend of an insignificant variation in the yields of **4a–4h** was probably due to the stereoelectronic effect of substituted functional groups. Likewise, *N*-allyl protected MBH carbonate **1i** reacted smoothly to furnish the corresponding spirooxindole fused benzo[*b*]thiophen-3(2*H*)-one **4i** in 46% yield (Scheme 4).



Scheme 4 Substrate scope of MBH carbonates and thioaurones. Reaction conditions: the reactions were carried out with MBH carbonate **1a** (0.115 mmol), thioaurone **2aa** (0.138 mmol), and DBU (0.115 mmol) in 2.0 mL of MeCN at room temperature. Isolated yield after column chromatography. Diastereomeric ratio >20 : 1 in all cases and determined by ^{1}H NMR. DBU: 2.0 equiv.

Later, we investigated the substrate scope of various thioaurones (**2ba–2ha**) with MBH carbonate **1a** under the standard reaction conditions (Scheme 4). Gratifyingly, all the reactions proceeded smoothly to afford the corresponding [3 + 2] annulation-hydroxylation products **4j–4p** in moderate yields (up to 54%, Scheme 4). Even the reaction of a thioaurone derivative with a 3,4-disubstituted aryl group with **1a** proceeded smoothly to furnish the desired product **4p** (Scheme 4). It is important to note that substrates containing electron-donating/-withdrawing groups at the *para* and *meta*-positions of the aryl moiety of thioaurones reacted smoothly, while the *ortho*-substituted and heteroaryl thioaurones did not react under the optimized reaction conditions. We observed that all the spirooxindole fused benzo[*b*]thiophen-3(2*H*)-ones (**4a–4p**) were obtained with high diastereoselectivity (>20 : 1 dr). Furthermore, the molecular structure of compound **4a** was established unambiguously using single-crystal X-ray diffraction analysis.[21] Based on analogy and other spectroscopic data, the structures of all other products were deduced.

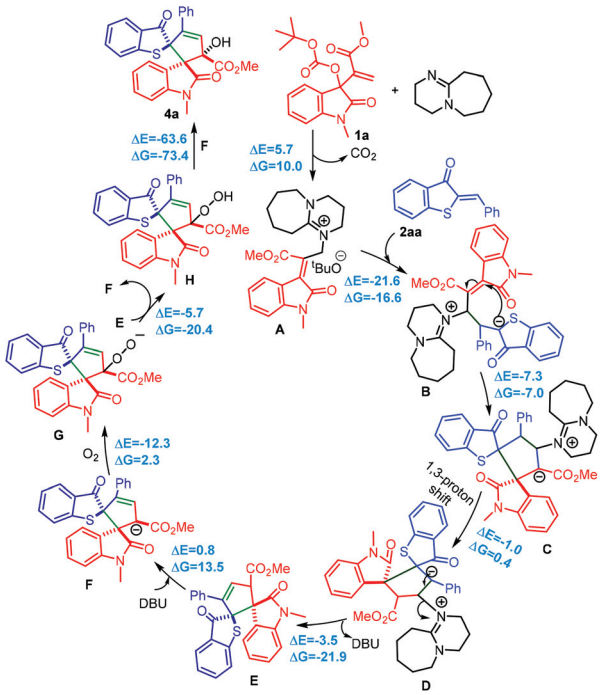
Furthermore, we carried out control experiments to understand the plausible mechanistic pathway of [3 + 2] annulation-hydroxylation reaction (Scheme 5). The addition of the radical scavenger 2,2,6,6-tetramethylpiperidinooxy (TEMPO) or butylated hydroxytoluene (BHT) under standard conditions did not inhibit the reaction and **4a** was obtained in 52% and 50% yield, respectively. These experimental results ruled out the involvement of a free-radical intermediate in this transformation. When we performed the reaction under an inert atmosphere, a trace amount of **4a** was obtained, thus supporting the essential requirement of molecular oxygen for this transformation. In order to gain further insight into the source of oxygen incorporation, we performed the labelling experiment using $^{18}O_2$. We observed the incorporation of labelled oxygen in the desired product **4aa**, thus supporting the essential role



Scheme 5 Control experiments.

This journal is © The Royal Society of Chemistry 2021

Published on 21 April 2021. Downloaded by Indian Institute of Science Education & Research Pune on 6/20/2025 12:51:17 PM.



Scheme 6 Proposed reaction mechanism for [3 + 2] annulation-hydroxylation.

of oxygen in the desired transformation (confirmed by HRMS, see the ESI, page S7†).

In accordance with previous reports[8] and based on our experimental results, and quantum chemical calculations (DFT-PBE/TZVP level of theory) a plausible mechanism is described in Scheme 6. The reaction is initiated by the nucleophilic attack of DBU on MBH carbonate **1a** to generate quaternary ammonium salt **A** with the liberation of CO_2 and *tert*-butoxide. As the intermediate **A** is relatively thermodynamically unstable (ΔG = 10 kcal mol^{-1}) it reacts with the *in situ* generated *tert*-butoxide to form an ylide. Then thioaurone **2aa** quickly reacts with the *in situ* generated ylide *via* favourable α-regioselective attack[22] to give intermediate **B** with a reaction free energy ΔG = −16.6 kcal mol^{-1}. Furthermore, the intermediate **B** undergoes intramolecular cyclization (ΔG = −7.0 kcal mol^{-1}) to form the spirocyclic intermediate **C**. Then this spirocyclic intermediate **C** undergoes a 1,3 proton shift to give the highly reactive intermediate **D**.[8c] This undergoes facile conversion to afford the corresponding spirocyclic intermediate **E** (ΔG = −21.9 kcal mol^{-1}; confirmed by HRMS, ESI, page S8†) by the elimination of DBU. Subsequently, the enolate intermediate **F** is formed during the course of reaction by the abstraction of an acidic proton by DBU.

The anionic intermediate **F** further reacts with oxygen (air) to give the peroxide anionic intermediate **G**, which in turn quickly abstracts the acidic proton (alpha to ester) from intermediate **E** to form the hydroperoxide intermediate **H** along with the generation of intermediate **F**. This reaction step proved to be highly facile as is evident from the reaction free energy value (ΔG = −20.4 kcal mol^{-1}). Finally, the enolate **F** attacks on the weak peroxide bond of a highly reactive intermediate **H** to furnish the final product **4a**.[17]

Conclusions

In summary, we have developed a protocol for the synthesis of cyclopentadiene- and cyclopentene-spirooxindole derivatives in a practical manner. We have successfully employed aurones and thioaurones as suitable C2 synthons in [3 + 2] annulation with MBH carbonates of isatin to construct structurally diverse and multi-functionalized spiro fused carbopentacyclic scaffolds using a suitable Lewis base. The structurally similar aurone and thioaurone showed different reactivities under different bases to afford spirooxindole fused cyclopentadiene and spirooxindole fused hydroxy cyclopentene derivatives, respectively. The experimental findings were further corroborated by DFT calculations to support the probable mechanism of the annulation reaction.

Conflicts of interest

There are no conflicts to declare.

Acknowledgements

R. G. B. thanks DST-SERB (CRG/2019/005753), Govt. of India for the generous research grant. The authors also thank IISER Pune for the financial assistance. P. K. W and A. S. S. thank the UGC, and R. D. thanks the CSIR, New Delhi, Government of India for providing fellowships. The authors also thank Dr Utpal Das for providing ^{18}O labelled oxygen and Dr T. Vijayakanth IISER Pune for obtaining crystal data. The support and the resources provided by 'PARAM Brahma Facility' under the National Supercomputing Mission, Government of India at the Indian Institute of Science Education and Research (IISER) Pune are gratefully acknowledged.

Notes and references

1 A. Ding, M. Meazza, H. Guo, J. W. Yang and R. Rios, *Chem. Soc. Rev.*, 2018, **47**, 5946–5996.
2 (*a*) Y. T. Yang, J. F. Zhu, G. Liao, H. J. Xu and B. Yu, *Curr. Med. Chem.*, 2018, **25**, 2233–2244; (*b*) S. S. Panda, R. A. Jones, P. Bachawala and P. P. Mohapatra, *Mini-Rev. Med. Chem.*, 2017, **17**, 1515–1536; (*c*) N. Ye, H. Chen, E. A. Wold, P. Y. Shi and J. Zhou, *ACS Infect. Dis.*, 2016, **2**, 382–392; (*d*) B. Yu, Y. C. Zheng, X. J. Shi, P. P. Qi and H. M. Liu, *Anticancer Agents Med. Chem.*, 2016, **16**, 1315–1324; (*e*) B. Yu, D. Q. Yu and H. M. Liu, *Eur. J. Med. Chem.*, 2015, **97**, 673–698; (*f*) L. M. Zhou, R. Y. Qu and G. F. Yang, *Expert Opin. Drug Discovery*, 2020, **15**, 603–625.

Published on 21 April 2021. Downloaded by Indian Institute of Science Education & Research Pune on 6/20/2025 12:51:17 PM.

3 (*a*) B. Yu, Z. Q. Yu, P. P. Qi, D. Q. Yu and H. M. Liu, *Eur. J. Med. Chem.*, 2015, **95**, 35–40; (*b*) Y. J. Zhao, A. Aguilar, D. Bernard and S. M. Wang, *J. Med. Chem.*, 2015, **58**, 1038–1052; (*c*) C. V. Galliford and K. A. Scheidt, *Angew. Chem., Int. Ed.*, 2007, **46**, 8748–8758.

4 (*a*) S. A. Babu, R. Aslam, N. A. Padmavathi and V. Rajkumar, *Nat. Prod. Chem.*, 2015, **46**, 227–339; (*b*) G. J. Mei and F. Shi, *Chem. Commun.*, 2018, **54**, 6607–6621; (*c*) A. K. Franz, N. V. Hanhan and N. R. Ball-Jones, *ACS Catal.*, 2013, **3**, 540–553; (*d*) D. Cheng, Y. Ishihara, B. Tan and C. F. Barbas, *ACS Catal.*, 2014, **4**, 743–762; (*e*) N. R. Ball-Jones, J. J. Badillo and A. K. Franz, *Org. Biomol. Chem.*, 2012, **10**, 5165–5181; (*f*) P. Saraswat, G. Jeyabalan, M. Z. Hassan, M. U. Rahman and N. K. Nyola, *Synth. Commun.*, 2016, **46**, 1643–1664; (*g*) R. Rios, *Catal. Sci. Technol.*, 2012, **2**, 267–278; (*h*) M. Meazza and R. Rios, *Chem. – Eur. J.*, 2016, **22**, 9923–9928; (*i*) X. Companyó, A. Zea, A. N. R. Alba, A. Mazzanti, A. Moyanoa and R. Rios, *Chem. Commun.*, 2010, **46**, 6953–6955.

5 (*a*) H. Kato, T. Yoshida, T. Tokue, Y. Nojiri, H. Hirota, T. Ohta, R. M. Williams and S. Tsukamoto, *Angew. Chem., Int. Ed.*, 2007, **46**, 2254–2256; (*b*) R. M. Williams, J. Cao, H. Tsujishima and R. J. Cox, *J. Am. Chem. Soc.*, 2003, **125**, 12172–12178; (*c*) E. V. Mercado-Marin, P. Garcia-Reynaga, S. Romminger, E. F. Pimenta, D. K. Romney, M. W. Lodewyk, D. E. Williams, R. J. Andersen, S. J. Miller, D. J. Tantillo, R. G. S. Berlinck and R. Sarpong, *Nature*, 2014, **509**, 318–324.

6 (*a*) J. Peng, X. Huang, L. Jiang, H. L. Cui and Y. C. Chen, *Org. Lett.*, 2011, **13**, 4584–4587; (*b*) J. Peng, G. Y. Ran, W. Du and Y. C. Chen, *Synthesis*, 2015, 2538–2544; (*c*) Y. Chen, B. D. Cui, M. Bai, W. Y. Han, N. W. Wan and Y. Z. Chen, *Tetrahedron*, 2019, **75**, 2971–2979.

7 (*a*) Z. C. Chen, Z. Chen, W. Du and Y.C. Chen, *Chem. Rec.*, 2020, **20**, 541–555 and references cited therein. (*b*) R. J. Yan, B. X. Liu, B. X. Xiao, W. Du and Y. C. Chen, *Org. Lett.*, 2020, **22**, 4240–4244; (*c*) K. Kumar and R. K. Rawal, *ChemistrySelect*, 2020, **5**, 3048–3051; (*d*) P. K. Warghude, A. S. Sabale and R. G. Bhat, *Org. Biomol. Chem.*, 2020, **18**, 1794–1799; (*e*) Z. C. Chen, Z. Chen, Z. H. Yang, L. Guo, W. Du and Y. C. Chen, *Angew. Chem., Int. Ed.*, 2019, **58**, 15021–15025; (*f*) P. Chen, Z. C. Chen, Y. Li, Q. Ouyang, W. Du and Y. C. Chen, *Angew. Chem., Int. Ed.*, 2019, **58**, 4036–4040; (*g*) L. N. Pan, J. Sung, R. G. Shi and C. G. Yan, *Org. Chem. Front.*, 2020, **7**, 3202–3208.

8 (*a*) P. K. Warghude, P. D. Dharpure and R. G. Bhat, *Tetrahedron Lett.*, 2018, **59**, 4076–4079; (*b*) M. S. Mei, Y. H. Wang, Q. Hu, Q. H. Li, D. Y. Shi, D. Gao, G. Ge, G. Q. Lin and P. Tian, *Chem. Commun.*, 2020, **56**, 10718–10721; (*c*) Y. Chen, B. D. Cui, Y. Wang, W. Y. Han, N. W. Wan, M. Bai, W. C. Yuan and Y. Z. Chen, *J. Org. Chem.*, 2018, **83**, 10465–10475; (*d*) F. Wei, H. Y. Huang, N. J. Zhong, C. L. Gu, D. Wang and L. Liu, *Org. Lett.*, 2015, **17**, 1688–1691; (*e*) S. K. Arupula, S. Guin, A. Yadav, S. M. Mobin and S. Samanta, *J. Org. Chem.*, 2018, **83**, 2660–2675; (*f*) J. Y. Du, Y. H. Ma, F. X. Meng, R. R. Zhang, R. N. Wang, H. L. Shi, Q. Wang, Y. X. Fan, H. L. Huang, J. C. Cui and C. L. Ma, *Org. Lett.*, 2019, **21**, 465–468; (*g*) X. Fan, H. Yang and M. Shi, *Adv. Synth. Catal.*, 2017, **359**, 49–57.

9 (*a*) Q. Luo, X. Y. Wei, J. Yang, J. F. Luo, R. Liang, Z. C. Tu and Y. X. J. Cheng, *Nat. Prod.*, 2017, **80**, 61–70; (*b*) A. B. Petersen, M. H. Rønnest, T. O. Larsen and M. H. Clausen, *Chem. Rev.*, 2014, **114**, 12088–12107; (*c*) Y. Malpani, R. Achary, S. Y. Kim, H. C. Jeong, P. Kim, S. B. Han, M. Kim, C. K. Lee, J. N. Kim and Y. S. Jung, *Eur. J. Med. Chem.*, 2013, **62**, 534–544; (*d*) J. Lin, S. Liu, B. Sun, S. Niu, E. Li, X. Liu and Y. Che, *Nat. Prod.*, 2010, **73**, 905–910.

10 (*a*) L. Huang, J. S. Lin, B. Tan and X. Y. Liu, *ACS Catal.*, 2015, **5**, 2826–2831; (*b*) K. C. S. Lakshmi, J. Krishnan, C. R. Sinu, S. Varughese and V. Nair, *Org. Lett.*, 2014, **16**, 6374–6377; (*c*) T. Zarganes-Tzitzikas, M. A. Terzidis, J. Stephanidou-Stephanatou, C. A. Tsoleridis and G. Kostakis, *J. Org. Chem.*, 2011, **76**, 9008–9014; (*d*) M. Braun, A. Hessamian-Alinejad, B. F. Lacroix, B. H. Alvarez and G. Fischer, *Molecules*, 2008, **13**, 995–1003; (*e*) C. B. Zhang, P. H. Dou, J. Zhang, Q. Q. Wei, Y. B. Wang, J. Y. Zhu, J. Y. Fu and T. Ding, *ChemistrySelect*, 2016, **1**, 4403–4407; (*f*) D. Kowalczyk, J. Wojciechowski and Ł. Albrecht, *Synthesis*, 2017, 880–890; (*g*) Z. P. Wang, S. Xiang, P. L. Shao and Y. J. He, *Org. Chem.*, 2018, **83**, 10995–11007.

11 (*a*) M. B. Isman and P. Proksch, *Phytochemistry*, 1985, **24**, 1949–1951; (*b*) O. Kayser, A. F. Kiderlen, U. Folkens and H. Kolodziej, *Planta Med.*, 1999, **65**, 316–319; (*c*) T. Nakayama, *J. Biosci. Bioeng.*, 2002, **94**, 487–491; (*d*) C. Zwergel, S. Valente, A. Salvato, Z. Xu, O. Talhi, A. Mai, A. Silva, L. Altucci and G. Kirsch, *Med. Chem. Commun.*, 2013, **4**, 1571–1579.

12 (*a*) C. Guo, M. Schedler, C. G. Daniliuc and F. Glorius, *Angew. Chem., Int. Ed.*, 2014, **53**, 10232–10236; (*b*) Z. Q. Liang, Z. H. Gao, W. Q. Jia and S. Ye, *Chem. – Eur. J.*, 2015, **21**, 1868–1872; (*c*) M. Wang, Z. Q. Rong and Y. Zhao, *Chem. Commun.*, 2014, **50**, 15309–15312; (*d*) F. Wang, C. Luo, Y. Y. Shen, Z. D. Wang, X. Li and J. P. Cheng, *Org. Lett.*, 2015, **17**, 388–391; (*e*) H. Ni, Z. H. Ni, Z. Yu, W. Yao, Y. Lan, N. Ullah and Y. Lu, *Chem. Sci.*, 2017, **8**, 5699–5704; (*f*) While we were about to communicate the manuscript, Chen and co-workers reported an article on the asymmetric [3 + 2] annulation of isatin derived MBH carbonates with aurones and thioaurones for the construction of spiroheterocycles, DOI: DOI: 10.1002/ajoc.202100078.

13 (*a*) W. H. Ding, A. M. Yu, L. Zhang and X. T. Meng, *Org. Lett.*, 2019, **21**, 9014–9018; (*b*) V. Dočekal, B. Formánek, I. Císařová and J. Veselý, *Org. Chem. Front.*, 2019, **6**, 3259–3263; (*c*) B. Formánek, J. Tauchman, I. Císařová and J. Veselý, *J. Org. Chem.*, 2020, **85**, 8510–8521; (*d*) M. Saktura, B. Joachim, P. Grzelak and Ł. Albrecht, *Eur. J. Org. Chem.*, 2019, 6592–6596; (*e*) A. Skrzyńska, A. Albrecht and

 This journal is © The Royal Society of Chemistry 2021

Published on 21 April 2021. Downloaded by Indian Institute of Science Education & Research Pune on 6/20/2025 12:51:17 PM.

Ł. Albrecht, *Adv. Synth. Catal.*, 2016, **358**, 2838–2844; (*f*) J. Jia, A. Yu, S. Ma, Y. Zhang, K. Li and X. Meng, *Org. Lett.*, 2017, **19**, 6084–6087.

14 (*a*) K. Eggers, T. M. Fyles and P. J. Montoya-Pelaez, *J. Org. Chem.*, 2001, **66**, 2966–2977; (*b*) S. Bhattacharya, T. K. Pradhan, A. De, S. R. Chaudhury, A. K. De and T. Ganguly, *J. Phys. Chem. A*, 2006, **110**, 5665–5673; (*c*) J. Plötner and A. Dreuw, *J. Phys. Chem. A*, 2009, **113**, 11882–11887; (*d*) S. Wiedbrauk, B. Maerz, E. Samoylova, A. Reiner, F. Trommer, P. Mayer, W. Zinth and H. Dube, *J. Am. Chem. Soc.*, 2016, **138**, 12219–12227.

15 (*a*) J. Z. Vlahakis, M. D. Wand and R. P. Lemieux, *Adv. Funct. Mater.*, 2004, **14**, 637–642; (*b*) D. Jacquemin, J. Preat, V. Wathelet, M. Fontaine and E. A. Perpete, *J. Am. Chem. Soc.*, 2006, **128**, 2072–2083.

16 (*a*) M. T. Konieczny, W. Konieczny, S. Okabe, H. Tsujimoto, Y. Suda and K. Wierzba, *Chem. Pharm. Bull.*, 2006, **54**, 350–353; (*b*) A. A. Mouineer, A. F. Zaher, A. A. Elmalah and E. A. Sobh, *Mediterr. J. Chem.*, 2017, **6**, 165–179.

17 (*a*) Y. Yang, F. Chin, W. Ma, T. Jiang and Z. Tan, *Org. Lett.*, 2012, **14**, 4762–4765; (*b*) M. Bai, Y. You, Y. Z. Chen, G. Y. Xiang, X. Y. Xu, X. M. Zhang and W. C. Yuan, *Org. Biomol. Chem.*, 2016, **14**, 1395–1401; (*c*) Y. Yang, Y. Li, C. Cheng, G. Yang, S. Wan, J. Zhang, Y. Mao, Y. Zhao, L. Zhang, C. Li and L. Tang, *J. Org. Chem.*, 2019, **84**, 2316–2324.

18 CCDC 2067873† contains the supplementary crystallographic data for compound **3a**.

19 CCDC 2067878† contains the supplementary crystallographic data for compound **3v′**.

20 T. B. Nguyen and P. Retailleau, *Org. Lett.*, 2018, **20**, 186–189.

21 CCDC 2067874† contains the supplementary crystallographic data for compound **4a** and CCDC 2067877† contains the supplementary crystallographic data for compound **4c**.

22 We believe that the α-regioselective attack may be preferable over γ-regioselective attack to avoid the steric crowding thus leading to higher diastereoselectivity.

OL Organic Letters

pubs.acs.org/OrgLett Letter

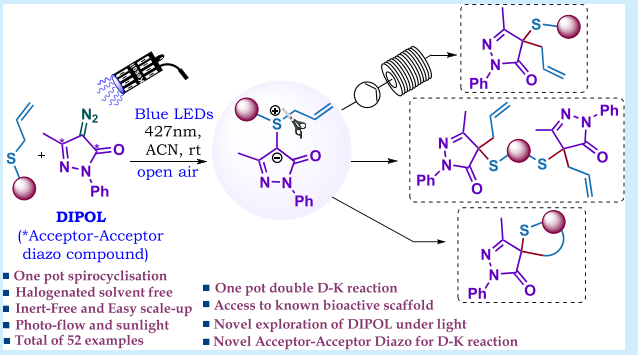
The Reactivity of Acceptor-Acceptor Diazo Pyrazolones with Allyl Thioethers under Visible Light: Access to Homoallyl Sulfides, Spiropyrazolones - Pesticide Analogues and Photoflow Synthesis

Onkar S. Bankar, Chhabi Pal, Debasish Laha, Abhijeet S. Sabale, and Ramakrishna G. Bhat*

Cite This: *Org. Lett.* 2024, 26, 9191−9197 Read Online

ACCESS | Metrics & More | Article Recommendations | Supporting Information

ABSTRACT: The novel reactivity of a less selective and more reactive acceptor-acceptor kind of diazo pyrazolone (DIPOL) has been explored under visible light for the first time. We have successfully demonstrated the reaction of DIPOL and different allyl thioethers under blue light to construct a wide variety of products including a pesticidal analogue exclusively in excellent chemoselectivity in good to excellent yields. Moreover, possible side products emanating from ketene were not observed. This protocol works smoothly in an environmentally benign solvent under inert free conditions. The practicality of the protocol has been extended to a photoflow reaction, and also, the reaction works smoothly under the direct exposure of sunlight.



Downloaded via IISER PUNE on June 20, 2025 at 11:49:41 (UTC).
See https://pubs.acs.org/sharingguidelines for options on how to legitimately share published articles.

The pyrazolone framework is a privileged structural motif and has been widely utilized in dyes as well as bioactive and pharmaceutical compounds due to its versatility and applicability in diverse fields.[1,2] This interesting scaffold is known to exhibit anti-inflammatory, antitumor, neuroprotective, antibacterial, antifungal, and antipyretic properties, and the newer pyrazalone derivatives have garnered a lot of interest in the pharmaceutical sector (Figure 1).[3] Spiropyrazolone derivatives are known to elicit anti-HIV properties, and they are also proven type-4 phosphodiesterase inhibitors (Figure 1).[4]

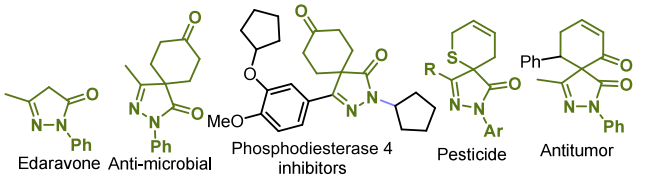


Figure 1. Functionalized pyrazolone and spiropyrazolone.

Likewise, diazo compounds are also known for their versatile reactivity to access different useful scaffolds in organic synthesis.[5] In particular, the cyclic diazo compounds have received special attention, as they are capable of showcasing intra/intermolecular reactivity under different catalytic conditions. Cyclic diazo compounds have been explored for C−H bond functionalization, cycloaddition, and rearrangement reactions, etc.[6] Surprisingly, the acceptor-acceptor cyclic diazo pyrazolone scaffold and its reactivity have been rarely explored through transition metal catalysis (Scheme 1A).[7] Moreover, the reactivity of diazo pyrazolones (DIPOL) under the irradiation of visible light or photolysis to generate carbene is unknown in the literature (Scheme 1A).[8]

The Doyle-Kirmse (D-K) reaction of diazo compounds and allylic sulfides under transition metal catalysis is known to furnish products via [2,3]-sigmatropic rearrangement of allyl sulfonium ylides formed in situ. Generating the allyl sulfonium ylides efficiently via D-K reaction is very useful and has been explored to construct bioactive compounds and natural products.[9] The D-K reaction has been extensively studied on different types of donor,[10] acceptor,[11] and donor−acceptor[12] diazo compounds (Scheme 1B). However, to the best of our knowledge, none of the acceptor-acceptor classes of diazo compounds have been explored for the D-K reaction until date probably due to their reactivity (Scheme 1C).

Recently, Xiao and Gryko have independently reported the visible-light-mediated D-K reaction with allyl phenyl sulfide and propargyl phenyl sulfide to access the [2,3]-sigmatropic rearrangement D-K reaction (Scheme 1D).[13] However, these interesting and elegant protocols rely on halogenated solvent, inert atmosphere, and a super stoichiometric amount of allyl

Received: August 22, 2024
Revised: October 12, 2024
Accepted: October 17, 2024
Published: October 23, 2024



ACS Publications © 2024 American Chemical Society

Scheme 1. Carbene Surrogates and Their Reactivity under Visible Light Diazo Pyrazolones (DIPOL)

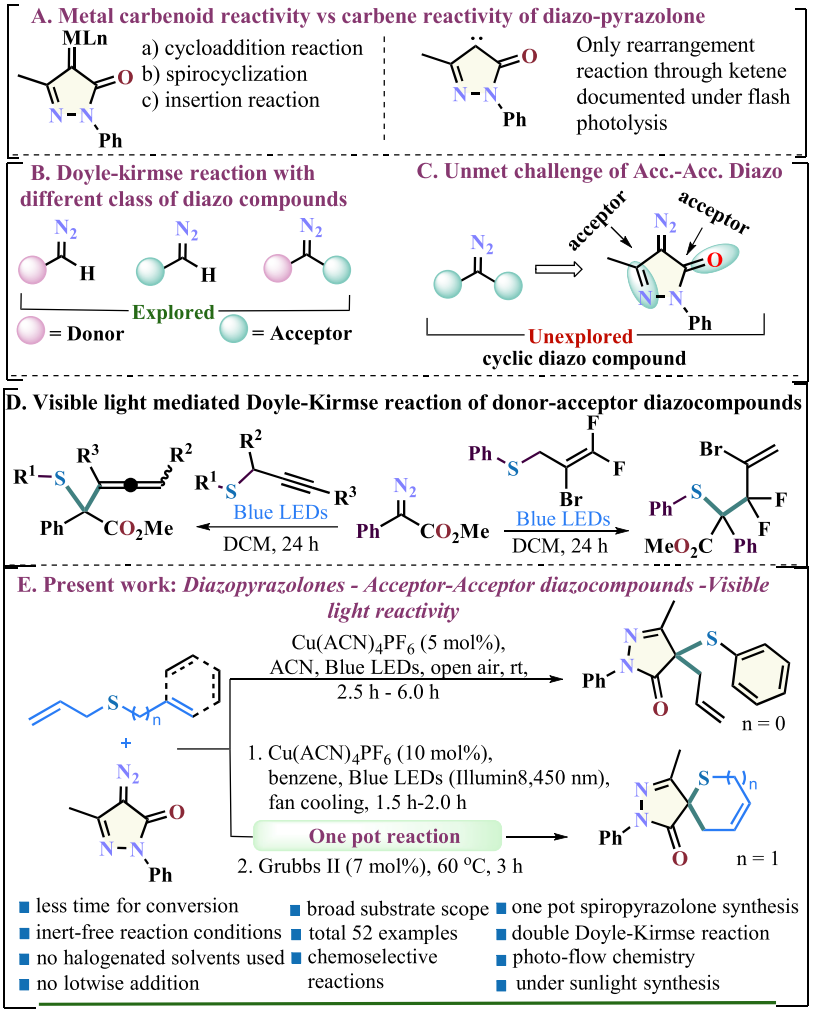
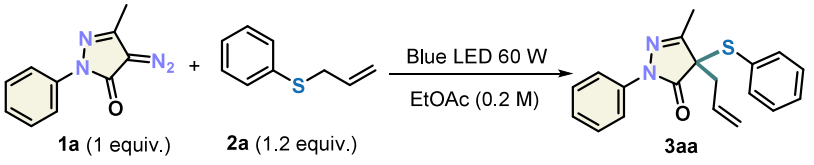


Table 1. Optimization Studies of the Visible-Light-Mediated Doyle-Kirmse Reaction[a]



Entry	Deviations from tested conditions[a]	Yield[b] (%) of **3aa**
1	None	28(26)
2[d]	ACN	60
3[d]	427 nm blue LEDs	68
4[d]	No light, 82 °C	NR
5[d]	427 nm, $AgSbF_6$	86
6[d]	**427 nm, $Cu(ACN)_4PF_6$**	**93(91)**
7[d]	No light, $Cu(ACN)_4PF_6$, 82 °C	NR

[a]Reaction conditions: DIPOL **1a** (0.2 mmol, 1.0 equiv), allyl phenyl sulfide **2a** (0.24 mmol, 1.2 equiv), EtOAc (c = 0.2 M), irradiated with blue LEDs (60 W) at room temperature (27 °C), 16 h. [b]Yields of **3aa** were determined by ^{1}H NMR spectroscopic analysis of the reaction mixture using 1,3,5-trimethoxybenzene as the internal standard. [c]Isolated yield of the products was given in the parentheses. [d]A. R. grade ACN was used. NR = No reaction.

thioethers and require a portion-wise addition of acceptor−donor diazo compound.

Owing to the importance of pyrazolones, we hypothesized that acceptor-acceptor diazo compounds such as DIPOLs may react under visible light. We believed that visible light of a suitable wavelength may assist dinitrogen extrusion to form a carbene intermediate, which in turn may undergo a D-K reaction with various allyl thioethers to furnish pyrazolone derivatives.[14]

https://doi.org/10.1021/acs.orglett.4c03117
Org. Lett. 2024, 26, 9191−9197

In order to validate our hypothesis, we commenced with a model reaction of diazo edaravone (DEDA) **1a** and allyl phenyl sulfide **2a** in EtOAc under the irradiation of blue LED light (60 W). Gratifyingly the reaction afforded the desired product **3aa** in modest yield (26%, Table 1, Entry 1). Interestingly, we did not observe any rearrangement products emanating through ketene. Encouraged by the initial result, we carried out further optimization by screening different solvents (see SI, Table S1, page 11). Among all, ACN proved to be the most advantageous to afford the desired product **3aa** in moderate yield (60%, Table 1, Entry 2). Halogenated solvents (DCM, $CHCl_3$) and polar aprotic solvents with nucleophilic sites such as THF or 1,4-dioxane proved to be incompatible (see SI, and Table S1). The reaction in polar protic solvents (H_2O, MeOH, EtOH) worked very sluggishly to afford the desired product in poor yields (up to 14%, 30 h, see SI Table S1). Later, we screened different light sources of specific wavelength, and among all, 427 nm blue LEDs proved to be the best for the efficient transformation to obtain the desired product **3aa** in higher yield in lesser time at rt (Table 1, Entry 3). The reaction in the absence of light (at room temperature as well at an elevated temperature of 82 °C) did not afford the desired product **3aa** (Table 1, Entry 4). Surprisingly, among all the additives, silver and copper salts enhanced the yield of **3aa** significantly (Table 1, Entries 5, 6). To confirm the exact role of a copper complex whether it acts as an additive or as a catalyst (which may form a copper-carbenoid with **1a**), we performed the reaction of **1a** and **2a** in the presence of $Cu(ACN)_4PF_6$ from rt to 82 °C (absence of light) in ACN (Table 1, Entry 7).

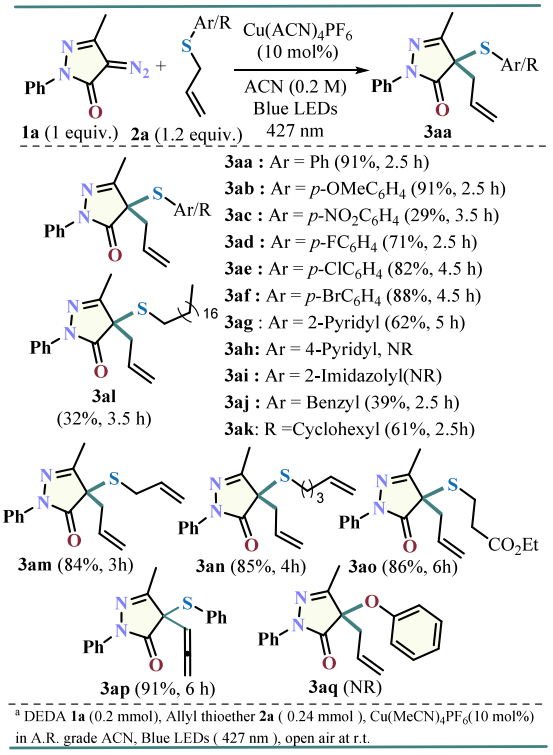
However, the reaction did not afford **3aa**, thus ruling out the formation of copper carbenoids, if any (thermal process). Based on the exhaustive screening, **1a** (1 equiv), allyl phenyl sulfide **2a** (1.2 equiv), and $Cu(ACN)_4PF_6$ (10 mol%) in ACN under blue LEDs (427 nm) at room temperature proved to be the optimum conditions to access **3aa** (Table 1, Entry 6).

Having optimized the reaction conditions so as to generalize the protocol, we explored the diverse substrate scope of allyl thioether (Scheme 2). In this regard, we synthesized a variety of thioethers **2b**−**2q** having saturated, unsaturated, cyclic, and acyclic groups. Initially, we focused on *para*-substituted-aryl sulfides and, upon treatment with DEDA **1a** under the optimized reaction conditions, successfully furnished the corresponding rearrangement products **3ab**−**3af** (up to 91%, Scheme 2). It is observed that the electron donating as well as electron withdrawing substituents on allyl phenyl sulfide furnish corresponding products **3ab** (91%) and **3ac** (29%) in excellent and modest yield respectively. This may be due to the influence of the electronic factor on the varied nucleophilicity of the sulfur atom. The allyl sulfide having deactivating groups (F, Cl, and Br) also worked well to afford the desired products (**3ad**−**3af**) (up to 88%). The heteroaromatic, benzylic, and cyclohexyl, long-chain-alkyl-derived allyl sulfides afforded the desired products (**3ag, 3aj, 3ak, 3al**), while the 4-pyridyl (**2h**)- and 2-imidazolyl (**2i**)-derived allyl sulfides did not react probably due to the lesser nucleophilic reactivity of sulfur (Scheme 2).

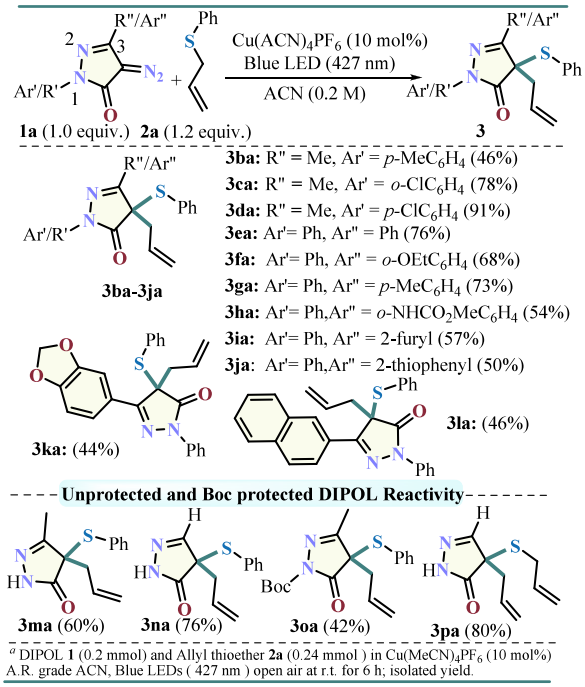
Allyl thioether containing terminal alkenes (**2m**−**2o**) also worked smoothly to furnish the corresponding products **3am**−**3ao** in very good yields (up to 86%). Gratifyingly, we did not observe any cyclopropanation side products emanating from the reaction of carbene and alkene. The phenyl propargyl thioether (**2p**) worked well to give the corresponding **3ap** in excellent yield (up to 91%). However, allyl phenyl ether **2q** under optimized conditions did not react to afford desired **3aq** (Scheme 2).

Later, we synthesized a variety of diazo pyrazolones (**1a**−**1r**) and explored their reactivity. Substrates containing substituents on *N*1 of DIPOL upon treatment with allyl phenyl sulfide **2a** afforded the corresponding desired products **3ba**−**3da** in moderate to excellent yields (Scheme 3). Variation in the

Scheme 2. Substrate Scope of Allyl Thioethers



Scheme 3. Substrate Scope of Diazopyrazolone

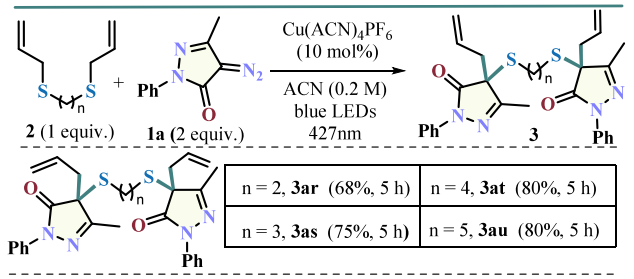


https://doi.org/10.1021/acs.orglett.4c03117
Org. Lett. 2024, 26, 9191−9197

outcome of yields is attributed to the ability to stabilize the negative charge of the ylide species during the course of the reaction. Aryl, heteroaryl substituents on C3 of *N*-phenyl diazo edaravone reacted smoothly with allyl phenyl sulfide **2a** to afford the corresponding desired products **3ea−3la** in moderate to good yields (up to 76%, Scheme 3). Gratifyingly, bulky naphthyl derivatives as well as dioxalane-derived substrates tolerated the reaction conditions well (**3ka, 3la**). More importantly, unprotected as well as protected pyrazolone derivatives reacted smoothly with **2a** to afford the corresponding products (**3ma−3pa**) in good to very good yields (up to 80%, Scheme 3). It is important to highlight that many bioactive scaffolds need a free NH group for hydrogen bonding for eliciting the bioactivity, and the protocol effectively avoided protection-deprotection as a proof of concept.

Encouraged by the initial success of the D-K reaction on the novel pyrazolone scaffold, we planned to synthesize a range of intriguing molecules by executing the double D-K reaction by strategically utilizing the long chain diallyl disulfides. In this regard, we synthesized various long-chain diallyl disulfides (**2r−2u**). Interestingly, the reaction of DEDA (2 equiv) with different diallyl disulfides (**2r−2u**) afforded the corresponding desired products (**3ar−3au**) in good to very good yields at rt (up to 80%) under standard conditions (Scheme 4).

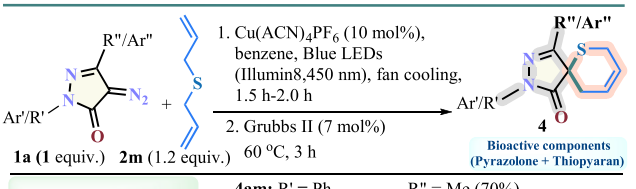
Scheme 4. Double Doyle-Kirmse Rearrangement



[a], DEDA **1a** (0.4 mmol) and Allyl thioether **2** (0.2mmol) and $Cu(MeCN)_4PF_6$ in a.r.grade ACN, Blue LEDs (427 nm) open air at r.t.; isolated yield.

Pyrazolone as well as thiopyran derivatives are known for their potent bioactivities.[3] Also, interestingly, pyrazolone fused thiopyrans (spiropyrazolone - shown in Figure 1, Scheme 5) are known as potent pesticides.[4] Encouraged by the success obtained through this protocol, we further planned to synthesize a few spiropyrazolones in one pot under visible light conditions. Gratifyingly, model substrates **1a** and **2m** under the reaction conditions afforded the desired product **3am** in good yield (84%). Later, **3am** under Grubbs metathesis conditions afforded the desired spiropyrazolone **4am** in 85% yield (see SI, Page S7).

Scheme 5. One Pot Synthesis of Spiropyrazolone



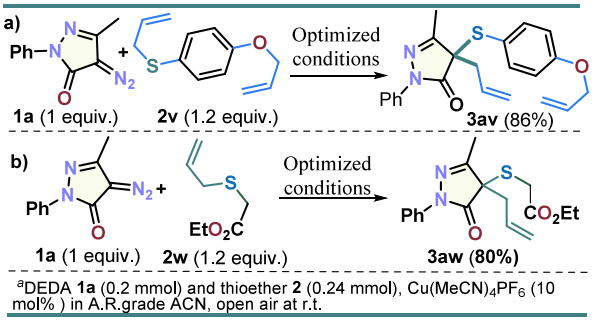
4am: R' = Ph, R" = Me (70%)
4bm: Ar' = *p*-MeC_6H_4, R" = Me (56%)
4cm: Ar' = *p*-ClC_6H_4, R" = Me (58%)
4em: Ar' = Ph, Ar" = Ph (62%)
4fm: Ar' = Ph, Ar" = *o*-$OEtC_6H_4$ (38%)
4im: Ar' = Ph, Ar" = 2- furyl (60%)
4lm: Ar' = Ph, Ar" = 2- napthyl (61%)

[a] DIPOL **1a** (0.2 mmol), Diallyl sulphide **2m** (0.24mmol), $Cu(ACN)_4PF_6$ (10 mol%) in A.R.grade Benzene (1mL), Blue LEDs (450 nm) at r.t.; Next, add Grubbs II (10 mol%) and heat reaction to 60 °C.

Inspired by this success, we planned to execute this reaction in one pot using a parallel synthesizer Illumin8 (450 nm blue LEDs).[15] In this regard, different DIPOLs (**1a−1c, 1e, 1f, 1i, 1l**), diallyl sulfide **2m**, and copper catalyst (10 mol%) were loaded in seven different reaction vessels of Illumin8 and were irradiated by blue LEDs (450 nm, 1.5−2 h, monitored by TLC). Afterward, the Grubbs II catalyst (10 mol%) was added to the crude reaction mixture and stirred for 3 h at an elevated temperature without irradiation of light. To our delight, we obtained the corresponding spiropyrazolone products by achieving the D-K reaction and ring closing metathesis in one pot (**4am−4cm, 4em, 4fm, 4im, 4lm**) in moderate to good yields (Scheme 5).

In order to examine the chemoselectivity of this transformation, we synthesized the substrate **2v** (having both *O*-allyl thio- and *S*-allyl ether moieties) that has two potential sites to form either a sulfur ylide or an oxygen ylide. Interestingly, the reaction of **2v** with DEDA **1a** under the optimized reaction conditions furnished the corresponding **3av** exclusively as a sole product (86% yield, Scheme 6a). This clearly indicated

Scheme 6. Chemoselectivity: D-K vs Stevens Reaction



[a]DEDA **1a** (0.2 mmol) and thioether **2** (0.24 mmol), $Cu(MeCN)_4PF_6$ (10 mol%) in A.R.grade ACN, open air at r.t.

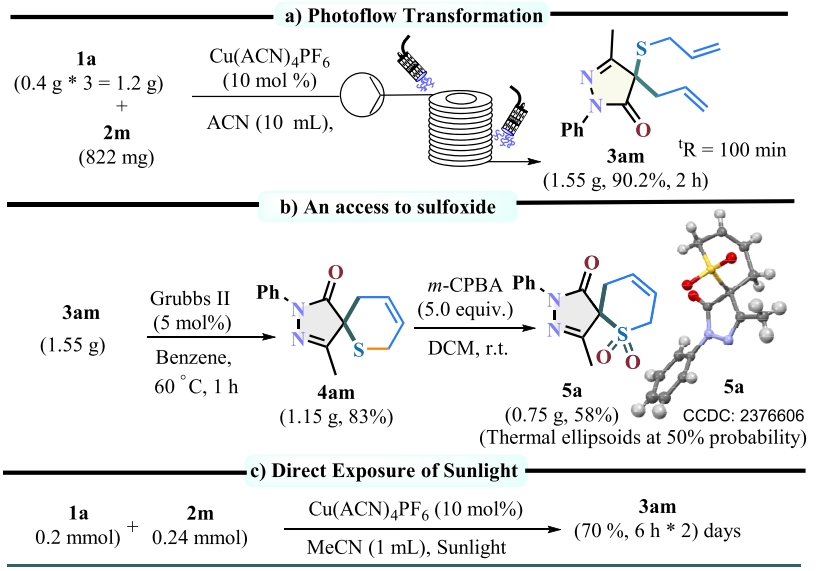
that sulfur ylide is more favorable and preferred over oxygen ylide, possibly due to the higher electronegativity of the oxygen atom that makes the oxygen ylide relatively less stable.

Later, we synthesized compound **2w** in order to examine the competitive reaction between the Doyle-Kirmse and [2,3]-Stevens reaction. The reaction of **1a** and **2w** exclusively favored the D-K reaction over the [2,3]-sigmatropic reaction to furnish desired product **3aw** in higher yield (80% yield, Scheme 6b).

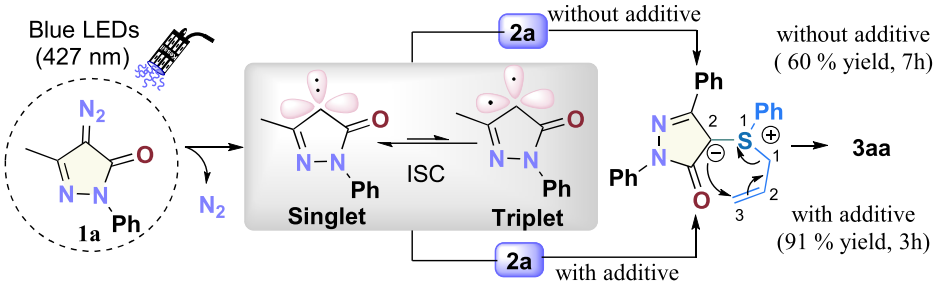
After successfully exploring the novel synthetic protocol for achieving the D-K reaction on newer diazo scaffold, we became intrigued in studying blue-light-induced carbene formation under continuous-flow conditions for further application. Flow chemistry is particularly well-suited for performing photochemical transformations due to the small channel diameters and large reaction surface area enhancing the penetration of photons into the reaction solution. In this regard, we carefully examined the photoflow reaction of the protocol in gram quantity. Unlike the traditional batch process (an average reaction time of 4.5 h), the coil reactor enabled quantitative conversion of DEDA **1a** (same light source as in the batch Process, 427 nm) to afford the corresponding desired product **3am** in excellent yield in a shorter reaction time (2 h, 90%, Scheme 7a, see SI for details). This result clearly highlights the potential of continuous flow processes for reaction intensifi-

https://doi.org/10.1021/acs.orglett.4c03117
Org. Lett. 2024, 26, 9191−9197

Scheme 7. Applications: Photoflow and Sunlight Reactions



Scheme 8. Plausible Mechanism of the Transformation



cation. This application provides access to reaction parameters that are not attainable in conventional batch chemistry.

Further in order to explore the late-stage application of this protocol, **3am** (1.55 g) was subjected to the ring closing metathesis to obtain the compound **4am** in excellent yield (Scheme 7b). This upon treatment with *m*-CPBA afforded the corresponding sulfoxidation product **5a** in a 58% yield (Scheme 7b). Later, we explored the reaction of **1a** and **2m** under direct exposure of sunlight while maintaining other optimized reaction conditions (Scheme 7c). Interestingly, we obtained desired product **3am** in good yield (70%).

In order to have some insights into the reaction pathway, we performed a series of control experiments, and a plausible mechanism is proposed (Scheme 8).

We have also carried out UV−visible studies and HPLC and FT-IR studies to understand the role of copper salt as a catalyst or additive and radical trapping experiment to study the nature of the reaction pathway (see SI for details). Based on the observation and available literature precedence, we propose **1a** undergoes photolysis to generate the singlet carbene, which further reacts with **2a** to afford the **3aa** via [2,3]-sigmatropic rearrangement, and the copper salt may be acting like a Lewis acid additive, not as a catalyst.

In summary, we have successfully demonstrated novel reactivity of an acceptor−acceptor diazo compound such as DIPOL under visible light irradiation to achieve the Doyle-Kirmse reaction. The bench-stable diazo pyrazolones have been effectively employed for the double Doyle-Kirmse reaction to access bis-allyl sulfides and spiropyrazolones under visible light. The established protocol demonstrated a wide substrate scope and a good functional group tolerance. The application of the protocol was further demonstrated on a continuous-flow setup, and the reaction also works under the direct exposure of sunlight. The method gives access to construct the bioactive pyrazolone fused thiopyran scaffold and pesticide analogue framework. The protocol is also proven to be scalable.

■ ASSOCIATED CONTENT

Data Availability Statement

The data underlying this study are available in the published article and its Supporting Information.

Supporting Information

The Supporting Information is available free of charge at https://pubs.acs.org/doi/10.1021/acs.orglett.4c03117.

The reaction optimization tables, procedure for reaction, series of control experiments, photoflow synthesis and sunlight synthesis procedure, characterization data for all new compounds, and copies of ^{1}H, $^{13}C\{^{1}H\}$, and $^{19}F\{^{1}H\}$ NMR spectra (PDF)

Accession Codes

Deposition Number 2376606 contains the supplementary crystallographic data for this paper. These data can be obtained free of charge via the joint Cambridge Crystallographic Data

https://doi.org/10.1021/acs.orglett.4c03117
Org. Lett. 2024, 26, 9191−9197

Centre (CCDC) and Fachinformationszentrum Karlsruhe Access Structures service.

AUTHOR INFORMATION

Corresponding Author

Ramakrishna G. Bhat − *Department of Chemistry, Indian Institute of Science Education and Research (IISER)-Pune, 411008 Pune, Maharashtra, India;* orcid.org/0000-0002-7739-9553; Email: rgb@iiserpune.ac.in

Authors

Onkar S. Bankar − *Department of Chemistry, Indian Institute of Science Education and Research (IISER)-Pune, 411008 Pune, Maharashtra, India*

Chhabi Pal − *Department of Chemistry, Indian Institute of Science Education and Research (IISER)-Pune, 411008 Pune, Maharashtra, India*

Debasish Laha − *Department of Chemistry, Indian Institute of Science Education and Research (IISER)-Pune, 411008 Pune, Maharashtra, India;* orcid.org/0000-0002-2479-6467

Abhijeet S. Sabale − *Department of Chemistry, Indian Institute of Science Education and Research (IISER)-Pune, 411008 Pune, Maharashtra, India*

Complete contact information is available at: https://pubs.acs.org/10.1021/acs.orglett.4c03117

Notes

The authors declare no competing financial interest.

ACKNOWLEDGMENTS

R. G. B. thanks Science and Engineering Research Board, Department of Science and Technology (SERB-DST), New Delhi, Government of India (File no: CRG/2023/004226 and CRG/2019/005753) for the generous research grant. The authors also thank IISER Pune for the financial assistance. O. S. B.; C. P.; A. S. S.; D. L. thank UGC New Delhi, The Government of India for providing fellowship.

REFERENCES

(1) Varvounis, G. Chapter 2 Pyrazol-3-ones. Part IV: Synthesis and Applications. *Adv. Heterocycl. Chem.* **2009**, *98*, 143−224.

(2) Li, Y.; Zhang, S.; Yang, J.; Jiang, S.; Li, Q. Synthesis and application of novel crosslinking polyamine dyes with good dyeing performance. *Dyes Pigm.* **2008**, *76*, 508−514.

(3) (a) Brogden, R. N. Pyrazolone Derivatives. *Drugs* **1986**, *32*, 60−70. (b) Yoshida, H.; Yanai, H.; Namiki, Y.; Fukatsu-Sasaki, K.; Furutani, N.; Tada, N. Neuroprotective Effects of Edaravone: a Novel Free Radical Scavenger in Cerebrovascular Injury. *CNS Drug Rev.* **2006**, *12*, 9−20. (c) Chande, M. S.; Barve, P. A.; Suryanarayan, V. Synthesis and Antimicrobial Activity of Novel Spirocompounds with Pyrazolone and Pyrazolthione Moiety. *J. Heterocycl. Chem.* **2007**, *44*, 49−53. (d) Bondock, S.; Rabie, R.; Etman, H. A.; Fadda, A. A. Synthesis and antimicrobial activity of some new heterocycles incorporating antipyrine moiety. *Eur. J. Med. Chem.* **2008**, *43*, 2122−2129.

(4) (a) Schmidt, B.; Scheufler, C.; Volz, J.; Feth, M. P..; Hummel, P.; Hatzelmann, A.; Zitt, C.; Wohlsen, A.; Marx, D.; Kley, H.-P.; Ockert, D.; Heuser, A.; Christiaans, J.; Sterk, G. J.; Menge, W. M. P. B. Pyrazolone derivatives as pde4 inhibitors. WO2008138939, 2010. (b) Hadi, V.; Koh, Y.-H.; Sanchez, T. W.; Barrios, D.; Neamati, N.; Jung, K. W. Development of the next generation of HIV-1 integrase inhibitors: Pyrazolone as a novel inhibitor scaffold. *Bioorg. Med. Chem. Lett.* **2010**, *20*, 6854−6857. (c) Doeller, U.; Shermolovich, Y. G.; Yemets, S. V.; Thönessen, M.-T.; Hempel, W. Pesticidal compositions containing 4-spirocyclic pyrazoles. WO2003022055, 2003.

(5) (a) Ye, T.; McKervey, M. A. Organic Synthesis with α-Diazo Carbonyl Compounds. *Chem. Rev.* **1994**, *94*, 1091−1160. (b) Davies, H. M. L.; Morton, D. Guiding Principles for Site Selective and Stereoselective Intermolecular C-H Functionalization by Donor/acceptor Rhodium Carbenes. *Chem. Soc. Rev.* **2011**, *40*, 1857−1869. (c) Davies, H. M. L.; Manning, J. R. Catalytic C-H Functionalization by Metal Carbenoid and Nitrenoid Insertion. *Nature* **2008**, *451*, 417−424. (d) Gillingham, D.; Fei, N. Catalytic X-H Insertion Reactions Based on Carbenoids. *Chem. Soc. Rev.* **2013**, *42*, 4918−4931. (e) Ford, A.; Miel, H.; Ring, A.; Slattery, C. N.; Maguire, A. R.; McKervey, M. A. Modern Organic Synthesis with α-Diazocarbonyl Compounds. *Chem. Rev.* **2015**, *115*, 9981−10080. (f) Candeias, N. R.; Paterna, R.; Gois, P. M. P. Homologation Reaction of Ketones with Diazo Compounds. *Chem. Rev.* **2016**, *116*, 2937−2981. (g) Cheng, Q.-Q.; Deng, Y.; Lankelma, M.; Doyle, M. P. Cycloaddition Reactions of Enoldiazo Compounds. *Chem. Soc. Rev.* **2017**, *46*, 5425−5443. (h) Davies, H. M. L.; Denton, J. R. Application of Donor/acceptor-Carbenoids to the Synthesis of Natural Products. *Chem. Soc. Rev.* **2009**, *38*, 3061−3071.

(6) (a) Hussain, Y.; Empel, C.; Koenigs, R. M.; Chauhan, P. Carbene Formation or Reduction of the Diazo Functional Group? An Unexpected Solvent-Dependent Reactivity of Cyclic Diazo Imides. *Angew. Chem., Int. Ed.* **2023**, *62*, e202309184. (b) Laha, D.; Bhat, R. G. Silver Catalyzed Epoxidation of Aldehydes Using Donor-/Acceptor-type Vinyl Diazosuccinimides to Access Spiro-Pyrrolidine-dioneoxiranes. *Asian J. Org. Chem.* **2020**, *9*, 918−921. (c) Inyutina, A.; Kantin, G.; Dar'in, D.; Krasavin, M. Diastereoselective Formal [5 + 2] Cycloaddition of Diazo Arylidene Succinimides-Derived Rhodium Carbenes and Aldehydes: A Route to 2-Benzoxepines. *J. Org. Chem.* **2021**, *86*, 13673−13683. (d) Hunter, A. C.; Schlitzer, S. C.; Stevens, J. C.; Almutwalli, B.; Sharma, I. A Convergent Approach to Diverse Spiroethers through Stereoselective Trapping of Rhodium Carbenoids with Gold-Activated Alkynols. *J. Org. Chem.* **2018**, *83*, 2744−2752. (e) Dar'in, D.; Kantin, G.; Glushakova, D.; Sharoyko, V.; Krasavin, M. Diazo Tetramic Acids Provide Access to Natural-Like Spirocyclic α, β-Butenolides through Rh(II)-Catalyzed O-H Insertion/Base-Promoted Cyclization. *J. Org. Chem.* **2024**, *89*, 7366−7375. (f) Bankar, O. S.; Laha, D.; Meher, K. B.; Bhat, R. G. Umpolung Reactivity of Diazo Arylidene Succinimides: Distal C-H Functionalization of α-Thiocarbonyls from the Reactive Carbenoid Center. *Chem Asian J.* **2023**, *18*, e202300774. (g) Laha, D.; Meher, K. B.; Bankar, O. S.; Bhat, R. G. Silver-Catalyzed One-Pot Access to Diastereoselective Benzo[5,6]oxepino[2,3-c]pyrroles via Formal (5 + 2)-Annulation of Donor-/Acceptor-Type Aryl Vinyl Diazosuccinimide with Ketones. *Asian J. Org. Chem.* **2022**, *11*, e202200062.

(7) (a) Zhang, Z.; Han, J.; Zhu, S. Facile synthesis of novel CF3-substituted ring-fused furo[2,3-c] pyrazoles through $Rh_2(OAc)_4$ catalyzed [3 + 2] cycloaddition of 4-diazo-1-phenyl-3-(trifluoromethyl)- 1H-pyrazol-5(4H)-one with aromatic alkynes. *Tetrahedron Lett.* **2011**, *67*, 8496−5101. (b) Zhang, K.; Zhao, G.; Cao, W. Construction of fluorinated pyrazole derivatives via a one-pot tandem CeH insertion/electrophilic fluorination reaction. *Tetrahedron Lett.* **2014**, *70*, 5659−5665. (c) Fang, F.; Hu, S.; Li, C.; Wang, Q.; Wang, R.; Han, X.; Zhou, Y.; Liu, H. Catalytic System-Controlled Divergent Reaction Strategies for the Construction of Diversified Spiropyrazolone Skeletons from Pyrazolidinones and Diazopyrazolones. *Angew. Chem., Int. Ed.* **2021**, *60*, 21327−21333. (d) Song, X.; Wang, K.; Xue, L.; Yu, H.; Zhang, X.; Lee, R.; Fan, X. Coupling Partner-Dependent Unsymmetrical C-H Functionalization of N-Phenoxy acetamides Leading to Sophisticated Spirocyclic Scaffolds. *Org. Chem. Front.* **2022**, *9*, 4583−4590. (e) Cai, X.; Song, X.; Zhu, Q.; Zhang, X.; Fan, X. Concise Synthesis of Spirocyclic Dihydro phthalazines through Spiro annulation Reactions of Aryl Azomethine Imines with Cyclic Diazo Compounds. *J. Org. Chem.* **2022**, *87*, 11048−11062. (f) Yu, C.; Xu, Y.; Zhang, X.; Fan, X. Selective Synthesis of Pyrazolonyl Spirodihydroquinolines or Pyrazolonyl Spiroindolines under Aerobic or Anaerobic Conditions. *Org. Lett.*

2022, *24*, 9473−9478. (g) Lai, R.; Xu, S.; Zhang, Q.; Zhou, H.; Luo, C.; Wang, Y.; Hai, L.; Wu, Y. Derivation of Benzothiadiazine 1,1 dioxide Scaffolds via Transition Metal-Catalyzed C—H Activation/ Annulation. *Chin. J. Chem.* **2023**, *41*, 1973−1978.

(8) (a) Padwa, A.; Woolhouse, A. D.; Blount, J. J. 1,3-Dipolar Cycloaddition Reactions of Diazopyrazolinones with Electron-Deficient Dipolarophiles. *J. Org. Chem.* **1983**, *48*, 1069−1074. (b) Umrigar, P.; Griffin, G. W.; Ege, S. N.; Adams, A. D.; Das, P. K. Reactive intermediates in the photochemistry of 4-diazo-2-pyrazolin-5-one. *Can. J. Chem.* **1984**, *62*, 2456−2463.

(9) (a) West, T. H.; Spoehrle, S. S. M.; Kasten, K.; Taylor, J. E.; Smith, A. D. Catalytic Stereoselective [2,3]-Rearrangement Reactions. *ACS Catal.* **2015**, *5*, 7446−7479. (b) Jana, S.; Guo, Y.; Koenigs, R. M. Recent Perspectives on Rearrangement Reactions of Ylides via Carbene Transfer Reactions. *Chem. Eur. J.* **2021**, *27*, 1270−1281. (c) Dong, S. X.; Liu, X. H.; Feng, X. M. Asymmetric Catalytic Rearrangements with α-Diazocarbonyl Compounds. *Acc. Chem. Res.* **2022**, *55*, 415−428. (d) Doyle, M. P.; Tamblyn, W. H.; Bagheri, V. Highly effective catalytic methods for ylide generation from diazocompounds. Mechanism of the rhodium-and copper-catalyzed reactions with allylic compounds. *J. Org. Chem.* **1981**, *46*, 5094−5102. (e) Doyle, M. P.; Griffin, J. H.; Chinn, M. S.; van Leusen, D. Rearrangements of Ylides Generated from Reactions of Diazo Compounds with Allyl Acetals and Thioketals by Catalytic Methods. Heteroatom Acceleration of the [2,3]-Sigmatropic Rearrangement. *J. Org. Chem.* **1984**, *49*, 1917. (f) Ma, M.; Peng, L.; Li, C.; Zhang, X.; Wang, J. Highly Stereoselective [2,3]-Sigmatropic Rearrangement of Sulfur Ylide Generated through Cu(I) Carbene and sulfides. *J. Am. Chem. Soc.* **2005**, *127*, 15016−15017. (g) Davies, P. W.; Albrecht, S. J. -C.; Assanelli, G. Silver-catalysed Doyle-Kirmse reaction of allyl and propargyl sulfides. *Org. Biomol. Chem.* **2009**, *7*, 1276−1279. (h) Miura, T.; Tanaka, T.; Yada, A.; Murakami, M. Doyle Kirmse Reaction Using Triazoles Leading to One-pot Multifunctionalization of Terminal Alkynes. *Chem. Lett.* **2013**, *42*, 1308−1310. (i) Yadagiri, D.; Anbarasan, P. Rhodium-Catalyzed Denitrogenative [2,3] Sigmatropic Rearrangement: An Efficient Entry to Sulfur-Containing Quaternary Centers. *Chem.-Eur.J.* **2013**, *19*, 15115−15119. (j) Lin, X.; Tang, Y.; Yang, W.; Tan, F.; Lin, L.; Liu, X.; Feng, X. Chiral Nickel (II) Complex Catalyzed Enantioselective Doyle- Kirmse Reaction of α-Diazo Pyrazole amides. *J. Am. Chem. Soc.* **2018**, *140*, 3299−3305.

(10) (a) Aggarwal, V. K.; Ferrara, M.; Hainz, R.; Spey, S. E. [2,3]-Sigmatropic rearrangement of allylic sulfur ylides derived from trimethyl silyl diazomethane (TMSD). *Tetrahedron Lett.* **1999**, *40*, 8923−8927. (b) Carter, D. S.; Van Vranken, D. L. Iron-Catalyzed Doyle-Kirmse Reaction of Allyl sulfides with (Trimethylsilyl)-diazomethane. *Org. Lett.* **2000**, *2*, 1303−1305.

(11) McMillen, D. W.; Varga, N.; Reed, B. A.; King, C. Asymmetric Copper-Catalyzed [2,3]-Sigmatropic Rearrangements of Alkyl- and Aryl-Substituted Allyl sulfides. *J. Org. Chem.* **2000**, *65*, 2532−2536.

(12) (a) Ma, M.; Peng, L.; Li, C.; Zhang, X.; Wang, J. Highly Stereoselective [2,3]-Sigmatropic Rearrangement of Sulfur Ylide Generated through Cu(I) Carbene and sulfides. *J. Am. Chem. Soc.* **2005**, *127*, 15016−15017. (b) Zhang, Z.; Sheng, Z.; Yu, W.; Wu, G.; Zhang, R.; Chu, W.-D.; Zhang, Y.; Wang, J. Catalytic asymmetric trifluoromethylthiolation via enantioselective [2,3]-sigmatropic rearrangement of sulfonium ylides. *Nat. Chem.* **2017**, *9*, 970−976. (c) Lin, X.; Tang, Y.; Yang, W.; Tan, F.; Lin, L.; Liu, X.; Feng, X. Chiral Nickel (II) Complex Catalyzed Enantioselective Doyle-Kirmse Reaction of α-Diazo Pyrazoleamides. *J. Am. Chem. Soc.* **2018**, *140*, 3299−3305. (d) He, F.; Jana, S.; Koenigs, R. M. Gold-Catalyzed Sigmatropic Rearrangement Reactions via Carbene Transfer Reactions. *J. Org. Chem.* **2020**, *85*, 11882−11891.

(13) (a) Orlowska, K.; Rybicka-Jasińska, K.; Krajewski, P.; Gryko, D. Photochemical Doyle-Kirmse Reaction: A Route to Allenes. *Org. Lett.* **2020**, *22*, 1018−1021. (b) Yang, J.; Wang, J.; Huang, H.; Qin, G.; Jiang, Y.; Xiao, T. gem-Difluoroallylation of Aryl Diazoesters via Catalyst-Free, Blue-Light-Mediated Formal Doyle-Kirmse Reaction. *Org. Lett.* **2019**, *21*, 2654−2657.

(14) An earlier version of this manuscript was filed on the preprint server ChemRxiv: Bankar, O. S.; Pal, C.; Laha, D.; Sabale, A. S.; Bhat, R. G. Reactivity of Acceptor-Acceptor Diazo-Pyrazolones with Allyl Thioethers under Visible Light: Access to Homoallyl and Bis-Homoallyl Sulfides, Spiropyrazolones-Pesticide Analogues and Photo-Flow Synthesis. *ChemRxiv*, **2024**, DOI: 10.26434/chemrxiv-2024-5s3zt.

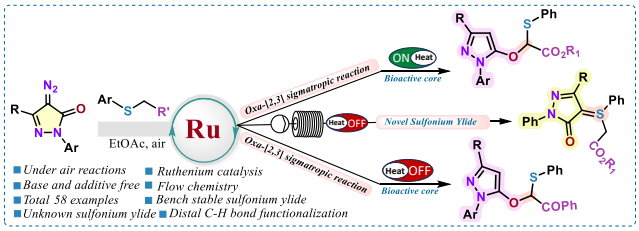
(15) The one-pot reaction of the Grubbs metathesis at room temperature was too sluggish and worked well at an elevated temperature (60 °C) in benzene. We also observed that acetonitrile is not advantageous for this one-pot reaction. In this regard, Parallel Reactor-Illumin8 was used with available LED cartridges (450 nm), and hence, it might have led to formation of desired products in relatively lower yields with comparison to 427 nm.

https://doi.org/10.1021/acs.orglett.4c03117
Org. Lett. 2024, 26, 9191−9197

Ruthenium Catalyzed Tunable Reactivity of Acceptor-Acceptor DIPOL with Different Thioether Derivatives: Access to Bench Stable Sulfonium Ylides and Alkoxy Pyrazoles

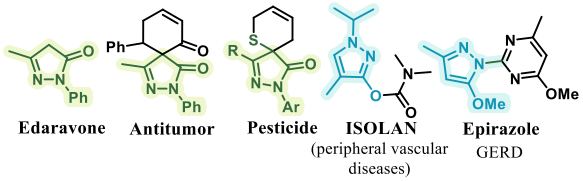
Onkar S. Bankar, Chhabi Pal, Bhavya, Abhijeet S. Sabale and Ramakrishna G. Bhat*

ABSTRACT: Unexplored reactivity of acceptor-acceptor kind of diazo pyrazolones (DIPOLs) has been effectively explored for the synthesis of novel bench stable sulfonium ylides and alkoxy pyrazoles. Umpolung reactivity of DIPOL with α-thioesters/ketones has been successfully tapped under ruthenium catalysis to achieve oxa-[2,3]-sigmatropic rearrangement. Important feature of this protocol is the exploration of tunable reactivity of DIPOL towards different thioethers to access stable sulfonium ylides as well as alkoxy pyrazoles. The protocol has demonstrated a wide functional group tolerance, excellent chemo- and regio-selectivity, and efficient rearrangement involving the carbonyl motif. As an application flow chemistry has been explored by using coil reactor as well continuous stir tank reactor for achieving the gram scale synthesis.



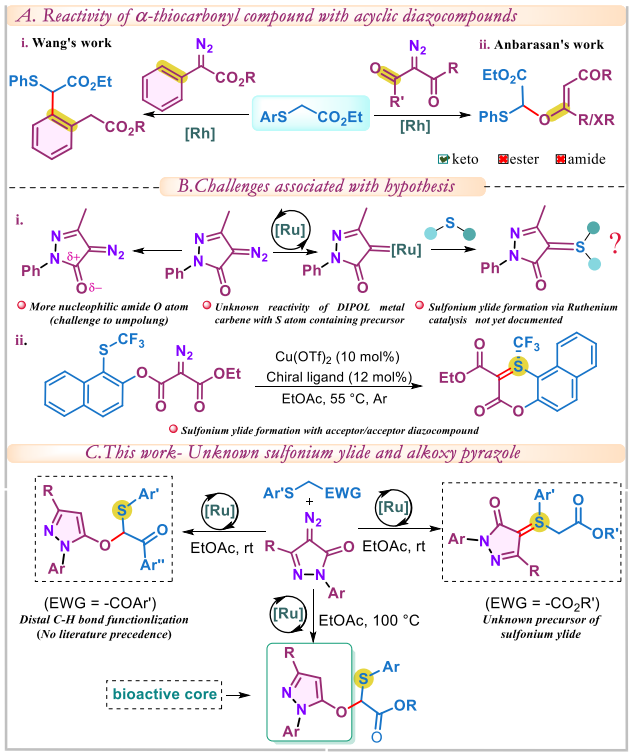
Diazo compounds have been utilized as useful synthetic precursors in organic synthesis for various synthetic transformations.[1] Decomposition of diazo compounds by a transition-metal catalyst has been widely used as an effective tool to generate reactive carbene intermediate for achieving different novel synthetic strategies.[2] Based on the substitution patterns on the diazo group, these compounds are primarily categorized into three types: acceptor-only, acceptor-acceptor, and donor-acceptor type compounds.[3] The substituents on the diazo group significantly influence both the stability and reactivity of diazo compounds, which in turn affects their behavior in various transformations.[4] Due to notable differences in stability and reactivity profiles, acceptor-acceptor diazo compounds have been less extensively studied compared to donor-acceptor diazo compounds. Particularly, cyclic acceptor-acceptor diazo compounds derived from pyarazolone scaffold are seldom explored in the literature due to its reactive nature.[5] Interestingly, there are many biologically active compounds that have pyarazolone/alkoxy pyrazoles backbone (see Figure 1) and usually these useful compounds have been synthesized using conventional synthetic approaches. [6]

Figure 1. Functionalized Pyrazolone and Alkoxypyrazole



Diazo compounds as surrogates of carbenes have been explored efficiently for a range of transformations, including sigmatropic rearrangements that involve nitrogen, sulfur and selenium ylides formed in situ.[7] In particular, sulfur ylides have gained significant interest due to their stability and they show diverse reactivity leading to various interesting and useful rearrangements. Some of the well-known sigmatropic rearrangements are Doyle–Kirmse[8] reaction and Stevens[9] reaction that are known to proceed via [2,3] and [1,2]-sigmatropic rearrangements respectively. Usually,

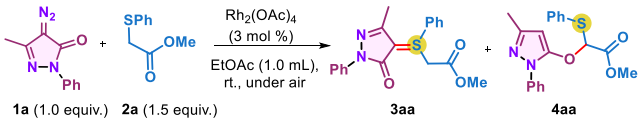
Scheme 1. Carbene surrogates and their reactivity under Ruthenium catalysis.



https://doi.org/10.26434/chemrxiv-2025-f6k87 **ORCID:** https://orcid.org/0000-0002-7739-9553 Content not peer-reviewed by ChemRxiv. **License:** CC BY-NC-ND 4.0

these rearrangements need allyl/alkyl sulfides as reacting partners under metal catalysis. Interestingly, α-thiocarbonyl compounds in presence of Rh(II)-carbenoids lead to [2,3]-sigmatropic rearrangement via 1,3 - proton shift. Also, different diazo compounds (varied electronic property) react differently with α-thiocarbonyl compounds to furnish interesting products. Wang and co-workers explored the thio Sommelet–Hauser rearrangement by treating the donor-acceptor diazo compounds with α-thiocarbonyl compounds under rhodium catalysis (Scheme 1Ai).[10] Interestingly, Anbarasan and co-workers observed the oxa-2,3-sigmatropic rearranged products when treated the acyclic acceptor-acceptor diazo compound with α-thiocarbonyl compounds under rhodium catalysis (Scheme 1Bii).[11]

Table 1. Optimization Studies of the Sulfonium Ylide and Alkoxy Pyrazole Formation reaction. [a]



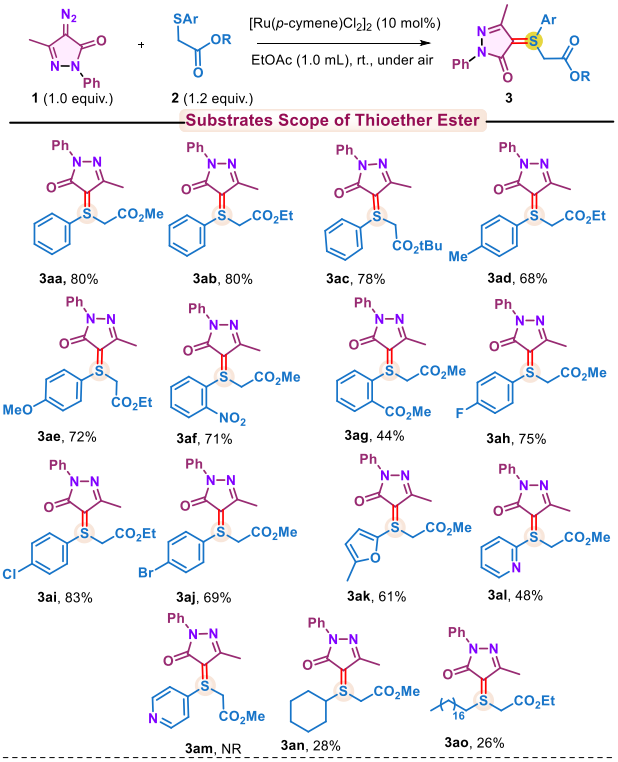
1a (1.0 equiv.) **2a** (1.5 equiv.) **3aa** **4aa**

Sr.No	Deviation from tested condition	Time (h)	Yield[b](%) **3aa**	Yield[b](%) **4aa**
1	None	48	NR	-
2	$Rh_2(OAc)_4$ at 78°C	12	34	-
3	$RuCl_2(p\text{-cymene})_2$	12	70(68)	-
4	$RuCl_2(p\text{-cymene})_2$	48	68	-
5	$RuCl_2(p\text{-cymene})_2$ at 78 °C	12	60	-
6[c]	**$RuCl_2(p\text{-cymene})_2$**	**6**	**82(80)**	**-**

[a]**Reaction conditions**: DIPOL **1a** (0.2 mmol, 1.0 equiv.), thioether ester **2a** (0.24 mmol, 1.2 equiv.), $Rh_2(OAc)_4$ (3 mol %), EtOAc (c = 0.1 M), at room temperature (27 °C), 12 h. [b]Yields of **3aa** were determined by ^1H NMR spectroscopic analysis of the reaction mixture using 1,3,5-trimethoxybenzene as the internal standard. [c]**1a** (1.2 equiv.), **2a** (1.2 equiv.), $RuCl_2(p\text{-cymene})_2$ (10 mol%) in EtOAc (0.1 M). Isolated yield of the products was given in the parentheses. NR = No reaction.

However, these interesting protocols are limited to flexible acyclic diazo compounds and, they rely on elevated temperature and halogenated solvent. Looking at the reactivity patterns of different diazo compounds, it would be highly challenging and desirable to examine the reactivity of DIPOLs (acceptor-acceptor) under metal catalysis as they have been rarely studied in the literature. Owing to the importance of pyrazolone scaffold, challenging reactivity of DIPOLs and also inspired by earlier reports we hypothesized that DIPOLs could undergo reaction with thiocarbonyl compounds to generate the corresponding sulfonium ylide intermediate in situ under suitable metal catalysis. The sulfonium ylide may eventually favour the sigmatropic rearrangement to offer the corresponding alkoxy pyrazole scaffold. However, the proposed hypothesis has a few challenges to overcome based on the literature survey. Also, the formation of sulfur ylide from DIPOLs are also not known in literature thus making it difficult to predict the outcome of the products based on the hypothesis. Also, there are not many reports associated with reactivity of acceptor-acceptor cyclic diazo carbonyl compounds such as DIPOLs via metal-carbenoid reactivity. Finally, mechanistically, oxygen of the pyrazolone amide is relatively more nucleophilic and it may pose hurdle for the proposed umpolung reactivity to obtain the desired transformation (Scheme 2Bi, 2Bii). As there are no reports of cyclic as well as acyclic amide containing diazo compounds, it demands a detailed and systematic investigation. In order to evaluate our hypothesis, we commenced with a model reaction using diazo edaravone (DEDA) **1a** (1.0 equiv.) and thioether ester **2a** (1.5 equiv.) in the presence of $Rh_2(OAc)_4$ at ambient temperature. The reaction did not work even under the prolonged reaction time (48 h) and both the substrates **1a** and **2a** were intact (Table 1, Entry 1). Later, we carried out the reaction of **1a** and **2a** in presence of $Rh_2(OAc)_4$ at an elevated temperature (78 °C, Table 1, Entry 2). Surprisingly, we isolated sulfonium ylide **3aa** albeit in lower yield (34%) and the anticipated alkoxy pyrazole derivative **4aa′** was not formed (Table 1, Entry 2). After gleaning through the literature, we learned that the sulfonium ylide **3aa** obtained is unknown in the literature.

Scheme 2. Substrate Scope of Thioethers Esters[a]



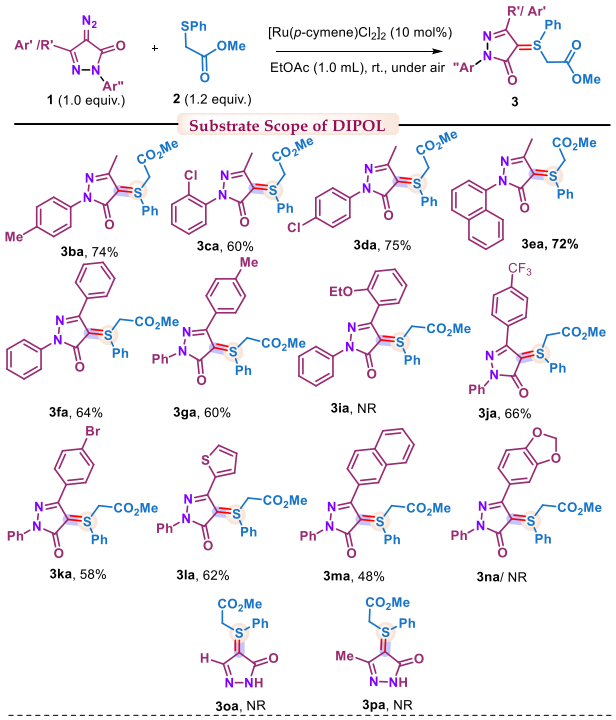
[a]**Reaction conditions:1** (0.2 mmol), **2a** (0.24 mmol), $[RuCl_2(p\text{-cymene})]_2$ (10 mol %), EtOAc (0.1 M)

In order to study and explore the reactivity of this new sulfonium ylide of DEDA, we further planned to optimize the reaction conditions so as to obtain the new sulfonium ylide efficiently. We screened different rhodium catalysts such as $[Rh_2(TFA)_4]$ and $[Rh_2(esp)_2]$ at room temperature. However, reaction did not work even under prolonged reaction time (see ESI, Table *S1*). Later, we screened different ruthenium catalysts such as $[RuCl_2(p\text{-cymene})_2]$, $[Ru(PPh_3)_3(CO)H_2]$, $[Ru(Phen)_3]Cl_2$, etc. at room temperature (see ESI, Table *S1*). Surprisingly, $[RuCl_2(p\text{-cymene})_2]$ (3 mol%) efficiently catalyzed the reaction of DEDA **1a** (1.0 equiv.) and thioether ester **2a** (1.5 equiv.) at room temperature to furnish the desired sulfonium ylide **3aa** in good yield (70%, 12 h, Table 1 Entry 3). The reaction under

https://doi.org/10.26434/chemrxiv-2025-f6k87 **ORCID:** https://orcid.org/0000-0002-7739-9553 Content not peer-reviewed by ChemRxiv. **License:** CC BY-NC-ND 4.0

prolonger reaction time as well as at an elevated temperature did not afford the product **4aa** (Table 1 Entry 4, 5). Among all the catalysts screened, [$RuCl_2$(*p*-cymene)$_2$] proved to be efficient for this transformation. Later, we screened the reaction in various solvents such as polar protic, aprotic, nucleophilic and non-nucleophilic solvents (See ESI, Table *S2*). Among all, ethyl acetate (EtOAc) proved to be advantageous for the efficient transformation. Based on the systematic screening (See ESI, Table *S3, S4*), **1a** (1 equiv.), **2a** (1.2 equiv.), [$RuCl_2$(*p*-cymene)$_2$] (10 mol %) in ethyl acetate at room temperature proved to be optimum reaction condition to obtain the stable sulfonium ylide **3aa.**

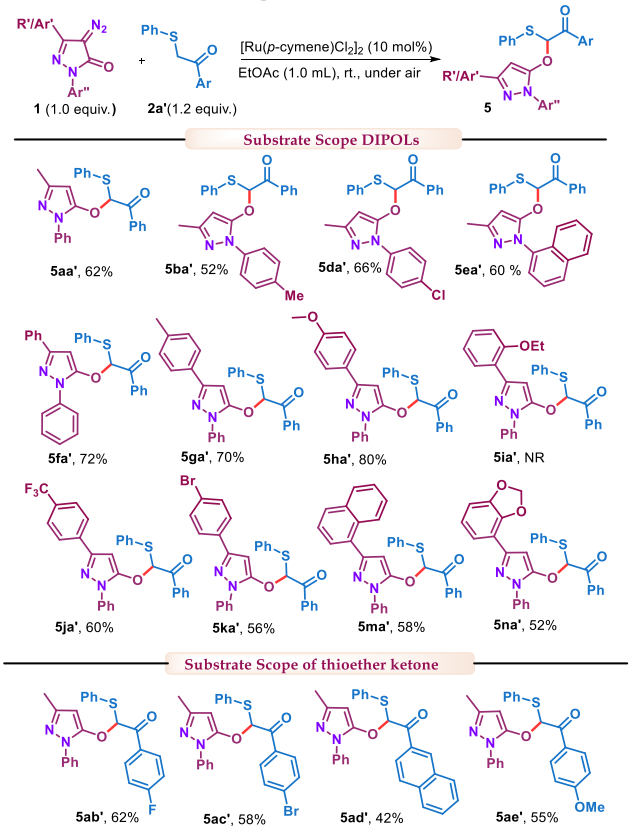
Scheme 3. Substrate Scope of Diazopyrazolone[a]



[a]**Reaction conditions:1** (0.2 mmol), **2a** (0.24 mmol), [$RuCl_2$(*p*-cymene)]$_2$ (10 mol %), EtOAc (0.1 M)

Having standardized the optimum reaction condition, we planned to explore the substrate scope and, in this regard, we synthesized a variety of aryl, heteroaryl, acyclic and cyclic alkyl derived thioether esters. The reaction of DEDA **1a** with methyl, ethyl and *t*-butyl thioether esters (**2a**-**2c**) under the optimum reaction condition afforded the corresponding desired products (**3aa**-**3ac**) in good yields (up to 80%). Aryl thioether esters having containing electron donating, electron withdrawing and electron deactivating substituents on phenyl group (**2d**-**2j**) worked smoothly under the optimum reaction conditions to furnish the corresponding products (**3ad**-**3aj**) in moderate to good yields (up to 83%, Scheme 2). Heteroaryl derived thioether esters such as 2-furyl, 2- pyridyl (**2k**-**2l**) derivatives reacted with **1a** smoothly to afford the corresponding sulfonium ylides (**3ak**-**3al**) in moderate yields (up to 61%). However, the 4-pyridyl thioether ester did not furnish the desired product **3am** probably owing to instability due to its electronic nature. Cyclohexyl and long chain alkyl derived thioether esters reacted sluggishly with **1a** to furnish the corresponding sulfonium ylides **3an**, **3ao** in lower yields (up to 28%). In order extend the generality and practicality of this protocol, we synthesized a variety of diazo pyrazolones (DIPOLs) such as *N*-aryl and C-4 substituted DIPOLs (**1b**-**1p**). To begin with we studied the reactivity of *N*-aryl DIPOL having electron-donating as well as deactivating groups (Me, Cl, Naphthyl) (**1b**-**1e**) with **2a** under optimum reaction condition furnished the corresponding products (**3ba**-**3ea**) in moderate to good yields (up to 74%, Scheme 3). Further DIPOLs substituted with C4 phenyl group having electron donating as well as electron withdrawing substituents (**1f**-**1i**) upon treatment with thioether ester **2a** afforded the corresponding products (**3fa**-**3ia**) in moderate yields (up to 64% yield, Scheme 3).

Scheme 4. Substrate Scope of Thioethers ketone[a]



[a]**Reaction conditions:1** (0.2 mmol), **2a** (0.24 mmol), [$RuCl_2$(*p*-cymene)]$_2$ (10 mol %), EtOAc (0.1 M)

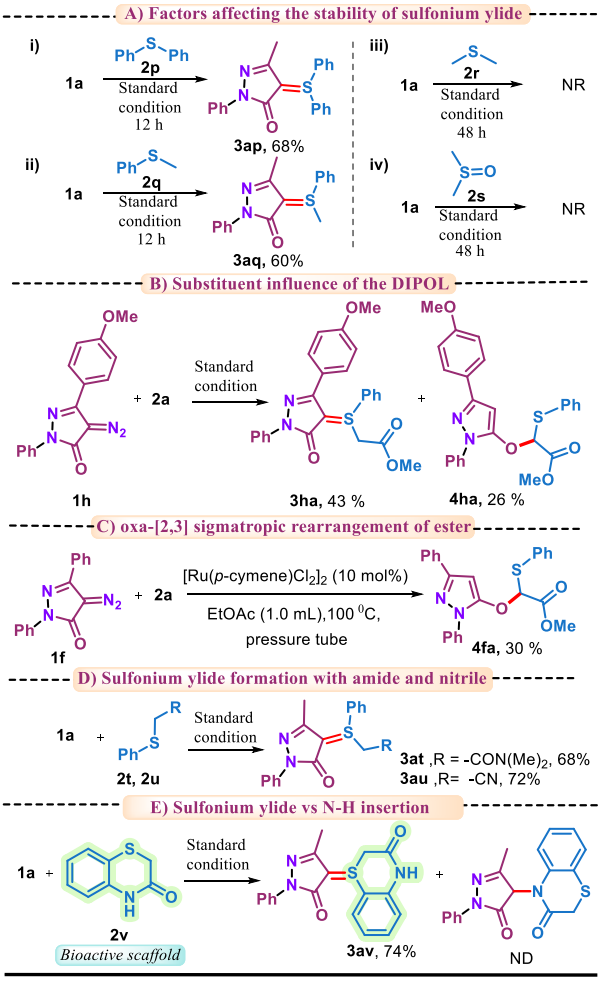
However, DIPOL with *o*-ethoxy phenyl group **1i** did not react probably due to the steric hindrance. DIPOL having C4-phenyl substituted with electron deactivating groups **1j** and **1k** react smoothy to obtained corresponding product **3ja** and **3ka** respectively. Some of other DIPOLs having 2-thionyl **1l**, and bulkier naphthyl **1m** reacted smoothly with **2a** under the reaction conditions to furnish the corresponding products (**3la**,**3ma**) in moderate to good yields (up to 62%, Scheme 3). The DIPOLs having benzodioxolane **1n** and protecting group free substrates (**1o**-**1p**, NH free) under optimum reaction conditions did not react at all (Scheme 3). Probably, unlike DEDA **1a** the free N-H in pyrazolone may be destabilizing the sulfonium ylide.

In order to enhance the generality of the protocol further, we planned replace the thioether ester **2a** with thioether ketone **2a′**. Surprisingly, the reaction of DEDA **1a** with thioether ketone **2a′** under optimum reaction condition offered the alkoxy pyrazole product **5aa′** unexpectedly in

https://doi.org/10.26434/chemrxiv-2025-f6k87 **ORCID:** https://orcid.org/0000-0002-7739-9553 Content not peer-reviewed by ChemRxiv. **License:** CC BY-NC-ND 4.0

moderate yield (62% yield). Excited as well as intrigued by this result, we planned to explore the diverse substrate scope of DIPOLs to so to investigate the reactivity pattern (Scheme 4). We explored the reaction of a variety of DIPOLs (**1a**–**1n)** having different *N*-arenes as well as alkyl/arene substituents at C4 position with thioether ketone **2a′** under optimum reaction conditions. C4 methyl substituted and *N*-arene substituted DIPOLs (**1b**, **1d** and **1e**) reacted smoothly with thioether ketone **2a′** to furnish corresponding alkoxy pyrazole products **5ba′**, **5da′** and **5ea′** respectively in moderate yields (up to 66 %).

Scheme 5. Control Experiments



Different N-aryl groups and aryl/heteroaryl groups at C-4 position of DIPOLs (**1f-1n**) reacted smoothly with thioether ketone **2a′** to afford the corresponding products (**5af′- 5an′**) in good yields (Scheme 4).

We observed that DIPOLs with C-4 phenyl group with electron donating groups reacted smoothly to afford the desired alkoxy pyrazoles in relatively in higher yields than that of C4-phenyl substituted with electron deactivating groups (Scheme 4). Whereas, C4-phenyl ring having *ortho*-ethoxy substituent DIPOL (**1i**) did not react under the optimum reaction condition probably due to the steric hindrance thus limiting the rearrangement. However, bulkier substituents such as naphthyl and benzodioxanyl at C4 position of DIPOLs reacted with **2a′** to afford the desired products albeit in moderate yields (up to 60%, Scheme 4). Later, in order to study the substrate scope of thioether ketones, we synthesized a variety of thioether ketones (**2b′**-**2f′**) having electron donating, electron deactivating and bulkier substituents. We observed that all the thioether ketones upon reaction with DEDA (**1a)** under optimum reaction condition furnished the desired alkoxy pyrazoles (**5ab′**-**5af′**) in moderate yields (up to 62%, Scheme 4).

Intrigued by the interesting results especially looking at the tunable reactivity of DIPOLs furnishing diverging products, we became interested in exploring the mechanistic insights in detail. In this regard, we explored a series of control experiments (Scheme 5).

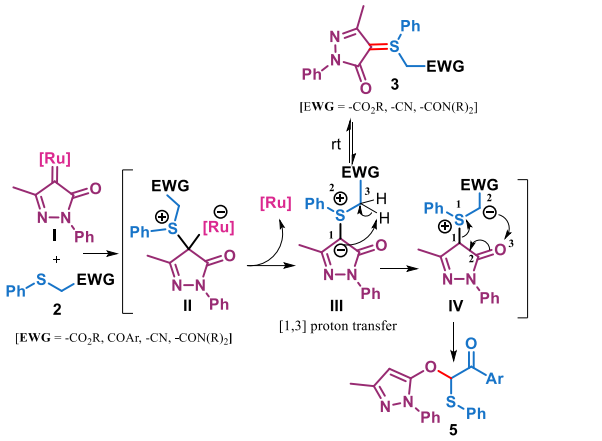
To begin with we studied the stability and the reactivity of sulfides towards DEDA. The reaction of diphenyl sulfide **2p** and methyl phenyl sulfide **2q** with DEDA **1a** under optimum reaction conditions afforded the corresponding products (**3ap**, **3aq**) in moderate yields (up to 68%, Scheme 5Ai, 5Aii). Interestingly, dimethyl sulfide **2r** did not react with the DEDA **1a** and the desired product was not obtained in trace even after prolonged reaction time. (up to 4h, Scheme 5Aiii). Also, dimethyl sulfoxide **2s** did not react with DEDA **1a** under optimized reaction conditions thus clearly indicating that the role of phenyl group for providing the stability to the sulfonium ylides (Scheme 5Aiv).

In order to understand the role of subsistent on phenyl group of **1** and its electronic effect on the overall transformation, we synthesized the electron rich *p*-methoxy phenyl substituted DIPOL **1h** (higher electron donating ability). Surprisingly, **1h** upon reaction with **2a** under standard reaction condition afforded corresponding sulfonium ylide **3ha** along with the alkoxy pyrazole derivative **4ha** though in modest yield (Scheme 5B). We believed that electron-donating methoxy group on the DIPOLs decreases the stability of the sulfonium ylide through cross resonance, thereby leading to oxa- [2,3] sigmatropic rearrangement via 1,3-proton transfer. This presumption is further supported by the exclusive formation of product **3ha** (see Scheme 3) wherein we did not observe any product emanating from oxa-[2,3] sigmatropic rearrangement due electron deactivating nature of CF_3 group. Further we hypothesized that electronic factors in turn influence the acidity of protons and the pKa also vary with the temperature. In this regard, we carried the reaction of **1a** and **2a** at an elevated temperature while maintaining the other standard conditions. Interestingly, we obtained the corresponding alkoxy pyrazole derivative **4fa** exclusively in modest yield along with inseparable side products (Scheme 5C). Later, we synthesized thioether amide **2t** as well as thioether nitrile **2u** and treated them with **1a** to obtain the corresponding the sulfonium ylides **3at, 3au** exclusively (Scheme 5D). These results indicate that higher acidity of protons in thioether ketones favored the facile 1,3-proton transfer to afford the corresponding alkoxy pyrazoles. While the thioether esters/amides/nitrile disfavor the facile 1,3-proton transfer probably due to lower acidity of protons compared to thioether ketones. Later, in order to examine the competitive reactivity of the sulfonium ylide versus the N-H insertion reaction, we synthesized compound **2v** a known bioactive scaffold [12] and subjected it to the reaction with **1a**. We obtained the corresponding sulfonium ylide product **3av** in 74% exclusively and we did not observe N-H insertion product even in trace.

https://doi.org/10.26434/chemrxiv-2025-f6k87 **ORCID:** https://orcid.org/0000-0002-7739-9553 Content not peer-reviewed by ChemRxiv. **License:** CC BY-NC-ND 4.0

Based on the control experiments and literature precedence[9f,11] the plausible reaction mechanism has been depicted in Scheme 6. DEDA **1a** in presence of $RuCl_2(p\text{-cymene})_2$ forms a ruthenium carbenoid intermediate **I**. This intermediate further reacts with thioether **2** to generate the corresponding sulfonium ylide **II** in situ which further leads to intermediate **III** by the regeneration of the catalyst.

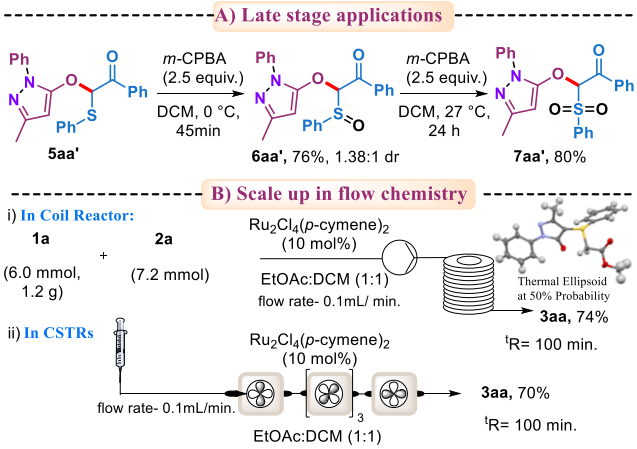
Scheme 6. Plausible Mechanism of the Transformation



Depending on the reactivity of thioethers, in situ generated intermediate **III** further affords either stable sulfonium ylide **3** or alkoxypyarazole **5**. The intermediate **III** derived from thioether ketones undergoes 1,3-proton shift to form intermediate **IV** which subsequently forms the desired alkoxy pyrazole **5** via oxa-[2,3]-sigmatropic rearrangement.

To explore the late-stage applications, substrate **5aa′** was treated with *m*-CPBA at 0 °C to obtain the corresponding mono-sulfoxide product **6aa′** in 76% yield (Scheme 7). We also, synthesized the corresponding sulfone product **7aa′** starting from the sulfoxide **6aa′** using *m*-CPBA (80%, Scheme 7). To further demonstrate the synthetic potential of this strategy, we carried out the flow synthesis on a gram scale using both a coil reactor as well as a continuous stirred-tank reactor after optimization (Scheme 7Bi, 7Bii; see more details in the ESI).

Scheme 7. Late Stage and Flow Synthesis.



In summary, we have successfully demonstrated novel reactivity of acceptor–acceptor diazo compound such as DIPOL under ruthenium catalysis to achieve novel class of sulfonium ylides and alkoxy pyrazole. These novel class of bench-stable sulfonium ylides have been effectively employed for the further application such as sulfoxidation, gram scale synthesis under flow chemistry as well. The established protocol demonstrated a wide substrate scope and good functional group tolerance. The also method gave an access to construct the bioactive alkoxy pyrazole. We have successfully explored the tunable reactivity of DIPOL with different thioether derivatives to access useful compounds.

ASSOCIATED CONTENT

Data Availability Statement

The data underlying this study are available in the published article and its Supporting Information.

Supporting Information

The Supporting Information is available free of charge on the Publications website. The reaction optimization tables, procedure for reaction, series of control experiments, flow synthesis procedure, characterization data for all new compounds and copies of ^{1}H, $^{13}C\{^{1}H\}$, and $^{19}F\{^{1}H\}$ NMR spectra (PDF). Data for the crystal structure reported in this manuscript have been deposited at the Cambridge Crystallographic Data Centre (CCDC) under the deposition number CCDC 2425665 (compound **3aa**).

AUTHOR INFORMATION

Corresponding Author

[a]Prof. Dr. Ramakrishna G. Bhat – Department of Chemistry, Indian Institute of Science Education and Research (IISER)-Pune, Dr. Homi Bhabha Road, Pashan, 411008, Pune, Maharashtra, India. orcid.org/0000-0002-7739-9553; Email: rgb@iiserpune.ac.in

Author Contributions

[a]Mr. Onkar S. Bankar, [a]Ms. Chhabi Pal, [a]Ms. Bhavya, [a]Mr. Abhijeet S. Sabale – [a]Department of Chemistry, Indian Institute of Science Education and Research (IISER)-Pune, Dr. Homi Bhabha Road, Pashan, 411008, Pune, Maharashtra, India. orcid.org/0009-0008-6701-9722

ACKNOWLEDGMENT

R. G. B. thanks Science and Engineering Research Board, Department of Science and Technology (SERB-DST), New Delhi, Government of India (File no: CRG/2023/004226) for the generous research grant. The authors also thank IISER Pune for financial assistance. O. S. B.; C. P.; B.; A. S. S. thank UGC New Delhi, The Government of India for providing fellowship. Authors also thank Sandeep Kaulage for kind help in obtaining SC-XRD data.

REFERENCES

(1) a) Ciszewski, Ł. W.; Rybicka-Jasiń ska, K.; Gryko, D. Recent Developments in Photochemical Reactions of Diazo Compounds. *Org. Biomol. Chem*. **2019**, *17*, 432–448. b) Zang, Z.; Stivanin, M. L.; Jurberg, I. D.; Koenigs, R. M. Visible light-promoted reactions with diazo compounds: a mild and practical strategy towards free carbene intermediates. *Chem. Soc. Rev*. **2020**, *49*, 6833–6847. c) Liu, Z.; Sivaguru, P.; Zanoni, G.; Bi, X. N- Triftosyl hydrazones: anew chapter for diazo-based carbene chemistry. *Acc. Chem. Res*. **2022**, *55*, 1763–1781.

(2) a) Kang, Z.; Wang, Y.; Zhang, D.; Wu, R.; Xu, X.; Hu, W. Asymmetric Counter-Anion-Directed Aminomethylation: Synthesis

https://doi.org/10.26434/chemrxiv-2025-f6k87 **ORCID:** https://orcid.org/0000-0002-7739-9553 Content not peer-reviewed by ChemRxiv. **License:** CC BY-NC-ND 4.0

of Chiral β-Amino Acids via Trapping of an Enol Intermediate *J. Am. Chem. Soc.* **2019**, *141*, 1473–1478. (b) Lin, X.; Tang, Y.; Yang, W.;Tan, F.; Lin, L.; Liu, X.; Feng, X. Chiral Nickel(II) Complex Catalyzed Enantioselective Doyle–Kirmse Reaction of α-Diazo Pyrazoleamides *J. Am. Chem. Soc.* **2018**, *140*, 3299–3305. (c) Guzman, P. E.; Lian, Y.; Davies, H. M. L. Reversal of the Regiochemistry in the Rhodium-Catalyzed [4+3] Cycloaddition between Vinyl diazoacetates and Dienes *Angew. Chem., Int. Ed.* **2014**, *53*, 13083–13087. (e) Xu, X.; Zavalij, P. Y.; Hu, W.; Doyle, M. P. Highly stereoselective Ru(ii)–Pheox catalyzed asymmetric cyclopropanation of terminal olefins with succinimidyl diazoacetate *Chem. Commun*. **2012**, *48*, 11522–11524.

(3) a) Davies, H. M. L.; Morton, D. Guiding Principles for Site Selective and Stereoselective Intermolecular C–H Functionalization by Donor/acceptor Rhodium Carbenes. *Chem. Soc. Rev*. **2011**, *40*, 1857–1869. b) Zhang, Z.; Gevorgyan, V. Visible Light-Induced Reactions of Diazo Compounds and Their Precursors. *Chem. Rev*. **2024**, *124*, 7214–7261. (c) Ford, A.; Miel, H.; Ring, A.; Slattery, C. N.; Maguire, A. R.; McKervey, M. A. Modern Organic Synthesis with α-Diazocarbonyl Compounds. *Chem. Rev*. **2015**, *115*, 9981–10080.

(4) (a) Candeias, N. R.; Paterna, R.; Gois, P. M. P. Homologation Reaction of Ketones with Diazo Compounds. *Chem. Rev*. **2016**, *116*, 2937–2981. (b) Cheng, Q.-Q.; Deng, Y.; Lankel ma, M.; Doyle, M. P. Cycloaddition Reactions of Enol diazo Compounds. *Chem. Soc. Rev*.**2017**, *46*, 5425–5443. (c) Davies, H. M. L.; Denton, J. R. Application of Donor/acceptor-Carbenoids to the Synthesis of Natural Products. *Chem. Soc. Rev*. **2009**, *38*, 3061–3071.

(5) (a) Cai, X.; Song, X.; Zhu, Q.; Zhang, X.; Fan, X. Concise Synthesis of Spirocyclic Dihydro phthalazines through Spiro annulation Reactions of Aryl Azomethine Imines with Cyclic Diazo Compounds. *J. Org. Chem*. **2022**, *87*,11048–11062 (b) Fang, F.; Hu, S.; Li, C.; Wang, Q.; Wang, R.; Han, X.; Zhou, Y.; Liu, H. Catalytic System-Controlled Divergent Reaction Strategies for the Construction of Diversified Spiropyr-azolone Skeletons from Pyrazolidinones and Diazopyrazolones. *Angew. Chem., Int. Ed*. **2021**, *60*, 21327–21333. (c) Yu, C.; Xu, Y.; Zhang, X.; Fan, X. Selective Synthesis of Pyrazolonyl Spiro dihydroquinolines or Pyrazolonyl Spiroindolines under Aerobic or Anaerobic Conditions. *Org. Lett*. **2022**, *24*, 9473–9478. (d) Bankar, O. S.; Pal, C.; Laha, D.; Sabale, A. S.; Bhat, R. G. The Reactivity of Acceptor-Acceptor Diazo Pyrazolones with Allyl Thioethers under Visible Light: Access to Homoallyl Sulfides, Spiropyrazolones - Pesticide Analogues and Photoflow Synthesis. *Org. Lett.* **2024**, *26*, *43*, 9191–9197.

(6) (a) Zhang, Z.; Han, J.; Zhu S. Facile synthesis of novel CF3-substituted ring-fused furo [2,3-c] pyrazoles through $Rh_2(OAc)_4$ catalyzed [3+2] cycloaddition of 4-diazo-1-phenyl-3-(trifluoromethyl)- 1H-pyrazol-5(4H)-one with aromatic alkynes. *Tetrahedron Lett*. **2011,** *67,* 8496-5101. (b) Zhang, K.; Zhao, G.; Cao, W. Construction of fluorinated pyrazole derivatives via a one-pot tandem CeH insertion/electrophilic fluorination reaction *Tetrahedron Lett*. **2014**, *70*, 5659-5665. (c) Fang, F.; Hu, S.; Li, C.; Wang, Q.; Wang, R.; Han, X.; Zhou, Y.; Liu, H. Catalytic System-Controlled Divergent Reaction Strategies for the Construction of Diversified Spiropyrazolone Skeletons from Pyrazolidinones and Diazopyrazolones. *Angew. Chem., Int. Ed*. **2021**, *60*, 21327–21333. (d) Song, X.; Wang, K.; Xue, L.; Yu, H.; Zhang, X.; Lee, R.; Fan, X. Coupling Partner-Dependent Unsymmetrical C–H Functionalization of N-Phenoxy acetamides Leading to Sophisticated Spirocyclic Scaffolds. *Org. Chem. Front*. **2022**, *9*, 4583–4590. (e) Cai, X.; Song, X.; Zhu, Q.; Zhang, X.; Fan, X. Concise Synthesis of Spirocyclic Dihydro phthalazines through Spiro annulation Reactions of Aryl Azomethine Imines with Cyclic Diazo Compounds. *J. Org. Chem*. **2022**, *87*, 11048–11062. (f) Yu, C.; Xu, Y.; Zhang, X.; Fan, X. Selective Synthesis of Pyrazolonyl Spirodihydroquinolines or Pyrazolonyl Spiroindolines under Aerobic or Anaerobic Conditions. *Org. Lett.* **2022**, *24*, 9473–9478. (g) Lai, R.; Xu, S.; Zhang, Q.; Zhou, H.; Luo, C.; Wang, Y.; Hai, L.; Wu, Y. Derivation of Benzothiadiazine-1,1-dioxide Scaffolds via Transition Metal-Catalyzed C—H Activation/Annulation. *Chin. J. Chem*. **2023**, *41*, 1973—1978.

(7) (a) Bankar, O. S.; Laha, D., Meher, K. B.; Bhat, R. G. Umpolung Reactivity of Diazo Arylidene Succinimides: Distal C–H Functionalization of α-Thiocarbonyls from the Reactive Carbenoid Center. *Chem Asian J*. **2023**, *18*, e202300774. (b) Laha, D.; Meher, K. B.; Bankar, O. S.; Bhat, R. G. Silver-Catalyzed One-Pot Access to Diastereoselective Benzo [5,6] oxepino [2,3-c] pyrroles via Formal (5+2)-Annulation of Donor-/Acceptor-Type Aryl Vinyl Diazosuccinimide with Ketones. *Asian J. Org. Chem*. **2022**, *11*, e202200062. (C) Inyutina, A.; Dar'in, D.; Kantin, G.; Krasavin, M. Tricyclic 2-benzazepines obtained via an unexpected cyclization involvingnitrilium ylides. Org. Biomol. Chem. 2021, 19, 5068–5071.

(8) (a) Kirmse, W.; Kapps, M. Reaktionen des diazomethans mit diallyl sulfide und allylathern¨ unter kupfersalz-katalyse. Chem. Ber. **1968**, *101*, 994. (b) Doyle, M. P.; Tamblyn, W. H.; Bagheri, V. Highly effective catalytic methods for ylide generation from diazo compounds. Mechanism of the rhodium- and copper-catalyzed reactions with allylic compounds J. Org. Chem. **1981**, *46*, 5094–5102. (c) Carter, D. S.; Van Vranken, D. L. Iron-Catalyzed Doyle–Kirmse Reaction of Allyl Sulfides with (Trimethylsilyl)diazomethane *Org. Lett.* **2000**, *2*,1303–1305. (d) Kato, Y.; Miki, K.; Nishino, F.; Ohe, K.; Uemura, S. Silver-catalysed Doyle–Kirmse reaction of allyl and propargyl sulfides *Org. Lett*. **2003**, *5*, 2619–2621. (e) Zhou, J.; Cao, C.-L.; Sun, X.-L.; Dai, L.-X.; Tang, Y. Doyle–Kirmse Reaction of Allylic Sulfides with Diazoalkane-Free (2-Furyl) carbenoid Transfer *Adv. Synth. Catal*. **2009**, *351*, 308–312. (f) Ellis-Holder, K. K.; Peppers, B. P.; Kovalevsky, A. Y.; Diver, S. T. Rhodium-Catalyzed Denitrogenative [2,3] Sigmatropic Rearrangement: An Efficient Entry to Sulfur-Containing Quaternary Centers *Org. Lett*. **2006**, *8*, 2511–2514.

(9) (a) Kantor, S. W.; Hauser, C. R. Rearrangements of Benzyl trimethyl ammonium Ion and Related Quaternary Ammonium Ions by Sodium Amide Involving Migration into the Ring *J. Am. Chem. Soc*. **1951**, *73*, 4122–4131. (b) Hauser, C. R.; Kantor, S. W.; Brasen, W. R. Rearrangement of Benzyl Sulfides to Mercaptans and of Sulfonium Ions to Sulfides Involving the Aromatic Ring by Alkali Amides *J. Am. Chem. Soc*. **1953**, *75*, 2660–2663. (c) Shirai, N.; Watanabe, Y.; Sato, Y. J. Intermediate in Sommelet-Hauser rearrangement of N, N-dimethyl benzyl ammonium N-methylides *J. Org. Chem*. **1990**, 55, 2767–2770. (d) Tanaka, T.; Shirai, N.; Sugimori, J.; Sato, Y. J. Selection of a Sommelet-Hauser or a Stevens rearrangement pathway of N, N-dimethyl(substituted benzyl)ammonium N-alkylides. *J. Org. Chem*. **1992**, *57*, 5034–5036. (e) Jana, S.; Koenigs, R. M. Rhodium-Catalyzed Carbene Transfer Reactions for Sigmatropic Rearrangement Reactions of Selenium Ylides *Org. Lett.* **2019**, *21*, 3653–3657. (f) Lin, X.; Yang, W.; Yang, W.; Liu, X.; Feng, X. Asymmetric Catalytic [2,3] Stevens and Sommelet–Hauser Rearrangements of a-Diazo Pyrazoleamides with Sulfides. *Angew. Chem., Int. Ed*. **2019**, *58*, 13492–13498.

(10) Liao, M.; Peng, L.; Wang, J. Rh(II)-Catalyzed Sommelet–Hauser Rearrangement. *Org. Lett*. **2008**, *10*, 693–696.

(11) Reddy, A. C. S.; Anbarasan, P. Rhodium-Catalyzed Rearrangement of S/Se-Ylides for the Synthesis of Substituted Vinylogous Carbonates. *Org. Lett*. **2019**, *21*, 9965–9969.

(12) Ellouz, M.; Sebbar, N. K.; Fichtali I., Ouzidan, Y.; Mennane, Z.; Charof, R.; Mague, J. T.; Urrutigoïty, M.; Essassi, El. M. Synthesis and antibacterial activity of new 1,2,3-triazolylmethyl-2*H*-1,4-benzothiazin-3(4*H*)-one derivatives. *Chemistry Central Journal* **2018,** *12*

https://doi.org/10.26434/chemrxiv-2025-f6k87 **ORCID:** https://orcid.org/0000-0002-7739-9553 Content not peer-reviewed by ChemRxiv. **License:** CC BY-NC-ND 4.0

https://doi.org/10.26434/chemrxiv-2025-f6k87 **ORCID:** https://orcid.org/0000-0002-7739-9553 Content not peer-reviewed by ChemRxiv. **License:** CC BY-NC-ND 4.0

ScienceDirect

Spirooxindole

Chemistry, Synthesis, Characterization and Biological Significance

2024, Pages 309-331

Chapter 12 - Synthesis of hybrid spirooxindoles

Prakash K. Warghude [1 2], Abhijeet S. Sabale [1], Ramakrishna G. Bhat [1]

Show more

Outline | Share Cite

https://doi.org/10.1016/B978-0-443-22324-2.00012-6 ↗

Get rights and content ↗

Abstract

Hybrid spirooxindoles represent a class of compounds that have gained significant attention in the realm of medicinal chemistry due to their diverse biological activities and promising pharmacological profiles. These unique structures, featuring a spirooxindole core, amalgamate various molecular scaffolds, offering a versatile platform for drug design and development. The synthesis and structural modifications of hybrid spirooxindoles have led to compounds exhibiting a wide array of biological properties, including anticancer, antimicrobial, antiinflammatory, and neuroprotective activities. Their potential as therapeutic agents have spurred intensive research efforts aimed at exploring their mechanisms of action and optimizing their pharmacokinetic properties.

Recommended articles

References (0)

Cited by (0)